Proceedings Of The Fourth Annual NASA And Department Of Defense Precise Time And Time Interval (PTTI) Planning Meeting

14-16 November 1972

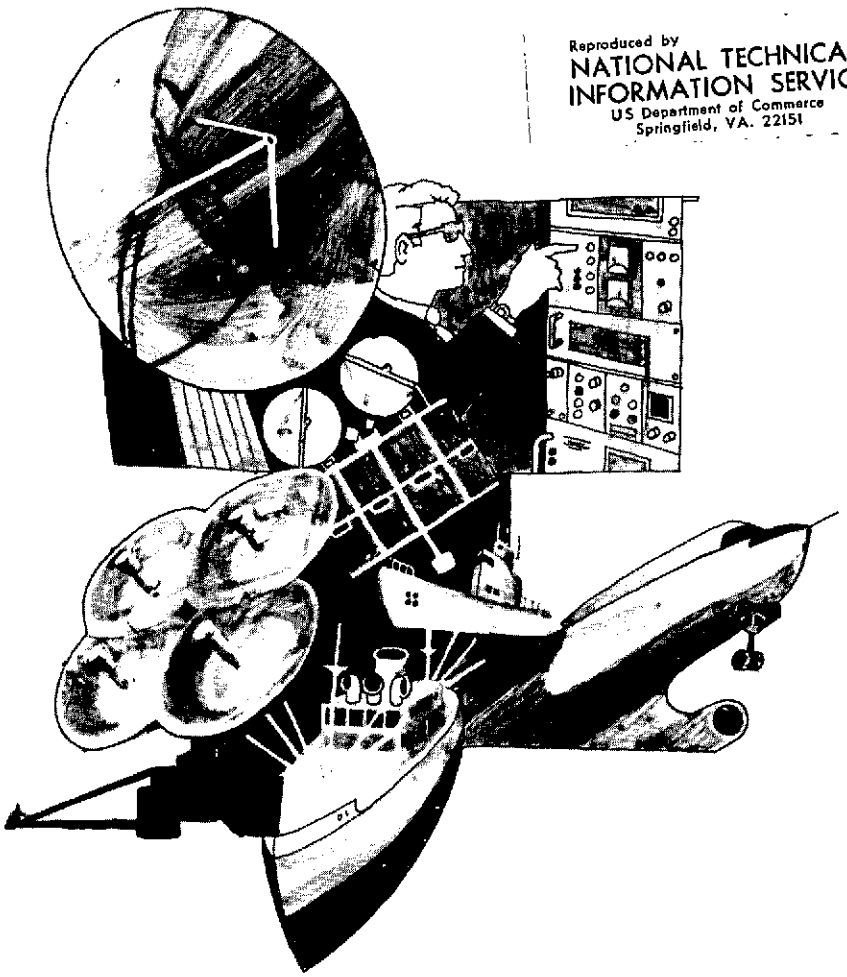

X-814-73-72

X-814-73-72

PROCEEDINGS

OF THE

FOURTH PRECISE TIME AND TIME INTERVAL PLANNING MEETING

Held at Goddard Space Flight Center
November 14-16, 1972

Compiled by
H. N. Acrivos
Clark Wardrip

Second Printing

Sponsored by
NASA Goddard Space Flight Center (GSFC)
U. S. Naval Observatory (USNO)
U. S. Naval Electronic Systems Command (USNESC)

Prepared by
GODDARD SPACE FLIGHT CENTER
Greenbelt, Maryland 20771

FOREWORD

This volume contains the papers and panel discussions presented at the fourth Precise Time and Time Interval (PTTI) Planning Meeting. The meeting was sponsored jointly by NASA/Goddard Space Flight Center, the U. S. Naval Observatory, and the U. S. Naval Electronic Systems Command. The meeting was held at Goddard Space Flight Center on November 14-16, 1972.

The objectives of the PTTI Planning Meetings are to:

- Disseminate and coordinate information at the user level associated with PTTI
- Review present and future PTTI requirements
- Inform Government engineers, technicians, and managers of precise time and frequency technology and its problems
- Provide an opportunity for an active exchange of new technology associated with PTTI

The proceedings are arranged into three sessions, namely:

I. Satellite Timing Techniques, Precision Frequency Sources, and VLBI applications.

II. Frequency Stabilities and Communications

III. VLF–UHF, Propagation and Use

A panel discussion on the papers and related subject matter was conducted by the session chairman after each session. The panels were composed of experts in the field covered by the particular session.

More than 300 people participated in the conference, either as attendees or registrants. Attendees came from the U. S. Government, from private industry, and from several foreign embassies. Twenty-eight papers were invited for presentation, covering areas of navigation, communications, satellite tracking, interferometry techniques, radio wave propagation, and frequency and time generation and synchronization.*

It is the hope of this year's PTTI officers that the close communication and cooperation that has been established between the various Government agencies will be maintained, perpetuated, and expanded to cover other PTTI-related fields in future meetings.

*"Use of Precise Time and Frequency Standards in the Very Long Baseline Interferometer Investigation of Celestial Radio Sources," by K. H. Johnston and S. H. Knowles of the Naval Research Laboratory, was presented but is omitted from these Proceedings.

It is with great pleasure that we acknowledge the support and contribution of the officers, session chairmen, panelists, speakers, and authors, and the many others who contributed to the success of this year's PTTI meeting.

Copies of the proceedings may be obtained from either the Goddard Space Flight Center or the U. S. Naval Observatory by sending a request to either:

S. Clark Wardrip
Head, Timing Systems Section
Code 814.2
Goddard Space Flight Center
Greenbelt, Maryland 20771

Harold N. Acrivos
Precise Time Operations Officer
Time Service Division
U. S. Naval Observatory
Washington, D. C. 20390

CONTENTS

CONTENTS (continued)

CONFERENCE OFFICERS AND COMMITTEES

General Chairman
Clark Wardrip, GSFC

Technical Program Committee Chairman
Harold N. Acrivos, USNO

Executive Committee
Harold N. Acrivos, USNO
Lcdr. Frank R. Johnson, Jr., USNO
Theodore N. Lieberman, NAVELECSYSCOM
Robert R. Stone, Jr., NRL
Clark Wardrip, GSFC

Arrangements

Exhibits:
Harold N. Acrivos, USNO
Paul Kushmeider, GSFC
Wilfred Mazur, GSFC
James A. Murray, Jr., NRL
John Wilson, NELC

Technical Assistance
Robert A. Howatt, GSFC
Donald Kaufmann, GSFC
James C. Perry Jr., GSFC

Finance Committee Chairman
Theodore N. Lieberman, NAVELECSYSCOM

Banquet Speaker
Dr. John A. O'Keefe, GSFC

Proceedings' Editors
Dr. R. Glenn Hall, USNO
Dr. William J. Klepczynski, USNO
Dr. Jayaram Ramasastry, GSFC

Call to Session
Clark Wardrip, GSFC

Opening Address
Laverne R. Stelter, GSFC

Introduction
Capt. John C. Bajus, NAVELECSYSCOM

Session I Chairman
Andrew R. Chi, GSFC

Session II Chairman
Dr. William Klepczynski, USNO

Session III Chairman
Dr. Gernot M. R. Winkler, USNO

Panel Discussions

Session I

Discussion Coordinator: *Andrew R. Chi,* GSFC

Panel Members:

Dr. Carroll O. Alley, Maryland University
Dr. William J. Hurd, JPL
Dr. Stephen H. Knowles, Maryland University
Dr. Arthur O. McCoubrey, Frequency and Time Systems, Inc.
Peter F. MacDoran, JPL
Dr. Jayaram Ramasastry, GSFC

Session II

Discussion Coordinator: *Dr. William J. Klepczynski,* USNO

Panel Members:

Lauren J. Rueger, APL
Dr. Gernot M. R. Winkler, USNO
Dr. John E. Lavery, GSFC
James A. Murray, Jr., NRL
Harold C. Folts, NCS
Jay B. Curtright, JPL
Robert R. Stone, Jr., NRL
Cdr. William K. Hartell, NESC
Eric R. Swanson, NELC
Dr. James C. Morakis, GSFC
John T. Stanley, NBS

Session III

Discussion Coordinator: *Dr. Gernot M. R. Winkler,* USNO

Panel Members:

Dr. Frederick W. Rohde, USATOPOCOM
Eric Swanson, NELC
Dr. Friedrich H. Reder, USAECOM

Panel Members Continued:

Dr. James Crouchley, Queensland University, Australia
James Britt, NELC
Andrew R. Chi, GSFC

OPENING ADDRESS

Laverne R. Stelter
Goddard Space Flight Center

On behalf of Dr. John Clark, the Director of Goddard Space Flight Center, I would like to welcome you here this morning. To those of you that have come in from out of town, I'm sorry about the wet weather. While driving into work this morning, I heard the weatherman report that the rain should stop by noon. Now, if the weatherman dealt with such precise subjects as time, he would be more accurate. We do hope the weather improves and that your stay here is a good one.

I would like to tell you briefly about what we do here at Goddard, especially for the benefit of those of you who have not been here before. And I would also like to tell you why we consider time and timing a very important subject.

There are about 4200 people here at Goddard, and about two-thirds of them are involved in managing, preparing, and launching earth-orbiting satellites. These satellites fall into two basic categories: the scientific type, for astronomy, earth physics, and so on – satellites like the Orbiting Solar Observatory (OSO) series; and the application satellites, such as the Advanced Technology Satellite (ATS) series, weather satellites like Nimbus, and more recently, the Earth Resources Technology Satellite (ERTS-1).

I might add that in many cases the satellite experiment instruments are built in-house here at Goddard, and in some cases the smaller satellites are actually constructed here. And most are also tested here. Those of you who take the tour Thursday will see the environmental test facilities – the classic "shake and bake" facilities.

The other one-third of the people here are involved with the ground-operations end of the business. This breaks down into two major categories – the tracking and data-acquisition function, and the data-processing function. Those of us in networks are involved in the engineering and operation of tracking stations around the world, with the global communications net that ties these stations together, and with the project control centers that take care of the health and maintenance of the spacecraft themselves.

Again, those of you who go on the tour will also see the heart of our communications net. You will also see a number of project control centers. From some of these centers, the earth-orbiting satellites are physically controlled.

The subject of timing is a very important ingredient in everything we do here. Speaking from personal experience, I first got involved with timing – and this may sound like some time ago, considering the young faces in the audience – back in the early 1950s. I was a red-hot engineer, just out of college, and one of my very first jobs in the U.S. Army Signal

Corps was to put out into the field a better way to measure frequency at our point-to-point transmitter and receiver station.

So I did a two-month survey of what was available in the state-of-the-art and ended up with General Radio frequency-measuring equipment. It was actually two racks of equipment, including a longitudinal-oscillating 100-Kc crystal, heterodyne oscillators, and so forth. The crystal was good to about one part in 10^6. This equipment was sent to the field and I remember thinking at the time that it was quite an achievement to consistently measure the output frequency of a transmitter operating in the HF band with an accuracy of better than 100 hertz.

Well, that was just about 20 years ago, and many advances have been made since that time. During Apollo-17 for instance, we measured the position of the lunar rover with respect to the lunar module to a positional accuracy of about one meter on the lunar surface. To do that, the frequency standards in use today in the tracking stations must have a short-term stability on the order of about one part in 10^{12}. We used the very long baseline interferometer (VLBI) technique and measured the relative arrival time of the wavefronts of the signals from the lunar module and from the lunar rover. Therefore, in 20 years, we've come a long, long way.

We see no end to the demand for very precise measurement of time, which is also obviously related to very good frequency stabilities. As we move into the area of very high precision orbit determination, techniques involving the measurement of lunar libration, and so forth, we are going to require better and better precision in everything we do.

It is conferences such as this that we feel are extremely beneficial in allowing interchange and exchange of information. We look forward to a continuing cooperation with all of you in attempting to further PTTI capabilities. We feel that a forum such as this goes a very long way in promoting advances in the state-of-the-art.

Once again, welcome to Goddard. We hope your stay here is a pleasant one. If there is anything we can do to help you out, let us know. We will do our best to accomodate you.

Thank you very much.

INTRODUCTION

John C. Bajus
U. S. Naval Electronic Systems Command

As a professional Naval officer and operating engineer, I want to welcome you on behalf of the U.S. Navy to this fourth Precise Time and Time Interval (PTTI) Planning Conference.

The two sponsoring agencies of the U. S. Navy, the U.S. Naval Observatory and the Naval Electronic Systems Command, are very fortunate this year to enjoy the co-sponsorship of the NASA/Goddard Space Flight Center. In particular, I want to express my appreciation to Dr. Clark and the people at Goddard for allowing us to utilize this beautiful facility. Thank you for your generous contribution to this conference.

One of the main reasons for this PTTI Planning Conference is the exchange of practical information. Therefore, I would like to discuss the recent changes within the Navy relative to management of this important aspect of our daily lives.

The Naval Observatory, like other government organizations, is resource limited, and even more so in these days. Its responsibility as the PTTI manager for the Department of Defense is in itself a full-time job. In the past, this dual role of Naval Observatory and Department of Defense manager has caused some problems, especially at tri-Service meetings. Therefore, in order to improve the situation, the Chief of Naval Material, Admiral Kidd, has been charged with the Navy management responsibility, and he is in the process of redelegating these responsibilities to us in the Naval Electronic Systems Command. This, we hope, will strengthen the Naval Observatory's capabilities for the execution of their proper mission. Which means, in the PTTI area, essentially the following:

- Provision of the time standard
- Management and consultation regarding the overall Department of Defense precise time and time interval effort
- The distribution of precise time and time interval down to the next level in the PTTI hierarchy, that is, to the precise time-reference stations

The Naval Electronic Systems Command will assume these additional management responsibilities for the Navy, including planning, programming, and budgeting for the complete research development and on into total life-cycle support. In addition, the Naval Electronic Systems Command will assist the Naval Observatory in the execution of its responsibilities as the manager for the Department of Defense.

As examples, we can mention the current effort to upgrade the time distribution over LORAN-C and the proposed establishment of precise time-reference stations at certain satellite communications ground terminals.

The choice of our command, NAVELECS, for this role is proper because of our expanding responsibilities in the Naval Material Command for command and control communications underseas and for space surveillance, navigation, and recently, electronics warfare. Each of these system areas will require PTTI as an indispensible element. Furthermore, it is the only common base for achieving integrated communications navigation and identification systems, and other such system concepts that cut across many electronics systems.

While NAVELECS has been charged with these additional responsibilities without a concomitant increase of resources, we welcome this challenge to do a good job and we will try our best to do so, for the Navy's operational requirements demand it.

In many tactical situations we find it is mandatory that several Department of Defense components be synchronized to a high order to complete a mission. We have to be on time. And I trust as we continue our deliberations these few days that we will maintain our time schedule. I sincerely hope that this conference will help us all in this endeavor.

SESSION I

Satellite Timing Techniques, Precision Frequency Sources, and VLBI Applications

TIMATION III SATELLITE

Charles A. Bartholomew
Naval Research Laboratory

This satellite is the third in a series of experimental satellites designed to investigate and demonstrate the techniques of a satellite navigation system. Timation III is designed to measure the error budget for a proposed system and provide one element of a navigation demonstration experiment. Table 1 lists the principal characteristics of the three satellites and shows the progressive development of the program.

Figure 1 is a drawing of the satellite showing the basic structure. It is an octagonal donut, 48 inches across the flats and approximately 23 inches in height. The solar panels, navigation and telemetry antennas, gravity gradient booms, and solar cell experiments are clearly visible. Figure 2 lists five auxiliary experiments to be conducted with the satellite.

Time management or time transfer is a natural fallout of most navigation systems. This satellite, in view for long periods of time and covisible over intercontinental ranges, will provide an excellent time transfer capability.

A joint service flavor has been added in the form of an Air Force experiment. This consists of a pseudo-noise modulated signal near 1580 MHz. This experiment requires relatively high power compared with the power system capability and therefore must be scheduled for limited periods of time. This experiment is being conducted principally for ionospheric scintillation measurements and ILS demonstration tests.

A NASA retroreflector panel for ranging measurements provides a second joint experiment. This independent measure of range is expected to provide valuable correlation data to the navigation measurements. The expected resolution for the NASA system is 10 cm.

Several radiation dosimeters are being considered to correlate measured radiation effects on the quartz oscillator and provide dose levels and rates at this new orbit altitude. Residual radiation effects can be seen in Figure 3 which is a plot of apparent aging rate versus time for the Timation II satellite. The aging rate prior to launch was approximately $+1pp10^{11}$ per day. During the initial orbiting period it was as high as $+3pp10^{11}$ per day and decreasing to almost $-5pp10^{11}$ per day. This effect has decreased to approximately $-1.4pp10^{11}$ per day at day 1000. Transient radiation effects can be seen in Figure 4, a plot of frequency versus time for days 204 through 239 in 1972. The abrupt frequency shift is associated with a solar storm.

Test solar panels will be included to provide long-term evaluation data of several new solar cell configurations in this operating environment.

Figure 5 is a list of the primary ground stations in the orbit determining net. The satellite is always in view of at least one ground station. The satellite is observed four times daily at each station with visibility times ranging from 40 to 140 minutes.

A set of four candidate oscillators is being evaluated for this satellite. These units were manufactured by Frequency Electronics Inc. of New York. Figure 6 is a plot of fractional frequency fluctuation versus averaging time and Figure 7 is a plot of frequency versus time to show aging rates.

Table 1
Timation Satellites.

Launch Date	May 31, 1967	Sept. 30, 1969	FY 74
Altitude	500 nm	500 nm	7,500 nm
Inclination	70°	70°	145°
Weight	85 lb	125 lb	415 lb
Frequencies	400 MHz	150 & 400 MHz	335 & 1580 MHz
Max. Mod. Freq.	100 KHz	1 MHz	6.4 MHz
Memory	No	No	Yes
Osc. Stab.	$3pp10^{11}$	$1pp10^{11}$	$1\text{-}5pp10^{12}$
D.C. Power	6W	18W	90W BOL

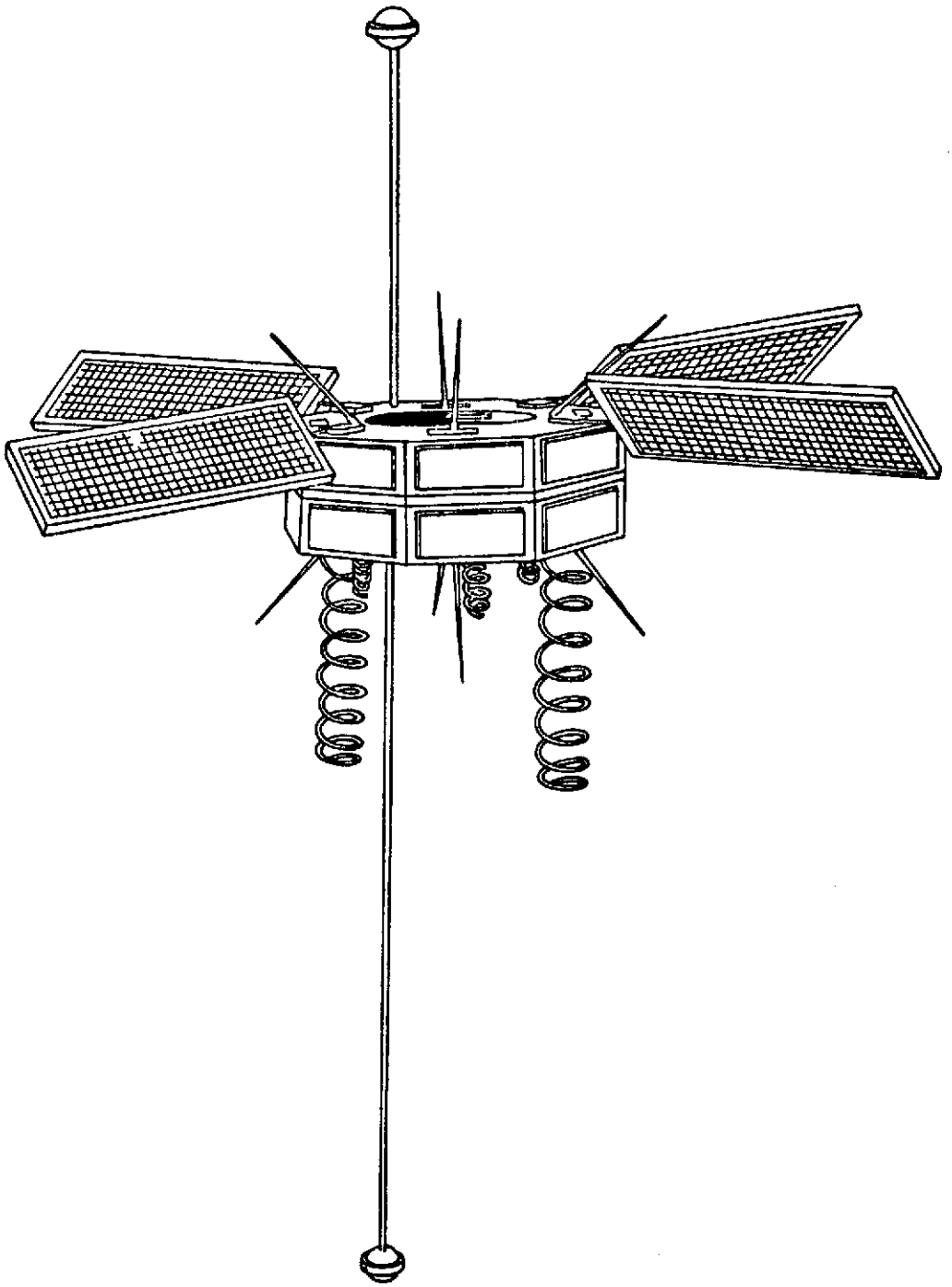

Figure 1. Drawing of Timation III.

TIME TRANSFER

PRN MODULATION (USAF)

RETROFLECTORS (NASA)

RADIATION DOSIMETERS

TEST SOLAR PANELS

Figure 2. Timation III experiments.

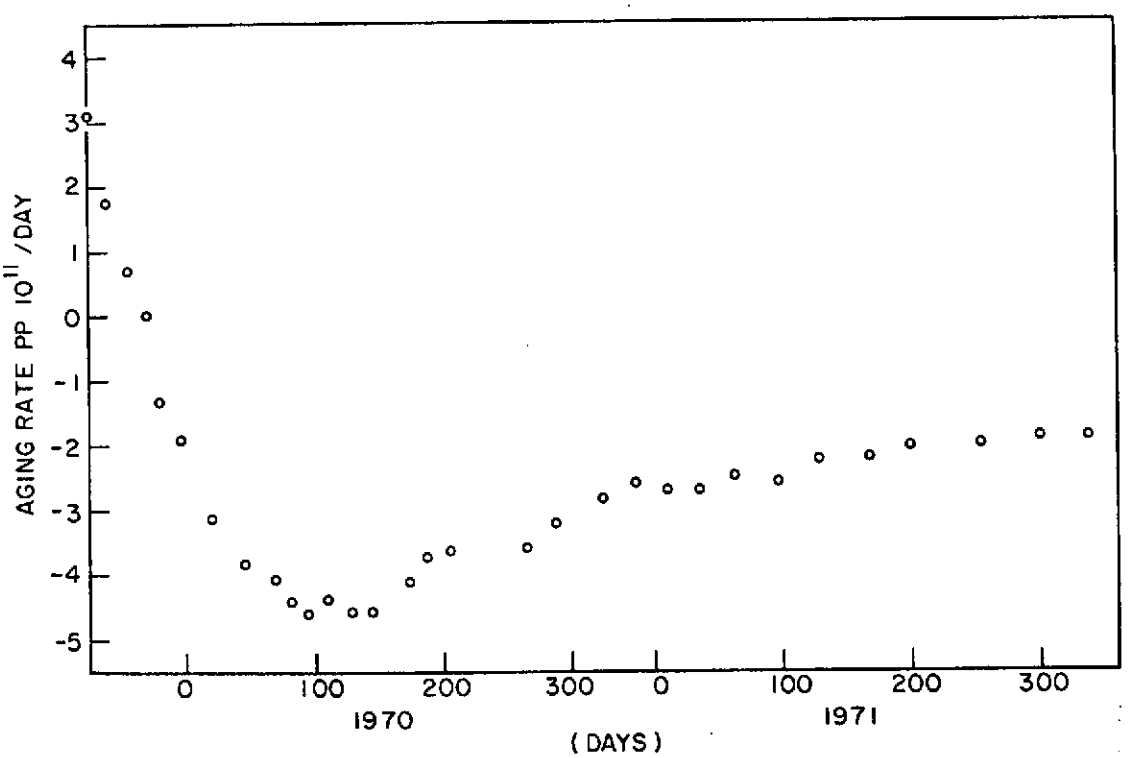

Figure 3. Apparent aging rate for Timation II.

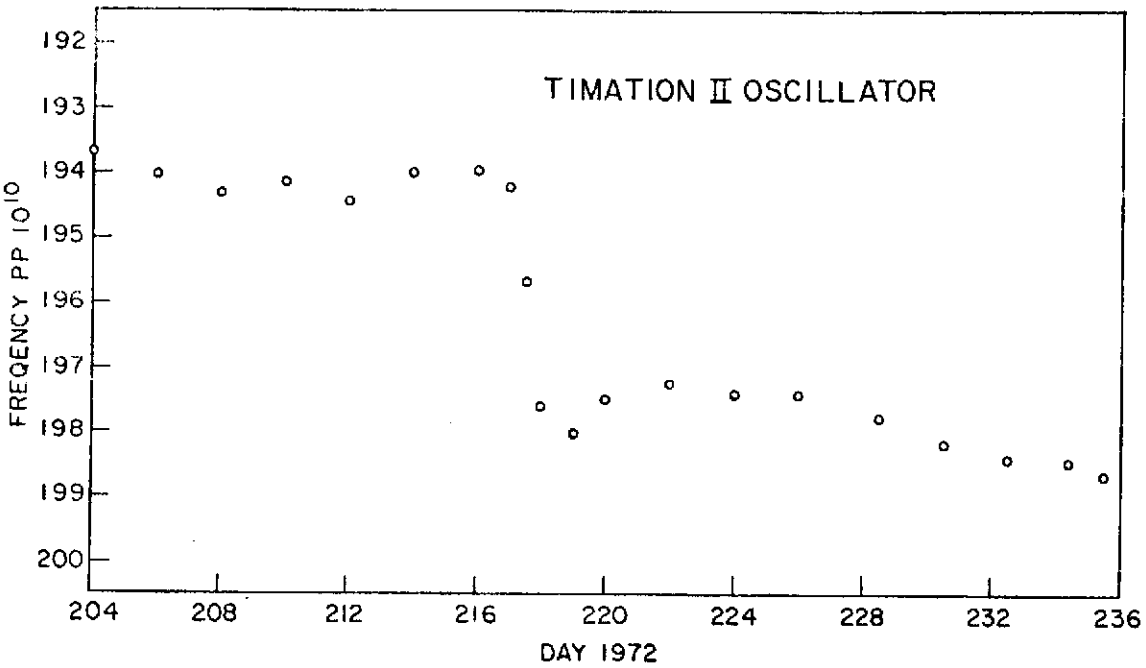

Figure 4. Transient radiation effects.

TRACKING SITES

MARYLAND

FLORIDA

SAMOA

GUAM

SEYCHELLES

Figure 5. Primary ground stations in the orbit determing network.

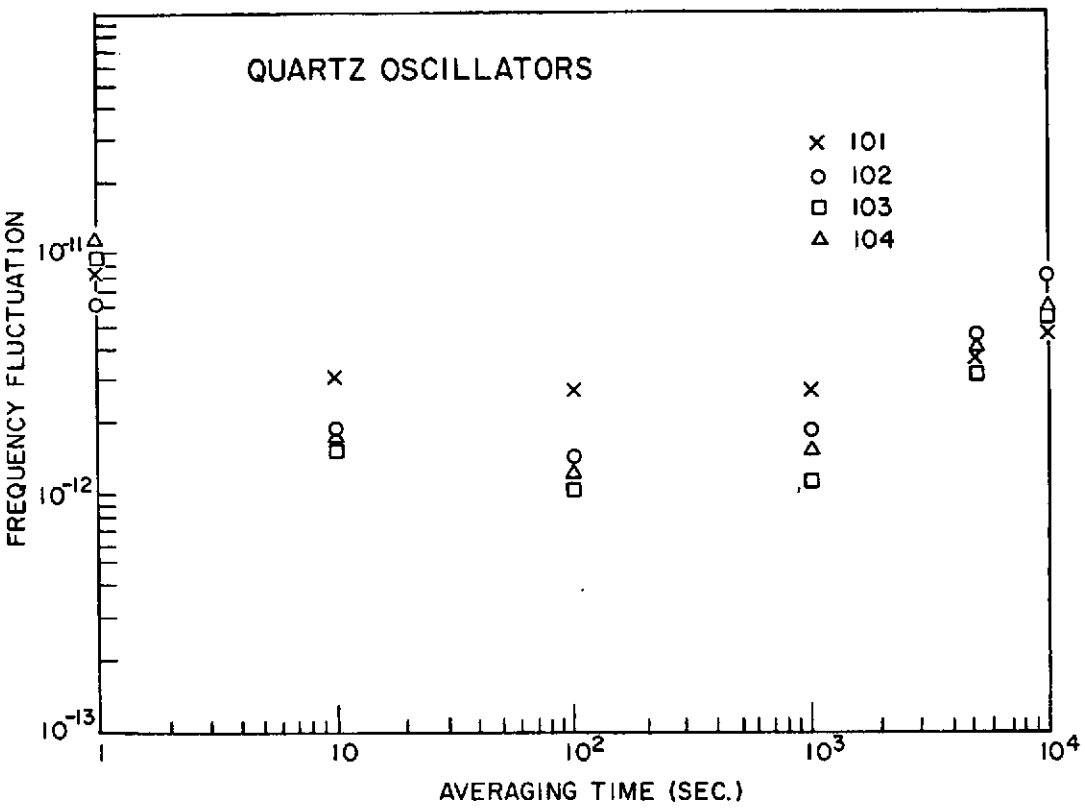

Figure 6. Fractional frequency fluctuation.

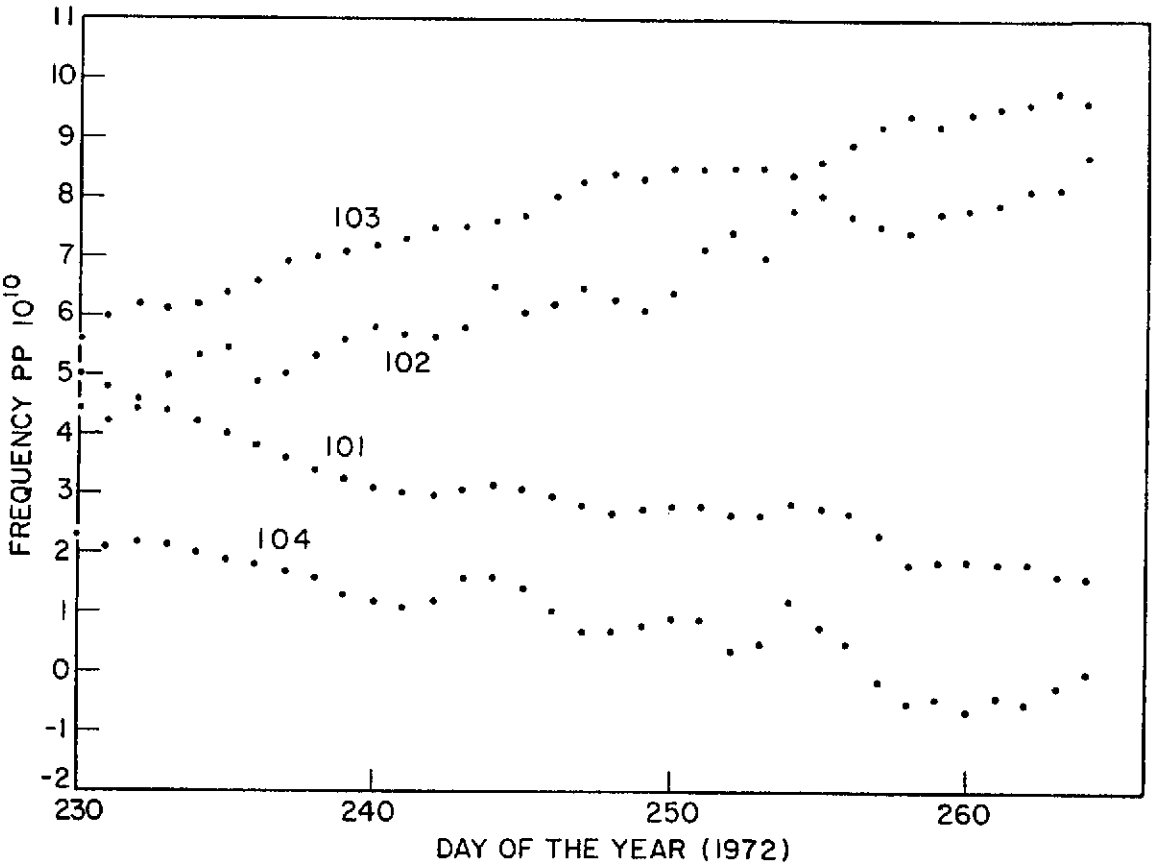

Figure 7. Oscillator aging rates.

BRITISH AMERICAN SATELLITE TIME TRANSFER EXPERIMENT

Roger Easton
Naval Research Laboratory

At last year's PTTI we ran an actual time transfer between two buildings approximately 300 feet apart. We did this by means of a satellite approximately 500 miles away. Figure 1 shows the results obtained.

This year the Naval Observatory asked that we perform a similar experiment with the Royal Greenwich Observatory (RGO). The Royal Greenwich Observatory, with headquarters in a fifteenth century castle, is at the site shown on the map (Figure 2).

The final data, which we will describe more fully, is shown in Figure 3. The two sets of data are displaced 15.2 microseconds. This displacement represents the difference between the Naval Observatory and RGO clocks as measured in this experiment.

Last year we showed a bit about the theory of time transfer. However, since there is always someone in the audience who is new and did not get the word, I will repeat myself briefly.

REVIEW

The satellite has four advantages for navigation and time transfer: (1) well-known position; (2) line-of-sight signal, which allows the use of UHF; (3) worldwide coverage; and (4) a celestial navigation solution identical to the one used in celestial navigation for 200 years (see Figure 4). The diagram indicates the observer on a ship and his method of measuring the range to the satellite. He knows the radius of the earth and the distance from the center of the earth to the satellite. Triangulation gives him the angle θ, the same angle a celestial navigator would have used to observe a star in the same geographical position of the satellite.

Figure 5 is a diagram of range measurement by phase measure. The satellite has a clock (in this case, a 100-kHz clock) that is counted down: 100, 10, 1, 0.1 kHz. The observer has a similar clock. The observer receives the signal from the satellite and compares the phase of the 100-kHz received signal to his own 100-kHz to get a phase reading; he repeats this step for the other frequencies. If the satellite clock is synchronized to the observer clock, this phase reading gives a measurement of the time delay between the satellite and the observer.

Figure 6 is a schematic of the actual procedure measured in 6800, 920, 18, and 8.6, 10 microseconds; with 100-cycle, 1000, and 10,000 microseconds countdown. The satellite clocks and the navigator clocks are synchronized in this case. However, by the time this signal gets from the satellite to the navigator, his clock has changed because it took 6800 microseconds for the signal to arrive. The phase comparison for the first clock is 0.68 of a cycle, which gives a rough reading of 6800 microseconds. For the second clock, the reading

is 0.92, so it should read 6920 microseconds. For the third clock the reading is 0.18, so it should read 6918 microseconds; and for the fourth clock it is 8.6, so it should read 6918.6 microseconds.

Figure 7 is an intercept chart invented a hundred years ago by St. Hilaire, a French naval officer. The precomputed chart shows the assumed position, the direction of the satellite at 16 minutes past the hour, and the computed time delays from the satellite at 16 minutes past the hour (10,870 microseconds). Thus, one can plot the predicted satellite positions for these times, compute the distance from the satellite to the assumed position, and convert this to time delay.

Figure 8 shows a fix determined on the intercept chart. At 16 minutes past the hour the time delay is read, a right angle is drawn, and a line of position (LOP) is established. Other LOPs are drawn in a similar fashion. If there are no errors, the fix is perfect. But more often than not, the result will be similar to that pictured in Figure 9, an intercept chart showing the effect of synchronization error on plot, which is identical to having an instrument error for a celestial fix. The navigator is at the center of the arc of the circle; and the radius is the time error between his clock and the satellite clock. Thus the use of this technique allows both navigation and time transfer.

Figure 10 is a photograph of the satellite in current use, Timation II. It was launched over two years ago on the aft rack of an Agena rocket. Table 1 lists the characteristics of Timation I (which failed after two years because of the failure of the gravity-gradient boom), Timation II, and Timation III (scheduled for launch in December 1972).

Table 1
Timation Satellite Characteristics.

	I	II	III
Launch Date	31 May 1967	30 Sept 1969	Proposed
Altitude	500 n.mi.	500 n.mi.	7500 n.mi.
Inclination	70°	70°	135°
Weight	85 lb	125 lb	425 lb
DC Power	6 W	18 W	90 W
Frequencies	400 MHz	150 and 400 MHz	400, 1600 MHz
Max Mod Freq	100 kHz	1 MHz	8 MHz
Osc Stab	$3pp10^{11}$	$.5\text{-}1pp10^{11}$	$1\text{-}2pp10^{12}$

Figure 11 shows the aging rates of the oscillators on Timation I and II. When the crystal oscillator on Timation II (which is tunable from the ground) was launched into space, it had a positive aging rate, 2 parts in 10^{11} per day. This rapidly decreased to more than minus 4 parts in 10^{11}, but has now come back up to minus 2 parts in 10^{11} per day. This would not be expected from any ground measurements. The rate of Timation I started at a much lower rate and gradually became more negative. The difference was caused by proton bombardment on the crystal. The reason for the different shapes of the curves is that Timation I had a much higher positive coefficient when it was launched and the proton bombardment (largely proton, some electron) compensated for it almost directly, thus the almost zero aging rate. Timation II had a much lower aging rate and the protons overcompensated for it, which caused the highly negative aging rate for part of the time. It was determined that the rate was largely caused by protons because Timation II had a lead shield that shielded out the electrons, and it still had almost the same rate that would have been expected without the lead shield.

THE RGO-NAVOBS EXPERIMENT

For the RGO experiment we used the same RCA receiver we showed last year. This receiver used the 10/1 frequency step in the satellite transmitter, thus resolving the ambiguity between tones to give a final answer on range delay. However, although this receiver resolves the ambiguity, it does not always do so correctly, as will be shown.

While we were making these measurements in England, other people were making similar ones here in Washington on other (and less ambiguous) equipment. Points were read once per minute at each site. However, England is far enough from Washington that no points were run concurrently. Figure 12 shows the data links used in the computations.

Figure 13 shows the relationship of the data for three near-consecutive passes as corrected postdiction for satellite position, satellite frequency, and satellite clock phase.

Figures 14 and 15 show expanded data for two of the passes shown on Figure 13. It is seen that the equipment used at RGO does contain some ambiguity. These ambiguous points caused some problems but were corrected by using the large number of good data points available.

Each pass was smoothed at the point of nearest approach to provide a single point in Figure 16. The results we obtained agree within 1.5 microseconds with LORAN C measurements made at RGO. A traveling clock check made before the experiment indicated a discrepancy of approximately 1.5 microseconds when compared to LORAN C. The next clock comparison is scheduled for later this year. So, while the absolute accuracy of the time-transfer technique used is not known, it appears that accuracies of one-half microsecond are readily available.

ACKNOWLEDGEMENTS

This experiment required a large effort by many people, including Donald W. Lynch, James Buisson, Thomas McCaskill, Cecelia Burke, and Hugh Gardner of NRL, and Humphry Smith, Henry Gill, Ann Strong, and Antony Seebrook of RGO. In addition the orbits were computed with the aid of NRL and TRANET people around the world.

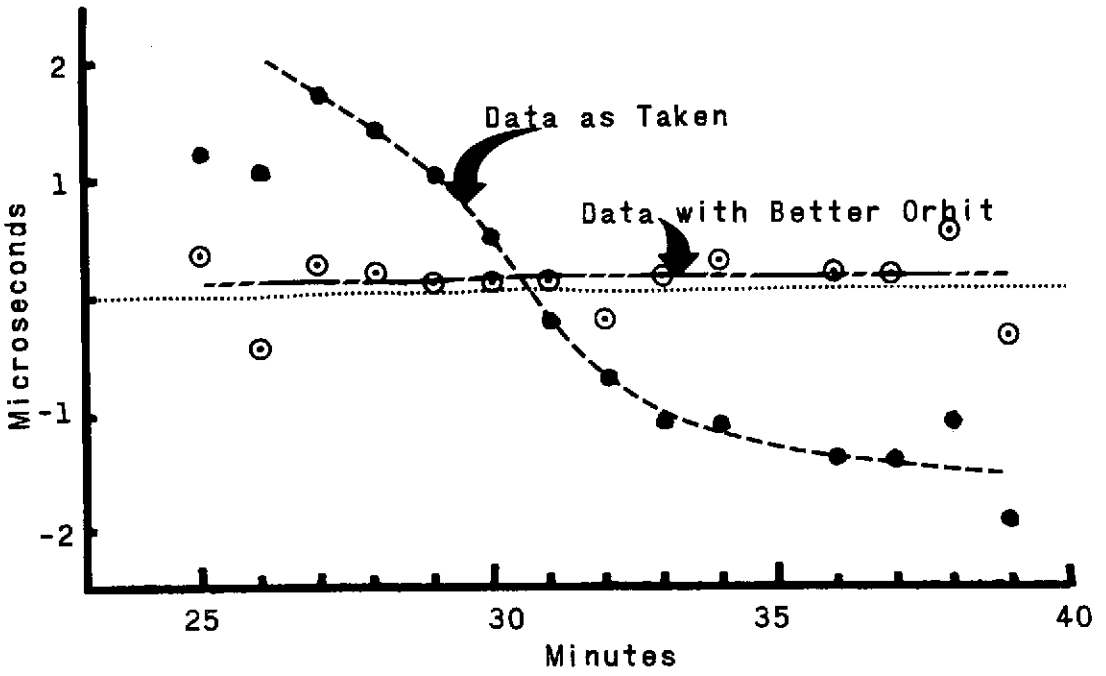

Figure 1

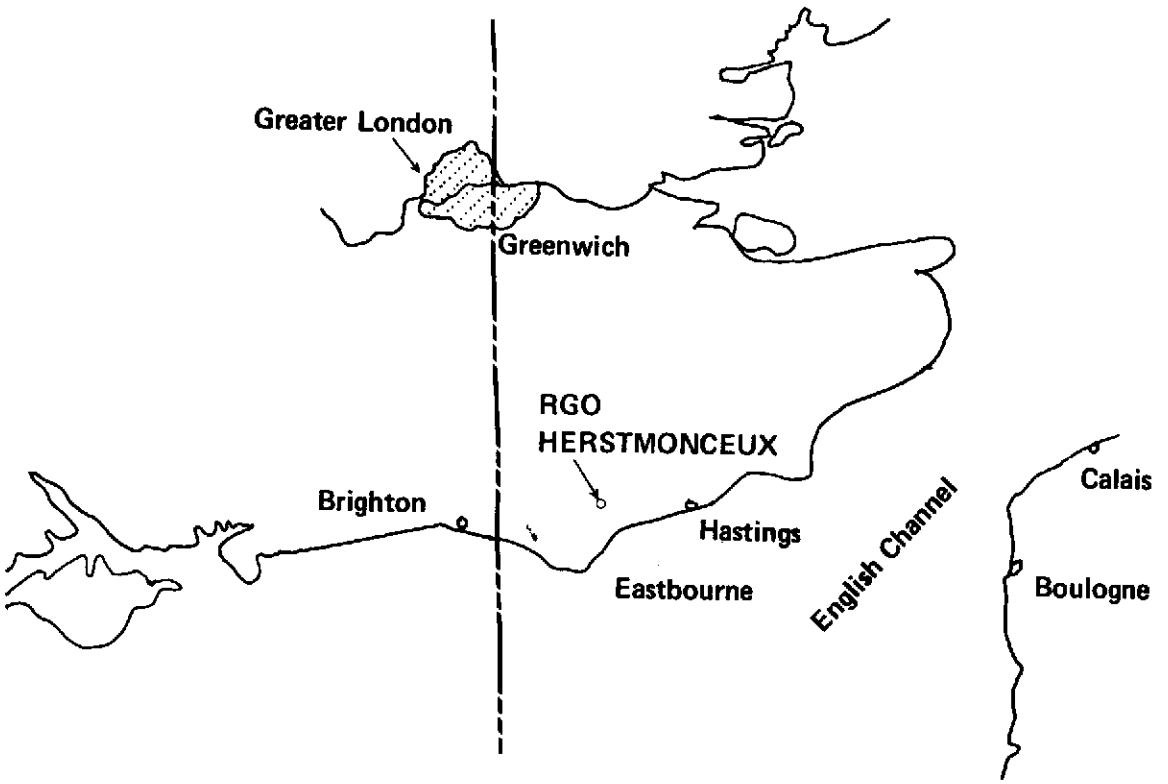

Figure 2. Location of the Royal Greenwich Observatory.

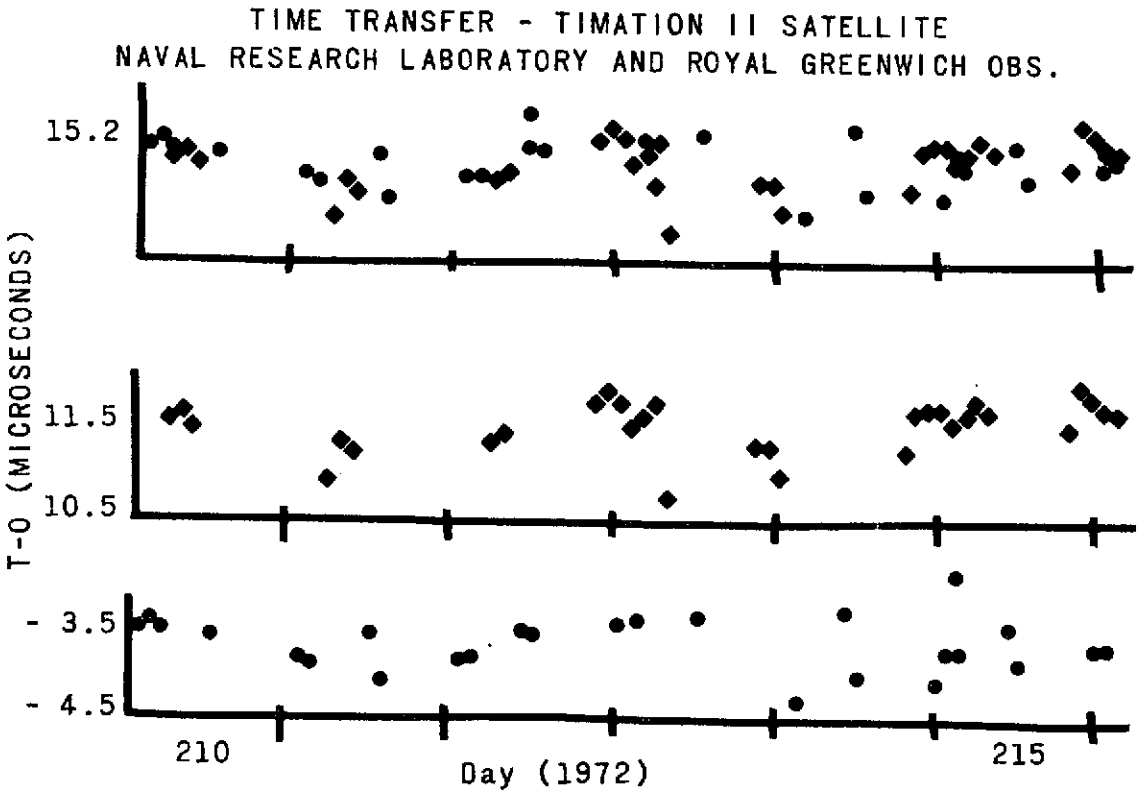

Figure 3. Timation II time-transfer experiment results.

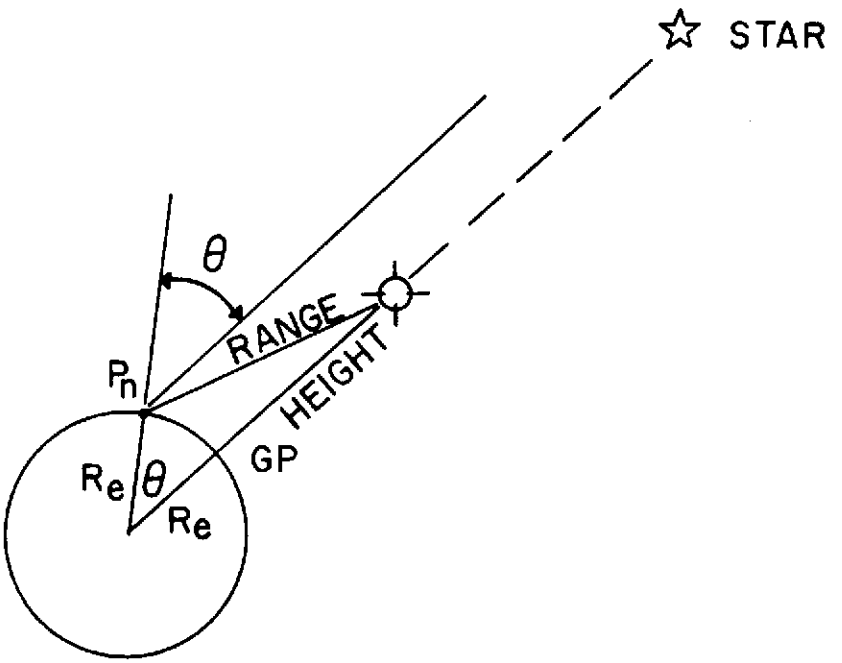

Figure 4. Transform to celestial navigation.

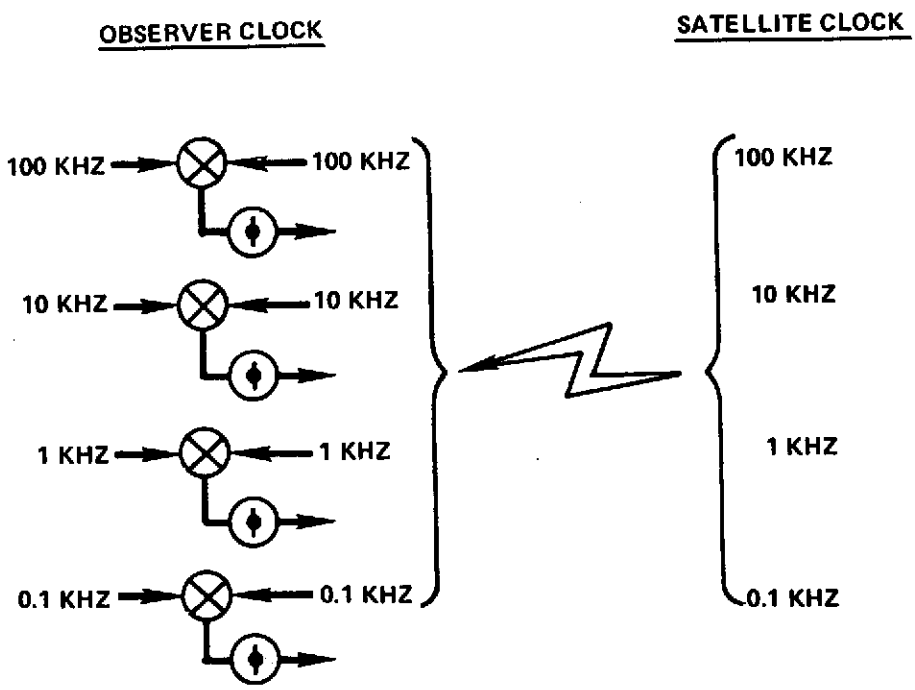

Figure 5. Range measurement by phase measurement.

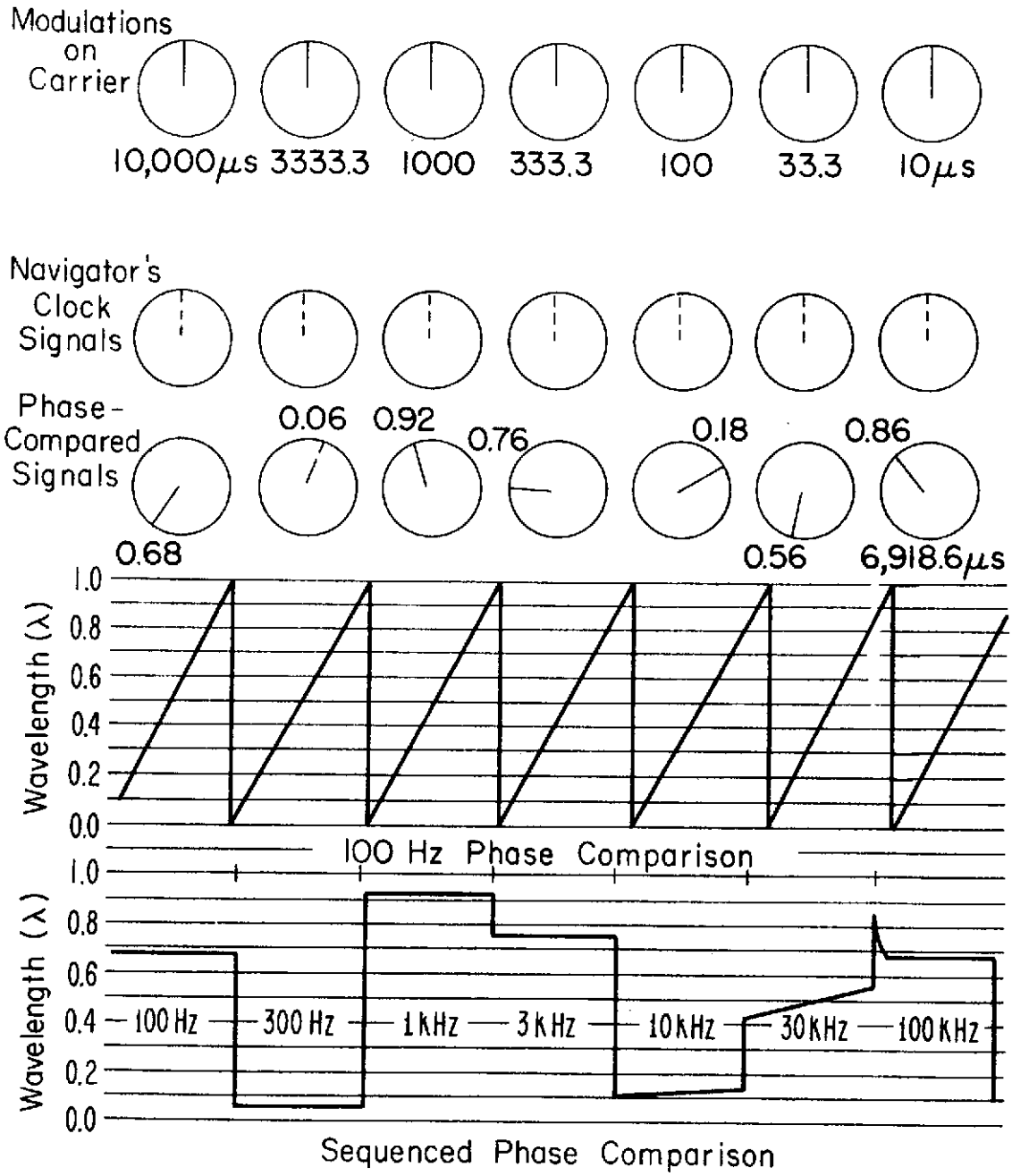

Figure 6. Schematic procedure.

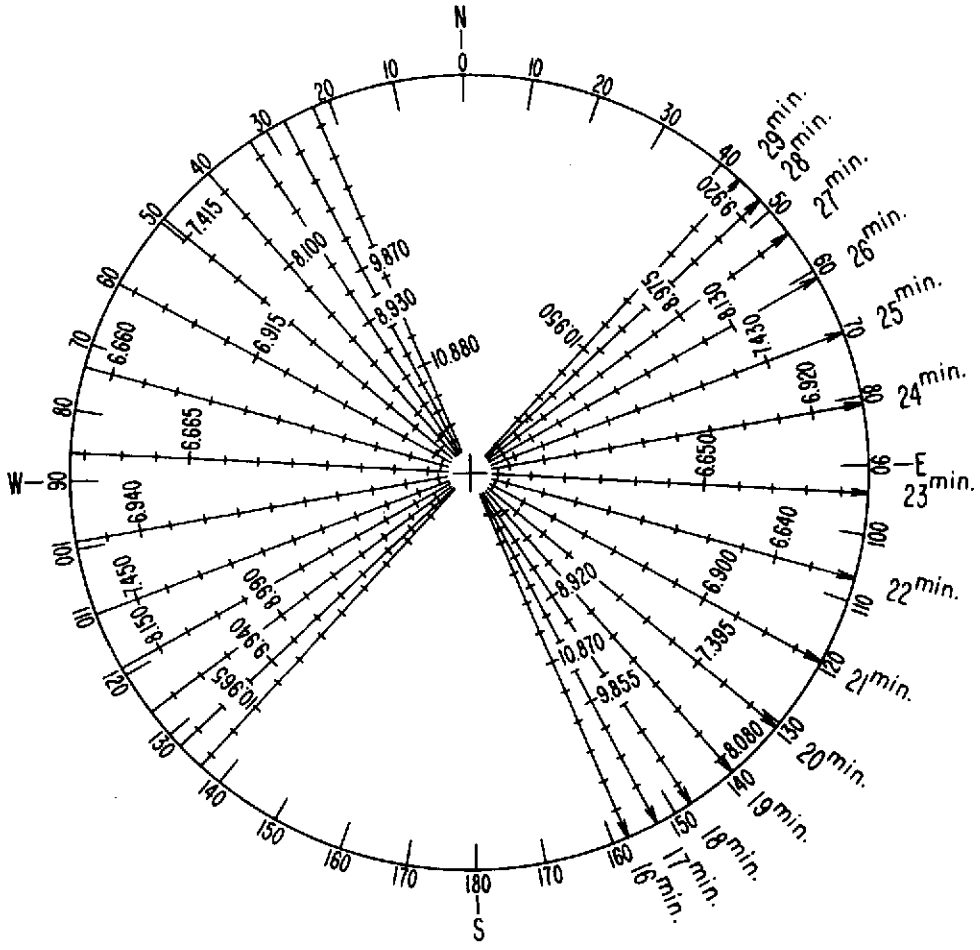

Figure 7. Precomputed intercept chart.

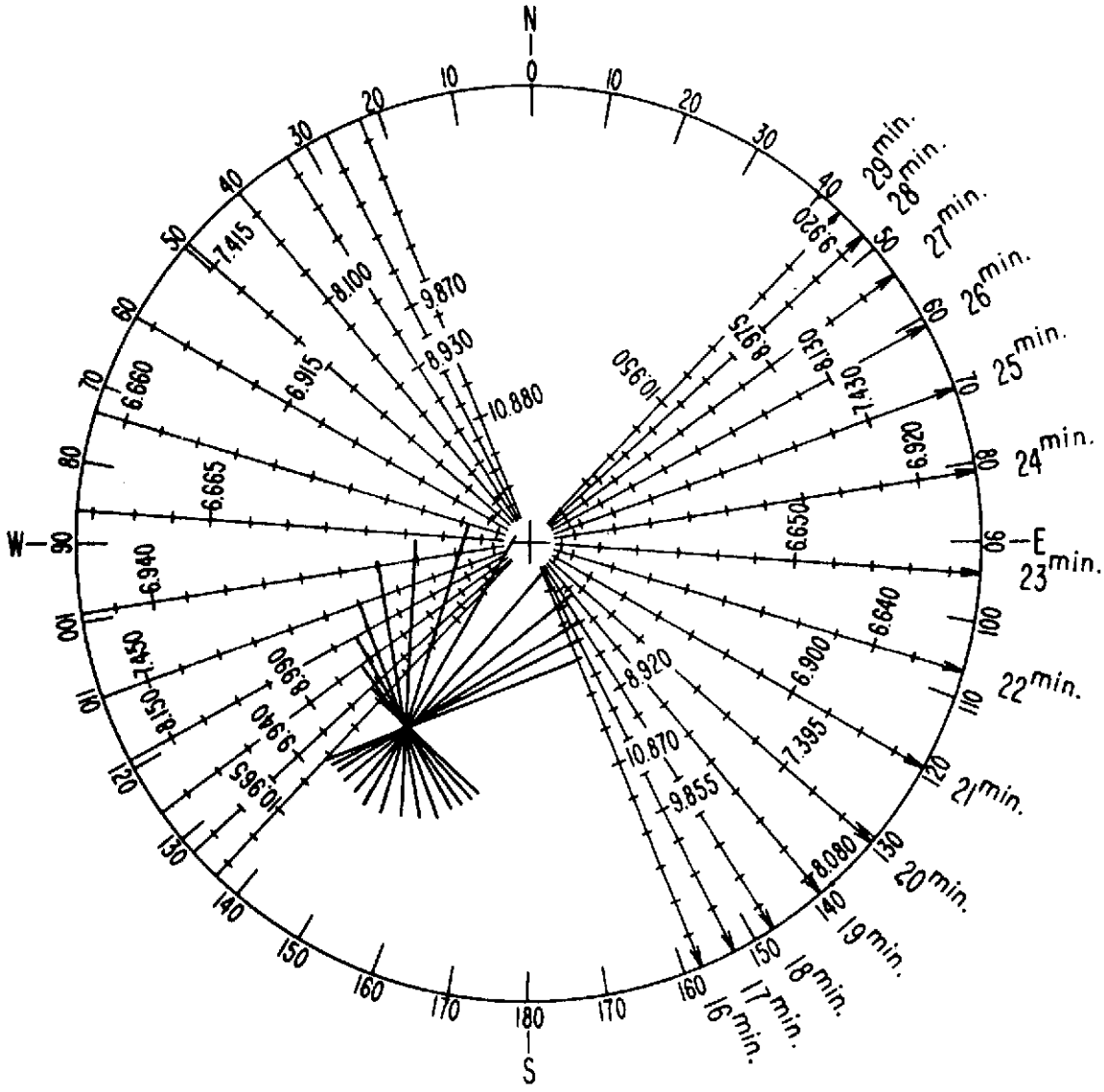

Figure 8. Fix determined on intercept chart.

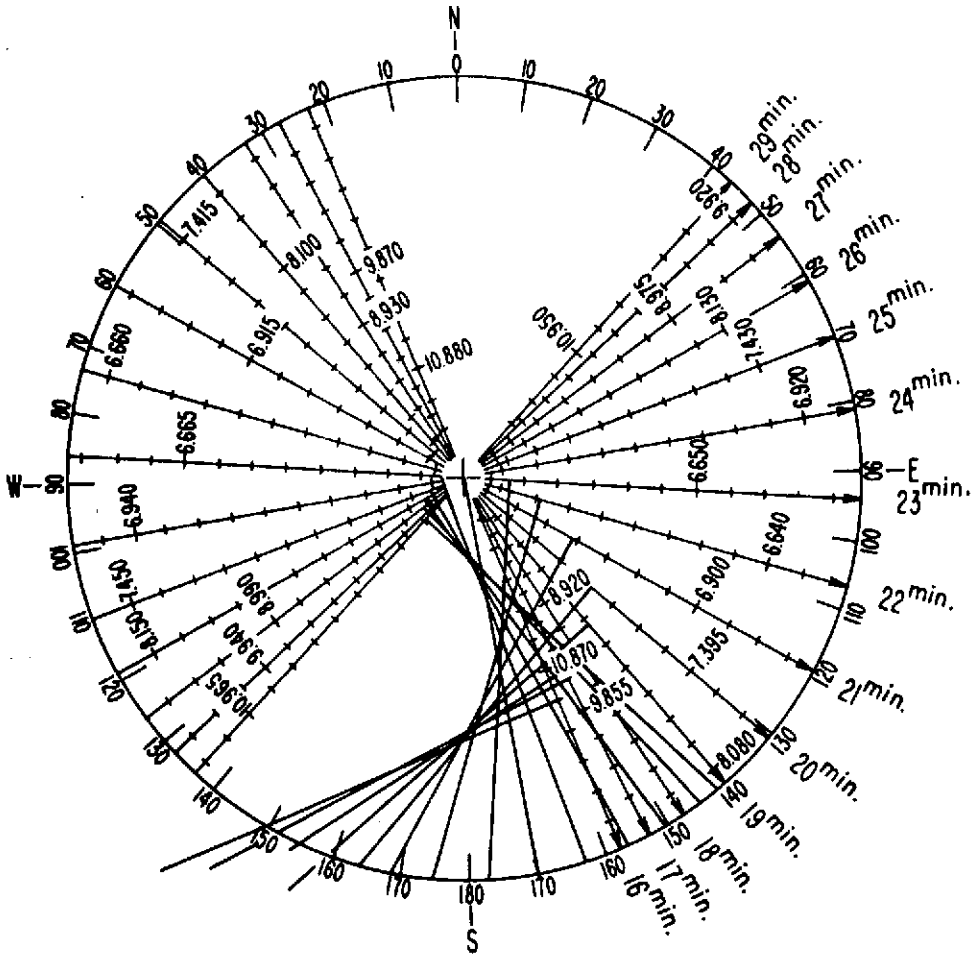

Figure 9. Intercept chart showing effect of synchronization error on plot.

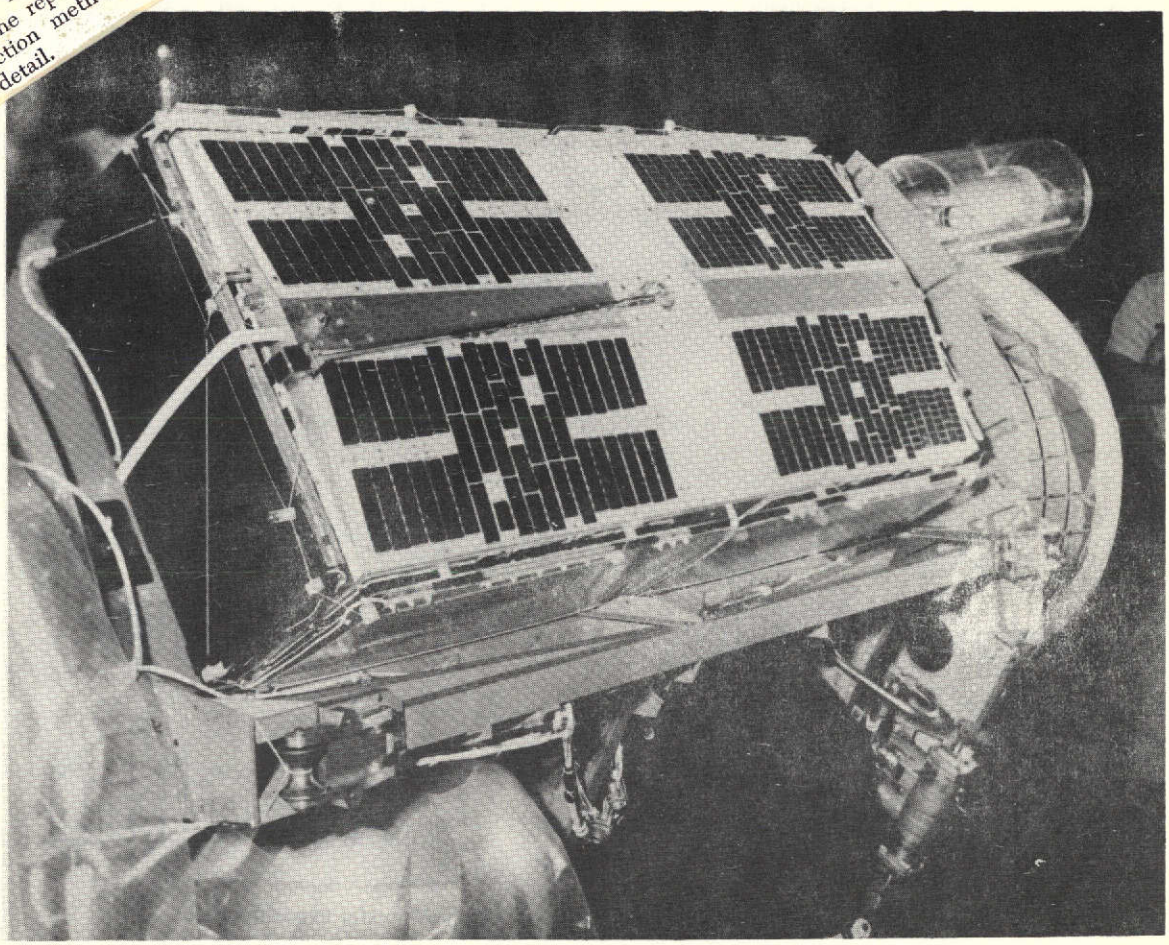

Figure 10. Timation II.

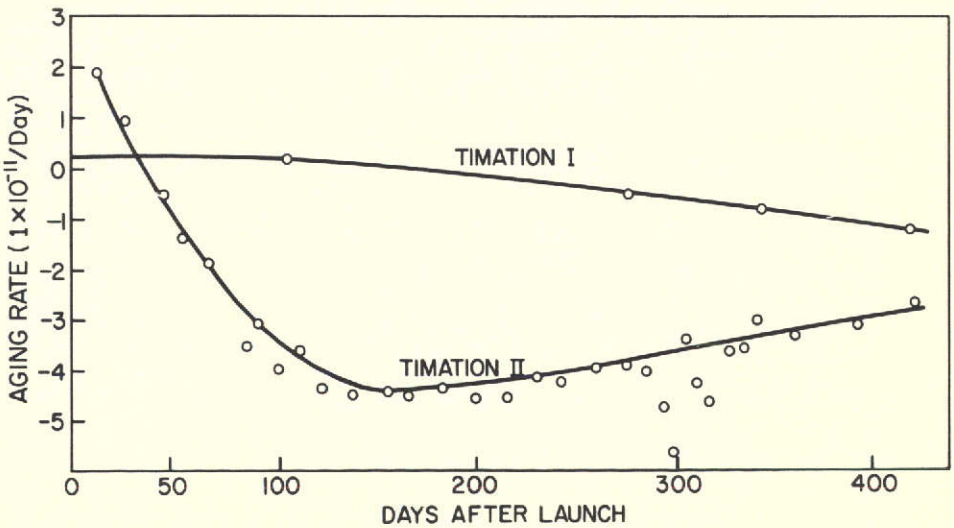

Figure 11. Aging rates of crystal oscillators.

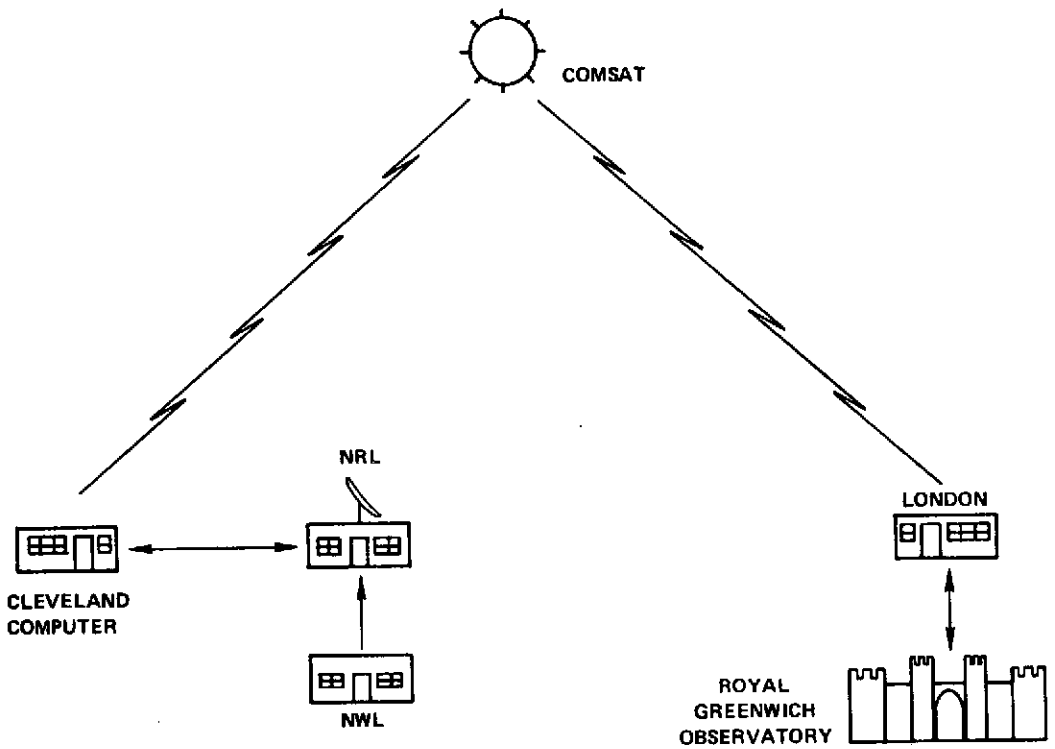

Figure 12. Data links for the NRL-RGO time-transfer experiments.

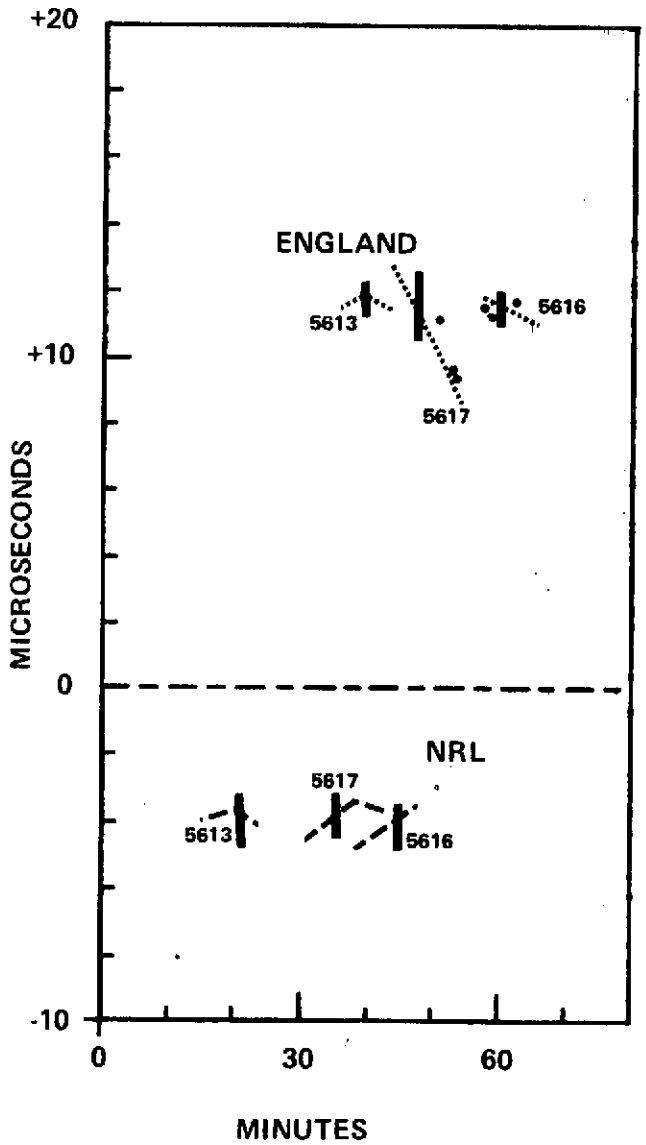

Figure 13. Relationship of data for three near-consecutive passes.

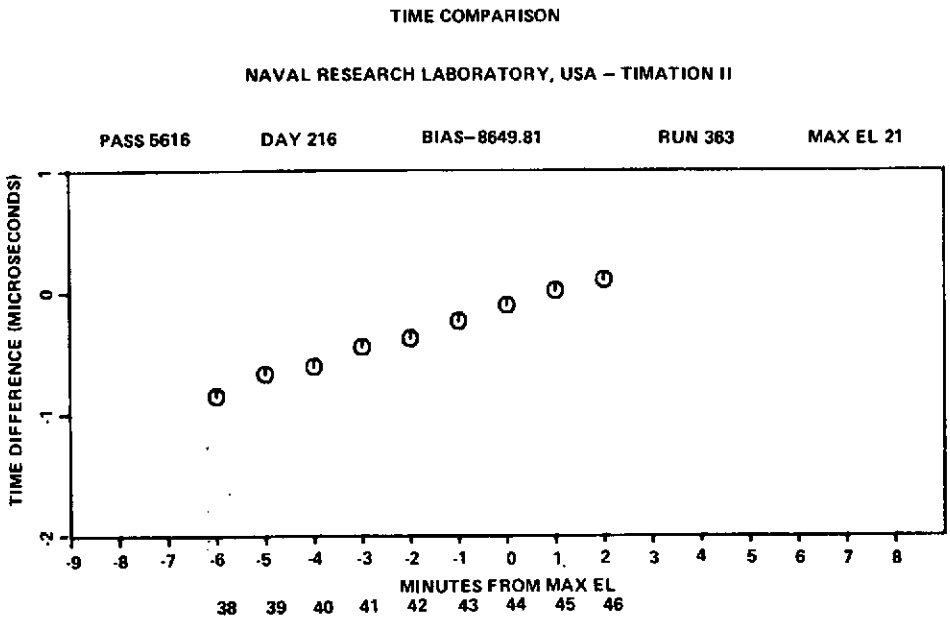

Figure 14. Expanded data from Figure 13.

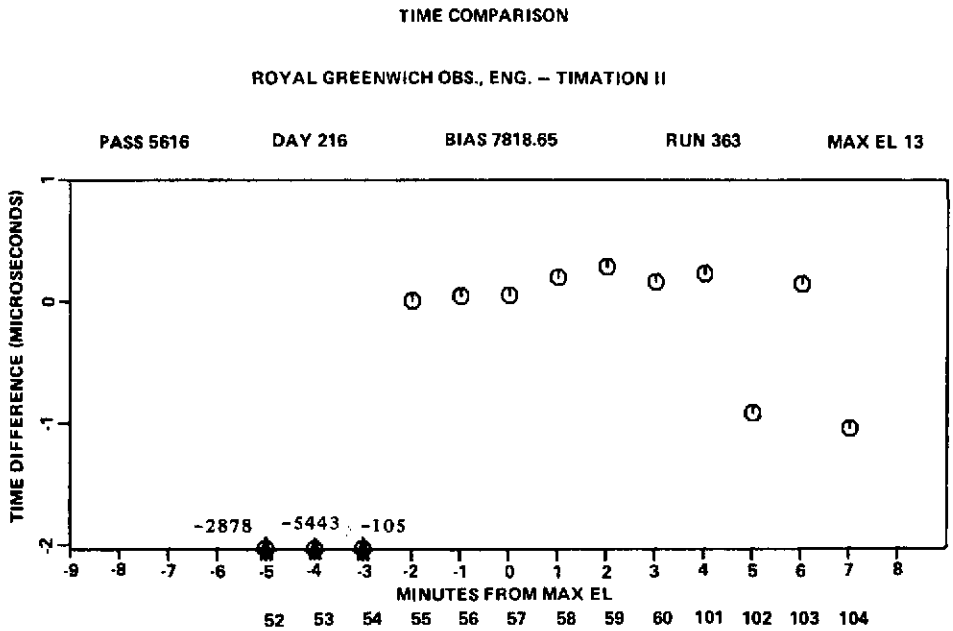

Figure 15. Expanded data from Figure 13.

PERFORMANCE OF THE NEW EFRATOM OPTICALLY PUMPED RUBIDIUM FREQUENCY STANDARDS AND THEIR POSSIBLE APPLICATION IN SPACE RELATIVITY EXPERIMENTS

Carroll O. Alley, Ralph Williams, Gurbax Singh, and John Mullendore
Department of Physics and Astronomy
University of Maryland

ABSTRACT

Comparison of the new Efratom units with cesium beam and hydrogen maser standards at the U.S. Naval Observatory showed stability of $\sim 5 \times 10^{-12}$ over two-week periods in a normal laboratory environment. Dependence of frequency upon the environmental parameters of pressure, magnetic field, temperature, supply voltage, and acceleration was measured. A package of three units with automatic phase comparison and recording was designed and constructed to allow a measurement of relativistic effects on time with high accuracy on the Apollo-17 lunar mission. Although NASA management declined to fly the experiment, some aspects of the design and the relativistic effects to have been expected are presented. The technique has applications for ground-based PTTI activities as well as for future space flights.

INTRODUCTION

It has been very gratifying to the first author and others who worked on the original concept of rubidium optically pumped frequency standards in the 1950s after they were invented by Professor Robert H. Dicke of Princeton to see the excellent engineering exhibited in the new Efratom units. When we looked at the room full of equipment used in the first experiments, we jokingly said that eventually it could be reduced to the size of a matchbox. Ernst Jechart and Gerhard Hubner at Efratom have almost succeeded in producing a package approaching a kitchen-size matchbox!

Dimensions:	10 cm-by-10 cm-by-10 cm
Weight:	1.3 kilograms
Power:	13 watts

This small size allowed us to think realistically of assembling a package of three atomic clocks which could be flown to the moon and returned in the command module of the Apollo-17 mission, to measure the gravitational potential effect of general relativity with increased accuracy and to provide a highly convincing demonstration of the reality of the relativistic effects on time.

The large time difference (about 300 microseconds) to be expected from relativistic effects had been recognized during the first manned circumnavigation of the moon by the Apollo-8

astronauts in December, 1968.[1] For the longer Apollo-17 flight, the expected time difference was about 700 microseconds, of which 5 percent was due to the velocity and 95 percent was caused by the gravitational potential difference.

By measuring and recording the three relative phase differences among the three frequency standards it seemed possible to measure the elapsed time with an uncertainty of about 200 nanoseconds over the 296-hour flight. It is to be emphasized that the changes of individual clock rates can be recorded in this way, since such changes do not occur at the same time for each frequency standard. This technique is very old and is regularly used at the U.S. Naval Observatory to improve substantially the accuracy obtainable from straight statistical averaging. It formed the basis for the round-the-world clock experiment of Hafele and Keating,[2] which seems to demonstrate the existence of the relativistic effects with the Hewlett-Packard cesium-beam recording clocks which they carried. (The accuracy of this demonstration was not high since the effects were small and there was difficulty in knowing accurately the velocity and position of the commercial aircraft used.) For the well-tracked Apollo-17 flight an accuracy of 0.03 percent seemed achievable with a package of three Efratom units and intercomparison electronics. The best existing measurement of the gravitational potential effect, the Mössbauer Effect measurements of gamma-ray frequency changes by Pound, Rebka, and Snider,[3] has an accuracy of 1 percent. The possible opportunity to improve this accuracy by a factor of 30, by a completely different method using returned recording clocks (about which there is still continuing controversy), in a very credible experiment using available commercial equipment, suggested an all-out effort to produce the experiment hardware and to attempt to persuade the National Aeronautics and Space Administration to include the experiment on Apollo-17. Although the Apollo-17 measurement would have an accuracy less by a factor of ten than that claimed for the future rocket-probe hydrogen-maser experiment being developed by Vessot,[4] it had the virtues of redundancy, recovery of operating clocks, and immediacy, as well as the dramatic element involving the astronauts, which would be of great value for establishing the reality of the relativistic effects on time in the public consciousness. There was initial encouragement from NASA and a formal proposal was submitted from the University of Maryland. The Office of Naval Research provided financial support to begin the construction of a flight-qualified package in early August 1972. The scientific community gave very strong endorsement to the experiment. In interaction with Apollo spacecraft engineers at the Houston Manned Spacecraft Center and at North American Rockwell it was determined that space, weight, and power were all available, and a copper/water-vapor heat-pipe solution to the heat-transfer problem was identified. Clock intercomparison electronics was designed and constructed using integrated circuits, and a hermetically sealed box to house the clocks and electronics was built to fit the space available in the command module. Nevertheless, it was finally decided in early October by the NASA Administrator, upon the recommendation of the Apollo Program managers, that the short time before the launch (scheduled for December 6) and limited

financial resources would result in risks to the mission if the atomic clock relativity experiment were carried, and the proposal was declined.

It is the purpose of this paper to record the performance characteristics of the Efratom frequency standards which we measured in preparing the experiment and to give some further details about the phase intercomparison electronics and packaging. It is expected that a self-contained ensemble of intercompared clocks will be of value for time synchronization trips and other PTTI applications, as well as in future space relativity experiments.

MEASURED PERFORMANCE OF EFRATOM FREQUENCY STANDARDS

The desirable properties of small weight, small volume, and low power consumption of these new units, which became available to us for tests only in July 1972, are further enhanced when associated with a frequency stability superior to that of most optically pumped standards and comparable over periods of hours with those of the typical cesium atomic beam standards. Data in support of this performance are displayed in Figures 1 and 2. The performance is much better than the manufacturer's specification of an upper bound for the frequency stability, $<10^{-10}$ per month, which was deliberately made conservative. The figures are portions of strip charts on which the phase of the output signal frequency (divided by two to yield five MHz) is compared with the phase of the USNO hydrogen maser. For ready comparison the phase of the signal from Hewlett-Packard Model 5061 cesium-beam clocks is displayed simultaneously. In Figure 2 the hydrogen maser reference frequency for the rubidium unit is progressively shifted in phase by an electronic "phase microstepper" so that rate changes of 10^{-13} can be identified. The fine performance of the rubidium unit is apparent. Similar performances have been seen in the other units tested, although two of the seven examined have exhibited a somewhat more noisy short-term performance.

The data which originally convinced us of the quality of the Efratom rubidium units are summarized in Figures 3 and 4. The changes of phase of Efratom unit No. 111 with respect to one of the cesium-beam master atomic clocks of the USNO for the period July 14 to August 1, 1972 are displayed in Figure 2. There was no environmental control other than air conditioning. It became clear that changes of barometric pressure were influencing the frequency when the rates were calculated and plotted as a function of time along with the barometric pressure for the same period, as shown in Figure 4. Subsequent measurements of the pressure dependence of frequency were made by placing the unit in an aluminum pressure chamber yielding a pressure coefficient of 1.4×10^{-13} per millibar change from standard atmospheric pressure. Apart from the slow changes produced by barometric pressure changes, rate changes of a few parts in 10^{12} do sometimes occur, separated by many hours of operation in which the rate is constant to within a few parts in 10^{13}.

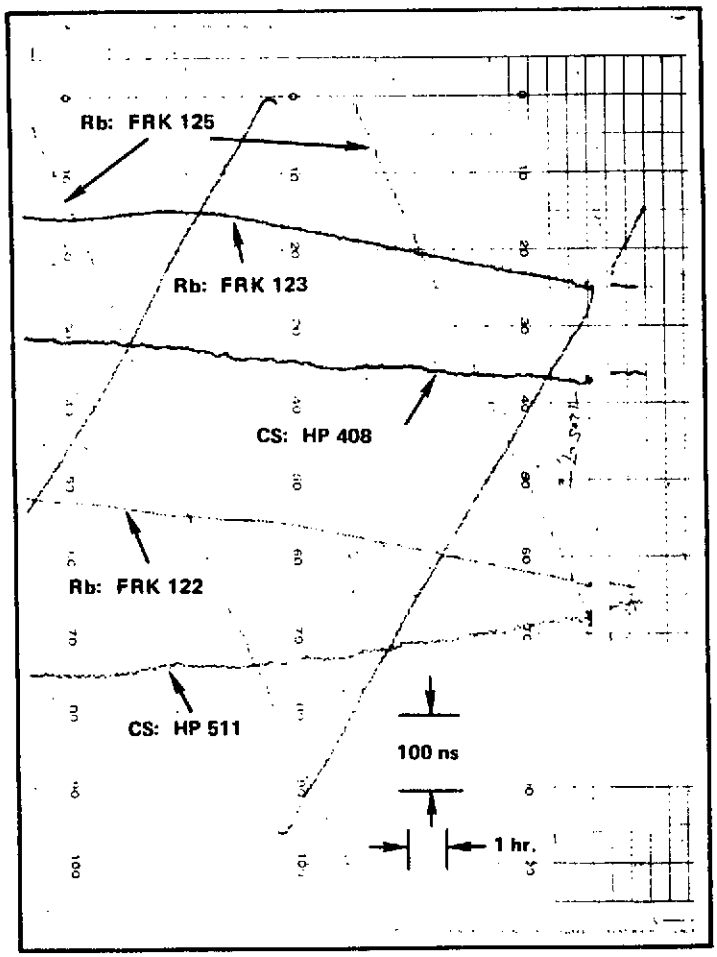

Figure 1. Plot of results of comparison of Efratom and cesium-beam frequency standards.

Other environmental effects on frequency have also been measured for Efratom unit No. 111. These include the dependence on external magnetic fields, temperature, and supply voltage. The magnetic field dependence was measured with 40-inch-diameter Helmholtz coils arranged to give a field in the direction of the local earth field, with a uniformity of 1 percent over the volume of the frequency standard. With the direction of the field in the plane of the cooling fins and 30° from the vertical, the coefficient for small changes about the earth field value was found to be about $+8 \times 10^{-12}$ per gauss. This relatively large coefficient even in the presence of the two mu-metal shields included in the commercial unit suggested the packaging of the unit in two additional mo-permalloy nested boxes having a wall thickness of 50 mils and separated from each

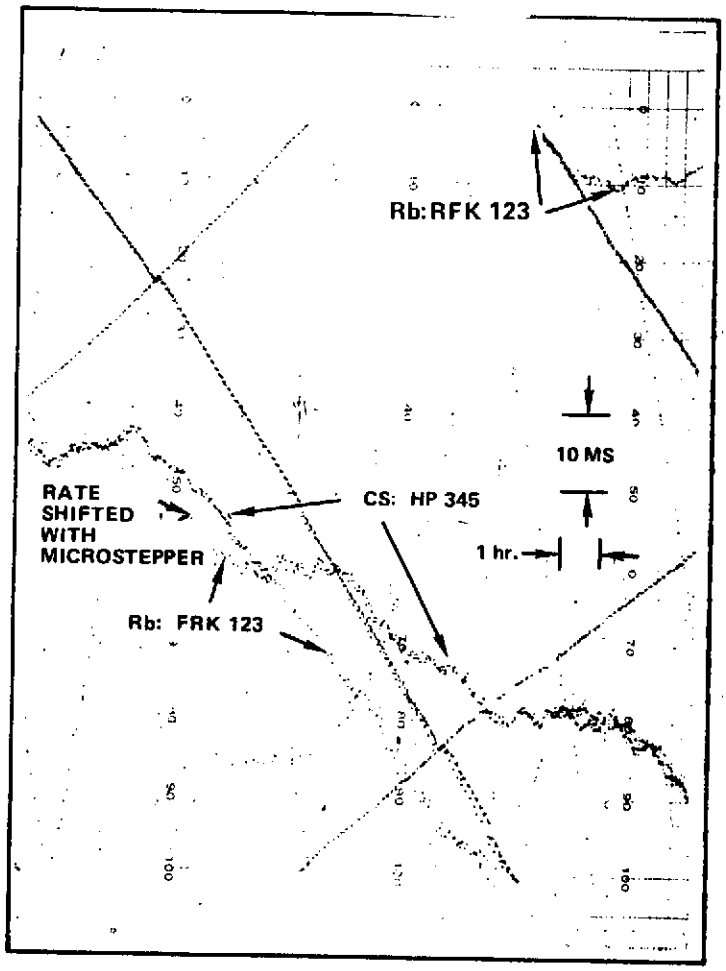

Figure 2. Plot of results of comparison of Efratom and cesium-beam frequency standards (continued).

other and from the mu-metal case of the frequency standard by about 1/8 inch. Tests with such shielding showed no discernible change in frequency (with resolution of 2×10^{-13}) for changes in the magnetic field equal to the value of the earth's field ($\sim$ 0.3 gauss) which would be experienced on a flight to the moon. The initial rough measurements on temperature dependence for unit No. 111 yielded a coefficient of $\sim +7 \times 10^{-13}$ per degree centigrade for the range 20°C to 40°C. Tests on the supply voltage dependence showed a coefficient of $+9 \times 10^{13}$ per volt for variations of a few volts about 28 volts.

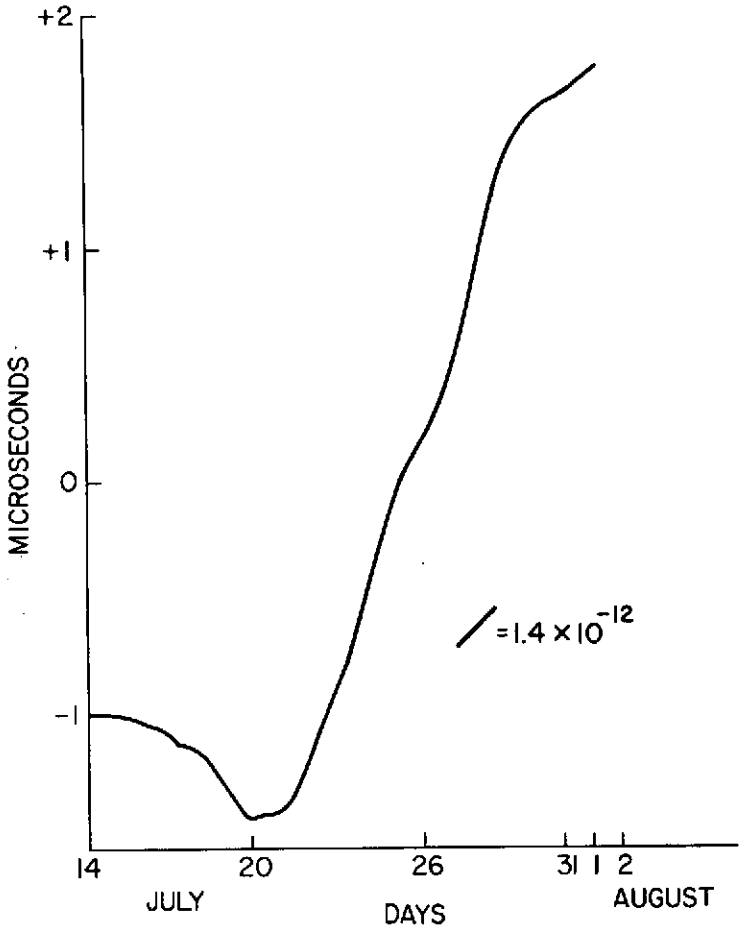

Figure 3. Phase of Efratom unit No. 111 versus USNO master clock, from July 14 to August 1, 1972.

The dependence of rate on the magnitude of acceleration was studied using the centrifuge at the Naval Research Laboratory. It showed a linear change of 8×10^{-11} in going by steps from zero to ten g along the optical pumping axis of the clock. No loss of phase lock was observed and recovery to the original rate was observed within the resolution available at that time for the field test ($\sim 10^{-12}$). Other tests have been carried out on the changes of rate produced by turning the unit upside down in the earth's gravity field. For unit No. 111, a change of 2 g along the pumping axis produced a change of $\sim 2 \times 10^{-11}$, consistent with the centrifuge results, with recovery to the original rate within a resolution of $\sim 2 \times 10^{-13}$. Smaller changes were observed for rotations about axes perpendicular to the pumping axis. It is clear that the accuracy of measurement of the relativistic effects in space flight will depend on our ability to predict from tests of this sort the effect of the transition from one g to zero g in free fall.

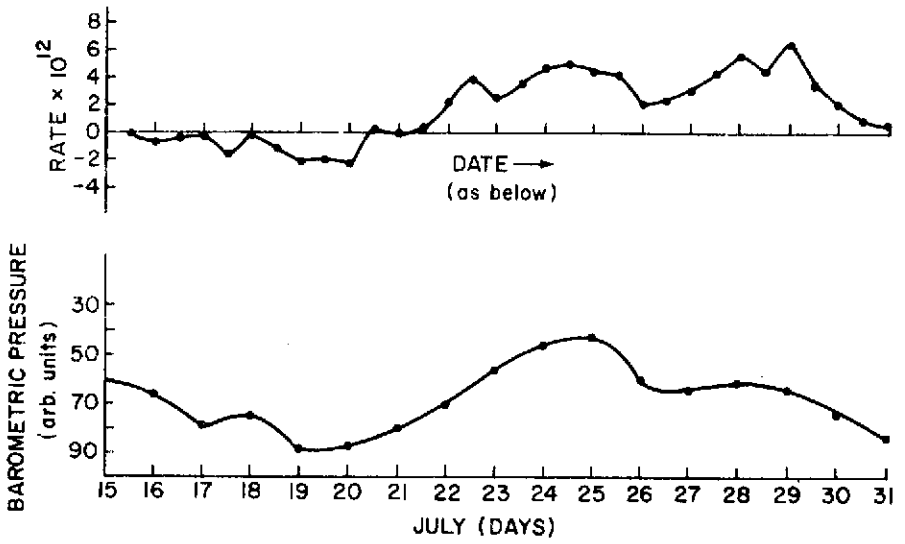

Figure 4. Effect of barometric pressure on Efratom unit No. 111 frequency rate: (top) rate obtained by plotting slope of phase graph (Figure 3); (bottom) barometric pressure over the same period – the points are daily means.

Vibration tests have not yet been conducted. Three units ruggedized for vibration were received from Germany on October 6. The ruggedization was accomplished by bonding certain electronic components to the circuit boards. The plans to conduct the vibration tests of these units before the Apollo flight-readiness test on October 15 had to be curtailed after the negative decision by NASA, since financial resources did not permit the round-the-clock work by large numbers of personnel which was required.

Three additional units have been examined for their frequency stability. They were found to perform as well on long term as Unit No. 111 and the three ruggedized units, although two units showed slightly more short-term noise.

To simulate the condition of no convective cooling which occurs in a free-fall environment, unit No. 111 was operated in its magnetic shields in a chamber evacuated to a pressure of 300 microns for a period of seven hours. Heat conduction was provided by fastening the inner mo-permalloy shield to the heat-transfer plate of the unit and providing a 1/8-inch copper plate between the inner and outer shields on the heat-transfer side of the nested boxes. This side of the package rested on the 1/2-inch aluminum bottom plate of the vacuum chamber. The temperature of the mu-metal case of the commercial unit was monitored using a thermistor. The temperature changed only from 44°C to 45.7°C, showing that a major part of the heat transfer is by conduction. The frequency was measured and showed no change within 2×10^{-12} during the vacuum operation except that change expected from the reduction of the pressure (a higher precision measurement was not attempted).

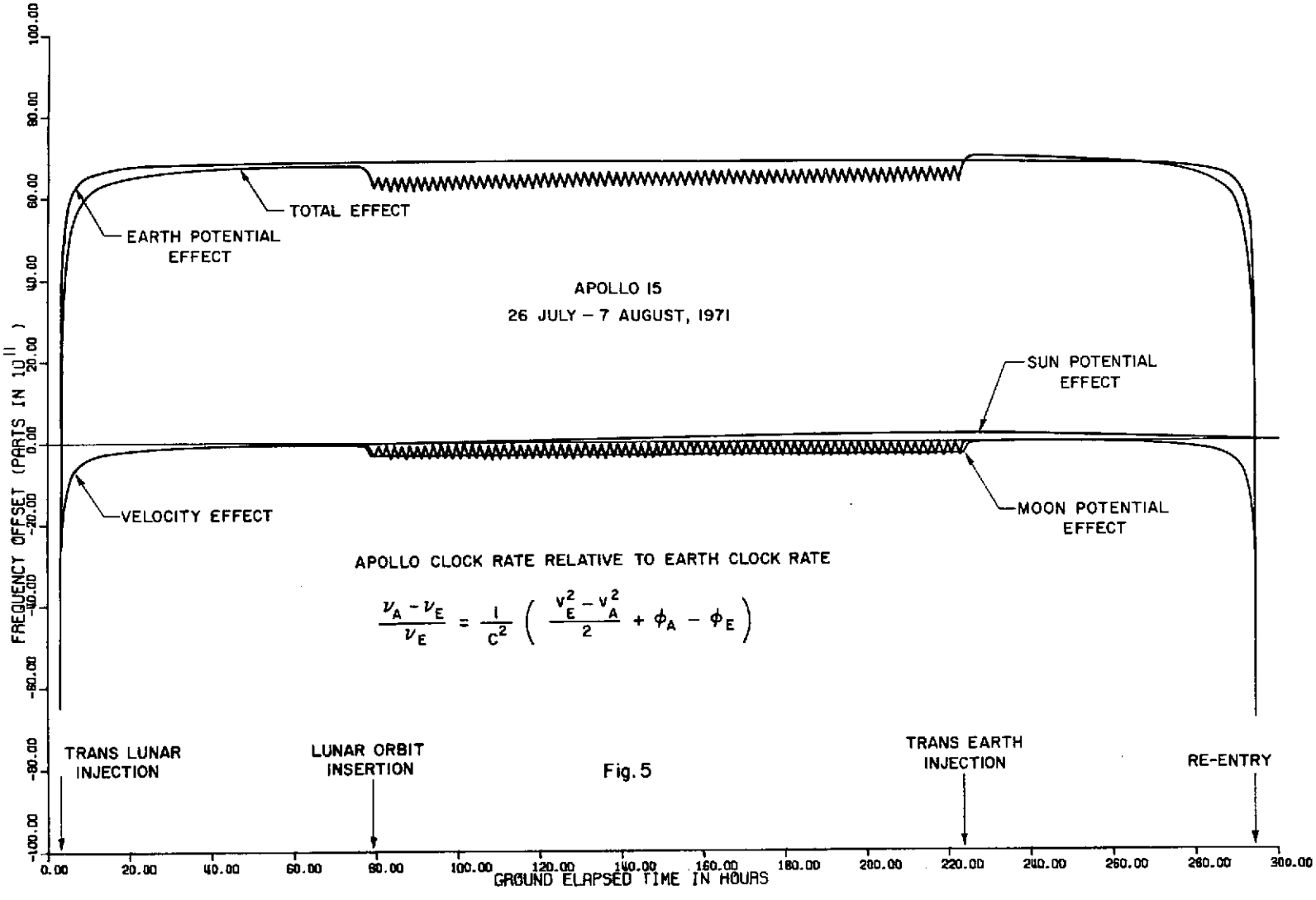

Fig. 5

Figure 5. Results of analysis of Apollo-15 trajectory data.

ELECTRONIC CIRCUITS

The measurement of the relative rates between pairs of clocks in the flight package is made possible by modern integrated circuit techniques requiring relatively little power and volume. It is also possible to measure critical environmental parameters at selected times and record their values in storage registers. Circuits to perform these functions have been designed and constructed by John Giganti and the Electronics Shop at the University of Maryland. They will be only briefly described here, but detailed circuit drawings are available upon request. Four 7-by-10-inch printed circuit boards were built to perform the functions of counting, phase, comparison, housekeeping, and programming.

To convert a *frequency standard* into a *clock*, count-down circuits are needed. The ten MHz frequency from each of the three Efratom units is counted by dividing down to the level of a pulse per second. This pulse is synchronous with the input frequency and is obtained by opening a gate after a series of ripple counting circuits to let through a shaped pulse of 5-ns rise obtained from the original ten-MHz sine wave. In order to provide additional certainty that no counts have been lost, the total number of 0.1 second intervals is stored in each channel for later readout. Outputs through buffer amplifiers are provided at 5 MHz, at 1 MHz, and at 1 MHz with phase reversal each second, as well as the 1-Hz pulses. A composite output is also provided with seconds pulses from clocks A, B, and C. Each counter can be stopped by applying a +10-volt signal through a light-emitting diode connection so that the seconds tick can be adjusted in epoch. To distinguish the three clocks, the seconds pulses from clocks A, B, and C have widths of 1, 2, and 3 microseconds, respectively, on this composite line.

Direct phase comparison at ten MHz is accomplished using hot carrier diode balanced mixers to compare A with B, B with C, and C with A, both directly and in quadrature. The sine and cosine outputs for each pair are quantized with an analog-to-digital converter in nine bits each (equivalent to 0.2 ns) and stored in a magnetic core memory having 4096 words of 18-bit length. This core memory was a back-up unit for the most recent Orbiting Astronomical Observatory and was loaned by the OAO Project Manager at Goddard Space Flight Center. For the Apollo flight of 300 hours, it was planned to sample once every 1500 seconds.

A separate board has been devoted to the programming of the phase measurements and to the routing of the information to the core memory. The sampling rate can be readily varied. For example, the package can be used to transfer time with high accuracy by carrying it to other points on the earth. During these trips, a sampling interval of 100 seconds might be convenient.

Another separate board has been devoted to "housekeeping" functions, which are defined as the monitoring of various environmental parameters. These include the pressure within the sealed box, and the temperature, supply voltage, and crystal-oscillator feedback voltage for each frequency standard. A total of twelve input voltages can be

sampled and these voltages quantized and stored in a shift register memory having capacity, for the Apollo-17, of sampling once every three hours.

Power conditioning is accomplished by use of a switching regulator to provide a constant 22.5 volt source for the frequency standards as the buss voltage varies away from 28 volts. It is also designed to accept power from two 28-volt silver-zinc batteries which were designed and space-qualified for the Apollo Lunar Communications Receiving Unit (LCRU) in the event of loss of power from the buss. Two power-converter units are fed from the switching regulator and these provide the voltages needed for the electronic circuits and core memory. The total power requirement is 56 watts.

MECHANICAL PACKAGE

Much attention was given to the problem of heat transfer from the frequency standards to the aluminum box in which they are housed. The temperature of the standards can not rise above 65°C because the optical pumping cell and cavity are thermostated at 72°C and some temperature differential is needed. Therefore vibration and shock isolators which provide some thermal conductivity were chosen. These are made by the Aeroflex Company and consist of spirals of stainless steel rope. Three isolators are used per unit, attaching the outer mo-permalloy magnetic shield to the floor and one wall of the box. It was necessary to add flexible straps of copper braid between each unit and the box for additional heat conduction to maintain a temperature differential of about 20°C when conducting 12 watts.

MAGNITUDE OF RELATIVISTIC EFFECTS FOR AN APOLLO MISSION

To first order, the fractional frequency offset of the Apollo clocks relative to the earth clocks as a function of velocity and gravitational potential is given by

$$\frac{\nu_A - \nu_E}{\nu_E} = \frac{1}{C^2}\left(\frac{v_E^2 - v_A^2}{2}\right) + \phi_A - \phi_E$$

A numerical evaluation using a computer was carried out by A. Buennagel of the University of Maryland for the actual Apollo-15 trajectory data and the result is plotted in Figure 5.[5] The oscillation due to the vector composition of velocity during the lunar orbits is interesting. It was planned to observe these changes by monitoring the transmitted 1-MHz frequency over the television data link while simultaneously measuring the range rate and range of the spacecraft using the unified S-band tracking system.

CONCLUSIONS

The advantages of using an ensemble of clocks which are regularly intercompared have been recognized at least since the time of Captain Cook's exploratory voyages to the South Seas. He carried a set of four chronometers to use in establishing longitude. It is now possible to build a compact self-contained set of small atomic clocks and intercomparison electronics as a result of the dramatic size reduction achieved by Efratom's design of optically pumped rubidium standards and the use of modern integrated circuit electronics. Such packages, which can readily incorporate a controlled environment —for example, constant pressure—can be used in many situations to increase accuracy and reliability. In particular such packages are well suited for future space flights and it is anticipated that not only will the relativistic effects on elapsed time be measured with high accuracy, but also the correction for such effects will become routine in space-navigation and time-transfer operations.

ACKNOWLEDGMENTS

It is a pleasure to thank the many people who encouraged and helped in this measurement and design effort:

U.S. Naval Observatory:	Gernot Winkler Glenn Hall Ken Putkovich
University of Maryland:	Douglas Currie Sherman Poultney John Rayner Charles Steggerda
NASA:	Harvey Hall Noel Hinners Chris Perner
Office of Naval Research:	Robert Morris Arnold Shostak William Condell
Frequency and Time Systems:	Robert Kern Arthur McCoubrey
Efratom:	Ernst Jechart Gerhard Hubner Bernard Schluter
Naval Research Laboratory:	Roger Easton Al Bartholomew Robert Moore

REFERENCES

1. C.O. Alley, Relativistic Clock Readings and the Apollo-8 Flight, University of Maryland Technical Note, December 30, 1968.

   "A Matter of Overtime." *Time*, March 7, 1969.

2. J.C. Hafele and R.E. Keating, *Science* **177**, 166 and 168, July 14, 1972.

3. R.V. Pound and G.A. Rebka, Physical Review Letters, **4**, 337, 1960.

   R.V. Pound and J.L. Snider, Physical Review **140B**, 788, 1965.

4. R.F.C. Vessot and M.W. Levine, *Proceedings of the Conference on Experimental Tests of Gravitation Theories,* Jet Propulsion Laboratory, Technical Memorandum 33-499, p. 54, 1971.

5. A similar computer calculation, stimulated by Reference 1 above, was carried out by J.E. Lavery, Relativistic Time Corrections, for Apollo-12 and Apollo-13. NASA Technical Note TN D-6681. August, 1972.

SECOND GENERATION TIMING SYSTEM FOR RANGING EXPERIMENT APOLLO LUNAR LASER *

Douglas G. Currie, Charles Steggerda, John Rayner, and Albert Buennagel
Department of Physics and Astronomy
University of Maryland

The following is a brief description of the current status of the timing electronics for the new Lunar Laser Ranging Station on Mt. Haleakala, on the island of Maui in Hawaii. The general aim of the Lunar Laser Ranging Experiment is to measure, with high accuracy, the distance from a fixed point on the earth, the observatory, to a retroreflector array which was placed on the lunar surface. In practice, we use three such arrays, placed on the surface during the flights of Apollo-11, -14 and -15. Measurements to these fixed fiducial marks permit an accurate analysis to be performed, in which the various parameters which affect the range may be separated.

The present operating procedure is to direct a short laser pulse through a telescope to the retroreflector on the surface of the moon. This retroreflector then returns the light in the direction from which it originated. The signal is received in the telescope, and the round trip travel time is measured. At present, this time interval is measured with an accuracy of the order of one nanosecond. This is achieved by averaging over about 150 laser shots or about ten received photoelectrons. Ranging attempts to the several reflectors are scheduled three times during each lunar day.

The general method of data analysis is to compare the ranges obtained over a long period of time to the predictions derived from integration of the lunar motion and from data on the earth rotation. The initial scientific objective of the experiment is the production of an improved lunar ephemeris. Following this, a study of the rotations of the moon about its center of mass can improve the values for the moments of inertia of the moon. This data addresses the question of a lunar core and the chemical differentiation of the moon. In addition, since the rotation of the earth produces a significant alteration to the range, one may extract information on the motion of the spin axis of the earth, variations in the rate of rotation of the earth, continental drift, and other similar phenomena. I will not go into the details of these questions, since they have been discussed elsewhere. Finally, the gravitation theory which describes how the moon travels about the earth may be tested to the level of being able to distinguish effects due to the Brans-Dicke theory and effects caused by the gravitational effect of gravitational self-energy of the earth.

*The NASA Lunar Laser Ranging Experiment team has the general responsibility for this work. The team consists of C. O. Alley, University of Maryland; P. L. Bender, Joint Institute for Laboratory Astrophysics; D. G. Currie, University of Maryland; R. H. Dicke, Princeton University; J. E. Faller, Joint Institute for Laboratory Astrophysics; W. M. Kaula, University of California/Los Angeles; G. J. F. MacDonald, Dartmouth College; J. D. Mulholland, University of Texas; H. H. Plotkin, Goddard Space Flight Center; E. C. Silverberg, McDonald Observatory; D. T. Wilkinson, Princeton University; and J. G. Williams, Jet Propulsion Laboratory. This work was supported in part by NASA grant number NGR 21-002-267.

At present, measurements with the full accuracy of 15 cm are accomplished on over about 50 percent of the attempts on the above mentioned schedule. The studies of short periods of data give results which are consistent with the 15-cm accuracy. The long-term fitting of the lunar orbit has an rms agreement of better than ten meters. This is believed to be due primarily to the difficulty in the libration theory of the moon. Adjustments are made in this long term fit to the fifteen parameters, which include reflector locations, earth station locations as well as initial conditions of the orbit. The primary effort at present, on the theoretical side, is the process of extracting, from the differences between the measured ranges and the numerically integrated orbit, the more interesting lunar orbit parameters, initial conditons for the integration, and so on. Due to correlations between certain of these parameters, some of these numbers are less accurate than the ten meter residuals of the long term fit.

The currently used timing equipment, developed by the University of Maryland for use at the McDonald Observatory, has a potential accuracy of 1/10 nanosecond. This is significantly better than the limit of about one nanosecond which is imposed by the length of the presently used laser pulse which is three to four nanoseconds. In order to obtain this accuracy, which is of the order of a part in 10^{10}, the determination is split into two separate parts. A start vernier measures the time interval from the time of detection of the outgoing laser pulse to the next pulse in a 20-MHz train of pulses. A digital counter then measures the interval in units of 50 nanoseconds. A stop vernier measures the time interval from the detection of the single photoelectron return, returning from the moon, to the next count of the 20-MHz counter. The return photoelectron also stops the counter, thus yielding the three components required to determine the accurate time interval. There are the attendant requirements in the McDonald System for epoch to an accuracy of about 50 microseconds and a knowledge of the frequency to the order of a part in 10^{10}. Both of these requirements are significantly more stringent than the minimum requirement to produce an uncertainty equal to that which results from averaging over a few returns. At McDonald we are operating once every three seconds so that we have a nice leisurely capability of firing off a pulse to the moon and sitting and waiting for it to come back before sending another. The state of the laser art at the time of station construction dictated a pulse width of three to four nanoseconds, which defined the accuracy of about one nanosecond. This is achieved by averaging over the pulse width since with less than one photoelectron per shot we are sampling the whole pulse width rather than the leading edge.

In the new Haleakala Station which is being coordinated by the Institute for Astronomy of the University of Hawaii, a new type of laser with a pulse width of 1/10 nanosecond will be used. It will have a firing rate of a few shots per second and is currently being developed under the direction of Dr. Plotkin at the Goddard Space Flight Center. Dr. Faller, formerly of Wesleyan University and now with the Joint Institute for Laboratory Astrophysics, is fabricating a specialized multielement telescope to receive the light from the moon. Our group at the University of Maryland is constructing the timing electronics and timekeeping system.

Several new problems are presented by the Haleakala installation. These are both due to new requirements on the equipment and also due to the 10,000 foot altitude of the station. Particular problems are the high repetition rate of the new laser, the large noise background rates, the short laser pulses which permit the use of better timing accuracy, and the need for increased automation due to the effect of altitude on human operators.

Although the new laser for use at the Haleakala Station will operate at a rate of a few pulses per second, similar types of lasers, which are being studied by Dr. C. O. Alley at the University of Maryland, may operate at rates of 30 to 100 pulses per second. The use of a timing system similar to the one which was developed for the McDonald station would then require the use of up to several hundred counters which is obviously ridiculous. To circumvent this we have gone from interval timing to event timing. More explicitly, in the McDonald System, we measured precisely the time interval between two events. In the Haleakala System, we measure the epoch of each event with high accuracy, so the difference of the two epochs yields the event time difference. Our equipment measures the epoch of outgoing and return pulses to a precision of 1/10 nanosecond. With this system, only one event timer is required, rather than many time interval counters.

The event timer consists of a 10-MHz synchronous counter with multiple latches and verniers. Until a triggered event arrives, the "latch" produces a binary output which is identical to the output of the pulse counter. Upon reception of the triggering event it "latches," that is, it holds the values which the pulse counter displayed at the time of the event. At the same time the vernier circuit starts to determine the time interval between the event and the time of which the counter is latched. The verniers are dual slope intergrators based on an EGG design. When an event comes, a capacitor starts charging at a fixed rate. It stops charging, and starts discharging when the counter is latched. An 80 MHz counter is gated on during the time the capacitor discharges back to zero. The rate of discharge is such that there is one count per 1/10 nanosecond.

Since the McDonald system goes dead after the first pulse in a predetermined gate interval is measured, a noise pulse from the sunlit moon can mask a photon returning from the retroarray. For this reason the large background noise rate, which occurs because of the high transmission and collecting area of the receiving optics, makes a multistop system desirable. Our new equipment supplies this by using four verniers and four counter-latches which are combined to permit four successive pulses from a photomultiplier-discriminator to be measured. When a particular vernier-latch unit is activated by an incoming pulse, it enables the next unit in the chain and it ignores all subsequent pulses. With this configuration, the pulses can then be fed in parallel to high impedence inputs on each unit and the incoming pulses do not have to be switched. This eliminates the problem of delays in the routing circuits. This system can measure pulses with separations down to 80 nanoseconds, which is less than the dead time for our photomultiplier discriminator.

The sequencing and activation of the timing electronics is controlled by a mini-computer, it also calculates predicted ranges for use in the temporal gating of the returns. For this task

the original McDonald system read precalculated ranges from a magnetic tape supplied by J.D. Mulholland of JPL. But with many laser shots per second, this is not feasible; both in terms of the amount of magnetic tape needed and the computer time necessary to precalculate the ranges for all possible operating times. The computer also reads the outputs of the latches and verniers, stores this data for real time processing, and records the data on magnetic tape. The computer time necessary could be reduced somewhat by an interpolation scheme but it is more efficient to calculate the ranges directly from a Tschebyscheff polynominal fit. This procedure will work to at least ten shots per second, but faster rates will require interpolation.

It is also desirable to have real-time operator feedback yielding the preliminary results of the ranging operation. This allows the crew to move on to the next reflector when sufficient returns have been accumulated and it indicates possible malfunction when no returns are received. In the McDonald System, this is accomplished by printing, for each received photoelectron, the residual (or difference) between the observed round trip travel time and the predicted round-trip travel time. Most of these will be noise. However, the laser returns appear bunched in one close time interval of a few nanoseconds. This may be displaced from the prediction for a variety of reasons. A monitoring program in the computer notes when a residual is within a few nanoseconds of a previous residual and produces an audible indication to permit real-time feedback to the person guiding the telescope. The higher data rate on the new station precludes printing the results for each shot so a histogram will be displayed by the computer on a CRT Monitor. The scale and offset of the histogram can be varied to allow a detailed examination of a small portion of the display. Due to the high background, small bins will be needed to distinguish the buildup due to real returns. Drafts in the prediction could then cause real returns to fall into several adjacent bins. To compensate for this, provision will be made to subtract a linear drift from the residual ranges before they are histogrammed.

The computer will also be used for the collection of data on the general operating parameters of the system (temperature and so on), specific data on the run (seeing, number of shots), and on the operation state of the housekeeping subsystem. The computer has a self-controlled crystal oscillator that is used to create an internal clock time-base which, though not very accurate, can serve to indicate gross malfunctions in the station block. The computer uses its internal clock to provide a digital display of the current time (operator reference) on the CRT monitor.

The main station clock consists of a stable crystal oscillator and a specially built counter to indicate the epoch. The station clock will be compared to Loran-C and perhaps a rubidium atomic standard. In order to match the overall distance measurement accuracy the station frequency must be maintained with a long-term accuracy of four parts in 10^{11}. It seems feasible to increase this to about four parts in 10^{12} and thus remove it as a source of error. This same free-running crystal oscillator is also used to provide the time base for the 2-1/2 second averaging times typical of the lunar range. The frequency changes due to aging are

monitored by the Loran-C comparison. The requirement that one be able to make an instantaneous determination of the nominal 2-1/2-second period to a precision of 1/10 nanosecond requires careful control of the ten-MHz signal. Subharmonics have appeared in the clocks we have studied and this must be controlled with careful filtering. Crystal filters were installed on the new station oscillator that lead to a jitter reduction of less than 0.1 nanosecond. The epoch of the measurement must be maintained to 50 μsec in order to match our overall measurement accuracy, since the earth rotates approximately 1.5 cm in this time. The previously mentioned comparison to Loran-C, along with periodical frequency adjustment, maintain the proper epoch. The epoch of the crystal with respect to Loran C, as well as to other standards such as VLF or the rubidium standard, is monitored by the computer and automatically recorded on tape 12 times per hour.

At present, the new equipment is in the final test stages. It will be run in parallel with the previously constructed equipment at McDonald in early February of the coming year. Installation at Haleakala should take place this summer.

PRECISION FREQUENCY SOURCES

Arthur O. McCoubrey and Robert H. Kern
Frequency and Time Systems, Inc.

INTRODUCTION

Program of F.T.S.

Frequency and Time Systems, Inc., is organized to supply state-of-the-art precision oscillators based upon internal development programs, advanced developments of affiliates in Switzerland, and precision oscillators available to us on the basis of distribution agreements when such opportunities complement the line of products.

Applications

With regard to applications we recognize that frequency and time interval standards, whether they are used in the laboratory or in the field, constitute only one important need for precision oscillators. Throughout the historical development of radio technology, there has been an increasing need for precision oscillators in communications and navigation. Densely packed communications channels have expanded toward higher frequencies and the development of time ordered communications has increased. Radio aids have been extended to larger regions of navigable space and higher levels of accuracy. For these reasons the need for precision oscillators of more and more advanced performance continues. In this connection it is essential to regard precision oscillators as subsystems which must be chosen and designed to meet the requirements of the larger systems into which they will be integrated. We, therefore, recognize that no single kind of precision oscillator and no particular configuration can be developed for the growing diversity of applications.

Scope of Paper

In this paper we will outline briefly the status of our internal development of new cesium beam stabilized oscillators. We will also discuss the status of the advanced state-of-the-art quartz oscillator soon to be available, and we will describe a new, very advanced and extremely practical rubidium stabilized oscillator which we are now in a position to supply. We will confine our discussion to application oriented information relating to these cesium, quartz and rubidium oscillators, and we will not go into operating principles which are thoroughly discussed in the literature and are not germane to this meeting.

With regard to performance data, our cesium development program has not yet reached the point at which typical results can be published. Likewise, the evaluation of production models of our new quartz oscillators has not been completed to the point of comparison with already published measurements of the engineering prototype. In the case of the

Table 1
Frequency and Time Systems, Inc.
Precision Frequency Sources.

	Oscillators			Resonators		
	Quartz	Rubidium		Cesium		Cesium
	B-5400	FRK	FRT	FTS-1		FTS-2
Output (MHz)	4 – 7	10	10 5 1 0.1			
Stability				Length	12.5 in	21 in
Short-Term	7×10^{-13} (1 sec)	5×10^{-11} (1 sec)	2×10^{-11} (1 sec)	Volume	110 in^3	412 in^3
Long-Term	1×10^{-10}/day	1×10^{-10}/mo	1×10^{-10}/mo	Weight	9 lbs	21 lbs
Temp. Range	-60°C +60°C	-25°C +65°C	-10°C +50°C	Accuracy	1×10^{-11}	1×10^{-11}
Power	2.4W (25°C)	13W (25°C)	50W (25°C)	Short-term Stability	5×10^{-11} (1 sec)	3×10^{-12} (1 sec)
Warm-up	30 min (2×10^{-7})	10 min (2×10^{-10})	10 min (2×10^{-10})			
Volume	50 in^3	72 in^3	780 in^3			
Weight	1.6 lbs	2.9 lbs	27 lbs			

miniature rubidium oscillator, performance information has been included in an earlier paper of this meeting.

While two of the precision oscillators which I will describe were developed and are presently manufactured outside the United States, I want to say at the outset that in addition to our role as distributors of such technologically advanced products, we also include in our plans licensed manufacturing, as required, to meet the conditions imposed by the Buy American Act.

PRECISION FREQUENCY SOURCES

Overview

Table 1 summarizes some of the characteristics of the quartz and rubidium oscillators and two cesium resonators which we will review in this paper. While two prototype cesium tubes have been constructed and operated in the course of our development program, it is still too early to make a direct comparison of the characteristics of oscillators based upon these tubes with the characteristics of quartz and rubidium oscillators. Such a comparison has been made in the case of the quartz and rubidium, however, and the significant characteristics are apparent. It may be noted here that the difference in size and weight between the rubidium and quartz oscillators is not particularly great as reflected by the new development I will discuss below. They are both very compact and power requirements, while different, are very small.

B-5400 Quartz Oscillator

The model B-5400 quartz oscillator is a refinement of new developments reported by Brandenberger, et al.[1] in 1971. These advancements involve the control of noise characteristics of critical circuit components in order to minimize their effects upon short term stability. In the sideband frequency range from 1 to 100 Hz the power in the frequency spectrum of the phase fluctuations, as reported at that time, was decreased by more than 10dB below that of earlier state-of-the-art 5 MHz oscillators. In the time domain, stability values were measured to be better than 1×10^{-12} from 0.1 seconds to averaging times well beyond 100 seconds.

The B-5400 has been designed at Groupe des Etalons de Frequence of Ebauches Company by Mr. Brandenberger. It incorporated the advances in short term stability and, at the same time, it is reduced in size to a very compact unit having a minimum power requirement.

A small preproduction group of B-5400 oscillators has been manufactured by Oscilloquartz, a subsidiary of Ebauches in Switzerland, in order to determine the practical limitations of

[1]H. Brandenberger, et al., "Proceedings of the 25th Annual Symposium on Frequency Control," (1971), p. 226.

factory processing. The evaluation of these units is in progress and we expect production oscillators of this type to be available within a few months. They will reflect the advances demonstrated by the development prototypes. Figure 1 illustrates one of the preproduction B-5400 units.

Cesium Resonators

Two cesium atomic beam resonator developments are in progress at Frequency and Time Systems. The FTS-1 Cesium Tube has been designed as a resonator for oscillators which will meet the requirements of the specification MIL-F-28734 Types 2 and 3. The second development, the FTS-2, is based upon the research carried out under the direction of Dr. Peter Kartaschoff at the Swiss Laboratory for Watch Research (Laboratoire Suisse de Recherches Horlogères). This work included the basic design of a high-performance cesium tube. The LSRH resonator uses a very effective system of atomic beam optics utilizing a hexapole deflection magnet at the source end and a double dipole deflection magnet at the detector end. FTS-2 is the first prototype which incorporates the LSRH design principles. It has demonstrated an excellent level of performance and we consider it to be the appropriate cesium tube to meet the requirements of MIL-F-28734 Type 1 frequency standards, as well as other high-performance laboratory instruments.

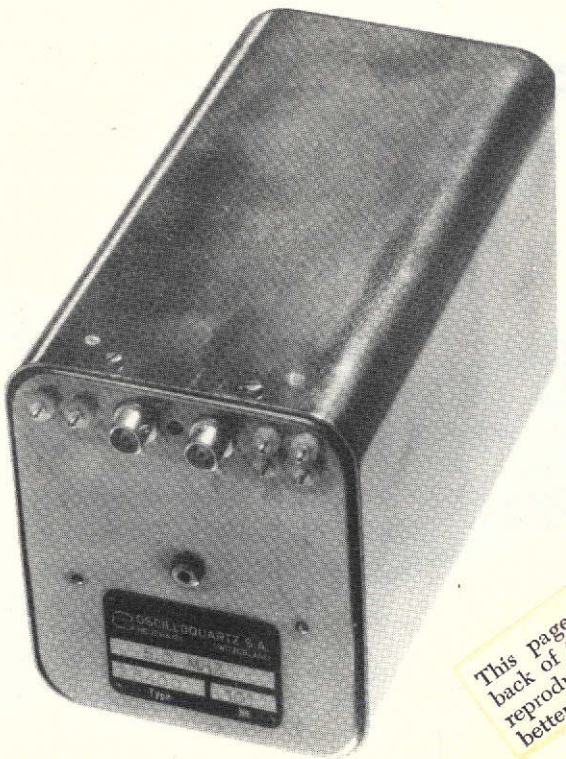

Figure 1. B-5400 high-performance quartz oscillator.

This tube also demonstrates new efficiency principles which are important in terms of cost per unit of operating time, a consideration which will certainly come into sharper focus.

The FTS-1 is illustrated in Figure 2. This tube is an advanced prototype which reflects most of the final design details which will be included in the production tubes. The design of a basic electronic system utilizing this tube is also in progress on the basis of coordinated work by Frequency and Time Systems, Groupe des Etalons de Frequence of Ebauches and Oscilloquartz.

The relationship between the two FTS cesium tubes and the requirements of MIL-F-28734 is illustrated graphically in Figure 3. The expected performance of the B-5400 quartz oscillator is also illustrated in this graph, and it is evident that this unit will also be an important component in high-performance atomic frequency standards.

Rubidium Oscillators

In the United States and Canada, Frequency and Time Systems distributes rubidium frequency standards manufactured by Efratom Elektronik in Munich, Germany. One of these units, the model FRK, is a modular oscillator which functions not only as a frequency standard, but also as a basic building block for systems that require highly stabi-

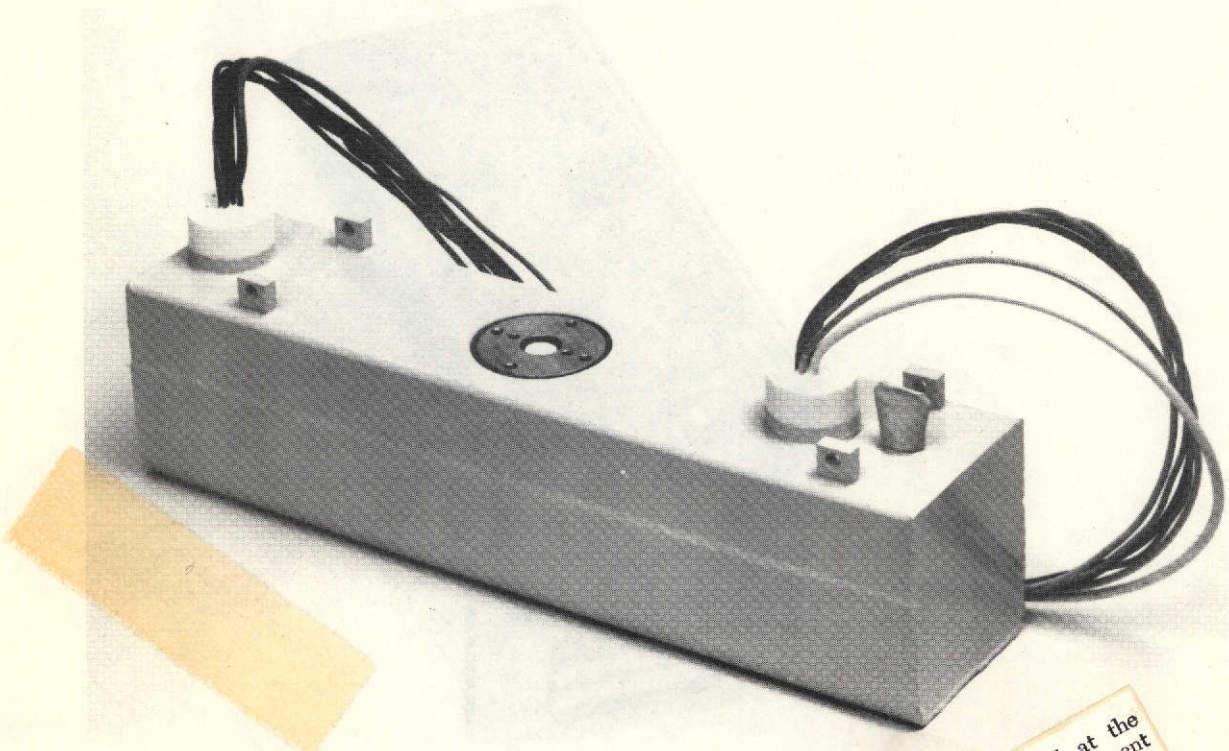

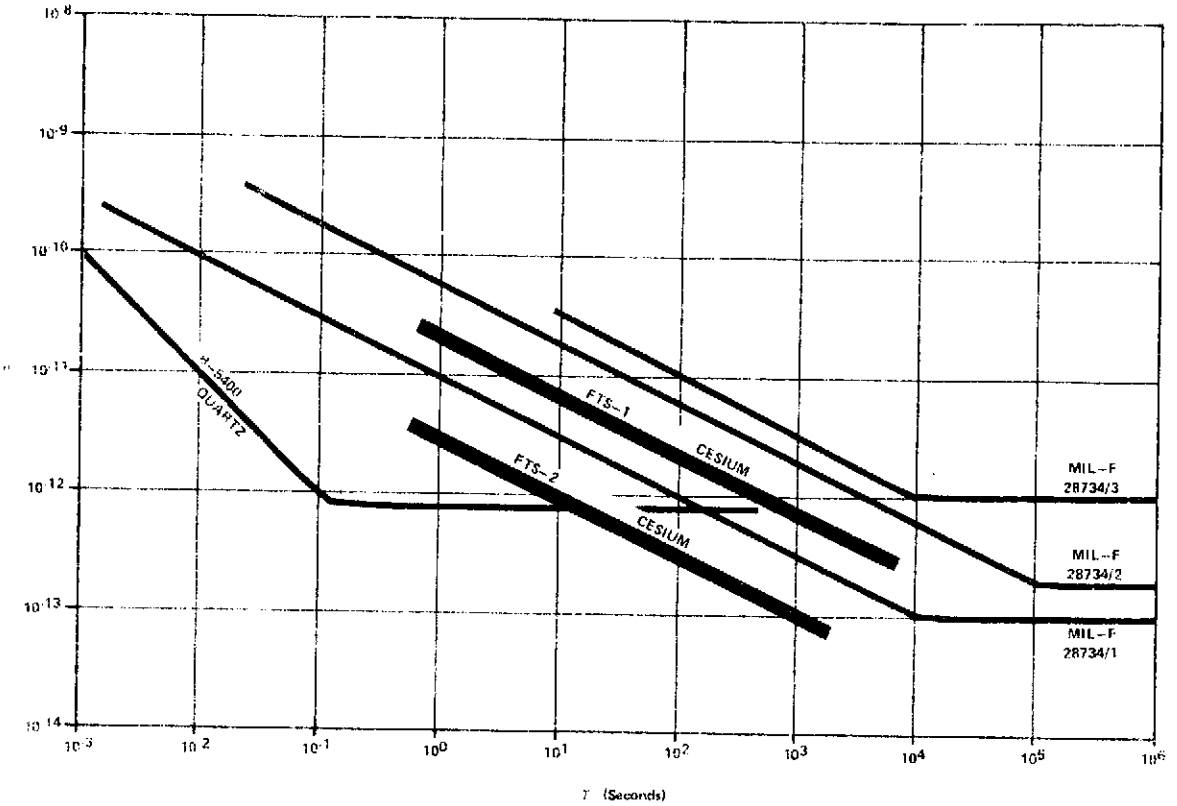

Figure 3. Precision frequency sources.

lized oscillators. The FRK is certainly the most compact atomic oscillator ever made and, while the specifications are conservative, its performance characteristics are equivalent to the most advanced devices of this type. Operating power requirements are minimal at 13 watts and, perhaps as important as the compact size, the warm-up and settling time following power turn on is extremely short. Following the application of power, the FRK locks up and delivers signal in about six minutes at 25°C. In ten minutes the frequency is well within the specified nominal value of 1×10^{-9}. This warm-up characteristic and the relative absence of the effects of shock and acceleration make it possible to utilize the FRK rubidium oscillator in field applications for which precision quartz oscillators could never be considered. The small size and power requirement assures that no significant system penalty will result.

The model FRT is a laboratory frequency standard based upon the miniature FRK. The FRT includes a power supply for operation from utility power lines and a stand-by battery with two hours reserve capacity. This instrument is well suited, therefore, to portable time transfer applications as well as reliable laboratory operation in the event of power failure. The commonly used standard frequencies are available with buffered dual outputs in each case.

Figure 4 illustrates the system organization of the miniature FRK. The output of a voltage controlled crystal oscillator is multiplied and combined with a signal from a synthesizer to produce the 6834-MHz rubidium frequency. This signal is applied to an Rb 87 resonance cell through which the light from a rubidium lamp also passes. When the signal frequency corresponds to the rubidium atomic resonance, the absorption of rubidium light in the cell increases. This effect is sensed in a photo detector and a control signal is generated which steers the frequency of the voltage controlled oscillator.

Figure 5 illustrates the FRK with the cover removed showing the voltage regulator circuit card nearest the cover, and the multiplier/synthesizer circuit card on the adjacent face.

Figure 6 is a view of the rubidium cell along with the microwave cavity into which it fits. The windings illustrated produce the magnetic "C" field which is necessary to the operation of atomic standards.

Figure 7 illustrates the FRK modular oscillator installed as a component in the Efratom Model FRT portable rubidium frequency standard. The heat sink may be used when there is no adequate heat transfer surface available for mounting. The stand-by battery shown in Figure 7 provides for two hours operation in portable applications and uninterrupted ser-

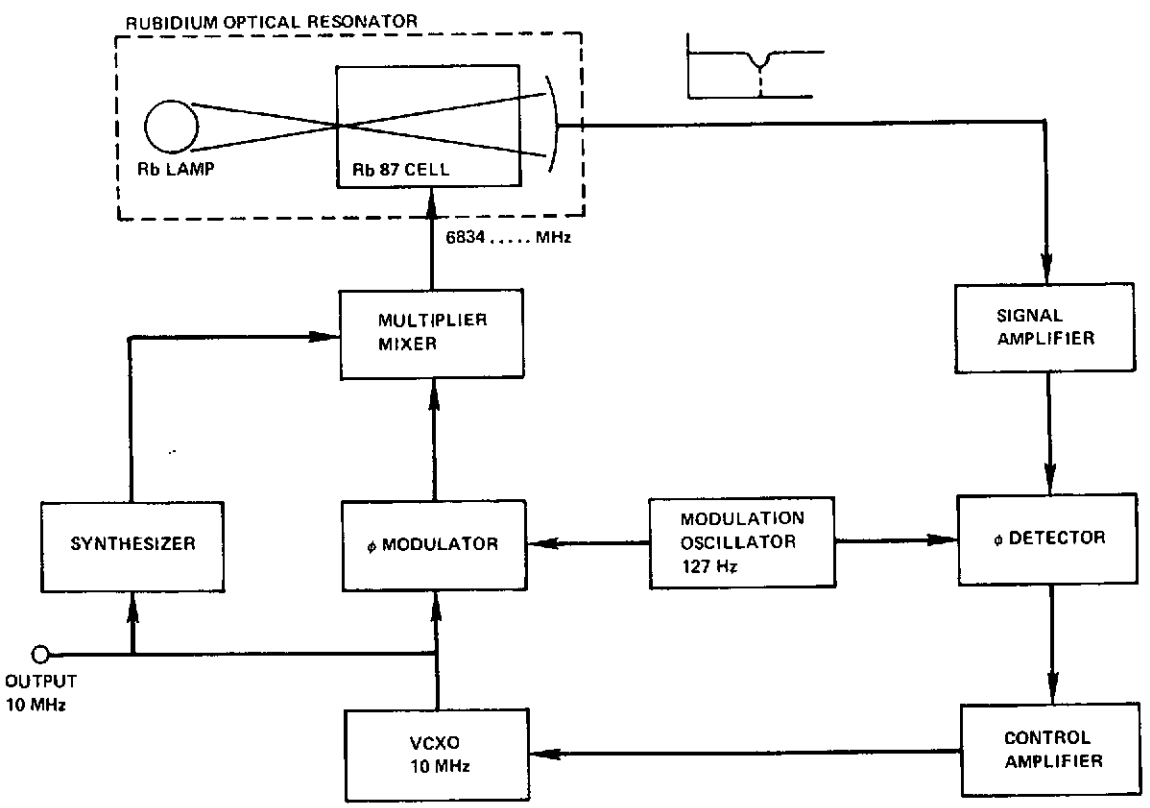

Figure 4. Block diagram of the FRK rubidium oscillator.

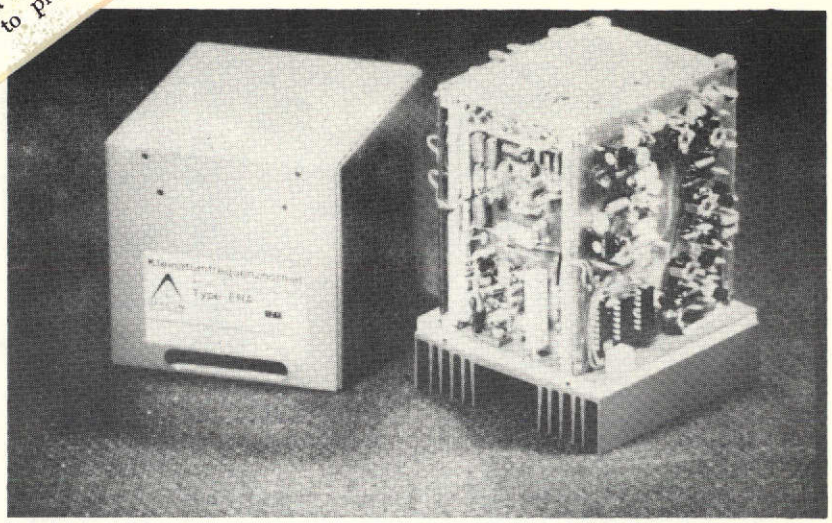

Figure 5. FRK rubidium oscillator.

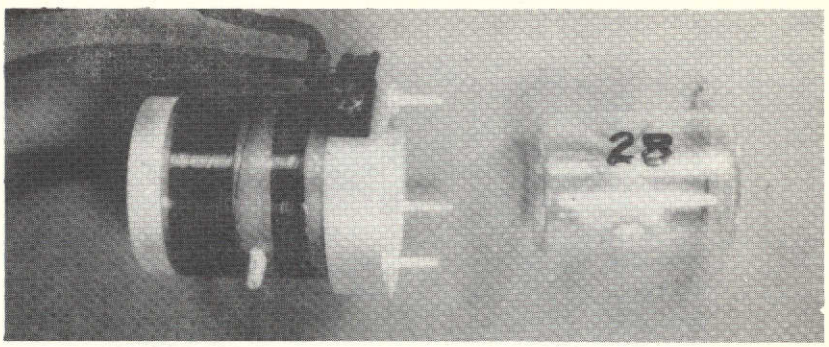

Figure 6. Rubidium cell in the FRK rubidium oscillator.

vice in the case of power failure. The power supply automatically charges the battery and provides all power to the unit while connected to utility lines.

The front view of the complete FRT is illustrated in Figure 8. Four commonly used standard frequencies are available from independent dual outputs at the front and rear of the unit. A meter and switch permit the important functions to be monitored and the frequency trim control is also available on the front panel.

CONCLUSION

Performance measurements of the FRK have already been discussed by Professor Alley and it is not necessary to repeat them here. The new rubidium frequency standards are available at the present time. In just a few months the new quartz oscillator will also be available.

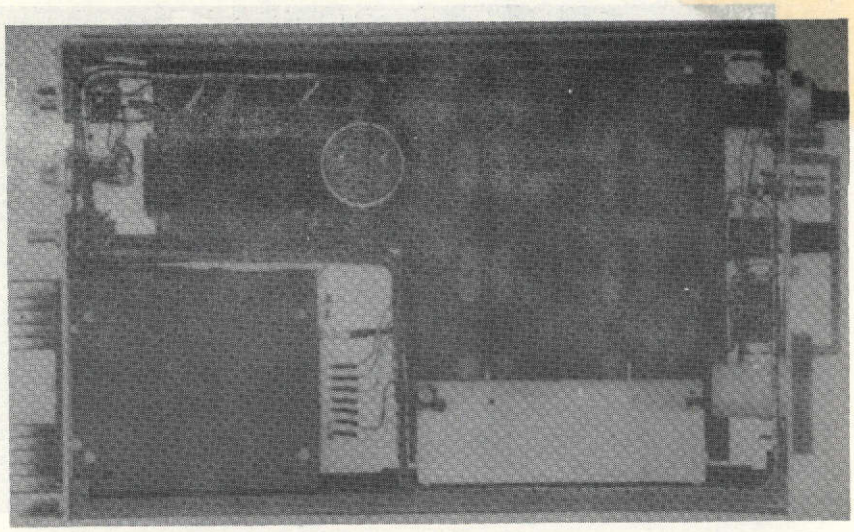

Figure 7. FRK modular oscillator installed in the Efratom Model FRT portable rubidium frequency standard.

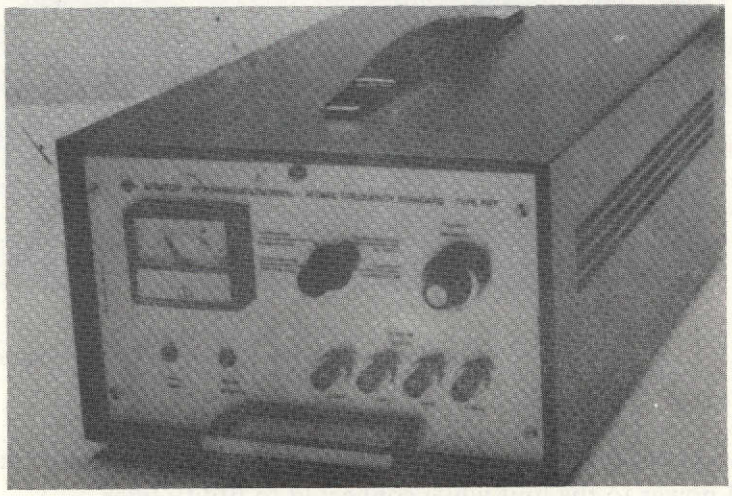

Figure 8. Model FRT portable rubidium frequency standard.

The demonstration and availability of our new cesium oscillators will follow at a later date; however, we expect to be able to discuss engineering tests related to performance in the relatively near future.

NASA HYDROGEN MASER ACCURACY AND STABILITY IN RELATION TO WORLD STANDARDS

Harry E. Peters
Goddard Space Flight Center

Donald B. Percival
U.S. Naval Observatory

ABSTRACT

Frequency comparisons were made among five NASA hydrogen masers in 1969 and again in 1972 to a precision of one part in 10^{13}. Frequency comparisons were also made between these masers and the cesium-beam ensembles of several international standards laboratories. The hydrogen maser frequency stabilities as related to IAT were comparable to the frequency stabilities of individual time scales with respect to IAT. The relative frequency variations among the NASA masers, measured after the three-year interval, were 2 ± 2 parts in 10^{13}. Thus time scales based on hydrogen masers would have excellent long-term stability and uniformity.

I. INTRODUCTION

Atomic hydrogen maser frequency standards, developed at Goddard Space Flight Center (GSFC) for field applications, have been used for several years at NASA tracking stations and other locations around the world. [1] This paper reports the results of measurements of accuracy, reproducibility, and long term stability of these masers. The results were acquired by comparing the masers with one another and with the time scales of several national laboratories which contributed to the international time scale (IAT) maintained by the Bureau International de l'Heure (BIH). [2]

Figure 1 illustrates the intercomparisons described. The five hydrogen masers to the left were designed at GSFC during 1966–1969. NX-1 was a fully operational experimental hydrogen maser which tested several design concepts; these were later incorporated into four field-operable prototype hydrogen masers (NP-1, NP-2, NP-3, and NP-4). NX-1 has operated since September 1967, as a basic frequency standard. The prototype hydrogen masers have operated almost continuously since their completions in 1968 and early 1969.

During construction and testing of the prototype hydrogen masers, measurements were made on all factors which affect their basic accuracy capability. In addition, careful intercomparisons determined the frequency relationships between them. Due to worldwide deployment for experimental applications since August 1969, only sporadic and inexact comparisons of the relative frequencies of the hydrogen masers were possible.

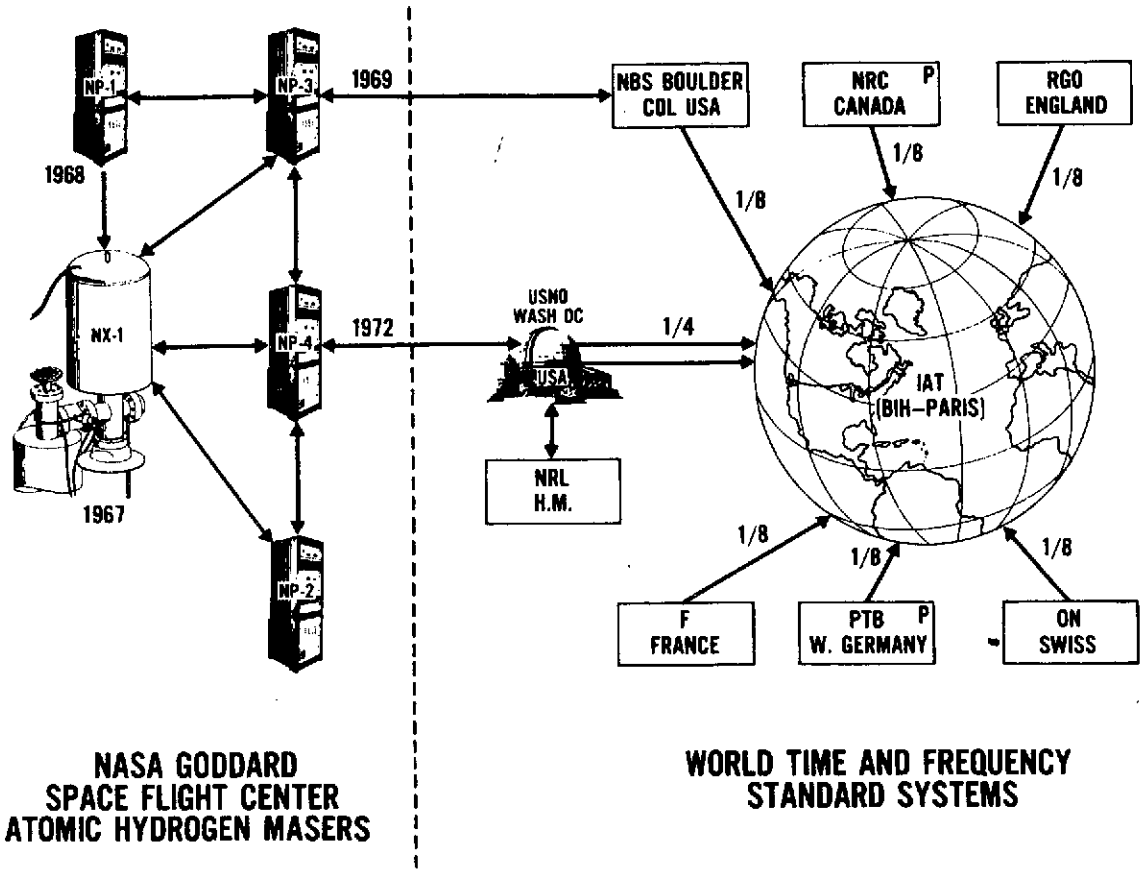

Figure 1. NASA hydrogen maser accuracy and stability measurement system.

In 1972 however, three of the prototypes were at GSFC simultaneously; precise frequency measurements were made among them and the NX-1 hydrogen maser. Combined with the 1968–1969 frequency measurements, these data allowed the determination of relative frequency differences, long term stability, and reproducibility of the four hydrogen masers over a three year interval. In addition, the remaining prototype maser, NP-3, which was at the NASA Apollo tracking station at Goldstone, California during 1972, was compared in frequency to the other masers, but it was compared with much less precision, using VLF, traveling clocks, and Loran-C.

Frequency measurements were also made between some of the NASA masers and various time scales.[3,4] For a three month period from late November 1969, to February 1970, NP-3 was compared at the National Bureau of Standards (NBS) in Boulder, Colorado with the NBS six clock ensemble. Some previously unpublished results of this comparison are given in this report.[5,6]

During 1972, through a collaboration of the United States Naval Observatory (USNO) and GSFC, the NP-4 maser was compared at the USNO for eight months with the USNO 16-

clock cesium ensemble. Simultaneously, NP-4's frequency was compared to the BIH's IAT time scale by using the USNO time scale as a link comparison. In turn, the BIH time scale provided a link to relate the frequency of the NP-4 maser to all the time standards laboratories associated with the BIH. [8,9] (See Figure 1.)

All laboratories contributing to the BIH time scale used a minimum of three Hewlett-Packard cesium-beam standards, which were maintained under good laboratory conditions. Under the weighting scheme used by the BIH to calculate IAT during 1972, the USNO time scale was given a weight of two, while the other six time scales were given a weight of unity. In addition, two laboratories (National Research Council of Canada, Ottawa, Canada, and Physikalisch-Technische Bundesanstalt, Braunschweig, West Germany) operated primary cesium beam frequency standards during 1972.

Besides its cesium-beam standards, the USNO operated a Varian H-10 hydrogen maser during part of 1972, as an interpolation oscillator to analyze frequency variations among cesium clocks. A microwave link between the USNO and the Naval Research Laboratory (NRL) gave the USNO access to two additional early Varian H-10 masers maintained by NRL. [10]

II. MEASUREMENTS RELATIVE TO STANDARDS LABORATORIES

Figure 2 gives the results of the 1972 frequency measurement between the NP-4 hydrogen maser and A.1 (USNO) (which is labelled USNO (MEAN) on the graph). A.1 (USNO) is the independent, uncoordinated, local atomic time scale derived by the USNO. While the net change in frequency between NP-4 and A.1 (USNO) was close to zero for the total period, there were clearly defined deviations from the average frequency of up to three parts in 10^{13}.

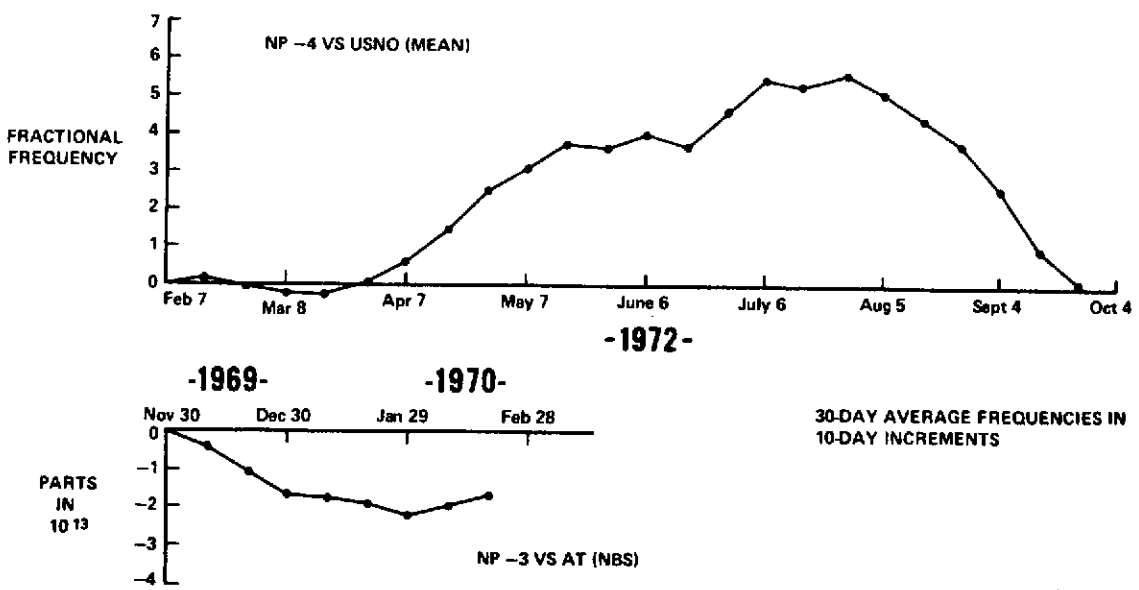

Figure 2. Frequency comparisons—NP masers versus U.S. standards labs.

Figure 2 also shows the results of the three-month frequency measurement between the NP-3 hydrogen maser and the six-clock NBS cesium ensemble in 1969–1970. An Allan variance analysis for 20-day sampling time gave a relative fractional frequency stability of seven parts in 10^{14}. The internal estimate of the variation in the NBS time scale was 4.5 parts in 10^{14}.

At both the USNO and NBS, the NASA masers operated in an average air-conditioned environment. The cavities of the masers were automatically tuned continuously with respect to a good crystal oscillator; for this mode of operation the automatic tuning system should limit cavity-related frequency excursions to less than one part in 10^{13}.[1] The variation of NP-4 with respect to A.1 (USNO) was approximately three times that expected, due to cavity-related frequency changes.

As discussed above, the algorithm used to compute A.1 (USNO) was designed to generate as uniform a time scale as possible. A.1 (USNO) has been evaluated from internal considerations to be stable to a few parts in 10^{14} for measurement periods from 10^6 to 3.10^7 seconds. However, estimation of frequency stability from internal consistency alone would be too optimistic if there were some unknown frequency shifts which were common to most cesium standards in an ensemble.[7] One effort to evaluate the stability of A.1 (USNO) against external standards has been made by B. Guinot and M. Granveaud.[9] Compared to IAT, A.1 (USNO) was found to have a stability of 0.6 to 1.3 parts in 10^{13} for averaging times of 60 days. (IAT, however, was not truly external to A.1 (USNO) since 25% of IAT was derived from the USNO time scale.) If this stability estimate were valid for the 240 day period in which A.1 (USNO) and NP-4 were compared, then the variation of A.1 (USNO) with respect to NP-4 was approximately three times that expected.

That time scales based on cesium ensembles do vary with magnitudes greater than expected from internal estimates of stability may be seen from Figures 3 and 4. Here the frequency variations of NP-4 and the contributors to the IAT time scale are plotted against IAT. (While the deviations in frequency between NP-4 and A.1 (USNO) shown in Figure 2 were definitely real, some of the frequency variations in Figures 3 and 4 were probably due to poor reception of LORAN-C signals, which were used to link the various time scales. This coordination error has been calculated as ± 1 part in 10^{13} on a 30 day basis.[9]) The variation of NP-4 against IAT was comparable to the variations of the contributing time scales against IAT. The NP-4 maser and the independent cesium ensembles agreed to within several parts in 10^{13} for the eight-month period.

Thus there was no clear, unambiguous conclusion as to the relative stabilities of a hydrogen maser and a system of cesium clocks. It would be of interest to conduct further comparisons which would involve more than one hydrogen maser of the NP type. Hopefully such comparisons would provide further data to evaluate the stability properties of hydrogen masers and cesium clock ensembles.

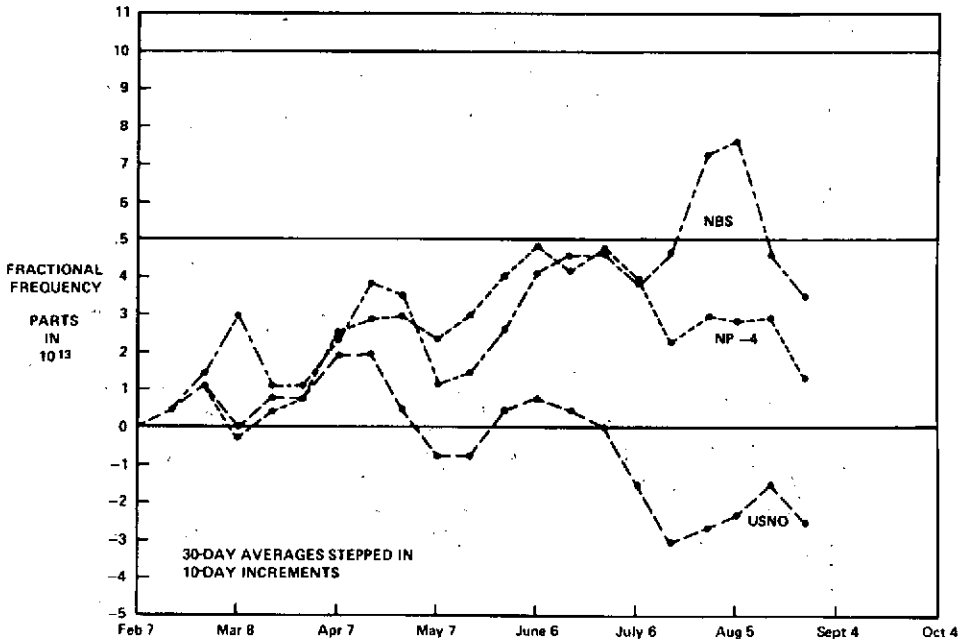

Figure 3. USNO, NBS and NP-4 maser frequency versus IAT.

III. MEASUREMENTS BETWEEN MASERS

Figure 5 shows frequency comparisons of the NASA prototype masers against the NX-1 maser in 1969 and 1972. The data have been corrected for second order doppler shift (with an error estimate of ±.0004 Hz), magnetic field measurement (±.0000013 Hz). and wall shift (± .0024 Hz). The errors associated with cavity tuning and the measurement technique were no greater than ± .00014 Hz. Since NP-3 was in Goldstone, California and was compared via traveling clock, VLF, and LORAN-C, there was an additional measurement error estimated at ± .0007 Hz.

Table 1 gives the 1972 absolute frequency of all of the NASA masers with respect to IAT. These values were referred to the 1972 NP-4 measurement reported previously. [8,9] The error estimate given for the average value of the absolute frequencies was that attributable to a single hydrogen maser since the major uncertainty, the wall shift, was a common systematic error. Table 1 includes a new value for the wall shift temperature coefficient associated with the hydrogen masers. The cavity temperature of NP-2 and NP-4 were lowered by 17°C. The resulting changes in the frequencies of NP-2 and NP-4 indicated that the previous value for the wall shift temperature coefficient was in error.*

*The value for f_H given herein differs by 0.0003 Hz from the value in Reference (8). This is due to the use of the present value of wall shift temperature coefficient, namely (0.008 ± 0.0003) Hz-in/°C. The previous value, assumed in Reference (8) to be (0.005 ± 0.0003) Hz-in/°C, was that given by Vessot et al. (12), and was only claimed to be valid for the temperatures from 25°C to 40°C, whereas the new value was measured for 35°C to 53°C. The 0.0003 Hz change is far less than the claimed error, so is not of great significance.

Due to operational requirements, immediate before and after measurements were not done, and the 1972 measurements were the first precise frequency comparisons of NP-2 and NP-4 and the other masers subsequent to the temperature changes. [12]

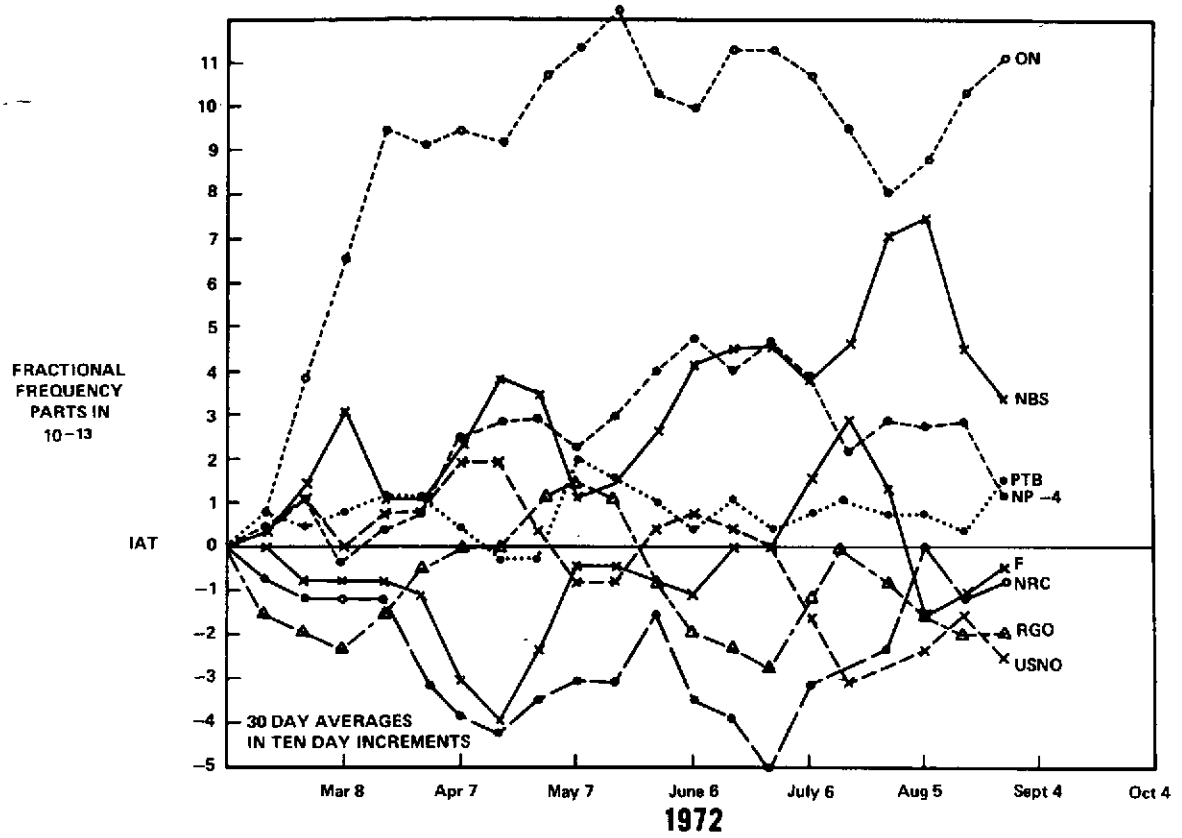

Figure 4. Frequency comparisons–International Standards Labs and NP-4 H-maser versus IAT.

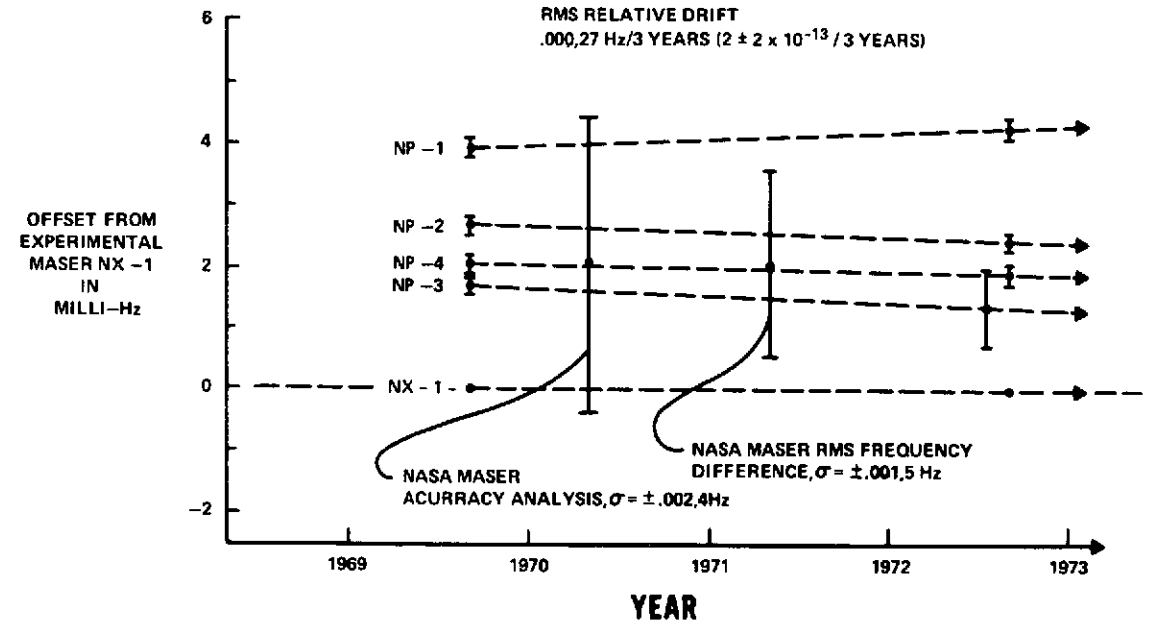

Figure 5. Frequency relationships–NASA NX-1 and NP-1, -2, -3, -4 atomic hydrogen masers.

Because of this temperature change, NP-2 and NP-4 in Figure 5 should only be compared to one another, and NP-1, NP-3, and NX-1 should only be compared to one another, in order to estimate the long term performance of the NASA masers.

Table 1

f_H = 1,420,405,751. + table value, H_z

Maser	NP-1	NP-2	NP-3	NP-4	NX-1
Value	.7782	.7764	.7753	.7758	.7740
Average value 0.7760 ± .0024 Hz					

The long-term stability inferred in Figure 5 should be valid if frequency variations due to magnetic field changes are either negligible or estimated by Zeeman frequency measurements. (In the 1972 NP-4/USNO measurement, the magnetic field was checked weekly. The variations in Zeeman frequency indicated an uncertainty in the maser frequency of ± .000014 Hz, with a negligible measurement error.) Under these conditions, a stability estimate for the NASA masers was 2 ± 2 parts in 10^{13} in three years.

An estimate of the intrinsic reproducibility of the NASA maser has been calculated from the RMS variation of all of the maser frequencies from their average frequency. The resulting value was 0.0015 Hz. Reproducibility may be improved significantly if the maser bulbs were removed and recoated; however, this was not done since these masers were in field usage for most of the three years. (For field applications, these absolute differences are easily removed or adjusted to any desired frequency by synthesizers.)

CONCLUSION

Hydrogen masers have already provided significant contributions to PTTI applications due to their excellent short-term stability. Their long-term stability, long operating life, and reproducibility demonstrate their usefulness in generating accurate, stable, and uniform time scales. The use of the hydrogen maser holds promise to improve time and frequency control with greater ease than presently possible with large ensembles of cesium clocks.

REFERENCES

1. H.E. Peters, T.E. McGunigal, and E.H. Johnson, "Hydrogen Standard Work at Goddard Space Flight Center," 22nd Freq. Cont. Symp. USAEC, Ft. Monmouth, N.J., 1968.

   H.E. Peters, T.E. McGunigal, and E.H. Johnson, "Atomic Standards for NASA Tracking Stations," 23rd Freq. Cont. Symp. USAEC, Ft. Monmouth, N.J., 1969.

   H.E. Peters, "Hydrogen Masers and Other Standards," Proc. 3rd DOD/PTTI Meeting, NRL, Washington, D.C., 1971.

   H.E. Peters, "Topics in Atomic Hydrogen Standard Research and Applications," NASA/GSFC X-524-71-408, 1971. (Also, in Proc. Seminar on Freq. Stds. & Meteorology, University Laval, Quebec, Canada, 1971.)

   H.E. Peters, E.H. Johnson, and T.E. McGunigal, "NASA's Atomic Hydrogen Standards," Proc. Colloque Int. De Chron., Paris, 1969.

2. B. Guinot, M. Feisel, and M. Granveaud, Bureau International De L'Heure Annual Report, 1970, Paris, 1971.

3. J. Lavery, "Operational Frequency Stability of Rubidium and Cesium Frequency Standards," Proc. 4th DOD/PTTI Meeting, NASA/GSFC, Greenbelt, Md., 1972.

4. A.R. Chi, F.G. Major, and J.E. Lavery, "Frequency Comparison of Five Commercial Standards with a NASA Experimental Hydrogen Maser," 24th Freq. Cont. Symp. USAEC, Ft. Monmouth, N.J., 1970.

5. A.S. Risley, et al., "Long Term Frequency Stability of a NASA Prototype Hydrogen Maser," (Summary), in CPEM Dig. 1970, IEEE, N.Y., N.Y., 1970.

6. D.W. Allen, "Statistical Modeling and Filtering for Optimum Atomic Time Scale Generation," Proc. Seminar on Freq. Stds. & Meteorology, University Laval, Quebec, Canada, Aug.-Sept. 1971.

7. D.W. Allen, J.E. Gray and H.E. Machlin, "The National Bureau of Standards Atomic Time Scales: Generation, Dissemination, Stability and Accuracy," IEEE Trans. I&M, Vol. IM-21, No. 4, Nov. 1972.

8. H.E. Peters, R.G. Hall, and D.B. Percival, "Absolute Frequency of an Atomic Hydrogen Maser Clock," Proc. 26th Freq. Cont. Symp. USAEC, Ft. Monmouth, N.J., 1972. (Also, in NASA Report X-524-72-225, GSFC 1972)

9. B. Guinot, and M. Granveaud, "Atomic Time Scales," IEEE Trans. I&M, Vol. IM-21, No. 4, Nov. 1972.

10. D. Phillips, R. Phillips, and J.O. Neill, "Time and Frequency Transfer Via Microwave Link," Proc. 24th Freq. Cont. Symp. USAEC, Ft. Monmouth, N.J., 1970.

11. G.M.R. Winkler, R.G. Hall, and D.B. Percival, "The U.S. Naval Observatory Clock Time Reference and the Performance of a Sample of Atomic Clocks," Metrologia, Vol. 6, No. 4, Oct. 1970.

12. R. Vessot, et al., "An Intercomparison of Hydrogen and Cesium Frequency Standards," IEEE Trans. I&M, Vol. IM-15, No. 4, Dec. 1966.

VERY LONG BASELINE INTERFEROMETRY (VLBI) EARTH PHYSICS*

Peter F. MacDoran
Jet Propulsion Laboratory

HISTORICAL ORIGINS OF VLBI

Historically, applications of interferometry have been primarily for astronomical purposes beginning with the work of A.A. Michelson and F.G. Pease in 1920. These early experiments used optical wavelengths to measure the angular diameters of stars. The method operated by combining starlight received from two separate optical paths, which had to be established and maintained at equal optical lengths (Figure 1). This task proved to be extremely difficult and prevented the primary mirrors from being separable by more than 20 ft., mainly because of atmospheric dissimilarities in the two interferometer arms. A dissimilarity in optical path of only 0.2μ (1/2 an optical wavelength) is sufficient to de-

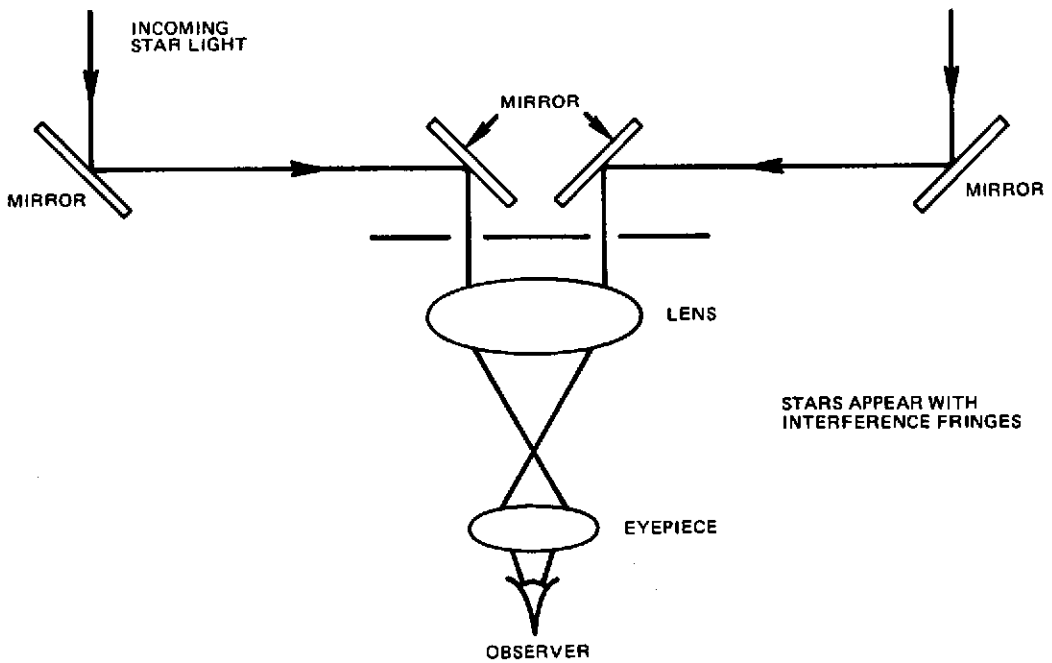

Figure 1. Michelson/Pease stellar interferometer.

*This paper presents the results of one phase of research carried out at the Jet Propulsion Laboratory, California Institute of Technology, Pasadena, California, under contract No. NAS 7-100, sponsored by the National Aeronautics and Space Administration.

stroy the interference pattern (or fringes) which is the output of any interferometer system.

With the emergence of radio astronomy as a discipline in the 1930s came the desire to create the analog of the Michelson/Pease stellar interferometer using radio waves instead of optical wavelengths. These early radio interferometers were the so-called hard-wired systems, because cables or some other phase-stable communications link was needed to derive the first local oscillator signals (Figure 2). As with its optical forerunner, the radio paths had to be stable to better than one-half an RF wavelength to maintain the fringe output of the interferometer. The practicality of laying cables has limited short baseline interferometers to about 1 km, whereas microwave relay links have allowed antenna separations up to about 100 km.

Because the resolving power of an interferometer is dependent on the ratio of the wavelength to the antenna separation, there was the inevitable desire to move the antenna spacing to intercontinental distances, if possible. The breakthrough in achieving these very long baselines occurred in 1967[1,2] because of improvements in quantum electronic frequency systems which afforded essentially identical performance of two or more separate devices for generating local oscillator signals. The improved frequency systems eliminated the need for a phase-stable link between the two receiving stations, making it possible for the stations to be separated by arbitrarily large distances limited only by the earth's diameter. This, then, was the origin of the radio astronomy technique of very long baseline interferometry (VLBI).

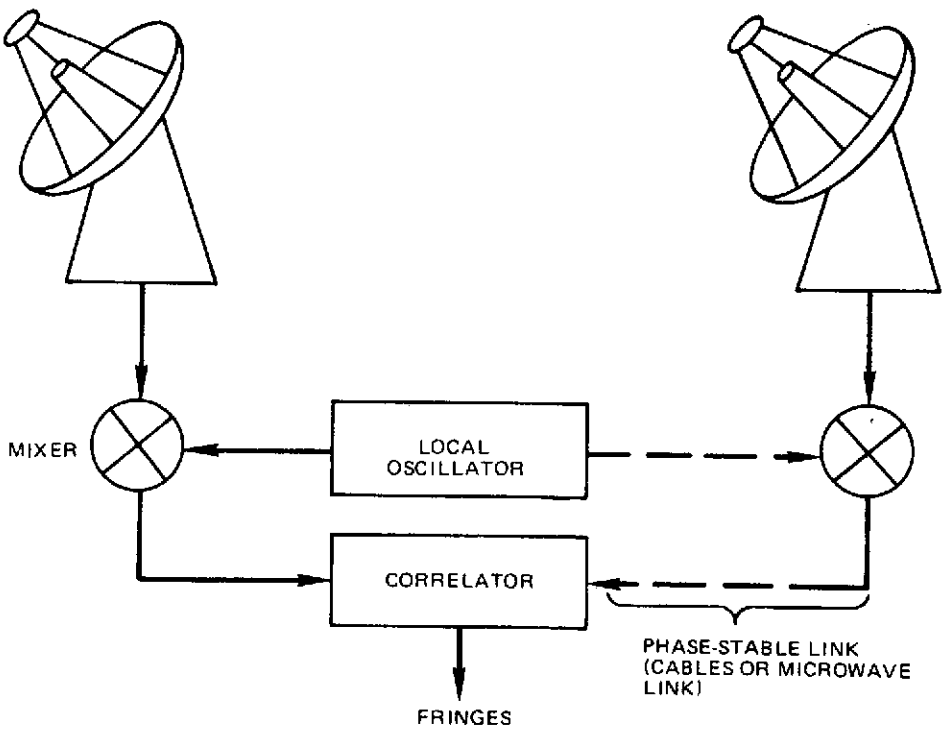

Figure 2. Conventional hard-wired radio interferometer.

Perhaps it would have been more apt to term the method independent station radio interferometry, so as not to imply that only very long baselines were allowed.

When the baselines are comparatively short, and phase-stable communication links are available, the outputs of the heterodyne receivers are conveniently combined at a common site to produce fringes. However, on a very long baseline the output of the receivers must be handled differently. The only method so far demonstrated consists of recording receiver output on magnetic tapes along with time codes from each station. Two implementations exist in this type of recording: an analog approach favored by the Canadians and a digital method used by virtually all U.S. teams. These magnetic tapes are brought together for cross-correlation processing, usually several days or weeks after the time they were recorded. It is the cross-correlation process which yields the fringe response of the interferometer. A schematic diagram of the VLBI technique is given in Figure 3.

Since the original experiments in 1920, interferometry has been used for astronomical applications and particularly for measuring the angular diameters of the sources of light or of radio waves. The early publications on VLBI, however, correctly identified applications to geophysics,[3,4] although the predictions of centimeter-level measurements are yet to be realized over very long baselines.

For those interested in the general VLBI literature and the use of this concept in the study of spatial structure of celestial radio sources, general survey articles[5,6] will be of interest.

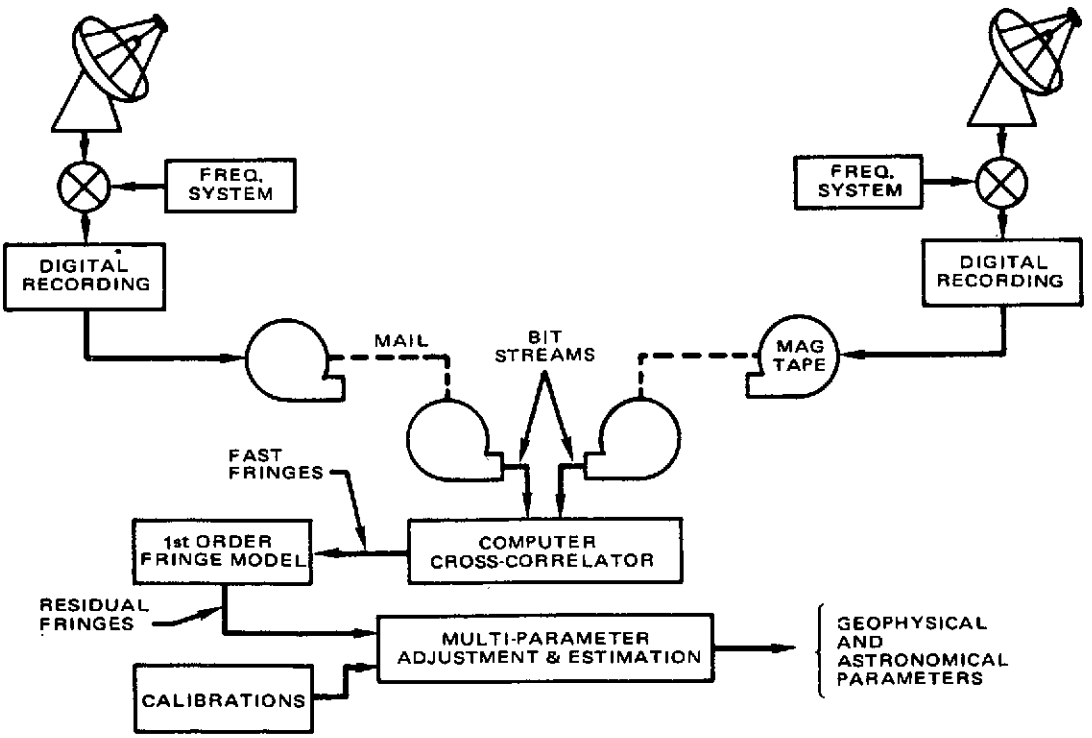

Figure 3. The VLBI technique.

THE VLBI TECHNIQUE

In VLBI measurements, the radio signal produced by a distant source is recorded simultaneously at two radio antennas. Because of a difference in ray paths, reception of the signal may be delayed in time at one antenna relative to the other. By cross correlating the two signals, the time delay and/or its time derivative may be determined.[7,8] When narrow-band recording equipment is used, only the derivative of the time delay may be measured with adequate precision. If the radio signal is generated by an extragalactic object, the radio source may be regarded as a fixed object because of its great distance.

The time variation of the time delay is due entirely to the earth's motion, but depends, of course, on the source location and the baseline vector between the two antennas. In general, measurement of the derivative of the time delay for many natural sources can lead, by means of a least-squares analysis, to the determination of source locations; the baseline vector; and earth-motion parameters, such at UT-1 and polar motion.

Figure 4 shows a schematic diagram of a radio interferometer station pair, while Figure 5 gives the geometry of the situation. As these two antennas are separated by a distance $|\vec{D}|$, there may be a difference in the time of reception of the signal at the two antennas. This delay, τ_g, is given by

$$\tau_g = \frac{D}{c} \cdot \hat{S} \tag{1}$$

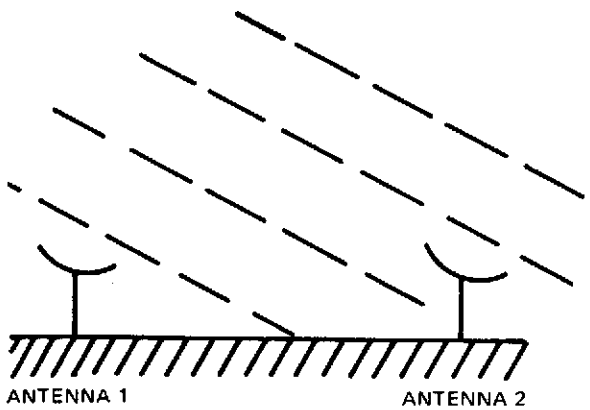

Figure 4. Interferometer pair.

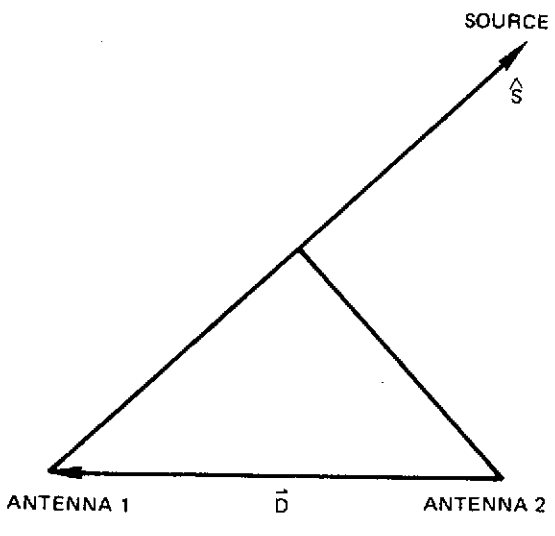

Figure 5. Interferometer geometry.

where c is the speed of light, and $\hat{s}$ is a unit vector opposite the direction of propagation of the wave front (assumed plane for simplicity only). This time delay has a maximum possible value of the earth's radius/c, or 0.021 sec. The quantity

$$\nu_F = \omega_0 \frac{\partial \tau_g}{\partial t} \tag{2}$$

is known as the fringe rate, where ω_0 is the received frequency and is just the negative of the Doppler shift between the two stations. In general, cross correlation of the two data streams allows the time delay τ_g and the fringe rate ν_F to be measured.

The dot product in Eq. (1) is most usefully expanded in terms of the equatorial coordinate system of date. In this system, the right ascension and declination of the source are given by α_s, δ_s while the equivalent quantities for the baseline vector $\vec{D}$ are α_b, δ_b.

Explicitly writing out the dot product in Eq. (1)

$$\begin{aligned} \tau_g &= \frac{|D|}{c} [\cos\delta_b \cos\alpha_b \cos\delta_s \cos\alpha_s \\ &\quad + \cos\delta_b \sin\alpha_b \cos\delta_s \sin\alpha_s + \sin\delta_b \sin\delta_s] \\ &= \frac{|D|}{c} [\sin\delta_b \sin\delta_s + \cos\delta_b \cos\delta_s \cos(\alpha_b - \alpha_s)] \end{aligned} \tag{3}$$

the fringe rate – Eq. (2) – is then

$$\nu_F = -\frac{|D|\omega_0}{c} [\cos\delta_b \cos\delta_s \sin(\alpha_b - \alpha_s)] \frac{\partial}{\partial t}(\alpha_b - \alpha_s) \tag{4}$$

If the equatorial projection of |D| is called r_b,

$$r_b = |D| \cos\delta_b$$

since

$$\frac{\partial}{\partial t}(\alpha_b - \alpha_s) = \omega_e \tag{6}$$

where ω_e is the angular velocity of rotation of the earth (0.73×10^{-4} rad/s),

$$\nu_F = \frac{\omega_0 r_b}{c} \omega_e \cos\delta_s \sin(\alpha_b - \alpha_s) \tag{7}$$

Eq. (3) emphasizes that cylindrical coordinates are the natural units for this problem. The problem, however, is also conveniently expressed in terms of a right-handed Cartesian coordinate system fastened to the earth with the x axis through Greenwich and the z axis along the instantaneous rotation axis.

If α_G (t) is the right ascension of Greenwich, and λ_b is the longitude of the baseline in the earth-fixed system, then

$$\lambda_b = \tan^{-1} \frac{y_2 - y_1}{x_2 - x_1} \tag{8}$$

where x_i, y_i, and z_i refer to the earth-fixed, geocentric coordinates of the ith station, and the right ascension of the baseline vector becomes

$$\alpha_b(t) = \lambda_b + \alpha_G(t) \tag{9}$$

In a system fixed to the earth

$$X = |D| \cos \delta_b \cos \lambda_b \tag{10}$$

$$Y = |D| \cos \delta_b \sin \lambda_b \tag{11}$$

$$Z = |D| \sin \delta_b$$

where X, Y, and Z are the projections of the baseline on the x, y, and z axes. The geometry of a typical baseline is illustrated in Figure 6.

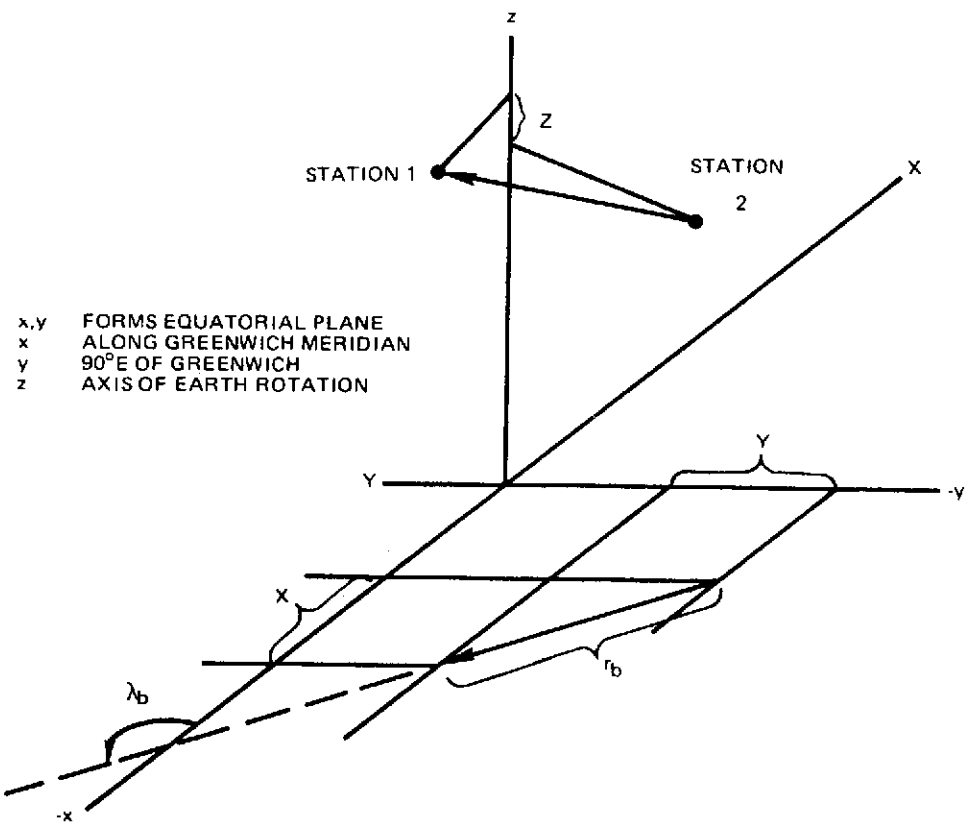

Figure 6. Intrinsic coordinates of an interferometer baseline vector.

Substituting Eq. (9) into Eq. (3), one can obtain

$$\tau_g = \frac{1}{c} \; Z \sin\delta_s + \cos\delta_s \; X \cos[\alpha_G(t) - \alpha_s] - Y \sin[\alpha_G(t) - \alpha_s] \tag{12}$$

and

$$\nu_F = -\frac{\omega_e \omega_0}{c} \cos\delta_s \; X \sin[\alpha_G(t) - \alpha_s] + Y \cos[\alpha_G(t) - \alpha_s] \tag{13}$$

RECENT HISTORY OF VLBI GEODETIC EXPERIMENTS

Various research teams have been active in the development of the VLBI technique for applications to geophysics. There has been considerable variety in demonstrated accuracies and lengths of baselines, as summarized in Table 1.

In order to give some insight into the progression of such research, the following is a brief historical account of the experience at JPL. VLBI earth physics experiments began by

Table 1.
VLBI Geodetic Experiments Summary.

Reporting Date	Group	Baseline
Apr 1970 (Ref. 9)	MIT	Haystack/Greenbank (845 km)
Sep 1971 (Ref. 10)	GSFC	Rosman/Mojave (3 Mm)
Oct 1971 (Ref. 11)	JPL	Goldstone only (16 km)
Apr 1972 (Ref. 10)	GSFC	Agassiz/OVRO (3.9 Mm)
Oct 1972 (Ref. 12)	MIT/GSFC	Haystack/Greenbank (845 km)
Dec 1972 (Ref. 13)	JPL	Goldstone/Madrid (8.4 Mm)
Dec 1972 (Ref. 14)	JPL	Goldstone only (16 km)

using two stations of the Goldstone Deep Space Communications Complex (DSCC), the 64-m Mars and the 26-m Echo antennas, separated by 16 km. In January 1971, a two-dimensional (equatorial components only) baseline measurement of 30-cm accuracy, relative to a ground survey, was obtained by fringe-frequency observations. Those fringe-frequency measurements were disturbed by instabilities at the first local oscillator. These instabilities were corrected for subsequent experiments by construction of a fixed frequency multiplier.

In the summer of 1971, a series of intercontinental baseline experiments were conducted between the 64-m Goldstone and 26-m Madrid stations of the Deep Space Network (DSN). The goals for the experiment were to measure variations in the earth's rotational rate UT-1, the equatorial components of this intercontinental baseline (approximately 8400 km), and to begin the establishment of a catalog of extragalactic radio sources. As reported by J.L. Fanselow at the American Geophysical Union meetings in San Francisco, California, on December 5, 1972, each of these goals was achieved. The variations in UT-1 were measured with a precision of the state-of-the-art (2 milliseconds) and found to be in agreement with those derived optically by the Bureau International de l'Heure (BIH), Paris, France. The equatorial baseline components were determined with an accuracy of 1.5 meter and found to be within 5.3 meters of the baseline derived by the DSN from Doppler tracking of interplanetary spacecraft. This difference is under investigation. A catalog of ten extragalactic radio sources has been determined with a relative accuracy of 0.1 to 0.01 arc second.

The experience gained from these Goldstone/Madrid measurements enabled a quantitative systems analysis to be made. The results indicated that a small antenna could be fielded for surveying over short, moderate, or even intercontinental baselines. With the assistance of the geophysical community, particularly the Caltech Seismological Laboratory, sites of geophysical significance were suggested, and perhaps more importantly, the requirement for extremely high measurement accuracy was clearly established. It became recognized that the major geophysical contribution which a VLBI-type measurement can make is the rate of earth crustal strain taking place over hundreds of kilometers on either side of earthquake fault zones. However, in order to be of short-term worth (within five years), measurements need to be made with five-centimeter or better accuracy in three dimensions. Because the strain rate can be at most about six cm per year, and resolution of at least two cm per year is required to adequately distinguish between various competing geophysical theories a measurement accuracy of five cm would require five years to achieve a rate determination uncertainty of two cm per year.

Since a radio interferometer had never achieved such high accuracies, it became necessary to conduct a series of feasibility demonstrations, and beginning in 1972, experiment emphasis returned to the Mars and Echo stations of the Goldstone DSCC. In April 1972, the first JPL test of two-channel bandwidth synthesis was made with a channel spacing of 10 MHz. Bandwidth synthesis schemes were pioneered by MIT[16] and allow the measurement of the time-delay interferometer function. The April experiment determined the third component of the baseline vector with an accuracy of 50 cm. Based on the April 1972 experiment, the radio system and computer software were redesigned to perform a synthesis over a 40-MHz

channel separation. As reported by J.B Thomas at the December AGU meetings in San Francisco, the results of three experiments (August 16, October 14 and 18, 1972) are 5 cm, 4 cm and 4 cm in three dimensions, respectively. The comparison of the interferometer determinations with an existing ground survey indicates good agreement in the length of the baseline, within the 20-cm uncertainty of the horizontal geodetic control.

In August 1972, a surplus U.S. Army transportable 9-m-diameter satellite communications station was transferred to NASA/JPL to become a portable radio interferometer station. This 9-m antenna will be used as the feasibility station to demonstrate the concept called ARIES (Astronomical Radio Interferometric Earth Surveying) for applications to monitoring earth crustal deformations for study of the earthquake mechanism. The ARIES concept is illustrated in Figures 7 through 11.

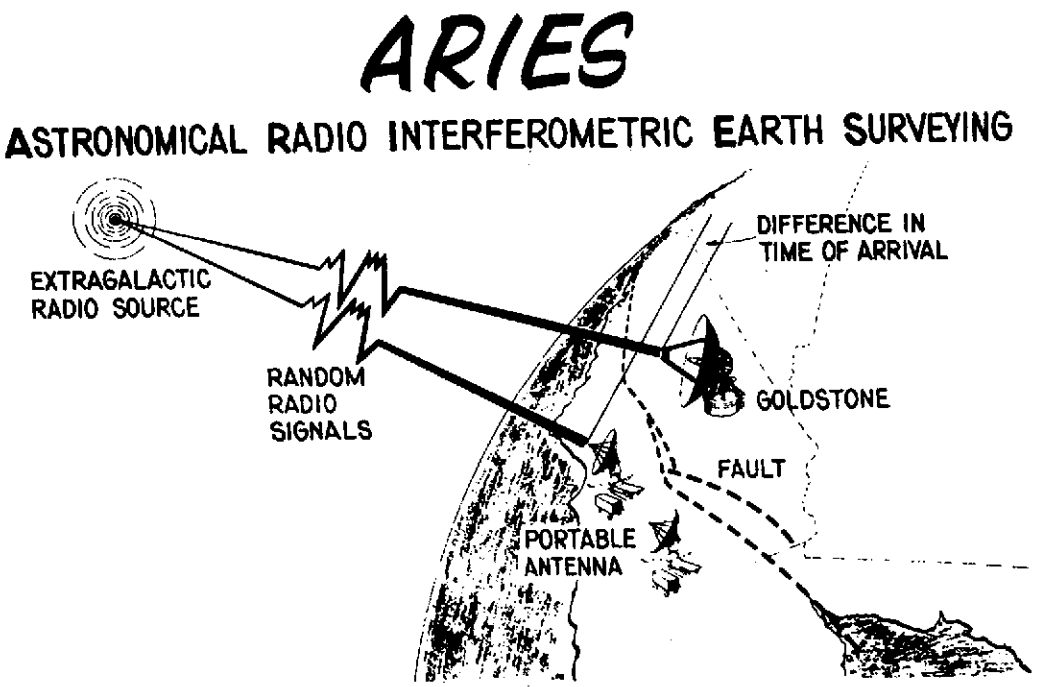

Figure 7. ARIES: astronomical radio interferometric earth surveying.

ARIES ♈

OBJECTIVE: TO DEVELOP A NEW INSTRUMENTAL TECHNIQUE FOR THE STUDY OF EARTHQUAKE MECHANISMS BY MEANS OF EARTH CRUSTAL DEFORMATION MONITORING.

APPROACH: REFINE THE TECHNIQUE OF VERY LONG BASELINE INTERFEROMETRY (VLBI) SO AS TO ACHIEVE 3 cm OR BETTER EARTH SURVEYING ACCURACY USING FIXED AND PORTABLE STATIONS.

♈ ASTRONOMICAL RADIO INTERFEROMETRIC EARTH SURVEYING

Figure 8. Objective and approach of the ARIES program.

EVOLUTION OF THE ARIES♈ CONCEPT

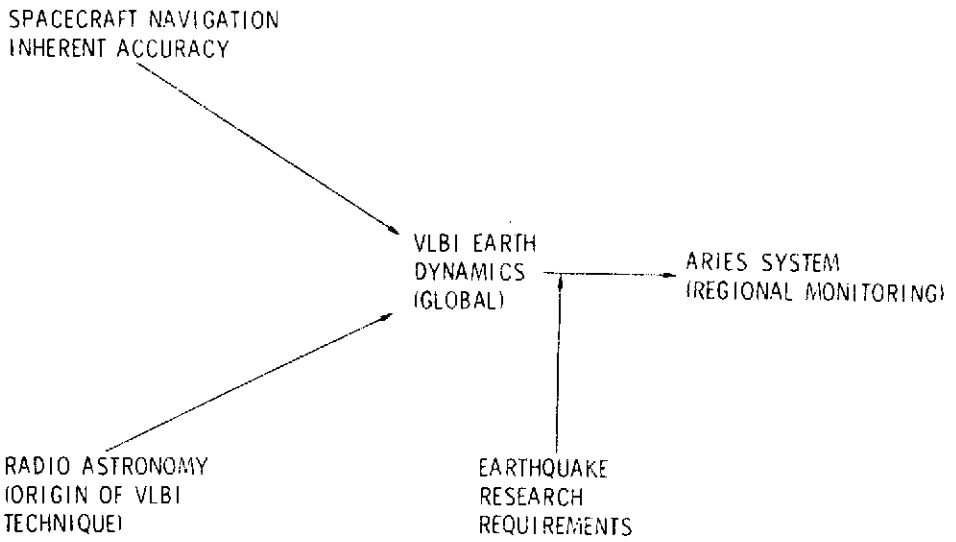

♈ ASTRONOMICAL RADIO INTERFEROMETRIC EARTH SURVEYING

Figure 9. Evolution of the ARIES concept.

- 10 cm MEASUREMENT ACCURACY IN A SINGLE DAY
- INHERENT ACCURACY INDEPENDENT OF BASELINE LENGTH
- REFERENCE EARTH LOCATIONS MEASURED IN THREE DIMENSIONAL GEOCENTRIC COORDINATES RELATIVE TO EXTRAGALACTIC RADIO SOURCES
- OPERATES IN VIRTUALLY ALL WEATHER
- NO TRANSMISSION OF LIGHT OR RADIO SIGNALS NECESSARY (NON-ELECTROMAGNETICALLY POLLUTING)
- INHERENTLY PASSIVE, USING ONLY NATURAL RADIO SIGNALS (NO CYCLOMATES)

Figure 10. ARIES system characteristics.

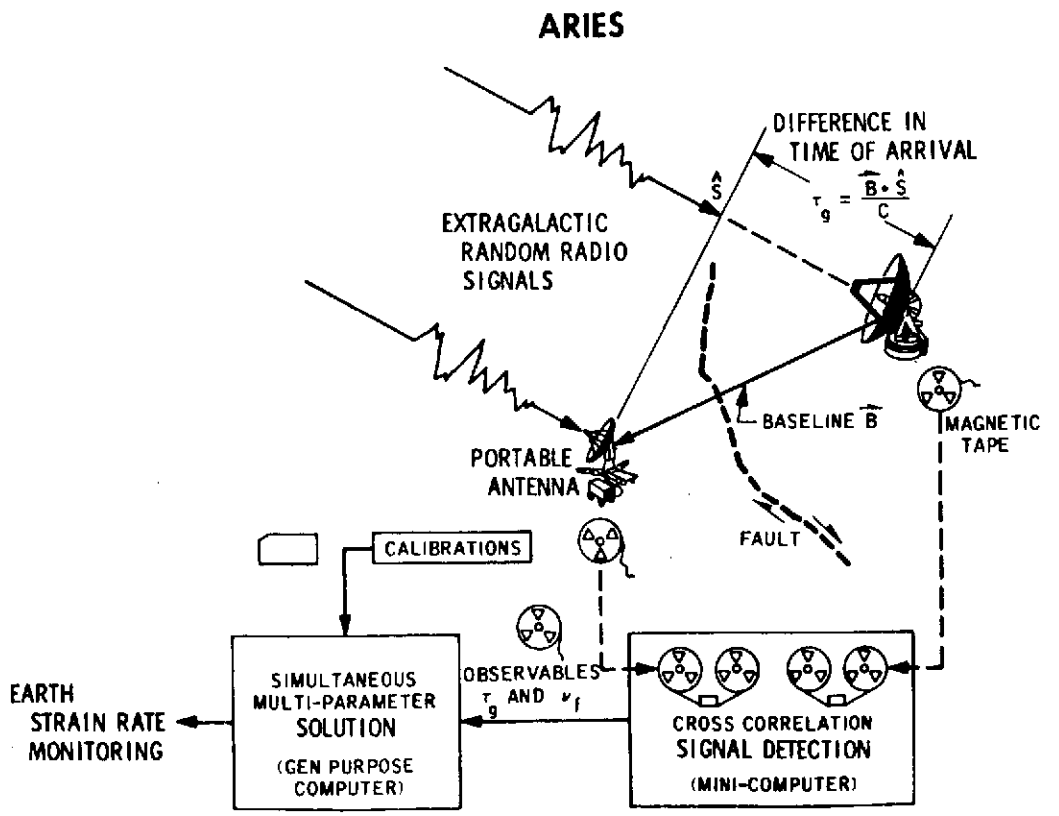

Figure 11. Schematic of ARIES implementation.

ACKNOWLEDGEMENTS

The author wishes to thank P.S. Callahan, H.F. Fliegel, J.L. Fanselow, J.B. Thomas, and J.G. Williams of the Jet Propulsion Laboratory and J.H. Whitcomb of the Caltech Seismological Laboratory for advice on the many diverse elements concerned in the preparation of this paper.

REFERENCES

1. N.W. Broten et al., "Long baseline interferometry: a new technique," *Science,* **156,** 1592-93, June 1967.
2. C. Bare et al., "Interferometer experiment with independent local oscillators," *Science,* **157,** 189-91, July 1967.
3. T. Gold, *Science,* **157,** 302, July 1967.
4. G.J.F. MacDonald, *Science,* **157,** 305, July 1967.
5. W.K. Klemperer, "Long-Baseline Radio Interferometry with Independent Frequency Standards," *Proc. IEEE,* **60,** No. 5, May 1972.
6. K.I. Kellermann, "Intercontinental Radio Astronomy," *Scientific American,* November 1971.
7. J.B. Thomas, An Analysis of Long Baseline Radio Interferometry, JPL Technical Report 32-1526, Vol. VII, February 1972.
8. J.B. Thomas, An Analysis of Long Baseline Radio Interferometry, Part II, JPL Technical Report 32-1526, Vol. VIII, April 1972.
9. H.F. Hinteregger et al., *Trans. Amer. Geophys. Union,* **51,** 267, 1970.
10. J. Ramasastry et al., Very Long Baseline Experiments for Geodynamic Applications, NASA/Goddard Space Flight Center, X592-73-380. March 1973.
11. J.L. Fanselow et al., The Goldstone Interferometer for Earth Physics, JPL Technical Report 32-1526, Vol. V, October 1971.
12. H.F. Hinteregger et al., "Precision Geodesy via Radio Interferometry," *Science,* **178,** 396-98, October 1972.
13. J.L. Fanselow et al., "The Equatorial Projection of a California/Spain Baseline and Irregularities in the Earth's Rotation Rate as Obtained by a Radio Interferometer," American Geophysical Union meeting, San Francisco, California, December 5, 1972.
14. J.B. Thomas et al., "Radio Interferometry: Feasibility Demonstration for Monitoring Tectonic Motion," American Geophysical Union meeting, San Francisco, California, December 5, 1972.
15. A.E.E. Rogers, "Very Long Baseline Interferometry with Large Effective Bandwidth and Phase Delay Measurements," *Radio Science,* **5,** 1239, October 1970.

PRECISION TIMING AND VERY LONG BASELINE INTERFEROMETRY (VLBI)

Thomas A. Clark
Goddard Space Flight Center

INTRODUCTION

Very long baseline interferometry (VLBI) is a technique which was developed by radio astronomers for investigating small angular features in galactic and extragalactic radio sources. If an interferometer is formed from two separate elements along a baseline vector $\overline{B}$ and operated at wavelength λ, interference fringes will result with an angular separation

$$\theta = \lambda/|\overline{B}| \text{ radians}$$
$$= 206265\ \lambda/|\overline{B}| \text{ seconds of arc}$$

For the Goldstone–Haystack ("Goldstack") baseline which will be discussed later, $B \cong 4000$ km and $\lambda \cong 4$ cm, so $\theta \cong 10^{-8}$ radians $\cong 2$ milliseconds of arc. The resultant fringes may be thought of as Doppler "beats" resulting from the differential velocities of the stations when viewed from the source. The resultant fringe frequency varies as a diurnal sinusoid which has a maximum frequency (when the baseline is "broadside" to the source) of

$$f \cong \frac{B' \cos \delta}{13713\ \lambda} \text{ Hz}$$

where B' is the equatorial component of the baseline and δ is the declination of the source. For sources at low declinations, the Goldstack interferometer has fringe rates of $\cong 7$ kHz.

An interferometer will respond only to signals which arise from sources smaller than a fringe. The various sources which have apparent angular sizes smaller than ~ 1 millisecond of arc include

- Nucleii of quasars and certain peculiar galaxies
- Maser-like galactic sources emitting in the OH ($\lambda \cong 18$ cm) and H_2O ($\lambda \cong 1.35$ cm) spectral lines
- Pulsars
- Man-made sources such as satellites and lunar beacons.

Table 1
Current VLBI Experimental Programs.

Program	Frequency	Stations	Collaborating Institutions
"Quasar Patrol" (to investigate the structure and variability of extragalactic radio sources)	7.8 GHz 14.5 GHz	Haystack-Goldstone Plus Onsala and Greenbank	GSFC-Univ. of Md. MIT Haystack Obs. JPL
Astrometric and Geodetic observations with VLBI	7.8 GHz	Haystack-Goldstone plus Fairbanks, Onsala, and Greenbank	GSFC-Univ. of Md. MIT Haystack Obs. NOAA Chalmers
Differential Astrometry		Haystack-Goldstone	GSFC-Univ. of Md.
• Quasar proper motions	7.8 GHz		MIT Haystack Obs.
• general relativity tests	8.1 GHz	Haystack-Westford-Greenbank	
• pulsar proper motions	2.3 GHz	Greenbank-Goldstone	GSFC-Univ. of Md. JPL
Meter wavelength VLBI	196.5 MHz	Greenbank	GSFC-Univ. of Md.
• studies of the Crab Nebula and associated pulsar	111.5 MHz	Sugar Grove	NRL
• studies of extragalactic radio source structure and spectra	73.8 MHz	Arecibo	Arecibo Obs.
• studies of the interstellar medium			
• supernova remnant mapping			
• interplanetary scintillations			
Decameter wavelength VLBI	26.3 MHz	Boulder-Haswell and Boulder-Ames	GSFC-Univ. of Md. NOAA Univ. of Iowa Iowa State Univ.
• (same as meter wavelength program)			
• studies of sporadic radio emission from Jupiter and Saturn			

Table 2
Telescope Employed In VLBI Program.

Telescope Location	Sponsoring Organization	Observing Frequency	Size	System Temperature	Site Time/ Freq. Standard
Haystack, Mass.	MIT-NEROC	7.8 GHz	120 ft	50-80K	Maser
Westford, Mass.			60 ft	200K	Maser
Goldstone, Calif.	JPL	14.5 GHz 7.8 GHz 2.3 GHz 2.3 GHz	210 ft 210 ft 210 ft 85 ft	40K 30K 20K 20K	Maser Maser Maser Maser or Rubidium
Fairbanks, Alaska	NOAA	7.8 GHz	85 ft	150K	Maser or Rubidium
Onsala, Sweden	Chalmers Inst. of Technology	7.8 GHz	84 ft	50K	Maser or Rubidium
Greenbank, W. Va.	NRAO	14.5 GHz 8.1 GHz 2.3 GHz 73-196 MHz	140 ft 3 @ 85 ft 140 ft 300 ft	100K 100K 100K 1000-2000K	Maser Maser Maser Rubidium
Sugar Grove, W. Va.	NRL	73-196 MHz	150 ft	1000-2000K	Rubidium
Arecibo, Puerto Rico	NAIC Cornell	73-196 MHz	1000 ft	1000-2000K	Rubidium
Boulder, Colo.	NOAA	26.3 MHz	Dipole Arrays 10^4 m^2 area	20000K	Rubidium
Haswell, Colo.					
Ames, Iowa	Univ. of Iowa and Iowa State				

The experimental programs currently being pursued by the GSFC*/University of Maryland VLBI team are shown in Table 1. Our emphasis is on astronomical observations utilizing the VLBI technique. It should be noted that these programs fall into two distinct categories. At frequencies $\geqslant$ 2 GHz, the program emphasis is on high-sensitivity receivers, large precision telescopes, and high-stability frequency standards (typically hydrogen masers). The meter and decameter wavelength programs also require large telescopes; but due to the bright sky, receiver performance is less critical. The lower observing frequency permits less precise frequency standards (rubidium). The long-wavelength programs are summarized in more detail by Clark and Erickson (1973). The properties of the telescopes we are using are given in Table 2 and the baselines we have formed over the past four years are shown in Figure 1.

TECHNIQUES

In order to form an interferometer such as the one shown in Figure 2, let us consider that the baseline is a vector $\vec{B}$ and that a unit vector $\hat{S}$ describes the location of a point source. Since we can egocentrically think of the sky as moving over the earth, $\hat{S}$ is a time variable, $\hat{S}(t)$.

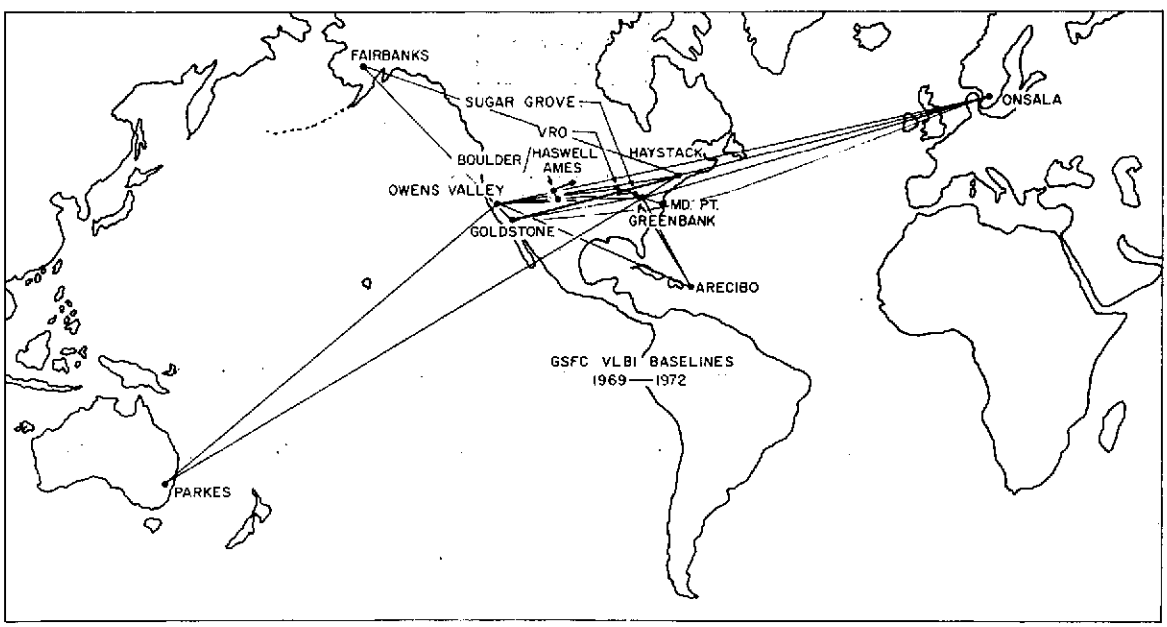

Figure 1. GSFC VLBI baselines; 1969-1972.

*There are two groups conducting VLBI investigations at GSFC. Dr. J. Ramasastry's group (Code 592) is involved in Earth Physics and Tracking Applications of VLBI. Dr. Clark's group (Code 693) is primarily involved in the Radio Astronomy aspects of VLBI. In this paper, GSFC refers to Dr. Clark's group.

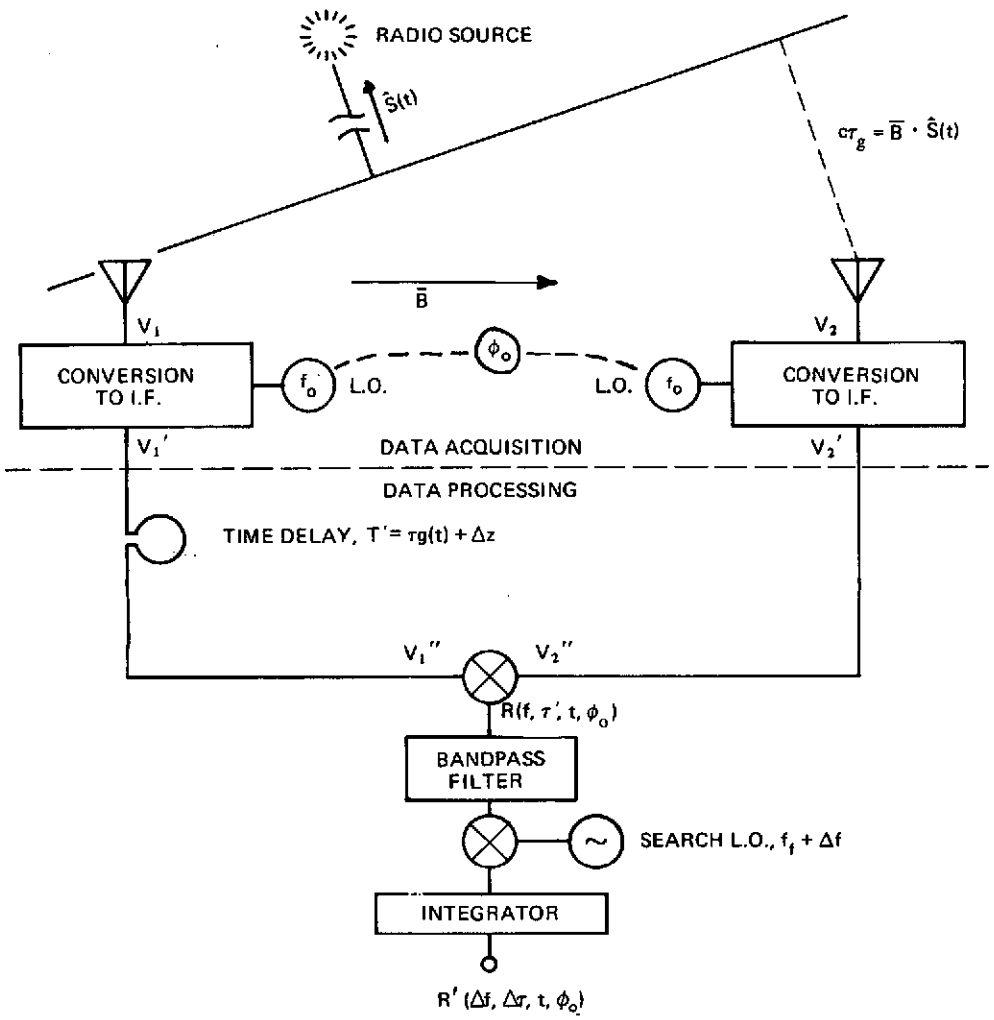

Figure 2. Simplified block diagram of an interferometer.

A wavefront from the source arrives at the left-hand station τ_g earlier than at the right-hand station, where

$$c\,\tau_g(t) = \bar{B} \cdot \hat{S}(t)$$

Our antennas have effective collecting areas A_1 and A_2, so the voltage induced by the source will be proportional to the incoming wave's electric field by

$$V_1 \propto \sqrt{A_1}\, E_o\, e^{2\pi i f t}$$

$$V_2 \propto \sqrt{A_2}\, E_o\, e^{2\pi i f (t-\tau_g)}$$

where f is the frequency of observation. To facilitate processing, the signal is amplified and converted to a convenient intermediate frequency (IF). This is done by heterodyning with a local oscillator at a frequency ν_o, where we permit a phase shift ϕ_o (which may be time variable) to exist between the local oscillator sources. Therefore, the outputs from the IF converters will be

$$V_1' \propto \sqrt{A_1}\, E_o\, e^{2\pi i(f-f_o)t}$$

$$V_2' \propto \sqrt{A_2}\, E_o\, e^{2\pi i[(f-f_o)t - f\tau_g]}\, e^{i\phi_o}$$

If the signal in the left-hand channel is now delayed by τ' (which is nominally = τ_g), then

$$V_1'' \propto V_1'\, e^{-2\pi i(f-f_o)\tau'} \propto \sqrt{A_1}\, e^{2\pi i(f-f_o)(t-\tau')}$$

$$V_2'' = V_2'$$

Note that the phase shift of the delay line τ' enters at the intermediate frequency $(f-f_o)$.

The cross correlator multiplies the two signals V_1'' and V_2''. If we assume that only the difference terms are passed by the bandpass filter, i.e., frequencies of $\sim 2f_{if} = 2(f-f_o)$ are attenuated, then

$$R(f,\tau,t,\phi_o) = V_1'' \cdot V_2''^*$$

$$\propto \sqrt{A_1 A_2}\, E_o^2\, e^{2\pi i f_o \tau_g}\, e^{2\pi i(f-f_o)(\tau_g - \tau')}\, e^{-i\phi_o}$$

$$\underbrace{\quad}_{A} \qquad \underbrace{\qquad\qquad}_{B} \qquad \underbrace{\quad}_{C}$$

The "A" term represents the fringes, since it is the variation of τ_g with time that results in a periodic sinusoidal interference pattern. Note that when the delay line τ' is "tracked" with τ_g, it is the local oscillator frequency f_o, and not the signal frequency f which describes the fringes.

In order to conveniently process these fringes, we next slow them down further by removing the nominal fringe frequency f_f, where

$$f_f = \frac{d}{dt}(f_o \tau_g) = f_o \cdot \dot{\tau}_g$$

By suitably "searching" about f_f we can define the true fringe frequency $f_f + \Delta f$. Since the output from this last heterodyning operation is at dc, we can now integrate for long periods of time. We are limited by the time interval t_c of the "C" term over which the local oscillators maintain coherence, i.e., when $< \phi_o(t + t_c) - \phi_o(t) > \sim 1$ radian. The uncertainty principle dictates that the fringe frequency can be measured with a accuracy of $\sim(2\pi \times$ integration time$)^{-1}$, or about 1 mHz for our normal three-minute recording time. The "B" term describes the phenomenon of the "white-light" fringe, which we more properly call the delay resolution function (DRF). In general, we observe a band of noise

frequencies, and not a discrete, unique frequency. For the extragalactic radio sources, the intrinsic radiation is so broadband that it may be considered as uniform over any realizable passband. (The OH and H_2O sources in our galaxy and manmade sources in general do not meet this criterion.)

If each of the IF converters had a filter with a power response $G(f_{if})$, where $f_{if} = f - f_o$, then the response of the correlator to broadband signals would be

$$R'(\Delta f, \Delta\tau, t, \phi_o) = \frac{\int G(f_{if}) R(f_{if}, \Delta f, t, \phi_o)\, df_{if}}{\int G(f_{if})\, df_{if}}$$

$$\propto \int G(f_{if})\, e^{-2\pi i f_{if} \Delta\tau}\, df_{if}$$

where $\Delta\tau = \tau' - \tau_g$. The latter relation should be recognized as the Fourier transform of the response function G, measured in residual delay ($\Delta\tau$) units. We call the envelope of $R'(\Delta\tau)$ the DRF. It has a characteristic width $\sim (2\pi \times \text{bandwidth})^{-1}$. For a rectangular passband of width ΔF_R, the DRF will have the form

$$R(\Delta\tau) \propto \frac{\sin(\pi \Delta F_R\, \Delta\tau)}{\pi\, \Delta F_R\, \Delta\tau}$$

which is ~ 3 μsec wide for our normal 360-kHz recording bandwidth. In order to narrow the DRF, we have developed a technique of synthesizing a wide bandwidth (Rogers, 1970; Hinteregger, 1972; Hinteregger et al., 1972) by sequentially sampling a number of discrete 360-kHz bands over a range of up to $\sim$ 100 MHz. Figure 3 shows an observed DRF utilizing the Goldstack configuration with five switching steps over $\sim$40 MHz. Note that the delay $\Delta\tau$ can easily be measured to a few nanoseconds (ns).

Let us briefly describe the actual VLBI recording system. We use adaptations of the "Mark-1" recording system developed at the National Radio Astronomy Observatory (Bare et al., 1967). This system records 360-kHz bandwidth noise at a 720 kbps rate on ordinary seven-track, 800 bites per inch computer tapes running at 150 inches per second. Data is blocked into 0.2-second records ($\sim$ 140 kb), and the time at which each bit was sampled (at a 1.4 μsec rate) is known to a few hundred ns with respect to a local UTC clock. Tapes are started at each station on a nominal (and prenegotiated) minute, and tape formatting (record counts + bit counts within a record) establishes synchronization. Tapes are then brought together at a later time and are played back on an ordinary digital computer. The computer calculates a priori values of τ_g and $\dot{\tau}_g$, changes the bit alighment by $\tau' \cong \tau_g \pm n$ bits (where n = 3,2,1,0) to allow for the finite width of the DRF and some clock errors, and cross-correlates the bits. Fringe rates ($f_o \dot{\tau}_g$) are then removed by phase rotations on the cross-correlation values. Small residual Δf's are measured by additional offset "oscillators" (actually by performing fast Fourier transforms) and best-fit values of $\Delta\tau$, Δf, $|R|$ and ϕ_o (t) are derived. These computer programs have been implemented for IBM 360 computers here at GSFC, where the bit correlations are done in software, and for the CDC 3300 computer at Haystack, where the bit correlations are done in a hard-wired integrated-circuit correlator.

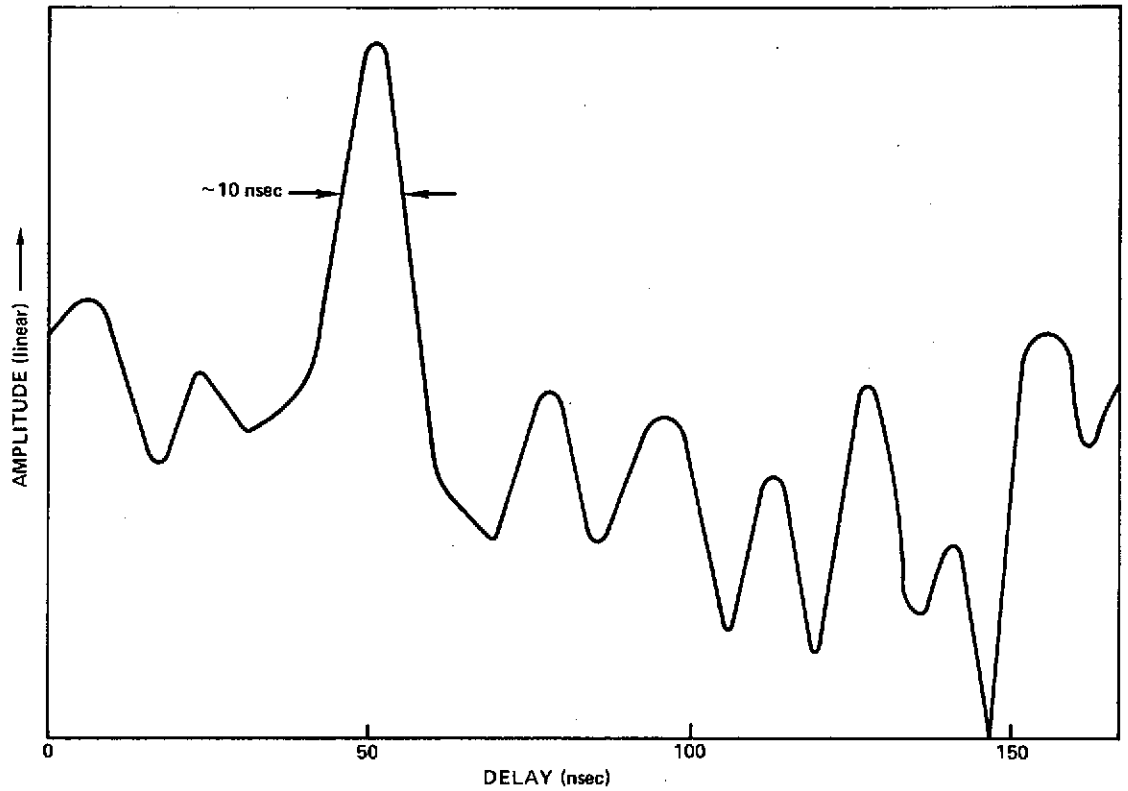

Figure 3. Delay resolution function, Goldstack, April 15, 1972. Source: VRO 42.22.01.

In order to minimize the number of trials necessary to process these data, we like to know that portion of $\Delta\tau$ which arises from the clocks which sample the bits and format the tapes to ~ 10 μsec or better. We further want the clocks to remain stable to ~ 1 μsec for the several days that an experiment may be in progress. Our long-term clock requirements therefore are at the $\Delta t/t \sim 10^{-11}$ to 10^{-12} level, well within the state-of-the-art, even for rubidium clocks.

In the previous discussion, we assumed that the local oscillators were similar and that their differences were characterized by a phase offset, $\phi_o(t)$. In order to "break the wires" of a conventional interferometer so that the stations can be separated by large distances, it is necessary that we have oscillators which are as nearly identical as possible. Since we can never hope to measure $\phi_o(t)$ explicitly, we must have frequency standards with good phase stability. A typical requirement is less than one radian rms phase perturbation accumulated in our integration period. We record data for three minutes on one tape, so at 8 GHz we need short term phase stability of

$$\frac{<\Delta\phi>}{\phi} = \frac{1}{2\pi \cdot 8 \cdot 10^9 \cdot 180} \cong 1 \times 10^{-13}$$

Many experiments we perform call for measuring times on several tapes, so 10-20 minute stability levels of $\sim 10^{-14}$ are desirable.

In order to achieve these levels of stability, we began collaborating with Mr. H. Peters of GSFC more than four years ago on deploying hydrogen masers to radio astronomy observatories, and on making masers and the associated local oscillator multipliers more stable and reliable. Mr. Peters has made available two older Varian H-10 masers which now reside at Greenbank, West Virginia, and at Haystack, Massachusetts. His NP masers have been successfully used at Haystack; Owens Valley, California; Fairbanks, Alaska; Maryland Point, Maryland; Tidbinbilla, Australia; Johannesburg, South Africa; Madrid, Spain; and soon Onsala, Sweden, for astronomical VLBI experiments. Masers built by Dr. Vessot of the Smithsonian have been used at Agassiz Observatory, Massachusetts; Owens Valley, California; and Madrid, Spain; while masers built by Dr. Sydnor of JPL are regularly used at the Goldstone 210-foot telescope. Haystack owns another H-10, which has been used for radar and VLBI for a number of years. The Canadian VLBI team owns two H-10s, which they have used extensively. Apologies are offered to those who have been slighted by omission from this list. It should be clear that VLBI requires the best standards available, and is one of the major users of those that are available in the field.

In Figure 4 we show the phase stability which we achieve with hydrogen masers at X-band. To form this plot we have removed the a priori fringe phase due to the source-interferometer geometry ($2\pi f_o \dot{\tau}_g$) and a 5×10^{-13} linear offset. The dotted line shows the trend of the mean phase as determined from three-minute observations. The short solid lines show the phase trend during each three-minute run. The data span 42 minutes. No correction for phase noise due to the neutral atmosphere was possible for these data. The ionospheric contribution should be negligible. These data show three distinct regions. During the first half two slopes appear, zero and -3×10^{-13}. The last half has a constant slope of $+4 \times 10^{-14}$. The phase during the three-minute runs fits the longer term curve well except for "glitches" at $\sim$ 0720 UT and 0735 UT. These short transients could easily be due to clouds passing through the beam of one of the telescopes, since the phase seems to return to the mean line after a few minutes.

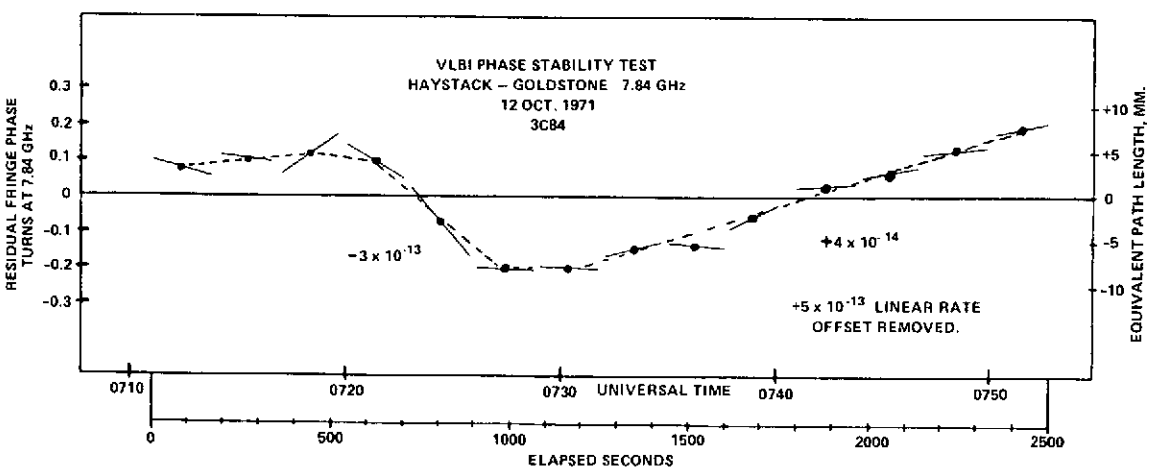

Figure 4. VLBI phase stability test, Haystack-Goldstone, 7.84 GHz, October 12, 1971, 3C84.

Some similar plots obtained with rubidium standards at meter wavelengths are shown in Figures 5 (from Erickson et al., 1972) and 6. Most of the phase noise at these low frequencies is due to the ionosphere since the stability required to give $\langle \Delta\phi \rangle \lesssim 1$ radian is only $\sim 10^{-11}$.

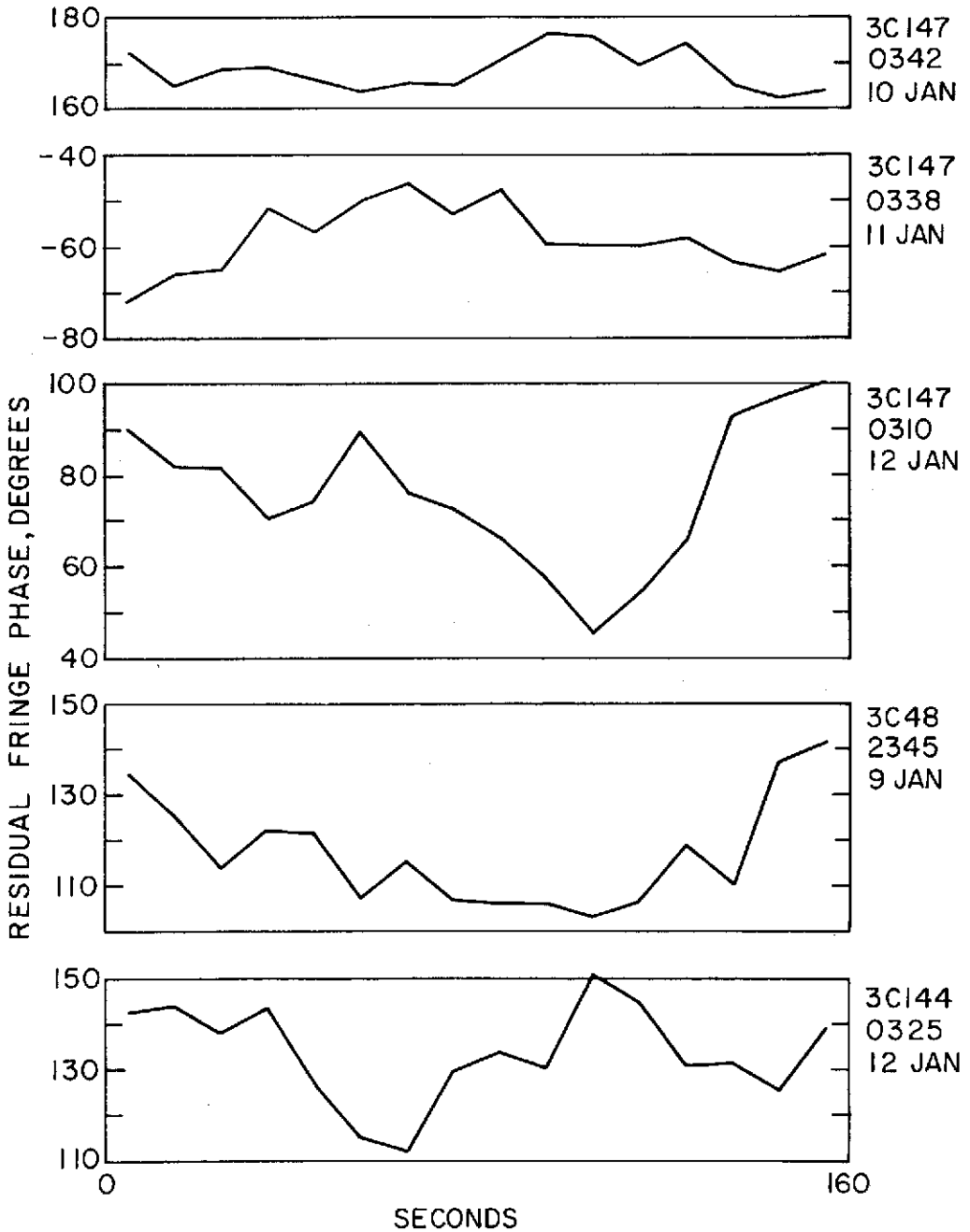

Figure 5. Phase stability plots with rubidium standards.

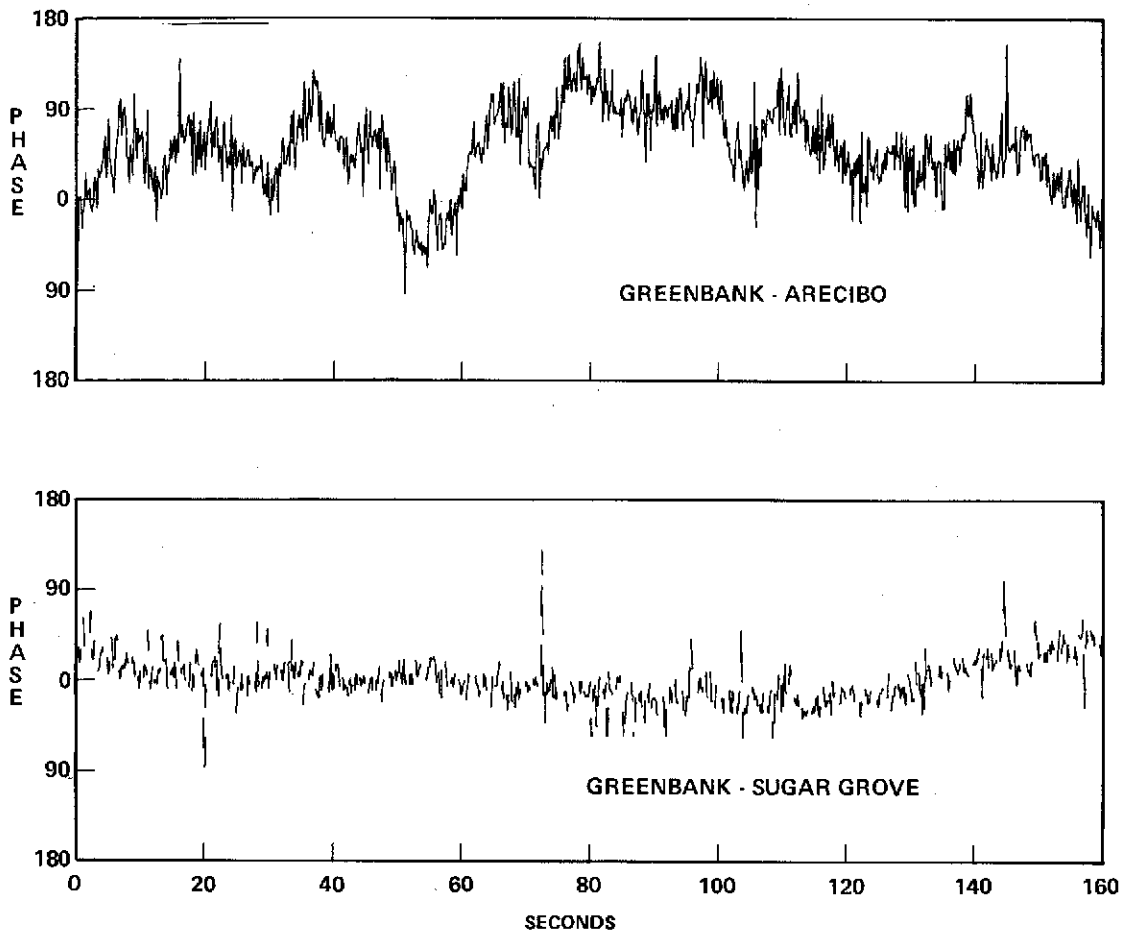

Figure 6. VLBI phase stability, 196.5 MHz, December 19, 1971, 3C287.

RESULTS

Let us now discuss some of the more interesting results from our VLBI program.

(1) Structure of Quasars: We began using the Goldstack configuration in the fall of 1970. Our initial experiment was to be a test of general relativity by measuring the change in position of the Quasar 3C279 as it is occulted by the sun (this is an annual event and has become our "Oktoberfest"). As a surprise to us, we found that 3C279 showed significant fringe amplitude variations (see Figure 7) which could be interpreted in terms of 3C279 being an equal double source with a separation of 1.55 ± 0.03 milliseconds of arc (Knight el al., 1971). When we repeated the experiment four months later, the spacing between components had increased to 1.69 ± 0.02 milliseconds of arc. The resultant expansion rate of 1.2 microsecond of arc per day corresponds to ten times the velocity of light if 3C279 is at the distance ($\sim 6 \times 10^9$ light years) indicated by its red shift (Whitney et al., 1971). Since this startling discovery, a number of other sources have also been observed

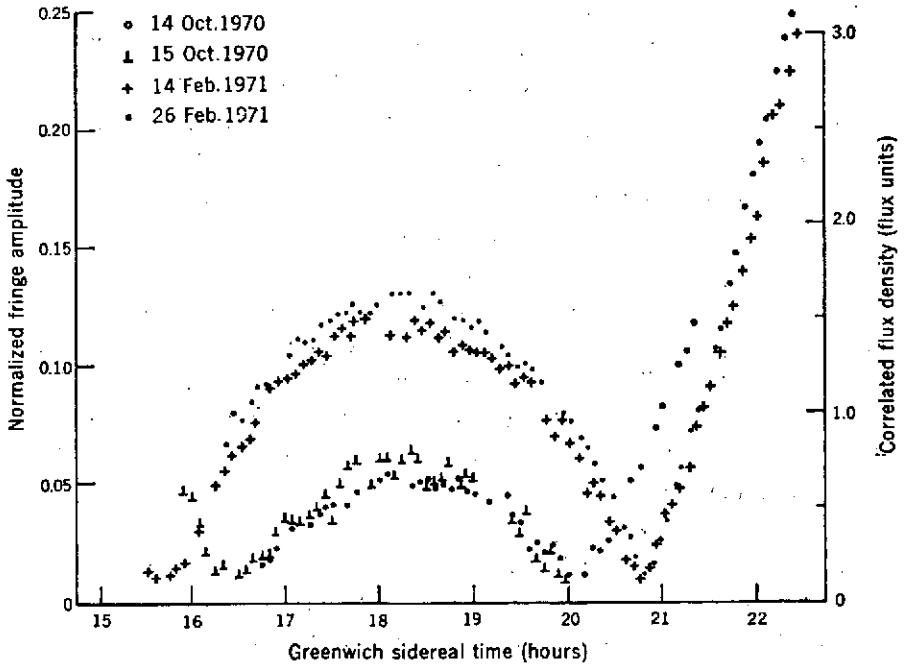

Figure 7. Significant quasar fringe amplitude variations.

to change their structure on short time scales and a synoptic observing program known as the "Quasar Patrol" has been set up to study these phenomena (Shapiro et al., 1973).

(2) Geodesy and Astrometry: VLBI shows great promise of being able to perform geodetic measurements over large distances to accuracies of better than one meter. Because of our inability to measure the phase offsets of the independent local oscillators [ϕ_o (t)], we will find it difficult to work to the levels of a fraction of a fringe in angle ($\lesssim$ 1 cm in length) directly. However, we can observe the fringe phase (2π f_o τ_g) either as a function of time to define the fringe rate

$$f_f(t) = \frac{1}{2\pi}\frac{d}{dt}\phi$$

or as a function of frequency to define the group delay

$$\tau_g(t) = \frac{d}{df}\phi$$

independent of the value of ϕ_o.

A least-squares fit on $f_f(t)$ and/or $\tau_g(t)$ for data spanning a number of hours of time on a number of sources permits the separation of the baseline and source geometry terms. We have demonstrated (Hinteregger et al., 1972) that we can perform geodetic measurements at the ~ 1 meter level in the length of $\bar{B}$ and a few meters in the orientation of $\bar{B}$ and our

most recent results are consistent to the sub-meter level. Some of the noise in the orientation determination is probably due to small polar-location irregularities in the noise level of the BIH publications, and some of the noise is due to residual uncorrectable atmospheric effects. Our least-squares fitting is performed with the MIT PEP planetary radar ephemeris to remove all known geometric effects. We have recently performed measurements on the Goldstack baseline and find that we are achieving better than the ~ 1 meter in length, few meters in orientation accuracy which we obtained on shorter baselines. Figure 8 shows some typical raw residuals (uncorrected for atmospheric effects) in fringe rate showing noise of 10^{-13} and systematic effects due to the atmosphere of ~ 10^{-12} to 10^{-11} at low elevation angles. Figure 9 shows the ensemble of group delay residuals from a fit which included a simple model atmosphere and ~ 25 hours of data from ten sources. The data were obtained on the Goldstack baseline, synthesizing a bandwidth of ~ 23 MHz with six frequency steps. Clearly the rms of residuals is only a few tenths of an ns, but some sources (such as 3C120) show systematic errors of up to ~0.8 ns. Work is in progress to uncover the causes of these systematic errors.

This data has also been analyzed to determine the astrometric positions of a number of extragalactic radio sources at the 0.1 Arc second level (Rogers et al., 1973); these are the most accurate position measurements achieved by astronomers to date.

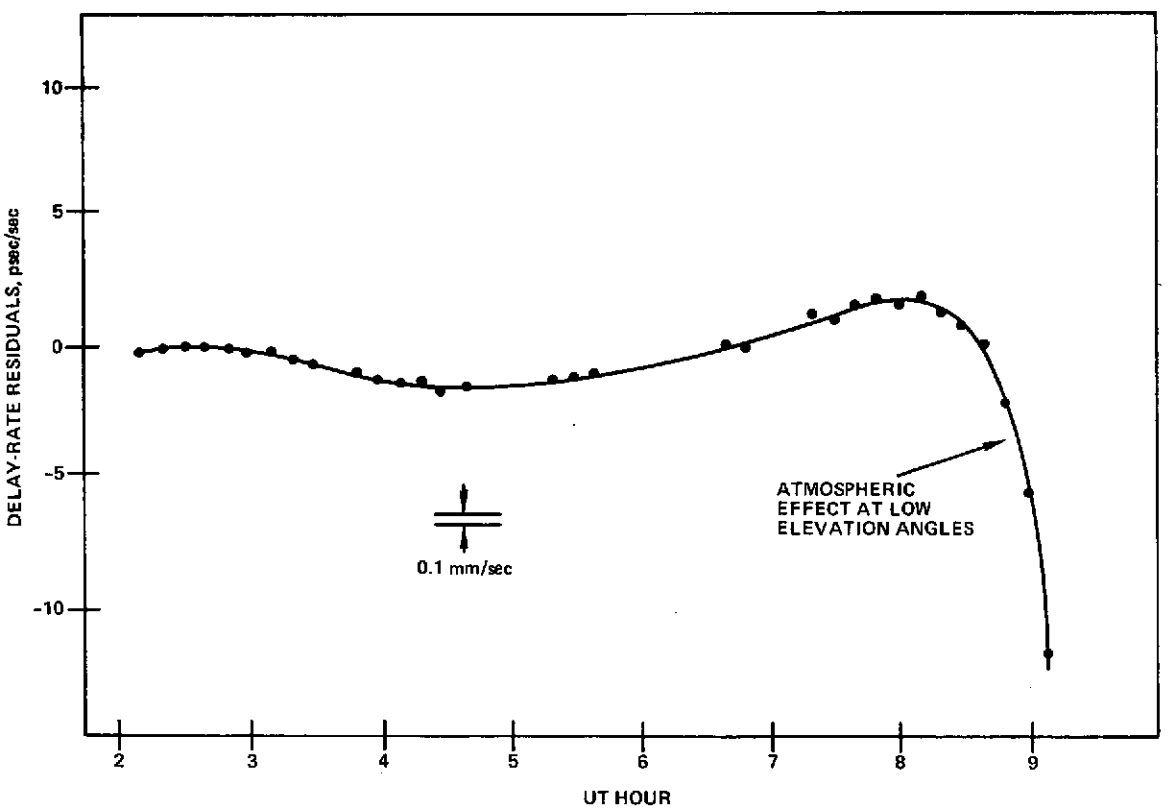

Figure 8. Typical raw residuals in fringe rate.

In principle we could utilize these techniques to synchronize clocks to the new ns level, and to check clock rates at the 10^{-13} to 10^{-14} level on intercontinental baselines. VLBI should be seriously considered when formulating requirements for such synchronization.

We have also employed the same techniques for manmade sources. In 1969 we successfully tracked the TACSAT synchronous satellite for ~ eight hours and were able to define an accurate orbit (Preston et al., 1972).

(3) Differential Astrometry: The programs just described also measure the coordinates of the extragalactic sources to the ~ 0.1 second of arc level. These sources are so distant that they define an excellent inertial frame which is not subject to the rather large proper motions with which optical astrometric measurements are plagued.

In order to push these measurements even further, we have also developed a technique for measuring differential source positions at the ~ 0.01 second level. If we consider two sources, the observed fringe phases will be

$$[2\pi f_o \tau_{g1}(t) + \phi_o(t)]$$

and

$$[2\pi f_o \tau_{g2}(t) + \phi_o(t)]$$

Providing we use the same local oscillator chains for observing, the $\phi_o(t)$ terms will be identical. If we now sample the phases on each source sufficiently often so that $\phi_o(t)$ is the same, i.e., we sample the sources at intervals small compared with the local oscillator coherence time, then the difference phase

$$2\pi f_o [\tau_{g1}(t) - \tau_{g2}(t)]$$

is independent of the local oscillators. We have accomplished this in two ways. For short arcs on the sky, we can utilize an ordinary two-element interferometer and simply switch the telescope beams back and forth. For the Goldstack baseline, the arc from 3C279 to 3C273 is about 10° on the sky. We are able to record two minutes on 3C279, move the telescopes, record one minute on the stronger source 3C273, and move back in a five-minute (and somewhat hectic) sequence. This is the mode we have utilized for our attempted Goldstack 1970 General Relativity tests, and for other convenient closely spaced source pairs.

For larger arcs, we utilize a four-element interferometer configuration where two telescopes at each end run coherent local oscillators, and assign one telescope to each source. For these experiments we have utilized the Haystack and Westford dishes in Massachusetts, and two of the three 85-foot telescopes comprising the NRAO interferometer in West Virginia. Reductions on these data are now proceeding and we hope to utilize the data for tests of General Relativity, to help form a more precise astrometric inertial reference grid of extragalactic sources, and to look for proper motions of extragalactic sources to help set the extragalactic distance scale. A program to measure pulsar proper motions against the extragalactic source reference grid is also in progress.

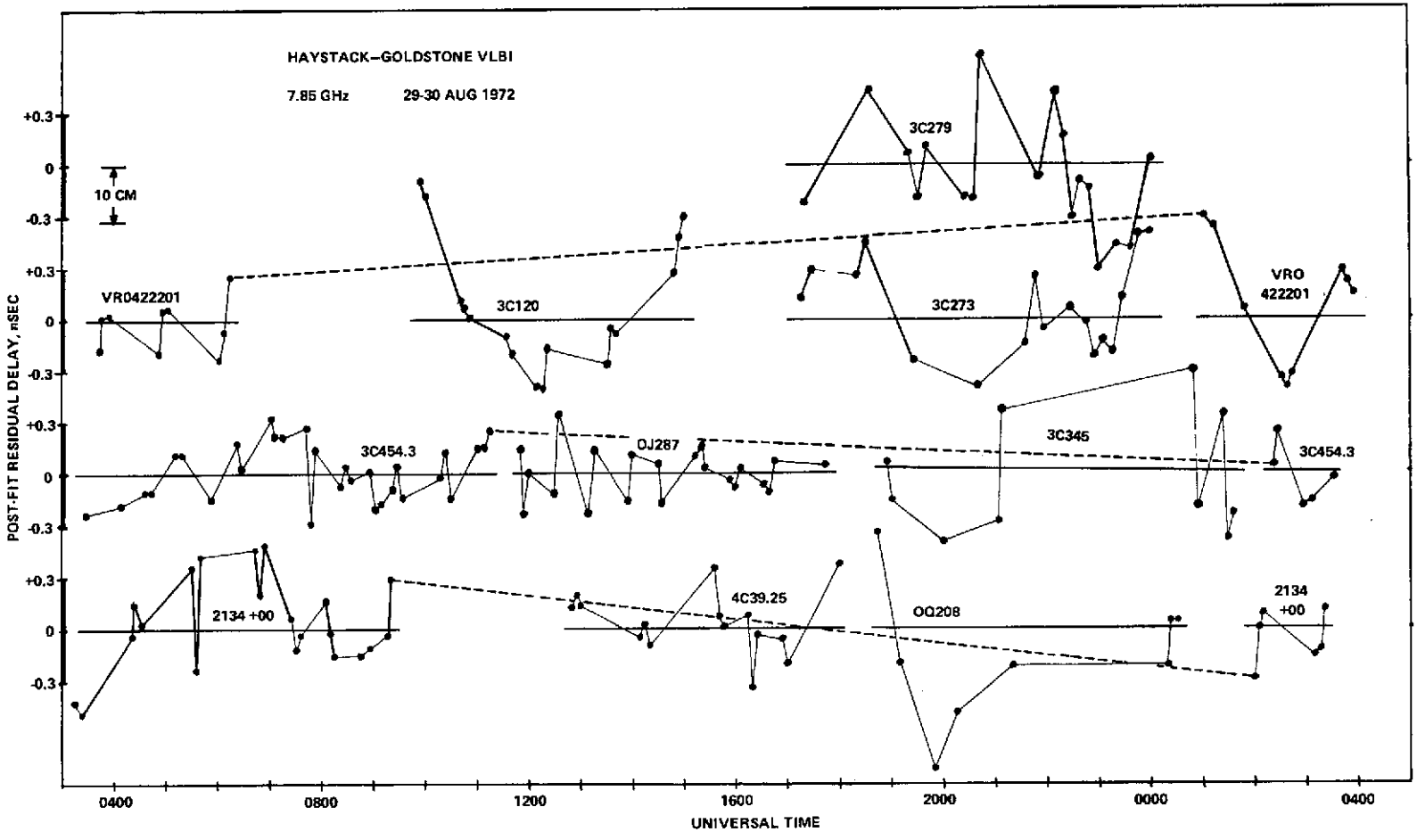

Figure 9. The ensemble of group delay residuals. Haystack-Goldstone VLBI, 7.85 GHz, August 29-30, 1972.

The lower frequency experiments are of purely astronomical interest and beyond the scope of this paper.

SUMMARY

In summary, VLBI is finding applications in a number of distinct areas, including

- Astronomical studies of quasars, pulsars, and so on
- Precision geodesy
- Tests of fundamental physical laws
- Satellite tracking

In order to perform VLBI measurements we need precise time and frequency standards. VLBI has been one of the main driving forces in the development of field-operational hydrogen masers. VLBI in return shows promise at achieving operational time and frequency coordination on an intercontinental basis. The continued progress of the technique requires the close cooperation of radio astronomers and the engineers developing advanced standards.

The work described in this report reflects the combined efforts of a number of individuals at a number of institutions. It would be futile to try to list them all, but the MIT members of our team (consisting of I. Shapiro, A. Rogers, A. Whitney, H. Hinteregger, C. Knight, D. Robertson, and a number of others) have spearheaded the geodetic and astrometric work described here. They derive financial support from the NSF and ARPA.

REFERENCES

C. C. Bare et al. *Science*, **157**, (1967). p. 189.

T. A. Clark and W. C. Erickson. *Proceedings IEEE.*, **61**, (1973, in press).

W. C. Erickson et al. *Astrophys. J.*, **177**, (1972). p. 101.

H. F. Hinteregger, Ph.D. thesis. MIT (1972).

H. F. Hinteregger et al. *Science*, **178**, (1972). p. 396.

C. A. Knight et al. *Science*, **172**, (1971). p. 52.

R. A. Preston et al. *Science*, **178**, (1972). p. 407.

A. E. E. Rogers. *Radio Science*, **5**, (1970). p. 1239.

A. E. E. Rogers et al. *Astrophys. J.* (1973, in press).

I. I. Shapiro et al. *Astrophys. J.* (1973, in press).

A. R. Whitney et al. *Science*, **173**, (1971). p. 225.

TRACKING THE LUNAR ROVER VEHICLE WITH VERY LONG BASELINE INTERFEROMETRY TECHNIQUES

Daniel Shnidman
Bendix Field Engineering Corporation

I. VERY LONG BASELINE INTERFEROMETRY (VLBI)

Very Long Baseline Interferometry is a highly accurate method for determining the angular positions of radio sources. This is done by recording the radio signal at two widely separated stations. The difference in arrival time of the signal at the two stations, τ, is used to determine the source angular position, θ, with the trigonometric relationship shown in Figure 1. A broad frequency signal is required to determine τ to a high resolution. A second method, not requiring a broad frequency signal, is to measure the frequency difference of the signal observed at the two stations. The frequency difference, which is proportional to the rate of change of τ, yields θ, the rate of change of the source angular position.

In early 1971, Mr. Irving Salzberg of the Metric Data Branch proposed using NASA's Unified S-band tracking network to interferometrically track the Lunar Rover as the astronauts drive across the surface of the moon.

II. THE UNIFIED S-BAND SYSTEM

Consider the capabilities of NASA's Unified S-band doppler tracking system for VLBI tracking. The system's ability to determine a change in θ, the source angular position, depends on its ability to determine a change in Δr, the range difference between the tracking stations and the signal source. That is,

$$B \cos \theta = \Delta r \tag{1}$$

Differentiating

$$d\theta = \frac{-d(\Delta r)}{B \sin \theta} \tag{2}$$

The USB doppler tracking system can observe range changes of less than 1 centimeter. The system is limited by the cesium frequency standard noise. Over a 10-second interval, the rubidium frequency standards show about half that noise. The H-master standards do not add appreciable noise to the 2 millimeter noise of the remainder of the system. Typical station separation is about 6000 kilometers.

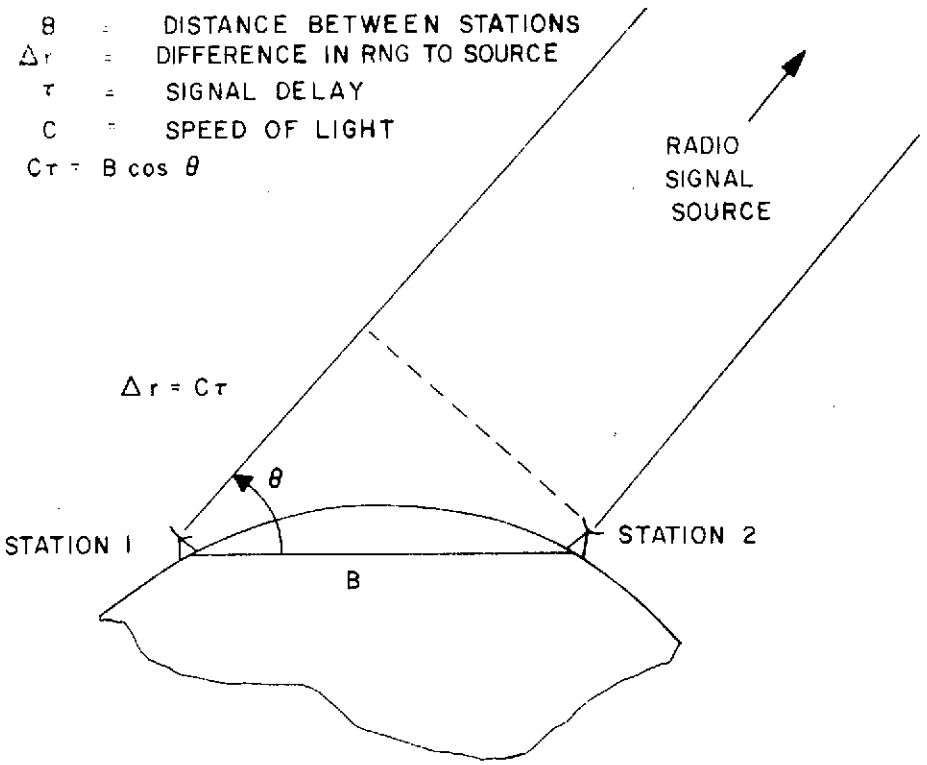

Figure 1. Very long baseline interferometry.

Solving for $d\theta$,

$$d\theta \approx \frac{10^{-2}}{5 \times 10^{6}} = 2 \times 10^{-9} \text{ radian} = 0.005 \text{ sec}$$

That is about the height of an ant at 100 miles! At lunar distances that amounts to 0.8 meters.

The present doppler tracking system can be used for Lunar Rover VLBI tracking without additional equipment. The data is recorded in a highly compact form; the hundreds or thousands of recording tapes normally needed for VLBI are not required. Weeks are not needed to reduce the data; real-time data processing is possible.

III. THE ANALYSIS METHOD

Figure 2 shows how doppler tracking is utilized for Lunar Rover tracking. The doppler frequency shift is a measure of the range-rate, the radial component of the source velocity.

$$\dot{r} = \hat{r} \cdot \vec{V} \tag{3}$$

The difference in radial velocity from the two stations is equal to the component of the velocity in the direction $(\hat{r}_1 - \hat{r}_2)$.

$$(\dot{r}_1 - \dot{r}_2) = (\hat{r}_1 - \hat{r}_2) \cdot \vec{V} \tag{4}$$

With a third station, one can measure the velocity component out of the plane of the page. The third velocity component is determined by constraining the Lunar Rover to the surface of the moon. The lunar surface features are modeled by adjusting the local lunar radius, R_L. The range-rate itself cannot be used to determine this third velocity component, since the Rover transmitter frequency, being only quartz crystal controlled, may be biased by one part in 10^5. In fact, the range-rate is used with the lunar ephemeris to solve for the transmitter frequency in the differential doppler reduction.

There are several problems associated with this method. During the course of a track the ionospheric phase path length may change several meters. A one meter change in the phase path length results in approximately a 100-meter error in the Lunar Rover position. A frequency standard bias of one part in 10^{12} produces a 100 meter per hour bias in the Lunar Rover tracking. Station location uncertainties produce similar errors.

These error sources are eliminated by doppler tracking both the Rover and the Lunar Module transmitters at each station. The Lunar Module is used as a reference benchmark and all Lunar Rover measurements are made with respect to the Lunar Module (Figure 3). By subtracting the Lunar Module doppler range-rate from that of the Rover, all systematic biases common to both signals, such as those due to the phase path medium, the frequency standard, station location and the lunar ephemeris cancel to the first order. If there are no

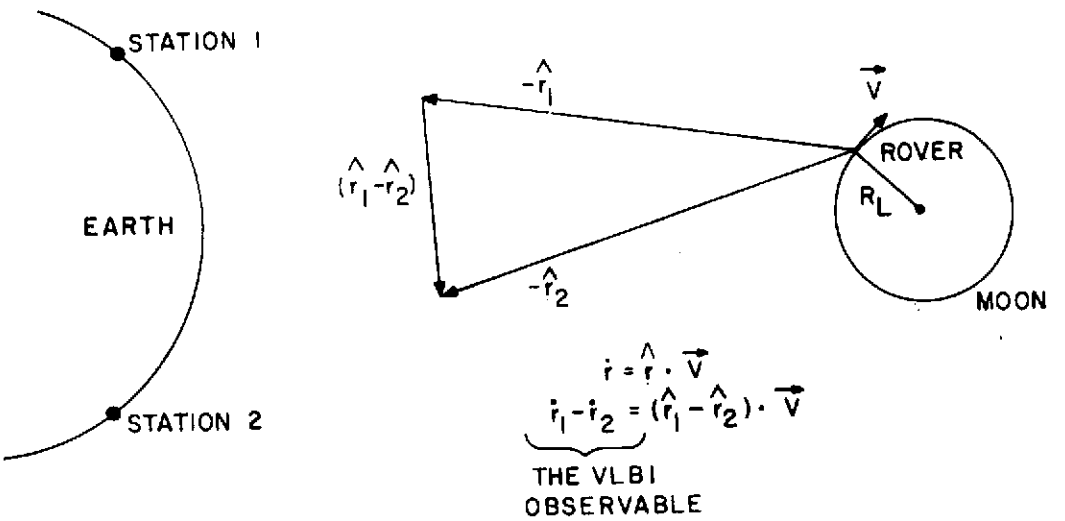

Figure 2. The VLBI observable.

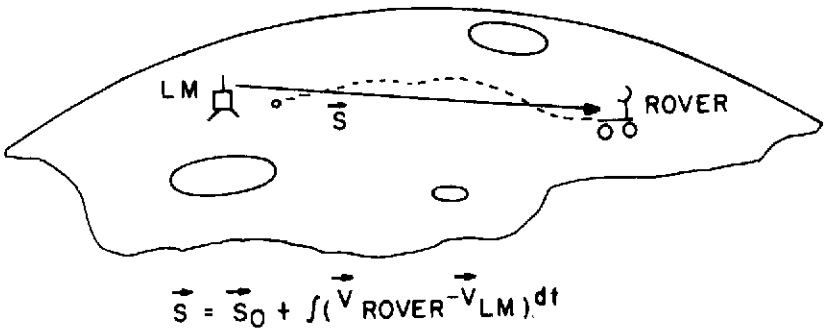

Figure 3. Lunar Rover tracking by differential VLBI.

inter-receiver phase drifts, only the differential VLBI observable remains as a first order quantity. The position of the Rover with respect to the Lunar Module, $\vec{S}$, is determined by integrating the differential velocity from the known initial position.

$$\vec{S} = \vec{S}_o + \int (\vec{V}_{Rover} - \vec{V}_{LM})\, dt$$

In summary, Lunar Rover VLBI tracking requires three widely separated stations, doppler tracking both the Lunar Rover and the Lunar Module.[1]

IV. APOLLO-16 LUNAR ROVER TRACKING

During the first Rover traverse of Apollo 16, four stations participated in Lunar Rover tracking. The four stations Madrid, Ascension Island, Merritt Island, and Goldstone are shown in Figure 4. MIL–ACN–MAD and GDS–ACN–MAD form the large triangles needed for sensitive Lunar Rover tracking. The triangle formed by GDS–MIL–MAD is only fair; that formed by GDS–MIL–ACN, very poor.

Figure 5 is a time line of the events during the traverse. There were three portions to the traverse. The first, from the Lunar Module area to Plum Crater, where the astronauts stopped for scientific activities. The second, from Plum Crater to Spook Crater for more rock collecting, then back to the Lunar Module. When the astronauts dismount from the Rover, they switch the Rover transmitter from PM to FM for TV transmission. The USB system is unable to doppler track an FM transmitter.

MAD, ACN, and MIL participated during the entire traverse, a total of 63 minutes of tracking. GDS participated only during the last two portions, for 34 minutes. The entire traverse totalled more than 4 km.

[1]See *STDN Metric Tracking Performance Apollo-16 Final Report*, NASA/Goddard X-832-72-203 for a discussion of the algorithm. The report is available at the Goddard Space Flight Center Library.

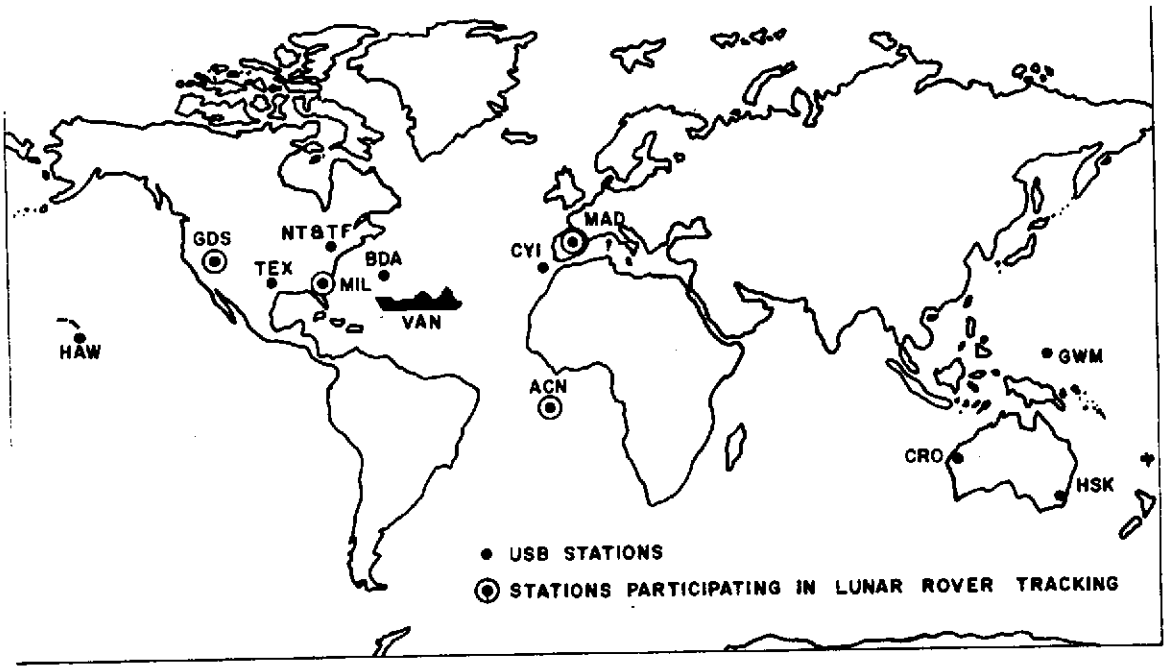

Figure 4. The USB Manned Space Flight Network.

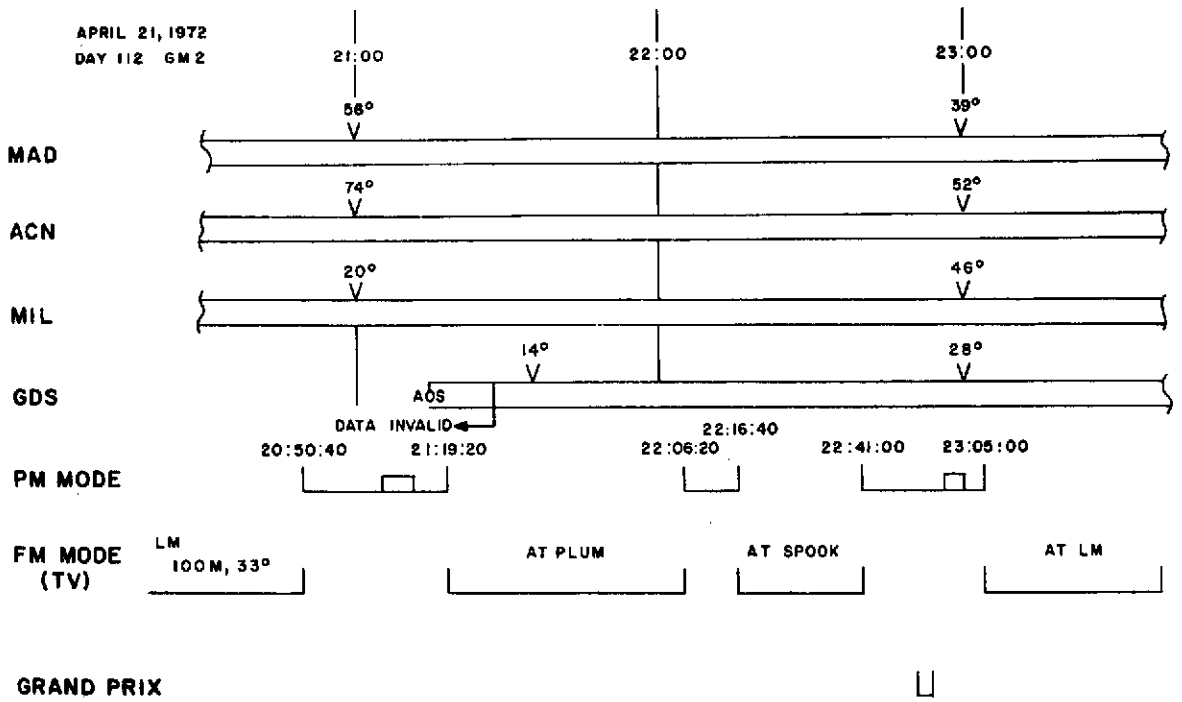

Figure 5. Events and time-line for traverse of EVA-1, Apollo-16.

V. APOLLO-16 TRACKING RESULTS

Figure 6 is a map of the Rover traverse determined by Lunar Rover tracking.[2] These results were compared to the astronauts readings of the Rover on-board navigation system. The Rover on-board navigation system has a granularity of 100 meters in range and one degree in bearing to the Lunar Module. Although the on-board navigation system is also susceptible to error from wheel slippage and alignment error, nevertheless, the on-board navigation results agreed with the Lunar Rover tracking results to well within 50 meters.

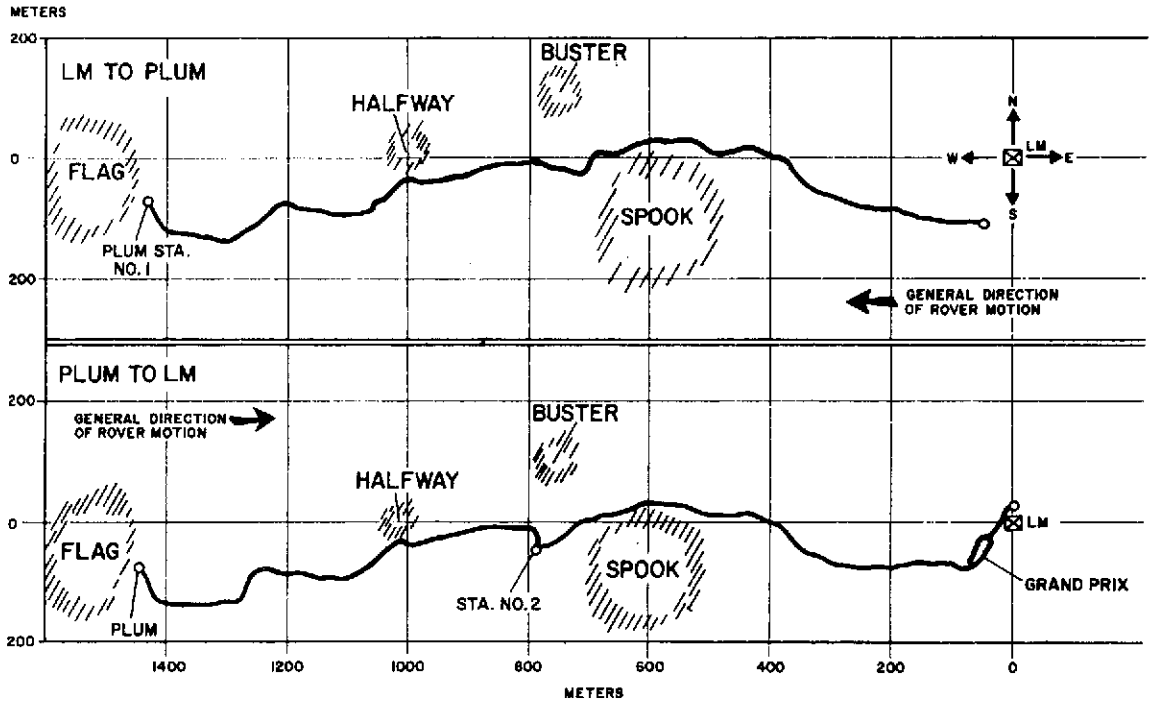

Figure 6. Map of the Lunar Rover track.

[2]A complete Lunar Rover Track ephemeris is contained in Bendix technical memorandum MDO-72-297 *Apollo-16 Lunar Rover Tracking - Final Results.* The memorandum is available from the Metric Data Evaluation Office; Bendix Field Engineering Corp.; 6811 Kenilworth Ave.; Riverdale, Md.

The 20-second incremental motion of the Lunar Rover during portion 1 is plotted in Figure 7. Note that a stationary period is clearly visible. This six-minute stationary period occurred just south of Halfway Crater (see Figure 6) while the astronauts debated with the Mission Control Center whether the crater they had just passed was Flag Crater or Halfway Crater. This vividly demonstrates the astronauts need for a reliable navigation system. A second stationary period occurred after the Gran Prix maneuvers while one of the astronauts was setting up mortar charges for a seismographic experiment. These two known stationary periods were used to evaluate the Lunar Rover tracking noise and drift. The drift and 1 σ noise of the MIL–ACN–MAD configuration is presented in Table 1.

The Mission Control Center reported that at the end of the first traverse the Lunar Rover parked a few meters north of the Lunar Module. This agrees very well with the Lunar Rover tracking results listed in Table 2.

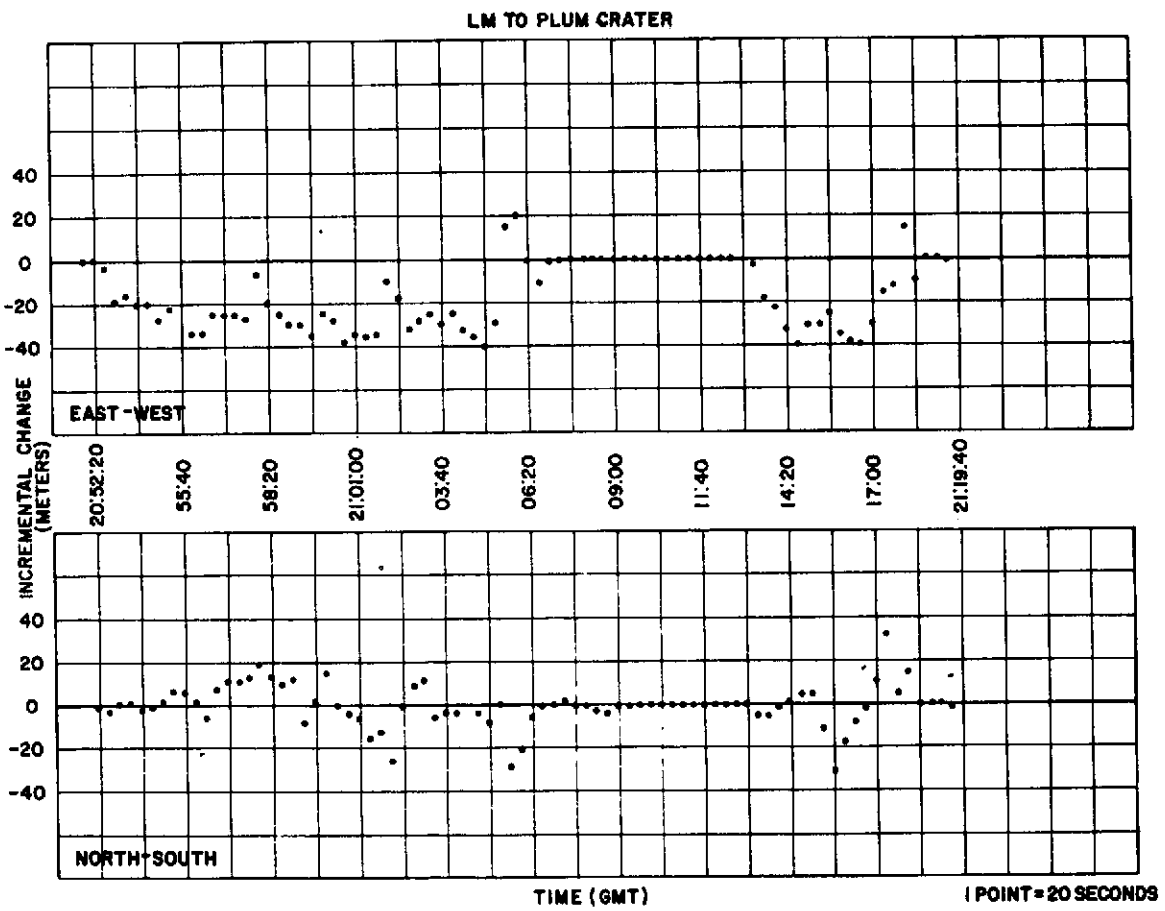

Figure 7. Incremental motion of the Lunar Rover.

Table 1
Lunar Rover Tracking--Noise and Drift.

Stationary Period (GMT)	Noise (Meters)	Drift (mm/sec)
21:06:04-21:12:40		
N-S	0.97	-8
E-W	0.40	-7
22:55:00-23:01:40		
N-S	0.69	-7
E-W	0.54	-4

Table 2
Lunar Rover Tracking–Closure Results.

Station Configuration	N-S (Meters)	E-W (Meters)
MIL - ACN - MAD	6.0	9.0
GDS - ACN - MAD	7.4	5.6
GDS - MIL - MAD	-8.8	0.3

VI. APOLLO-17

For the coming Apollo-17 mission, Lunar Rover tracking has been scheduled to support all three Rover traverses. This amounts to about seven hours of tracking covering 34 kilometers. The tracking information is needed to aid the astronauts' navigation and to provide an accurate traverse map for the Traverse Gravimeter and the Surface Electrical Properties experiments. The data will be processed in semireal-time. That is, the data will be received at Goddard Space Flight Center in real-time and will be batch processed within ten minutes of each Lunar Rover stop.

[3] Personal communication.

VII. FUTURE APPLICATIONS

Recently a modification to the tracking station receiver has been designed and tested by Dr. Hinteregger of MIT. This modification, shown schematically in Figure 8, will permit the direct recording of the differential doppler phase of two signals with only one receiver. The IF signal is wide enough to carry both transmitter signal frequencies. The receiver is locked onto one signal frequency while the other signal frequency, which contains the differential doppler phase, is tapped of the IF signal and converted to a frequency acceptable to the doppler recorder. The resulting differential doppler phase shows a stability improvement in noise and drift of more than two orders of magnitude.[3] This stability improvement is gained with a 33 percent reduction in the tracking network resource requirement.

The differential VLBI tracking technique makes a large set of tracking methods and scientific experiments now possible. For example, lunar librations are presently being measured by differential tracking of the ALSEP scientific transmitters on the moon. Results to within one second of selenographis arc, a factor of ten improvement in our present knowledge, are expected. Other applications include the measurement of wind velocity on

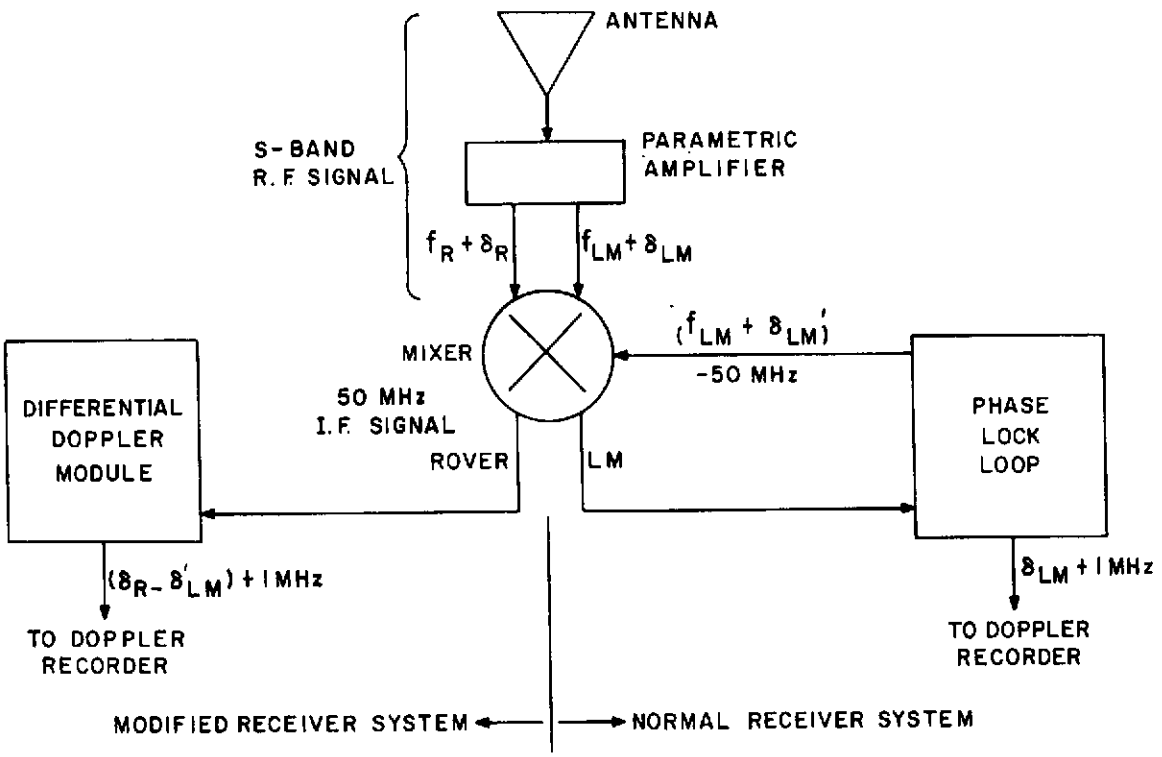

Figure 8. Receiver modification for recording differential doppler frequency.

Venus, mother-daughter satellite tracking, the measurement of the lunar mascons, and the measurement of planetary gravitational fields.[4,5]

In conclusion, differential VLBI has been used to track the Apollo-16 Lunar Rover with better than 25-meter accuracy and noise of less than one meter. This technique, which will support Apollo-17 Lunar Rover experiments and navigation, has application to a wide range of future space navigation and astrophysical experiments.

---

[4]Counciiman, C. C., H. F. Hinteregger, and I. I. Shapiro, *Science,* vol. 178, pp. 607-608.

[5]Invaluable support in the theory and the reduction techniques of differential VLBI was provided by Drs. Hinteregger, Counciiman, and Shapiro, of MIT.

AN ANALYSIS AND DEMONSTRATION OF CLOCK SYNCHRONIZATION BY VLBI

William J. Hurd
Jet Propulsion Laboratory

ABSTRACT

A prototype of a semireal-time system for synchronizing the DSN station clocks by radio interferometry was successfully demonstrated on August 30, 1972. The system utilized an approximate maximum likelihood estimation procedure for processing the data, thereby achieving essentially optimum time synchronization estimates for a given amount of data, or equivalently, minimizing the amount of data required for reliable estimation. Synchronization accuracies as good as 100 nsec rms were achieved between DSS 11 and DSS 12, both at Goldstone, California. The accuracy can be improved by increasing the system bandwidth until the fundamental limitations due to position uncertainties of baseline and source and atmospheric effects are reached. These limitations are under ten nsec for transcontinental baselines.

I. INTRODUCTION

It is well known that the clocks at widely separated antenna ground stations can be synchronized by the techniques of very long baseline interferometry (VLBI). The objectives of this work are to optimize the signal processing of VLBI data and, utilizing the processing techniques developed, to demonstrate an operationally feasible time-synchronization system for the Deep Space Net (DSN). Although the results are discussed with application to the 26-m and 64-m antennas of the Deep Space Station (DSS) of the DSN, the analysis and techniques are applicable to any similar networks.

There are two reasons that an operational VLBI time-synchronization system may be desirable for the DSN. First, accuracies an order of magnitude better than currently attained by the moon-bounce system may be attainable with little initial investment and with operational costs which should be no higher than for the existing system. Second, VLBI may be the only operationally feasible method for achieving the 10- to 20-nanosecond (ns) accuracies required for two-station tracking of deep space probes. [1, 2]

The time-synchronization accuracy attainable by interferometry over very long baselines is fundamentally limited by the uncertainties in the differential time delay from the radio source to the antennas. These uncertainties, which increase with baseline length, are caused by errors in the estimates of the source positions and antenna location and by the variable propagation delays in the atmosphere. It is anticipated that the antenna locations will soon be known to within about one meter, and source position errors can be reduced to this same level by interferometry. The atmospheric effects depend on frequency in a

known manner, and can be calibrated by receiving on two frequencies, say S- and X-band. The fundamental limitation of accuracy can probably thus be reduced to ten ns or less for intercontinental baselines.

Until the fundamental limit is approached, the synchronization accuracy depends primarily on the utilized bandwidth, provided that the signal-to-noise ratio is high enough for reliable detection. The experiment reported on here confirms the two most important analytical results: First, that reliable estimates can be achieved with a small enough amount of data, about 1 million bits, so that semireal-time processing is feasible; and second, that with this amount of data, the rms errors are less than 0.1 times the inverse system bandwidth, so that rms errors of less than ten ns can be achieved with system bandwidths of only about ten MHz.

II. DESCRIPTION OF EXPERIMENT

As a first step in demonstrating the feasibility of an operational system for DSN clock synchronization by VLBI, an experiment was conducted on August 30, 1972, between the 26-m antennas at DSS 11 and 12, both at Goldstone. The experiment was implemented using a minimum of special interfacing hardware in addition to standard DSN station equipment. The data were acquired and processed following the approximate maximum-likelihood method described in the Appendix and in Reference 3.

A simplified block diagram of the experiment is shown in Figure 1. At each station, the received signals were demodulated in two-phase quadrature channels, filtered, quantized to one bit, and buffered into an XDS 920 TCP computer. Besides the receivers, the TCP computers are the major portion of the system. The special equipment for the experiment consisted of the two-channel demodulators, the filters, limiters, and samplers; and the buffers from the sampler to the TCP computers. This was all contained in one small chassis for each station, plus cables to interface to the computers.

The experiment procedure was to initiate sampling at the same time at each receiver according to the station master clocks, and to fill the TCP computer memories with data at the highest possible sampling rate. The computer speeds limited the data rate to 500 kbps, or 250 kbps per channel, so that the system bandwidth was limited to 250 kHz. Furthermore, the maximum number of samples which could be taken at this rate was limited by the memory sizes to approximately 320,000 bits. In an operational system, the data could be transmitted directly from the computers to JPL over the high speed data lines and processed within a few minutes in the Network Control System (NCS) or other computers. In the experiment, however, real-time operation was not required, but instead it was desired to make a number of independent estimates of time synchronization using each of several radio sources. Therefore, the data were written onto magnetic tape and processed later on a Sigma-5 computer at JPL. Five different radio sources were observed, with a total of 504 batches of data taken at ten-second intervals.

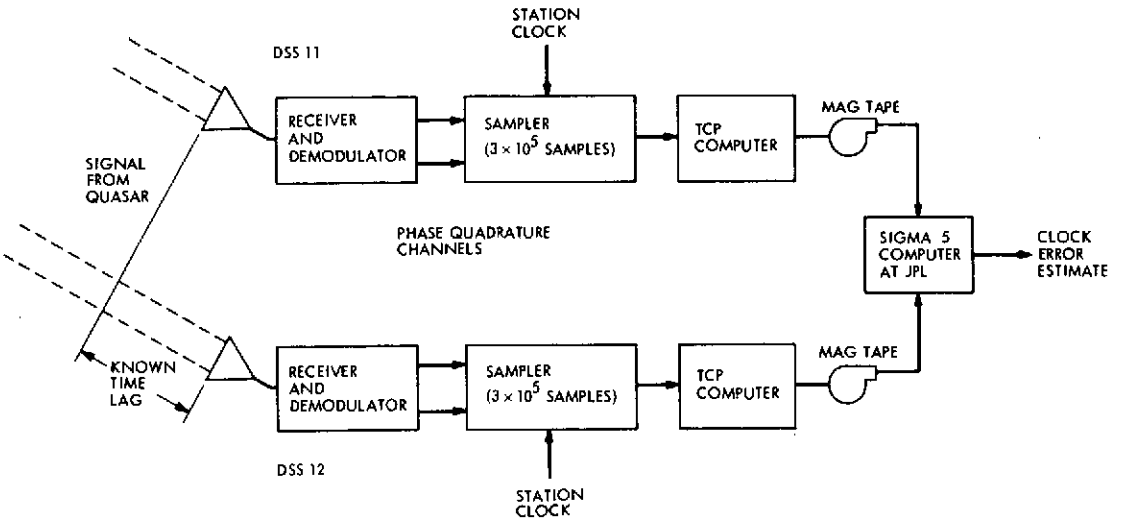

Figure 1. VLBI time-synchronization experiment block diagram.

III. PRINCIPAL RESULTS AND SYSTEM IMPLICATIONS

The desirability of an interferometry time synchronization system for the DSN depends on the ability to achieve reliable results with a reasonable amount of data. This, in turn, depends on the availability of radio sources with enough correlated flux, that is, with enough electro-magnetic flux which appears to be from an ideal point-source when viewed by the long baseline interferometer. In this section, we set a standard for the required source intensity for various system configurations based on experimental and analytical results, and show that adequate sources are available to result in an operationally feasible system.

The experimental results were limited by the system parameters of two 26-m antennas with temperatures of 16.3K and 37K, 250-kHz bandwidth, and 3.2×10^5 bit buffer size. The theoretical and experimental results are compared in Figure 2. Also shown are the theoretical results for a 2.5-MHz bandwidth, which could be realized by removing the sampling rate restriction from the current (Block III receiver) system, and for a 25-MHz bandwidth, which can be realized with the future DSN Block IV receivers. For the three strongest radio sources, rms processing errors of 96, 228, and 403 ns were achieved, in close agreement with theory. The results for the weakest of these sources, with an estimated correlated flux of 4.6 fu, are most significant for two reasons: First, the estimates were reliable even though the signal-to-noise ratio was somewhat lower than the desirable minimum, and second, the results were in close agreement with theory, indicating that the theory does not break down until the signal-to-noise ratio is reduced below this level. Based on both the theoretical and experimental results, we conclude that a source intensity of 5.5 fu would have been adequate to reliably achieve an rms error of less than 0.4 μsec, or less than one-tenth of the inverse of the system bandwidth. Whenever possible, higher accuracies should be achieved by increasing the system bandwidth and not the amount of

data or the signal-to-noise ratio, both because few sources have more than two to three fu of correlated flux over long baselines, and because increasing the amount of data is expensive in terms of buffer storage, computer time, and ground communications facility (GCF) usage.

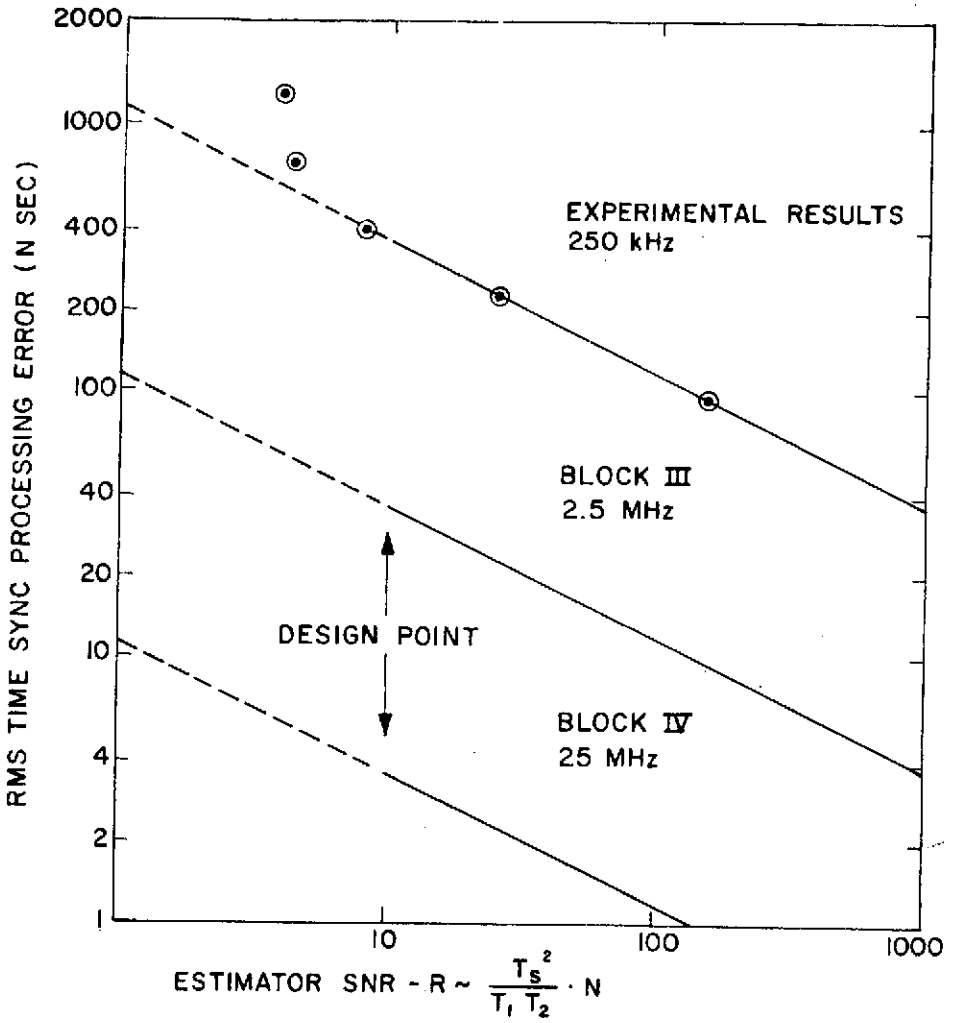

Figure 2. Theoretical and experimental time-synchronization error versus signal-to-noise ratio and bandwidth.

Table 1 presents the source intensities required to achieve the reliable performance level of one-tenth of the inverse system bandwidth for various antenna sizes and receiver noise temperatures in the DSN. Two buffer sizes are considered, the 0.32 megabit usable in the TCP computers, and 1.0 megabit, which is a practical size to consider if special-purpose memories are used for wider bandwidths. In utilizing Table 1, one should keep in mind that the system temperatures increase at low elevation angles, so that the required fluxes might increase by a factor of about 1.5.

Table 1
Source Intensity Required for Various System Parameters.

Antenna Diameters (m)		System Temperatures (k)		Amount of Data or Buffer Size (10^6 bits)	Source Intensity (fu of Correlated Flux)
26	26	17	37	0.32	5.50
26	26	17	37	1.0	3.48
26	26	17	17	0.32	3.70
26	26	17	17	1.0	2.34
64	26	17	37	0.32	2.24
64	26	17	37	1.0	1.26
64	26	17	17	0.32	1.51
64	26	17	17	1.0	0.86
64	64	17	17	0.32	0.61
64	64	17	17	1.0	0.35

The availability of known radio sources was surveyed using Reference 4 and a computer program for mutual visibility devised by J.G. Williams of the JPL Tracking and Orbit Determination Section. Considering sources to be jointly visible only when the elevation from both stations is 10 degrees or greater, there is always at least one source of 1.3 fu or stronger visible by the station pairs at Goldstone and Spain, Goldstone and Australia, and Spain and South Africa. Sources of 2.0 fu are available for most of the day, and sources of 3 to 6 fu are normally visible for at least a few hours each day. The source 3C-454.3, which is sometimes as strong as 6.38 fu,[4] is visible to each of the above pairs for at least three hours a day, but unfortunately it has at other times been observed to be considerably weaker, and similar variations occur with some of the other strong sources. It is therefore not desirable to base a system on the strongest few sources.

Considering both the source intensities required and their availability, it is safe to say that station pairs with at least one 64-m antenna can be synchronized at will to within one-tenth of the inverse system bandwidth with 1.0 megabit of data. That is, there would be little if any operational restriction as to time of day due to lack of mutual visibility of adequate sources. Synchronization of two 26-m antennas could be accomplished with some restrictions on time of day, or by using more data. It is important to note that the amount of data used is not restricted by the high-speed buffer size, but convenience is sacrificed if it becomes necessary to fill the buffer several times, store the data on magnetic tape between fills, and then transmit a larger amount of data to the central computer for processing.

We conclude that a system with 1.0-megabit buffers would be operationally feasible. It would be less restricted than the X-band moon-bounce system, for which moon visibility restricts the time of day, and even the time of year for two northern hemisphere stations.

IV. ESTIMATION PROCEDURE

The estimates of time-synchronization error were made using the approximate maximum-likelihood method derived in the Appendix and in Reference 3. This method is distinguished from normal cross-correlation methods in that the cross-products are multiplied by appropriate weighting functions before being summed or envelope detected. This weighting accounts for changes in clock offset during the measurement time, and provides an optimum method for resolving the time estimates to greater accuracy than the time between samples. Approximate maximum-likelihood estimates of fringe frequency, phase, and signal-to-noise ratio also result.

The demodulation, filtering, and sampling procedures are shown in Figure 3, and are described in detail in Section V and in the Appendix. The ith samples in the phase-quadrature channels after demodulation, filtering, and limiting are denoted by X_i and Y_i for DSS 11 and by Z_i and W_i for DSS 12. These signals have cross correlations which depend on i and on ρ, τ, δ, ω, and ϕ where

$$\rho^2 = \frac{T_c^2}{T_{11} T_{12}}$$

is the product of the input signal-to-noise ratios, and

T_c = increase in system temperatures due to correlated flux from source

T_{11}, T_{12} = total system noise temperatures at DSS 11 and 12, including total source, flux, correlated or otherwise

δ = difference in path length from source to the two stations, in seconds (often called τ_g)

τ = error in clocks, or actual time difference between first samples at the two stations.

ω = stopped fringe frequency, or apparent doppler difference after demodulation, in rad/sec

ϕ = stopped fringe phase

As shown in the Appendix, the cross correlations, that is the expected values of the cross-products, can be expressed as

$$E(X_i Z_j) = \frac{2}{\pi} \rho\, a_{ij}(\tau, \delta) \cos(j\Delta + \phi) \tag{2}$$

$$E(X_i W_j) = \frac{2}{\pi} \rho\, b_{ij}(\tau, \delta) \sin(j\Delta + \phi) \tag{3}$$

$$E(Y_i Z_j) = \frac{2}{\pi} \rho\, c_{ij}(\tau, \delta) \sin(j\Delta + \phi) \tag{4}$$

and

$$E(Y_i W_j) = \frac{2}{\pi} \rho\, d_{ij}(\tau, \delta) \cos(j\Delta + \phi) \tag{5}$$

where $\Delta = \omega \cdot 4\,\mu$sec and it is assumed that the timing is such that the cross products are uncorrelated expept for $i \approx j$. The factor $2/\pi$ arises due to the hard limiting, and the coefficients a_{ij}, b_{ij}, c_{ij}, and d_{ij} are determined by the particular filtering and sampling method.

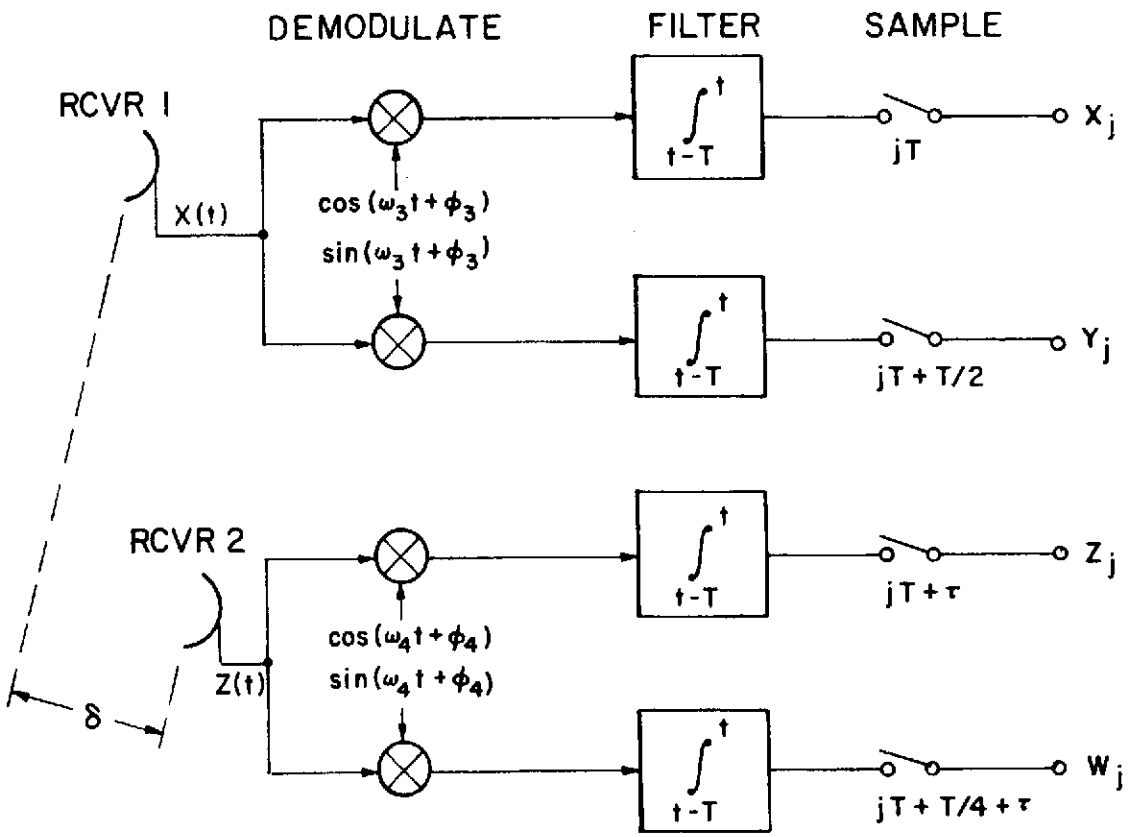

Figure 3. Demodulation, filtering, and sampling.

In general, for long baselines and measurement times, the fringe rate cannot be assumed constant, and $j\Delta$ must be replaced by a phase angle $\theta(j)$ which is known by the geometry. There is no significant difference in the estimation procedure. We assume here that the fringe rate is constant, for convenience and because this is valid for the short baseline of this experiment.

The approximate maximum-likelihood estimation procedure is derived in the Appendix. The implementation is to maximize the estimator function, G, over assumed values for τ and ω, for the actual received data samples. In calculating G, the stopped fringe rate ω is first normalized by subtracting out known quantities. Thus the frequency variable becomes

$$f = \frac{1}{2\pi}(\omega - \omega_0) \tag{6}$$

where ω_0 is the a priori estimate of the stopped fringe frequency. Two factors contribute to ω_0: the fringe rate as calculated from the geometry, and the difference in local oscillator frequencies, or effective receiver-center frequencies, at the two stations. The frequency f is the sum of the errors due to geometry and to oscillator instabilities, and the estimate of f is the estimate of these errors.

The steps in the estimation procedure for τ and f are:

(1) Assume a value of τ, say τ_k

(2) Form all cross-products whose cross correlations are nonzero for $\tau = \tau_k$

(3) Multiply the cross-products by the cross correlations for $\tau = \tau_k$ neglecting the sinusoidal terms, that is, form $X_i Z_j a_{ij}(\tau_k, \delta)$, and so on

(4) Assume a value for f, say f_j

(5) Evaluate $G(\tau_k, f_j)$

(6) Maximize $G(\tau_k, f_j)$ over the region of uncertainty in f by looping back to step 4

(7) Maximize $G(\tau_k, f_j)$ over the region of uncertainty in τ by looping back to step 1

(8) The estimates $\hat{\tau}$ and $\hat{f}$ of τ and f are the values of τ_k and f_j which maximize G

The distinguishing feature of this procedure is in weighting the cross-products by their assumed τ-dependence before envelope detecting. This gives a natural and optimum method for resolving the estimate of τ to greater resolution than the time between samples, and for accounting for the filtering and sampling methods and for the changes in τ over the measurement time.

V. TOWARDS OPTIMUM FILTERING AND SAMPLING

Although the ML estimation procedure is the same for all filtering and sampling methods, the statistics of the estimator function and of the estimates do depend on the filtering and

the sampling. In this experiment, the utilizable bandwidth was restricted by the maximum possible sampling rate to much less than the receiver bandwidth. Thus the filters could be chosen essentially arbitrarily. For this case, it is shown in Reference 3 that a filter which integrates over the time between samples (a sliding window integrator) is nearly ideal in the sense of maximizing both the minimum and the average signal-to-noise ratios of the estimator function. In conjunction with this filter, the sampling times in the various channels should be staggered as shown in Figure 3. Both the cosine and sine channels at both receivers are sampled with a uniform interval of T = 4 μsec between samples, but the sine channel is sampled T/2 later than the cosine channel at one receiver, and T/4 later at the other receiver.

The optimization problem is considerably different when the utilized bandwidth is limited by the receiver RF bandwidths. In this case the receiver transfer function may be the principal factor determining the effective filter characteristics, and the primary design parameters to optimize are the sampling rate and phase relationships.

VI. PROPERTIES AND EXAMPLES OF THE ESTIMATOR FUNCTION

The statistics of the estimator function have been evaluated both analytically and by simulation.[3] We summarize here some of the key statistics, and then examine graphically some typical sample functions which were observed in the experiment.

The estimation procedure is considered to be reliable when the probability is high that the estimates are in the general vicinity of the correct values of the parameters, rather than being completely extraneous. This depends on the probability distributions of G for the correct and widely erroneous values of the parameters. Once the form of the distributions are known, the performance can be well predicted by a figure of merit which we call the signal-to-noise ratio of the estimator. It is defined as the square of the difference in the means of G for the correct and incorrect values of the parameters, to the variance of G at the correct values. When G is normalized in the natural manner, its mean is unity for widely incorrect assumed values of the parameters, and is unity also when $\rho = 0$, so

$$R = \frac{[E\{G(\tau, f)\} - 1]^2}{\text{Var } G(\tau, f)} \tag{8}$$

The estimator signal-to-noise ratio varies approximately as ρ^2, i.e., as the product of the input signal-to-noise ratios, or alternatively as the square of the source flux density. For the particular filtering and sampling method used, it is given by

$$R = \frac{1}{2} \frac{r}{1 + \left(\frac{1}{2r}\right)} \approx \frac{r}{2} \tag{9}$$

where

$$r = 0.267 \rho^2 N$$

and N is the number of samples in each channel at each receiver. Since the system bandwidth is the inverse of the time between samples in one channel, N is also the system time-bandwidth product.

Estimation will be reliable whenever R exceeds about 10, because the maximum value of G will almost always occur in the vicinity of the correct values of τ and f unless the initial uncertainty in these parameters is large. For example, when the initial uncertainty in f is negligibly small, the number of independent values of G which must be calculated is approximately equal to the time uncertainty times twice the system bandwidth. For the 250 kHz bandwidth of this experiment, time uncertainties of ±10 to ±100 μsec would require calculation of only 10 to 100 independent values of G. It can be seen from the curves of Reference 3 that, for these uncertainties, the results would be reliable about 98 to 99 percent of the time with R = 10.

The resolution of the estimates depends on the peakedness of G more than on R. An approximation to the rms error is estimation of τ is presented in Reference 3, and is

$$\sigma_\tau = \frac{0.79T}{\rho N^{1/2}} \tag{10}$$

where T is the time between samples in one channel, or the inverse system bandwidth. In terms of R,

$$\sigma_\tau \approx \frac{0.289T}{R^{1/2}}$$

so that R = 10 is sufficient to reduce the rms error to less than 0.1 T as well as to result in reliable estimation.

Insight into the capabilities of the estimator function to resolve time and frequency can be gained by studying the function at high signal-to-noise ratios. Figure 4 shows a plot of an actual sample function of $G(\tau_k, f_j)$ observed for a fairly high intensity source, 3C279, with R estimated to be 24.8. The maximum of G is 52.844 and occurs for f_j = -0.20, τ_k = 40.97, so that these are the estimates $\hat{f}$ and $\hat{\tau}$ of f and τ. In the time domain, G is nominally symmetrical, and decreases to half its maximum in under ± 2 μsec, and approximately to zero in ±4 μsec. In the frequency domain, G is also nominally symmetrical about the actual value of f, although this is not apparent from the sample function because the maximum did not occur at f_j = 0. The measurement time of the experiment was NT ≈ 0.64 sec., and the effective bandwidth of G is slightly less than the inverse of this time. It is observed that for different f_j, the maximum of G occurs at very close to the same value of τ_k. This implies that it may be unnecessary to maximize over f_j when only estimates of τ are required, provided that the initial uncertainty in f is small compared to 1/NT, say less than ±0.1/NT.

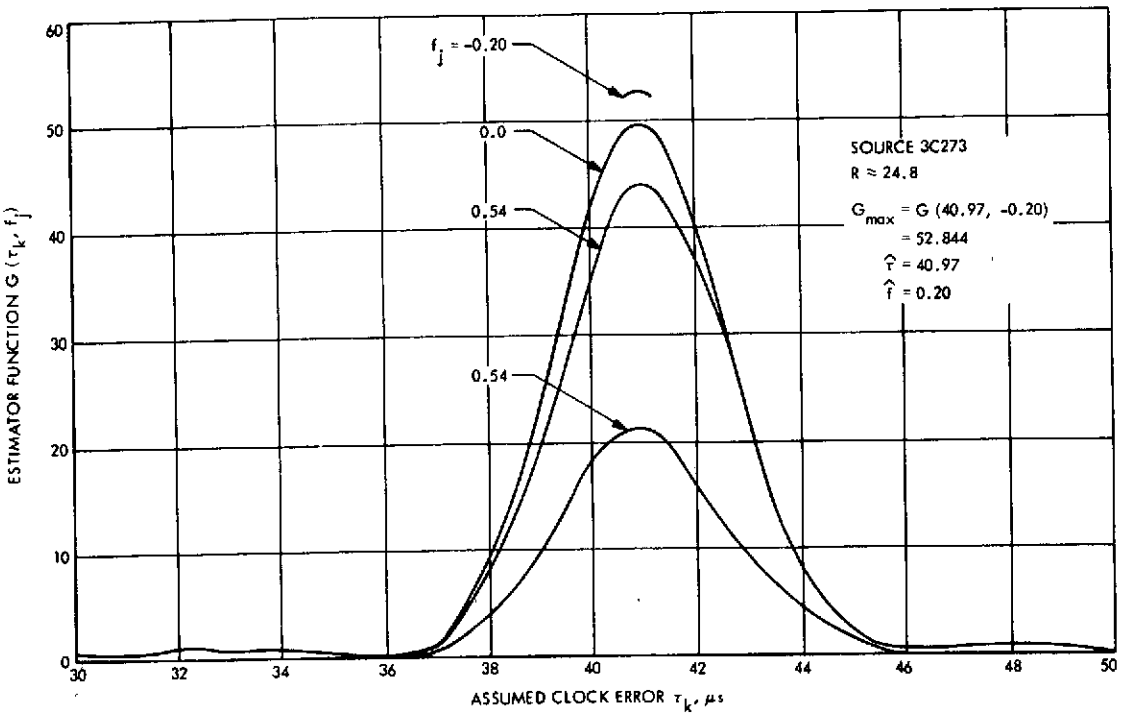

Figure 4. An estimator sample function at a high signal-to-noise ratio.

The performance of the estimator when the noise is significant is illustrated in Figures 5 and 6. Each presents three sample functions from different realizations of the experiment, with the time dependence shown only for the frequency variable fixed at the nominal value, $f_j = 0$. Figure 5 is for a weaker source, 4C39.25, with R estimated to be 3.81, which is significantly below the suggested design value of 10. In one of the three cases, the maximum of G occurs near $\tau_k = 21$ μsec, far removed from the true value which is near 41 μsec. Extraneous results like this occur frequently at these low signal-to-noise ratios. Figure 6 is for source P1127-14, with R estimated to be 8.20, which is only marginally below the design point of 10. Fairly wide variations in the maximum value of G occur at this signal-to-noise ratio, but no extraneous maxima were observed in the 72 sets of data taken for this source.

VII. DETAILED RESULTS

A total of 504 sets of data were taken using five different radio sources, and independent estimates of the time and frequency differences at the two receivers were made for each set of data. The most important results are the means and standard deviations of the estimates of τ and f as a function of the estimator signal-to-noise ratio, R. In order to present these results, it was necessary to estimate R from the data. The method for estimating R is presented later.

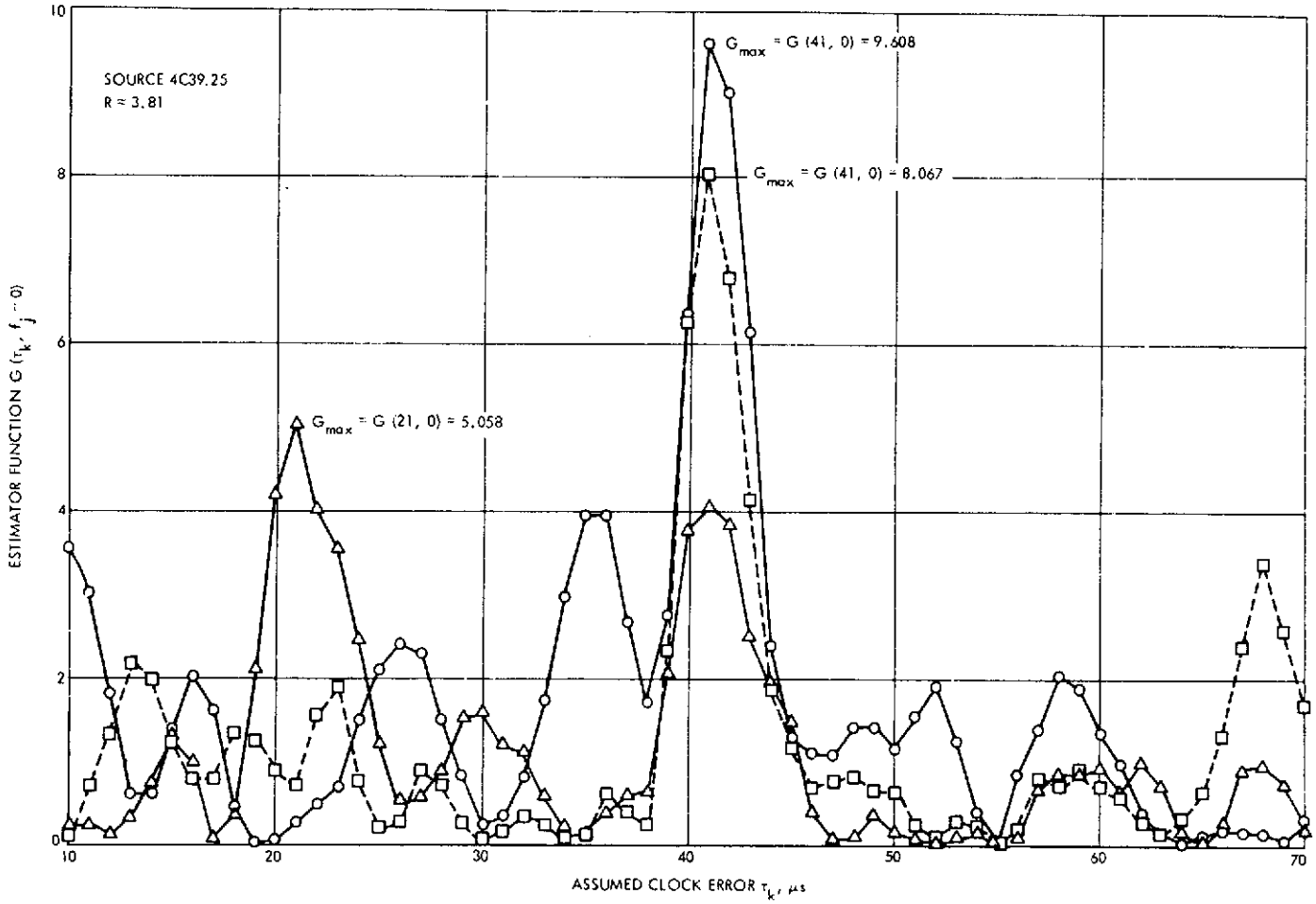

Figure 5. Three estimator sample functions at a low signal-to-noise ratio.

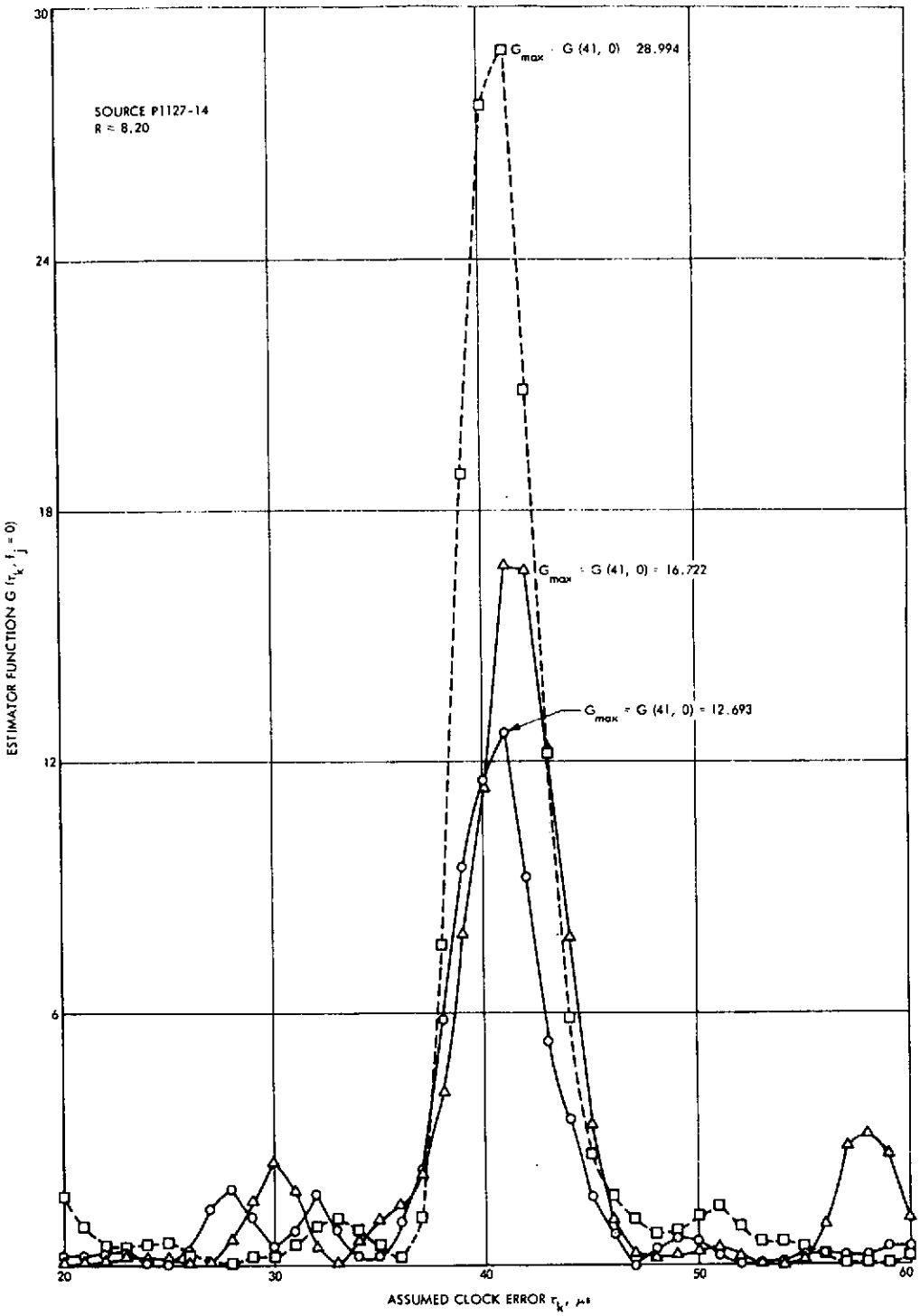

Figure 6. Three estimator sample functions at a marginal signal-to-noise ratio.

Joint Estimate of τ and f

Table 2 presents the results of the joint estimation of τ and f for the five sources. The statistics are based on 144 independent estimates for each of the two strongest sources, 3C273 and 3C279, and on 72 cases for the other sources. Since the true values of τ and f were not known, it was not possible to compute the actual rms errors, therefore, the standard deviations were estimated from the data using the estimates of the means. The standard deviation of the mean estimate for one source is equal to the standard deviation of one estimate for that source, divided by the square root of the number of cases. None of the mean estimates of τ differ from the value 40.97 by more than two standard deviations. All variations in the mean estimates can thus be attributed to noise. There is no evidence to suggest any effects due to errors in source or station positions, changes in the clock synchronization during the experiment, or errors in data processing.

The statistics of the estimates of f cannot be attributed entirely to noise, because of local oscillator instabilities. A hydrogen maser was used for the S-band reference at DSS 12, and rubidium was used at DSS 11, so the rubidium standard contribution dominated. Both the long- and short-term stabilities are on the order of one part in 10^{11}. Errors in the nominal value of f of up to 0.1 Hz were anticipated, as were short term variations with a standard deviation on the order of 0.01 to 0.1 Hz.

Due to noise alone, the standard deviation of f should vary as $R^{1/2}$, provided R is ~ 10 or greater. This relationship was nominally satisfied for the second and third strongest sources, with R = 24.8 and 8.20, and standard deviations of 0.0946 and 0.159 Hz. For the strongest source, the frequency instability was not negligible compared to the noise. Therefore, its effect was estimated from the results for two strongest sources, assuming the noise and instability errors to add in the mean square. The rms error due to frequency instability was estimated at 0.036 Hz, which is well within the range of uncertainty of this effect. The rms frequency estimation error due to noise is then approximately

$$\frac{0.468}{R^{1/2}} \quad \text{Hz}$$

This relationship was also closely satisfied for the next weakest source. An R of 10 thus results in an rms error in frequency estimate of less than 0.1 divided by the measurement time of 0.64 sec, just as it results in a timing error of less than 0.1 divided by the bandwidth.

Estimation of τ For Fixed f

When the a priori uncertainty in frequency is small, τ can be estimated by maximizing G over τ only, assuming no frequency error, that is, f = 0. This results in better estimates of τ than does joint estimation of τ and f when the long- and short-term frequency instabilities are very small. Before this experiment was actually performed, it was felt that the frequency stabilities would be sufficiently good to omit maximization over f, and this was confirmed in the experiment. However, the amount of long-term drift is random, and the

Table 2
Joint Estimation of τ and f.

Radio Source	Estimated SNR of Estimator (R)	ESTIMATION OF τ		ESTIMATION OF f	
		Mean (μsec)	Standard Deviation (μsec)	Mean (Hz)	Standard Deviation (Hz)
3C273	148.0	40.955	0.0956	-0.0807	0.0503
3C279	24.8	41.00	0.228	-0.0799	0.0946
P1127-14	8.20	40.95	0.403	-0.0810	0.159
DW0742+10	4.24	40.95	0.719	-0.0772	0.239
4C39.25	3.81	40.78	1.26	-0.0355	0.249

frequency offsets in the local oscillators might have been too large on another day. It was, therefore, necessary to process the data in both manners, in order to be able to predict future performance.

The results of estimation of τ for f fixed at zero are presented in Table 3. The theoretical rms errors in estimation of τ are also presented, as calculated for the estimated values of R. For the three highest signal-to-noise ratio cases, the observed and calculated rms errors were very close. For the lowest two signal-to-noise ratios, the observed errors were significantly higher than the calculated values. This is because the theory breaks down when R is low enough so that extraneous results occur.

The observed rms errors at low signal-to-noise ratios would have been still higher if the assumed region of uncertainty in τ had been greater, because there would have been more extraneous results due to noise. Throughout the experiment, the uncertainty region was assumed to be from 30 to 50 μsec.

Table 3
Estimation of τ for f = 0.

Radio Source	Estimated R	Estimation of τ		Theoretical rms Error in τ (μsec)
		Mean (μsec)	Standard Deviation (μsec)	
3C273	148.0	40.955	0.0978	0.095
3C279	24.8	41.00	0.224	0.232
P1127-14	8.20	40.95	0.408	0.403
DW0742+10	4.24	40.98	0.641	0.560
4C39.25	3.81	40.92	0.952	0.591

Comparison of Estimation Methods

In comparing the results of estimating τ jointly with f and with f fixed at zero, it is seen that there is negligible difference in the standard deviations of the estimates for the three highest signal-to-noise ratio cases, and that all are close to theory. For the two lower signal-to-noise ratios, the errors are significantly higher when f is estimated instead of assumed to be zero. There are two reasons for this. First, the estimates of f are poor enough to degrade the estimate of τ. Second, more extraneous estimates occurred, because there were effectively more independent calculations of G for noise only.

Estimation of R, ρ, and Flux Density

For each independent case, the approximate maximum likelihood estimate for ρ is the square foot of the maximum value of G, divided by the proper normalization factor. This is the best estimate of ρ only because the maximum value of G occurs at the best estimates of τ and f. A better estimate of ρ would be obtained from value of G at the correct values of τ and f. Therefore, since it was desired to have the overall best estimates of ρ, and hence of R, the values of ρ were estimated using the best overall estimates of τ and f. These best estimates were taken as τ = 40.955 and f = 0.0807 Hz, the values obtained from the strongest source. The overall estimates of ρ for each source were taken as the average of the estimates of ρ for all of the cases] or that source.

The estimates of R were obtained from the estimates for ρ according to equations 8 and 9. To estimate the correlated fluxes, it was assumed that the system temperatures at DSS 11 and 12 were the cold sky temperatures of 37K and 16.3K, respectively, raised by the source total flux at the rate of 0.11K per flux unit. Then the correlated fluxes are given by Equation 1.

Table 4 presents the estimated flux densities, input signal-to-noise ratios, and estimator signal-to-noise ratios for the five sources.

Table 4
Estimated Flux Densities and Estimator SNR's.

Radio Source	Number of Cases	Total Flux [Ref. 4] (fu)	Estimated Correlated Flux (fu)	Estimated Geo. Mean Input SNR (ρ)	Estimated Estimator SNR (R)
3C273	144	39.0	22.0	0.0834	148.0
3C279	144	12.2	8.1	0.0344	24.8
P1127-14	72	6.2	4.6	0.0199	8.20
DW0742+10	72	3.7	3.3	0.0145	4.24
4C39.25	72	3.8	3.1	0.0138	3.81

APPENDIX

This appendix presents a precise formulation of the problem and the notation, and the derivation of the approximate maximum likelihood estimation procedure. The optimization of the filtering and sampling, an analysis of the statistics of the estimator function, and an approximation to the rms error of the time estimate are presented in Reference 3.

Problem Formulation and Data Sampling

Figure 3 illustrates the demodulation, filtering, and sampling of the radio-source signal and receiver noise at the two ground stations. The radio energy emitted by the radio point source is essentially white and gaussian. However, because we can only observe the energy in the bandwidth of our receivers, we can consider the signal to be a narrowband gaussian process. The signal plus noise at the outputs of the two receivers can be represented as

$$X(t) = [n(t)+s(t)] \cos(\omega_1 t+\phi_1) + [m(t)+r(t)] \sin(\omega_1 t+\phi_1) \quad (A1)$$

and

$$Z(t) = [p(t)+s(t-\delta)] \cos(\omega_2 t+\phi_2)+[q(t)+r(t-\delta)] \sin(\omega_2 t+\phi_2) \quad (A2)$$

where

t = time

$\delta = \delta(t)$ = time lag from receiver 1 to receiver 2

$\omega_1 - \omega_2$ = difference in doppler shift, or actual fringe frequency

ϕ_1, ϕ_2 = random phase angles

$s(t)$, $r(t)$ = noise processes representing signal

$n(t)$, $m(t)$, $p(t)$, $q(t)$ = receiver noise

All of the noise processes are assumed independent and bandlimited only by the receivers. The difference frequency $\omega_2 - \omega_2$ and difference phase $\phi_1 - \phi_2$ are assumed to be constant over the observation time, however, the time delay $\delta(t)$ varies due to the rotation of the Earth. We can assume this to be linear and known, $\delta(t) = \delta_0 + \delta t$. The difference frequency and phase are essentially constant only because the change in δ is small compared to the reciprocal of the difference frequency.

Suppose now that we observe $X(t)$ beginning at $t = 0$, and $Z(t)$ beginning at $t = \tau$. This time offset τ is not precisely known, because the clocks at the two stations are not precisely synchronized. We desire to form an estimate $\hat{\tau}$ of τ from the received signals, and to use this estimate to synchronize the clocks.

In order to extract the maximum information from the received signals, both the sine and cosine components of the random processes must be processed. The received signals are thus demodulated to baseband in two channels, using quadrature phase reference signals

derived from rubidium frequency standards which we require to be frequency and phase stable over the observation interval. The signals are then filtered and sampled, with the filtering assuring that all samples in each channel are independent of one another. The demodulated and filtered signals, with * denoting convolution, are

$$x(t) = [X(t) \cos(\omega_3 t+\phi_3)] * h_x(t) \tag{A3}$$

and

$$y(t) = [X(t) \sin(\omega_3 t+\phi_3)] * h_y(t) \tag{A4}$$

at the X receiver, and

$$z(t) = [Z(t) \cos(\omega_4 t+\phi_4)] * h_z(t) \tag{A5}$$

and

$$w(t) = [Z(t) \sin(\omega_4 t+\phi_4)] * h_w(t) \tag{A6}$$

at the Z receiver. We have represented the filtering by convolutions with h_x, h_y, h_z, and h_w, the filter weighting functions.

Since the frequency and phase reference for a narrowband process can be chosen arbitrarily, we can choose the frequency and phase reference of either X or Z arbitrarily. For convenience, we chose $\omega_1 = \omega_3$ and $\phi_1 = \phi_3$, and we define $\omega = \omega_2 - \omega_4$ and $\phi = \phi_2 - \phi_4$. The difference frequency ω, also called the stopped fringe rate, is determined by the relative doppler between X and Z, as reflected by ω_2, and by the reference ω_4. The difference or fringe phase ϕ is random, and uniformly distributed. With this simplification, the observed processes are

$$x(t) = [n(t)+s(t)] * h_x(t) \tag{A7}$$

$$y(t) = [m(t)+r(t)] * h_y(t) \tag{A8}$$

$$z(t) = \{[p(t)+s(t-\delta)] \cos(\omega t+\phi) + [q(t)+r(t-\delta)] \sin(\omega t+\phi)\} * h_w(t) \tag{A9}$$

and

$$w(t) = \{[q(t)+r(t-\delta)] \cos(\omega t+\phi) - [p(t)+s(t-\delta)] \sin(\omega t+\phi)\} * h_w(t) \tag{A10}$$

The four observables are now sampled, all at a uniform and identical rate, with a sampling interval T. Independence of the samples in each channel is assured by having the weighting functions be zero outside of the interval (O, T), and by the whiteness of the noise processes. A remaining parameter which can be varied is the relative times of the samples in the sine and cosine channels, so we leave this arbitrary. As references, we assume that the sampling

of x(t) begins at t = 0, and the sampling of z(t) begins at t = τ, that is, at the delay we wish to estimate. The samples of y and w occur Δ_1 and Δ_2 after the samples of x and z. Thus the samples are

$$X_j = x(jT)$$

$$Y_j = y(jT+\Delta_1)$$

$$Z_j = z(jT+\tau)$$

and

$$W_j = w(jT+\tau+\Delta_2)$$

At this point we make the further assumption that ω is a very low frequency compared to the sampling rate, so that the factors $\cos(\omega t + \phi)$ are constant over T and can be brought outside of the convolution integrals. This assumption is reasonable, since ω can be chosen by the experimenter.

We now normalize the observables to unit variance, and express the observable covariances as

$$E(X_i Z_j) = A_{ij} = \rho a_{ij} \cos(jT\omega + \phi) \quad \text{(A11)}$$

$$E(X_i W_j) = B_{ij} = \rho b_{ij} \sin(jT\omega + \phi) \quad \text{(A12)}$$

$$E(Y_i Z_j) = C_{ij} = \rho c_{ij} \sin(jT\omega + \phi) \quad \text{(A13)}$$

$$E(Y_i W_j) = D_{ij} = \rho d_{ij} \cos(jT\omega + \phi) \quad \text{(A14)}$$

The a_{ij}, b_{ij}, c_{ij}, d_{ij} reflect the dependence on τ-δ (t), and are constant for fixed i-j when τ-δ is constant. In any case, they vary slowly in i-j. Also, the sinusoidal variation in the covariances is slow in j, because $\omega T \ll 1$. Thus for each i-j there is a range of j for which the covariances are essentially constant.

Derivation of Approximate Maximum Likelihood Estimator

The general procedure of maximum-likelihood estimation is to maximize the a posteriori probability density function (PDF) of the observables, conditioned on the unknown parameters. The values of the parameters which maximize the PDF for the given set of observables are chosen as the maximum-likelihood (ML) estimates. The parameters to be estimated here are ρ, τ, ϕ, and ω. In this section, we derive approximate maximizations of the PDF with respect to ρ and ϕ. The resulting function must then be maximized numerically with respect to τ and ω in order to obtain estimates of all the parameters.

The first step in our problem is to find the joint PDF of the observables X_i, Y_i, Z_i, and W_i, conditioned on the unknown parameters ρ, ϕ, τ, and ω. This PDF depends only on the conditional covariance matrix, since the observables are jointly gaussian and zero mean.

Suppose we define a row vector U having as its components all of the observables:

$$U = (X_1, X_2, \ldots, X_N, Y_1, Y_2, \ldots, Y_N, Z_1, Z_2, \ldots, Z_N, W_1, W_2, \ldots, W_N) \quad \text{(A15)}$$

where N is the number of samples of each variable.

Then the covariance matrix of U is

$$\Lambda = \begin{pmatrix} I & O & A & B \\ O & I & C & D \\ A^t & C^t & I & O \\ B^t & D^t & O & I \end{pmatrix} \quad \text{(A16)}$$

where A, B, C, and D are the covariance matrices with elements A_{ij}, B_{ij}, and so on, given by equations (A11) through (A14), and the conditional PDF of the observables is

$$P(U\rho, \phi\tau, \omega) = \frac{C}{|\Lambda|^{1/2}} \exp\left[-\tfrac{1}{2} U\Lambda^{-1}U^t\right]$$

The covariance matrix Λ depends on the parameters ρ, ϕ, τ, and ω, and c is a constant.

The major problem at this point is to invert the covariance matrix. We can do this only in series form, and it is the truncation of this series in the maximization procedure which causes our estimator to be only approximately maximum likelihood.

To proceed we define a matrix P such that

$$\Lambda = I + P \quad \text{(A18)}$$

The matrix P has at most four non-zero elements in each row and column, because A, B, C, and D have at most two non-zero elements in each row and column. Furthermore, the non-zero elements of P are proportional to ρ and do not exceed ρ in absolute value. Since ρ is small ($< 10^{-2}$), we can expand Λ^{-1} in a power series, and bound the terms:

$$\Lambda^{-1} = I - P + P^2 - P^3 + \cdots \quad \text{(A19)}$$

Since the two principal quadrants of P are zero, the principal diagonal elements of P^n are zero for odd n. The other elements are bounded by

$$\begin{aligned} \max_{i,j} \left| (P^n)_{ij} \right| &\leqslant 4\rho \max_{i,j} \left| (P^{n-1})_{i,j} \right| \\ &\leqslant 4^{n-1} \rho^n \end{aligned} \quad \text{(A20)}$$

where $(P^n)_{ij}$ denotes the ij elements of P^n.

Closer bounds can be obtained utilizing properties of the cross covariances for particular cases.

The conditional pdf can now be written as

$$P(U|\rho,\phi,\tau,\omega) = c \exp -\left[\tfrac{1}{2} U(I+P)^{1} U^{t} - \tfrac{1}{2} \log \det (I+P)\right] \tag{A21}$$

Using a well-known matrix identity,

$$\log \det (I+P) \equiv \mathrm{Tr} \log (I+P) = \mathrm{Tr}(P - \frac{P^2}{2} + \frac{P^3}{3} - \frac{P^4}{4} + \cdots \tag{A22}$$

The odd power terms can be deleted, since the principal diagonal of P^n is zero for odd n. Thus

$$\log \det (I+P) = -\mathrm{Tr} (\frac{P^2}{2} + \frac{P^4}{4} + \cdots) \tag{A23}$$

We now define a likelihood function $L_1(U|\rho,\phi,\tau,\omega)$ as the exponent of the conditional pdf, and maximization of L_1 is equivalent to maximization of the pdf.

$$L_1(U|\rho,\phi,\tau,\omega) = -\tfrac{1}{2} U(I - P + P^2 - + \cdots)U^t + \tfrac{1}{2} \mathrm{Tr} (\frac{P^2}{2} + \frac{P^4}{4} + \cdots) \tag{A24}$$

It is not feasible to maximize L_1 analytically with respect to any of the parameters without neglecting terms in P of higher order than P^2. With this approximation, we can maximize with respect to ρ and ϕ. Since normally τ and ω are the parameters of primary interest, the approximate solutions for ρ and ϕ usually suffice, but greater accuracy can be obtained numerically if required.

To proceed, we define a new matrix Q by

$$Q = \frac{1}{\rho} P = \frac{1}{\rho} \begin{pmatrix} 0 & 0 & A & B \\ 0 & 0 & C & D \\ A^t & C^t & 0 & 0 \\ B^t & D^t & 0 & 0 \end{pmatrix} \tag{A25}$$

Next we drop the U I U^t term in L_1, which is independent of the parameters, to obtain

$$L_2(U|\rho,\phi,\tau,\omega) \approx \tfrac{1}{2} U(\rho Q - \rho^2 Q^2)U^t + \tfrac{1}{4} \rho^2 \mathrm{Tr}(Q^2) \tag{A26}$$

By differentiating with respect to ρ, we see that L_2 is maximized for the conditional estimate of ρ

$$\hat{\rho} = \frac{UQU^t}{2UQ^2U^t - \mathrm{Tr}(Q^2)} \tag{A27}$$

The denominator of this expression can be approximated by its mean, which is $Tr(Q^2)$, so

$$\hat{\rho} \approx \frac{UQU^t}{Tr(Q^2)} \tag{A28}$$

The variance of the denominator of equation (A27) is also on the order of $Tr(Q^2)$. Therefore, since $Tr(Q^2) \approx 4N$, the approximation is good when N is large, say 10^4 or greater, which will always be true in VLBI problems.

A new likelihood function is now obtained by substituting the value of $\hat{\rho}$ into equation (A26), and again approximating uQ^2u^t by $Tr(Q^2)$:

$$L_3(U|\rho,\phi,\tau,\omega) \approx \frac{[UQU^t]^2}{Tr(Q^2)} \tag{A29}$$

Since the elements of Q vary slowly except for the sinusoidal variation, $Tr(Q^2)$ is essentially independent of Q and ω so long as $N\Delta\omega \gg \pi$. This can be assured by controlling ω by selecting the local oscillator frequencies. Neglecting any slight variation of $Tr(Q^2)$, L_2 can be maximized over ϕ. To do this, Q is expressed

$$Q = R\cos\phi + S\sin\phi \tag{A30}$$

where R and S do not depend on ϕ and are given by

$$R = \begin{pmatrix} 0 & R_o \\ R_o^t & 0 \end{pmatrix} \tag{A31}$$

$$S = \begin{pmatrix} 0 & S_o \\ S_o^t & 0 \end{pmatrix} \tag{A32}$$

where

$$R_o = \begin{pmatrix} (a_{ij}\cos j\Delta\omega & (-b_{ij}\sin j\Delta\omega) \\ (c_{ij}\sin j\Delta\omega) & (-d_{ij}\cos j\Delta\omega) \end{pmatrix} \tag{A33}$$

$$S_o \quad \begin{pmatrix} (-a_{ij}\sin j\Delta\omega) & (-b_{ij}\cos j\Delta\omega) \\ (c_{ij}\cos j\,\Delta\omega) & (-d_{ij}\sin j\Delta\omega) \end{pmatrix} \tag{A34}$$

The derivative of the likelihood ratio with respect to ϕ is then

$$\frac{d}{d\phi} L_3 = \frac{2(UQU^t)\, U(S\cos\phi - R\sin\phi)\, U^t}{Tr(Q^2)} \tag{A35}$$

and the value of ϕ which maximizes L_3 is

$$\hat{\phi} = \arctan \frac{USU^t}{URU^t} \tag{A36}$$

The new likelihood ratio is the maximum of L_3, that is, $L_3(\hat{\phi})$, which we renormalize to obtain the final estimator function G:

$$G(\tau,\omega) = \frac{(URU^t)^2 + (USU^t)^2}{4Tr(Q^2)} \tag{A37}$$

This is as far as we can proceed analytically. To find the final approximate ML estimates of all the parameters, G is maximized numerically over τ and ω. When only $\hat{\tau}$ is required, ω is usually known a priori, so that the numerical maximization is only over one parameter, τ.

ACKNOWLEDGEMENTS

The author acknowledges the assistance of P.F. MacDoran, J.G. Williams, and D.S. Spitzmesser, who shared their knowledge and experience in VLBI experiments, and of S.S. Brokl and the station personnel at DSS 11 and 12, who assisted in implementing the experiment.

REFERENCES

1. C.E. Hildebrand, V.J. Ondrasik, and G.A. Ransford, "Earth-Based Navigation Capabilities for Outer Planet Missions," AIAA/AAS Astrodymanics Conference, Palo Alto, California, September 11-12, 1972. AIAA Paper No. 72-925.
2. V.J. Ondrasik, C.E. Hildebrand, and G.A. Ransford, "Preliminary Evaluation Radio Data Orbit Determination Capabilities for the Saturn Portion of a Jupiter-Saturn-Pluto 1977 Mission," DSN Progress Report, JPL TR 32-1526, Vol. X, August 15, 1972, pp. 59-75.
3. W.J. Hurd, "DSN Station Clock Synchronization by Maximum Likelihood VLBI," DSN Progress Report, JPL TR 32-1526, Vol. X, August 15, 1972, pp. 82-95.
4. K.I. Kellermann, et.al., "High Resolution Observations of Compact Radio Sources at 13 Centimeters," Astrophysical J., Vol. 151, September 1970, pp. 803-809.

TIME AND FREQUENCY REQUIREMENT FOR THE EARTH AND OCEAN PHYSICS APPLICATIONS PROGRAM*

Friedrich O. von Bun
Goddard Space Flight Center

My talk will outline some of the time and frequency requirements we have for the Earth and Ocean Physics Applications Program (EOPAP). I will divide my talk into two major parts, since many of you may not know what this program is about. First I will explain what the program is and what it consists of, and then I will try to answer the question: "Why do we need certain requirements in time and frequency to accomplish these metric tasks we have given ourselves?"

I have to mention at this time that EOPAP is not yet fully approved by NASA, although we are lucky to have gotten our first spacecraft at least to the Bureau of the Budget. As you may know, it is difficult at this time to start anything new, so I cannot complain.

First, I will talk about the program itself, and the accuracies needed as far as frequency and time are concerned. Then I will try to translate these requirements, which come from ultra-precision orbital requirements, into those of time and frequency. Actually there are three parts to this, as you can see in Figure 1.

The Earth and Ocean Physics Applications Program has specific goals, and we need to perform specific experiments to achieve these goals. We must also fly certain spacecraft to reach these goals. We also have certain accuracy requirements which relate directly to time-frequency requirements.

A. THE EOPAP
- GOALS AND EXPERIMENTS
- SPACECRAFT

B. ACCURACIES NEEDED FOR THE PROGRAM
- MEASUREMENT REQUIREMENTS SUMMARY

C. TRANSLATE THESE REQUIREMENTS INTO
- TIME
- FREQUENCY

} REQUIREMENTS

Figure 1. The Earth and Ocean Physics Applications Program.

*This is the edited transcript of the recorded oral presentation.

The program consists of two major parts (Figure 2), namely earth dynamics and ocean dynamics. I'll explain a little bit later on what I mean by that, and, as I mentioned before, I will talk about the goals and the spacecraft, including the launch schedule.

MAJOR GOALS AND EXPERIMENTS

- **EARTH DYNAMICS**
- **OCEAN DYNAMICS**

SPACECRAFT AND LAUNCH SCHEDULE

Figure 2. The main parts of the program.

The major goals in earth dynamics are shown in Figure 3 and include earthquake hazard assessment and alleviation. Can we do something with present spacecraft or future spacecraft? What have we learned over the last ten years on space techniques which we can apply to problems we have on the ground? That is the driving force, really, for that program.

To give you an example, we are presently performing an experiment in the San Andreas Fault area to measure the motion between the American plate and the Pacific plate, utilizing laser techniques, laser-ranging techniques to be more accurate, with the BEC spacecraft equipped with laser corner reflectors.

Some time ago – I think about a year ago – we finished a polar motion experiment. We determined the motion of the pole to an accuracy of about one meter, utilizing only one single laser station and the BEC spacecraft. We could do this within six hours to the accuracy of one meter.

On global surveying and mapping, we are trying to determine the gravity field, particularly for the ocean dynamics program. We have considerably improved our station locations, particularly for the laser station. We have also improved the magnetic field for surveying and mapping.

EARTHQUAKE HAZARD ASSESSMENT AND ALLEVIATION

- **SAN ANDREAS FAULT EXPERIMENT (SAFE, LASER, VLBI)**
- **PLATE MOTION EXPERIMENT (VLBI, LASER) (U.S., JAPAN)**
- **SOLID EARTH TIDES (LASER, ATS-G)**
- **POLAR MOTION (LASER, VLBI)**
- **UT-1 (VLBI, LASER)**

GLOBAL SURVEYING AND MAPPING

- **GRAVITY FIELD DETERMINATION, R, $\dot{R}$, $\measuredangle$ LASER, GEM1-4 (SST, ALTIMETER)**
- **GEOID AND GRAVITY FINE STRUCTURE (ALTIMETER, R, $\dot{R}$, $\measuredangle$ (SST)**
- **MAGNETIC FIELD DETERMINATION, MAGNETOM, ORBIT**
- **INTERNATIONAL SATELLITE GEODESY EXPERIMENT, $\measuredangle$ ISAGEX, R, $\dot{R}$, LASER**

Figure 3. Major goals and experiments in the earth dynamics area of EOPAP.

The major experiments and goals in the area of ocean dynamics (Figure 4) are twofold. We try to determine the currents and the circulation by measuring the geostrophic uplift in the ocean. For this we would need an altimeter with at least a high resolution to, say, 10 centimeters.

As you may know, in 1974, we are flying the GEOS-C spacecraft, which will be equipped with an altimeter with an accuracy of about a meter or two. In addition, this spacecraft will be tracked from the ATS-F spacecraft by means of satellite-to-satellite tracking (SST) to help us in the orbit determination.

This will be the first satellite equipped with an altimeter which may give us a more detailed view of the ocean, particularly the ocean surface or, more specifically, the variation of the mean ocean surface. We will evaluate the ocean surface condition from the altimeter data. We may further get the sea state, the wind direction, and storm searches, all important factors, for instance, for shipping.

OCEAN CURRENTS AND CIRCULATION

- **OCEAN SURFACE CONDITIONS, GEOID, SLOPES, (ALT., SST, OTHERS)**
- **GENERAL CURRENTS AND CIRCULATION (ALT., TRACERS, SST, OTHERS)**
- **OPEN OCEAN TIDES, TSUNAMIES (ALT., SST, OTHERS)**

OCEAN SURFACE CONDITION MONITORING

- **SEA STATE, WAVE DIRECTION (ALT., SCATT., SST, OTHERS)**
- **SURFACE WINDS, MAGNITUDE, DIRECTION (ALT., SCATT., SST, OTHERS)**
- **STORM SURGES (ALT., SST, OTHERS)**

Figure 4. Major goals and experiments in the ocean dynamics area of EOPAP.

Now let me give you an idea (Figure 5) of measurements we're trying to make in order to accomplish the tasks outlined. We have to determine, for instance, the crustal motion, say to within one centimeter a year, if we want to determine what energy is stored in fault lines.

MEASUREMENT	ACCURACY
• CRUSTAL MOTION	1 CM/YEAR
• POLAR MOTION, EARTH ROTATION	2 CM/0.5 DAY
• SATELLITE ORBITS	10 CM
• GRAVITY FIELD/GEOID	10 CM
• SEA SURFACE TOPOGRAPHY	10 CM
• SEA STATE/WAVE HEIGHT	1 ÷ 3 M
• SURFACE WINDS	2 ÷ 5 M/S, $< 20^{\circ}$
• MAGNETIC FIELD	2 GAMMA, 0.5 ARCMIN

Figure 5. Measurements requirements summary.

We would like to determine polar motion to two centimeters' accuracy in a half a day's time. There seems to exist a correlation between polar motion and earthquakes. To do all this we need extremely precise satellite orbits (gravity field). Further, we need to have the sea state and wave height determined between, say, one and three meters. The surface winds we would like to determine to five meters a second, with a directional angle of at least 20 degrees; less if we can. We will further try to determine the magnetic field of the earth to about ± two gamma and a half-minute of arc. Right now we know the magnetic field to a few gammas but only the magnitude, not the direction.

In order to do this we have come up with a couple of flight missions, shown in Figure 6. And as I mentioned before, the first spacecraft, which is a large geodetic satellite, is at the Bureau of the Budget. This satellite is just a simple, heavy ball equipped with laser corner reflectors, which will have a polar orbit of roughly 3000 to 5000 kilometers and will act as a reflecting reference station in space. We hope to determine the orbit very accurately, say in the 10-centimeter range, so that we can determine motion of the poles, UT-1, and tectronic plate motions.

The next satellite we are planning is a SEASAT-1 – which stands for sea satellite – and which is, in essence, an oceanographic spacecraft equipped with a very accurate, perhaps a 30- to 50-centimeter-type altimeter, to determine ocean surface variation. Obviously other instruments will be carried, not of interest as far as time and frequency are concerned.

The next spacecraft is the Geopause, like "magnetopause." It means the satellite is so far away that it is out of the "noise field" of the gravity of the earth. At 30,000 kilometers, only six or seven of the gravity coefficients of the earth play a role; for a near-earth spacecraft at say 300-kilometer height, one needs perhaps 600 to 900 coefficients to determine a very accurate orbit. This is why we are going far out, and using that spacecraft as an "anchor" station to measure range rate using SST techniques. By doing so we can determine the exact variation of that low-orbiting satellite. SEASAT-2 is thought of as an operational sea satellite.

LAGEOS			S		▲						
SEASAT-1			S			▲					
GEOPAUSE				S				▲			
GRAVSAT				S				▲			
SEASAT-2							S				▲
CAL YEAR	72	73	74	75	76	77	78	79	80	81	82

S = START
▲ = LAUNCH

Figure 6. EOPAP spacecraft.

As you can see, the program plan covers the years up to 1982, but at the present time we are just talking about the first 1973 spacecraft, LAGEOS, and SEASAT-1.

This should give you an idea what we want to do, and the reason why—apply what we know and have learned in the past to problems we have on earth.

Let me try now to translate orbital accuracies into those of time and frequency. Take the orbit, say, of the LAGEOS, and we are talking about a two-centimeter range, which means we need a timing accuracy on the order of two or three microseconds (Figure 7).

What is the time synchronization needed if we perform range and range rate tracking from a satellite which is in a nearly synchronous orbit? Again we go through some basic arithmetic and we come up with roughly a microsecond, as the calculations shown in Figure 8 demonstrate. In order to sense the gravity variation of the earth's field by observing variations in the height of the low-orbiting satellite we need this kind of accuracy, and we hope with the Geopause spacecraft in orbit we can achieve this goal.

We have already planned – and hardware is being built – an ATS/Nimbus satellite-to-satellite tracking experiment, and hope to get 0.07 centimeter per second. And these spacecraft will be in orbit by 1974. Thus we will have some idea of what we can do and cannot do in the near future.

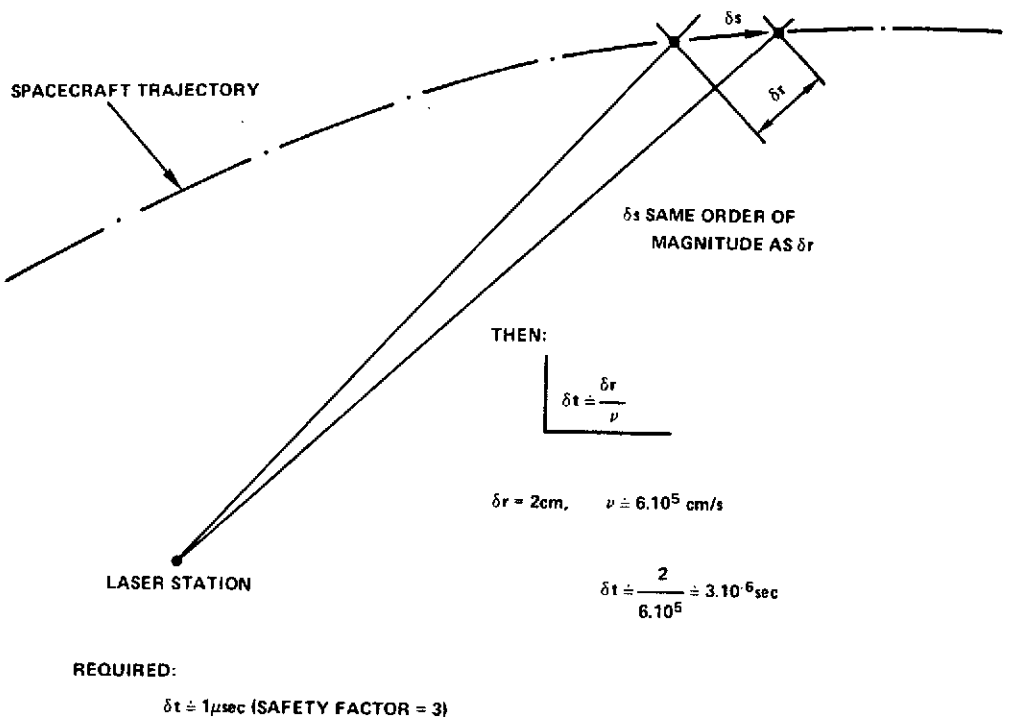

Figure 7. Time synchronization for orbital range tracking with LAGEOS.

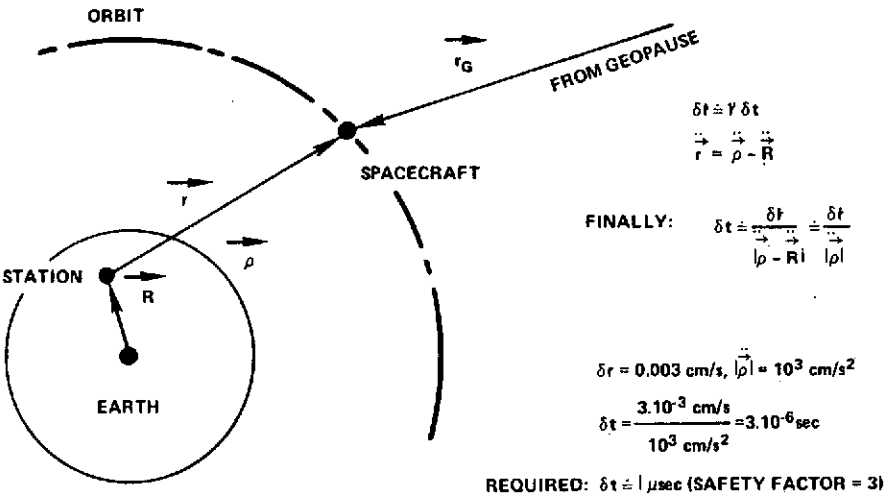

Figure 8. Time synchronization for orbital range-rate tracking with Geopause.

What time synchronization do we need, for instance, if we fly an altimeter (Figure 9)? And here we see it is a rather relaxed one. For an altimeter spacecraft experiment we need only one-third of a millisecond time synchronization between the stations, because it is really not too important where the spacecraft is in a horizontal direction. A millisecond corresponds to about one meter, yet the footprint is 10^4 times larger. This results from the variation of the height of the spacecraft, since one always has an orbit with a finite eccentricity.

HEIGHT VARIATION: $\dot{h} \doteq \nu . e \sin \eta$ **for** $e \leqslant 0.1$

AND: $\delta t \doteq \dfrac{\delta h}{\dot{h}}$

FOR: $\nu = 8.10^5$ cm/s, $e = 0.0125$, $\dot{h} = 100$ m/s

USING: $\delta h = 10$ cm

$\delta t = 10^{-3}$ sec $= 1$ msec

REQUIRED: $\delta t \doteq 1/3$ msec (SAFETY FACTOR = 3)

Figure 9. Time synchronization for a radar altimeter.

What frequency stability do we need if we have a two-way ranging system as we have right now on the Goddard network? We need a frequency stability $\delta\nu/\nu$, as in Figure 10, of 10^9, say over one second, again with the safety factor of three, if we want to determine a range rate to, say, 0.003 centimeter per second.

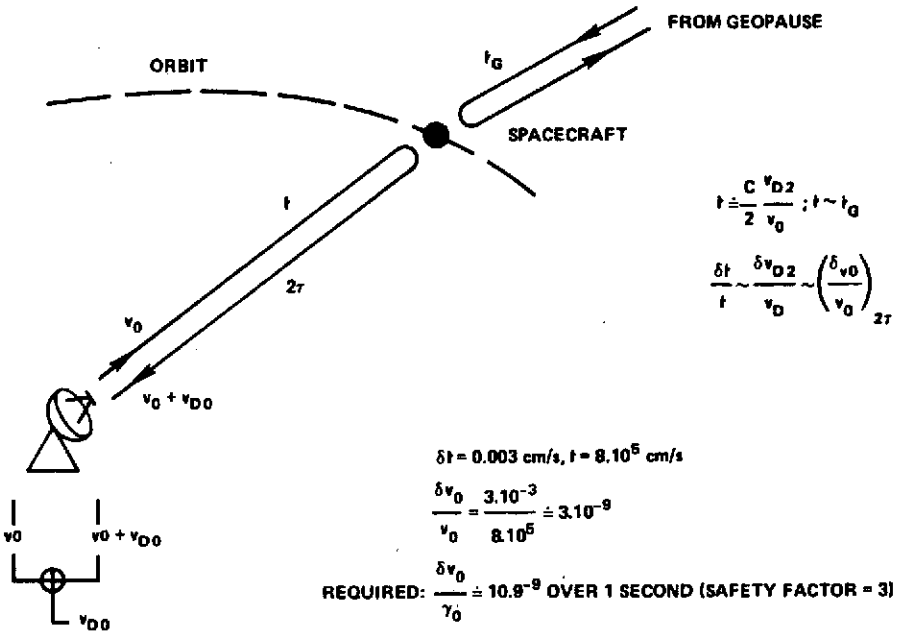

Figure 10. Frequency stability for a two-way range-rate system.

The frequency synchronization for a three-way ranging system is more stringent, as Figure 11 indicates. If one sends a signal up and receives it someplace else, any time bias error would introduce a range rate error. If I don't know the other stations' frequency, I would interpret the error as a doppler shift. In this case, we would need one part in 10^{13}, again with a safety factor of three.

1. FREQUENCY STABILITY PROBLEM SAME AS BEFORE
2. FREQUENCY OFFSET BETWEEN STATION 1 AND 2 WILL NOW BE INTERPRETED AS RANGE RATE' THUS INTRODUCING AN ERROR:

$$\left(\frac{\delta v_{12}}{v_0}\right) \doteq 2\frac{\delta t}{C}$$

$\delta t = 3.10^{-3}$ cm/s, $C = 3.10^{10}$ cm/s, $v_0 = 2.10^9$ Hz

$$\frac{\delta v_{12}}{v_0} = 2\frac{3.10^{-3}}{3.10^{10}} \doteq 2.10^{-13}$$

REQUIRED: $\frac{\delta v_{12}}{v_0} \leq 10^{-13}$ (SAFETY FACTOR = 3)

Figure 11. Frequency synchronization for a three-way range-rate system.

Figure 12 summarizes what I just said and tells what time synchronization we need for range and range-rate stations, as well as for satellite-to-satellite tracking. We're looking forward to, say, a one microsecond time synchronization between tracking stations. The frequency stability for a two-way range-rate system needs to be one part in 10^9, and a frequency synchronization for a three-way system needs to be one part in 10^{13}.

I hope I have given you some idea what we need for the new program both in frequency and in time synchronization.

- **TIME SYNCHRONIZATION:** $\delta t \doteq 1\ \mu sec$

  (FOR RANGE AND RANGE-RATE STATIONS, SATELLITE-TO-SATELLITE TRACKING)

- **FREQUENCY STABILITY:** $\frac{\delta \nu_0}{\nu_0} \leqslant 10^{-9}$ **(1 sec)**

  (FOR TWO-WAY RANGE RATE)

- **FREQUENCY SYNCHRONIZATION:** $\frac{\delta \nu_{12}}{\nu_0} \leqslant 10^{-13}$

  (FOR THREE-WAY RANGE RATE)

Figure 12. Summary of EOPAP requirements.

DR. WINKLER:

I think I have to ask a question here. If we understand your last requirement, one part to 10^{13}, is that absolute accuracy? Or is it frequency stability, or synchronization of . . . ?

DR. VON BUN:

It's really a frequency offset, and not an absolute accuracy.

DR. WINKLER:

So that would be frequency difference in the oscillators, and it has to be maintained to be within that?

DR. VON BUN:

Yes.

DR. WINKLER:

I see. Over what period of time?

DR. VON BUN:

Over the interval in which you make the measurements (minutes to hours, for example).

DR. WINKLER:

Over seconds?

DR. VON BUN:

No, over this measuring interval.

DR. WINKLER:

I understand. But that means you will have to use hydrogen masers at these stations?

DR. VON BUN:

That's right. We have actually used hydrogen masers at our tracking stations.

PANEL DISCUSSION

Andrew R. Chi, Moderator
Goddard Space Flight Center

MR. CHI:

In a discussion period, usually there's not enough discussion unless there is some stimulation. What I have tried to do is to cover the three themes of the papers given today. The three themes are: the frequency sources; the distribution of frequency and time; and the application of frequency and time.

Since there are five panel members and we have about one hour's time, I would like to limit the time to about five minutes per panel member, after which there will be a short discussion. After we go through the series of presentations and discussions, if we have time we can go into other areas.

The sequence which I would like to follow is to give those panel members who did not have a chance to speak today the first opportunity. So I will first call Dr. Knowles. His will be in the area of characteristics of radio sources and how to select them for applications.

DR. KNOWLES:

I actually don't have any prepared discussion, so my remarks will be quite brief.

I think the means of selecting radio sources for VLBI applications is rather simple and obvious. You want a source which is a point source and which does not vary. There has been considerable work done in the field of radio astronomy toward selecting these sources. We have pretty well listed the sources by now: a list of quasars, which are known to be point sources over baselines of the diameter of the earth; and also lists of the spectral line sources.

It's interesting to note that it turns out that the earth is a very good interferometer for natural sources for both spectral line sources and for quasars. Most of these sources are, quite clearly, heavily resolved by the time you get to a baseline the length of the earth.

Now the problem with this is that for possible applications, such as navigation systems, you have a fairly small percentage of sources to work with. For example, with the water vapor sources that Dr. Johnson spoke of, we expect that only between 10 and 25 percent of them will be visible over baselines of the length of the earth. And this definitely limits the utility of such sources and is a factor which hasn't quite been brought out in the literature on station locations, navigation systems, and related topics.

I might mention that, in the case of water-vapor sources, we discovered this resolution problem during one experiment involving three sources.

The other thing I'd like to mention is for purposes of using these sources on any routine basis for either navigation systems, which the Navy has asked our group to look into, or for station location or geodesy, it is quite important to have some program of systematic observations of the positions of all these sources concurrently and any observations of proper motion. I think this is being done by a couple of groups with regard to the quasars. We are doing it to some extent with the water vapor sources. But I think more long-term systematic program study of the source characteristics is a necessary part of any attempt to use these on a routine basis for measuring station position, for uses in navigation systems, or for anything like that.

MR. CHI:

The next topic will be in the area of VLBI applications for position determination and the comparison of this technique with other techniques such as lasar tracking and so on. Our panel member is Dr. Jayaram Ramasastry.

DR. RAMASASTRY:

What I would like to talk about is this: We all have been doing VLBI experiments up to now, fighting at centimeter levels, and submeter levels. But I'd like to focus attention on what kind of frequency stabilities or fractions frequency deviations we have been observing, what geodynamic problems we will be trying to investigate, what kind of philosophical approach we should adopt in the future, no matter who does the experiment.

First of all, I think we should thank Harry Peters of GSFC and Dr. Vessot of SAO and several others in the precise time and frequency field for supporting all the major VLBI experiments up to now, and pray God to give them long life and good health so that they can be of use to us all the time.

Coming to the frequency deviations, most of us doing credible work have been seeing one part in 10^{13} frequency stabilities, sometimes better, sometimes lower.

It is now understood that it is no use doing a VLBI experiment without reliable and well-performing primary-frequency sources. In the end, I will be talking about what I consider to be five commandments of good conduct for geodetic investigators. I think that's what we should keep in mind in planning future experiments.

The four major areas of geodynamic investigations that we are concentrating on in our Earth Physics Program are UT-1, polar motion, solid earth tides, and plate motion. I will go in that order in my discussion. In UT-1, seasonal variations of randomness have been observed, and the conventional technique like the PZT (photographic zenith tubes) and the transit circles have not been able to give anything better than about 5 milliseconds each. It seems that VLBI can provide about a half a millisecond or better. We have demonstrated this in our latest VLBI experiment between Agassiz and Owens Valley. And that's one area where I think that VLBI can contribute signficantly to geodynamic research.

The second area is polar motion, which is really the motion of the earth's mass around the rotation axis of the earth. In this area, VLBI, as has been shown, can really provide very significant data, even though no direct measurements have come up to date. However, I would like to point out that Doppler tracking data of Anderle and others have provided polar motion components at the one-to-two-meter level. As far as lasers are concerned, Dr. David Smith of GSFC is, I think, the only person who has come up with what I consider to be credible polar motion determination from a few hours (six) of laser ranging data.

And it is not really well known now whether laser ranging is going to be a better technique, or VLBI is the one for geodynamic applications. It doesn't matter, as long as we are going to solve the problems confronting us.

I'm just reporting here that lasers are providing these types of polar-motion data, and VLBI has not yet come up with it, but we hope we will soon be able to do so.

The third area concerns solid earth tides, where measurement of the tidal oscillations with gravimeters has yielded sufficiently good-quality data. There is another area where VLBI can also contribute.

Plate motion and fault motion are the areas where VLBI can make very significant contributions. We have been planning short-baseline experiments with combinations of a transportable dish and a main dish for fault-motion studies, and at the same time we are working on transcontinental baselines with the idea of measuring the relative motions between the transcontinental plates. In this area VLBI can give much less than ten centimeters resolution, and it seems as though in the next four years we should be able to settle down to what I consider to be the observatory type of experiment. At present, we have measured transcontinental baselines with an accuracy on the order of 40 to 100 centimeters. Within the next two years, we should be able to improve this to the five-centimeter level. That means we will not be experimenting anymore with VLBI; but will be investigating geodynamic phenomena.

Let me now summarize all the problems that are involved. In this context, I would like to discuss the five commandments of good conduct which I mentioned earlier. They are:

1. Never conduct experiments using stations of no geodynamic value.
2. Never conduct experiments without stable frequency sources and wideband recording systems.
3. Never, under any circumstances, improvise any hardware and software in any experiment.
4. Know the difference between precision and accuracy.
5. Tell the truth always. It pays to be honest in the long run.

VLBI should receive its share of material support if all the major error sources, including atmospheric effects, are to be resolved in order to realize the five-centimeter level absolute accuracy. Otherwise, VLBI will simply remain a radio astronomy tool.

DR. KNOWLES:

I might just add a word seconding Dr. Ramasastry on the importance of frequency standards and adding to his comments, thanking those who have made them for us. I might also add that it's clear that the whole field of frequency standards is changing rapidly. We are now getting improved rubidium and cesium instruments which may be more competitive with hydrogen masers at a greatly reduced cost, and this is well worth following up. It's really important to make these experiments economical and feasible.

And one more comment in that regard, while we are talking of the tools of the trade, let us not forget the important expense and difficulty of making a good wideband recording system for use in the separated interferometer technique. The so-called Mark-1 technique, and other narrowband systems are now pretty well under control. But there are at least several groups - I know the spectral line people are one of them - to whom it is very important to have this wideband and long recording-time capability, which is only available on one system now, the Mark-2 system, which has been developed by NRAO, but it's still in the process of development. They have many more engineering hours to go. It's possible that yet a third system, which would be very noticeably better than the others, could be developed by somebody with enough time and effort.

DR. RAMASASTRY:

I have one more comment to make. I have been working on a system which can provide the instantaneous 28-megahertz bandwidth using the 2-megahertz instrumentation tape recorders that are presently available at the STDN stations. One other person who has been working on the same problem is Dr. Hans Henteregger of MIT. The instrumentation tape recorders already exist at NASA/STDN stations, and they have 14 channels. They could be used directly. No frequency switching is involved: the recorder consists of 14 channels of 2 MHz each, which gives you 28 megahertz instantaneous bandwidth.

DR. ALLEY:

I just happen to know, from experiments being conducted at the University of Maryland by Dr. Currie, that they are leading towards long baseline interferometry in the optical region. And I wonder, since the discussion has centered a good bit on applications of VLBI to obtaining geodetic and geophysical information, whether he might like to make some comment at this point on the advantages of optical VLBI techniques.

DR. CURRIE:

I think the implication for geodesy is--it has the same level of the VLBI in the radio, but there are a number of advantages. I think that as far as this conference is concerned, it is perhaps less significant because of the lack of a need of precision clocks. It has the advantage that one can use rather ordinary clocks in the comparison. It does permit determination (in the initial straightforward form) of positions of the pole with respect

to the station longitude, certainly less than the meter level, probably down to the 10- to 20-centimeter level.

In a later version, it will also permit the study of UT. But it is something that test measurements have been made at the baselines of five million wavelengths, and these results have been used to resolve objects that have a diameter of about 20-thousands of a second of arc. But at present those measurements are made on a large optical telescope, and the use of separate aperatures has not been initiated yet.

MR. CHI:

This is the first time that I see we have the people who are in the frequency and time field, and their users. And the requirements start to catch up with the capability. Now, I'd like to call Dr. Hurd, who covered more or less the same area of applications, the signal processing requirement and approach for the VLBI applications.

DR. HURD:

I don't really have any prepared remarks at this point. I think I would like to comment a little more on getting wider bandwidths. People seem to be synthesizing wider bandwidths up to the receiver bandwidth by taking two narrowband segments, one at each end of the spectrum. But for signal processing the important problem is to minimize the amount of data you need, because this is the big problem: storing and processing data, and the computation time is going to be proportional to the number of bits of data required.

Now, to get wide bandwidths, core memories and even semiconductor memories are becoming very, very cheap, like a penny a bit. Anyone – almost anyone – can afford a million bits of memory and can make this memory as high-speed as you want just by paralleling the bits.

Take a batch of data at twice the bandwidth of your system, according to the Niquist rate. And if you need more than a million bits of data or so, or more data than the amount of memory, well, write this out onto magnetic tape at your leisure and then take another batch of data. And this is the natural way to achieve wide bandwidth utilization in the system. I think it's becoming competitive these days with the cheaper memories. And I think it's really the natural way to do it, and that it will minimize processing costs and system complexities.

Most people seem to have been processing VLBI data, even extracting the fundamental fringe rate and phase and the time delay by the least-squares technique. And I think maybe the maximum-likelihoood approach that I've taken might be somewhat beneficial in this regard. I'm not sure exactly what the computation-time rate also would be, but it seems like a very natural approach to me.

It leads very naturally into the interpolation between the sampling times. In my system, the samples were taken four microseconds apart, but with the minimum signal-to-noise ratio required for reliable detection, this naturally led to an interpolation down to an rms accuracy of one-tenth of the time between samples. So if you can sample every ten nanoseconds or so, you are down to the one nanosecond level, just at the minimum signal-to-noise ratio.

DR. CLARK:

Just in regard to the previous comments, as Dr. Knowles pointed out, the problems that you are going to face in time synchronization is one of available, relatively strong sources, especially when you start synchronizing over longer baselines.

The sensitivity you can achieve is a function directly of the number of bits -- and only the number of bits -- you can record phase coherently. Therefore, your end bits can be distributed in any way in the frequency domain to achieve the same detectability of sources. Your idea of distributing them over as wide a frequency range as possible is very fine. I would point out that with our relatively conventional cross-correlation techniques we are routinely doing time synchronization in the same sense that you described time synchronization, to the tenth of the sampling period interval which, for the Mark-I recording system, is in the 100- to 200-nanosecond time range. That's kind of our instantaneous level on a per-tape basis time accuracy, although we have demonstrated we can actually do it on what we call a record of data, which is two-tenths of a second of data, that is 140,000 bits; that we can achieve the same kind of accuracies if the sources are strong enough.

We also find that very frequently we can work down to things more like four or five times the rms noise level, still achieving a tenth of the sampling interval, providing that we integrate to get to those kinds of sensitivities, to take as much data as we need to do that. But we find that we can get those accuracies at the 5 sigma level rather than the 10 sigma level.

MR. MACDORAN:

There is, perhaps, a point that is not well understood by some members of the audience with regard to what it takes in the way of time synchronization.

For instance, in the results which I have sort of previewed and which are going to be given at the AGU with regard to the four centimeters in three dimensions. It is not fair to conclude that time synchronization per se was achieved at the 150 picosecond level.

The way that we have achieved the three-dimensional measurement is by the scheme that Dr. Hurd alluded to, which is a kind of synthesis process that I suppose is due mainly to Dr. Rogers at MIT. What we're doing – in the JPL work at least – is taking two windows that are separated by 40 megahertz, deriving the fringe phase at each of those two windows, and allowing those two phase patterns to beat against one another.

What one comes out with is a measure of the difference between the geometric time delay and the one that you have a priori modeled in the computer, so that you can adjust the model parameters to get the baseline parameters, for instance.

Now, each of the individual channels themselves – at least in the JPL work has been recorded at a 48-kilobit-per-second rate. So we must be able to extract that phase from each of those two channels, which are rather narrow. So what we had to do was to get the bits aligned to the sample time, which is about 21 microseconds.

So if you asked what was the time synchronization requirement for that experiment, the answer is something like ten microseconds. And on that basis of that ten microseconds we take it down and beat the two signals together and deduce a parameter which we can interpret in a geophysical sense equivalent to about one tenth of a nanosecond. And it's kind of a trick, it has a certain convenience, and it has the homely virtue that it can be done.

DR. WINKLER:

I just would like to repeat my request that if there is any operational capability anywhere nearby, that we would like to know about that. It would be extremely useful, for instance, to have traveling clocks in laboratories which have been synchronized to, let's say, 100 nanoseconds. It would be really useful in studying a number of things which are quite puzzling at the present time. That is one remark in regards to the clock synchronization.

I have another remark on the question of polar motion and UT-1 determination. And that is that it seems to me that one should look for some agreement in the scientific community about reference observatories, similar to what we actually use today as a definition of the conventional pole, the OCIs defined by location of five latitude stations. The latitude has once more been defined, and that is the origin of the international convention origin. Something like that is lacking in these more recent experiments and the consequence of that, what we are all referring to, is changes or differences of latitude, or changes or differences in UT-1.

I feel, scientifically speaking, that it would be desirable to propose and agree to a reference system for these other purposes. That would seem to me the only way that one can really study longer-period phenomena extending, let's say, over 10 years or 25 years.

DR. JOHNSTON:

Still going to the VLBI's application to the earth's rotation, interferometry has a sensitivity to absolute declination. But the parameters involved in the earth's rotation are sort of free-floating. There are three sensitive parameters: the longitude of the baseline, the right ascension of the radio source, and the universal time.

So if you want to start it, it must be a start by fiat, and I would suspect that one cannot fiat such a start until there is some degree of consistency, or an agreement on the part of

how the data is going to be taken and how it is going to be reduced. It's kind of an arbitrary thing and I would suppose one could back up, you know, and if we discover later that current applications were good enough in principle we could just back it up. Things have been backed up to 1900 for origins in the past, so I guess we could do it again.

DR. VON BUN:

I just want to make some comments on Dr. Winkler's thoughts of just a minute ago. First of all, I think we just started out, as I said before. To my knowledge, nobody had determined the polar motion with one station in six hours, and it was just a preliminary experiment to see if it worked and if so how well.

I agree with his statement but at the present time I think it's just too early to discuss this. As soon as we get some additional results from the VLBI and the laser stations, I think these questions will be resolved.

For instance, we just finished the San Andreas Fault experiment. We operated two laser stations over the last three months to determine ultimately the motion between the plates, but at the same time these measurements will be used to determine the pole motion. At the present time only relative motions are measured of course, and absolute motion will come with time, I think, maybe in two or three years, I would guess.

MR. MACDORAN:

Can you give us some inclination or some early information on how the "SAFE" experiment on the San Andreas went?

DR. VON BUN:

No, because we just finished the experiment and are collecting the data at this time. It looks like, very preliminarily, that we probably could determine the distance between the two stations to maybe 10 or 15 centimeters. It is better than we hoped for. Again, this is just the first trial run that we did this year, and we expected it would be in the 20-centimeter range but it looks like the data are better than expected. The lasers we are using right now are 20-centimeter lasers. We are bringing these instruments back – as a matter of fact they are just on their way now to be modified to a 5- or 10-centimeter range. Next year we'll send these back again, to continue the experiment. Right now I would say we are in the 15- to 20-centimeter range, safely.

MR. MACDORAN:

How well will you be able to independently confirm the accuracy of the measurements? I'd guess this is about an 800-kilometer baseline.

DR. VON BUN:

We will try to determine the distance in two or three batches and then see how they compare relative to each other. I really can't give you an exact answer to this because we haven't evaluated the data yet.

From the polar motion experiment we did, where we had lasers in the 30-centimeter range, we are coming down to the 30-centimeter accuracy in the baseline. So, assuming a linearity, I would assume if we have a 10-centimeter laser, we may come down to the 10-centimeter distance, and with a 5-centimeter laser we may come to a 5- or 10-centimeter distance.

But at the present time we just finished the experiment taking the data and no analysis has been made yet. As a matter of fact, we don't have the data here yet; we still have it at the station.

MR. MACDORAN:

Do you see an opportunity any time soon for collocation with the VLBI?

DR. VON BUN:

I hope so, because I consider this as an important experiment, because if we do something either with VLBI or with laser you will really never know what the absolute accuracy is; and I think a very good independent test will have to be made, and I hope we can soon make it, putting two lasers side by side with the VLBI system and really determining the distance between the two stations independently with both systems. We have both the laser and the VLBI capability at GSFC, so such an experiment is not a problem to us.

MR. MACDORAN:

In the Goldstone experiment we have a design featuring that experiment to compare against the National Geodetic Survey over that 16-kilometer baseline, and the National Geodetic Survey guarantees their work at the 20-centimeter level, and we have a comparison to within 12 centimeters of that. So I guess I take a little bit of issue with the strict interpretation.

DR. VON BUN:

Well, let me give you an example on the polar-motion experiment. We determine not only the polar motion but also the distance between Goddard and the station in Seneca; when we evaluated the distance, it fell exactly within the range we got from a survey, which I think is a coincidence because I just can't believe we determined the position of the two stations to 30 centimeters, and this is – in three dimensions – exactly what we got from a survey which was taken a year before the instrument was started.

DR. MCCOUBREY:

Andy, I just have a question about the very long baseline interferometry. In the discussion today I didn't hear any discussion of the possiblility that the presence of the earth between these sensors, between the antennas, may lead to effects, and I wonder if it does. The advancing plane wave must certainly be disturbed by the presence of the earth between the sensors, and I wonder if this is taken into account or if any large effects actually do occur?

MR. MACDORAN:

Well, on my bar chart, there were three separate bars that addressed that. There's something labeled ionosphere and the wet and dry troposphere. And those were phase delays, and that's the concern here rather than, say, a ray-bending type of thing.

DR. MCCOUBREY:

My question really relates more to the ray bending. Every part of the surface of the earth becomes a scattering point, and signals from those points must interfere with the advancing plane wave before it comes. . . .

MR. MACDORAN:

You mean scattering from the ground around?

DR. MCCOUBREY:

Right.

MR. MACDORAN:

Oh, well, the antennas themselves reject that to a very high degree. I mean just the natural beamwidth of the antenna itself given by the received wavelength in the aperture of the antenna will, you know, cancel out the things in the background.

You get such effects as spillover. We have a microwave receiver looking down into the optics, and there's a diffraction pattern that tends to see the ground around it and raise the system temperature, but the attenuation of the scattered signals is very far down, 30, 40, 50, 60 dB.

DR. MCCOUBREY:

These other effects you mentioned – the troposphere and the wet and dry atmosphere and so on – really lead to refractive effects, don't they?

MR. MACDORAN:

We tend to interpret it more conveniently in how the wave is slowed down rather than how it is bent, but one could make an interpretation in bending; it's just not as useful.

DR. RAMASASTRY:

I just want to comment a bit. The parabolic reflectors have a strong rejection capability as compared to the hemispheric antennas. There is definite antenna pattern, and sidelobes are a smaller fraction of the main lobe. Diffraction patterns due to ground are mainly rejected. So this is not a serious problem.

MR. CHI:

I'd like to go on to the next area, that is in the relativistic time correction. There is much talk about the measurement and the theory to prove the theory. Once the theory is proven to be correct, when or where is the correction of time needed? I'll ask Dr. Alley to discuss this.

DR. ALLEY:

I'd like to supplement some of the remarks I made this morning about the way in which one could use a traveling package of accurate clocks to distribute accurate time once one has convinced oneself that the relativistic corrections that are normally calculated do indeed describe the situation.

We have undertaken the development of a small compact package of clocks to serve not only for this possible space relativity experiment, but also to serve the USNO in actual clock trips. That is, the ability to have a very small package with the infer comparison of relative phases quite frequently as one does in the master clock system there, and have this all done automatically, would let one transmit the time with an accuracy of perhaps 100 nanoseconds over a trip of reasonable length.

Now, when you come to trying things in satellites, I point out that for Skylab the combined velocity and potential effects lead to a rate change of -3.3 parts in 10^{10} which is a change in epoch of the recording clocks of about 1.01 microsecond per hour for the orbit of Skylab (~400 km).

Now, one important aspect of the proposed space relativity experiment is that there are communication links on these manned spacecraft, namely, the frequency modulated TV link which is also used for high bit rate telemetry dumps, which has a bandwidth of about 2 megacycles. And one can readily transmit seconds ticks down. We have designed into the package a composite output which consists of 3 seconds ticks, one from each clock, clock A being 1 microsecond wide; clock B, 2 microseconds; clock C, 3 microseconds; and the rise on these pulses is very sharp. It's determined by opening a gate to let through a shape portion of the 10-megacycle rise sine wave, and we have something like a 5-nanosecond rise.

Now, the 2-megacycle bandwidth of this transmitter will limit you to something like half a microsecond rise, but receiving this pulse repeatedly, you can do a certain amount of averaging, and I think it's quite reasonable to expect 100 nanoseconds or so with that kind of a bandwidth.

Now, if you could have a wider bandwidth—which is very practical it seems for low orbit satellites—I mean, at the distances of the moon it becomes very expensive to transmit anything more, but at a few hundred kilometers very wide bandwidths are certainly possible. In fact, one could even go to optical transmitting systems—for example, semiconductor junction lasers with pulse rise times of a few hundred picoseconds – and be

able to use these transmitters to synchronize ground clocks to this accuracy as the satellite goes around. Such a technique obviously requires knowledge of the satellite distance to high accuracy so that the propagation delay can be corrected for. This is readily accomplished with laser ranging techniques. Subnanosecond-range time measurements are being routinely made in the lunar laser ranging experiment.

Now, one of the uncertainties in all of this is how the clocks perform in a zero-gravity environment, when they go into free fall, and this is practically impossible to simulate on the earth. The best you can do is turn the clocks upside down in the earth's gravitational field, do that about various axes, and we have been doing some of that, and we'll be doing more. The proposed space-flight relativity test has aroused some considerable interest at high levels in the Department of Defense for possible future systems where one might want to fly lightweight, low-power, small-volume clocks and where performance in an O-g environment is a very important aspect of such systems.

So, just to summarize, not only is it important to carry clocks out into space, get large relativistic effects, and bring them back to convince all the doubters that these effects are really there to high accuracy, but one could leave a package of clocks in orbit, and we would like to see some clocks left on-board Skylab and have some minimal power maintained, if this could be done, if the experiment could be flown, so that once the relativity measurement has been made, this kind of system can be used for distribution of time, as has been done with crystal oscillators on the Timation satellites that Roger Easton and Al Bartholomew and others have been working on.

Well, let me just stop there to see if there are questions.

DR. WINKLER:

I would like to second the comments by Professor Alley. In fact, I agree 100 percent with his first statement, the utility of knowing and being able to trust corrections to be applied for relativity effects. This capability could really be very useful. As a matter of fact, during the recent general assembly in Warsaw, the URSI assembly, just to get the discussion going I made a provocative statement which I want to repeat here, maybe to see what you have to say to that.

I believe that we will always have to have as a last calibration reference a portable atomic clock or clocks, and after the experiments done by Hefele and Keating, I want to remind you that in their analyses, as published in *Science*, the larger effect was not the performance of the clocks; it was in our ability with presently available navigation methods to exactly assess the relativity effects, even assuming that they are accurate.

In that extrapolation of the effect, or the prediction of the effect, the precision was in the order of 20 nanoseconds. Whereas the one sigma value of the agreement of these four clocks using the correlated rate-change method, as Hefele and Keating call it, there the sigmas were in the order of seven to ten nanoseconds.

So we have to keep that in mind, and I want to repeat that maybe a portable set of clocks will remain the most precise way to synchronize, to certify synchronization between any two points provided that they can really trust the theoretical relativity corrections, and that has to be established with high precision.

DR. ALLEY:

Could I just add – it is obviously essential to know the velocity and gravitational potential in which the satellite finds itself. Now, one of the very attractive features of these manned space flights is that this is all done routinely with the unified S-band system. Repeatedly one gets the range to 15 meters or so with the pseudorandom noise code, and one has the Doppler tracking to millimeters per second so limited by the atomic clocks at the tracking stations. One would have to continue keeping that information. For example, on the transfer of the seconds ticks you have got to take into account the propagation delay. That is, you've got to have a combination of radar plus clocks on board the spacecraft, and it's this combination of the two that I think lends great strength to the accuracy of time dissemination by means of satellites.

And, again, one can get the range exceedingly accurately by passive means, with ground-based lasers. It's so striking how the developments in quantum electronics keep coming up over and over again at this meeting, not only atomic clocks, but in other areas.

DR. WINKLER:

Can I add to these comments again? My only point of slight hesitancy in endorsing everything you said down to the last comma is in regards to the utility of systems. When we look for operational distribution of time, we certainly want to use a system where forever, or for the duration of the system, the bookkeeping and orbit calculations are being done routinely as they are being done in the Transit system or as they are being done even with the Timation navigation system. It is for these reasons that I feel that for operational dissemination of time to passive users, a navigational satellite system is the one to concentrate on.

Now, this does not mean that I do not agree that it would be a good idea to leave such a clock maybe on board of an experimental satellite to make these measurements, but I just want to be sure that we understand when we, as part of our conference intends to, look into the future for the design of systems and specifications of how do we want to bring time to the user, to a large number of users; I think the navigation satellite will play a very important role.

DR. ALLEY:

Yes. I think leaving a clock package on Skylab is not likely. I think it's going to be very difficult to maintain that. But I think a satellite dedicated to that purpose, perhaps along with related purposes, and continuous replacement of such satellites is going to be needed in the future.

MR. CHI:

I'd like to call on Dr. McCoubrey. In 1965 he had a very good review article on the status of frequency standards and their capability. At this time, I would like to ask him to review again and perhaps project into the future the capabilities of precise frequency sources.

DR. MCCOUBREY:

Well, I think it is useful to look backwards and see what has happened in the past several years to precise frequency sources and then perhaps to try to look ahead and see at least what the driving forces are that are going to cause the changes in the next several years and perhaps be sure that we recognize these guiding forces and know what they are.

I'm not sure I could really do a very good job of this now, but I'm sure that there are others here who will have ideas to add, and I think they should do, but in just looking back at the paper which is several years ago now, and looking at what happened, there have been some changes, of course. Many of the changes have been caused by the applications which have during that time become important in the case of all of the atomic oscillators. They've become much more reliable generally through the experience that people have had in using them and in refining the details of their operation, and I think this happens – this applies to the hydrogen masers, the rubidium oscillators and the cesium oscillators and standards.

In the case of the cesium, of course, there have been substantial advances in the direction of high performance – high performance particularly with regard to short-term stability which makes it possible to use them in relatively short periods of time, shorter periods of time.

Also, there have been advances in making them more compact, compatible with systems, such as collision avoidance systems, and a good deal of experience in using them in the environments of such systems.

I think in the past several years there have been questions; in the case of the cesium, pushing the sigma tau plots out into longer period of time, times where the parts in 10^{14} are becoming important, and I think there's a lot still to understand there – what is the true nature of the statistics, statistical performance of these standards out in these areas of a part 10^{13} out towards a part in 10^{14}; what is the physics of the operation of the system. I think there are some frontiers still to be advanced into.

In the case of the rubidium just looking at the figures we talked about this morning and where it was 5 or 6 years ago is a little easier to do. Five or six years ago we didn't have the heart of the rubidium standard separated from the rest of the electronics that make it into a useful frequency standard–it's power supply and things of that sort. So, one can't make a direct comparison, but it is possible to compare a rubidium frequency standard of that day with what's available now, and at that time 1000

cubic inches was roughly what was available in the smallest configuration that you could plug into the wall and use as a frequency standard.

Now, you can do the same thing with something that's about 750 cubic inches. I'm talking about a little more than the modular oscillator, but that has a standby battery in it which will operate for a couple of hours, and so I think probably the volume has come down effectively by a factor of two or so. The weight should certainly come down by a factor of two on the same basis.

Cost in the rubidium case has come down more than it has in the other cases – to perhaps three-quarters of what it was five or six years ago.

In the case of hydrogen, it's harder for me to comment. I think Harry Peters has done this very well. Certainly there have been a lot of refinements that relate to the convenience of using them and the confidence in what they do. Refinements involving the automatic turning of the cavity to correspond to the frequency of the maser oscillations, nominal frequency of the hydrogen resonance; there's been a good deal of advance in their reliability, and I think generally this has come out of the experience in working with them and in making the changes dictated by this experience – generally, engineering changes.

I think there remains a good deal to do as far as the wall shift is concerned in gaining more confidence in the stability of this wall shift. There is good evidence now to the effect that it has remained constant for a number of years, but a larger volume of measurements is certainly necessary.

One other matter comes up in looking backwards, and that's the question of what new inventions have occurred in this area, and I'm not sure, but I don't think any of them have been mentioned during the day yet. The one that occurs to me involves the methane stabilized laser, and I think in a few minutes it might be interesting to ask the Bureau of Standards people – either Dave Allen or Roger Beeler to comment on the status of that.

But I'd just like to comment on the importance of it. Certainly this is an important step in linking – coherently linking the radio spectrum to the infrared spectrum, and it holds out the prospect for linking the radio spectrum right into the optical spectrum. I'm sure this has many important consequences, only one of which is the possibility for a single length and time standard.

I think I'm going to leave those comments now and try to look ahead a little bit and ask – or raise the question of: Just what are the driving forces which are going to cause the changes in the future? I feel that there's no pressing need for new advances or new inventions in any case. There's much to do in terms of application and the refinements of the present technology which is available. I think the emphasis is certainly going to be on the applications and the choice of a right type of a precision oscillator, the right configuration of that type of oscillator to do a particular job with particular applications.

Certainly it will become more important for systems, particularly those that will require a large number of precision oscillators. It will become more important for attention to be given to this question of how much does it cost to run one for an hour. And, or run one for a year, or whatever length of time that is important in this application. In the case of satellites, for the lifetime of the satellites.

As far as cost is concerned, it seems to me that it's really a question of: What is the scale of the application? How many are going to be used? Actually, if you consider a frequency standard or precision oscillator, there's really less technology in it than there is in a television set, and the only difference I think really is in the scale of the application, and that scale is cetainly going to affect the advances towards lower costs, smaller sizes, and so on.

Other questions of advances which may be desirable or necessary: In the case of rubidium, I think it would be desirable to see a better understanding of the aging effects. It's my own opinion there are several physical effects involved there, some depending on the physics of the situation, others depending on the chemistry of the situation. And, while I think advances would be desirable, I don't think the application of the rubidium standards is in any way contingent upon these advances, and the applications will occur even with the technology as it stands insofar as aging is concerned.

I think the rubidium standard is going to be a contender for many of the applications of quartz crystal oscillators in the past. I mentioned one figure this morning I think which may be a little bit in error that I learned later, namely, this question of warm-up time, the rubidium oscillator can warm up very rapidly now, and I think this morning I suggested perhaps the state-of-the-art is such that a rubidium oscillator can be warmed up, up to 1000 times faster than a quartz oscillator. Since this morning, I have discovered that Hewlett-Packard has quartz oscillators that warm up in 30 minutes to within a part in 10^9.

In the case of the hydrogen maser, I've already mentioned the wall shift. I think more understanding of the wall shift is going to be more important and those resources that can be applied to this question should lead to a clarification.

I'd like to suggest that we ask Roger Beehler or Dave Allen to say something about the status of that methane-stabilized laser.

DAVID ALLEN:

Helman Helwig at the Bureau of Standards has published some results on that and his results at that time which were superior to any stability results of any oscillator. And that was essentially stability to one part 10^{13} in a sample time of ten seconds.

Since then, some better stability results have been achieved, but interestingly enough these have been in nonquantum electronic standards. Stein and Ewer at Stanford, using a superconducting niobium cavity have achieved stabilities better than this with an X-band source. In the future, this appears to be a real competitor.

The methane device, of course, has a very impressive stability, and one has to ask the question, "How can you use it?" At this date, doing synthesis in the optical or the infrared is very difficult. This undoubtedly will improve as time goes on and is improving right now. But currently you can't really utilize it.

I would like to, if I may, backtrack a little on Dr. Winkler's comment regarding portable clocks and whether or not you always need to rely upon this system. If you look at systems in general, the optical region of the spectrum is the one with the greatest bandwidth and has some extremely impressive promise in my mind. If you look at a portable clock, all it is, is a portable transmitter, and you use a coaxial cable to propagate the signal. The stabilities in the optical are very impressive, say, from satellite distances. The corner reflected signal from the moon is at such a large distance that using it decreases your signal-to-noise quite significantly, but, if you had a corner reflector on a satellite; and if you fully utilized, say, synthesis using methane-stabilized lasers in the optical region, to me the assumptions of reciprocity in this region might lead to future time-synchronization methods in the subnanosecond region. Theoretically this seems achievable, so this is kind of a projection on your comment that perhaps the ultimate system will be a portable clock on a satellite.

MR. BEEHLER:

NBS is about ready, we hope, to go into an operational phase on our new NBS five-frequency standard. Now, of course, this is far different from anything we've been talking about here today, because this is a sub-20-foot-long ultimate cesium standard which is designed strictly for laboratory standards use.

But, in terms of performance, it is also perhaps the kind of ultimate in that we envision an absolute accuracy for this device of one part in 10^{13} and a 1-second stability of about two parts in 10^{13}. The standard is put together, it is under vacuum; we are, we think, within a few days of observing the first beam in the standard.

MR. CHI:

I'd like to take this opportunity to thank the panel members, the authors of the papers, and the audience. I also want to remind you that one reason we have these discussions is in the hope that we can exchange knowledge and viewpoints between the users and the people who actually generate frequency and time. I'd now like to turn the meeting over to Mr. Wardrip.

MR. WARDRIP:

My thanks to you, Andy, and also to the speakers and panel members of today's session, and, of course, the audience.

SESSION II

Frequency Stabilities and Communications

TRANSIT IMPROVEMENT PROGRAM TIMING EXPERIMENTS

Lauren J. Rueger
The Johns Hopkins University

ABSTRACT

The most recent TRANSIT satellite launched introduces new system timing capabilities of the Navy Navigation Satellite System. The characteristics of these features are described and the results of in-orbit experiments relating to precision time measurements are given in this classified paper.

Anyone interested in obtaining a copy of the paper may make a request to The Johns Hopkins University/Applied Physics Laboratory.

INTERMEDIATE TERM FREQUENCY MEASUREMENTS WITH THE HP COMPUTING COUNTER IN THE USNO CLOCK TIME SYSTEM

Gernot M. R. Winkler
U.S. Naval Observatory

I. INTRODUCTION

High precision frequency measurements with various integration times τ can be made with conventional counters by using variable gate times. The Hewlett-Packard (HP) computing counter allows such measurements over a very wide range of frequencies and measurement times. This instrument can also convert period measurements into frequency by means of its arithmetic capabilities: The program library contains programs to facilitate frequency stability measurements $[\sigma_y(\tau)]$ in the most direct and convenient way.

An important limitation exists, however, in that measurement intervals are restricted to $\tau < 100$ seconds.

For long measurement intervals ($\tau \geqslant 1$ day), conventional phase difference recording provides a simple and economic frequency measurement capability at described frequencies (Reference 1).

At the USNO this method was used as the basis for all time scale computations (Reference 2), until requirements for highest resolution justified the development of an automatic data acquisition system as described by K. Putkovich (Reference 3). The phase measurements are now being made with the HP computing counter (with time interval plug-in unit) under program control from the HP "System Programmer," which in turn is interfaced with an IBM "1800" system. The "1800" controls the coaxial switch system through which the start and stop signals can be directed to the time interval meter.

Each phase measurement consists of an average of 256 individual measurements. This allows such a precision of measurement and a flexibility of operation that evaluation of frequency standards and clocks can be performed on line for $\tau > 100$ seconds, thereby closing the gap mentioned above.

This paper will discuss details of this phase measurement technique and its application in the evaluation of precision oscillators.

II. PHASE MEASUREMENTS WITH THE TIME INTERVAL UNIT (HP COMPUTING COUNTER, MODEL 5360)

1. The "Fly-Back" Subroutine

Successive phase measurements that are to be averaged must be checked against the previous measurement (φ-) to avoid averaging of widely divergent values near the "zero" or "full-period" point. The flow chart of our "fly-back" subroutine is shown in Figure 1. It occupies locations 160-200 in the system programmer and is called after every time interval measurement which contributes to an average. P is the period used (one second for tick-to-tick, 2×10^{-7} seconds for five-MHz signals) and is entered through the "external data" (switch) input.

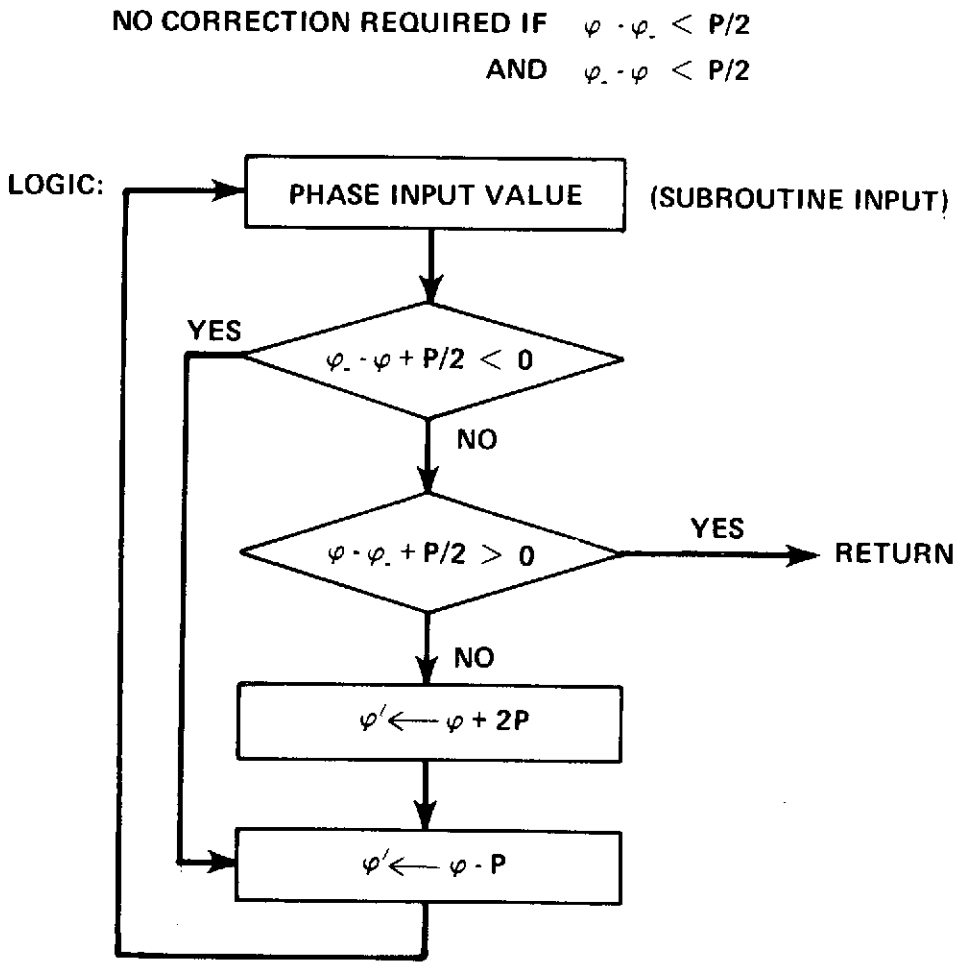

Figure 1. Fly-back subroutine.

2. Trigger Level Instability

The "start" and "stop" trigger levels are set at zero for phase measurements. Even very small additive noise will, however, contribute to measurement scatter. In order to minimize this noise contribution, five-MHz signals for phase measurements are used. Figure 2 compares time interval measurement scatter as a function of rise time (frequency of the sine wave input).

During preliminary performance tests, significant differences between our HP 5360 counters became evident. Table 1 summarizes our computing counters as far as it is pertinent to this report.

	Sine Waves 1 V_{rms}		
	100 khz	1 MHz	5 MHz
Peak to peak variation of Δt (10^4 samples)	2.8	1.0	0.7
σ of these p-p values	0.5	0.1	0.2
σ ($\overline{\Delta t}$)	0.4	0.14	0.1

Figure 2. Measurement scatter of a short time interval Δt as a function of rise time (taken with SER #863) (values in nanoseconds, Δt = 10).

Table 1
HP 5360 Counters in Use at the USNO.

Serial No.	Application
312	Used in preliminary tests until April 1972. Low calibration noise. Warranty repair of display module.
603	Used by Hefele and Keating in their global clock experiments. Average noise. (Resolution 10^{-15} in 1/2 day.) Presently on line.
863	Used as "system unit" May to October 1972. High calibration noise (10^{-14} in 1/2 day).
1048	Warranty repair (high noise level).

3. Quantization and Interpolator Noise (Q&I)

The resolution of a simple time interval measurement with the HP 5360 is 0.1 nanosecond. Since two interpolators provide input to the time interval routine, a naive expectation would be that Q&I noise could contribute as much as four nanoseconds peak to peak, if the interpolators are fully stabilized. Table 2 was derived with counter #312. A comparison of the computed σ (average) with the actually measured σ (by measuring a number of groups of n measurements each) indicates the presence of long-term instability which cannot be improved upon with our 256 measurement averaging routine.

The operational program which we use allows the collection of both calibrator readings (nominal value 1000 ± 1) during each measurement cycle as a routine check of the counter. Figures 3 and 4 give samples of calibrator readings of counter #863. It is evident that particularly "N2" is affected by additional noise. Figures 5 and 6 give the corresponding probability density functions and the power spectrum. The noise is white and nearly Gaussian (note the small side peak of N1). The power spectrum is given in relative values over a time period in days.

It should be emphasized that this additional noise encountered is the worst case we saw.

Counter #312 (Table 2) performed about ten times better. Figure 7 gives an updated version of Figure 6 of Reference 2 and is based on the measured σ of an average of 256 measurements as listed in Table 2. The presently used Counter #603 is only slightly inferior in the actual performance (10^{-15} in 1/2 day, Figure 8).

4. Cycle Resolution

The choice for five-MHz signals for the phase measurements was dictated by the desire to minimize trigger level noise contribution. A price to be paid for this benefit is the rather short period of only 200 nanoseconds. The Observatory has adopted the positive cycle crossover as the time reference mark; one-pulse-per-second ticks are used to identify a particular cycle. Caution must be exercised, however, in the use and adjustment of all

Table 2
Measured Time Delays of a Four-Foot RG58 Cable
With a One-MHz Signal From an HP Rubidium Oscillator

Number of Measurements (picosec)	$\overline{\Delta t}$	σ	$(\sigma AV)^{Comp}$	$(\sigma AV)^{Meas}$
40	6819	65	19	47
400	6809	75	3.5	7
4K	6805	76	1.00	3.5
40K	6811	77	0.33	4.2
400K	6813	77	0.1	2.3

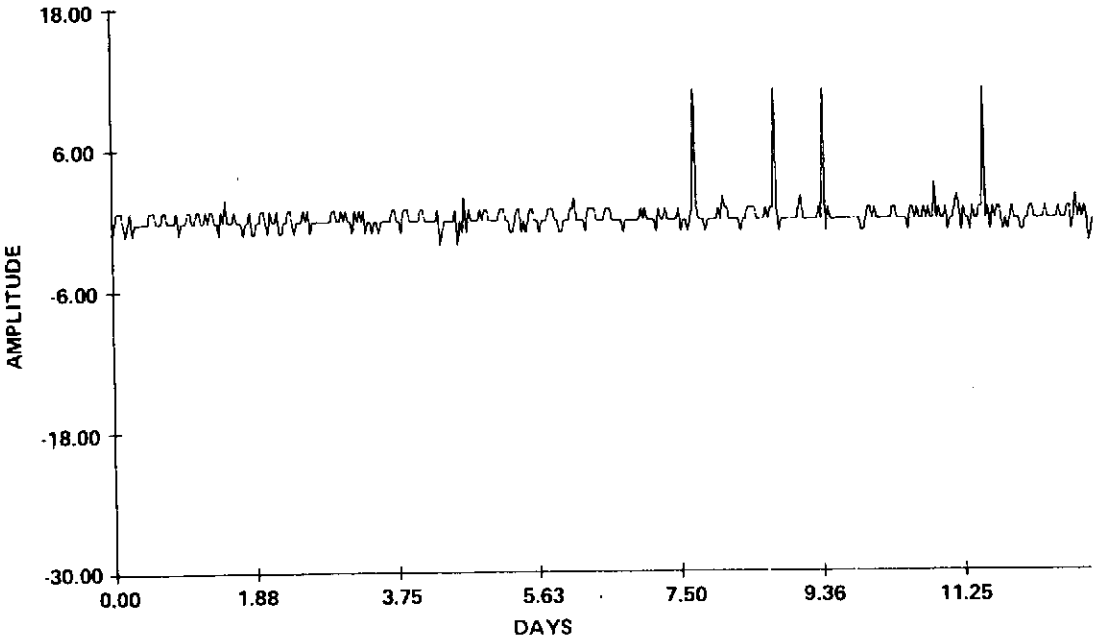

Figure 3. N1 calibration.

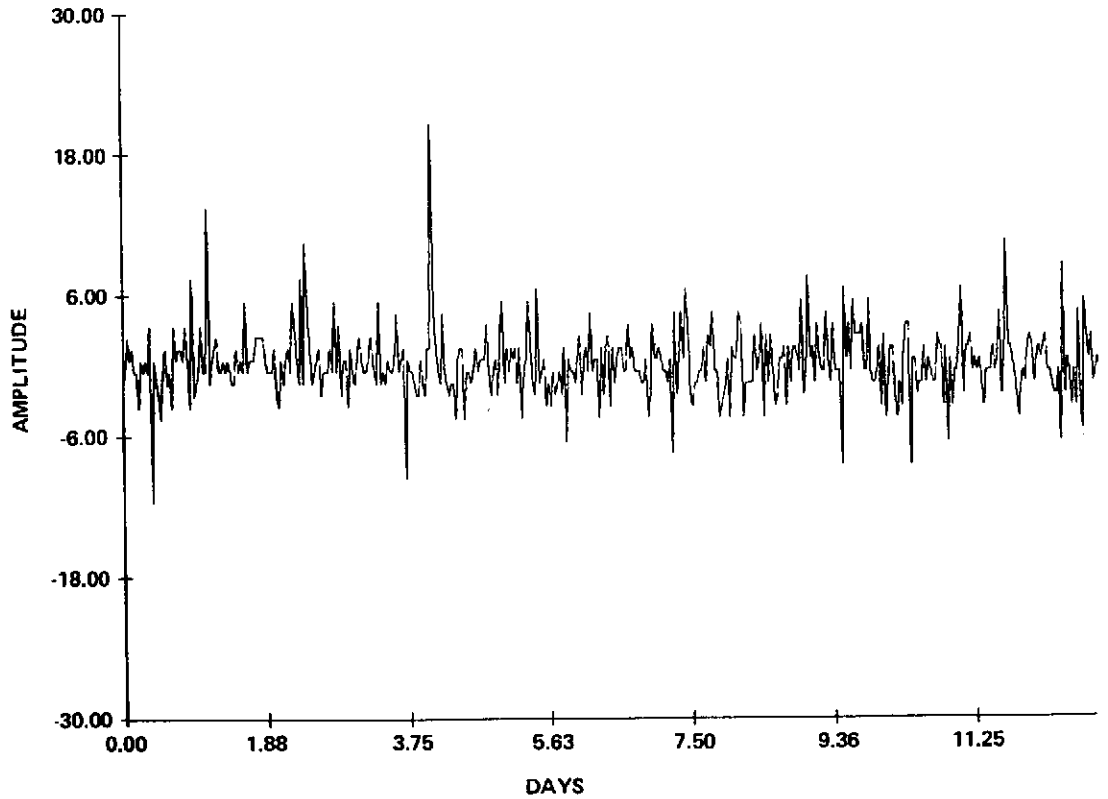

Figure 4. N2 calibration.

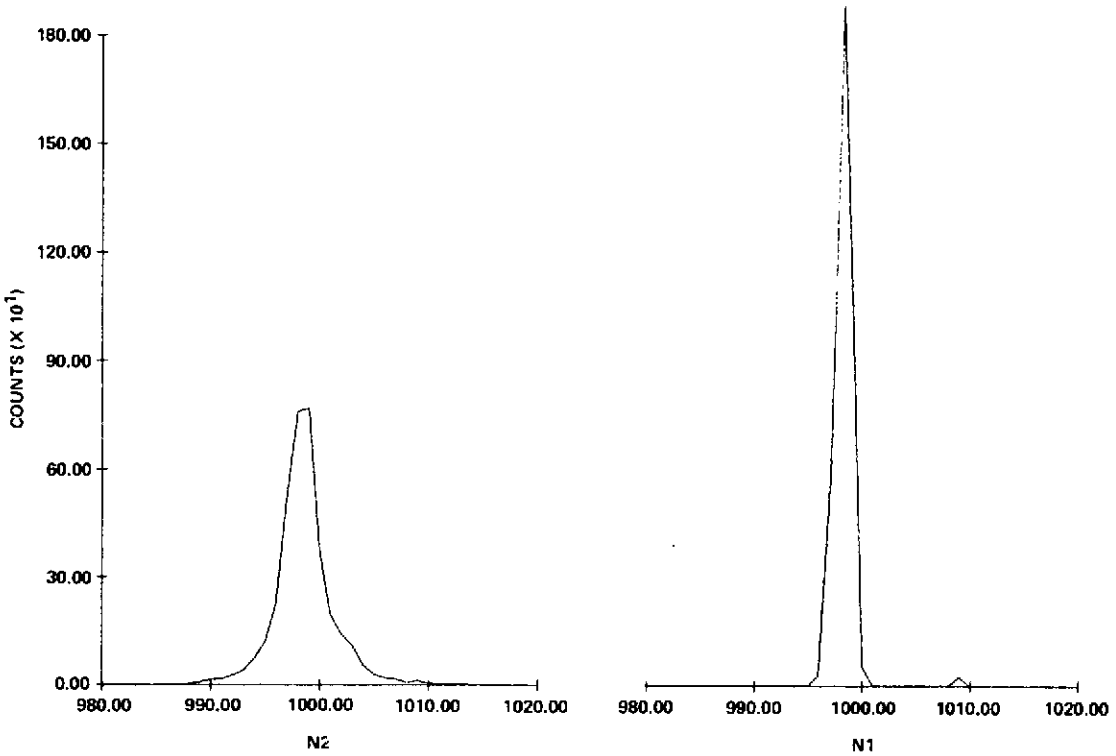

Figure 5. N2, N1 frequency distribution.

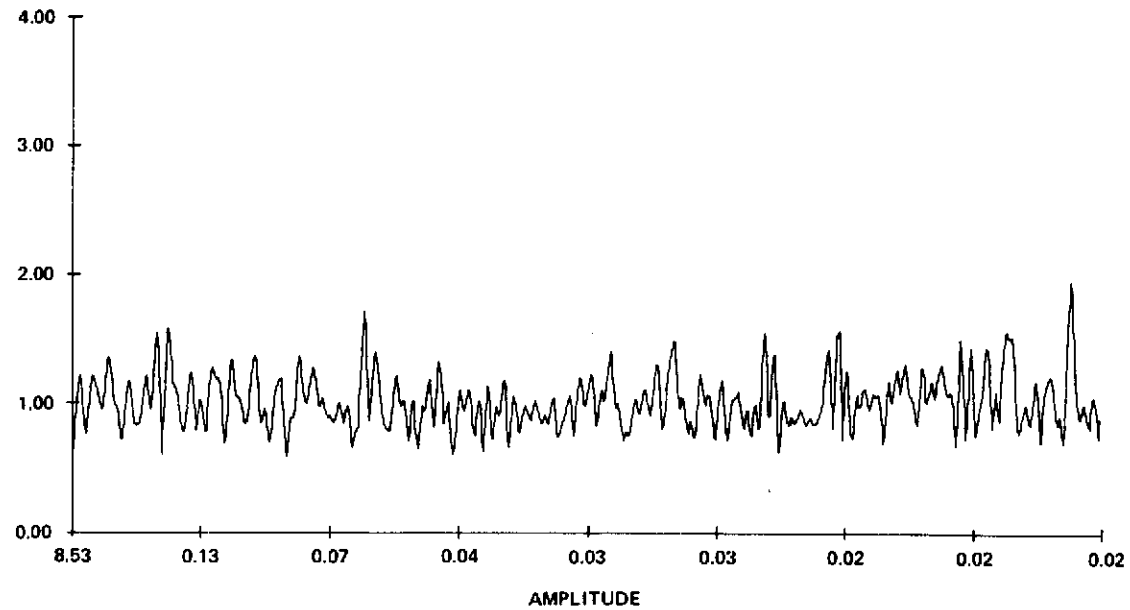

Figure 6. N2 calibration.

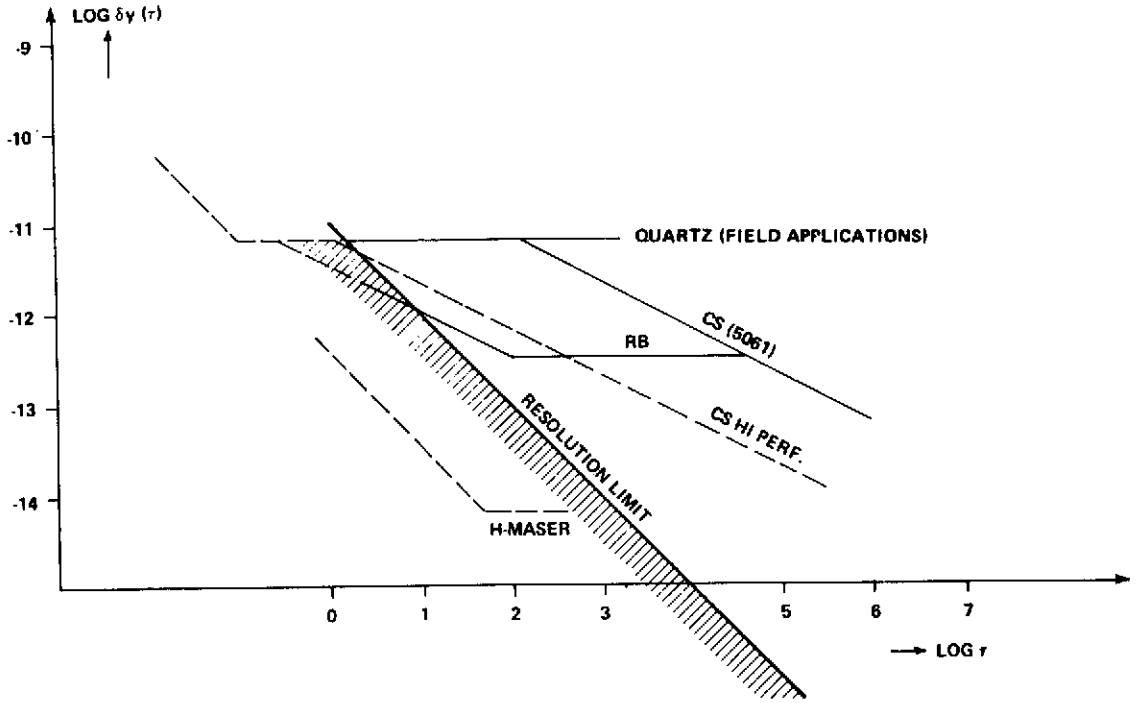

Figure 7. Schematic of expected limit of resolution in comparison with clock performances.

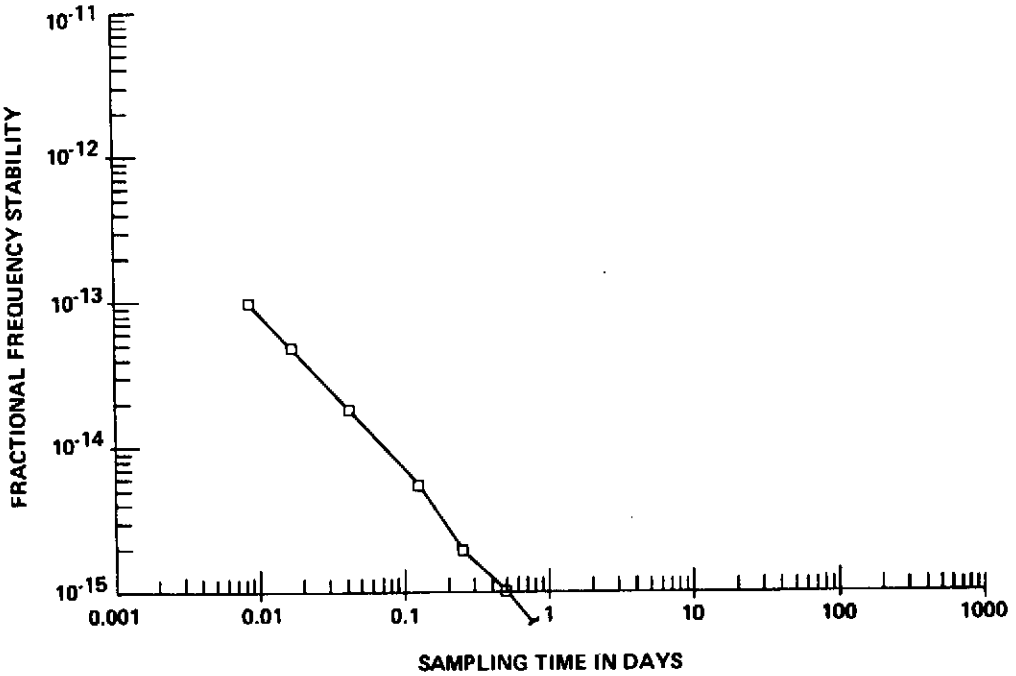

Figure 8. Overall system noise with counter #603.

distribution amplifiers in the system. Figure 9 gives an example of variations in the tick-to-phase relationship of our former reference system #2 (it has since been replaced with an improved version similar to system #1). These tick-to-phase measurements are simple (not averaged) data points. The interpolator noise, if present, enters in full magnitude in this case.

III. EXAMPLES OF SIGMA-TAU MEASUREMENTS

The present data collection at the USNO is programmed for a full measurement cycle of all clock differences and environmental parameters every hour on the hour. This measurement takes about four minutes. Each average of 256 phase-to-phase measurements takes about 1/2 second. The more time-consuming measurements are the tick measurements, where only 16 are being made for each average (17 seconds each). The tick-to-phase measurements are presently single.

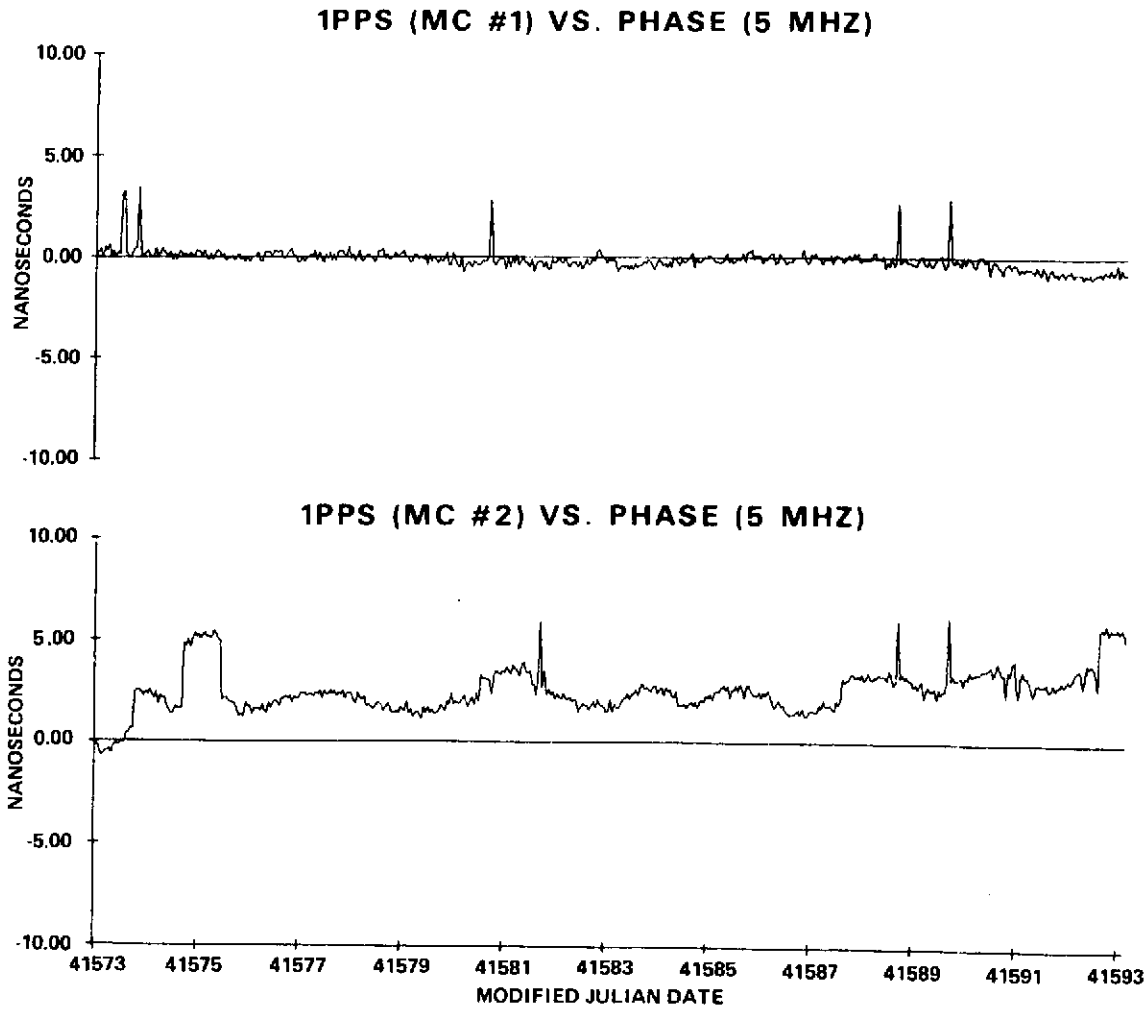

Figure 9. Examples of variations in the tick-to-phase relationship.

1. Experimental Scan

In addition to the above, a fast scan of 1 X 10 measurements is being done every 720 seconds (five times per hour). The NP4 hydrogen maser, on loan from the Goddard Space Flight Center (H. Peters design), was used as the "start" input against itself through a cable loop (for noise-level checks of the overall system) and against about ten other "stop" signals. This is a fast measurement (six seconds), and it allows stability measurements of clocks entirely independent of the USNO time scale. The reference signal has recently been replaced with the H-10 USNO maser.

As explained in Reference 2, the USNO clock time scale "MEAN (USNO)" is computed in five-day intervals. Its purpose is the provision of a clock time scale of superior reliability and long-term stability. Within the five-day intervals, however, the low frequency filtering inherent in the iterative procedure (Reference 2, Appendix) loses its effectiveness as we go to shorter averaging times τ.

For stability measurements $\sigma(\tau)$ where a hydrogen maser can be considered superior, direct comparisons of the clock with a hydrogen maser will produce reliable estimates of this clock's frequency stability. In cases where we deal with clocks of comparable performance, we can evaluate them in groups of three. By measuring rate variations of pairs of clocks (1 and 2, 2 and 3, 3 and 1) and by allowing for the contribution of the system noise (expressed as variance σ_N^2), one can solve the equations as listed in Figure 10.

In practice, several problems arise. First, one must use data which are homogeneous for the whole set; i.e., they must be collected nearly simultaneously. Second, one should expect frequent failures (imaginary results) due to the statistical variance in the measured estimates of $\sigma(\tau)$. One should not include clocks of widely different performance if the noise is high. Thirdly, one must realize that the environment is never perfect nor are the clocks truly stationary in their behavior. Any comparison of performance must take into account these factors. Nevertheless, this method can give consistent estimates of $\sigma(\tau)$.

MEASURED:

$$\sigma^2_{1,2}(\tau) = \sigma^2_{11} + \sigma^2_{22} + \sigma^2_{NOISE}$$

$$\sigma^2_{2,3}(\tau) = \sigma^2_{22} + \sigma^2_{33} + \sigma^2_{NOISE}$$

$$\sigma^2_{3,1}(\tau) = \sigma^2_{33} + \sigma^2_{11} + \sigma^2_{NOISE}$$

COMPUTED:

$$\sigma_{11} = \sqrt{\frac{\sigma^2_{12} + \sigma^2_{13} - \sigma^2_{23} - \sigma^2_{N}}{2}}$$

ETC.

Figure 10. Frequency stability measurements with clock triplets.

2. Examples

Examples of $\sigma(\tau)$ measurements (defined according to Reference 1) are given in Figures 11-13 taken with computing counter #863, and in Figure 14, from computing counter #603. Estimates of individual stabilities are listed in Table 3.

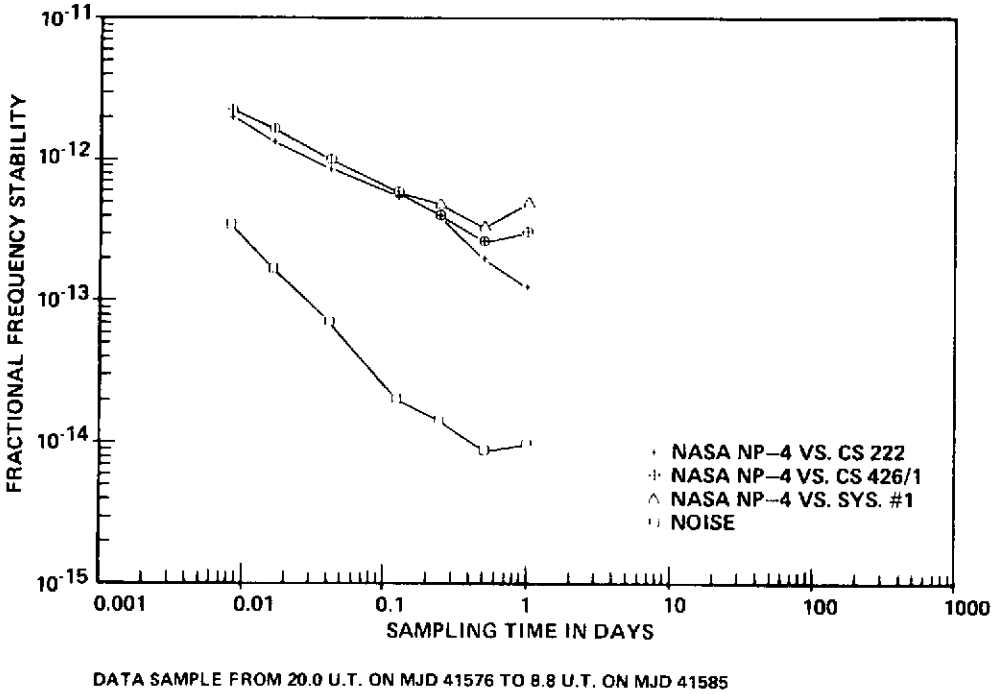

Figure 11. Frequency stabilities measurements – set 1.

Table 3
$\sigma(\tau)$ of Six Oscillators

Sec	Days	NP4 (NASA)	Cs(HP) 431	Rb(HP) 272	Cs(HP) 549	Cs(HP) 426	H_{USNO}	Noise
720	0.008	(0.9)	3.66	1.9	11.7	21.3	-⩽0.06	3.35
1,440	0.017	0.7	2.3	1.4	8.2	15.7	-⩽0.06	1.62
3,600	0.042	0.5	1.6	1.7	9.5	9.5	-⩽0.06	0.62
10,800	0.125	0.3	0.9	1.8	3.8	5.6	⩽0.06	0.19
21,600	0.250	0.3	0.7	2.0	2.2	3.8	0.1	0.14
43,200	0.500	0.3	0.5	2.0	2.4	0.2	0.08	
86,400	1.000	(0.4)	0.6	2.0	1.0	(0.6)		

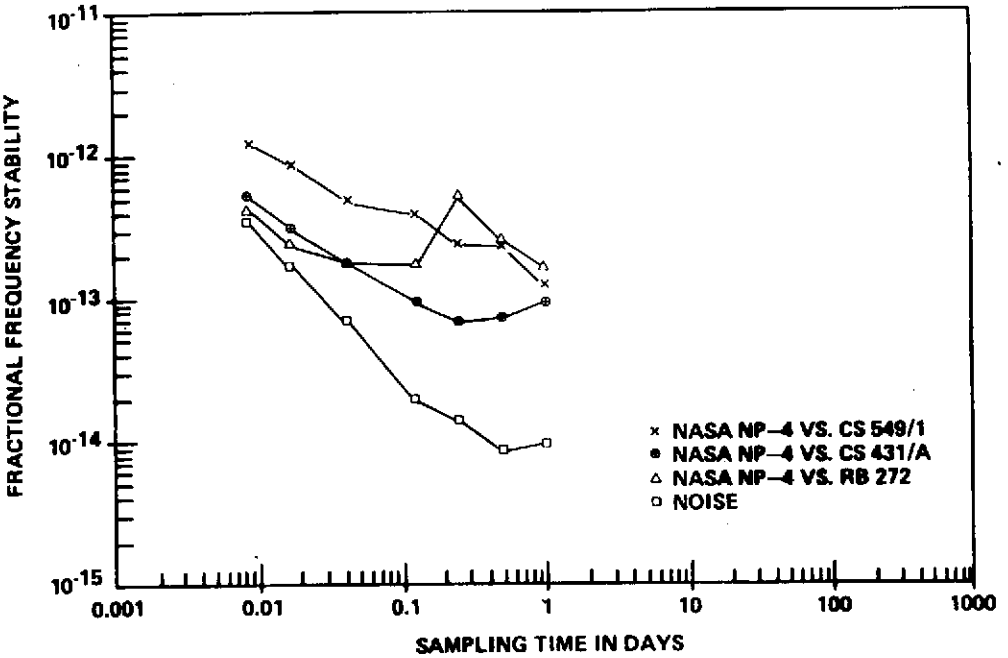

Figure 12. Frequency stabilities measurements – set 2.

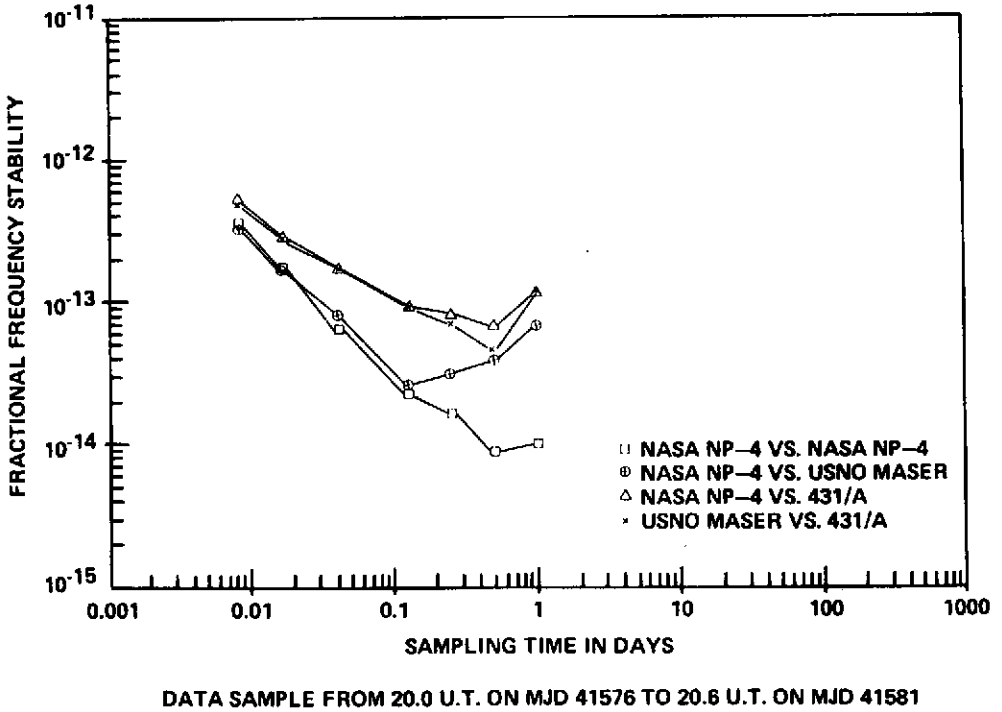

Figure 13. Frequency stabilities measurements – set 3.

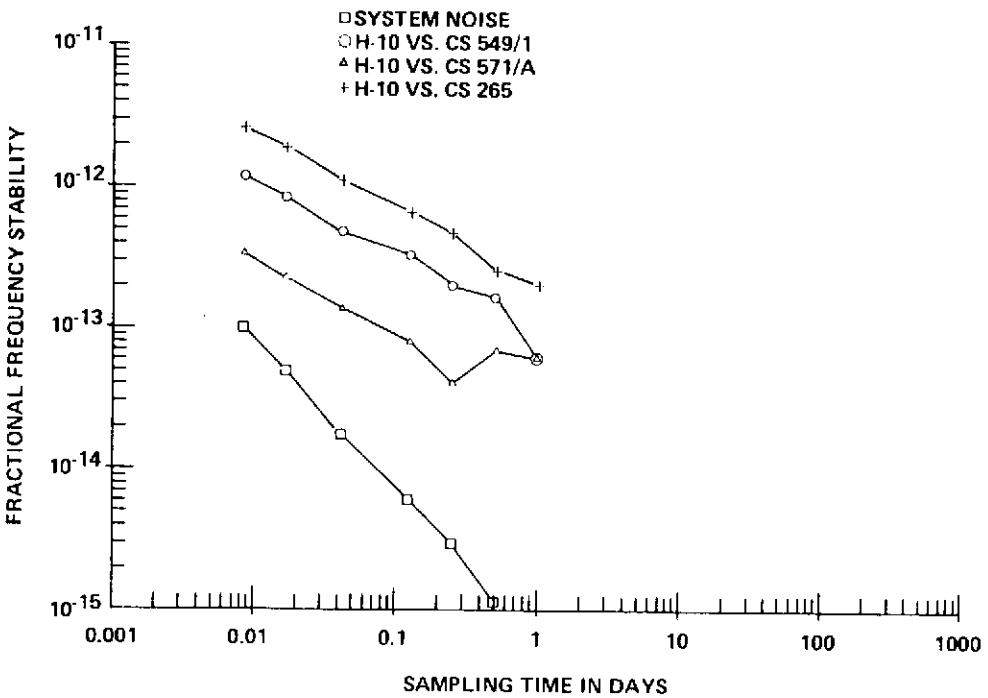

Figure 14. Frequency stabilities measurements – computing counter #603.

The routines used in preparing the $\sigma(\tau)$ plots mentioned above also include a tabulation of variances for the parameter $N \neq 2$ in order to allow for another indication of the noise type actually affecting the clock performance as originally discussed by David Allan (Reference 4). Almost all the practical utility of such stability parameters seems to reside, however, in the column labeled N = 2 (Tables 4 and 5).

IV. DISCUSSION AND CONCLUSIONS

The practical results of the stability measurements described can be summarized (at least for the commercially available cesium and rubidium clocks) in two parameters, if we restrict our interest to "clock" applications (we ignore "spectral purity") for $\tau > 100$ seconds.

The first parameter κ_s describes an oscillator's performance in the (Gaussian & White) FM region according to the model

$$\sigma(\tau) = \frac{\kappa_s}{\tau_s} \qquad \text{(Reference 2, p. 128)}$$

Table 4
Results of Sigma Computations
for USNO Maser versus 431/A (Old High-Performance Cesium).

τ (days)	N = 2 RMS Sigma		N = 4 RMS Sigma		N = 8 RMS Sigma	
	Complete Groups	($\times 10^{-13}$)	Complete Groups	($\times 10^{-13}$)	Complete Groups	($\times 10^{-13}$)
0.017	150	2.74	75	2.66	37	2.67
0.042	60	1.74	30	1.68	15	1.63
0.125	20	0.90	10	0.94	5	0.93
0.250	10	0.72	5	0.69	2	1.05
0.500	5	0.44	2	1.01		

Data sample from 20.0 UT on MJD 41576
to 20.6 UT on MJD 41581

Reduced on November 8, 1972.

Computing Counter No. 863.

Table 5
Results of Sigma Computations
for H-10 versus CS 571/A (New High-Performance Cesium).

τ (days)	N = 2 RMS Sigma		N = 4 RMS Sigma		N = 8 RMS Sigma	
	Complete Groups	($\times 10^{-13}$)	Complete Groups	($\times 10^{-13}$)	Complete Groups	($\times 10^{-13}$)
0.017	255	2.24	127	2.23	63	2.20
0.042	102	1.36	51	1.33	25	1.31
0.125	34	0.79	17	0.72	8	0.85
0.250	17	0.40	8	0.65	4	0.75
0.500	8	0.68	4	0.74	2	0.75

Data sample from 8.2 UT on MJD 41634
to 21.0 UT on MJD 41642

Reduced on November 25, 1972

Computing Counter No. 603

The second parameter is value τ_F, where the $\sigma(\tau)$ plot levels off into a flicker noise performance. (We know that for a very large τ, all clocks will show noise behaviors that correspond to models of even larger dispersion, random walk FM, "drift" noise, etc.)

In general then, we found evidence that aging of atomic standards will increase κ_s. We also found that inclement environmental conditions (except vibration, which also increases κ_s) will only reduce τ_F. Table 6 attempts to give representative values for these parameters.

Table 6
The Parameters κ_s and τ_F
(τ_F,' refers to less than ideal environments).

Clock	κ_s	τ_F	τ_F
Rb HP #272	5.3×10^{-12}	1/2 day	1/2 hour**
Cs HP #265 (5060, 1967 vintage with original beam tube)	7×10^{-11}	20 days	Unknown
Cs HP #549 (5061, vintage 1972)	3.2×10^{-11}	10 days	5 days***
Cs HP #431 (5061, with Hi-Perf tube, 1-1/2 years old)	1×10^{-11} *	10 days	1/2 day**
HP #571 (5061 with option 04) new	8×10^{-12}	10 days***	1 day***

*Cs 431 achieved $1.- \times 10^{-14}$ for τ = 10 days in Spring 1972 ($\kappa_s = 9.3 \times 10^{-12}$).

**The main cause of this poor showing is temperature sensitivity.

***Insufficient data.

V. ACKNOWLEDGEMENT

I owe all data preparation to D. B. Percival, and all of the indispensable hardware design and operation to K. Putkovitch, both of the USNO.

REFERENCES:

1. J.A. Barnes, et al., "Characterization of Frequency Stability," *IEEE Transactions on Instrumentation and Measurement*, vol. IM-20 (May 1971), pp. 105-20.

2. G.M.R. Winkler, R.G. Hall, and D.B. Percival, "The USNO Clock Time Reference and the Performance of a Sample of Atomic Clocks," *Metrologia*, 6 (no. 4, October 1970), pp. 126-34.

3. K. Putkovich, "Automated Timekeeping," *IEEE Transactions on Instrumentation and Measurement*, vol. IM-21, (November 1972). pp. 40-405.

4. David W. Allan, "Statistics of Atomic Frequency Standards," *Proc. IEEE*, vol. 54 (no. 2, February 19, 1966). pp. 221-30.

OPERATIONAL STABILITY OF RUBIDIUM AND CESIUM FREQUENCY STANDARDS

John E. Lavery
Goddard Space Flight Center

INTRODUCTION

In the course of testing various rubidium and cesium frequency standards under operational conditions for use in NASA tracking stations, about 55 unit-years of relative frequency measurements for averaging times from 10 to 10^7 s have been accumulated at Goddard Space Flight Center (GSFC). Statistics on the behavior of rubidium and cesium standards under controlled laboratory conditions have been published by many institutions (see example, Ref. 1), but it was not known to what extent the lesser controlled environments of NASA tracking stations affected the performance of the standards. The purpose of this report is to present estimates of the frequency stability of rubidium and cesium frequency standards under operational conditions based on the data accumulated at GSFC.

Table 1.
Atomic Frequency Standards Used
in Experiments.

Serial no. or designation	Manufacturer
Rb 107	Varian Associates
Rb 136	Varian Associates
Rb 138	Varian Associates
Cs 110	Hewlett-Packard Co.
Cs 136	Hewlett-Packard Co.
Cs 137	Hewlett-Packard Co.
Cs 138	Hewlett-Packard Co.
Cs 139	Hewlett-Packard Co.
Cs 152	Hewlett-Packard Co.
Cs 182	Hewlett-Packard Co.
Cs 185	Hewlett-Packard Co.
Cs 186	Hewlett-Packard Co.
HM:	
H-10 no. 2	Varian Associates
NX-1	(a)

[a]An experimental hydrogen maser developed at GSFC. See Ref. 2.

DATA DESCRIPTION

The three rubidium gas cells (designated Rb) and nine cesium beam frequency standards (Cs) on which the measurements were made, as well as the two hydrogen masers (HM) used as references for many of the tests, are listed in Table 1 along with their serial numbers or designations and their manufacturers. During the tests the standards were kept in a laboratory at GSFC. Except for the shielding built into the standards themselves, there was no special control of the ambient magnetic, electric, vibration, and temperature conditions. The ambient magnetic and electric conditions were typically noisy. The standards were driven by ac power and were in no way isolated by transformers. Vibration from nearby air-conditioning equipment and from trucks at a nearby loading platform was not shielded in any way. The ambient temperature was typically between 298 and 303 K. There were, however, several brief excursions to temperatures as low as 291 K and as high as 313 K, due to equipment problems. These conditions are less controlled than those in the NASA tracking stations. Hence the stabilities of the standards when operating in the tracking stations should be at least as good as the stabilities calculated in this paper.

The measurements made on the standards consisted of average relative frequency measurements for varying averaging times. In some of the data sets, average relative frequency measurements were missing or were bad because of ac power failure or recorder failure. All such points were a posteriori linearly interpolated from the nearest earlier (in epoch time) good average relative frequency measurement and the nearest later (in epoch time) good average relative frequency measurement.

The total number of measurements made for all types of data used in this report is given in Table 2. Data sets are said to be of the same type when the following parameters are the same for each set: test unit,[1] reference unit, duration or averaging time τ_0 of each average relative frequency measurement, and dead time d between successive measurements (that is, the time during which no measurement was taken). The servo time constants are indicated only for the cesium standards and only when $\tau_0 \leqslant 1000$ s. The difference in effect of a 10- and a 60-s time constant for $\tau_0 \leqslant 3600$ s can be neglected because the time constants in such cases are too small with respect to standards to have an appreciable effect. The rubidium standards tested all have a fixed servo time constant which is on the order of 1 ms.

Neither temperature effects nor long-term frequency drift was removed from the data before analysis because the object of the tests was to measure the stability of the frequency standards under operational conditions, where both temperature flucuations and long-term frequency drift are present.

[1] Although there are sometimes significant differences in the frequency stabilities of various rubidium standards, the three rubidium standards listed in Table 1 all had mutually close stabilities. For this reason, these rubidium standards will be considered to be identical. Because the nine cesium standards listed in Table 1 all had mutually close stabilities, they too will be considered to be identical.

Table 2
Average Relative Frequency Data Sets.

Type of data				Number of data sets m	Number of measurements	
Test unit	Reference unit	Averaging time τ_0, s	Dead time d, s		Total[a]	Interpolated
Rb	Rb	3 600	0.0	2	3 090	0
Rb	Cs (10-s TC)	10	2.3	1	1 076	18
Rb	Cs (10-s TC)	100	2.2	1	538	1
Rb	Cs (10-s TC)	1 000	2.7	1	223	0
Rb	HM	10	2.3	13	8 473	67
Rb	HM	100	2.2	10	6 405	16
Rb	HM	1 000	2.7	9	5 126	15
Rb	HM	3 600	.0	7	13 320	308
Cs	Cs	3 600	.0	3	8 851	263
Cs (10-s TC)	HM	10	.2	8	4 841	0
Cs (10-s TC)	HM	100	.2	8	4 871	11
Cs (10-s TC)	HM	1 000	.2	8	4 787	25
Cs (60-s TC)	HM	10	.2	8	4 634	0
Cs (60-s TC)	HM	10	2.3	3	1 904	2
Cs (60-s TC)	HM	100	.2	8	4 706	0
Cs (60-s TC)	HM	100	2.2	3	2 496	0
Cs (60-s TC)	HM	1 000	.2	8	4 804	3
Cs (60-s TC)	HM	1 000	2.7	1	692	0
Cs	HM	3 600	.0	13	37 404	1391
Cs	HM	604 800	.0	1	88	6

TC = time constant.
[a]Total number of measurements for all m data sets, including the interpolated measurements.

STATISTICAL ANALYSIS

Let there be given a set of m identical test frequency standards and a set of m identical reference frequency standards. Let ϕ_n (t), $1 \leqslant n \leqslant m$, denote the instantaneous fluctuations (measured in time units) of the epoch time output of the nth reference standard. Let y_n (t) be the instantaneous (fractional) frequency fluctuation of the nth test standard compared with the nth reference standard; i.e.,

$$y_n(t) \equiv \frac{d\phi_n(t)}{dt} \qquad (1$$

Let $\bar{y}_n$ (t) be the average relative (fractional) frequency fluctuation of the nth test standard compared with the nth reference standard:

$$\bar{y}_n(t) = \frac{1}{\tau}\int_t^{t+\tau} y_n(t)\,dt = \frac{\phi_n(t+\tau) - \phi_n(t)}{\tau} \qquad (2$$

The constant τ is called the averaging time of y(t). The Allan standard deviation $\sigma(2, T, \tau)$ of the frequency fluctuations of the set of test standards compared with the set of reference standards is defined to be (Ref. 3)

$$\sigma(2, T, \tau) = \sqrt{\frac{1}{m}\sum_{n=1}^{m} \langle \text{var}\,[\bar{y}_n(t+T) - \bar{y}_n(t)]\rangle} \qquad (3$$

where the symbol $\langle\ \rangle$ denotes infinite epoch time average. The analysis of all data listed in Table 2 consisted in the calculation of an estimate, which is denoted by $s(2, T, \tau)$ in th following manner.

Taking any type of data from Table 2, let the number of average relative frequency measurements in the nth data set, $1 \leqslant n \leqslant m$, be m_n. Denote this nth set of average relative frequency measurements by $y_n(i)_{i=1}^{m_n}$. For $i = 1, 2, \ldots, m_n - 1$, denote the variance of the two average relative frequency measurements $y_n(i)$ and y

$$v_n(i) = \frac{[\bar{y}_n(i+1) - \bar{y}_n(i)]^2}{2} \qquad (4$$

The square root of the average over both i ($1 \leqslant i \leqslant m_n - 1$) and n ($1 \leqslant n \leqslant m$) of these $v_n(i)$ is the desired estimate of $\sigma(2, \tau_0 + d, \tau_0)$:

$$s(2, \tau_0 + d, \tau_0) = \sqrt{\frac{\sum_{n=1}^{m}\sum_{i=1}^{m_n-1} v_n(i)}{\sum_{n=1}^{m}(m_n - 1)}} \qquad (5$$

From the original data sets $y_{n\ i=1}^{m_n}$, $1 \leqslant n \leqslant m$, new data sets with averaging time $\tau_1 = 2\tau_0$ and dead time d (assumed small with respect to τ_0) can be approximated by defining

$$\bar{y}_n(i; 1) = \frac{\bar{y}_n(i+1) + \bar{y}_n(i)}{2} \tag{6}$$

$i = 1, 2, \ldots, m_n - 1$ and $n = 1, 2, \ldots, m$. Denote the variance of $y_n(i; 1)$ and $y_n(i + 2; 1)$ by $v_n(i; 1)$:

$$v_n(i; 1) = \frac{[\bar{y}_n(i+2; 1) - \bar{y}_n(i; 1)]^2}{2} \tag{7}$$

$i = 1, 2, \ldots, m_n - 3$ and $n = 1, 2, \ldots, m$. Estimate $\sigma(2, \tau + d, \tau_1)$ by[2]

$$s(2, \tau_1 + d, \tau_1) = \sqrt{\frac{\sum_{n=1}^{m} \sum_{i=1}^{m_n - 3} v_n(i; 1)}{\sum_{n=1}^{m} (m_n - 3)}} \tag{8}$$

Let k be the exponent of the largest power of 2 contained in any of the m_n, $1 \leqslant n \leqslant m$. For $j = 2, 3, \ldots, k - 1$, the data set $\{\bar{y}_n(i; j)\}_{i=1}^{m_n - 2^j + 1}$ with averaging time $\tau_j = 2^j \tau_0$ and dead time d is successively calculated from the data set $\{\bar{y}_n(i; j-1)\}_{i=1}^{m_n - 2^{j-1} + 1}$ by pairwise averaging:

$$\bar{y}_n(i; j) = \frac{\bar{y}_n(i + 2^{j-1}; j-1) + \bar{y}_n(i; j-1)}{2} \tag{9}$$

$i = 1, 2, \ldots, m_n - 2^j + 1$; $n = 1, 2, \ldots, m$; j fixed. Denote the variance of $\bar{y}_n(i; j)$ and $\bar{y}_n(i + 2^j; j)$ by $v_n(i; j)$:

$$v_n(i; j) = \frac{[\bar{y}_n(i + 2^j; j) - \bar{y}_n(i; j)]^2}{2} \tag{10}$$

[2]Throughout this paper the convention is adopted that whenever a summand, e.g., $m_n - 3$ in $\sum_{n=1}^{m} (m_n - 3)$, is less than zero, it is treated as zero; and whenever a summation, e.g., $\sum_{i=1}^{m_n - 3} v_n(i; 1)$, has an upper limit that is less than the lower limit, it also is treated as zero.

$i = 1, 2, \ldots, m_n - 2^{j+1} + 1$ and $n = 1, 2, \ldots, m$. Estimate $\sigma(2, \tau_j + d, \tau_j)$ by

$$s(2, \tau_j + d, \tau_j) = \sqrt{\frac{\sum_{n=1}^{m} \sum_{i=1}^{m_n - 2^{j+1}+1} v_n(i; j)}{\sum_{n=1}^{m} (m_n - 2^{j+1} + 1)}} \tag{11}$$

An example of this procedure for zero dead time is presented in Figure 1. The quantity v represents the variance between the ordinates of the two lines to which the dotted line near v points.

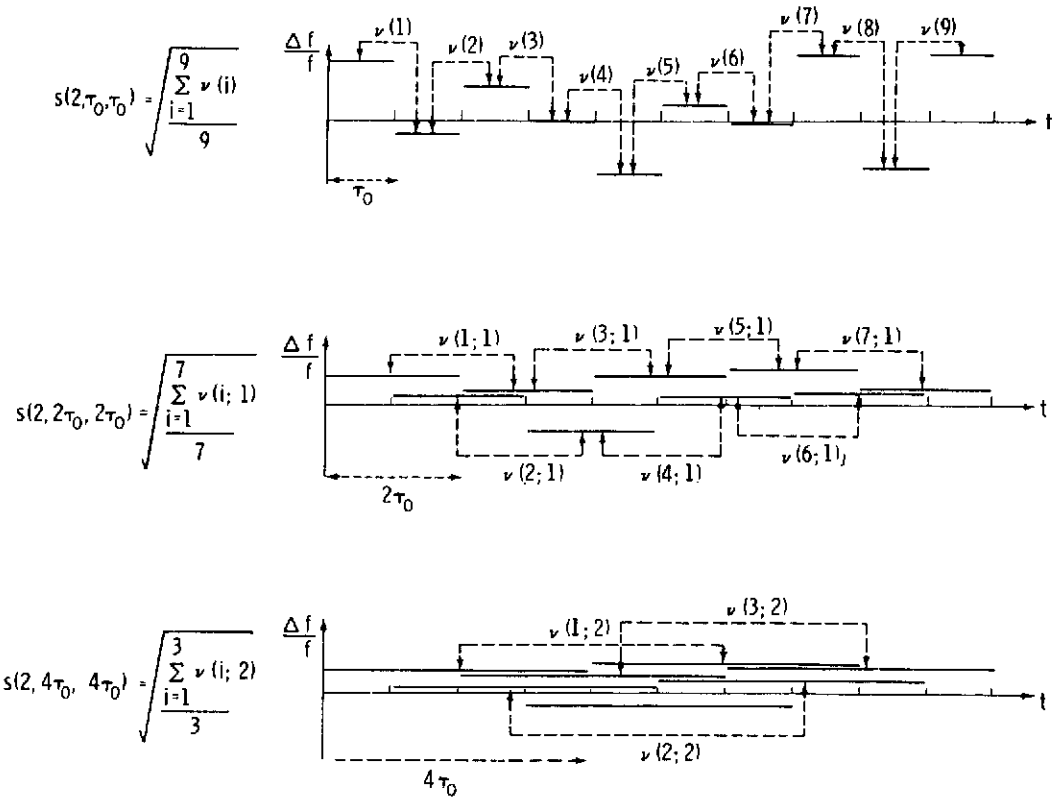

Figure 1. Calculation of $s(2,\tau,\tau)$.

RESULTS

For each type of data listed in Table 2 and for each averaging time $\tau_j = 2^j\tau_0$, $0 \leq j \leq k - 1$ (τ_0 and k change with the type of data), the estimate $s(2, \tau_j)$ of $\sigma(2, \tau_j + d, \tau_j)$ was calculated.[3] The results are presented in Table 3 and Figure 2 for all data involving a rubidium standard as either the test or the reference unit and in Table 4 and Figure 3 for the cesium versus cesium and cesium versus hydrogen maser data.

In order to use the data in Tables 3 and 4 to estimate the frequency stability of the rubidium and cesium standards tested, rather than the relative frequency stability of a comparison of two of these standards or of a comparison of one of these standards to a hydrogen maser, the following procedure is used. Denote the Allan standard deviations of the test standard versus a hypothetical perfect standard, the reference standard by $\sigma_T(2, \tau + d, \tau)$, $\sigma_R(2, \tau + d, \tau)$, and $\sigma_{T\text{-}R}(2, \tau + d, \tau)$ respectively. Because the variances $\sigma_T^2(2, \tau + d, \tau)$ and $\sigma_2(2, \tau + d, \tau)$ are linear functions (in fact, weighted integrals) of the respective power spectral densities of the test and reference standards (Ref. 3); and because the power spectral density of the comparison of two frequency standards is the sum of the power spectral densities of each of the standards, the following relation occurs:

$$\sigma_{T\text{-}R}^2(2, \tau + d, \tau) = \sigma_T^2(2, \tau + d, \tau) + \sigma_R^2(2, \tau + d, \tau) \tag{12}$$

For comparisons of two identical standards (rubidium standard versus rubidium standard and cesium standard versus cesium standard), $\sigma_R(2, \tau + d, \tau) = \sigma_T(2, \tau + d, \tau)$. Hence, from relation (12),

$$\sigma_T(2, \tau + d, \tau) = \frac{\sigma_{T\text{-}R}(2, \tau + d, \tau)}{\sqrt{2}} \tag{13}$$

For all data for which a hydrogen maser was used as a reference, it is assumed that the instabilities of the maser were sufficiently small so as to have

$$\sigma_T(2, \tau + d, \tau) \approx \sigma_{T\text{-}R}(2, \tau + d, \tau) \tag{14}$$

The normalized standard deviation $\sigma_T(2, \tau, \tau)$ can be calculated from $\sigma_T(2, \tau + d, \tau)$ by the relation

$$\sigma_T(2, \tau, \tau) = \frac{\sigma_T(2, \tau + d, \tau)}{\sqrt{B_2(r, \mu)}} \tag{15}$$

where $B_2(\tau, \mu)$ is a bias function (defined in ref. 4); $\tau = (\tau + d)/\tau$; and μ, representing the type of noise of the standard for the fixed averaging time τ and fixed dead time d, is determined from

$$\sigma_T(2, \tau + d, \tau) \propto \tau^{\mu/2} \tag{16}$$

[3]The analysis was carried out by programs E00016 and E00036 of the GSFC Computer Program Library. Program E00016 is for input relative phase data; program E00036 is for input relative frequency data. Although program E00016 reads relative phase data as input, its output is the Allan Standard deviation of relative frequency $s(2, \tau_j + d, \tau_j)$ defined in eqs. (5), (8), and (11). These two programs are based on a program written by David W. Allan of the National Bureau of Standards, Boulder, Colo.

Table 3.
Rubidium Standard Frequency Stability

Type of data				$s(2, \tau + d, \tau)$, $\times 10^{-12}$	Type of data				$s(2, \tau + d, \tau)$, $\times 10^{-12}$	Type of data				$s(2, \tau + d, \tau)$, $\times 10^{-12}$
Test unit	Reference unit	τ, s	d, s		Test unit	Reference unit	τ, s	d, s		Test unit	Reference unit	τ, s	d, s	
Rb	Rb	3 600	0.0	1.128			3 200	2.2	2.023			3 200	2.2	1.881
		7 200	.0	.874			6 400	2.2	1.405			6 400	2.2	1.447
		14 400	.0	.991			12 800	2.2	.708			12 800	2.2	.877
		28 800	.0	1.254			25 600	2.2	.387			25 600	2.2	.783
		57 600	.0	1.481	Rb	Cs (10-s TC)	1 000	2.7	4.015	Rb	HM	1 000	2.7	1.057
		115 200	.0	1.542			2 000	2.7	2.736			2 000	2.7	.917
		230 400	.0	1.493			4 000	2.7	2.092			4 000	2.7	.782
		460 800	.0	1.559			8 000	2.7	1.553			8 000	2.7	.677
		921 600	.0	1.893			16 000	2.7	1.310			16 000	2.7	.721
		1 843 200	.0	2.211			32 000	2.7	1.466			32 000	2.7	.829
Rb	Cs (10-s TC)	10	2.3	32.092			64 000	2.7	1.950			64 000	2.7	.717
		20	2.3	26.099	Rb	HM	10	2.3	22.844			128 000	2.7	.857
		40	2.3	18.610			20	2.3	29.558			256 000	2.7	1.011
		80	2.3	12.680			40	2.3	39.497	Rb	HM	3 600	.0	2.633
		160	2.3	9.782			80	2.3	31.205			7 200	.0	2.783
		320	2.3	6.584			160	2.3	5.432			14 400	.0	2.691
		640	2.3	4.452			320	2.3	5.673			28 800	.0	2.368
		1 280	2.3	3.902			640	2.3	2.404			57 600	.0	1.867
		2 560	2.3	5.389			1 280	2.3	1.945			115 200	.0	1.740
		5 120	2.3	10.868			2 560	2.3	1.125			230 400	.0	1.784
Rb	Cs (10-s TC)	100	2.2	9.972	Rb	HM	100	2.2	12.655			460 800	.0	1.629
		200	2.2	7.746			200	2.2	8.568			921 600	.0	1.637
		400	2.2	5.708			400	2.2	5.308			1 843 200	.0	1.700
		800	2.2	4.177			800	2.2	3.877			3 686 400	.0	2.788
		1 600	2.2	2.723			1 600	2.2	2.587			7 372 800	.0	4.549

Table 4.
Cesium Standard Frequency Stability.

Type of data				$s(2, \tau + d, \tau)$, $\times 10^{-12}$	Type of data				$s(2, \tau + d, \tau)$, $\times 10^{-12}$	Type of data				$s(2, \tau + d, \tau)$, $\times 10^{-12}$
Test unit	Reference unit	τ, s	d, s		Test unit	Reference unit	τ, s	d, s		Test unit	Reference unit	τ, s	d, s	
Cs	Cs	3 600	0.0	1.825			256 000	0.2	.190	Cs (60-s TC)	HM	1 000	0.2	2.199
		7 200	.0	1.266	Cs (60-s TC)	HM	10	.2	5.391			2 000	.2	1.523
		14 400	.0	.918			20	.2	4.524			4 000	.2	1.099
		28 800	.0	.728			40	.2	4.510			8 000	.2	.790
		57 600	.0	.594			80	.2	4.529			16 000	.2	.590
		115 200	.0	.546			160	.2	4.140			32 000	.2	.435
		230 400	.0	.579			320	.2	3.149			64 000	.2	.360
		460 800	.0	.616			640	.2	2.287			128 000	.2	.343
		921 600	.0	.440			1 280	.2	1.786			256 000	.2	.375
		1 843 200	.0	.333			2 560	.2	1.201	Cs (60-s TC)	HM	1 000	2.7	3.885
		3 686 400	.0	.352	Cs (60-s TC)	HM	10	2.3	6.080			2 000	2.7	2.963
Cs (10-s TC)	HM	10	.2	14.269			20	2.3	5.321			4 000	2.7	2.170
		20	.2	11.743			40	2.3	5.582			8 000	2.7	1.542
		40	.2	8.941			80	2.3	5.875			16 000	2.7	1.042
		80	.2	6.508			160	2.3	5.912			32 000	2.7	.672
		160	.2	4.721			320	2.3	5.039			64 000	2.7	.409
		320	.2	3.232			640	2.3	3.636			128 000	2.7	.262
		640	.2	1.886			1 280	2.3	2.217			256 000	2.7	.340
		1 280	.2	1.484			2 560	2.3	1.943	Cs	HM	3 600	.0	1.777
		2 560	.2	1.740	Cs (60-s TC)	HM	100	.2	4.149			7 200	.0	1.249
Cs (10-s TC)	HM	100	.2	6.014			200	.2	3.687			14 400	.0	.923
		200	.2	4.332			400	.2	2.962			28 800	.0	.732
		400	.2	3.090			800	.2	2.144			57 600	.0	.615
		800	.2	2.166			1 600	.2	1.535			115 200	.0	.572
		1 600	.2	1.616			3 200	.2	1.072			230 400	.0	.566
		3 200	.2	1.218			6 400	.2	.760			460 800	.0	.570
		6 400	.2	.936			12 800	.2	.580			921 600	.0	.556
		12 800	.2	.690			25 600	.2	.595			1 843 200	.0	.555
		25 600	.2	.388	Cs (60-s TC)	HM	100	2.2	5.699			3 686 400	.0	.590
Cs (10-s TC)	HM	1 000	.2	1.934			200	2.2	5.535			7 372 800	.0	.612
		2 000	.2	1.413			400	2.2	4.840	Cs	HM	604 800	.0	.464
		4 000	.2	1.073			800	2.2	3.690			1 209 600	.0	.337
		8 000	.2	.838			1 600	2.2	2.750			2 419 200	.0	.239
		16 000	.2	.729			3 200	2.2	1.931			4 838 400	.0	.181
		32 000	.2	.674			6 400	2.2	1.318			9 676 800	.0	.167
		64 000	.2	.481			12 800	2.2	1.003			19 353 600	.0	.114
		128 000	.2	.459			25 600	2.2	.883					

It is of interest to note that for the τ and μ of the data analyzed in this report, $B_2(\tau, \mu)$ differs from unity by less than 0.1 percent and can be ignored. Hence, for the data in this report,

$$\sigma_T(2, \tau, \tau) \approx \sigma_T(2, \tau + d, \tau) \tag{17}$$

Of course, relation (17) is an exact equality whenever $d = 0$.

Using the estimates $s(2, \tau + d, \tau)$ of $\sigma_{T\cdot R}(2, \tau + d, \tau)$ from Figures 2 and 3 in relations (13) and (14) and using relation (17), the standard deviations $\sigma_T(2, \tau, \tau)$ of the rubidium and cesium standards tested can be estimated. These estimates of $\sigma_T(2, \tau, \tau)$ are presented in Figure 4 as the "operational environment" curves. Also shown in Figure 4 are curves taken from References 1 and 5 representing the performance of rubidium and cesium standards in a "controlled environment." By "controlled environment" is meant an experimental environment shielded from magnetic, electric, vibration, and temperature effects much more than the "operational" environment in which the data presented in Figures 2 and 3 were taken.[4] The upper curve for rubidium standards under a controlled environment in Figure 4 is taken from Reference 5 and represents the measured performance of Varian rubidium standards under controlled conditions. The lower curve for rubidium standards under a controlled environment and the curve for cesium standards under a controlled environment in Figure 4 are taken from Reference 1 and represent the measured performance of Hewlett-Packard rubidium and cesium standards under controlled conditions.

CONCLUSIONS

From Figure 4 it is apparent that an operational environment degrades the performance of the rubidium standards (by up to one order of magnitude) for frequency averaging times between 10 and 10^3 s and that it degrades the performance of the cesium standards (by up to one order of magnitude) for frequency averaging times between 3×10^4 and 2×10^7 s. For all other averaging times in the range covered by the data in Figure 4, the stabilities of the standards are not degraded by the operational conditions.

ACKNOWLEDGEMENTS

Special credit is due to S. C. Wardrip and John H. Roeder who obtained all the relative frequency data used in this report. Thanks are due to Andrew R. Chi who supervised this program of relative frequency data acquisition as well as to Harry E. Peters, Thomas E. McGunigal, and Edward H. Johnson who operated the experimental hydrogen masers.

[4]For Reference 1, these conditions were verified by G. M. R. Winkler (private communication). It is assumed that the data presented in Reference 5 were obtained in a similarly controlled environment.

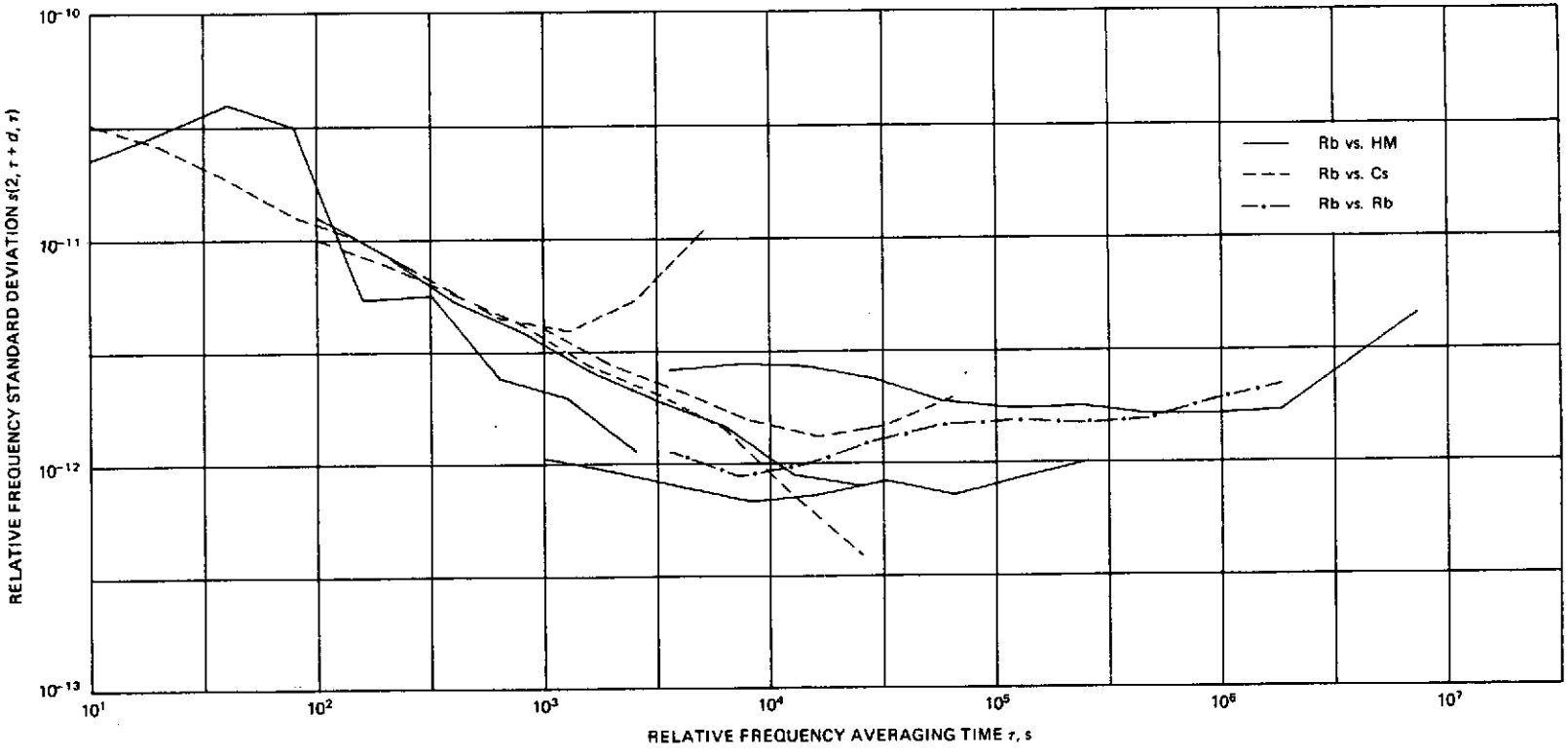

Figure 2. Rubidium standard relative frequency stability.

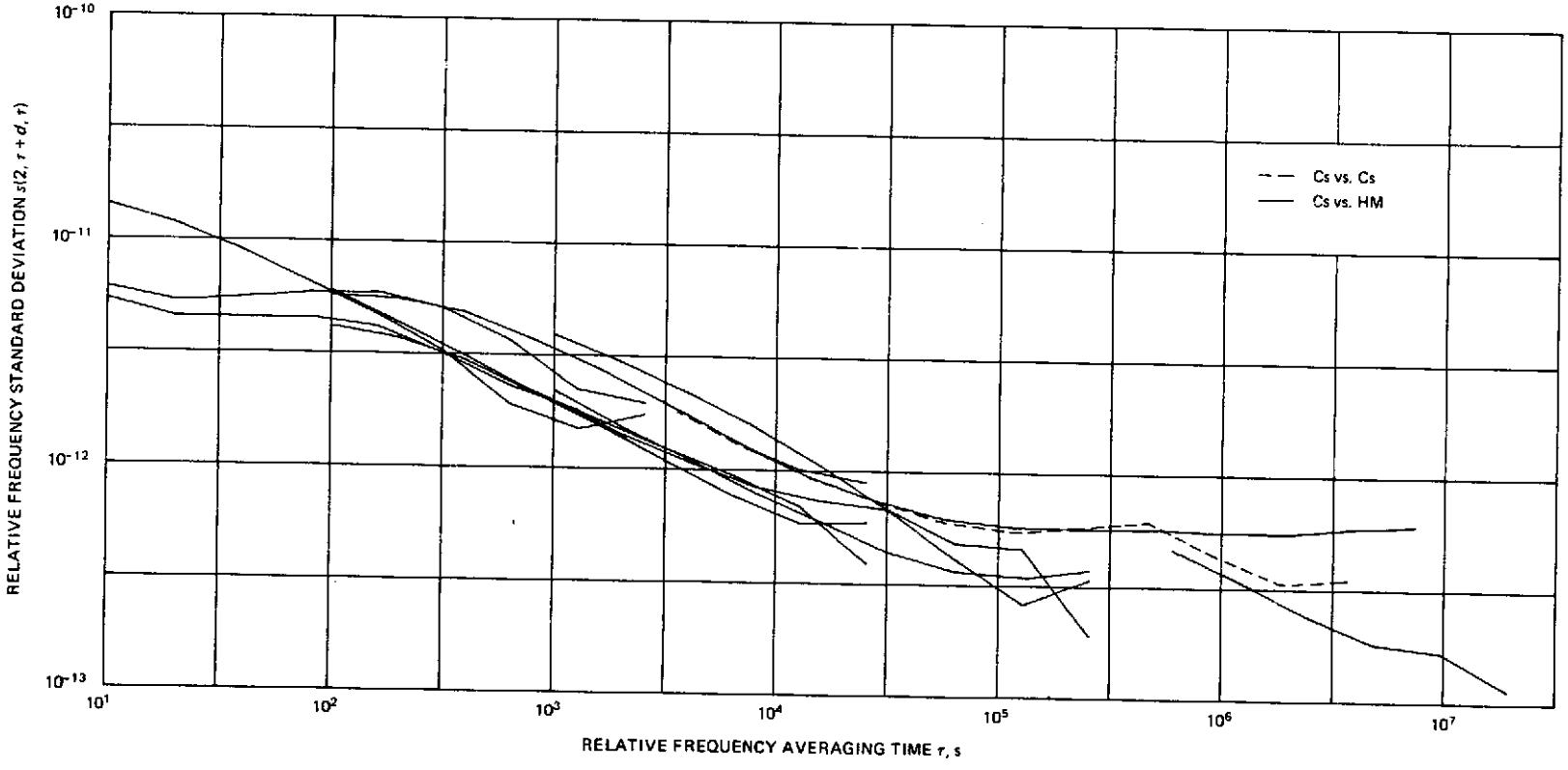

Figure 3. Cesium standard relative frequency stability.

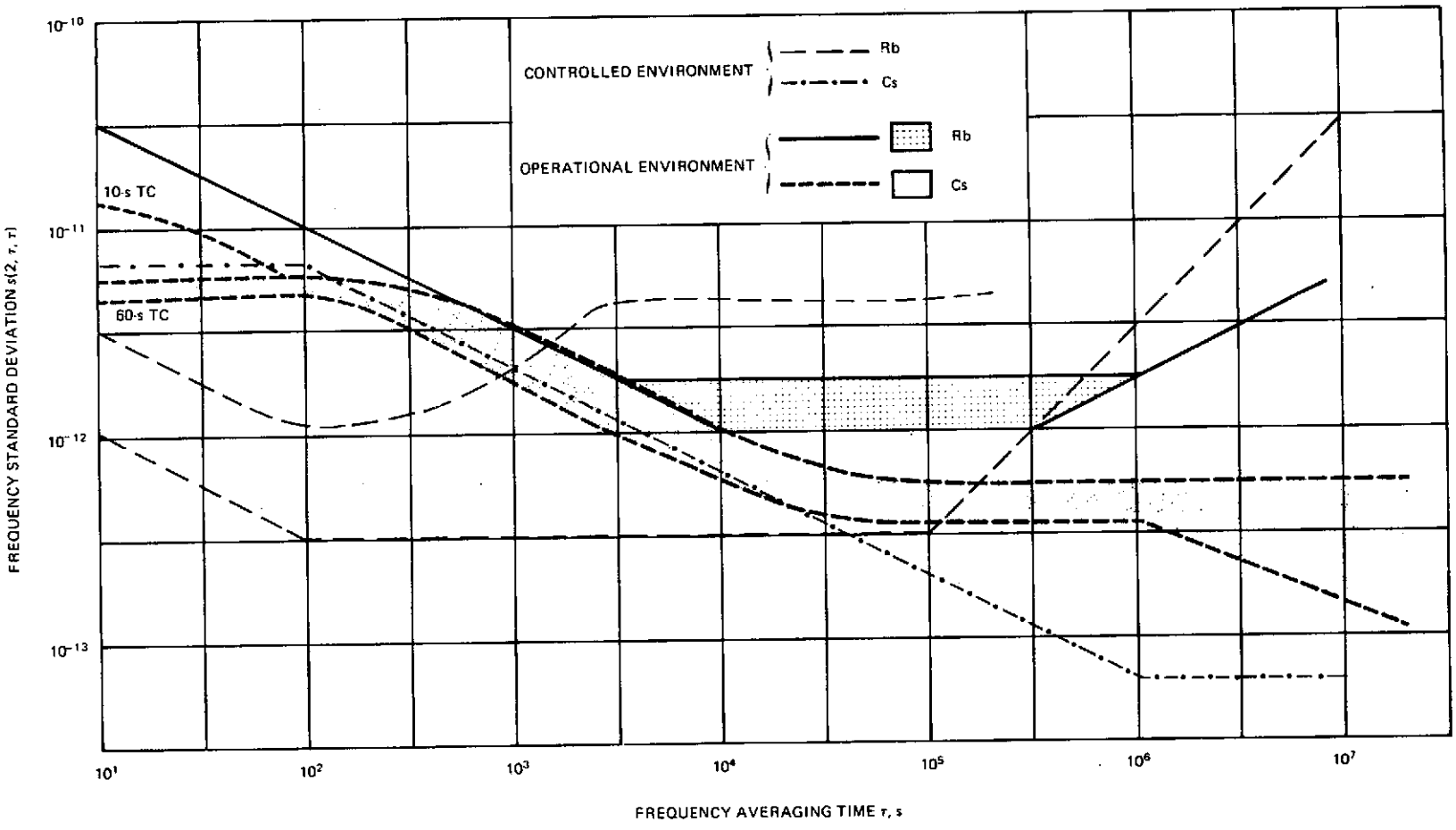

Figure 4. Rubidium and cesium standard frequency stabilities.

REFERENCES

(1) G. M. R. Winkler. "Path Delay, Its Variations, and Some Implications for the Field Use of Precise Frequency Standards." *Proc. IEEE* 60(5): 522-529, 1972.

(2) H. E. Peters, T. E. McGunigal, and E. H. Johnson. "Hydrogen Standard Work at Goddard Space Flight Center." *Proc. 22nd Annu. Symp. Freq. Control,* U. S. Army Electronics Command (Fort Monmouth, N.J.), 1968, pp. 464-492.

(3) J. A. Barnes, et al. "Characterization of Frequency Stability." *IEEE Trans. Instrum. Meas.* 20(2): 105-120, 1971.

(4) J. A. Barnes. *Tables of Bias Functions,* B1 *and* B2, *for Variances Based on Finite Samples of Processes With Power Law Spectral Densities.* NBS Tech. Note 375, Jan. 1969.

(5) A. O. McCoubrey. "A Survey of Atomic Frequency Standards," *Proc. IEEE* 54(2): 116-135, 1966.

HAWAII PTTI TEST BED

James A. Murray
Naval Research Laboratory

The Navy's Precise Time and Time Interval (PTTI) program concerns many systems having to do with communications, navigation, and other time-coordinated activities. To assess the ability of the current PTTI research and development efforts to serve these systems, a test bed is being established. The Naval Communication Station at Wahiawa, Hawaii, was selected for the site because of its involvement in or proximity to a number of activities that are either dependent upon the Naval Observatory as a common reference, or could benefit from the presence of accurate time and frequency standards.

A prime goal in the effort is to develop a repertoire of techniques and equipment that will permit communications facilities to be served most effectively by their ties to a common time reference. The test bed will provide guidance for the implementation of precise time and frequency discipline at other facilities.

One product of the test-bed problem will be an assessment of the accuracy of the time-discipline chain from the Observatory to each level of use. While it is possible to estimate potential accuracies from equipment and media characteristics, the practical accuracies attainable in an operational environment must be verified or ascertained.

Current Naval Research Laboratory (NRL) test-bed development work is being done under Naval Electronic Systems Command (NAVELEX) sponsorship with financial support for equipment construction by the Naval Communications Command (COMNAVCOMM). A site survey at Wahiawa in October 1971 attended by representatives of NRL, NAVELEX, COMMAVCOMM, Naval Shore Electronics Engineering Activity (NAVSEEAPAC), and the Defense Communications Agency (DCA-PAC) was employed to establish reasonable goals and to acquire specific information about potentially affected equipment. The basic plan for the test bed was then drawn up by NAVSEEAPAC at Pearl Harbor. The plan was later modified to make best use of currently available funds, time, and talent.

The system of time standards and transfers involved in establishing a reference at Wahiawa is illustrated in Figure 1. In this sort of chain, where time transfers are not made continuously, inaccuracies may be contributed by each time-transfer process and by each secondary standard. Inaccuracies due to the transfer processes are mainly functions of equipment and transmission media, while those due to the standards depend upon rate inaccuracies of the standards and the schedules by which they are updated.

Management practices can influence the accuracy substantially. However, if the time transfers over the links from the Observatory to Brandywine and from Brandywine to

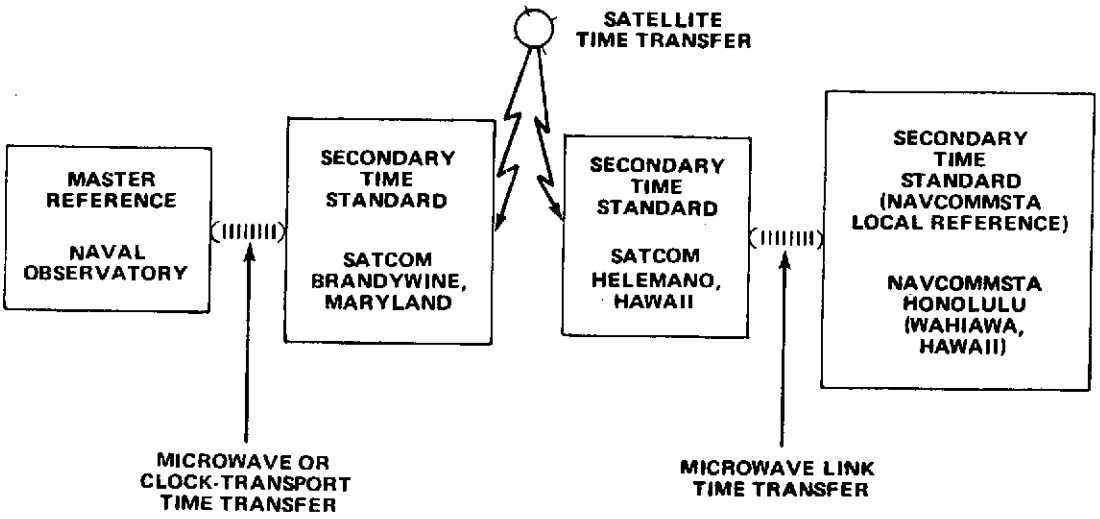

Figure 1. Timing chain from the Naval Observatory to NAVCOMMSTA Honolulu.

Helemano are made almost simultaneously, the rate error of the Brandywine standard is not important. The rate error of the Helemano standard can be similarly neglected if the time reference is passed to Wahiawa as soon as it is received from Brandywine. It would be possible then to check the Wahiawa standard against the Observatory with only the inaccuracy of three time transfers. Assuming an error of 0.1 microsecond (μs) per transfer, the standard could be checked to within 0.3 μs of the Observatory reference. Then assuming a rate error of one part in 10^{12} for the Wahiawa standard, a once-per-week update with 0.3 μs accuracy would keep the standard within 1 μs of the Observatory reference.

Experience with the test-bed operation should yield reasonable working values for the various accuracy factors. A figure of 1 μs for the Wahiawa standard, however, is not considered optimistic.

Most of the systems utilizing the Communication Station (COMMSTA) reference are located in the same building or nearby, and may be fed through transmission lines with fractional microseconds added inaccuracy. Any system requiring the full accuracy of the reference may be compensated for the small, fixed delay of the transmission line. Most systems require no correction.

Stabilization of the Radio Transmitting Facility (RTF) at Lualualei would employ an additional time transfer over an existing microwave link. The standards maintained at Lualualei might also be checked at reduced accuracy by monitoring the Transmitting Facility's very low frequency (VLF) broadcasts at Wahiawa. The receiving site near the Control Center at Wahiawa could be fed by coaxial line, but probably will not be implemented at this time.

The SATCOM facility at Helemano (Figure 2) not only acts as a link in the chain from the Observatory to Wahiawa, but also functions as a key terminal in distributing precise time to other satellite terminals in the western Pacific. Using a pseudorandom-noise satellite time transfer technique, many Defense Communications Agency earth terminals are being equipped for time transfer with cesium-beam clocks and time transfer equipment.

A cesium-beam clock at Helemano is its principal time standard. This clock is backed up by a disciplined time and frequency oscillator (DTFO). Under normal operation, the cesium-beam is updated periodically by time transfers from Brandywine, Md., and the DTFO is slaved to the cesium clock. The DTFO operates independently upon failure of the cesium-beam standard.

Timing signals and standard frequencies are generated by the two frequency standards and their time signal generators. An electronic counter is used for periodic checks of the time error between the two standards. The counter also serves as a readout for the time transfer unit, which is used either with the normal communications modem for time transfers with other SATCOM stations, or with a specially designed time transfer modem for clock comparisons with Wahiawa over a microwave link. Although it is not illustrated in the diagram,

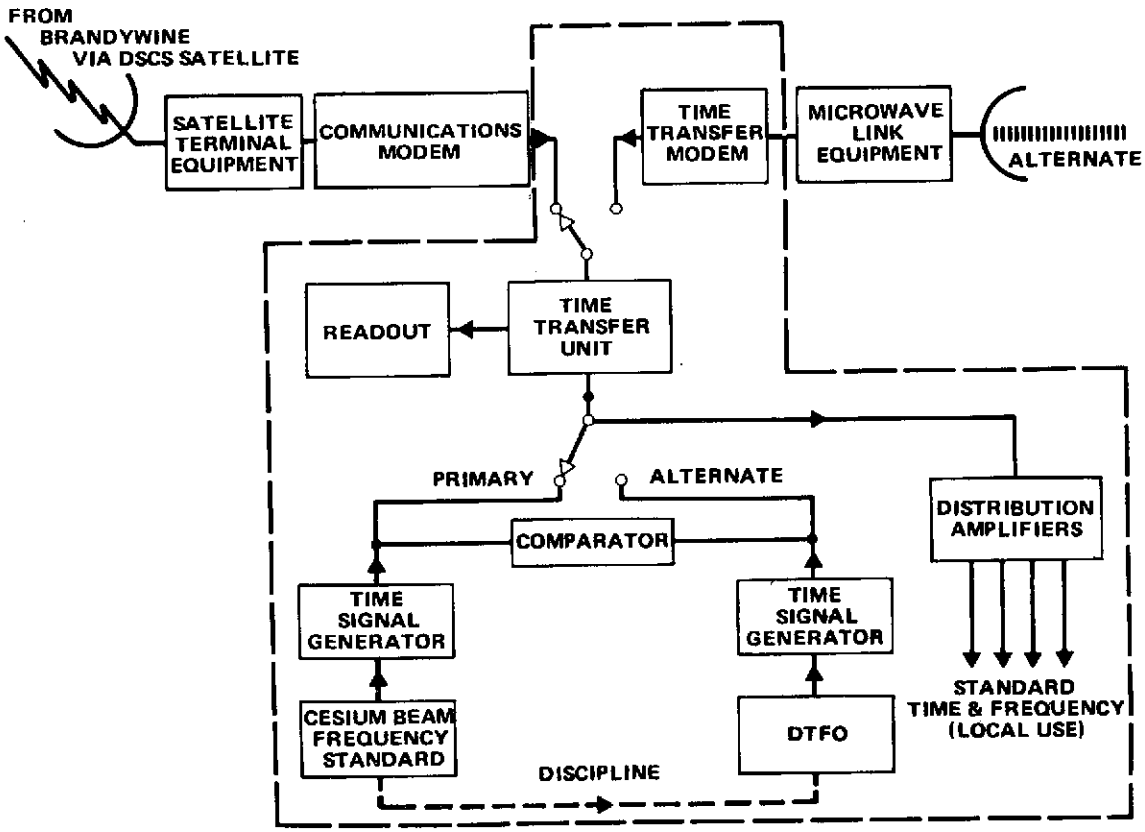

Figure 2. Helemano SATCOM time/frequency standard.

the time-transfer modem may be used with the satellite terminal to make time transfers with other satellite terminals that are not equipped with communications modems.

The time and frequency reference maintained at the communication control center at Wahiawa (Figure 3) is almost identical to the SATCOM facility standard at Helemano. The only difference is in the switching arrangements, because the Wahiawa standard does not interface with a communications modem.

Note that the Wahiawa reference may be checked at any time with the cesium-controlled references of Helemano and Lualualei. This fact gives each of the three time standards a double backup from standards of approximately equal precision.

If the cesium-beam at Helemano should fail, for example, its DTFO would then become that facility's local standard. It may be compared as often as required with Wahiawa, and indirectly with Lualualei, to maintain the required time accuracy. The Helemano DTFO may also perform the function of transfer standard between Brandywine and Wahiawa with little decrease in accuracy if it is maintained fairly well on frequency and if time transfers are passed along to Wahiawa soon after they are received from Brandywine.

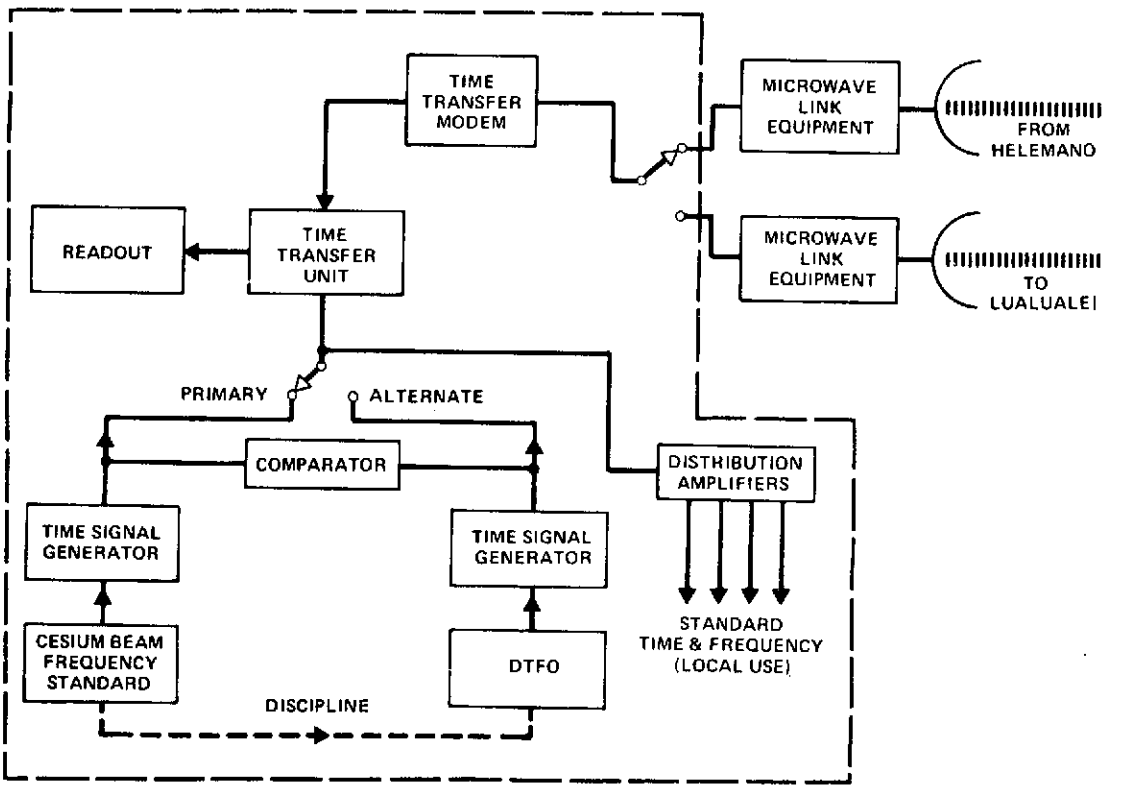

Figure 3. Wahiawa time/frequency standard.

Catastrophic failures of the major timing links may be handled in a variety of ways:

A prolonged failure of the Helemano-to-Wahiawa microwave link could be handled, for example, by transporting an accurately calibrated DTFO or cesium-beam standard from one site to the other or by simultaneously monitoring the VLF transmissions of Lualualei at the two sites.

An extended outage of the satellite link to Brandywine could be treated by reverting to indirect monitoring via the OMEGA navigation system, or the VLF transmissions of Lualualei. The link could also be replaced by occasional flying clock visits to one of the affected sites. A well established cesium-beam standard, however, may be relied upon for a frequency accuracy of nearly one part in 10^{12} and would gain or lose less than a microsecond per week after being set adrift. It is expected, therefore, that clock transports or indirect monitoring would be used rarely, if at all.

Examples of the methods of control and types of equipment served by the frequency standard at Wahiawa are shown in Figure 4. Sinewave signals are available from the standard at the usual frequencies of 100 kHz and at one and five MHz. Other available signals are one pulse per second, a once-per-second time code, and a one-MHz square wave that is coherent with the one pulse per second and time code.

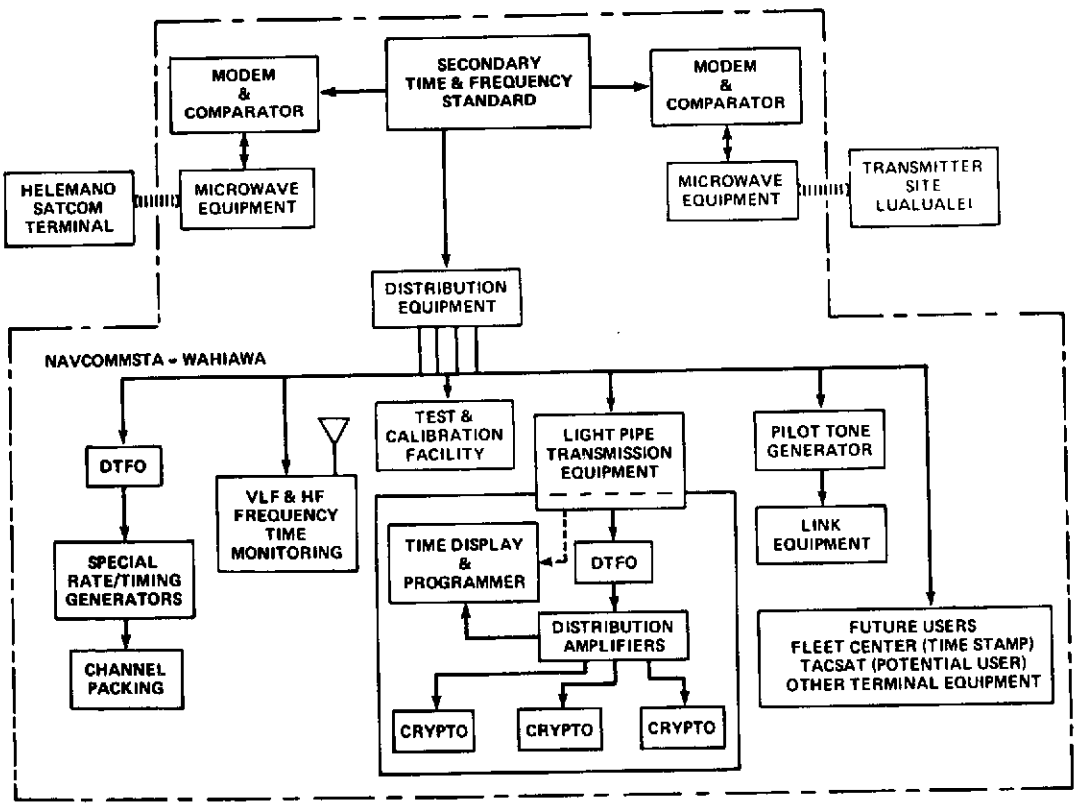

Figure 4. Precise time and frequency distribution for the Communication Control Center at Wahiawa.

It is hoped that a standard distribution format can be derived from experience with the several modes to be employed in the test bed. The time code is designed to be employed in a number of ways. A reference marker at the beginning and subsequent reference features permit equipment to be synchronized to a resolution determined largely by the bandwidth of the propagation medium between the time signal generator and the user system. The code also gives, in serial digital form, the hours, minutes, and seconds of the time of day. Data rates were selected to permit their transmission over normal voice circuits, although resolution is limited when such small bandwidths are used. Further encoding once each minute permits audible recognition of the minute and second of the hour.

A remote clock has been designed for use with the time code in varying degrees of sophistication. As a minimum function (and at minimum cost) the clock would simply read the code and display the time of day in hours and minutes; or hours, minutes, and seconds. An option will permit the clock to initiate an operation precisely at any selected second of the day. Inclusion of a controlled oscillator or use of an external 1-MHz standard frequency in another option would allow the clock to initiate an operation at precisely any microsecond of the day and to provide a fixed compensation for transmission line delay. The options employ printed-circuit cards already designed for the time signal generators at Helemano and Wahiawa.

The time display and programmer shown in the crypto area uses still another scheme to produce on-time output. The 1-Hz envelope of the time code is treated as an input frequency. The on-time leading edges of the code are counted to generate a parallel output which is decoded to drive a time-of-day display. A parallel comparator generates an output pulse when the time of day entered into a set of thumbwheel switches is reached by the counter. The time code that drives the device is also detected and updates the counter if it disagrees with the time code.

Timing signals from the Wahiawa standard will be transmitted to the crypto area through light-pipe equipment under development by the Naval Electronics Laboratory Center (NELC). DTF oscillators and automatic switching equipment will provide reliable standard frequencies to run the equipment, while the time display and programmer will provide precise timing events for equipment synchronization.

The channel packing program will be served by special timing generators to maintain accurate rates. Two DTF oscillators will provide a reliable reference to control the rates and will maintain alignment with respect to a one-pulse-per-second signal.

Although it is not scheduled for the present test bed installation, provisions can easily be made to monitor the frequency and timing of VLF and high-frequency (HF) broadcasts from the radio transmitting facility at Lualualei. When timing is eventually added to the keystream of the VLF transmissions, it may be effectively monitored and disciplined by Wahiawa, which is relatively free of unbalanced pickup from the two towers of Lualualei.

Frequency dividers will be provided for the test and calibration facility at Wahiawa. Test signals of 1 MHz and 1 kHz will be supplied.

A pilot tone-generator will provide an accurate 96 kHz frequency to discipline a microwave link network.

The availability of an accurate time and frequency reference at the communication station will permit equipment and systems to be simplified by relieving them from independently having to establish and maintain time and frequency accuracy. Among the potential beneficiaries are the Fleet Center, which could use precise message dating equipment and time-of-day displays, and the TACSAT communications system.

The receiver site illustrated in Figure 5 is not currently scheduled to be a part of the test bed, but could benefit by standard-frequency distribution to drive the frequency synthesizers of its receivers. In this application, spectral purity is important, because a noisy input may produce a noisy output.

The DTF oscillators at the receiving site make the site independent of the control-center standard during any distribution system failure. They also provide spectrally clean signals to the receivers, even if the line between the control center building and the receiving site picks up some noise.

Accuracy is degraded gradually after the DTFO loses its reference. During a distribution system outage, an unattended DTF oscillator would maintain a frequency accuracy better

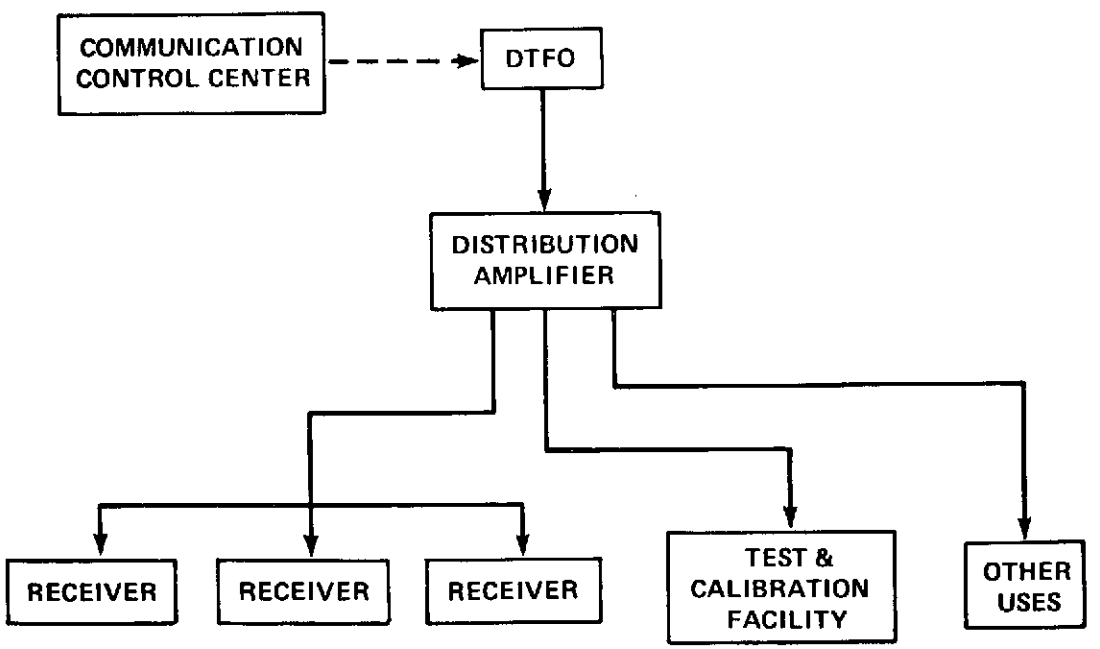

Figure 5. Precise time and frequency distribution for the receiver site at Wahiawa.

than one part in 10^9 for 20 days. This exceeds the requirements of the receivers by a sizable margin. One practical advantage of a distribution system of this type is the elimination of maintenance otherwise required to calibrate numerous individual frequency standards. As in the control center, standard frequency test tones and signals may be easily provided for frequency counters, signal generators and other frequency-dependent instruments.

The transmitter site (Figure 6) may be brought under the guidance of the NAVCOMMSTA time and frequency reference at Wahiawa through time transfers over an existing microwave link between the two sites. Only one additional time transfer modem would be needed, because Wahiawa will already possess such a unit for time transfers with Helemano.

One of the two cesium-beam frequency standards that now control the VLF transmitter would be moved to the Lualualei microwave terminal and serve as the transmitting facility reference. Each transmitter building or building wing would contain a DTFO that is disciplined by the reference. Transmitter spectral purity and accuracy requirements are similar to those of the receivers.

Because of the large distances between buildings (a mile or more in some cases), and the very strong high-frequency electromagnetic fields present throughout the site, distribution

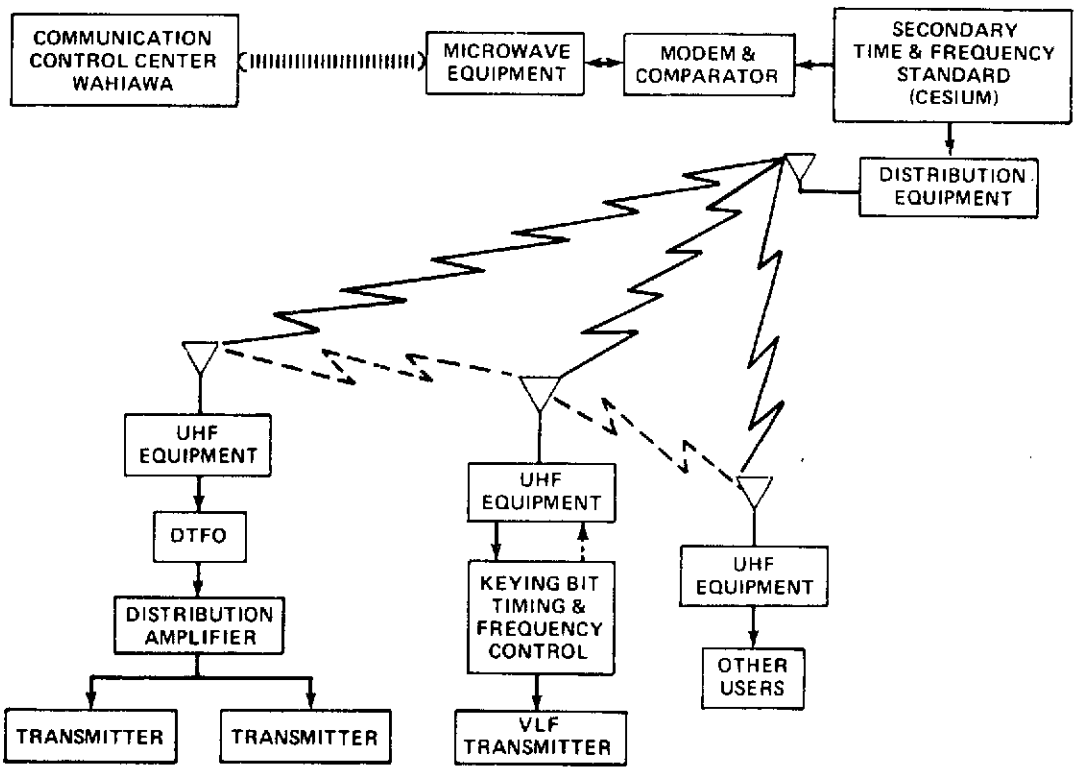

Figure 6. Precise time and frequency distribution for the transmitter site at Lualualei.

by coaxial cable could be both expensive and noisy. Current plans are to distribute the reference via low-power ultra-high-frequency (UHF) signals broadcast from the site of the reference. A UHF transmitter at the VLF site, the location of the other cesium-beam standard, could take over during any extended outage of the transmitter facility reference.

A format for the UHF broadcasts has not yet been chosen. A standard-frequency signal, amplitude- or frequency-modulating the UHF carrier would serve all of the transmitters except for the VLF and could be filtered effectively because of its narrow-band nature. However, the VLF transmissions must be controlled in time, and a time code is preferred.

Distribution of standard frequencies within the transmitter buildings by light pipes to avoid ground-loop problems in those high-field areas has been considered.

One of the first considerations in the implementation of any distribution system must be the consequences of its failure. A failure that would cause only a momentary malfunction of one user system might be catastrophic to another. The momentary loss of a standard frequency to a radio receiver, for example, might cause it to miss a few bits of data or a word of speech. The same momentary loss to a timing system could render it inaccurate forever afterwards. There are users subject to all degrees of inconvenience between these extremes.

The crypto-equipment at Wahiawa is a group of systems for which continuity of standard-frequency input is important. A passive auto-switch shown in Figure 7 has been designed to provide that continuity by selecting an available signal from one of two input lines. The switch is passive in that it operates completely from power supplied by the input signals.

One signal supplies the output and suppresses the other signal channel. If the first signal fails, the second channel becomes active and suppresses the first. The switch can be manually set to either channel, provided that it has an input of sufficient amplitude. Loss through the active channel is approximately three decibels (dB) at one volt root-mean-square (rms), and the inactive channel is suppressed approximately 25 to 30 dB. A slight discontinuity occurs at the instant of switching, but should not amount to more than a few microseconds.

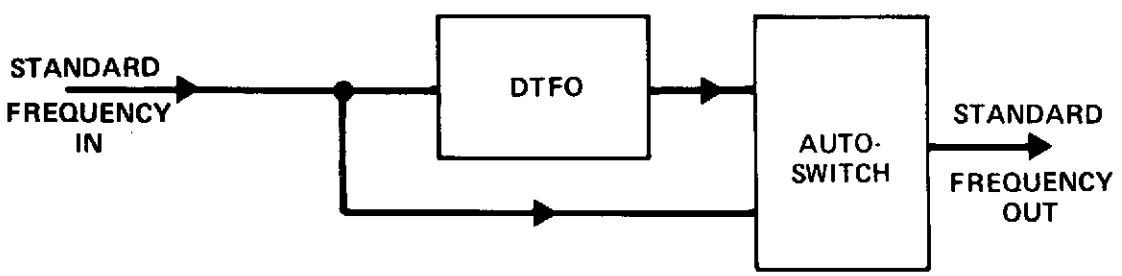

Figure 7. Passive autoswitch for timing applications.

The diagram illustrates one possible use of the switch. Under normal circumstances, the standard frequency input is routed through the switch. But if it fails, the DTFO output is channeled through instead.

The test bed effort has required the development of a number of new equipments, which are now in various stages of completion. The baud rate generator illustrated in Figure 8 produces basic frequencies to discipline a microwave system, the channel-packing modem, and a digital communications system. The microwave pilot tone and the basic channel-packing frequencies are maintained in alignment with a 1PPS input. One or more baud rate divider amplifiers driven by the generator produce square waves of 75 Hz X 2^n up through 9.6 kHz with positive-going edges on time with 1PPS.

The status of the generating system, which includes a servo-controlled crystal oscillator is displayed on the front panel. Normally, the reference for the check is 1PPS, but the 9.6 kHz reference may be selected for a rarely required maintenance procedure.

Battery backup is accommodated in this unit as in all other critical equipments for the test bed by provision of a connector for an external battery and appropriate automatic-internal switch-over circuitry. Nominal battery voltage is 24 volts, while some units can also accept 12 volts. Normal operation is at 115 volts 50-400 Hz.

The crypto-equipment is driven by a specially shaped 100-kHz square wave that is produced by amplifiers of the type shown in Figure 9. Each amplifier has 12 outputs; each of which can drive one or two machines. This unit can accept battery backup at 12 or 24 volts.

Distribution of the time code, 1PPS, and the timed one MHz is provided by the line driver of Figure 10. The unit contains four independent amplifier cards, each containing three output amplifiers. The inputs and outputs of individual cards may be made balanced or unbalanced, by switch selection. And high impedance or 50-ohm inputs may also be selected.

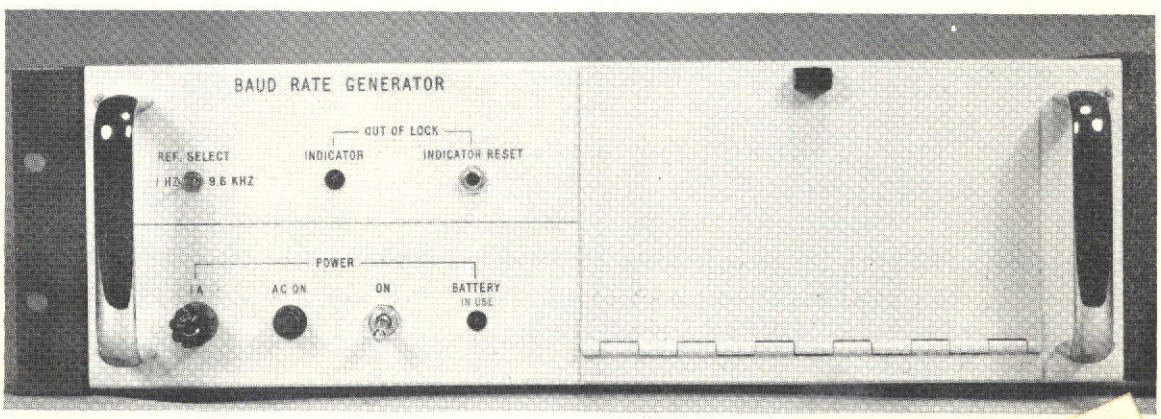

Figure 8. Baud rate generator.

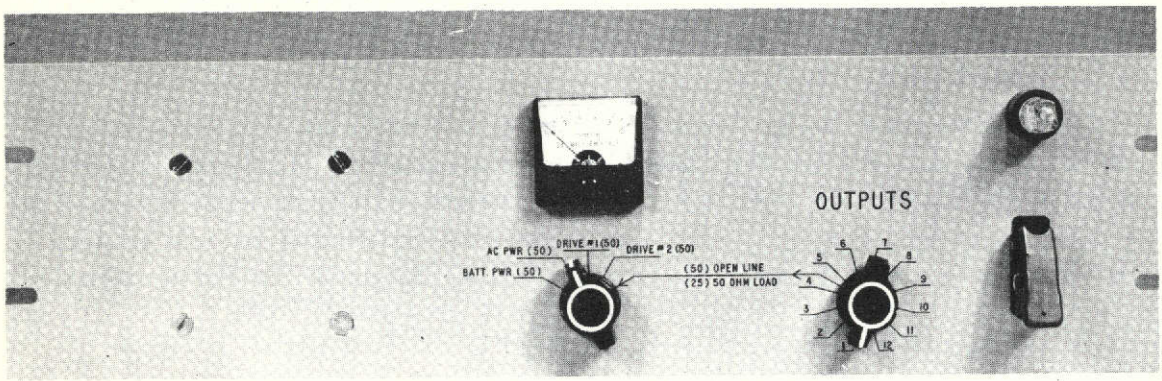

Figure 9. Distribution amplifier for crypto equipment.

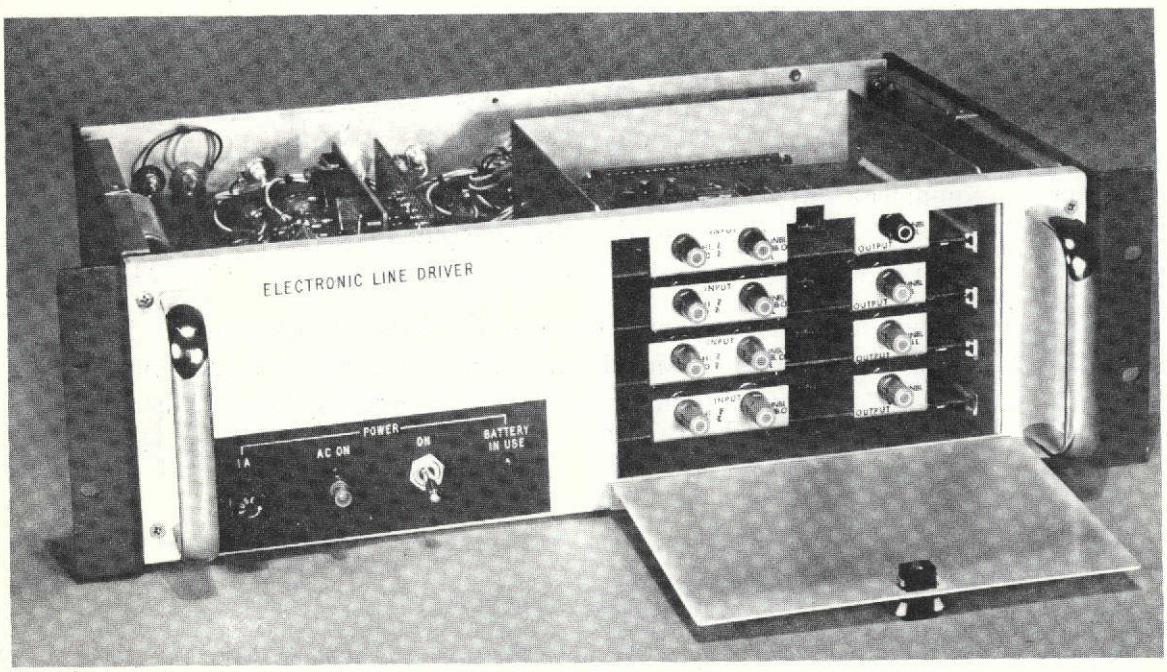

Figure 10. Timing signal distribution amplifier.

Time transfers between Helemano and Wahiawa will be made with the time transfer modem (Figure 11). This unit employs a pseudo-random noise code as a vehicle for effectively sending very short pulses from one site to another.

The modem is capable of operation over satellite links as well as fixed microwave links. Input and output are at a nominal 70 MHz, but a baseband interface is also provided for operation with certain link equipment. Bit rates from 1.25 MHz to 10 MHz may be selected to match bandwidth availability.

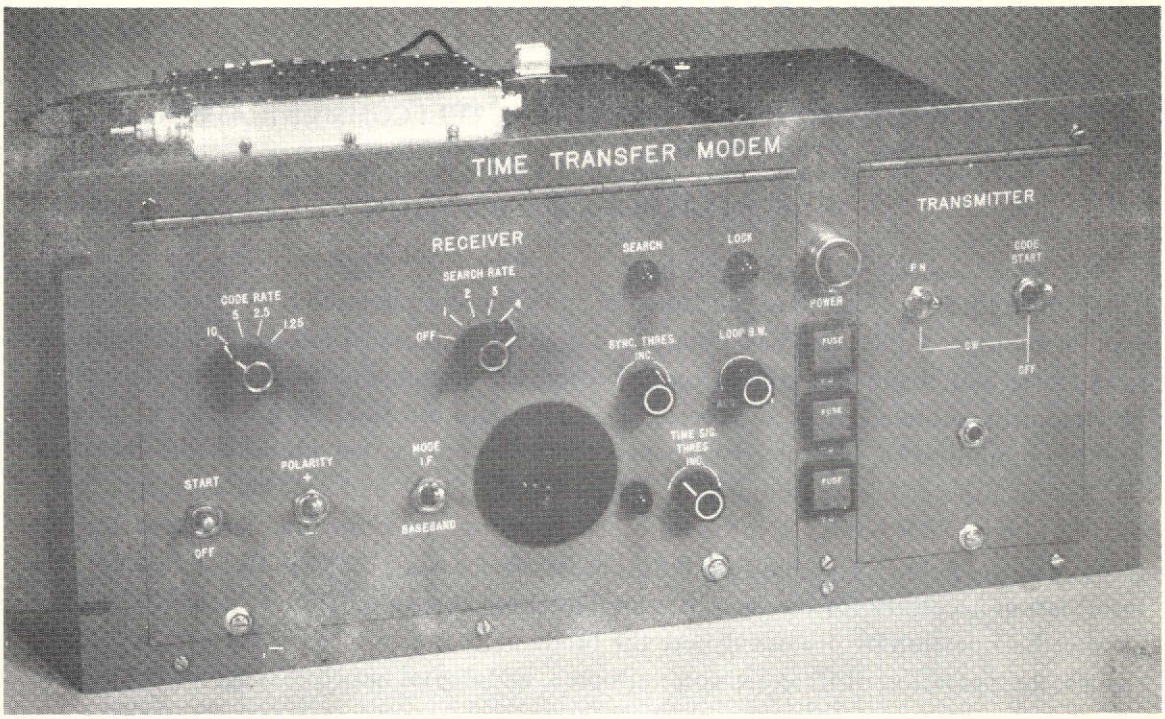

Figure 11. Time transfer modem.

Since the modem may be operated at a large bandwidth and below the level of interfering signals, the modem may be used in a lightly populated channel without significant mutual interference. This mode of operation has been used on the satellite links. For the line-of-sight microwave circuits in Hawaii, however, the channels are heavily occupied; and the modem spectrum will be reduced in width and converted to a lightly occupied region of the channel.

The time-transfer modems are used with time-transfer units in a two-way process that effectively cancels out the propagation time, and therefore gives direct clock comparisons without requiring a distance correction. Accuracy is in the order of 0.1μs for all bit rates and is limited primarily by the readout resolution of the counter at the higher bit rates.

The remaining units designed for the test bed, including the time signal generator, the time display and programmer, the test-signal interface, the auto switch, and selector switch panels are currently under construction and should be completed in about a month.

TIME AND FREQUENCY FOR DIGITAL TELECOMMUNICATIONS

Harold C. Folts
National Communications System

Time and frequency (T&F) are fundamental and pervasive parameters of telecommunication technology. Advancing development of digital communications using data modulation rates above 2400 baud and time-division multiplex in complex network configurations is now requiring more accurate and precise T&F reference information for efficient operation of telecommunication systems. Past papers that I have presented addressed the concept of T&F facilities at telecommunication stations in the field[1] and a system concept for distribution of T&F reference information via telecommunication and navigation systems to users in the field.[2] The question that is most often asked, "Why is T&F reference information necessary for the operation of digital telecommunication systems?" I will answer this question by discussing here the fundamental ideas of processing binary digital signals, the operation of time-division multiplex, and digital network synchronization.

A schematic diagram of a general communication system as conceptualized by Shannon and Weaver[3] is shown in Figure 1. This diagram is very general and can depict any type of communication. The information source selects a specific message which is encoded and sent through a communication channel. Enroute, the signal is subjected to perturbations from environmental noise. The received signal is then decoded and delivered to its destination. Through the process, the message may undergo many spurious changes, resulting in a loss of information content in the delivered message as compared to the original selected message. In digital telecommunication systems, loss of information content of the signals can be attributed to noise, distortion of waveshape, and loss of synchronization.

Digital signals are basically a series of binary digits (bits) occurring at a fixed rate of time. As shown in Figure 2, each bit represents one of two possible logical states (1 or 0) and is held for an equal time interval (t). The sequential combinations of logical states represent

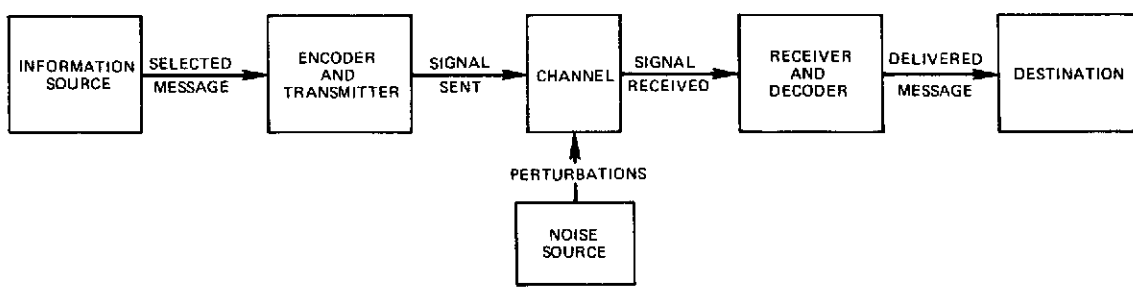

Figure 1. Schematic diagram of a general communication system.

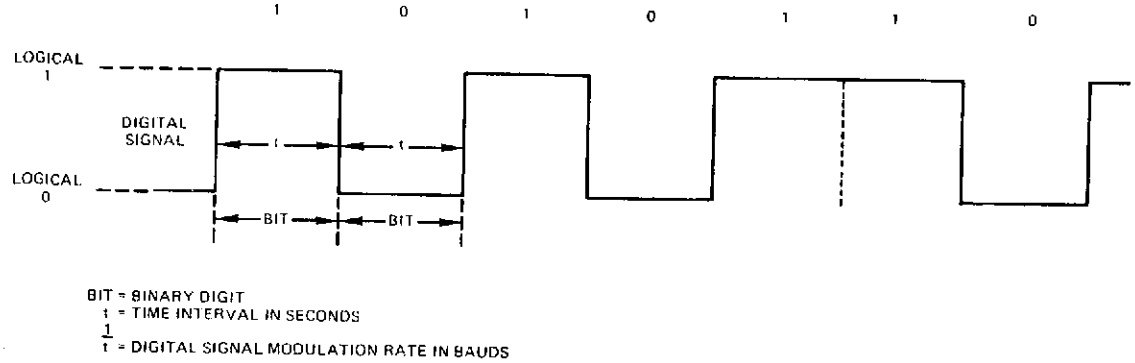

Figure 2. Basic digital signal.

the encoded information of the selected message. The reciprocal of the time interval of a bit gives the modulation rate in bauds for transmission of the digital signal.

There are also digital signals that may contain bits of different time intervals for identification of groups of bits as information characters. This is normally associated with conventional low-speed electromechanical teletype operation and has no significance in this discussion. Under consideration here are the serial digital signals with bits of constant time interval as normally used for data communications at a modulation rate of 2400 baud or higher.

The generation of a digital signal requires a source of time-interval reference information (often called *clock*) for timing the signal at a given modulation rate. Normally the timing-signal modulation rate is twice that of the associated digital signal. The relationship of the timing and digital signals is shown in Figure 3. The timing signal is a series of alternating logic states of equal time interval. One timing period consisting of a "1" and a "0" determines the interval duration of one bit in the digital signal. The logic state of the encoded information is detected by the "0" to "1" transition of the timing signal. This state is then reflected as one bit in the resulting digital signal for the duration of one timing period.

The detection of a digital signal also requires a source of time interval reference information. As shown in Figure 4, the received timing signal is normally twice the modulation rate of the digital signal and in the same phase relationship as at the digital signal source. However, the sampling of the digital signal is accomplished by the "1" to "0" transition of the timing signal, which is coincident with the center of the bit. This portion of the bit has the least probability of being perturbed by the transmission channel. Therefore, the chance of detecting the wrong logic state is minimized.

Now it becomes readily apparent that if the time interval (or frequency) of the timing signal is different from that of the received digital signal there will be a relative continuous change in phase between the two signals. Therefore, the point of detection will shift either toward the leading or the trailing edge of the bit. Eventually the detection point could change over

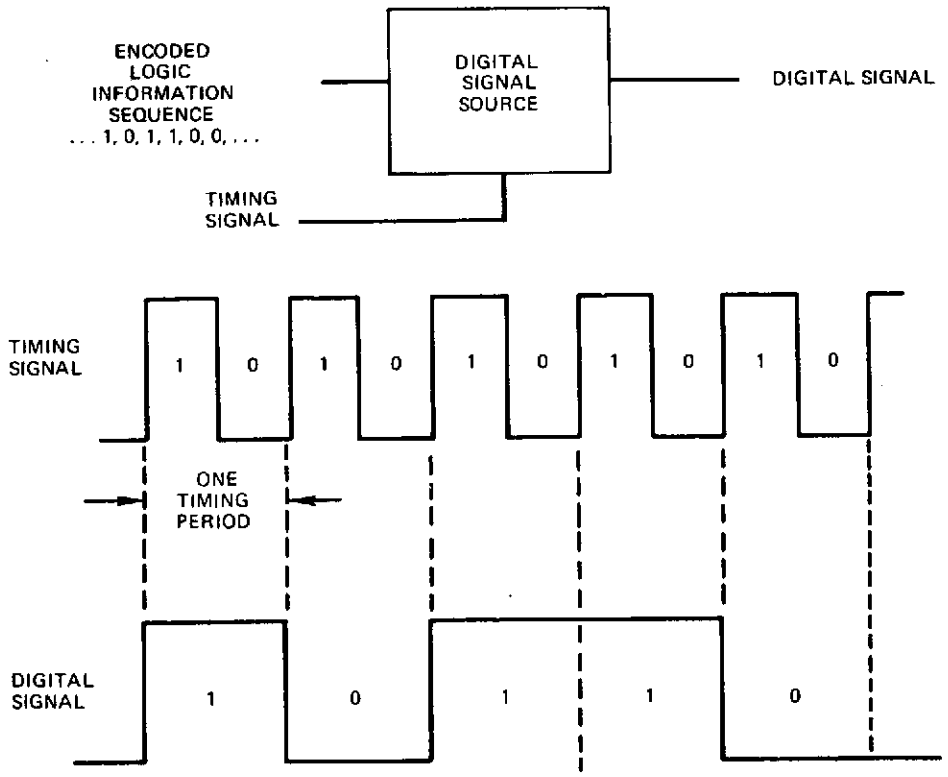

Figure 3. Generation of a digital signal.

to an adjacent bit. This would cause what is known as loss of bit-count integrity and result in loss of the information content of the signal. Even before loss of bit-count integrity, as the sampling point drifts into a perturbed portion of the data bit, the wrong logic state may be sensed.

A number of digital signals can be combined into a single digital signal by a time-division multiplexer (TDM). This is accomplished by reducing the time duration of the bits of the input signals and interleaving the bits (or groups of bits) into a single serial signal of a higher modulation rate. The rotating selector shown in Figure 5 functionally illustrates the process of time-division multiplexing. Rotating at a rate of one revolution per input-channel-bit time interval, the selector samples each channel sequentially for one quarter of a revolution. The resulting output signal has a modulation rate of four times that of the input channels. The first four bits of the multiplexed signal are the first bits of each input channel in the order that they are sampled. This sequence is then repeated as the selector continues to rotate.

Demultiplexing the signal is just the reverse of the multiplexing process. Functionally, a rotating selector in synchrony with the multiplexer distributes the bits of the incoming multiplexed signal to their respective output channels.

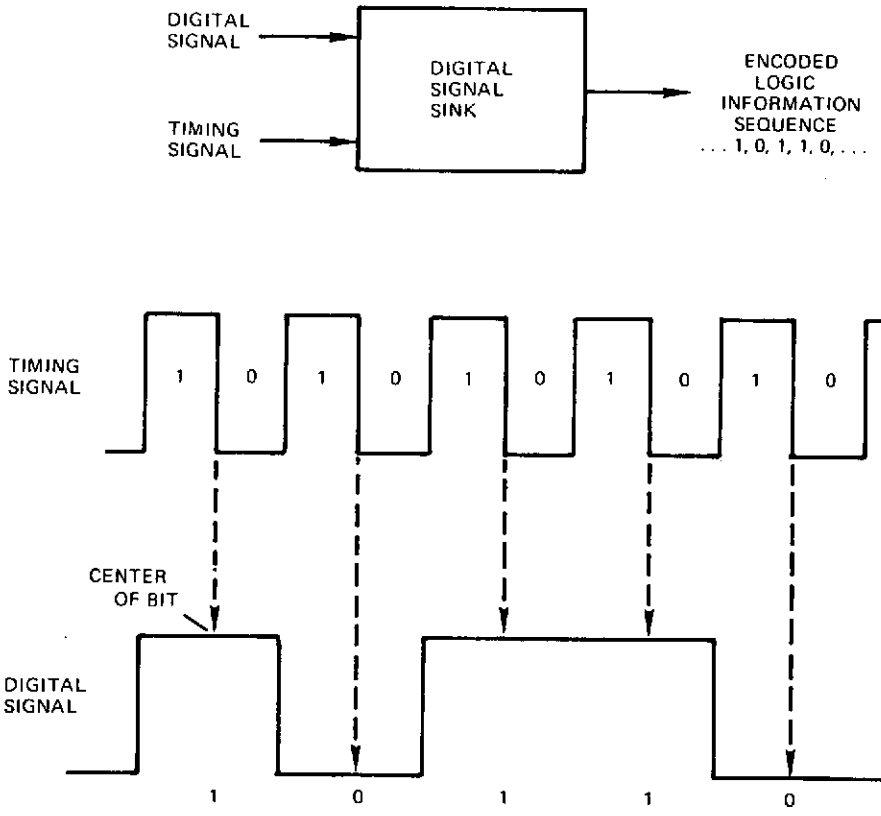

Figure 4. Detection of a digital signal.

A major problem in the design of digital communications is synchronization of the TDM and the terminal equipments. The synchronization problem for point-to-point operation as most commonly used up to this point in time, is relatively simple. However, this problem becomes acute with the evolution of complex network configurations.

Point-to-point synchronization requires only that the receiver be synchronized with the transmitter. This is typically achieved as shown in Figure 6 by recovering the time interval information from the received signal to phase lock a local oscillator which provides the timing for sampling the incoming digital signal. The receive timing is, therefore, slaved to the send timing, but contains any timing perturbations that may have occurred to the digital signal during transmission through the communication channel.

This basic scheme, however, is not adequate for network timing. All major nodes shown in Figure 7 must be synchronized with each other. Within a nodal facility, the digital signals must be exactly synchronous in order to allow interchange of signals between channels of various interconnecting routes. The synchronization must be accomplished in a manner that will prevent any instability throughout the network resulting from feedback of timing perturbations through network loops.

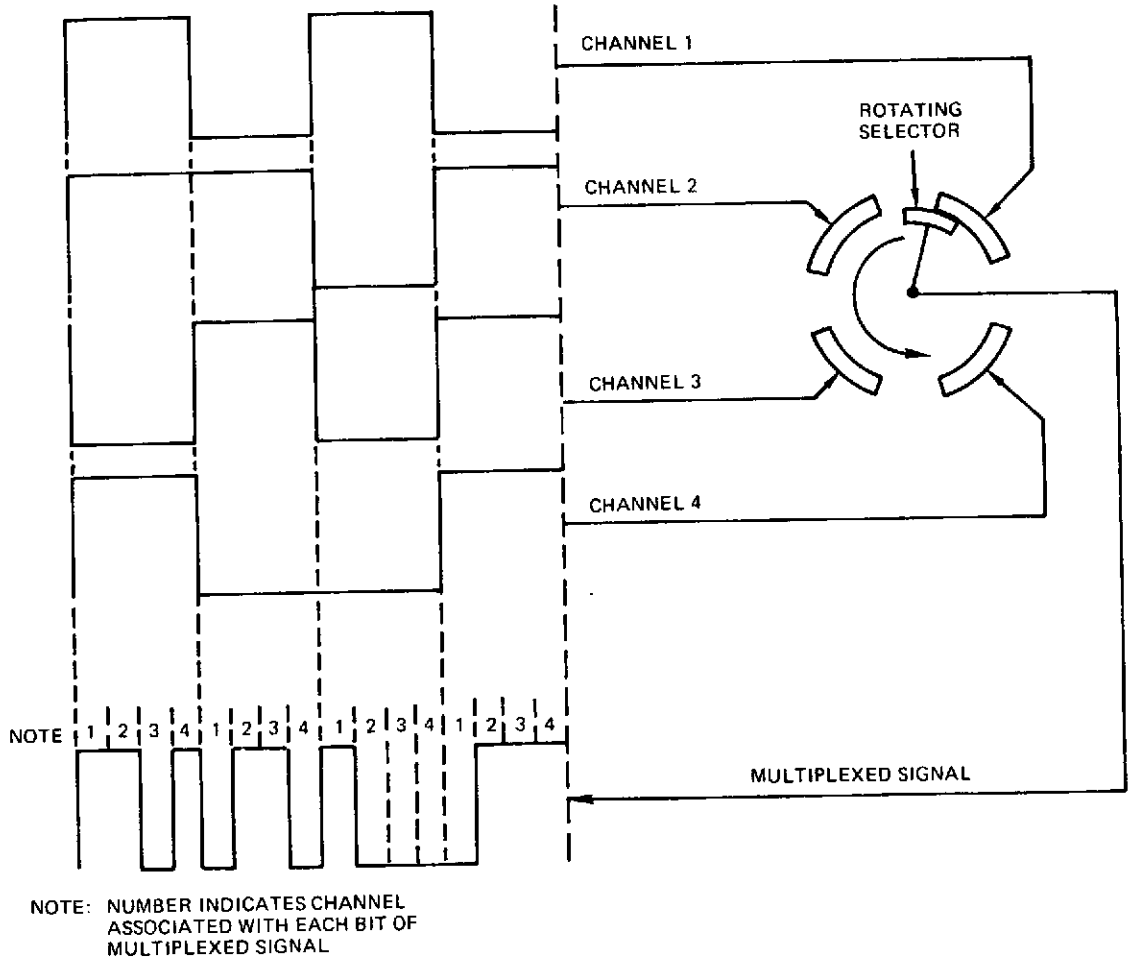

Figure 5. Time division multiplexer.

There are two basic factors that create the problems in synchronization. The first is that of maintaining a frequency coherence between the transmit-timing signals and the receive-timing signals. As discussed earlier, a difference in the time interval (the reciprocal of frequency) between the receive timing and the receive digital signals can cause the point of detection to drift into adjacent bits, resulting in a loss of bit-count integrity.

The other problem is due to a phenomenon associated with the transmission media. As discussed by R. Day[4] last year, communication circuits "breathe" by effectively changing length over a period of time. This produces a doppler effect on the signal by increasing or decreasing its frequency. This problem is most acute with satellite circuits where a few milliseconds of cyclic drift over a period of 12 hours may be experienced due to the movement of the satellite. On cable or microwave circuits, this may be only a few microseconds at the most. When operating at modulation rates in the megabaud range, however, this could cause a slip in the detection of several bits in the digital signal.

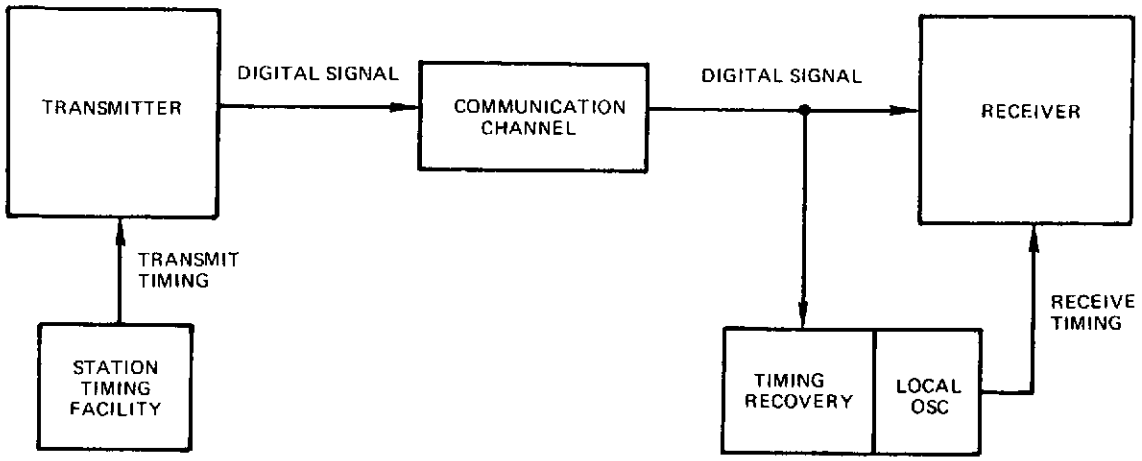

Figure 6. A typical point-to-point synchronization scheme.

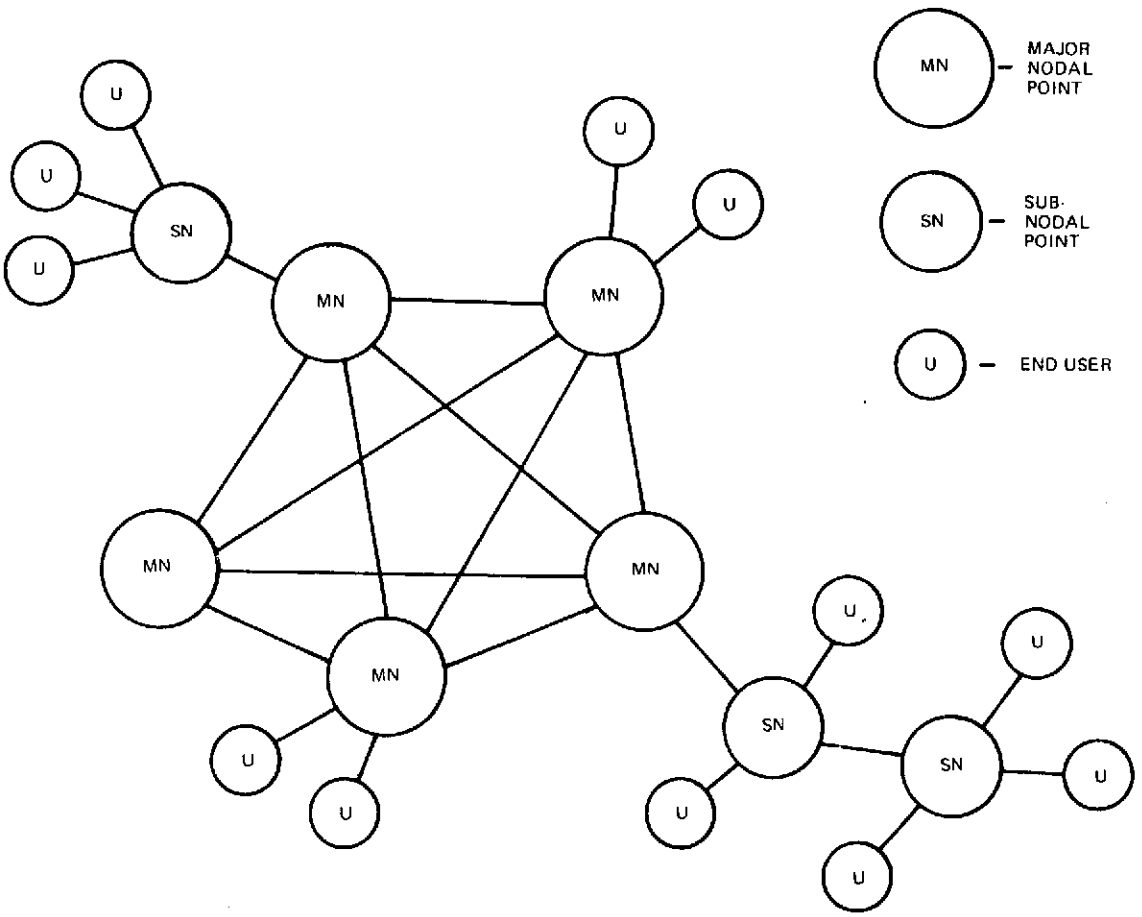

Figure 7. Typical communications network.

There have been several synchronizing techniques proposed,[5,6] but there has been no general agreement as to the best approach to be taken. The various proposals include use of nodal precise timing facilities tied into a T&F distribution subsystem, digital buffers, atomic clocks, pulse stuffing, frequency averaging, and discrete control correction.

The solutions to the synchronizing problems can be considered to fall into two categories, corrective and compensative. The solution to the difference in time interval of the transmit and receive timing signals can be one of a corrective nature, although it could also be one of compensation. The cyclic breathing of a communication channel requires a solution of compensation, since little is understood of this phenomenon and no practical corrective solutions are known. Another fundamental consideration is that the breathing phenomenon has a limit which can readily be determined for any particular application. The breathing is cyclic over a period of time and will average out to a mean value. The difference in the frequency of the transmit and receive timing signals, however, creates a continuous drift in time which does not have a limit.

A corrective solution to the timing signal frequency difference problem can be realized through the implementation of a T&F distribution subsystem[2] with precise T&F facilities at each nodal point in the network. This will ensure maintenance of timing coherence throughout the network, while each node is independent of each other node for its reference information. By retiming the digital signals at each node, timing perturbations are blocked and cannot propagate through to other nodes. Therefore, stability will be maintained throughout the network because feedback through network loops will not be possible.

A compensative solution to the timing perturbations due to the transmission media can be achieved by using digital buffers, adaptive queues, or elastic store devices. These devices are essentially the same in operation. The incoming digital signal is "written" into a temporary storage device by timing recovered from the received signal as shown in Figure 8. During initial synchronization the storage capacity is generally allowed to fill halfway. At this midpoint, the timing signal from the local station source "reads" the digital signal out

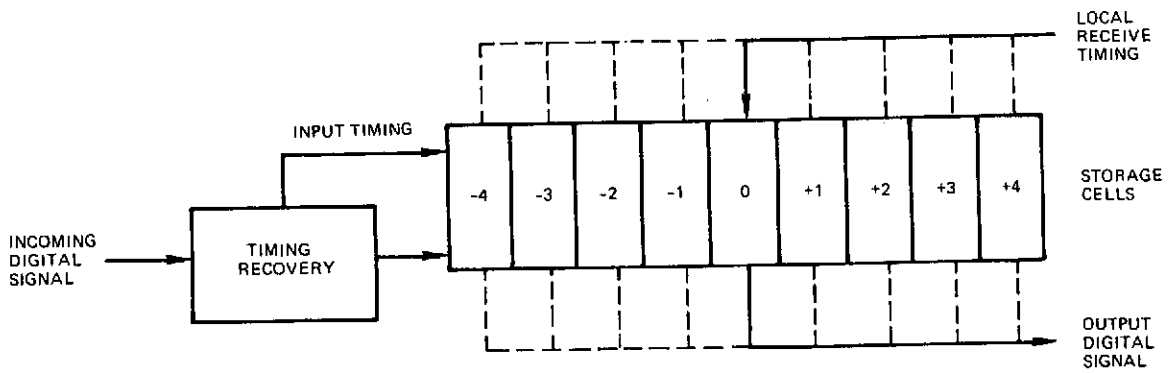

Figure 8. Digital buffer.

the storage to the receive equipment. As the input digital signal changes rate, the storage fill increases or decreases accordingly. The output sampling point then shifts to the appropriate cell to "read" the output signal at the correct time phase relationship.

The limit of timing variation that can be accommodated by the digital buffer depends on its storage capacity and the modulation rate of the signal. It is readily apparent that the dimension characteristic of the buffer naturally lends itself to compensating for the cyclic breathing phenomenon of transmission media. As long as the limits are not exceeded, there should be no requirement for periodic resynchronization. Further refinements have been incorporated into buffer devices to provide an adaptive queue which will compensate for any change in the transmission path over extended signal outages. Each time the circuit is restored a round-trip path-delay measurement is made to determine if an effective change in length has occurred. If so, the buffer fill is adjusted accordingly to allow reading the output from the correct cell.

If the digital buffer is also used to compensate for timing signal frequency differences, the change in fill of the storage cells will be continuous in one direction. This will eventually result in an overflow (or underflow) when the buffer limit is exceeded. In effect the mean point of the cyclic variation will shift in one direction until the storage capacity is exceeded. Thus periodic resynchronization will be required.

Most other synchronization techniques are compensative in nature, although some are a combination of corrective and compensative approaches. More complicated compensative techniques such as bit-stuffing require complex and costly logic circuitry. Also many of the bits in the digital signal are required for control, leaving only part of the signal to carry the actual message information. Once the modulation rates reach a level that exceeds the practical limit of coherent timing facilities, however, additional compensative techniques to ensure maintenance of network synchronization and stability will be necessary. Such a technique developed by R. Bittel[6] and called "discrete control correction" is a good example of what may be seen in the future.

Regardless of the type of digital-network synchronization technique used, a reliable precise source of T&F reference information will be required to ensure effective operation. The techniques are now available for economical distribution of T&F. Therefore, digital system designers must maintain cognizance of T&F technology for appropriate application in their discipline.

REFERENCES

1. H.C. Folts, "Precise Time/Frequency for the Defense Communications System," *Proceedings of the Third Annual Department of Defense Precise Time and Time Interval (PTTI) Strategic Planning Meeting,* Washington, D.C. November 16-18, 1971, pp. 83-190.

2. H.C. Folts, "Precise Time and Frequency is a Communication System," *Proceedings of the 26th Annual Symposium on Frequency Control,* Atlantic City, N.J., June 6-8, 1972, pp. 4-7.

3. C.E. Shannon and W. Weaver, *The Mathematical Theory of Communication,* Univ. of Illinois Press, Urbana, 1949.

4. R.A. Day, Jr., "The Effect of Changes in Absolute Path Delay in Digital Transmission Systems," *Proceedings of the Third Department of Defense Precise Time and Time Interval (PTTI) Strategic Planning Meeting,* Washington, D.C., November 16-18, 1971, pp. 195-209.

5. J.W. Pan, "Synchronization and Multiplexing in a Digital Communications Network," *Proceedings of the IEEE,* May 1972, pp. 594-601.

6. R.H. Bittel, *Network Timing and Synchronization,* Defense Communications Agency, Systems Engineering Facility, Reston, Va., Report 720.5-2, May 1972.

PRECISION TIME DISTRIBUTION WITHIN A DEEP SPACE COMMUNICATIONS COMPLEX

Jay B. Curtright
Jet Propulsion Laboratory

The Precision Time Distribution System (PTDS) at the Goldstone Deep Space Communications Complex is a practical application of existing technology to the solution of a local problem. The problem was to synchronize four station timing systems to a master source with a relative accuracy consistently and significantly better than 10 microseconds. The solution involved combining a precision timing source, an automatic error detection assembly and a microwave distribution network into an operational system. Upon activation of the completed PTDS two years ago, synchronization accuracy at Goldstone (two station relative) was improved by an order of magnitude. It is felt that the validation of the PTDS mechanization is now completed. Other facilities which have site dispersion and synchronization accuracy requirements similar to Goldstone may find the PTDS mechanization useful in solving their problem. At present, the two station relative synchronization accuracy at Goldstone is better than one microsecond.

The necessity for developing the PTDS evolved from the basic mission of the Goldstone Complex. Goldstone stations have been assigned the responsibility of obtaining telemetry (tracking) from deep space probes; i.e., those spacecraft which operate at distances and beyond the moon's orbit. In 1958, when the first deep space probe, Pioneer III, was tracked by Goldstone's 26-meter antenna, tracking ended when the spacecraft transmitter failed at a distance of just over 100,000 km from earth. By 1962, Goldstone tracked the first Venus probe at a range exceeding 30 million kilometers. Today, with the capability of the 64-meter Mars Station antenna, Pioneer X is being tracked at a range of over 3 AU (approximately 450 million kilometers).

During the same time frame that tracking range capability rapidly increased, other spacecraft and ground support functions had to be improved to keep pace. One of the most important improvement sequences was in the field of spacecraft control. For example, in the field of lunar exploration, the first series of probes transmitted TV pictures back to earth as the spacecraft descended toward an impact on the lunar surface at a speed over 8000 kilometer per hour. The next series of probes landed on the surface at a speed of less than 2 meters per second. After landing, the spacecraft took thousands of frames of video, performed simple chemical and mechanical analysis experiments and even lifted off the lunar surface and flew 10 feet laterally. All experiments were under direct control from earth.

In the field of planetary exploration, the first Venus probe in 1962 had a miss distance of approximately 35,000 km. The first Mars probe, launched two years later, came within approximately 9800 km of the planets surface.[1] By 1969, improvements in the control of spacecraft trajectory resulted in a Mars flyby within 3400 km of the surface.[1] In November 1971, the most recent of our Mars probes went into orbit around the planet at a planned periapsis altitude of 1650 km.[2] Each of the advances in control capability mentioned above required improved timing capability at the tracking stations.

The first precision timing system at Goldstone used a crystal oscillator for a source. In 1964, crystal oscillators were replaced by first generation rubidiums, and these were in turn replaced by second generation rubidiums in 1967. Over a period of four years, oscillator accuracy improved from 1×10^{-9} to 1×10^{-11}. Timing accuracy improvements, however, were not the only advancements needed to handle the increasingly more stringent mission requirements. Station timing synchronization had to be improved if the advances in oscillator accuracy were to be utilized fully.

Using HF radio, synchronization accuracy was gradually improved from a guaranteed two-station relative error of 5 milliseconds to an error of 1 millisecond. In 1967 the DSN started the Moon Bounce experiments,[3] which resulted in an improvement to first 20 microseconds and then 10 microseconds for two-station relative synchronization for all DSN stations around the world. The accuracy was further improved by using portable clocks but this method was extremely expensive and service was irregular. What was needed was low-cost dependable system. The PTDS project was started as a result of this requirement.

The following goals were established when the Precision Time Distribution System Project was started at the Goldstone Deep Space Communications Complex:

- Synchronize four remotely located precision timing systems to one master time source with microsecond accuracy
- Automatically monitor and record system errors for later analysis
- Use the existing communications system at Goldstone to reduce implementation costs

The first step in translating the PDTS goals into an operational system was the design and building of the Complex Microwave Timing Source (CMTS) shown in Figure 1. The CMTS contains two major subsystems, the precision timing source and the error-detection assembly. Design of both CMTS subsystems used off-the-shelf hardware to the maximum extent possible to reduce cost and construction time. A block diagram of the CMTS is shown in Figure 2.

The first block represents a commercially available cesium oscillator accurate to within one part in 10^{11} or approximately 0.864 microseconds per day. The oscillator output used is 1 MHz.

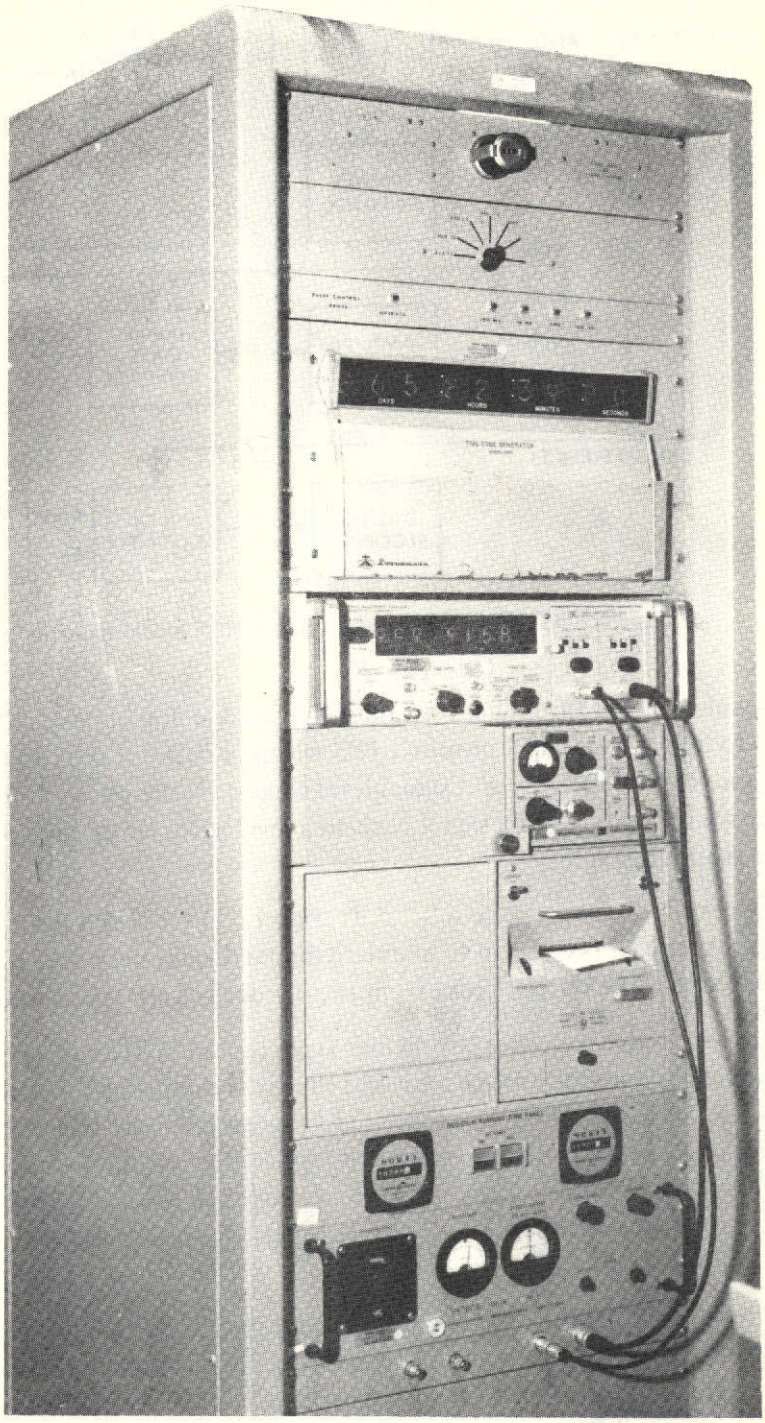

Figure 1. Complex microwave timing source assembly.

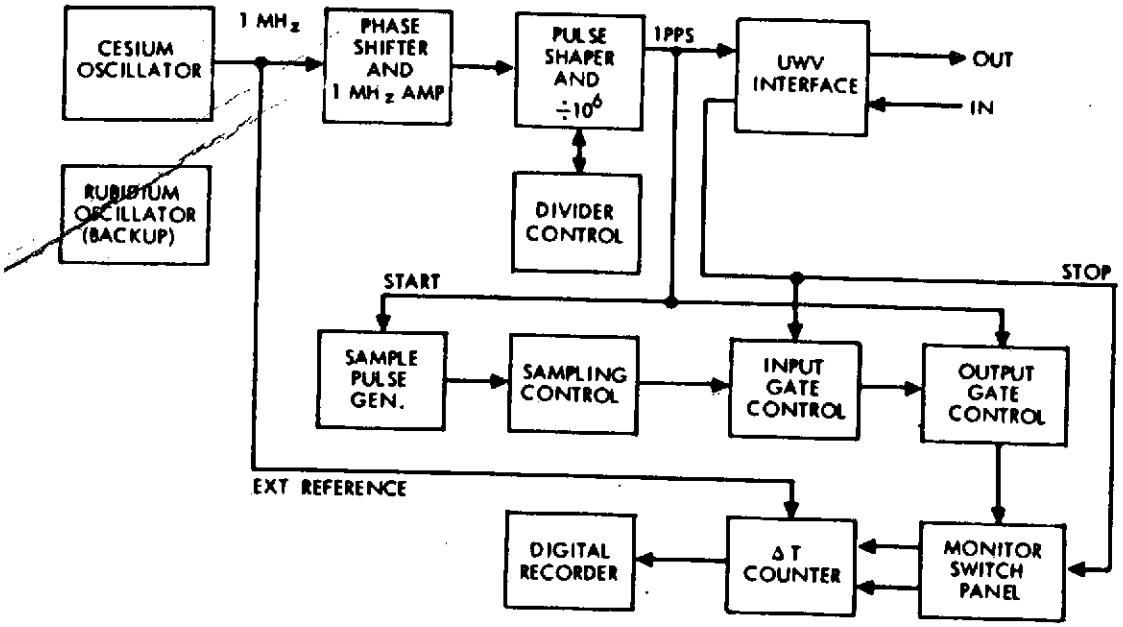

Figure 2. Complex microwave timing source block diagram.

The 1-MHz signal is passed through a continuously variable 360° phase shifter. The phase shifter is used to adjust the CMTS output 1 PPS within a range of 0.02 to 100 microseconds. Because of the 20-dB loss in signal level caused by the phase shifter, a tuned 1-MHz amplifier is used to boost the signal back to a level sufficiently high to drive the next stage with the required stability.

The shaper-divider block first stage is a Schmitt trigger. The 1-MPPS train of square waves out of the Schmitt trigger is coupled to standard digital divider network ($+10^6$) which outputs one pulse each second; the output pulse from the divider has a 50 percent duty cycle.

The 500-millisecond pulse from the last divider stage is used in several ways. One output from the last divider is passed through a second shaper, a monostable multivibrator (one shot), to produce 50-microsecond-duration pulses spaced precisely one second apart. This 50-microsecond pulse is fed to the microwave interface, the sampling circuits and the delay counter (ΔT). A second output of the last divider is used to drive the divider control block. The function of the divider control is to provide the capability for delaying the output 1 PPS from 0.1 milliseconds to 1 second if required.

To be of use, the 1 PPS must be distributed to all the stations at Goldstone. Figure 3 is a map of the Goldstone Complex which shows the intersite distances and indicates the conformation of the hills surrounding each site. The hilly terrain around Goldstone site is ideal for providing the required RF isolation between sites. Several spacecraft are often tracked simultaneously by Goldstone, each by a different station. With transmitters operating at +60 to +70 dBm or more and received signal levels ranging from -140 to -170 dBm, RF isolation is a necessity. The hills surrounding Goldstone sites provide 75 dB or better RF isolation between each pair of sites.

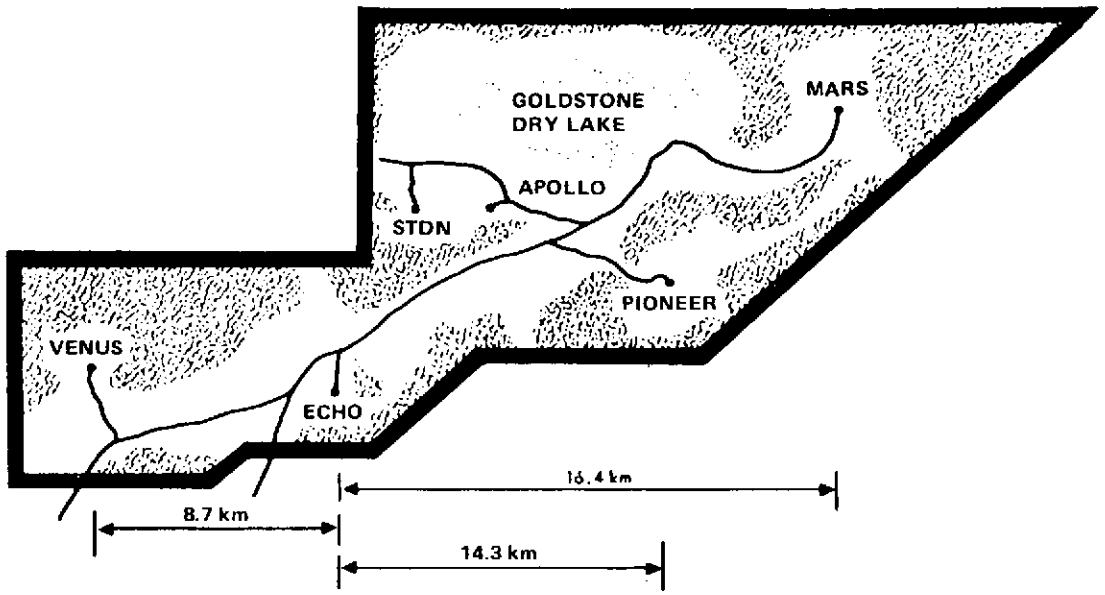

Figure 3. Goldstone complex map.

To provide the wide-bandwidth intersite communications required by Goldstone, a microwave link has been installed from the main communications center at Echo site to each of three remote sites (Figure 4). (The communications link between the Echo tracking station and the Echo site communications center uses coaxial cable since the two facilities are only

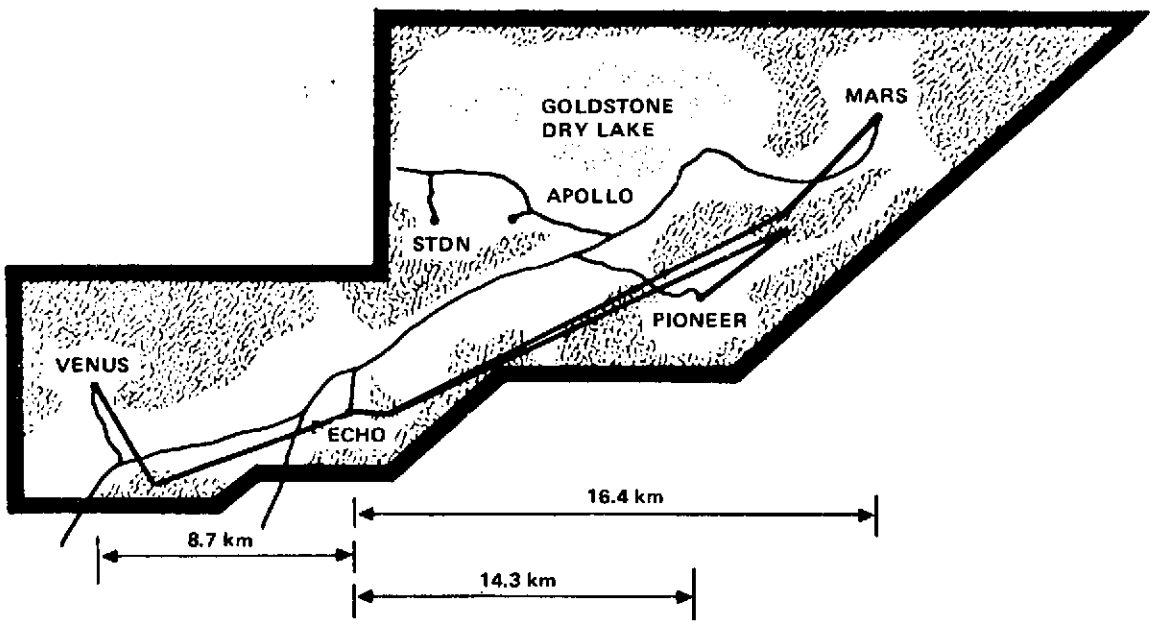

Figure 4. Goldstone complex map with microwave links shown.

about 200 meters apart via cable tunnels.) The CMTS is physically located in the communications center and is connected to the microwave equipment by short runs of 75 ohm coax.

Referring to Figure 5, the 1-PPS, 50-microsecond-duration pulse from the shaper divider is appropriately attenuated and then transmitted to the complex intersite microwave communications system. The notable items in this completely off-the-shelf communications link are the signal degradation and system drift. Figure 6 compares typical outgoing and return pulses; the outgoing pulse was taken from the output of the line driver amplifier of one station channel and the return pulse was taken from the same station return channel video amplifier. For basebands frequencies above 2.5 MHz the rise time of the return signal, between 10 percent and 90 percent of the slope, was approximately 0.4 microseconds, which was quite adequate, as compared to the slightly less than 0.2 microseconds rise time for the input pulse. Both pulses are extremely stable and exhibit almost undetectable jitter. Early in the project basebands above and below 2.5 MHz were tried. It was found that baseband frequencies above 2.5 MHz passed the pulse equally well but significant degradation in rise time occurred below a frequency of 2.5 MHz.

During this project, careful measurements were made of system drift as evidenced by variations in recorded round-trip delay times. Drifts of up to ±0.2 microseconds were noted on all three microwave links. Since the changes were somewhat cyclic, it is believed probable

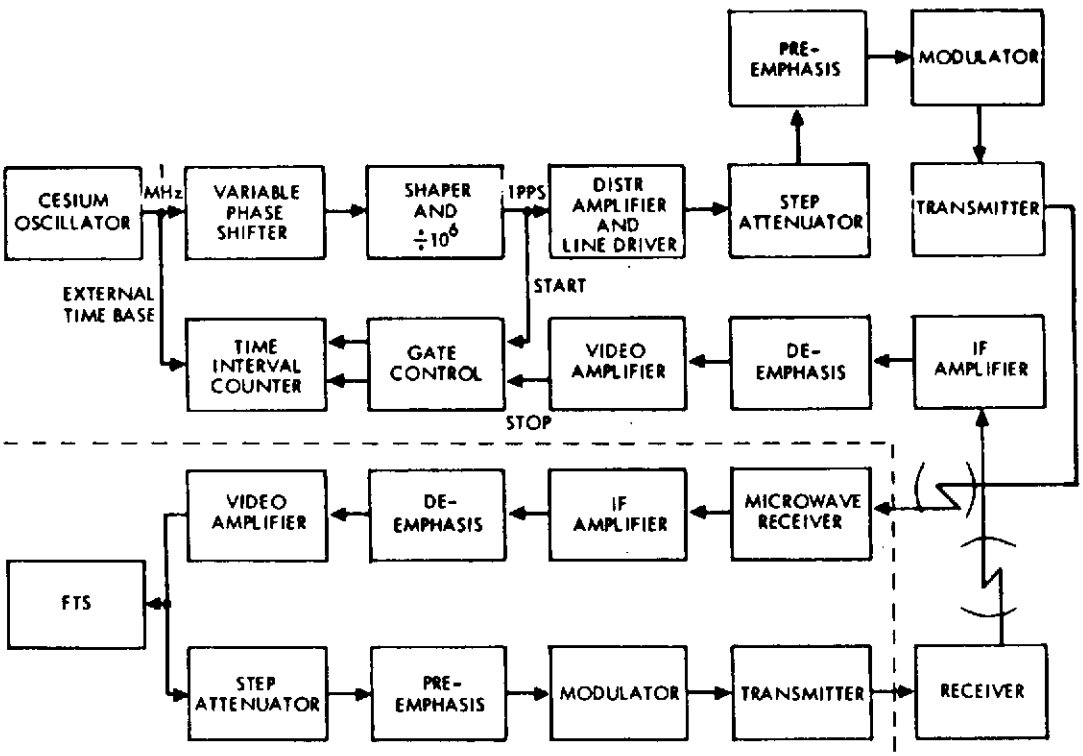

Figure 5. Precision time distribution system block diagram (1 channel).

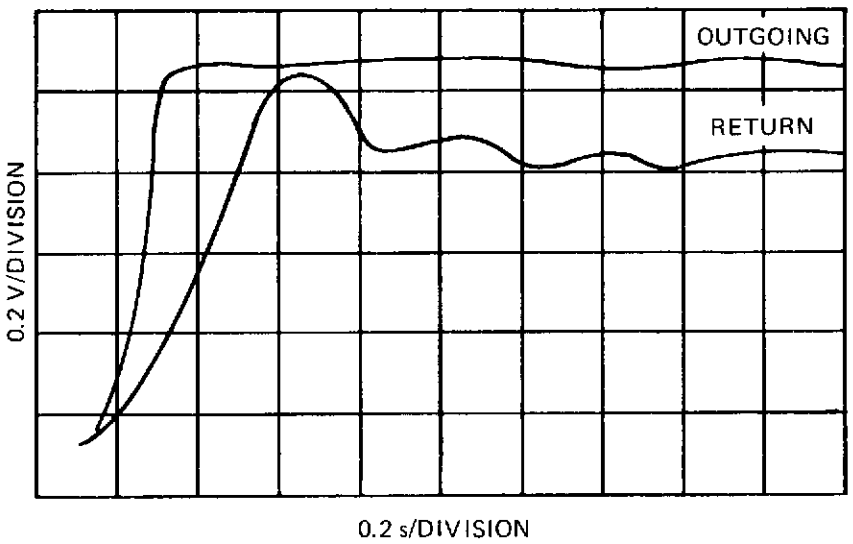

Figure 6. Microwave link waveform comparison.

that changing weather conditions were the prime cause of the drift. Cyclic variations of 20° C or greater than 40 percent relative humidity in 24 hours are, of course, not uncommon in the desert. In addition, during some windstorms, very large amounts of dust occlude the propagation path of the microwave link. Figure 7 is a plot of the drift of one channel of microwave over a period of 10 days. The diurnal cycling of the system is, of course, quite obvious. However, the causes of the longer period drift envelope, as evidenced by the 2-1/2 day cycle in the center of the plot, have not been fully determined. Investigation of system drift cycles is continuing. The correction of these drift problems is not particularly pressing at this time. Total excursion of the drift is less than 70 nanoseconds, which is more than an order of magnitude better than is presently required.

Referring again to Figure 2, the 1 PPS is also used to drive the error detection sampling logic of the system and provide the start pulse to the ΔT counter. First a combination of divider circuits is used to generate the several time periods involved in the sampling process. Pulse

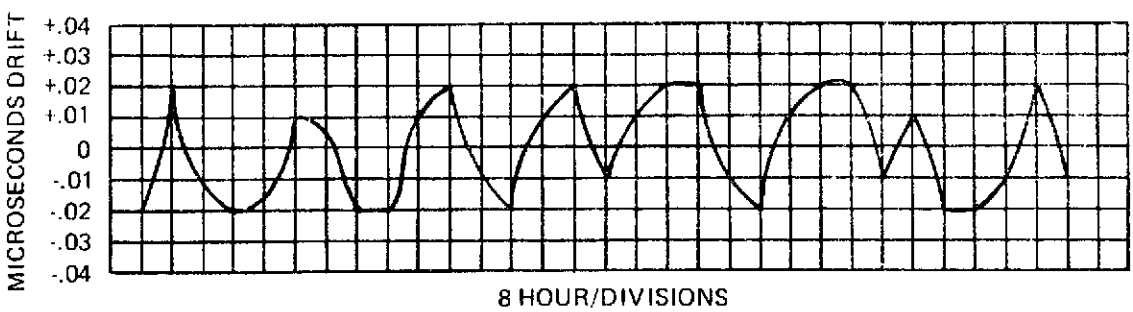

Figure 7. Microwave channel drift; ten-day period.

outputs for 1, 2, 4, and 64 minutes are used in the control logic. Each 64 minutes the prime sampling enable signal is generated, starting the sequence. Through the control of a series of coincidence gates, the round-trip delay time of each of the four stations is sampled in sequence and printed out 30 times in a 30-second period. The CMTS 1 PPS starts each sample count in the ΔT counter, and the 1 PPS returned from the station stops the sample. The sequence is completely automatic. No identification is used to "tag" the counter printouts since the sampling sequence is always the same and the wide disparity between round-trip times permits easy identification. Table 1 gives the time frames and approximate round-trip delay times for each of the four stations monitored. A complete schematic of the sampling control circuits and the precision timing circuits is shown in Figure 8 for readers who wish to study the CMTS in more detail.

Table 1
Time Frames and Delay Times.

Station	Time Frame	Delay* (μs)
Pioneer	T0-T30	94
Echo	T60-T90	3.5
Venus	T120-T150	58
Mars	T180-T210	112

*Delays are not actually figures, but are for use in identifying the stations from which samples are taken.

One feature of the PTDS that has not been previously mentioned is the clock reference for the cesium oscillator. The DSN Reference Standards Laboratory (RSL) clock located at Echo site is the standard used by all stations in the worldwide network. The RSL clock is continually maintained at within ± 2 microseconds of the National Bureau of Standards Clock-8.

The CMTS assembly receives the timing signal of the RSL clock by coaxial cable. The RSL also supplies a set of predictions of their best estimate of the difference between the NBS-8 and the RSL clock. By comparing the RSL daily predictions with the actual difference between the RSL clock and the CMTS oscillator, Goldstone has been able to maintain the CMTS at within ± 2 microseconds of NBS-8. Thus, for the past two years, Goldstone stations timing accuracy has been maintained at within ± 3 microseconds of NBS-8 and at better than one microsecond synchronization accuracy from station to station.

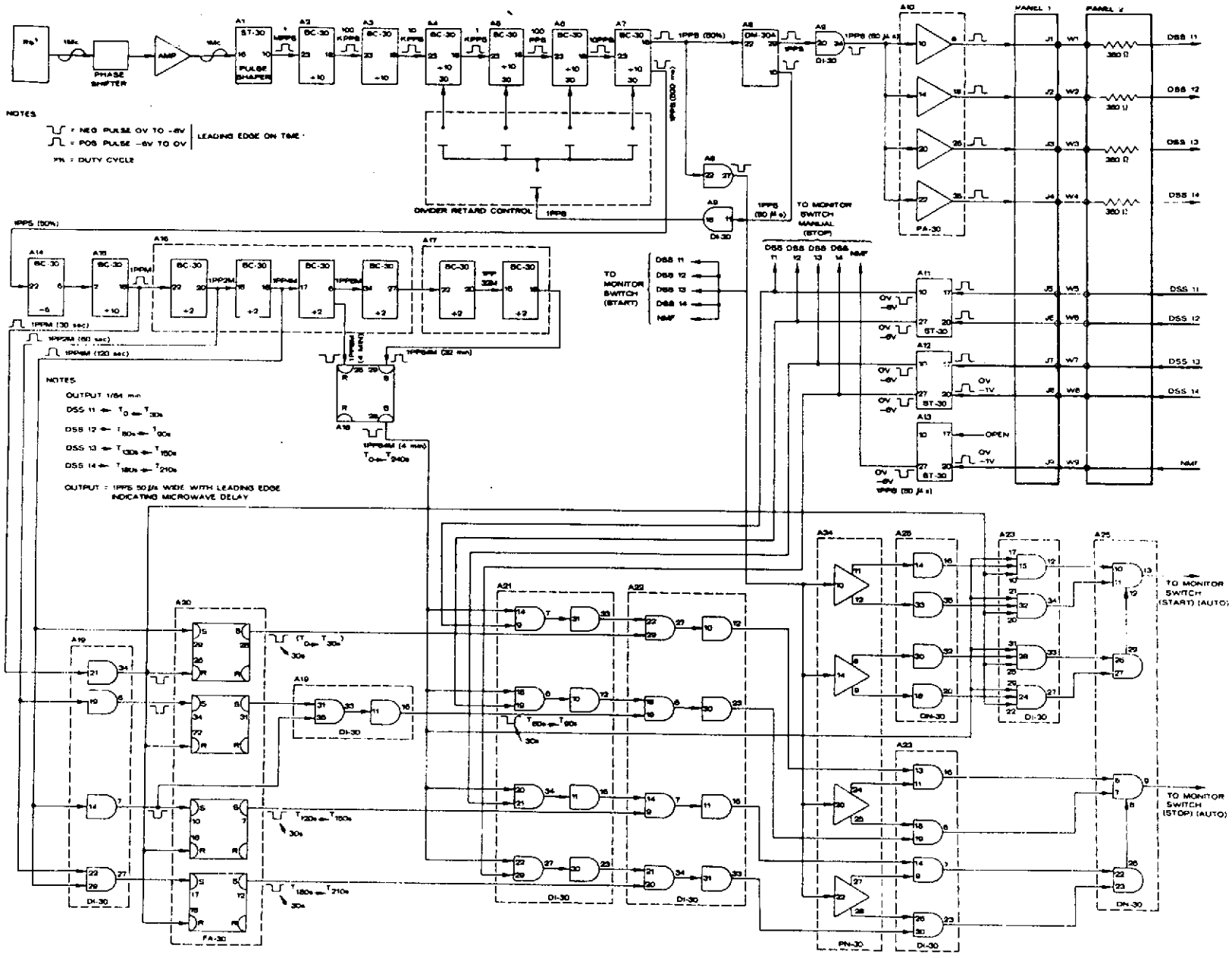

Figure 8. Complex microwave timing source logic diagram.

REFERENCES

1. NASA Pocket Statistics History, Program and Special Reports Division, Executive Secretariat, National Aeronautics and Space Administration, Washington, D.C., pp. A 28, A 35, A 62, July 1972.
2. "Mariner Mars 1971 Status Bulletin No. 22," JPL Internal Document, Jet Propulsion Laboratory, Pasadena, Calif., January 12, 1972.
3. W. H. Higa, "Time Synchronization via Lunar Radar," IEEE Proceedings, vol. 60, No. 5. pp. 552-557, May 1972.

UTILIZATION OF FSK COMMUNICATIONS FOR TIME

Robert R. Stone, Jr.
Thomas H. Gattis
Naval Research Laboratory

Theodore N. Lieberman
Naval Electronic Systems Command

The original purpose of this paper was to present off-the-air data on the recovery of a time stream transmitted by the VLF station NBA at Summitt, Canal Zone. Due to unforeseen difficulties in the procurement of some critical components required in the antenna portion of the system, the commencement date for transmission was delayed until January 1973. No actual data has been received from the station at this time; however, the system has been simulated in the laboratory.

This presentation will be divided into two parts:

- The first part discusses the method of time control employed at NBA for time-signal transmission. It also describes methods of extracting a "recovered clock" at the receiver and presents data derived in an experiment at the Naval Research Laboratory (NRL) and from a signal received from NLK/NPG, located at Oso, Washington.
- The second part of the presentation discusses requirements for adapting PTTI control to Naval Communications Systems. It describes a method for reducing the time required for synchronization or identification of messages and the fallout from the communication system to passive timekeeping users.

FSK COMMUNICATIONS FOR TIME

Figure 1 shows the stations, locations, assigned frequency, and nominal radiated power of the Naval VLF high-powered transmitting stations. At the present time, all of these transmissions are frequency/phase stabilized and are monitored by the Naval Observatory. The local station clocks are derived from cesium-beam oscillators which are maintained in frequency to within several parts in 10^{11}. These stations operate in an FSK mode with the lower carrier on the assigned frequency and the upper carrier offset by 50 cycles. It operates at 50 baud in 7.0 teletype code. In all stations except Northwest Cape Australia, only the on-frequency carrier is phase controlled. The offset frequency phase will vary to compensate for variations in the bit-stream timing. At Northwest Cape the bit stream is retimed.

In order to realize the full capabilities of the VLF system for PTTI purposes, it is necessary to control all time aspects of the signal. A block diagram of the NBA control system

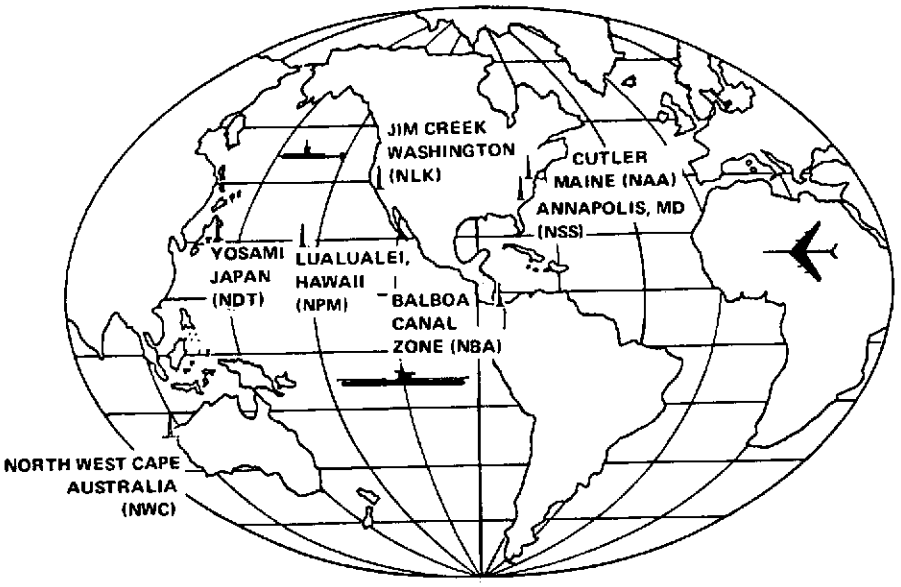

STATION	LOCATION	FREQUENCY (kHz)	NOMINAL RADIATED POWER (kw)
NAA	CUTLER, MAINE 44°38 9N, 67°16 9W	17.80	1,000
NBA	BALBOA, CANAL ZONE 09°-03 N 79°-39 W	24.00	150
NDT	YOSAMI, JAPAN 34°58 N 137°01 E	17.40	50
NLK	JIM CREEK, WASHINGTON 48°12 1N, 121°55 OW	18.60	250
NPM	LUALUALEI, HAWAII 21°-25 -N 158°-09 -W	23.40	140
NSS	ANNAPOLIS, MD. 38°-59 -N 77°-27 -W	21.40	85
NWC	NORTH WEST CAPE, AUSTRALIA 21°49 OS, 114°09 8E	22.30	1,000

Figure 1. The Naval VLF high-powered transmitting stations.

is shown in Figure 2. This system differs significantly from previous control systems since it will provide for not only phase control of both carriers but also the time of transition. All of the driving signals and time references are provided by a cesium-beam clock system which is coordinated in time by the Naval Observatory. The input keying information is stored and retimed in the storage buffer unit. The output from this unit keys the coherent FSK keyer, which provides the signal for driving the transmitter. The output of the transmitter is monitored at the antenna. Both of the carrier frequencies are tracked in the comparator. The positive going-zero crossings of these tracked frequencies are detected and divided down to produce 20-millisecond time streams. These time streams are then compared with a 20-millisecond time-stream reference from the clock. The error signal between the clock stream and the divided-down on-frequency carrier is used to phase control all of the signals required by the storage buffer and the coherent FSK keyer. The error signal produced from the comparison of the clock 20-millisecond stream and the divided-down off-frequency carrier is used to control the differential phase between the on-frequency carrier and the off-frequency carrier. In this manner, an output signal format is produced as shown in Figure 3. The positive going-zero crossings of the carriers are held on time. Selection of a particular cycle in each 20-millisecond segment is accomplished in the digital division. The divided signal marks the point of phase coincidence between the two carriers. This point can then be adjusted in calibration to occur at any selected point in the FSK transition. The center point on a transition was chosen to provide an easily identifiable spot for systems employing discriminators. Once set and calibrated, the control points will hold to within ± 200 nanoseconds of the reference clock.

An experiment was conducted using the block diagram shown in Figure 4 to determine the effects of noise on the recovered clock and to make a comparison between a discriminator demodulator and a coherent demodulator. A communication receiver, BRR-3, was employed. In normal noncoherent operation, the discriminator demodulator is used, but for coherent demodulation a special demodulator unit was developed which demodulates the IF output frequencies and phase locks the local oscillator in the BRR-3 receiver to a stable reference source. The recovered clock was compared in a phase meter with the local clock and displayed on a recorder. A simulated signal attenuated to the normal expected input level was fed into the receiver and a VLF antenna was also connected so that noise conditions would be nearly the same as those encountered when receiving an actual transmission.

Figure 5 shows the results of these tests at three levels of input signal with noise level essentially the same in all cases. The signal level in the upper chart is equivalent to that normally received in Washington from NBA. Note that the width of the line in this case is about 50 microseconds. If the signal is further averaged, ten microseconds can easily be obtained. This is sufficient to identify the cycle of the tracked on-frequency carrier. Even though epoch timing control has not been installed at the other VLF transmitters, the stability of the input keying is sufficient to produce periods of 15 to 20 minutes of stable

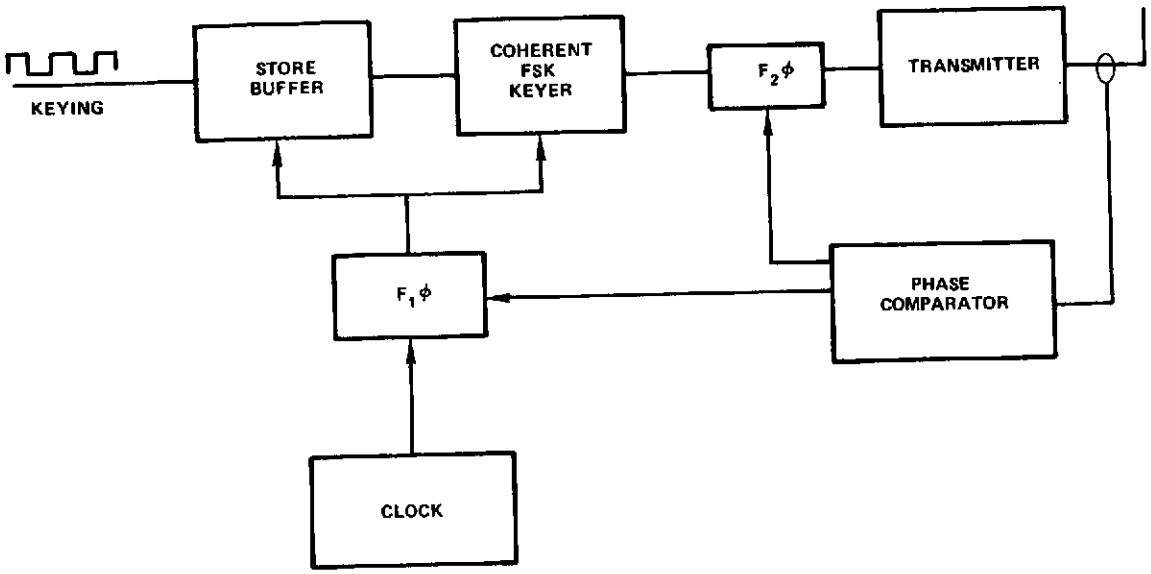

Figure 2. VLF time.

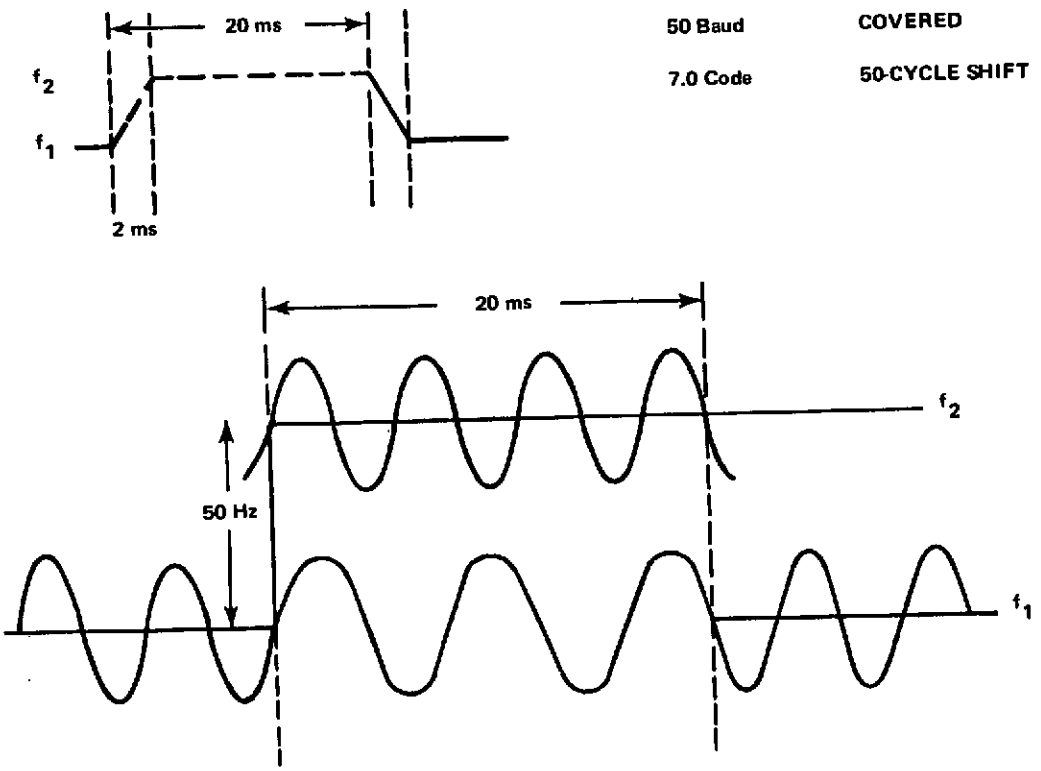

Figure 3. VLF/FSK signal format.

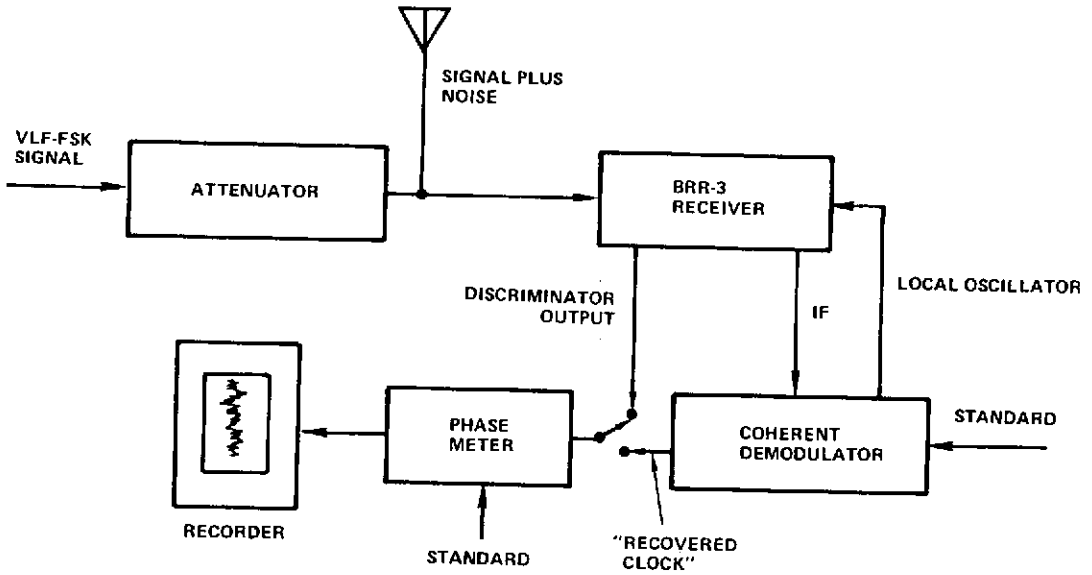

Figure 4. Measurement of VLF/FSK coherent/noncoherent timing transitions.

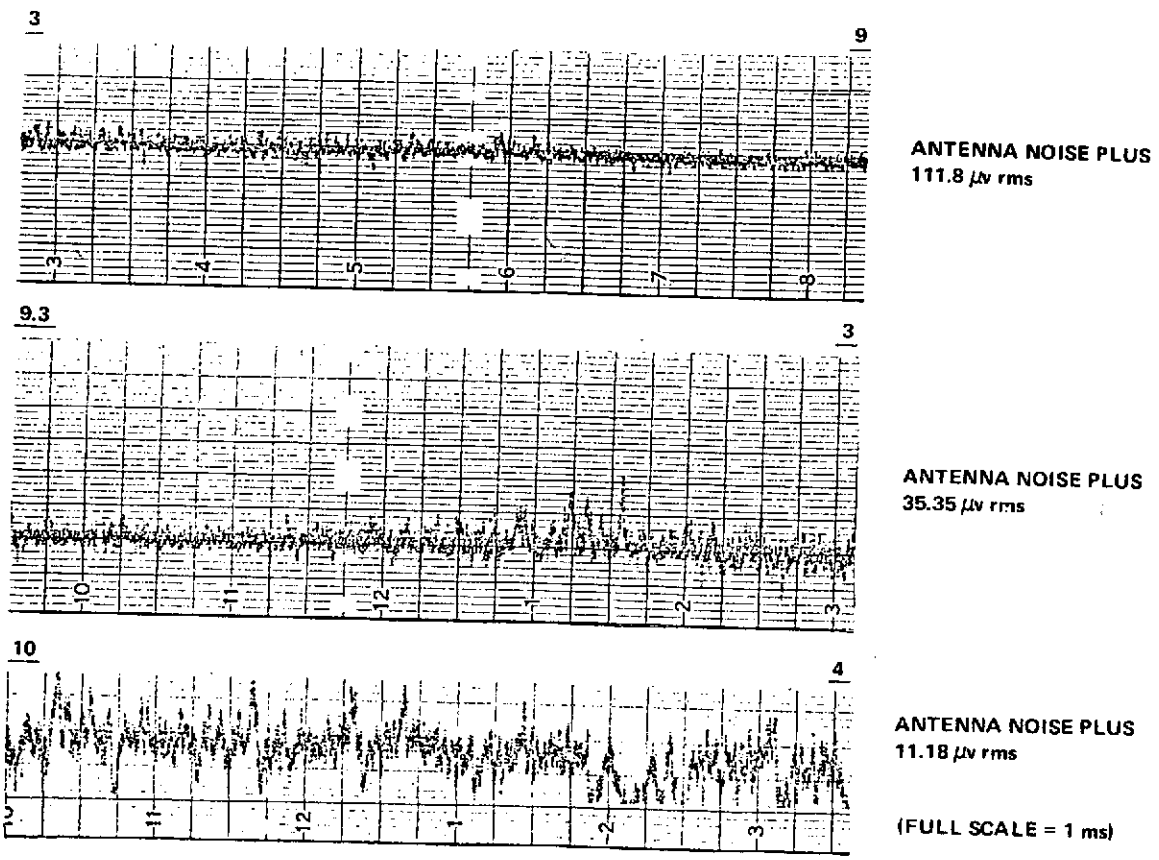

Figure 5. Recovered clock from VLF/FSK signal.

timing. Figure 6 shows data taken from the signal received from NPG/NLK at 18.6 kHz. The left portion of the graph shows the operation with the receiver's discriminator and the right portion of the graph shows the operation with the coherent demodulator. The abrupt shifts in the line were caused by changes in the phase of the offset frequency. The straight portions of the line indicate the stability of the recovered clock. These preliminary data indicate that the system will operate well for timekeeping purposes.

NBA is expected to be on the air in January, and at that time data should be obtained that will permit a more complete evaluation of the system.

PRECISION TIME AND TIME INTERVAL (PTTI) IN NAVAL COMMUNICATIONS

As a result of the application of new technology, the Naval Communications System is rapidly evolving into a high-speed digital network consisting of fixed, mobile, and itinerate users. Such a system portends multiplexing hierarchies based upon command levels, priorities, geographical locations, and so on. A fundamental limiting factor in such a system is network timing and synchronization. Basic to the success of such a system is the ability to define and discipline time interval and time-of-event.

The PTTI program addresses itself to the definition and coordination of precision time and time interval. A communication system may take the form shown in Figure 7. Here several communication nodes or functions are involved. These nodes may originate or transfer communication information and they may operate in a one-way or two-way mode. Furthermore, they may consist of synchronous or asynchronous systems. A rather complex situation is created wherein the interleaving of synchronous, asynchronous, high-speed, and low-speed data streams may be required. In addition, the time required for processing within the nodes, transit between the nodes, and variations in these time lengths must be considered. Unless a discipline is imposed on the bit, frame, link, and network synchronization or an intolerably large buffer is included, the system will be subject to a high error rate. The implementation of the PTTI concept will provide each node with a knowledge of time coordinated from a single point, with an error which is small compared to the length of the bit. It will also provide a means for the precision control of the timing aspects of the station, which will result in an ability to precisely control bit lengths and the position in time of code streams.

A PTTI-coordinated communication node may appear as shown in Figure 8. Bit timing will be coordinated at each node so that as each bit is transmitted by the node, the bit's leading edge will be synchronized to coordinated time. Frame, link, and network timing should be referenced to coordinated time and predesignated according to operational constraints. Predesignation may be made by preassignment, preamble, program, hierarchical level, or operational decision. In any event, the receiving node should be cognizant of the predesignated times so that code-stream presynchronization may be accomplished relative to the station PTTI-coordinated clock.

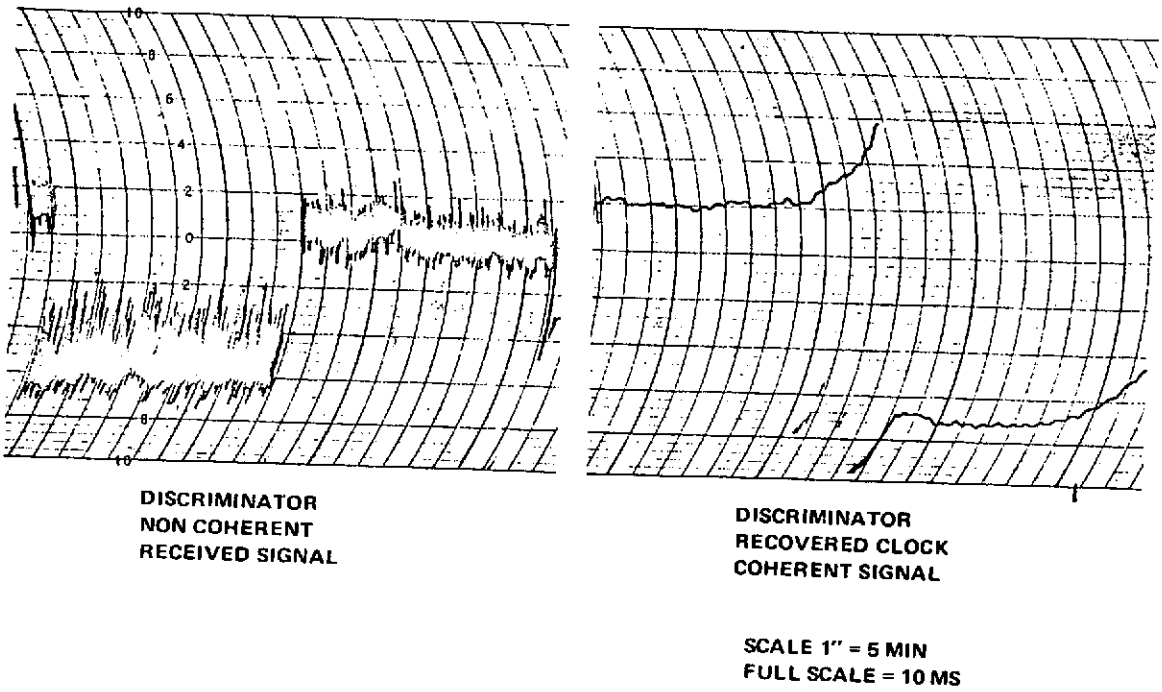

Figure 6. Data summary sheet.

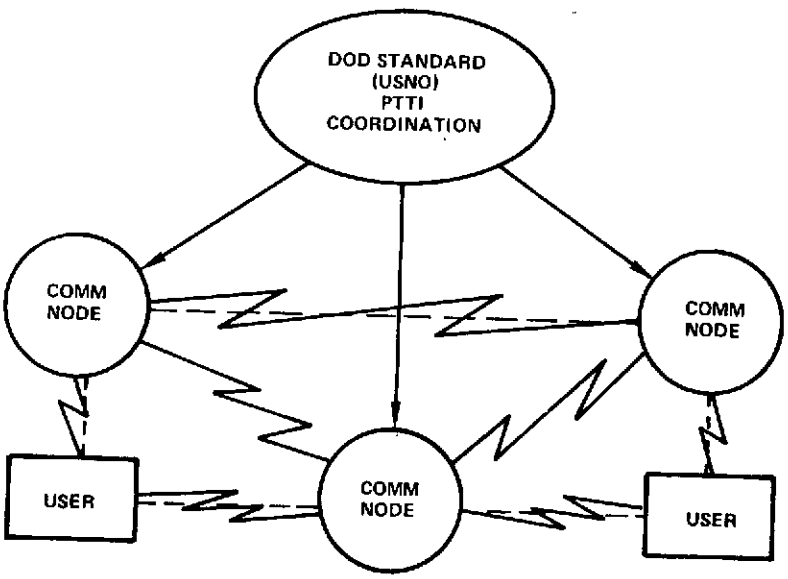

Figure 7. Communications network concept.

PTTI implies that at each communication juncture or node, a time reference be maintained which is sufficiently stable in its long-term average to provide a time of event in which the error is small relative to the length of the bit and to provide this time of event even after considerable periods of no communication. The stability and synchronization of the local reference clock are basic requirements. PTTI assumes the utilization of any available method for synchronization, including both active and passive systems (Figure 9). Any transmission containing a characteristic which can be identified in time can be utilized for time transfer and the subsequent synchronization of a local clock. Two-way systems have a capability for the correction of propagation delays. The time-transfer accuracy will be a function of the system precision. The accuracy of one-way systems will naturally be dependent upon not only the precision of the system but the predictability of the transmission delay as well. At the present time, the most accurate operational method of time transfer over long distances is through the DSCS Satellite System, which can provide coordinated time anywhere in the world to 1/10th of a microsecond. Other systems, such as Loran C, VLF, UHF, or HF, are dependent upon the proximity of the user to the transmitter. The VLF system, for instance, can provide coordinated time on a worldwide basis to within a few microseconds. It is expected that all major areas, such as short-communications stations, shipyards, or any major rendezvous point for ships, would maintain high-precision time and would have the capability for the transfer of this time over short distances to mobile units such as ships or aircraft. It must also be recognized that the systems which are utilized by the communication nodes have a capability for time synchronization (see Figure 8). Extraction of this information can be accomplished without interfering with the normal communication aspects. The ability to keep time and to control time interval is dependent upon the stability and drift rate of the reference oscillators. Two basic modes of operation are envisioned by the PTTI program; namely, one which utilizes a nearly invariant standard, such as the cesium molecular-beam device, and one which utilizes standards which have drift rates and which require updating, such as crystal oscillators or rubidium standards. The basic difference lies in the fact that the frequency or time interval which is produced from a cesium molecular-beam device is based upon the statistical average of the actions of a natural phenomena which essentially remains invariant. The time interval in this case is known within one part in 10^{11} and can be relied upon without reference to other standards. The time-error accumulation in such a system also varies in a straight-line fashion and can be easily predicted over long periods of time. Crystal oscillators have inherent in their mechanical nature, drift rates which are affected by environmental changes. The required stability of an oscillator used for PTTI purposes will be dependent not only upon its inherent drift rate but also on the frequency at which it can be recalibrated.

Figure 10 shows typical frequency drifts of various frequency/time references. Figure 11 indicates the accumulated time error which would result from these drifts. It would be expected in a major communication node, such as a shore communication station, that a cesium molecular-beam reference standard would be utilized as the PTTI source and a

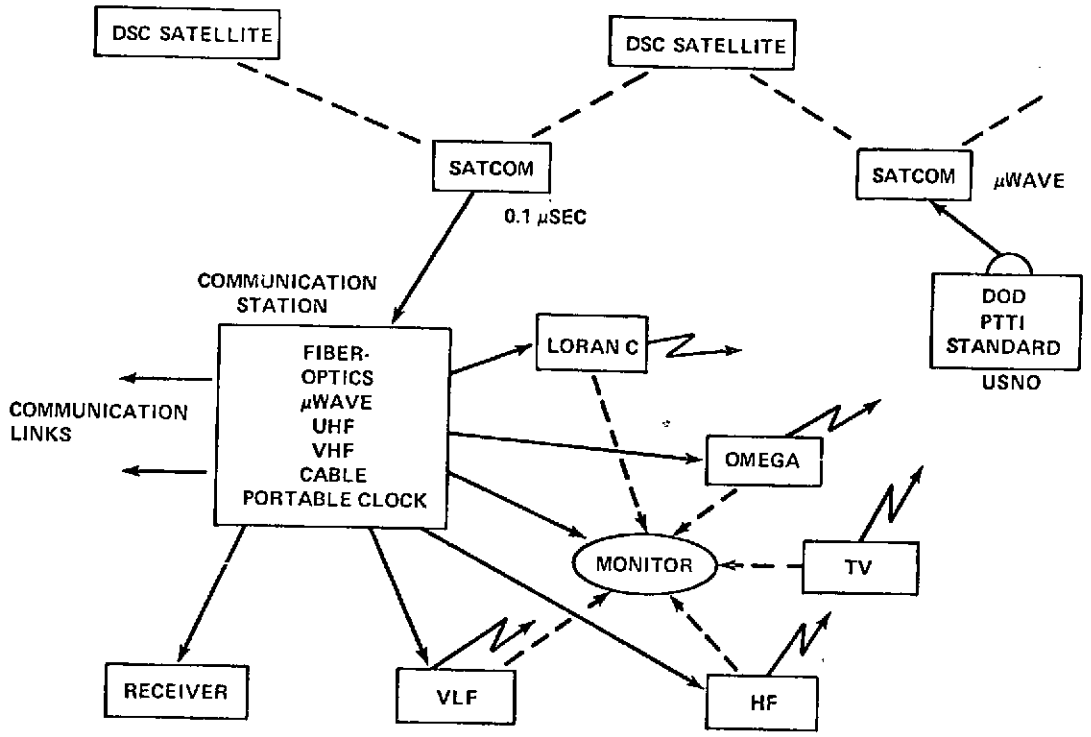

Figure 8. PTTI communication coordination.

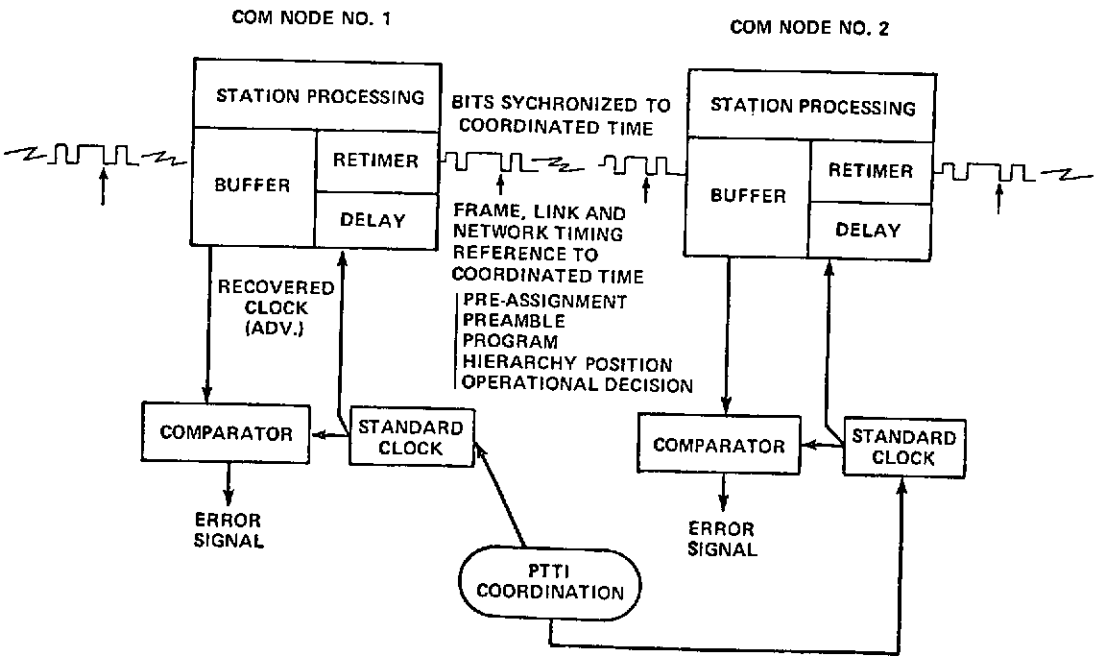

Figure 9. PTTI dissemination.

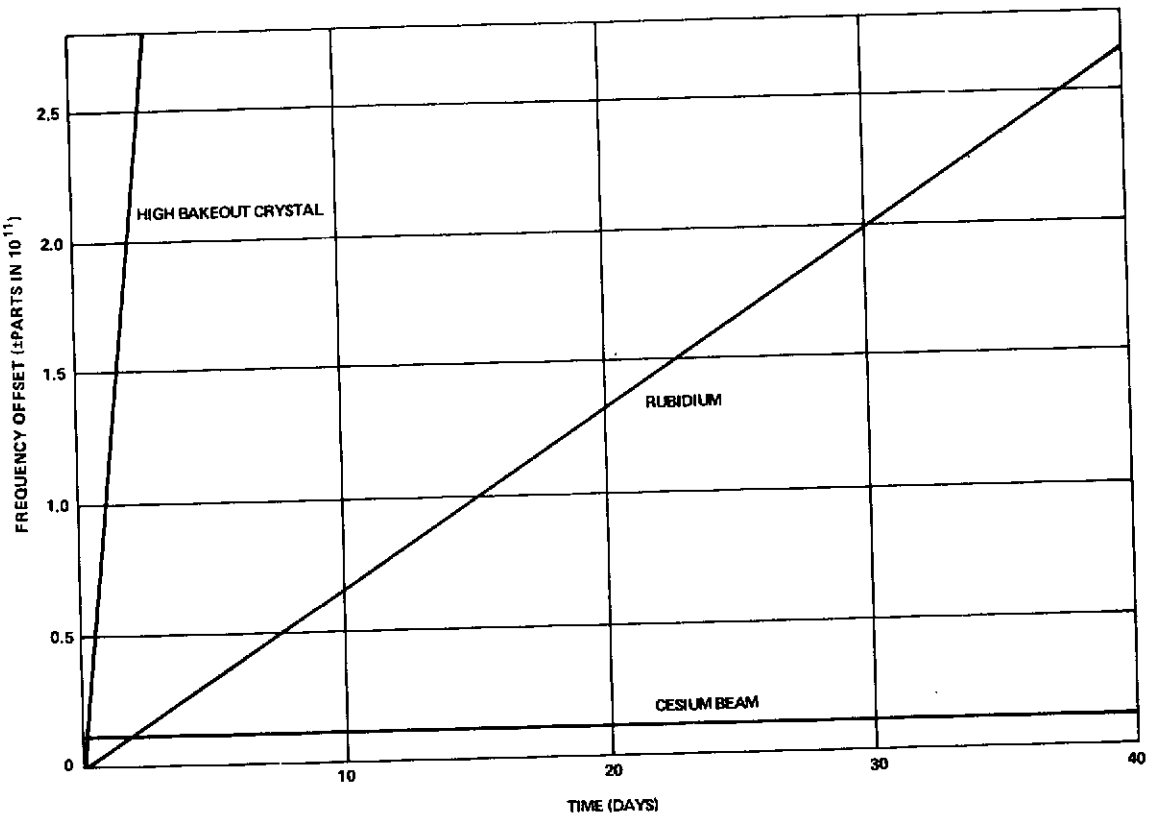

Figure 10. Probable maximum frequency offset without correction.

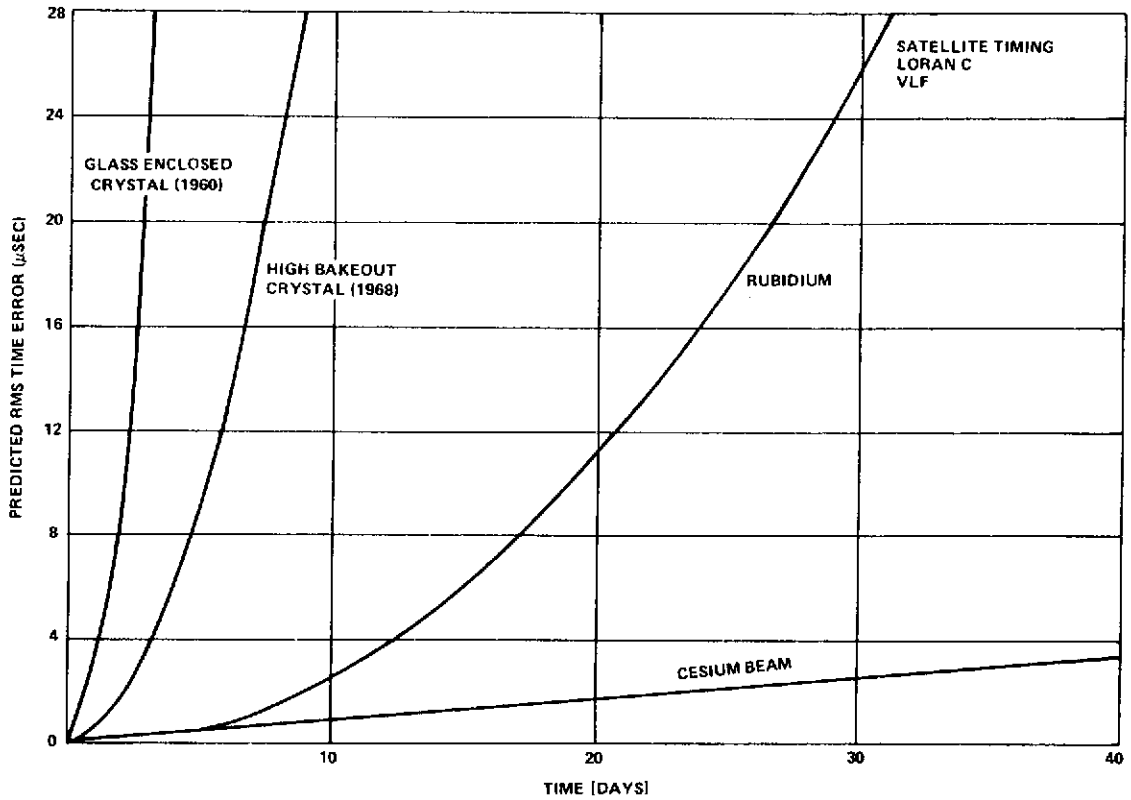

Figure 11. Probable maximum time error without correction.

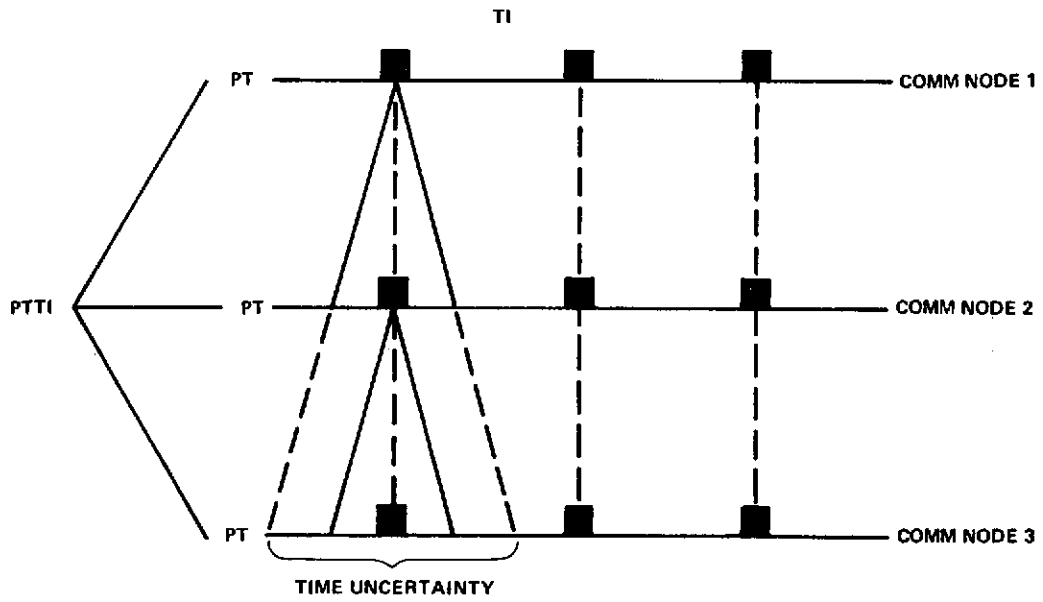

Figure 12. Precision retiming.

distribution made throughout the station. Discipline time/frequency oscillators would be utilized at user points. Synchronization of time kept by the standard clock could be accomplished by the most accurate or the optimum available method. Many COMSTAs have direct access to DSCS terminals. In the case of mobile units, means should be provided for direct synchronization with a major node (at the beginning of the mission).

One of the problems which exists in PTTI discipline of communication systems is that of delays arising from communication paths, instrument errors, or asynchronous systems. The solution to this problem lies in the ability to identify a predesignated time. Original broadcasts can be synchronized to start in a designated time relative to the standard clock. When a transmission is retransmitted after reception by a second communication node, its beginning must be delayed in sufficient time to account for any delays which occurred in the first transmission. One solution would be to normalize transmissions so that they would begin only at predesignated points, for instance, at each second. Another solution would be to designate the transmission start in accordance with the position of the node in the hierarchy. Since the transmission modes and patterns are known by the receivers, the precise beginning of message transmission from any given station would be officially designated. Either of these methods allows the station to presynchronize for any prescribed transmission. Network timing and synchronization can be made inherent in such a system, and the total delay involved in the transmission of a particular message could be reduced to the optimum. Time required for synchronization, resynchronization, or synchronization during jamming periods would be greatly reduced or eliminated. The advantage of retiming can be readily seen from Figure 6. The error introduced in the transmission path would be virtually eliminated when retransmitted from the following node.

In practice, the PTTI system will provide to the communication system a stable base for time-interval control and a coordinated reference for time-of-event control. It will utilize, where possible, characteristics of the communication links to maintain or verify the coordinated time. Under this system, a digital transmission would operate with all of its time-frequency aspects controlled relative to real time. The beginning of the code sequences would be designated by the operational constraints and would be subject to operational control. Such a method of operation permits the transfer of time to the nearest time increment through the communication, without interference. It also allows users who need only the time information the ability to extract it without the necessity of extracting communication information. Under this system many of the communication links would be automatic-position-location points which could be readily utilized by a tactical situation to determine propagation distances or position location.

TIMING REQUIREMENTS FOR THE SANGUINE ELF COMMUNICATIONS SYSTEM

Bodo Kruger
Naval Electronic Systems Command

SUMMARY

The requirements for transmitter stations clocks are 0.3ms (1σ) ± 1 ms for receiver clocks. It is of interest to note that for Sanguine, as in other coherent systems, the clock requirements are obtained as phase or time rather than as frequency.

1. INTRODUCTION – BRIEF SYSTEM OVERVIEW

The Navy has proposed to build an ELF communications system for communications primarily with submerged submarines. This system has been named Sanguine. The need for Sanguine follows from the following considerations:

In order for a weapon to be an effective deterrent it must be highly survivable. Weapon systems based in the world's ocean waters are the most survivable systems. Consequently, a great deal of emphasis is given to sea-based weapon systems such as the presently operating Polaris/Poseidon weapon system aboard nuclear submarines (SSBNs). The purpose of Sanguine is therefore to provide survivable command and control capability for sea-based and other forces, and in particular, to deliver High Priority Operational Messages.

The basic requirements for a command control and communications (C^3) system are:

- Deliver high priority operational messages, almost worldwide, pre- and post-attack, to SSBNs at speed and depth, and to other U. S. forces
- Survive physical attack (conventional and nuclear)
- Survive the electromagnetic pulse from low and high altitude nuclear bursts
- Be resistant to attack on the propagation path
- Be resistant to electromagnetic attack (jamming)

The C^3 problem has been studied for many years and the only solution which satisfies the above requirements is an ELF system, Sanguine. Sanguine will operate within the frequency band of 30 to 100 Hz; the most likely carrier frequency being 45 or 75 Hz. Figure 1 shows the free-space 45-Hz wavelength compared to the United States. This frequency band has the following characteristics:

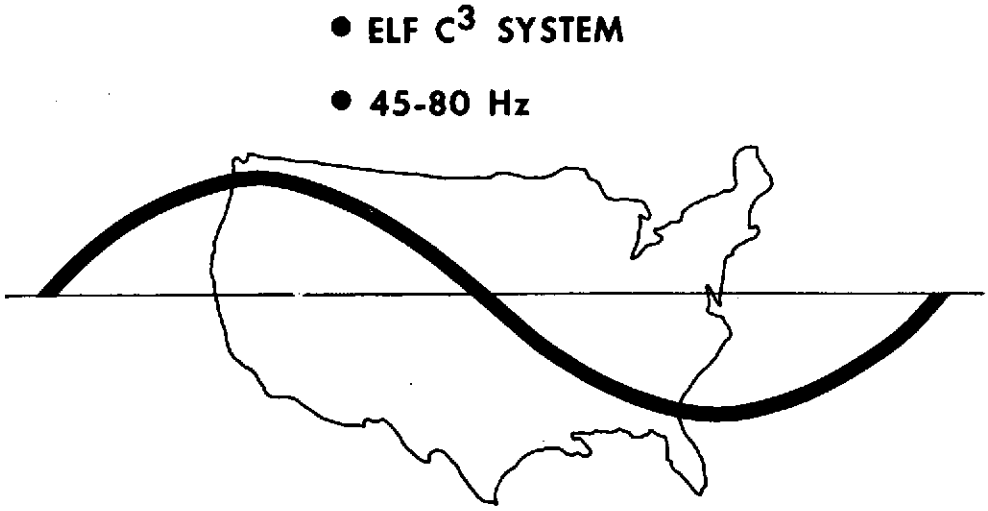

Figure 1. Free-space wavelength at 45 Hz.

Low Atmospheric Attenuation – permits reliable, almost worldwide, communication coverage from a CONUS-based transmitter and denies a jammer the range advantage it would have at higher frequencies

Low Sea Water Attenuation – permits ELF reception at considerable depths

Least Affected by Disturbed Propagation Path – attenuation is not severely increased by nuclear detonations along the propagation path

An illustration of the Sanguine concept is shown in Figure 2.

The transmitting antenna excites electromagnetic waves in the spherical cavity bounded by the ionosphere and the surface of the earth. ELF frequencies are well below the cut-off frequency of the first order mode (≈ 1700 Hz) in the cavity so that only the zero-order mode transverse magnetic waves will propagate.

The general vertical polarized E-field has a small horizontal component which propagates downward through sea water. This component can be sensed by an E-field submarine antenna.

The cost of the Sanguine transmitter will be an order of magnitude higher than the cost of all the receivers. In order to reduce system cost, signal and receiver design have been optimized to allow for the lowest signal-to-noise ratio compatible with C^3 requirements. Coherent detection is therefore used, which imposes timing requirements both on the transmitter and the receivers.

2. THE TRANSMITTER

Transmitter survivability is achieved by a combination of redundancy and hardened antenna and transmitter station design. The basic antenna element is shown in Figure 3; it can be viewed as a loop antenna. One part of the loop is an isolated cable grounded at each end, and the loop is closed by the earth return path. The cable can be buried, so it is very survivable. A power amplifier in a hardened transmitter station drives the current in the loop.

From 1000 to 10,000 of these basic elements will be combined in a transmitter array. Each transmitter station will be unmanned and will operate independently of the other transmitter stations; there will be no communications between stations. Each station must therefore have its own clock.

If each antenna element carries the current ΔI with relative phase as shown in Figure 4, then the resultant current I from N elements is

$$I = \sum_{1}^{N} \Delta I \cos \varphi^{i} = \Delta I \sum (1 - \tfrac{1}{2} \varphi_i^2 + \cdots)$$

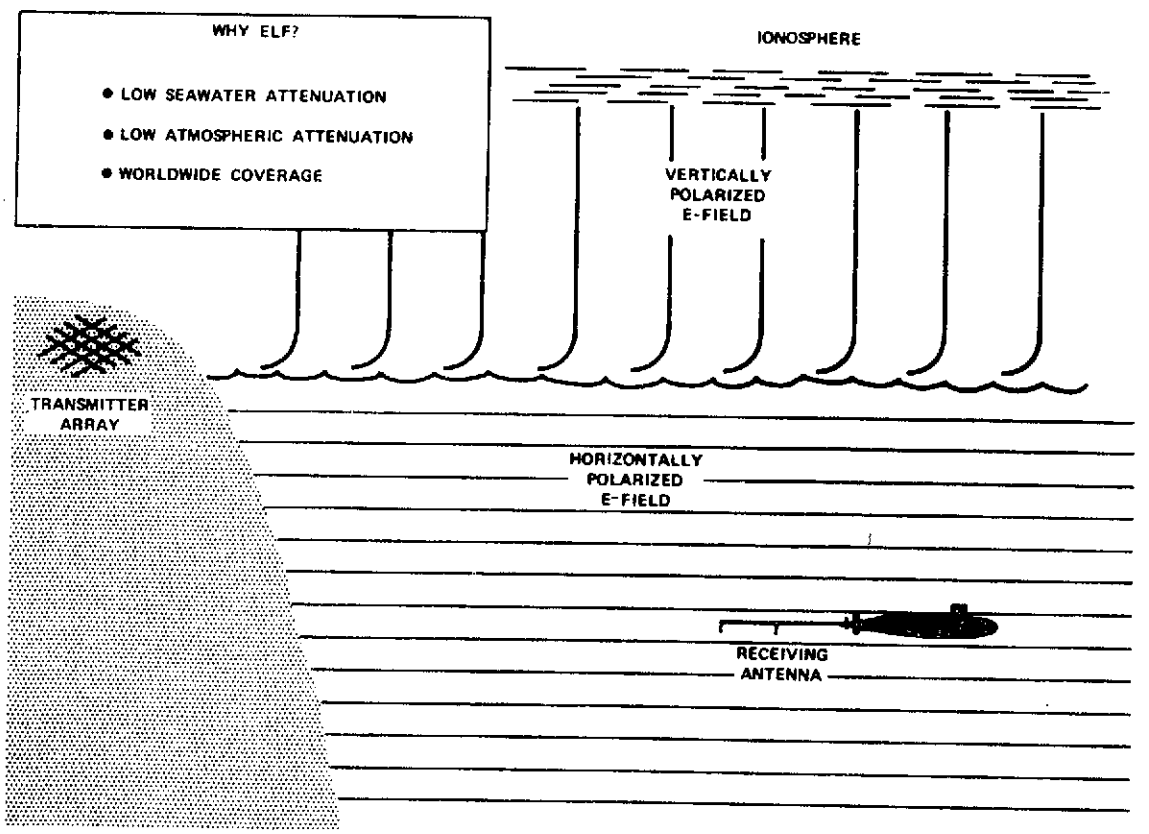

Figure 2. The Sanguine concept.

or

$$I = I_0 \cos \sigma_\varphi \tag{1}$$

where

$$I_0 = N \Delta I \tag{2}$$

$$\sigma_\varphi^2 = \frac{1}{N} \sum_1^N \varphi_i^2 \tag{3}$$

Thus $\cos \sigma_\varphi$ is the loss due to phase or timing errors at the transmitter stations. Table 1 shows the time accuracies required for 0.1 and 1 dB loss. Also shown is the required frequency stability obtained from

$$\frac{\Delta f}{f} = \frac{\Delta T}{T} \tag{4}$$

where T = 1 month.

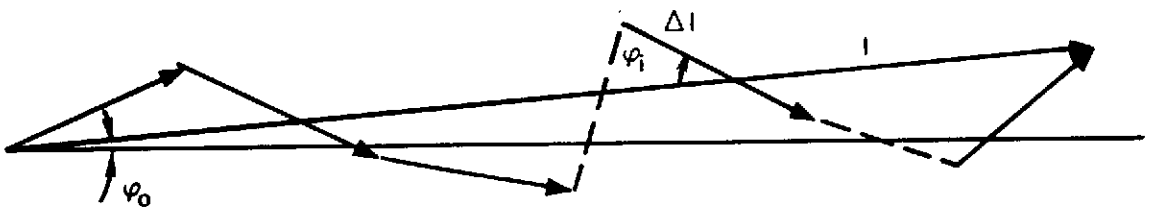

Figure 3. Basic Sanguine antenna element.

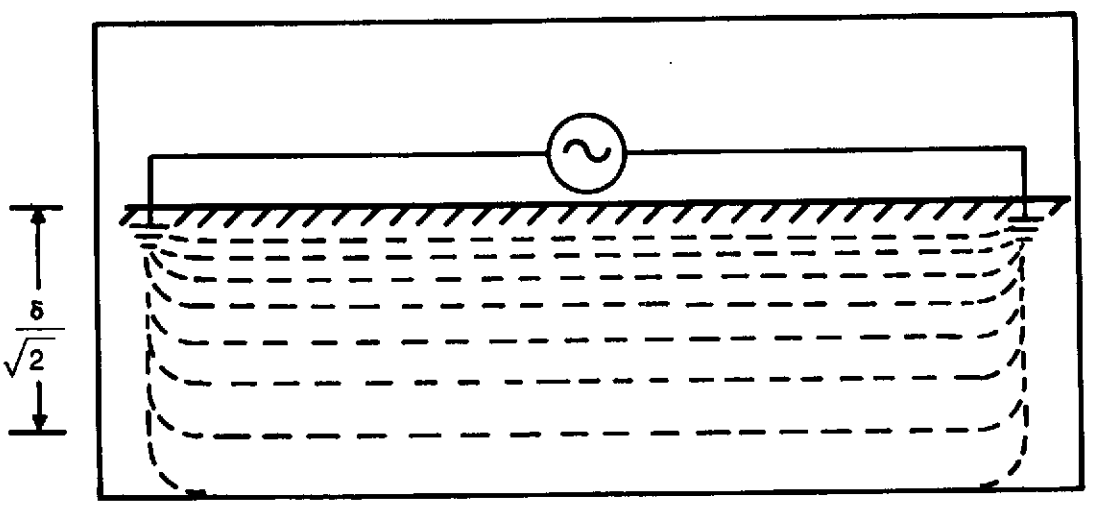

Figure 4. Summation of contributions from each antenna element.

Table 1
Time and Frequency Accuracy Required at Transmitter Stations.

	Phase Error	Time Accuracy		Frequency Accuracy	
Loss	(1σ)	(1σ)		Δf/f	(1σ)
(dB)	(Radius)	45 Hz	75 Hz	45 Hz	75 Hz
0.1	0.15	0.5 ms	0.3 ms	2.5×10^{-10}	1.5×10^{-10}
1	0.47	1.7 ms	1.0 ms	7.7×10^{-10}	4.6×10^{-10}

For the phase angle φ_0 of the resultant I, we have

$$\tan \varphi_0 = \frac{\sum_1^N \sin \varphi_i}{\sum_1^N \cos \varphi_i} \tag{5}$$

and for small angles

$$\varphi_0 = \frac{1}{N} \sum_1^N \varphi_i \tag{6}$$

and

$$\sigma_{\varphi_0} = \frac{1}{N} \sigma_\varphi \tag{7}$$

σ_{φ_0} is thus small and σ_0 can therefore be tracked by the receiver phase estimator described below.

3. THE RECEIVER

Minimum Shift Keying (MSK) has been selected for Sanguine as the most effective modulation scheme. MSK is a form of frequency-shift keying where the two frequencies f_1 and f_2 are orthogonal over one chip. Or if viewed as phase modulation $\exp\{ j(\omega_0 t + \phi(t)\}$, the phase $\phi(t)$ changes linearly $\frac{\pi}{2}$ during one chip. Several chips are combined to one channel symbol.

The phase of f_1 and f_2 will be obtained by a phase estimator in the receiver. The transmitter phase error φ_0 will thus be tracked by the receiver and will not degrade system performance.

For correlation of the chips, time is required. The signal loss due to a timing error is given by the correlation function $R(\tau)$. Following Source 3 we obtain

$$R(\tau) = (1 - \frac{|\tau|}{2T_c}) \cos(\frac{\pi\tau}{2T_c}) - \frac{1}{\pi} \sin(\frac{\pi|\tau|}{2T_c}) \quad (8)$$

where T_c is the chip time. A plot of Equation (8) is shown in Figure 5.

It is seen that $|\tau|/T_c = 0.1$ only results in 0.1 dB degradation. We thus can allow a total time error.

$$|\tau| = 0.1\ T_c$$

Due to antenna bandwidth limitations T_c will be 40 ms or longer, thus $|\tau| \geq 4$ ms. τ includes propagation path uncertainties and it seems reasonable to allot 1 ms to clock error out of the total 4 ms. The accuracy requirement for the receiver clock is therefore ±1 ms.

SOURCES

1. B. Kruger, "Project Sanguine – FBM Command and Control Communication," Naval Engineers Journal, Vol. 84, No. 3, June 1972. (This unclassified reference gives a SANGUINE System overview.)

2. "Engineering in the Ocean Environment," Record from IEEE International Conference at Newport, Rhode Island, Sept. 1972, IEEE publication 72 CHO 660-1 OCC. (This unclassified reference contains 22 papers on Sanguine.)

3. Sanguine System Design Study (SSDS) (U), Dec 1970. (This Classified report treats the technical aspects of Sanguine in detail.)

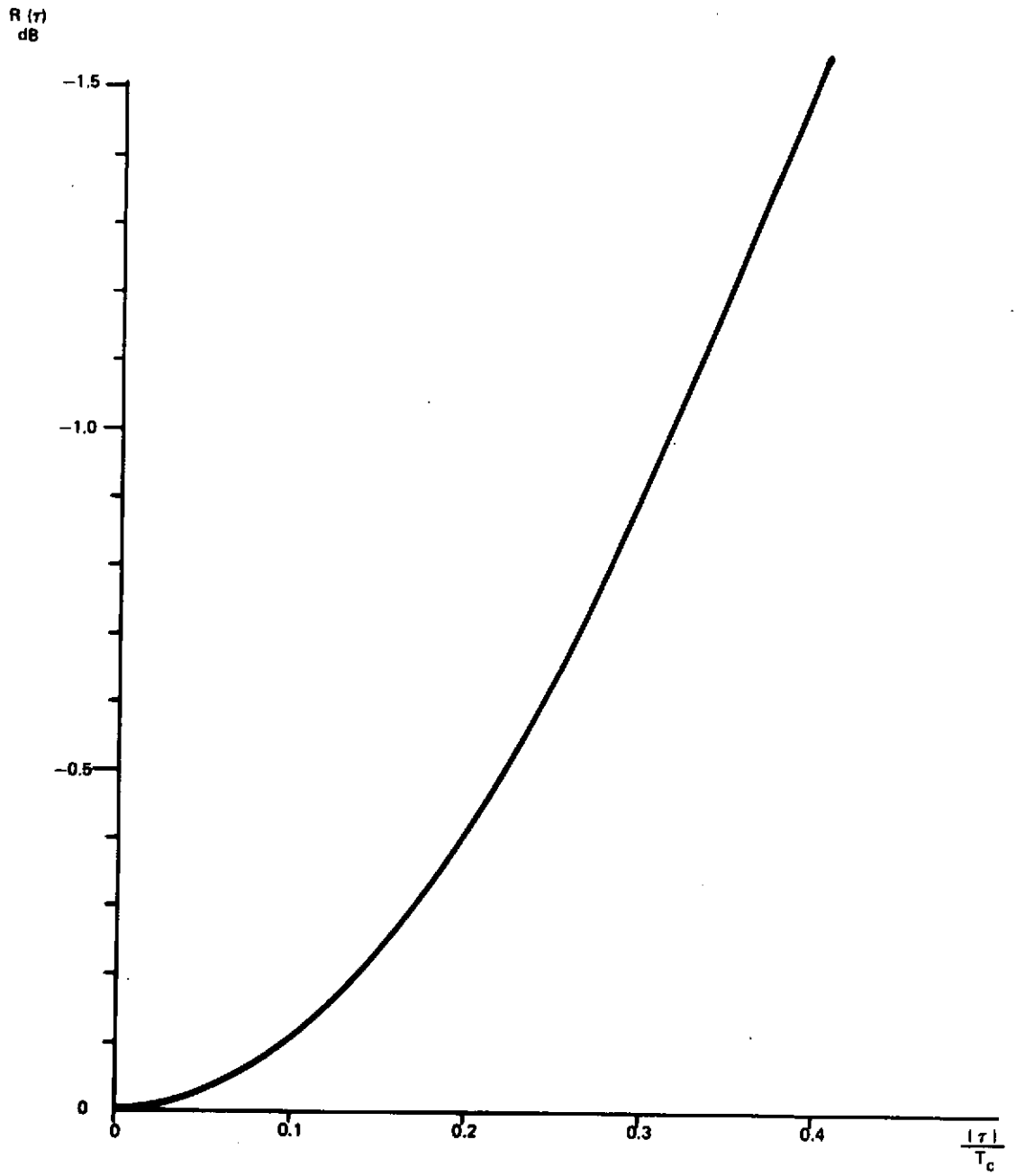

Figure 5. Correlation function R (τ) for chip detection.

CALIBRATED VLF PHASE MEASUREMENTS: SIMULTANEOUS REMOTE AND LOCAL MEASUREMENTS OF 10.2-kHz CARRIER PHASE USING CESIUM STANDARDS

Eric R. Swanson, Richard H. Gimber, and James E. Britt
Naval Electronics Laboratory Center

ABSTRACT

An investigation of spatial irregularity of VLF phase due to nearby objects and terrain is discussed. It is shown that the phase is regular to the microsecond accuracy of the instrumentation, and that a grounded steel tower in close proximity to a whip antenna will not affect the phase measurement. However, antennas coupling to trees may cause an anomalous phase shift.

INTRODUCTION

During the past ten years, increased use has been made of VLF phase measurements for navigation, time dissemination, and frequency distribution. Additional techniques have been proposed, such as differential OMEGA, in which a local monitor is used to calibrate a given area. In differential OMEGA, errors are not caused by overall phase fluctuations over the long propagation path, but are introduced only insofar as the local phase is irregular, or as phase fluctuations are decorrelated within a local area. Differential OMEGA and similar techniques thus place high requirements on the spatial regularity of phase and the constancy of phase measurements to the local environment. The purpose of this study was to investigate local phase regularity and immediate environment through the use of two matched equipments.

A generalized block diagram of the receiving instrumentation is found in Figure 1. The output of a cesium frequency standard is fed through a phase shifter into appropriate synthesizing equipment to develop a 10.2-kHz injection signal to be fed into the front end of the antenna system. The antenna system consists of a ten-foot vertical whip and appropriate coupler.

Signals were fed into a Tracor 599R receiver modified to four-minute time constants. An internal commutator was used to select the remote stations to be tracked, and also the local calibration signal which was inserted on an otherwise unused segment of the OMEGA commutation pattern. The receiver output was then recorded on analog recorders. Prior to commencement of the task, the equipment was assiduously checked in the laboratory not only to determine adequate function in the equipment, but also as part of an evaluation of Tracor 599R receivers. The remote equipment was then transferred from the laboratory into a station wagon and installed in as nearly the same relative component position as possible.

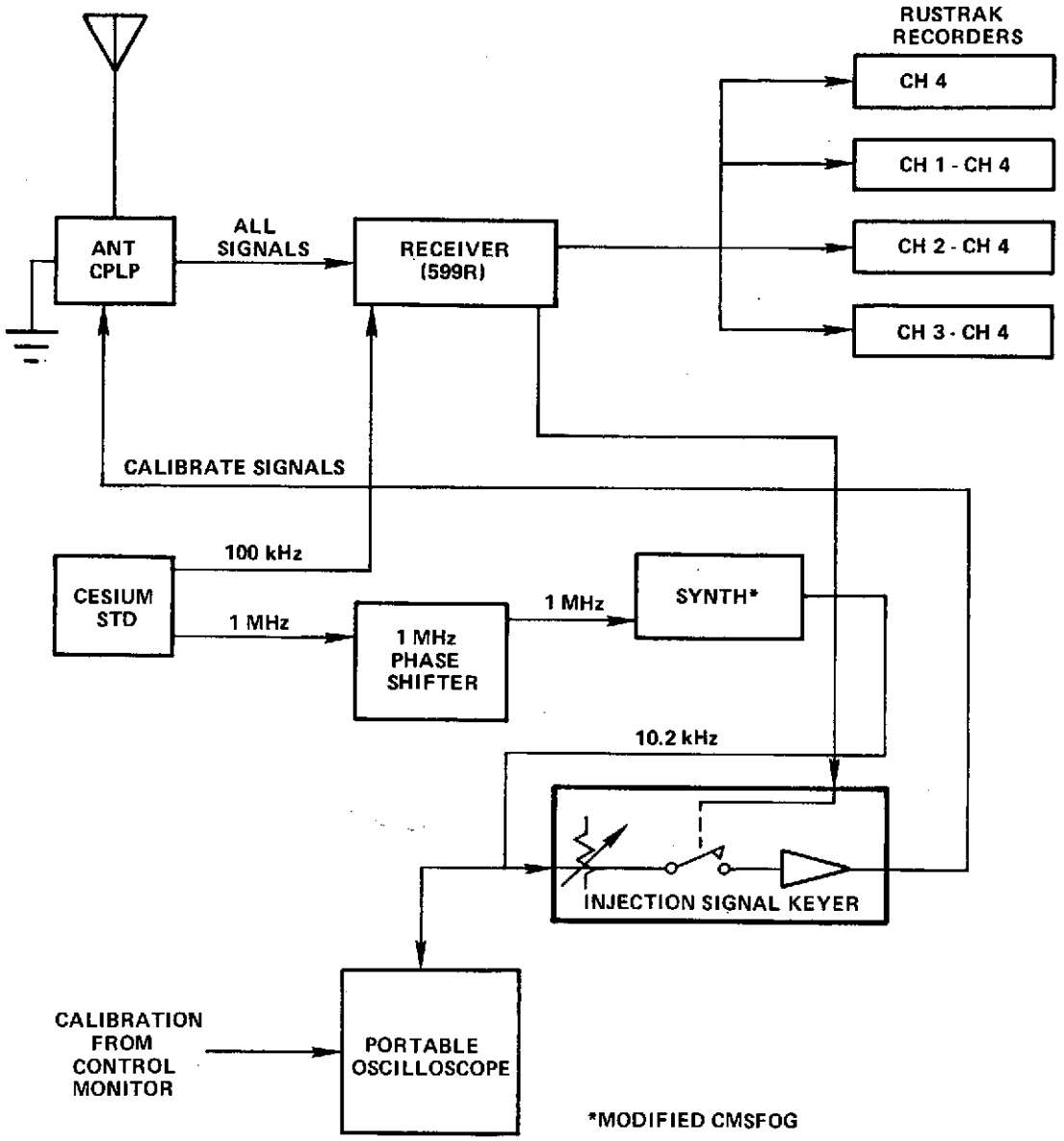

Figure 1. Block diagram of receiving instrumentation.

One of the receivers was left at the Naval Electronics Laboratory Center (NELC) for the duration of the tests. This receiver was operated from a ten-foot whip. Signals were fed from the antenna coupler at the base of the antenna through approximately 70 meters of coaxial cable to the receiver's location. This receiver operated from commercial power and was rack mounted, together with a second Tracor being used for measurements at 13.6-kHz and being served from the same coupler. The Tracor phase measurement output was then recorded using a multipoint analog recorder.

The remote receiver was operated from lead acid batteries, using a ten-foot whip mounted atop the station wagon roof. Recordings were made on four Rustrak dc recorders of one percent accuracy.

The experimental procedure consisted of parking the station wagon at a point outside the laboratory near the room housing the fixed receiver. The epoch as presented on the 10.2 kHz calibration of the output from the fixed receiver was then fed over approximately 30 meters of twin-ax to the station wagon. There the fixed epoch was compared with the epoch from the remote receiver and the phase shifter adjusted until coincidence was achieved. The phase calibration signals on remote and local receivers were thus matched to within a few tenths of a microsecond; the difference being due entirely to the differences in propagation velocity in cable lengths between the local receiver and the remote calibration receiver. The calibration procedure was conducted before each day of monitoring and again at the conclusion of each day of monitoring.

After calibration, the equipment was operated continuously as the vehicle was driven to a variety of receiving sites. Typically, the coordinates of the sites were determined from local topographic maps at a scale of 1:24000. Although the whip antenna was normally tied back during transit, the receiver was usually able to track signals even at freeway velocities, although serious quadrature error may sometimes have occurred. Once a recording site was reached, the antenna was elevated and 15 to 20 minutes were then allowed for the phase measurements to stabilize. The measurements were then made, strip-chart recorders marked, antennas tied back, and the vehicle was driven to the next site. Data was generated by two different means. In the first, the exact measurements were compared with simultaneous measurements made at the laboratory. Secondly, all records were reveiwed and compared for similarity. It was found that in most instances, the remote record exhibited behavior similar to the fixed record within the five minutes preceding movement from the remote site. In this case, the period for similar records was chosen, usually ranging from five to ten minutes. The entire period was then averaged, and the result used as the effective value. This latter approach apparently reduced experimental scatter, and is therefore the method employed to obtain measurements cited herein.

After the first two days of field monitoring, it was determined that there was a little leakage between the 10.2-kHz injection generator and the antenna system on the vehicle. The leakage was corrected; the data from the first two days of monitoring have been retained if the relative amplitude readings were not less than 10 decibels. Under these conditions, the phase perturbation would be negligible.

The test may be divided conveniently into two parts. The first part, the spatial regularity of phase was studied by conducting various measurements throughout the San Diego area. The second part consisted of a detailed investigation of the phase shift associated with antenna siting adjacent to a tree and a tower.

PART I: SPATIAL REGULARITY OF PHASE

General

It is important to note that there are several potential causes for spatial irregularity of phase and that the present study was designed especially to note only those associated with possible terrain or local environmental factors. Phase may vary irregularly from point to point due to imperfect spatial correlation of temporal variations; that is, long-term averages might vary regularly, but short-term test results exhibit scatter. Effects of the spatial decorrelation of temporal variations are best investigated by long-term measurements at a few fixed receiver sites rather than by the methods described herein. Phase may also vary irregularly as a function of distance from a transmitter if the propagation structure is due to several waveguide modes. This structural irregularity is expected to be the dominant irregularity at short distances from transmitters and may be significant up to several thousand kilometers or more at night.

Site Descriptions

The measurements to determine the spatial regularity of phase were designed to take maximum advantage of the extremely varied topography of San Diego County. Measurements were made from sea level to an elevation of 6000 feet and from the coast to the desert. Measurements were made on coastal bluffs, plains, promontories, in valleys, and in foothills. Weather conditions were generally sunny, although fog was sometimes experienced near the coast, and patches of snow remained on the ground at higher elevations.

The topography of the eastern sites is especially noteworthy. Mt. Laguna is on a ridge line running approximately north-south. An escarpment to the east is particularly abrupt, falling over 2000 feet in the first mile and over 4000 feet in the first four miles. The site at Ocotillo is located in the desert and separated from the ridge line by about one wavelength. Accordingly, if reflections off the escarpment were significant, the measurements at Ocotillo would probably be perturbed. The site at Devils Wash was located at the foot of the escarpment, at the 1000-foot contour level.

Several measurements were made in the immediate vicinity of NELC on Point Loma, a promontory separating San Diego Bay from the Pacific. Point Loma is approximately one mile wide and 400 feet high. Measurements were taken on the top and both sides of Point Loma. Additional measurements were made near the coast at Camp Pendleton and Imperial Beach. In general, every effort was made to obtain data from diverse geographic conditions. A description of the sites is given in Table 1. Data used to determine the spatial regularity of phase included only those sites at least 30 meters from trees, power lines, and other structures.

One of the receivers was left at the Naval Electronics Laboratory Center (NELC) for the duration of the tests. This receiver was operated from a ten-foot whip. Signals were fed from the antenna coupler at the base of the antenna through approximately 70 meters of coaxial cable to the receiver's location. This receiver operated from commercial power and was rack mounted, together with a second Tracor being used for measurements at 13.6-kHz and being served from the same coupler. The Tracor phase measurement output was then recorded using a multipoint analog recorder.

The remote receiver was operated from lead acid batteries, using a ten-foot whip mounted atop the station wagon roof. Recordings were made on four Rustrak dc recorders of one percent accuracy.

The experimental procedure consisted of parking the station wagon at a point outside the laboratory near the room housing the fixed receiver. The epoch as presented on the 10.2 kHz calibration of the output from the fixed receiver was then fed over approximately 30 meters of twin-ax to the station wagon. There the fixed epoch was compared with the epoch from the remote receiver and the phase shifter adjusted until coincidence was achieved. The phase calibration signals on remote and local receivers were thus matched to within a few tenths of a microsecond; the difference being due entirely to the differences in propagation velocity in cable lengths between the local receiver and the remote calibration receiver. The calibration procedure was conducted before each day of monitoring and again at the conclusion of each day of monitoring.

After calibration, the equipment was operated continuously as the vehicle was driven to a variety of receiving sites. Typically, the coordinates of the sites were determined from local topographic maps at a scale of 1:24000. Although the whip antenna was normally tied back during transit, the receiver was usually able to track signals even at freeway velocities, although serious quadrature error may sometimes have occurred. Once a recording site was reached, the antenna was elevated and 15 to 20 minutes were then allowed for the phase measurements to stabilize. The measurements were then made, strip-chart recorders marked, antennas tied back, and the vehicle was driven to the next site. Data was generated by two different means. In the first, the exact measurements were compared with simultaneous measurements made at the laboratory. Secondly, all records were reveiwed and compared for similarity. It was found that in most instances, the remote record exhibited behavior similar to the fixed record within the five minutes preceding movement from the remote site. In this case, the period for similar records was chosen, usually ranging from five to ten minutes. The entire period was then averaged, and the result used as the effective value. This latter approach apparently reduced experimental scatter, and is therefore the method employed to obtain measurements cited herein.

After the first two days of field monitoring, it was determined that there was a little leakage between the 10.2-kHz injection generator and the antenna system on the vehicle. The leakage was corrected; the data from the first two days of monitoring have been retained if the relative amplitude readings were not less than 10 decibels. Under these conditions, the phase perturbation would be negligible.

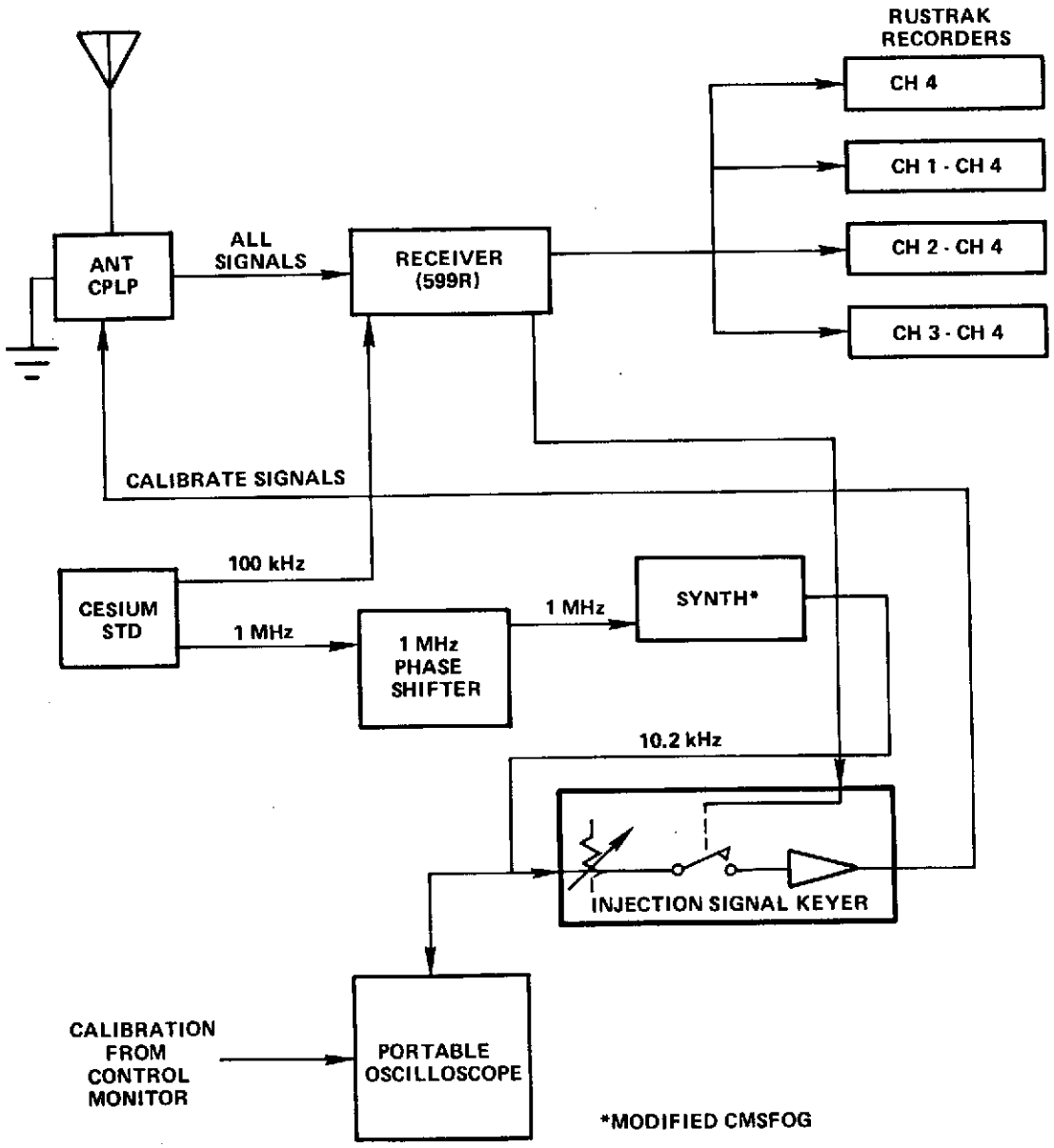

Figure 1. Block diagram of receiving instrumentation.

Table 1
Sites.

Sites	Location		Elev (Feet)	LOP			Site Description (Remarks)
	Latitude Deg Min	Longitude Deg Min		TR	HK	FP	
Cabrillo	32°40.26′	117°14.44′	405	209.275	142.114	130.380	Exposed promontory overlooking Pacific Ocean. No power lines. Unknown antenna 100 meters south.
Pt. Loma	32°42.96′	117°15.62′	300	209.304	142.127	130.305	Adjacent to large tree; 8 ft from high-voltage power line.
Sunset Cliffs	32°43.80′	117°15.33′	25	209.360	142.094	130.308	Cliff overlooking Pacific. No power line.
NELC No. 1	32°42.52′	117°14.67′	365	209.311	142.119	130.318	Poor location adjacent to building.
NELC No. 2	32°42.53′	117°14.67′	360	209.311	142.120	130.318	60 ft further from building than site 4 above.
Harbor Drive	32°43.68′	117°12.73′	5	209.223	142.231	130.195	Next to bay; clear location.
Shelter Island	32°42.49′	117°13.84′	5	209.268	142.163	130.281	Clear location surrounded by water on three sides.
Wooded Area	32°42.97′	117°14.70′	310	209.318	142.123	130.308	Residential area surrounded by trees, no power lines nearby.
Warner	32°42.96′	117°14.66′	305	209.316	142.124	130.306	Open site in residential area.
Mt. Laguna	32°52.32′	116°24.69′	6050	206.815	144.822	127.724	Southeast edge of mountain near top. Visibility 100 miles to N, E, and S. Some snow on ground nearby.
Ocotillo	32°44.14′	115°59.62′	390	205.415	146.084	126.840	Small desert community.
Devils Wash	32°43.63′	116°03.78′	1000	205.626	144.861	127.046	Good site just entering foothills.
Laguna Site No. 2	32°48.62′	116°30.70′	4085	207.086	144.481	128.118	
Glencliff Camp Ground	32°48.01′	116°29.97′	3810	207.040	144.438	128.102	In clear area.
Imperial Beach	32°36.05′	117°07.73′		208.880	142.438	130.210	
Camp Pendleton	33°36.18′	117°24.27′		210.147	141.864	129.793	

Results

Phase measurements were obtained by driving to the various sites in the San Diego Area and simultaneously measuring the phase at the sites and at NELC. The phase measurements, amplitude readings, and times for daytime readings taken on Trinidad, Hawaii, and Forestport from the remote sites together with the simultaneous phase measurements recorded at NELC are contained in an informal technical note describing the experiment.[1]

Assuming that there are no spatial irregularities of phase and that the true prevailing propagation velocity is used to define the circular line of position (LOPs), then the phase from any transmitter received at the remote site (ϕ_R) should equal

$$\phi_R = \phi_N + (LOP_R - LOP_N)$$

where ϕ_N is the phase at NELC and LOP_R and LOP_N are the 0.9974 range-range LOPs at the remote site and at NELC, respectively. Since the maximum separation from NELC was less than four wavelengths, the typical error due to dispersion would be about 0.1 cec even if the true prevailing relative velocity was several parts in 10^4 from the assumed v/c = 1.0026. Discrepancies in ϕ_R may then be interpreted as position errors or timing errors due to irregularities, instrumentation, etc. The discrepancies are tabulated in Reference 1. The overall rms discrepancy for sites appropriately removed from trees and other objects was 2.3 cec (2.3 μs). The discrepancies can be compared with estimated experimental errors.

The sources of expected experimental magnitudes are estimated in Table 2. The summation of the experimental error contributions is especially dependent on the S-curve error per channel. S-curve error arises through leakage or other nonlinearity in the phase-tracking circuitry of each phase-tracking channel. The amount of S-curve error depends on the actual phasing of the tracking channels within the receiver. Synthesized error estimates thus depend on the number of active phase-tracking channels as shown in Table 3. With four tracking channels active (references and signal on both NELC and remote receivers), the most likely experimental scatter would thus be about 1.8 cec rather than the 2.3 cec actually obtained. However, the reference phase at NELC was not changed during the experiment and thus at most three channels were active, while at least one contained an unknown bias. In practice, the received signal phase is fairly repeatable from day to day, and hence the signal channels for each of the various stations will also tend to reflect bias rather than scatter if diurnal change is not important. Further, the injection phase to the remote monitor was varied only infrequently and hence might have tended to contribute as either a bias or scatter. Accordingly, although the best estimate for the experimental rms should be computed allowing for four S-curve errors, it is likely that the actual experimental conditions may have produced significant biases and scatter, indicative of only one or two active tracking channels. Table 4 shows statistics computed for phase measurements on each

[1] Naval Electronics Laboratory Center Technical Note 1778, *Calibrated VLF Phase Measurements*, by E. R. Swanson, R. H. Gimber, and J. E. Britt, December 4, 1970. (Note: NELC technical notes are informal documents intended primarily for use within the Center.)

Table 2
Expected Errors.

Estimated Variation (cec)	Quasimaximum Variation (cec)	Source of Error
0.5	0.7	Noise
0.7	1.0	Field recorder nonlinearity
0.1	0.2	NELC recorder nonlinearity
0.4	0.5	Field reading
0.1	0.1	NELC reading
0.2	0.2	Phase variation with amplitude
0.5	0.7	Time synchronization between NELC and remote
0.1	0.1	Map coordinates
0.7	1.0	S-curve receiver tracking error per channel

Table 3
Synthesized Error Estimates.

No. of Active Tracking Channels	Estimated Scatter (cec)	Estimated Maximum Bias due to S-curve
4	1.8	0
3	1.6	1
2	1.5	2
1	1.3	3

of the individual remote signals unaffected by trees or other objects. Apparently, the rms errors differ significantly between the various stations, presumably depending on biases in the reference channels and bias generated by nearly constant phase measurement at NELC. The standard deviations confirm the expected behavior. The phase of Hawaii and Forestport remained relatively constant at NELC throughout the experiment and hence the scatter should reflect primarily S-curve error in tracking signals with the remote monitor and, to a lesser extent, whatever scatter may have been introduced by changes in the injection phase for the remote monitor. Thus, for Forestport and Haiku, the estimated scatter would be between 1.3 and 1.5 cec which is greater than the actual scatter of 1.1 cec. The discrepancy may be due to pessimistic error estimates for noise effects and strip-chart timing errors on Hawaii and Forestport. The noise and timing esti-

Table 4
Experimental Errors (cec).

Statistic	Transmitter		
	Trinidad	Haiku	Forestport
RMS	2.0	3.3	1.1
Bias	0.4	3.2	0.3
Scatter (Standard Deviation)	2.0	1.0	1.1

mates were nominal and may be expected to be pessimistic for the relatively clean and constant Hawaiian and New York signals and somewhat optimistic for Trinidad. The 2.0 cec observed scatter for Trinidad is indeed slightly larger than the 1.5 or 1.6 cec which should be expected due to the effects of diurnal variation on two tracking channels and possible scatter due to injection changes on the remote reference. Of course, to some extent, individual station differences may also be due to some variation on the S-curve errors of the particular receiver channels. Nonetheless, the typical scatter (1.5 cec is essentially equal to that predicted by the error analysis, while the details of the analysis tend to confirm the error model. The error model may also be extended to predict a quasimaximum likely error of about 7 cec, which is indeed greater than any observed discrepancy. It is therefore concluded that irregular phase variations due to terrain features must be less than about one cec (one microsecond) on 10.2-kHz OMEGA signals during the day.

PART II: PHASE SHIFT ASSOCIATED WITH ANTENNA SITUATED ADJACENT TO TREES AND TOWERS

Reception Near a Tree

As was mentioned earlier, phase fluctuations may occur in a local area because of an irregular local environment. A phase shift near a tree can be assumed to be the result of tree movement and not the propagation path to the given area.

Measurements for the tree experiment were made in the neighborhood of a 60-foot eucalyptus tree in the vicinity of NELC. Distances from the tree ranged from an open area 500 feet from the tree to directly beneath the tree where the branches nearly touched the antenna. Two smaller trees were also within 100 feet of the tree, and a five-foot chain-link fence was approximately 100 feet from the tree. Measurements made at 94 feet and closer to the tree were between the tree and Hawaii, while partially in the shadow with respect to Trinidad and Forestport. For the 90 minutes during which the measurements were taken, the weather conditions were a heavy overcast with sprinkles.

Equivalent Circuit

An equivalent circuit was used as a model for the effects of the tree on the antenna, as can be seen in Figure 2. V_a is the induced voltage in the whip antenna caused by an electric

field (E = electric field strength) and is by definition

$$V_a = E\, h_a \cos\theta$$

where h_a is the effective height of the antenna at an angle of θ with respect to the electric field. If the effective height of the tree is $6h_a$, then the voltage induced in the tree is

$$V_t = 6V_a$$

This approximation is reasonable if the effective height of the tree is close to half its physical height. The loss resistance typically dominates the radiation resistance, while at the same time the input reactance is mostly capacitive and much larger than the resistive term. For the present case, the loss resistance and radiation resistance are assumed negligible and are not shown in Figure 2.

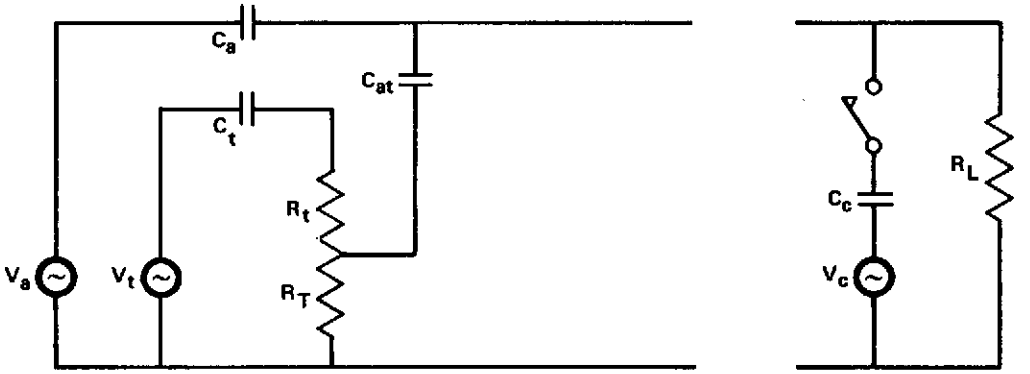

V_a = Incoming signal to antenna
C_a = Input coupling
V_t = Incoming signal to tree
C_t = Input coupling to tree

R_t, R_T = Resistance of tree
C_{at} = Coupling of tree to antenna
V_c, C_c = Internally generated frequency standard injected into antenna
R_L = Load resistance

Figure 2. Equivalent circuit for the tree experiment.

The coupling of the antenna to the tree will be distributed over the height of the antenna. It is difficult to say exactly how the leaves, branches, moisture, and other features of the tree effect its capacitance, but it seems clear the capacitance will increase in regions near the tree. A resistive term will be introduced in the coupling of the antenna to the tree since the resistance of the tree is nonzero. For the purposes of our circuit, the antenna was assumed to be coupled to the tree at the ten-foot level of the tree, so $R_t = 5R_T$. The resistance of the tree (1.5K Ω/six feet for dc) was determined by driving nails six feet apart into the tree and measuring the resistance across the nails.

With the superposition principle and a look at Figure 2, it is clear that the signal applied to the load is the sum of the component signals from the antenna and the tree. It is anticipated that a phase shift will occur when the phase component from the tree differs from that of the antenna. Clearly, the phase from the antenna (ϕ_a) is -90°. The phase injected from the tree should be a function of the coupling of the tree to the antenna, the effective resistance in the coupling of the tree to the antenna, and of the coupling of the tree to the signal. C_{at} should be small at large distances from the tree, reaching a maximum under the tree. For small values of the effective coupling resistance, there is a potential for the phase component from the tree to reach -180°. Assuming that the signal injected from the tree is much greater than that from the antenna, a phase shift of as much as 90° is possible. The signal from the tree may be dominate if C_c is much greater than C_a.

Results of the Tree Experiment

The results of the tree experiment are tabulated in Reference 1 and the phase readings are normalized to readings taken at 94 feet in Table 5. As can be seen in Figure 3, the phase shift is substantial in regions near the tree, while at the same time there is up to an 80 percent reduction in amplitude. Although the phase readings are not entirely reliable for amplitude readings below 5 dB, the phase on the three transmitters appears to be equally affected for reception near the tree.

Comparing the results that the model predicts with the observed data requires assigning values to the different components in the circuit. As an approximation for an antenna directly under the tree, the following values were estimated:

$R_L = 56k\ \Omega$

$V_t = 6V_a$

$C_t = 200$ pF (assume 35-ft. whip has 150 pF) $X_t = 75k\Omega$

$R_t = 15k\ \Omega$

$R_T = 3k\ \Omega$

$C_a = 25$ pF $X_a = 600k\ \Omega$

$C_{at} = 250$ pF $X_{at} = 60k\ \Omega$

Since C_{at} is much greater than C_a the signal from the tree will be dominant. The signal at V′ then will be

$$V' \approx 6V_a \sqrt{75^2 + 18^2} \cdot 3 \approx V_a/4 \text{ advanced } 76^\circ$$

Our model predicts both the observed drop in amplitude and the phase shift in the proper direction. Admittedly, the model was developed to fit the data and admittedly, it is an oversimplification to assign lump values to a distributed circuit, but it should be noted that the assumptions of circuit values are not unreasonable and that the model does account fairly well for the phenomena observed.

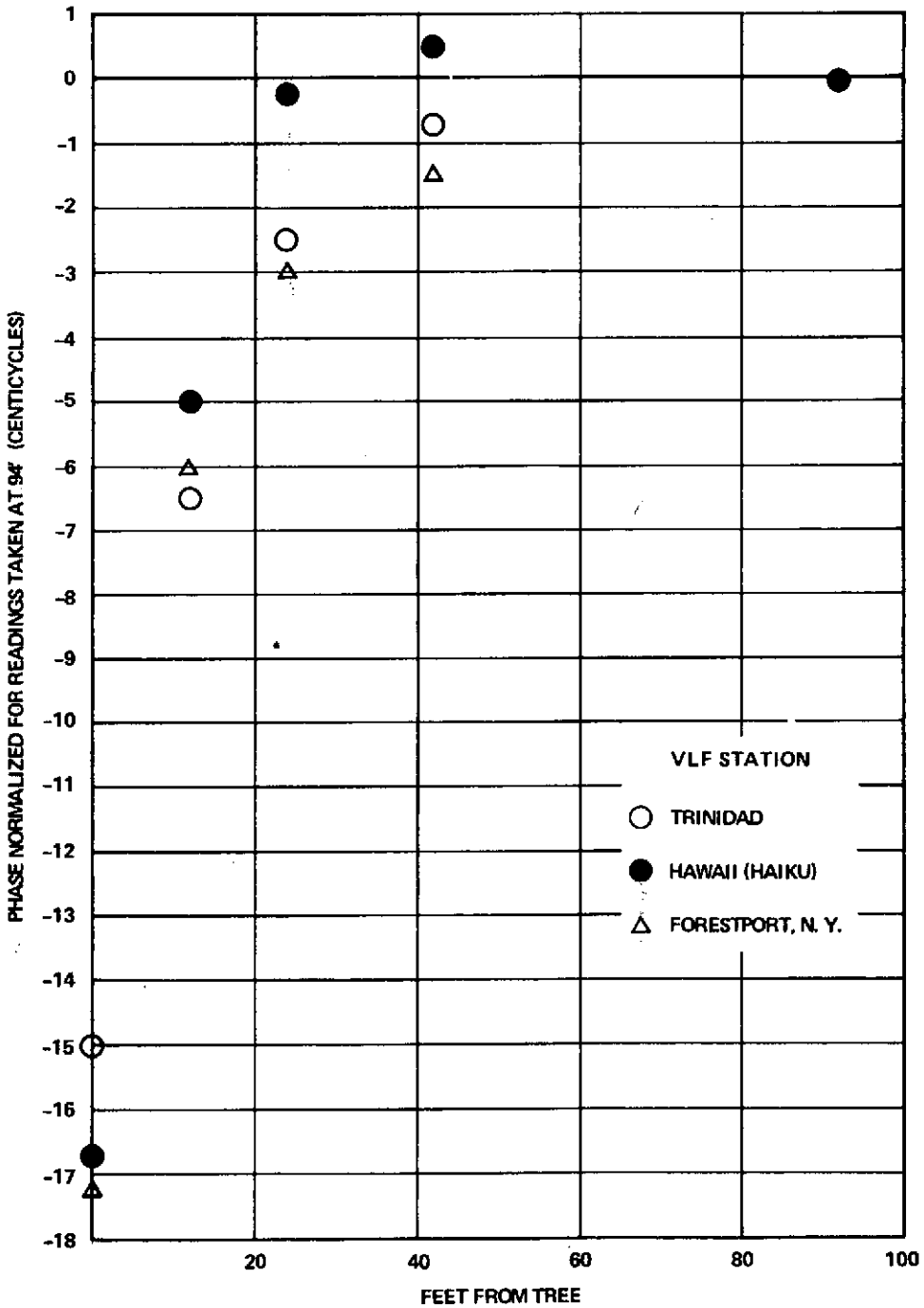

Figure 3. Phase shift versus distance from a 60-foot Eucalyptus tree (10.2 kHz).

Table 5
Phase Shift (cec)
(Normalized to Readings at 94 Feet).

TR	HK	FP	Distance From Tree
0.0	0.0	0.0	94 feet
-0.7	0.5	-1.5	42 feet
-2.5	-0.2	-3.0	24 feet
-6.5	-5.0	-6.0	12 feet
-15.0	-16.7	-17.3	Beneath tree

Measurements were also taken at three residential sites within 300 feet of one another. Warner (Site 9) was a clear area free of trees and power lines. Pt. Loma (Site 2) was adjacent to a large tree and eight feet from a high-voltage power line. The wooded area (Site 8) was completely surrounded by trees. The wooded area and Warner were on the same street while the site called Pt. Loma was around the corner from them. As can be seen from Table 6, those sites in close proximity to trees showed a substantial phase shift, while the open site at Warner, in the same vicinity as the two near trees, showed no corresponding phase shift.

Table 6
Tree Experiment
(LOP Errors for Hawaii).

Site	Date	Time	Amp	Raw Error (cec)	Bias Error (cec)	Remarks
Pt. Loma	March 24	1856	18	-11.4	-13.9	Adjacent to large tree.
	March 25	1719	16	- 8.7	-11.2	
Wooded Area	March 24	2243	12	-17.8	-20.3	Surrounded by trees.
Warner	March 25	1702	25	1.9	- 0.6	Clear area.

Reception Near a Tower

Signal behavior in the vicinity of a metal tower may be computed using the same equivalent circuit as was employed in analyzing the effects of being in the proximity of a tree (Figure 2). For a tower, the internal resistance will be negligible while the resistance between the effective point of antenna coupling and ground will usually be zero or infinite, depending upon whether the tower is perfectly grounded or ungrounded. The circuits of Figure 4 may thus be used to approximate Figure 2 for grounded or ungrounded towers.

From Figure 4, it is clear that no phase shift will occur at the receiver input as long as the reactance of the coupling capacitance between the tower and the antenna dominates the receiver input impedance. However, the amplitude may be significantly affected: If the tower is ungrounded, the signal will be enhanced; if grounded, the signal will be reduced.

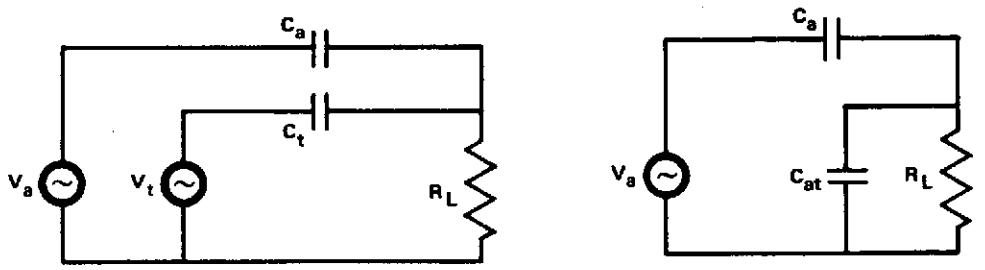

Figure 4. (a) Circuit for ungrounded tower; (b) circuit for grounded tower.

Measurements taken near a 100-ft grounded tower at NELC are given in Table 7. The measurements show no significant phase shift.

Table 7
Phase Shift Near Tower.

Trinidad		Haiku		Forestport		Difference (cec)			
Tower	Ref	Tower	Ref	Tower	Ref	TK	HF	FP	Feet from Tower
θ	θ	θ	θ	θ	θ				
77	76	46	45	72	73	1	1	-1	130
78	76	46	45	74	74	2	1	0	70
78	77	46	45	75	74	1	1	1	30
82	81	47	45	75	75	1	2	0	18
87	85	47	45	77	75	2	2	2	7

Reception Near Objects

The foregoing discussion of reception near trees and towers may be generalized to reception on a whip antenna near any object. The important considerations are (1) the capacitative coupling between the antenna and the object, and (2) the self-induced voltage on the object in the coupling region. Since both the coupling capacitance and the induced voltage depend on the size of the object, a convenient rule for siting antennas might be to provide separation from nearby objects equal to or greater than one-half their height. In practice, ordinary care in siting antennas should be more than adequate to avoid detrimental coupling.

It is particularly noteworthy that the experimental results can be explained by a simple model using direct coupling, rather than a more complex model using reflections such as might be expected at higher frequencies. Anomalous phase shift will thus be equal on all signals received at the same frequency independent of the station azimuths and local geometry. Accordingly, phase difference measurements made for navigational purposes will be unaffected no matter how close the receiving antenna is placed to other objects. (Assuming, of course, that adequate signals are available for phase tracking.) However, timing information obtained from various stations using an improperly sited antenna will be consistent, but incorrect.

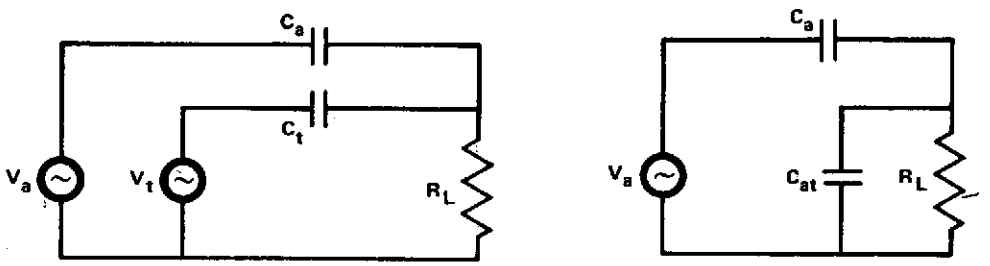

Figure 4. (a) Circuit for ungrounded tower; (b) circuit for grounded tower.

Measurements taken near a 100-ft grounded tower at NELC are given in Table 7. The measurements show no significant phase shift.

Table 7
Phase Shift Near Tower.

Trinidad		Haiku		Forestport		Difference (cec)			
Tower	Ref	Tower	Ref	Tower	Ref	TK	HF	FP	Feet from Tower
θ	θ	θ	θ	θ	θ				
77	76	46	45	72	73	1	1	-1	130
78	76	46	45	74	74	2	1	0	70
78	77	46	45	75	74	1	1	1	30
82	81	47	45	75	75	1	2	0	18
87	85	47	45	77	75	2	2	2	7

Reception Near Objects

The foregoing discussion of reception near trees and towers may be generalized to reception on a whip antenna near any object. The important considerations are (1) the capacitative coupling between the antenna and the object, and (2) the self-induced voltage on the object in the coupling region. Since both the coupling capacitance and the induced voltage depend on the size of the object, a convenient rule for siting antennas might be to provide separation from nearby objects equal to or greater than one-half their height. In practice, ordinary care in siting antennas should be more than adequate to avoid detrimental coupling.

It is particularly noteworthy that the experimental results can be explained by a simple model using direct coupling, rather than a more complex model using reflections such as might be expected at higher frequencies. Anomalous phase shift will thus be equal on all signals received at the same frequency independent of the station azimuths and local geometry. Accordingly, phase difference measurements made for navigational purposes will be unaffected no matter how close the receiving antenna is placed to other objects. (Assuming, of course, that adequate signals are available for phase tracking.) However, timing information obtained from various stations using an improperly sited antenna will be consistent, but incorrect.

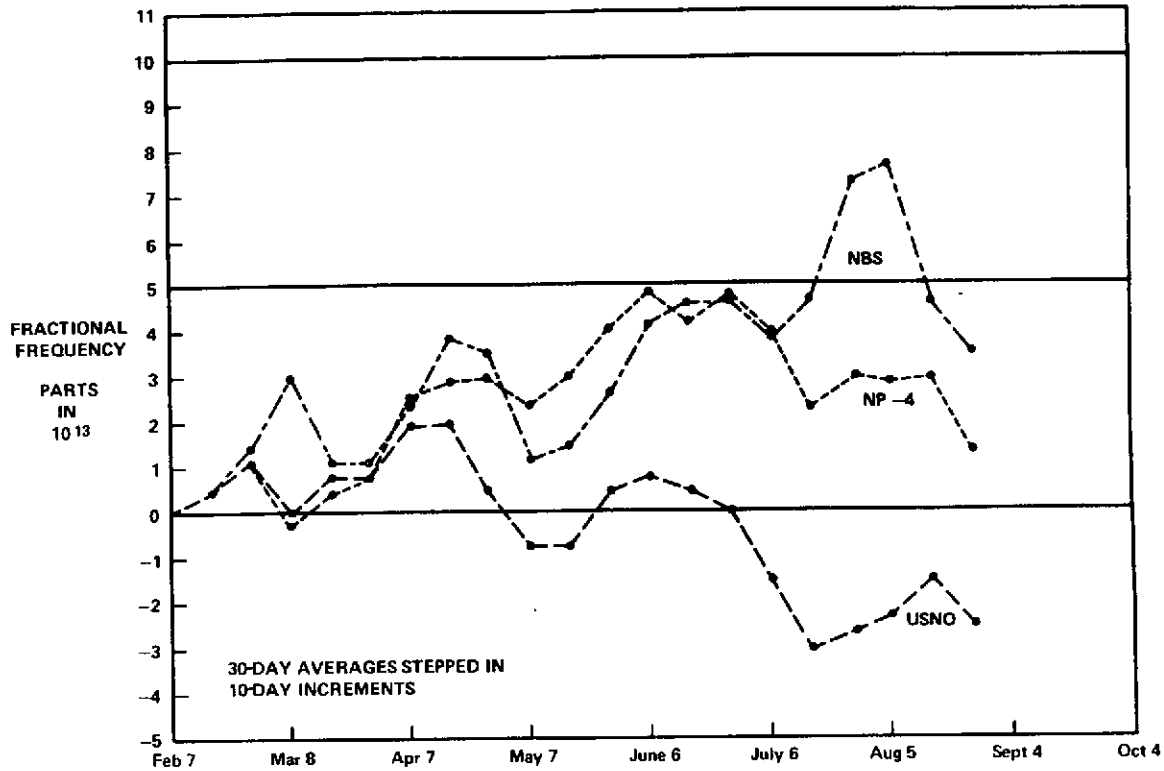

Figure 3. USNO, NBS and NP-4 maser frequency versus IAT.

III. MEASUREMENTS BETWEEN MASERS

Figure 5 shows frequency comparisons of the NASA prototype masers against the NX-1 maser in 1969 and 1972. The data have been corrected for second order doppler shift (with an error estimate of ±.0004 Hz), magnetic field measurement (±.0000013 Hz). and wall shift (± .0024 Hz). The errors associated with cavity tuning and the measurement technique were no greater than ± .00014 Hz. Since NP-3 was in Goldstone, California and was compared via traveling clock, VLF, and LORAN-C, there was an additional measurement error estimated at ± .0007 Hz.

Table 1 gives the 1972 absolute frequency of all of the NASA masers with respect to IAT. These values were referred to the 1972 NP-4 measurement reported previously. [8,9] The error estimate given for the average value of the absolute frequencies was that attributable to a single hydrogen maser since the major uncertainty, the wall shift, was a common systematic error. Table 1 includes a new value for the wall shift temperature coefficient associated with the hydrogen masers. The cavity temperature of NP-2 and NP-4 were lowered by 17°C. The resulting changes in the frequencies of NP-2 and NP-4 indicated that the previous value for the wall shift temperature coefficient was in error.* Because of this temperature change NP-2 and NP-4 in Figure 5 should only be compared to one another, and NP-1, NP-3, and NX-1 should only be compared to one another, in order to estimate the long term performance of the NASA masers.

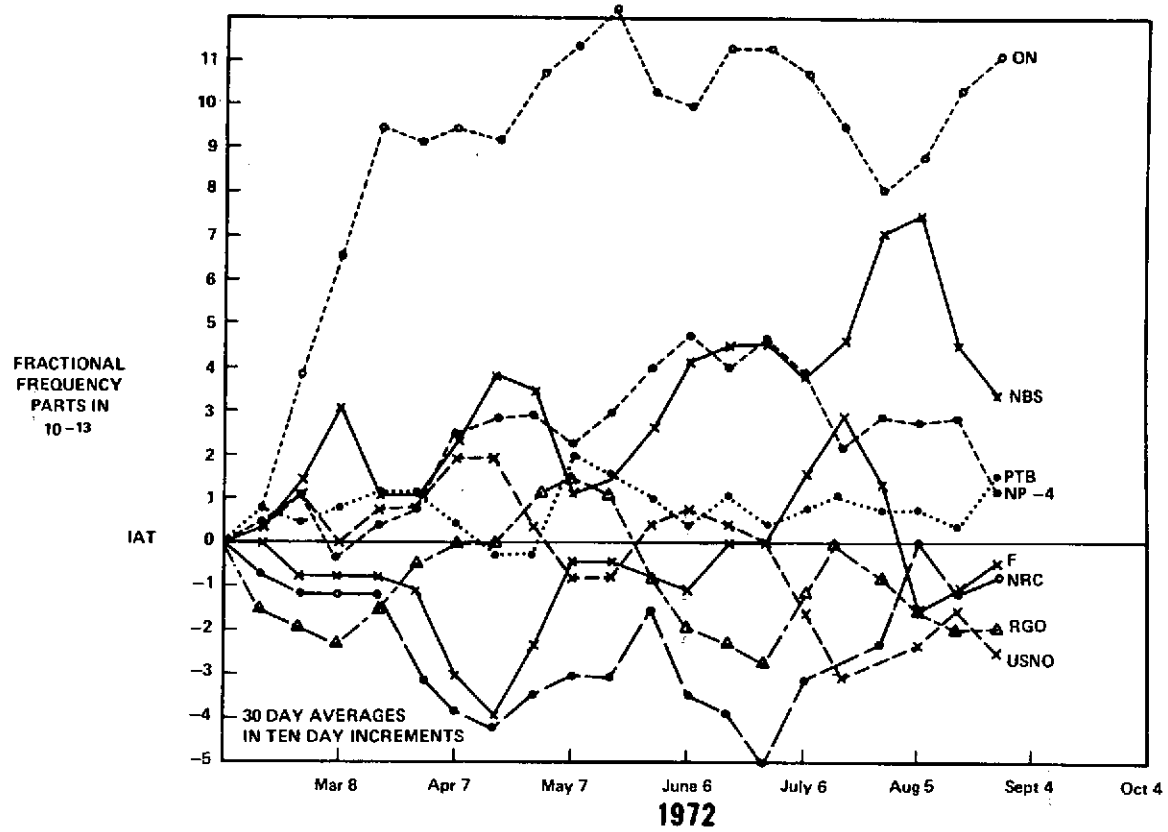

Figure 4. Frequency comparisons–International Standards Labs and NP-4 H-maser versus IAT.

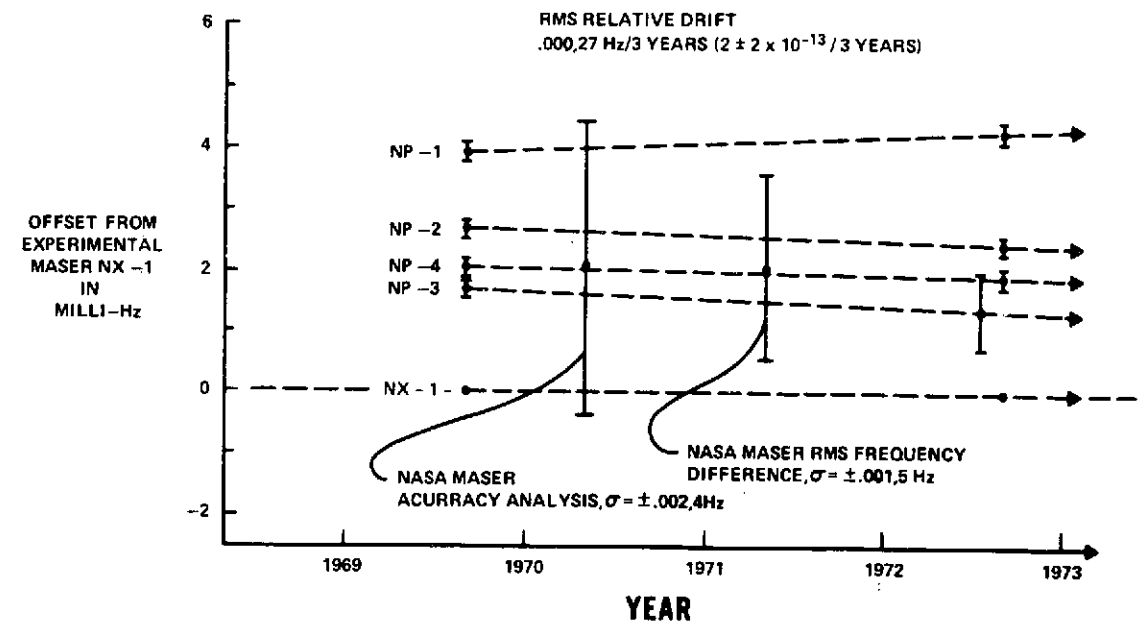

Figure 5. Frequency relationships–NASA NX-1 and NP-1, -2, -3, -4 atomic hydrogen masers.

The test may be divided conveniently into two parts. The first part, the spatial regularity of phase was studied by conducting various measurements throughout the San Diego area. The second part consisted of a detailed investigation of the phase shift associated with antenna siting adjacent to a tree and a tower.

PART I: SPATIAL REGULARITY OF PHASE

General

It is important to note that there are several potential causes for spatial irregularity of phase and that the present study was designed especially to note only those associated with possible terrain or local environmental factors. Phase may vary irregularly from point to point due to imperfect spatial correlation of temporal variations; that is, long-term averages might vary regularly, but short-term test results exhibit scatter. Effects of the spatial decorrelation of temporal variations are best investigated by long-term measurements at a few fixed receiver sites rather than by the methods described herein. Phase may also vary irregularly as a function of distance from a transmitter if the propagation structure is due to several waveguide modes. This structural irregularity is expected to be the dominant irregularity at short distances from transmitters and may be significant up to several thousand kilometers or more at night.

Site Descriptions

The measurements to determine the spatial regularity of phase were designed to take maximum advantage of the extremely varied topography of San Diego County. Measurements were made from sea level to an elevation of 6000 feet and from the coast to the desert. Measurements were made on coastal bluffs, plains, promontories, in valleys, and in foothills. Weather conditions were generally sunny, although fog was sometimes experienced near the coast, and patches of snow remained on the ground at higher elevations.

The topography of the eastern sites is especially noteworthy. Mt. Laguna is on a ridge line running approximately north-south. An escarpment to the east is particularly abrupt, falling over 2000 feet in the first mile and over 4000 feet in the first four miles. The site at Ocotillo is located in the desert and separated from the ridge line by about one wavelength. Accordingly, if reflections off the escarpment were significant, the measurements at Ocotillo would probably be perturbed. The site at Devils Wash was located at the foot of the escarpment, at the 1000-foot contour level.

Several measurements were made in the immediate vicinity of NELC on Point Loma, a promontory separating San Diego Bay from the Pacific. Point Loma is approximately one mile wide and 400 feet high. Measurements were taken on the top and both sides of Point Loma. Additional measurements were made near the coast at Camp Pendleton and Imperial Beach. In general, every effort was made to obtain data from diverse geographic conditions. A description of the sites is given in Table 1. Data used to determine the spatial regularity of phase included only those sites at least 30 meters from trees, power lines, and other structures.

The coupling model should also be applicable to the analysis of antenna performance on ships, buildings, or near various other structures. If the electrical parameters of the structure remain constant, then coupling is immaterial for normal navigation providing only that signals are adequately received. For timing, calibration of the antenna would be necessary if coupling was significant. Slow variation of the electrical parameters of a nearby structure would be unimportant for hyperbolic navigation but potentially unacceptable for timing. Fast variations, such as might occur on a ship due to roll or vibration causing intermittant electrical connections between various masts and guys, could cause rapid anomalous phase shift at the receiver which would appear as noise.

III. INTERPRETATION OF RESULTS

Application to Timing

The experimental results can be applied directly to assess possible local effects on timing accuracy using OMEGA. Timing accuracies have been parenthetically inserted in previous discussions by noting that one centicycle at 10.2 kHz can be interpreted as corresponding to about one microsecond. As previously noted, the effect of terrain irregularities is thus less than one microsecond. However, trees or structures may cause significant timing error if the receiving antenna is very poorly sited. If trees or structures introduce timing errors, the same error will be introduced on all 10.2-kHz OMEGA signals, and thus redundant measurements will not improve timing. Poor antenna siting is, however, usually easy to avoid.

The experiment also shows that OMEGA provides a means of providing accurate relative time between moderately separated sites.

Application to Navigation

The experimental results are also applicable to assessment of navigational errors and, in particular, evaluation of differential OMEGA, rendezvous accuracy, or relative positioning. Basic hyperbolic OMEGA navigation will include errors due to local phase irregularities. As a result of this experiment, local phase irregularities on 10.2-kHz OMEGA signals are negligible during the day.

The performance of differential OMEGA and the relative accuracy of OMEGA are especially dependent on local phase irregularities and decorrelation of phase fluctuations between two separated sites. As the experiment reflects errors of either type, the results obtained imply no significant limitation of differential accuracy due to local terrain features, antenna siting, or the decorrelation of phase fluctuation over the spatial extent of the experiment. In particular, in the absence of complicated signal structure due to propagation by various modes, it is unlikely that rms differential phase errors on circular lines of position in a differential system could be larger than one centicycle over spatial separations in the range 0 to about 100 km.

CONCLUSIONS

OMEGA phase measurements using whip antennas are unaffected by local terrain features to the experimental accuracy of about one centicycle. No anomalous phase shift is introduced by trees or towers unless the receiving antenna is placed sufficiently close so that significant capacitive coupling can occur. If phase measurements are taken adjacent to trees or within a forest, the anomalous phase shift will be the same for all OMEGA signals at the same frequency, and hence will not affect hyperbolic navigation. However, consistent through erroneous time estimates could occur.

ACKNOWLEDGEMENTS

Measurements were made in the spring of 1969 in conjunction with the field checkout of equipment developed for synchronized monitoring of OMEGA signals at Wales, Alaska. The experimental program was supported by the OMEGA Navigation System Project Office of the Naval Electronic Systems Command. Because of scheduling, various persons in addition to the authors helped in making the measurements and the contributions of Messrs. Rider, Kugel, and Gallenberger are gratefully acknowledged. Analysis was sponsored jointly by the OMEGA Project Office and by Mr. Andrew Chi of NASA.

THE USES AND LIMITATIONS OF HF STANDARD BROADCASTS FOR TIME AND FREQUENCY COMPARISON

John T. Stanley
National Bureau of Standards

ABSTRACT

The most practical methods of using high-frequency (HF) broadcasts for frequency and time comparison are reviewed briefly. Although standard broadcast and receiving equipment has improved vastly throughout the past fifty years, the HF propagation medium is no more stable today than it was a half century ago. Doppler shift resulting from changes in the effective height of the ionosphere typically limits the usable accuracy of received high frequencies to a few parts in 10^7. At locations beyond groundwave range of the transmitter, uncertainties in path delay generally restrict the usable accuracy of HF time signals to the order of a millisecond. Signal-averaging techniques are sometimes employed to extract frequency or time signals from a noisy background.

GENERAL DISCUSSION

Since 1904 or thereabouts we have witnessed increasing use of radio as a medium for dissemination of time and frequency information. Recent listings by the International Telecommunications Union and other authorities reveal that more than forty countries are now engaged in radio broadcasts of time and frequency standards. Presently, there are upwards of twenty stations transmitting frequency-time standards on regular schedules in the high-frequency (HF) band alone. Additional stations are broadcasting frequency-time standards in the low-frequency (LF) and very-low-frequency (VLF) bands.

In the United States, radio has been a principal means of transferring frequency-time standards for more than half a century. In fact, March 6, 1973 will mark the fiftieth anniversary of radio station WWV as a frequency-time service of the National Bureau of Standards (NBS).

During the first decade of its existence, WWV transmitted standard frequencies with accuracy no better than one part per million. As finer frequency-control measures were developed, the accuracy of WWV's transmissions steadily improved until it approached a few parts in 10^{12} where it remains today. Daily comparisons using the television line-ten technique ensure that the WWV time signals are synchronized within three microseconds to the UTC (NBS) scale, which in turn agrees within five microseconds to the UTC (USNO) scale at all times.

A second NBS station, WWVH, has been operating since July 1971, from near Kekaha, Kauai, Hawaii, to provide coverage for areas of the Pacific which are not served adequately

by WWV. Through time comparisons via portable clocks, Loran C, and LF transmissions of WWVB, the standards broadcast by WWVH and WWV are kept in the closest possible agreement. WWVH and WWV together serve more than two-thirds of the earth's surface, although no single radio-frequency channel is likely to be 100 percent reliable under all propagation conditions. As in the case of WWV, the standard frequencies transmitted by WWVH are accurate to within a few parts in 10^{12}.

Consistent progress has been made toward improving the accuracy of frequency-time standards as actually broadcast. However, the ionosphere is no more stable now than it was during the early 1900s, as shown in Figure 1. Consequently, beyond groundwave range the usable accuracy of standard HF broadcasts is little better today than during the years of World War II.

Doppler effect arising from motion of the ionosphere still limits the typical usable accuracy of standard frequencies propagated over skywave paths to a few parts in 10^7, or perhaps a part in 10^8 under good conditions. Uncertainty in determining propagation delay generally restricts to the order of one millisecond, the best accuracy that can be relied upon for time markers transmitted on HF carriers along skywave paths. Because of the severe degradation brought about by ionospheric factors over which we have no control, I expect no further major improvements to be made in the frequency generation equipment at WWV or WWVH for their present role as HF ground-based stations.

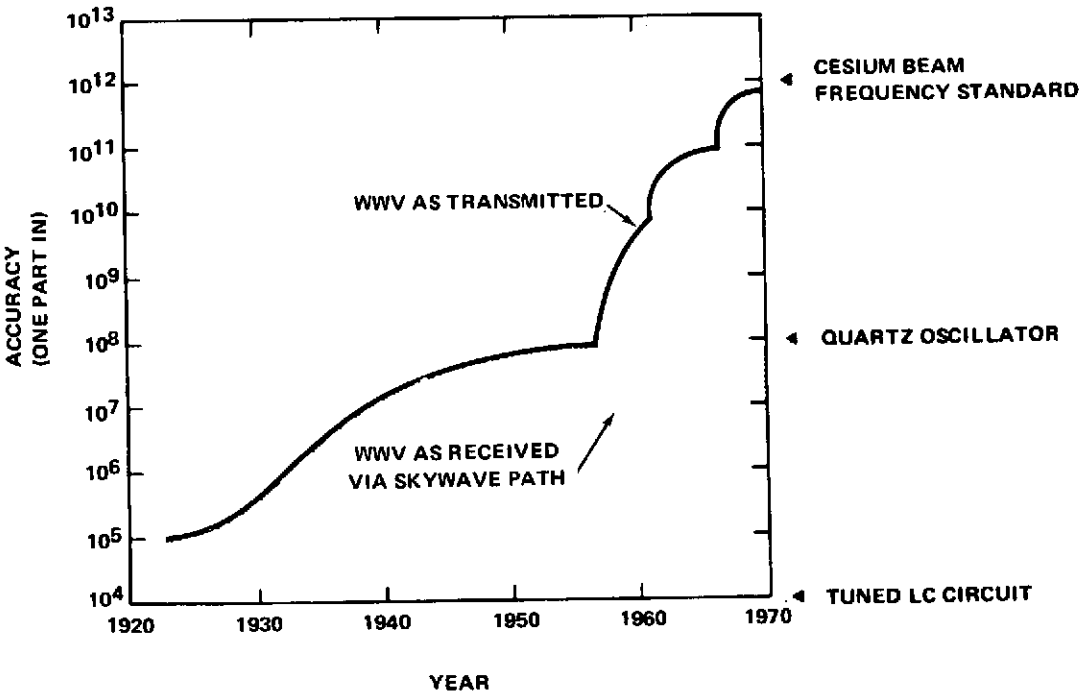

Figure 1. WWV broadcast accuracy.

Just as broadcast equipment has improved with the state-of-the-art, so too have standard broadcast formats evolved to satisfy changing needs. Beginning July 1, 1971, stations WWV and WWVH adopted totally new program formats, (Figure 2) in response to preferences registered during a nationwide survey of user requirements. Principal changes included more frequent voice announcements of time; the elimination of Morse code keying and its replacement in some cases with voice announcements; the continuous broadcast on a 100-Hz subcarrier of a binary time code very similar to the IRIG-H code; the use of male and female voices by WWV and WWVH respectively as an aid in distinguishing the broadcasts of the two stations from each other; the inclusion of 500-Hz standard audio tones in addition to standard tones of 440 Hz and 600 Hz; and the provision of certain 45-second segments every hour for voice announcements of public and scientific interest by agencies of the U.S. Government.

On January 1, 1972, further modifications were made in accordance with international agreement to eliminate the frequency offset of -300 parts in 10^{10} which had been a feature of most standard frequency broadcasts since the 1960s. Because the UTC rate is no longer changed continuously to keep in close agreement with the earth's rotation rate, UTC now departs more rapidly than before from the astronomical time scale, UT1. To prevent this difference from exceeding 0.7 second, occasional step adjustments of exactly one second (called leap seconds) are made as directed by the International Time Bureau (BIH). The first leap second in history occurred on June 30, 1972. The next one is scheduled to occur on December 31, 1972. The leap seconds ensure approximate agreement between the UTC scale and the UT1 scale needed by navigators and land surveyors.

Faced with ever-increasing demands for more stringent standards, researchers are exploring a variety of new methods for time and frequency dissemination. HF broadcasts fall far short of providing the extremely accurate standards required to support precision geodesy, satellite tracking, aircraft traffic control, atomic-clock synchronization, and advanced digital communications. It appears certain that no amount of money or effort can increase appreciably the effectiveness of the HF mode beyond its present capabilities.

On the other hand, the standard time and frequency broadcasts of stations such as WWV, WWVH, CHU, and JJY are more than sufficient for the everyday needs of most users. As attested by the growing number of frequency-time stations operating between three MHz and 30 MHz, the HF mode is still the most popular one for dissemination of time and frequency standards. Hardly any place in the world is outside the coverage area of one or more HF standard stations. Within the accuracy limitations previously cited, frequency calibration and clock synchronization can be achieved quite conveniently through HF standard broadcasts using relatively simple and inexpensive equipment at the receiver end.

Heterodyne Method

When high accuracy is not required, probably the simplest and fastest way of comparing the frequency of an oscillator to a broadcast standard is the familiar heterodyne or zero-beat method. To carry out this procedure a radio receiver is tuned to a standard carrier

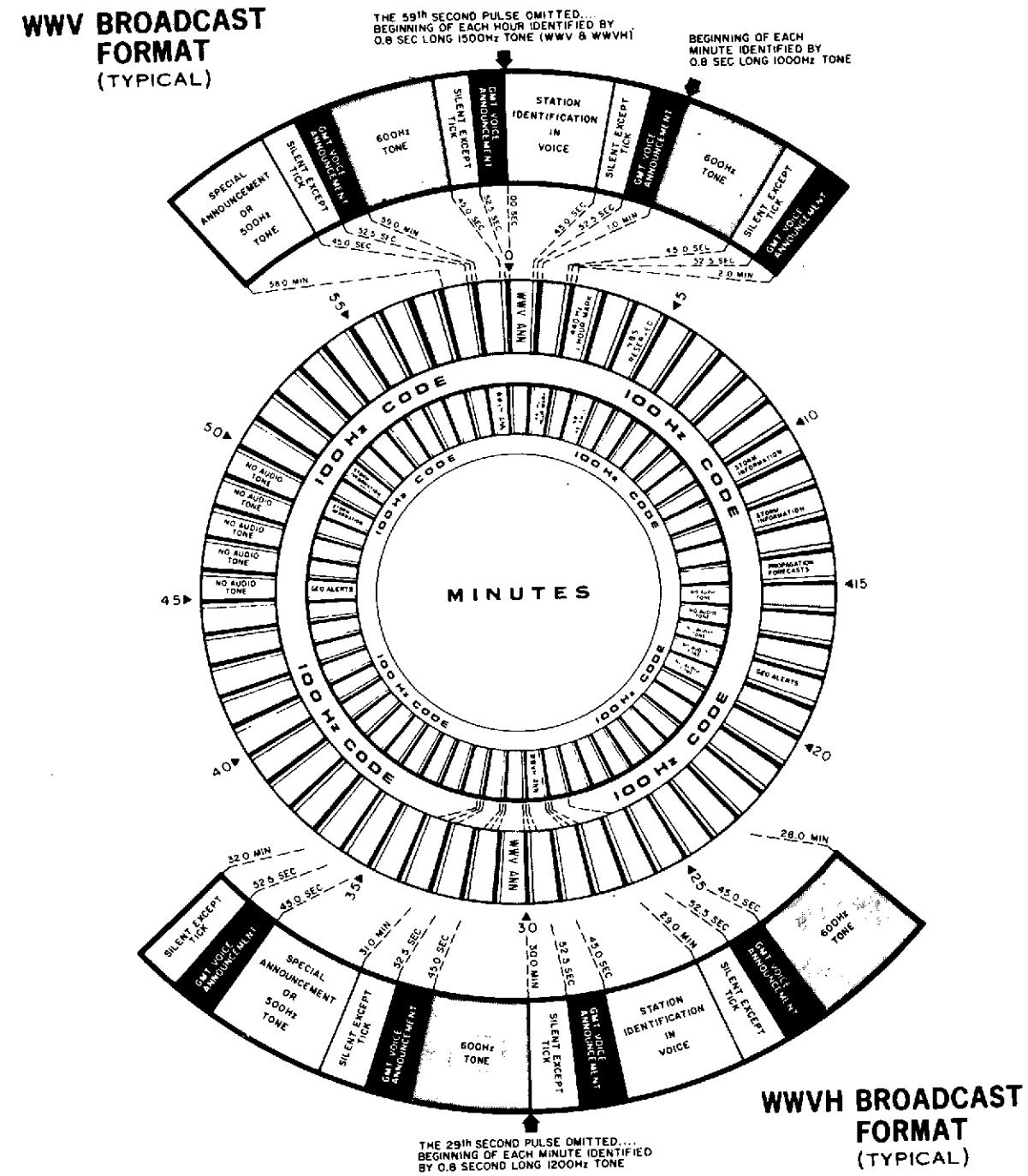

Figure 2. Typical broadcast formats.

frequency, say ten MHz, while the output of the oscillator is loosely coupled to the receiver antenna. Depending upon the fundamental frequency of the oscillator, it may be necessary to employ frequency multiplication or division to obtain a common frequency for comparison.

To achieve maximum modulation, energy from the oscillator should be adjusted so that it is approximately equal to that of the received broadcast signal. The resulting beat frequency can then be observed as a Lissajous pattern on an oscilloscope screen or can be measured directly with a counter (Figure 3). If the beat note is found to be one Hz, for example, when the comparison frequency is ten MHz, then the oscillator is off-frequency by one part in ten million, or 1×10^{-7}.

If desired, the oscillator could be adjusted until the beat note or difference frequency is reduced to zero, at which point the oscillator frequency would be correct to within the accuracy limits of the comparison process. Usually, however, it is difficult to adjust an oscillator to exactly zero beat with an HF carrier beyond the groundwave range of the transmitter. The problem arises from rapid fluctuations in the received signal strength and from propagation flutter in the received frequency.

When reception conditions are good, the best results can be obtained by counting the beats over a continuous interval of several minutes. If severe fading is experienced, however, it may be preferable to count the beats over an interval of only a few seconds and average the results of several successive comparisons.

As a general rule low-beat frequencies can be determined more accurately with an electronic counter by measuring period rather than frequency; the accuracy can be enhanced further by using the multiple-period feature which is common in most general-purpose counters today. The more periods over which a signal is averaged, the better the resolution that can be attained. In all measurements made with an electronic digital counter, the characteristic ambiguity of plus-or-minus one count must be taken into consideration.

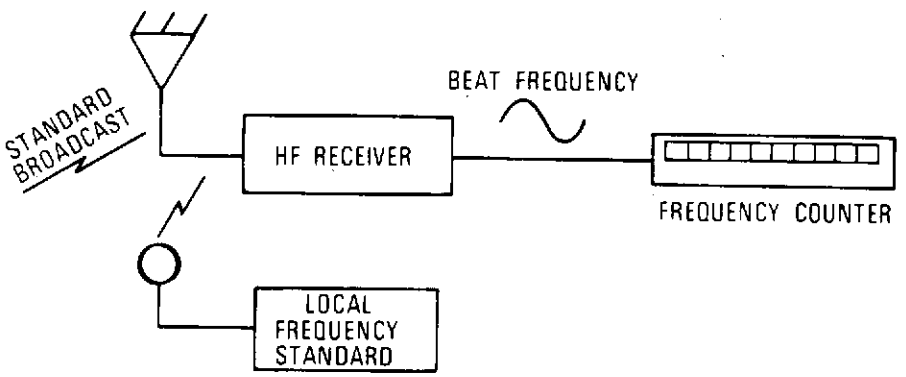

Figure 3. Heterodyne method.

As mentioned previously, skywave signals are subject to Doppler shifts brought about by vertical movement of the ionospheric layers during the course of the measurement. The error introduced by Doppler effect could be computed if sufficient data were known at the time of the measurement. The received frequency is shifted by a fractional amount equal to the rate of change in path length divided by the propagation speed of the radio wave. But ionospheric density, and hence path length, varies according to the time of day, season, sunspot cycle, geographic location, and so forth. Whereas average conditions of the ionosphere are predictable, one must realize that the conditions may deviate greatly from the norm at any particular instant.

Experience has shown that Doppler shifts of approximately three parts in 10^8 are typical for single-hop propagation via F-layer reflection. The effective change per hop increases slightly for multi-hop modes because of the higher departure angles encountered. An approximation to the overall effect of Doppler shift may be obtained merely by multiplying the estimated change per hop times the total number of hops involved, although it is very unlikely that the Doppler shift will be of equal magnitude at all reflection points along the path.

TIME-MARKER PHASING

An indirect method of frequency comparison uses standard time markers as a reference. Here the oscillator under test is used to drive an electronic clock, the output pulses of which are applied to the external trigger terminal of an oscilloscope while time markers from the receiver are applied to the vertical amplifier (Figure 4). The frequency offset of the oscillator is indicated by the rate at which the pattern drifts across the screen.

The second pulses, or ticks, transmitted by WWV consist of five cycles of 1000-Hz tone. The second pulses of WWVH comprise six cycles of 1200 Hz. In either case the duration of a complete pulse is five milliseconds with the leading edge of the first cycle on-time at its zero crossing. If the ticks are relatively free of jitter at the receiver output, time interval readings to ±10 microseconds may be resolved by expanding the sweep.

Like the direct comparison of frequencies, however, time comparisons are also subject to errors arising from propagation effects. Since the reference marker is on-time when it leaves the transmitter, corrections must be made for the propagation delay between the transmitter and receiver. A slight additional delay is encountered within the receiver itself, but for HF receivers having a bandwidth of 2000 Hz or greater the internal delay is usually negligible. The one-way transmission of time signals then requires some way of determining propagation delay time if reasonable accuracy is to be achieved.

Propagated at the speed of light, the time markers will arrive three milliseconds late for every 1000 kilometers traveled between the transmitter and receiver. Because HF groundwave propagation is confined to distances of only 160 kilometers or so, we will assume skywave propagation for the more general case. Except during the daytime when E-layer reflections sometime occur, long-distance HF reception usually results from F-layer reflection at an average virtual height of about 350 kilometers.

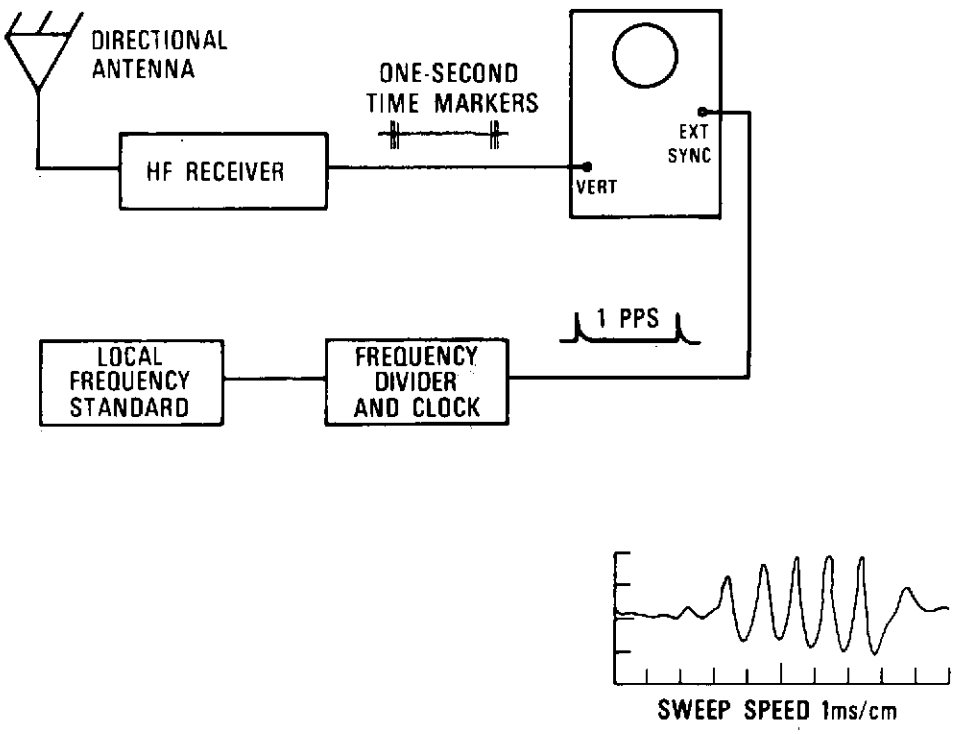

Figure 4. Time-marker phasing.

The maximum distance that can be spanned by F_2 reflection is about 4000 kilometers. For great-circle distances greater than 4000 kilometers, therefore, it is apparent that more than one reflection must generally occur. The fewest number of hops between the transmitter and receiver sites is the integer higher than the great-circle distance of 7000 kilometers. Division by 4000 yields a quotient of 1.75, which rounds off to 2 as the next higher integer. Thus two hops can be predicted for the shortest probable path. The same type of calculation leads to a prediction of three hops for great-circle distances from 8000 to 12,000 kilometers and four hops for distances between 12,000 and 16,000 kilometers. Once the number of hops is established, the distance traveled by the HF wave can be computed from the estimated height of the reflecting layer and the geometry of the path.

If several modes are being received, as indicated by jitter or the appearance of multiple ticks on the oscilloscope display, one should consider only the pulse with the earliest arrival time. Round-the-world echoes and interference from other frequency-time stations may cause problems unless a highly directional antenna is used with the receiver. Interlayer reflections, ionospheric turbulence, scattering, and other propagation anomalies may also cause excessive jitter.

The effects of jitter and the precision of measurement can be minimized by making observations over a long period of time. Fairly good results can be obtained with a long-persistence oscilloscope which permits several pulses to be superimposed and viewed together.

From such a display the operator can readily discern the pulse of earliest arrival. Similar results can be obtained from a multiple-exposure photograph of the oscilloscope display.

Under typical conditions it may be necessary to record data from an HF standard station for several days to average out the anomalies and approach high precision. For an observation period of 24 hours, the precision may be on the order of one part in 10^8; for a week to ten days, one part in 10^9; and for a month, one part in 10^{10}. In the HF spectrum the limit of accuracy is established by the propagation medium regardless of the duration of the observation interval. After plotting the measurement results for several days or weeks, one should disregard those points which do not conform with the others, or else correct the measurements to a more likely propagation mode.

Best results can generally be attained by tuning the receiver to the highest frequency that provides consistent reception. The optimum working frequency seems to be at about 85 percent of the maximum usable frequency. Operation at the optimum working frequency serves to reduce interference from high-order modes and usually results in the best reception over the greatest possible distance.

Because the density of free electrons in the ionosphere is greater during the day than at night and also greater in summer than in winter, it follows that the critical frequency is likely to be highest at noon and during midsummer. Throughout periods of peak sunspot activity the critical frequencies become abnormally high.

It is evident that in the interest of accuracy, the time or frequency comparisons should be made when the ionosphere is most stable. This condition generally prevails when the entire path of propagation is in total darkness or total daylight, that is, when midnight or noon occurs approximately midway between the transmitter and receiver sites. Because of Doppler effect, received frequencies are slightly high in the early morning hours when the path length is decreasing, and slightly low in the evening while the path is extending.

By carefully choosing the frequency, the mode of propagation, and the time of day for a measurement or comparison, an observer can obtain optimum results with HF time standards. Under ideal conditions the attainable accuracy may be ± 0.1 ms or better. At the opposite extreme, if the propagation path is highly disturbed the accuracy may deteriorate to worse than ± 10 ms. The nominal accuracy is ± 1 ms.

Several instrumentation variations are possible. A more elaborate arrangement might include a time comparator in conjunction with the oscilloscope. In lieu of the oscilloscope it is usually feasible to use a digital counter capable of time-interval measurement. If a continuous record of the comparison is desired, the counter may be outfitted with a digital-to-analog converter and recorder.

INTERFERENCE AND FADING

Mutual interference by two or more stations on shared channels is more serious now than ever before. In the HF spectrum, however, it is not unusual for a single station to interfere

with itself. Multipath reception often leads to alternate constructive and destructive interference at the receiver location without a second broadcast station being involved. The result is fading and distortion of the received signal.

Fadeouts may also result from other factors, such as ionospheric storms, solar flares, magnetic storms, and sporadic E-layer reflection. Nuclear explosions at altitudes between 15 and 60 kilometers have been reported as causing HF blackouts for periods of several minutes within a few hundred kilometers of the detonation site.

Interference problems can be attacked at the receiver most economically by using a directional antenna that favors the preferred signals azimuth and angle of arrival. Additional precautions may be taken by scheduling measurements for a time when the undesired signals are known to fade out.

Diversity receiver systems have long been used to combat the effects of fading in the field of radio communications. Such systems take advantage of the fact that if two or more receivers are separated by space, by frequency, by antenna polarization, or by angle of arrival, the fading often occurs independently at each receiver. Although diversity receivers are available for HF channels, the technique has not been widely exploited for frequency-time applications. Perhaps the added cost has been a deterrent.

NOISE

Additive noise has reached serious proportions throughout the HF spectrum. Atmospheric noise is generally high during the spring and summer months; but man-made noise may predominate at any time, especially in urban areas. As more radio stations increase their effective radiated power in an effort to overcome electromagnetic noise levels, the interference problem is compounded. Signal-averaging is an effective means of extracting time signals or other periodic waves from random noise.

For our present purposes random noise is considered to be that form of noise for which the average amplitude at any particular frequency is zero. Now let us assume a uniform periodic event, such as a time tick, that occurs in the presence of random noise. If the same point on the periodic pulse is examined every time the pulse recurs, an average voltage could be associated with that point. This follows from our assumption that the true signal amplitude at the point is constant whereas ultimately the random noise voltage at that point must average out to zero. The time required for the average signal voltage to emerge depends upon the extent and nature of the noise.

A signal-averager examines numerous points on the periodic wave and stores the instantaneous voltage of each point in a memory bank. Each time the wave recurs the same points are examined and the respective voltages are stored in the same memory elements. Eventually each memory element will contain the average voltage from its associated point on the waveform. At some prescribed moment the memory elements are strobed sequentially and the stored voltages displayed on an oscilloscope. The result is a reconstruction of the

average waveform without the distracting noise. The waveform is composed of many discrete voltage levels read out from the memory bank.

REFERENCES

(1) Hewlett-Packard Co., *Frequency and Time Standards*, Application Note 52 (Hewlett-Packard Co., Palo Alto, 1965).

(2) International Telecommunications Union, *List of Radio Determination and Special Service Stations*, List VI, 5th edition (ITU, Geneva, 1971).

(3) Jespersen, J.L., Blair, B.E., and Gatterer, L.E., "Characterization and Concepts of Time-Frequency Dissemination," *Proceedings of the IEEE*, pp. 502-521 (May 1972).

(4) Morgan, A.H., Precise Time Synchronization of Widely Separated Clocks, Technical Note No. 22 (NBS, Washington, 1959).

(5) National Bureau of Standards, *NBS Frequency and Time Broadcast Services*, Special Publication 236, 1972 edition (NBS, Washington, 1972).

(6) Stanley, J.T. and Milton, J.B., *Basic Laboratory Methods for Measurement or Comparison of Frequencies and Time Intervals*, Report 10744 (NBS, Boulder, 1972).

THE GLOBAL RESCUE ALARM NET (GRAN) EXPERIMENT

James C. Morakis
Goddard Space Flight Center

ABSTRACT

The OMEGA Position Location Experiment (OPLE) was performed in 1967 by the Goddard Space Flight Center in order to demonstrate a position location and data collection system. OMEGA navigation signals were received at a remote site and retransmitted via a synchronous satellite to a ground processing center where data collecting and position determination were performed. Recent technological advances have made it possible to develop an Advanced OPLE System towards a global search and rescue application. This application generated some new problem areas such as the OMEGA lane ambiguity, random access, location accuracy, real-time processing, and size and weight of the Search and Rescue Communications (SARCOM). This experiment will demonstrate the feasibility of instantaneous alarm and position location by using a relatively inexpensive, battery operated, three-pound package. This package can transmit the alarm and position through a synchronous satellite to a search and rescue station in less than three minutes, in an environment of 50,000 to 100,000 subscribers drawn from the maritime, aircraft, and recreational communities.

INTRODUCTION

The advanced OPLE (OMEGA Position Location Equipment) concept was chosen by NASA, the Navy, and the U.S. Coast Guard (USCG) as the best suited system for search and rescue application. From a number of systems that were considered, this concept was the only one that satisfied the requirements of continuous global coverage using already existing OMEGA navigation signals.* Furthermore, this system concept is already under development at NASA GSFC for this and other applications; thus, the adaption of this system for search and rescue results in further savings in development time and cost. The above rationale led to a proposal for a joint NASA, Navy, USCG Global Rescue Alarm Net (GRAN) experiment.

The four essential elements of these experiments are; (1) the OMEGA navigation signals, (2) mobile Search and Rescue Communicators (SARCOM), (3) the geosynchronous satellite, and (4) the central data acquisition and processing station.

*By 1974 all eight OMEGA stations are expected to be operational.

The very low frequency (VLF) OMEGA signals will be received by the SARCOM and retransmitted to the geosynchronous satellite at UHF along with identification data. Next they will be relayed to the central data acquisition and processing station.

There, the location of the SARCOM will be determined from the VLF data, and the name of the distressed party will be obtained from the ID data.

The following technological objectives have been selected:

1. Demonstrate a low cost search-and-rescue system
2. Reduce SARCOM size, weight, and cost
3. Resolve the ambiguity inherent in the OMEGA navigation system
4. Provide real-time position determination and identification readout
5. Improve position location accuracy
6. Increase subscriber capacity while maintaining good accuracy and low probability of self-interference

The first objective will be achieved at the time of the experiment. The second objective will be effected by utilizing a modificiation of the ATS/OPLE design for the SARCOM. Major changes will be conversion from a VHF to a UHF uplink frequency of 402 MHz and a reduction in size, weight, and prime power requirements while the ERP remains the same. The unit will not require an interrogation receiver since transmission will be initiated at the SARCOM. The circuitry will be miniaturized so that it can be hand held and provide approximately 30 minutes of operation, although not necessarily continuous.

Through studies initiated at NASA/GSFC, the feasibility of reducing the present data collection platform volume and weight to less than 1000 cm^3 and 5 pounds has been established. SARCOM specifications call for the following requirements:

Volume	1000 cm^3
Weight	1 kg
Output Power	5 watts max
Frequency	402 MHz
Bandwidth	2.5 kHz
Operation	3-minute broadcasts repeated at approximately 20-minute intervals
Data	Social Security number (36 bits) or other unique identifier

These specifications will require the use of miniaturization techniques. An effort is well underway to demonstrate this feasibility. The OPLE platform circuitry has been bread-boarded utilizing recent developments in integrated and linear circuits of standard size and configurations. Partitioning of circuit functions is complete and large scale integrated circuits are being fabricated. The major building blocks will be the transmission sequence

timer, frequency dividers to generate offset frequencies, ID data generator, and UHF driver and power amplifiers.

The position location ambiguity in the OMEGA system as now implemented results in a lane width of 72 nm which is clearly inadequate for search and rescue applications. The simplest technical solution requires that two additional OMEGA navigational tones be provided to the already existing three OMEGA transmission format; this situation will result in a more complex and therefore more costly SARCOM. Since the above result is contrary to the philosophy of trading simplicity in the SARCOM for complexity in the ground station, the following possible solutions to the lane ambiguity problem will be attempted.

SIGNAL-TO-SIGNAL RATIO COMPARISON

This method is based on the fact that the amplitude of VLF signals decreases in strength approximately inversely with distance. Preliminary computations indicate a location accuracy of ± 300 nm at the baseline between OMEGA stations and ± 750 nm at the furthest location from the baseline, which is certainly within the 1800 nm accuracy required. An understanding of this technique may be derived from the following example:

Consider a platform located at some distance P off the baseline of OMEGA station A and B, which might be some 5000 nm apart as shown in Figure 1.

In particular, consider the case where the platform at position P is 1000 nm from A and 4190 nm from B. Let the platform be relocated by 300 nm to position P in a direction perpendicular to the LOP so that position P is approximately 1290 nm from A and 3900 nm from B. Referring to Figure 2, the signal from A then decreases by about 8 dB and the signal from B increases by about 7 dB.

Inspection of the 10 kHz curve in Figure 2 indicates that the change in signal strength per 300 nm (550 km) is generally larger than 7 dB, an easily measurable quantity.

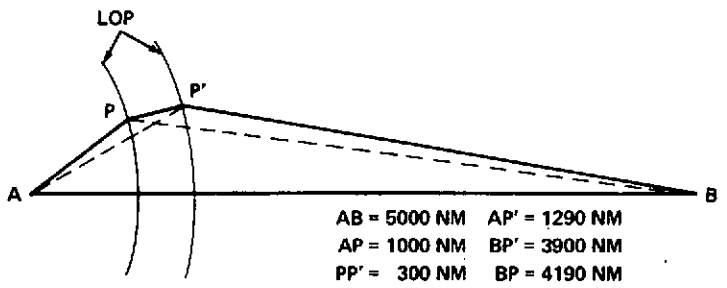

Figure 1. A typical two-station OMEGA configuration.

The two signal-to-noise ratios from A and B are first measured. Since the noise level is constant during the measurement the difference of the two signal-to-noise ratios in dB can be calculated and a hyperbolic line of position obtained.

The OMEGA signal strength will be plotted for several points on the earth to assess the amount of agreement with already collected data.

MULTIPLE LINES OF POSITION (MLOP) (KALMAN FILTERING)

This well known iterative estimation process would utilize the redundant lines of position using signals from four or more OMEGA stations. It may be seen in Figure 3 that three LOP's intersect perfectly only at the true location. At the present four OMEGA stations are in operation and by 1974 eight will be in operation to provide global coverage. Some preliminary results have already been obtained that indicate that this technique is feasible.

DIFFERENCE IN TIME OF ARRIVAL

This technique uses the whole waveform transmitted by the OMEGA stations. The effect is that the ambiguity frequency is ten seconds, the repetition period of the OMEGA transmission. The signals from the two OMEGA stations could, in concept, be cross correlated to obtain the difference in time of arrival; however, the required level of quantization is not practically achievable in view of the magnitude of the ambient noise. To overcome this problem the configuration of Figure 4 is used. A calibration platform is located in the vicinity of OMEGA station A. The signal from station A is transmitted to the satellite through two paths, the calibration platform and the platform P. The cross correlation of these two signals is maximized to obtain the difference in time of arrival τ_1, where $\tau_1 = t_{p1} + t_s - t_{c1} - t_1$. Where these parameters are shown in Figure 4; t_{c1} and t_1 are known, and τ_1 is measured by the correlation technique.

Similarly for the signal from OMEGA station B the difference in time of arrival of the signal throughout the platform P and the calibration platform P is $\tau_2 = t_{p2} + t_s - t_{c2} - t_2$ where t_{c2} and t_2 are known and τ_2 is measured by autocorrelation techniques; subtracting τ_2 from τ_1.

$$\tau_{1\text{-}2} = t_{p1} - t_{p2} + t_{c2} - t_{c1}$$

or

$$t_{p1} - t_{p2} = \tau_1 - \tau_2 + t_{c1} - t_{c2}$$

The right-hand portion of the equation is either measurable or known.

Dividing by the propagation velocity we obtain $x_{p1} - x_{p2}$ = constant, where x_1, x_2 are the distances of the platform from A and B. The above equation indicates a hyperbolic line of position with no ambiguity. Obviously this technique requires less than eight calibration platforms.

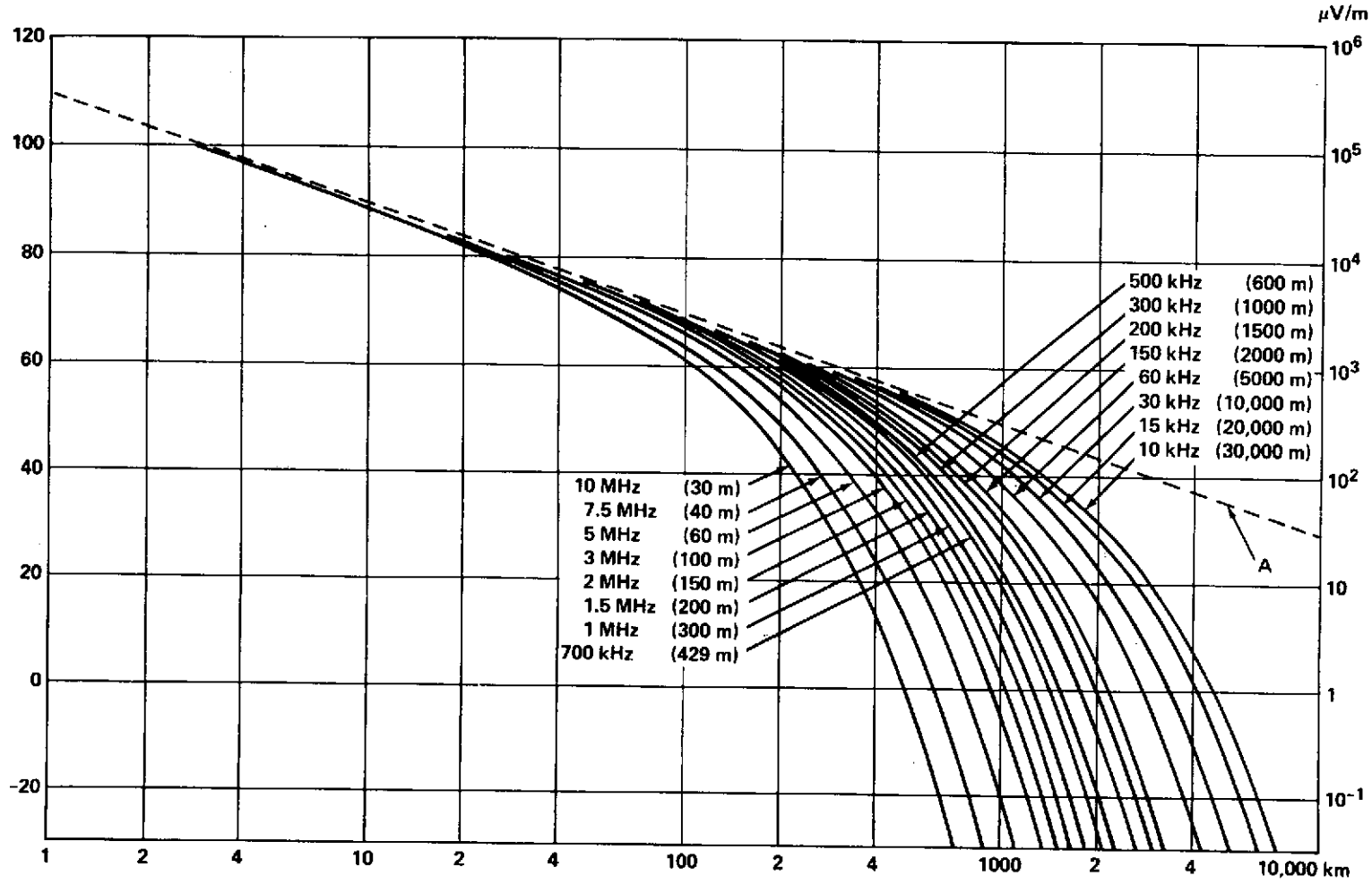

Figure 2. Groundwave propagation curves.

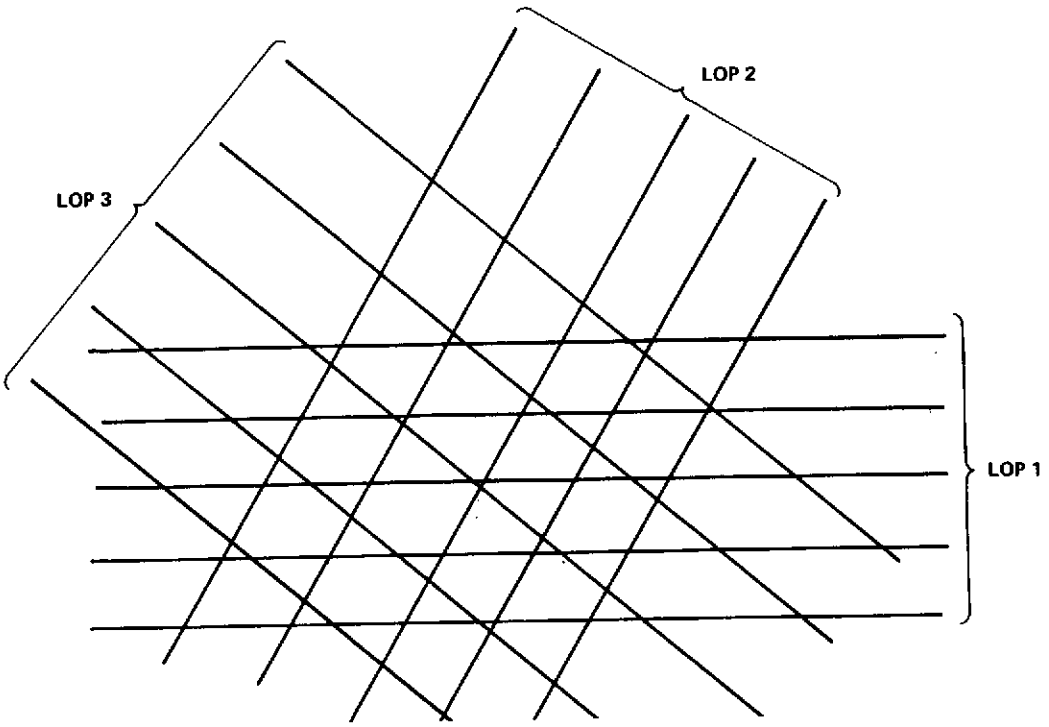

Figure 3. Geometry of redundant grid points.

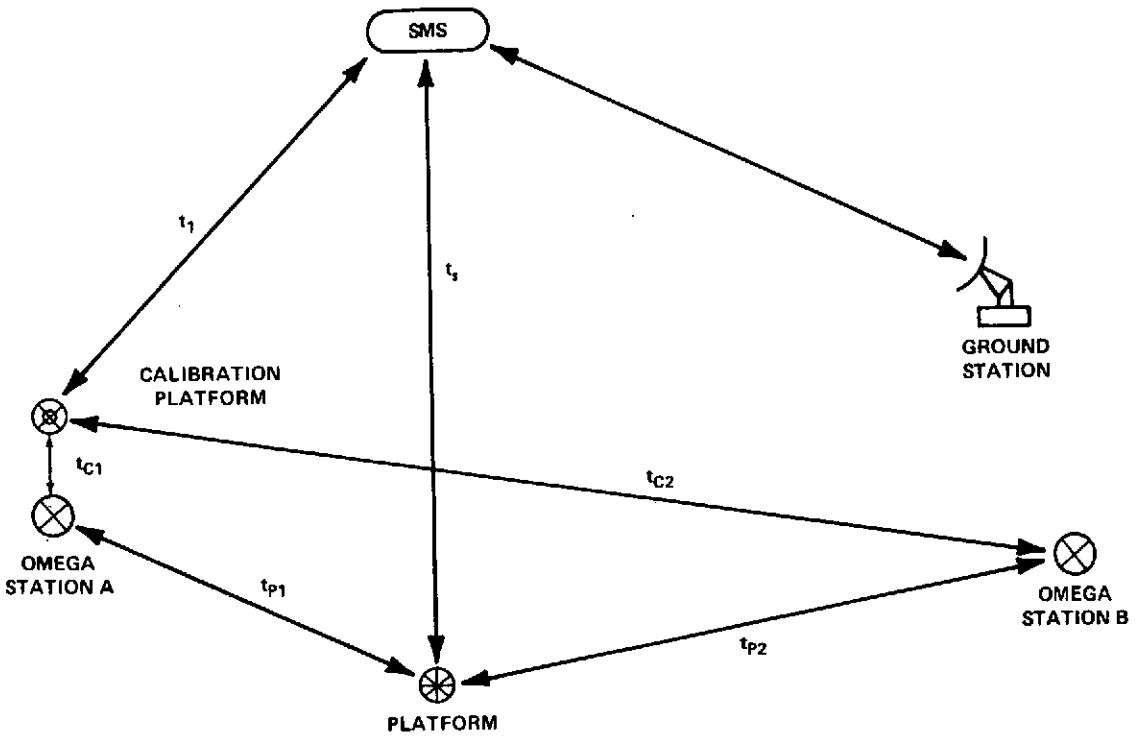

Figure 4. Time-of-arrival technique.

ADDITIONAL OMEGA TONE (10.88 kHz)

The extra OMEGA tone of 10.88 kHz would result in a lane width of 360 nm compared to 72 nm obtained with the present three-tone pattern.

The 10.88 kHz tone is a submultiple of the basic frequency of 816 kHz at the OMEGA ground stations and does not interfere with the existing 10.2 kHz and 11.3 kHz OMEGA tones. Thus, it can be easily implemented by modifying the frequency synthesizer at a cost of less than $100,000.

The difference between 10.88 kHz and 11.33 kHz is 0.453 kHz, while the difference between 10.88 kHz and 10.2 kHz is 0.68 kHz. The difference between 0.68 kHz and 0.453 kHz is 0.227 kHz, which corresponds to the 360 nm lane width above.

The optimum combination of one or more of the above techniques with respect to cost, accuracy, reliability, and complexity are subjects of a current study, which indicates that all of the methods discussed are feasible and can be implemented.

Real-time operation can be achieved by further effort in software and an appropriate increase in the size of the computer. The above-mentioned effort includes a trade-off study that depends on parameters such as CPU size and storage capacity in the computer, software changes, hardware changes and probability of missed alarms due to computer overload.

Presently an rms accuracy of 1 to 2 nm is obtained with OPLE equipment by utilizing skywave correction for the 10.2 kHz tone from published tables and computing a correction (off-line). This method of correction obviously supplies an average error but not the actual error in real world conditions spatially and time-wise. In this experiment for advanced OPLE we intend to deploy several calibration SARCOMs throughout the area of experimentation at known locations. Real-time propagation data from these platforms will supply the control center with spatial and time information on the skywave propagation error that will enable us to increase the location accuracy. (It is possible that these platforms could be used for ambiguity resolution by correlation and differential OMEGA techniques between the calibration SARCOMs and the distress SARCOM.)

Further improvement in accuracy will be achieved by more efficient VLF signal handling and antenna design at the SARCOM to enhance the VLF signal handling and antenna design at the SARCOM to enhance the VLF signal-to-noise ratio.

To increase subscriber capacity presently the WARC has allocated 100 MHz at VHF (at 406.0 MHz to 406.1 MHz for uplink search and rescue application). The present SARCOM utilizes 2.5 kHz for its information bandwidth, thus resulting in 40 search-and-rescue channels. As the number of users becomes larger, the probability of simultaneous transmission increases, thus increasing the risk of two or more users transmitting in the same channel during the same transmission time interval. This risk can be decreased by decreasing the transmission interval or the bandwidth required. The former will result in lower

accuracy and the latter may increase the complexity and power requirements at SARCOM. This is clearly a trade-off problem. Preliminary results indicate that with one hundred available channels and five or more simultaneous alarms, the probability of two or more SARCOM being on the same channel is about 5 percent. This trade-off analysis will require more data on accident statistics which will be supplied by the U.S. Coast Guard. The determination of cost functions or pertinent parameters such as false alarm, missed alarm, and so on will facilitate decisions on system design.

SUMMARY

The techniques outlined in this paper should not be considered finalized at this time since the experiment itself will be used as a vehicle to perform optimization and trade-off of the various possible solutions to the search and rescue problem.

The Development of an Advanced OPLE concept will also offer a capability for other user applications. It is anticipated that interest will be solicited among data collection users for additional experiments. The U.S. Naval Oceanographic Office has a requirement for real-time buoy tracking experiments to improve ocean current forecasting techniques. Interest has also been expressed by scientists in meteorology and ecology for a real-time data gathering system.

PANEL DISCUSSION

William J. Klepczynski, Moderator

DR. KLEPCZYNSKI:

I would like to start off the discussion by asking one question and seeing how things develop. First, I would like to find out if anybody would want to comment on the use of the lead second. Have there been any difficulties with respect to the users? Has it satisfied everybody's needs? Is everybody happy? Are there many complaints?

DR. WINKLER:

Please also comment on the usefulness of the UT-1 code, and any criticism you may have about that.

DR. KLEPCZYNSKI:

I was wondering if Mr. Stanley from the National Bureau of Standards has any user reaction?

MR. STANLEY:

Yes, I indeed have, especially in regard to the DUT-1 code. As most of you are probably aware, we transmit DUT-1 corrections from WWV as a series of double ticks every minute. Some of the seconds markers between the first and 15th seconds are doubled, and by simply counting the number of ticks that are doubled, one can obtain a coarse approximation of the difference between our times field as transmitted and UT-1.

For example, if two of the ticks are doubled, the DUT-1 correction to be applied is two-tenths of a second.

Now, I have received some complaints that the double ticks as transmitted by WWV cannot be distinguished clearly, especially during times of high atmospheric noise. The Canadian station, CHU, uses a similar procedure, but their keying tone is of longer duration and it appears to be much easier to discern their double tick than it is in the format that we are using at WWV. I would be interested in any comments that some of you may have.

DR. WINKLER:

I think one of the problems that we have is that we of the PTTI community are really not directly representative of the many people who use these time signals. And I would like to encourage each one of us who has some interface with that community so that we get some reaction. That community we are talking about is not represented anywhere. Because these are the people on radio receivers and they do not speak up or do not talk back – if you want to say that.

So we really have a problem. I think we will expect in the next year, and continuing, a discussion on the usefulness of the present arrangements, and their possible improvement. I would very much appreciate any ideas or criticisms, because we need these ideas.

MR. LAVANCEAU:

As one of the users of the DUT-1 code, I would like to know what can be done to have the Navy Department transmit the DUT-1 code properly. I notice that many times the DUT-1 code transmitted by Navy stations is not the correct code.

I think that users should be guaranteed the correct UT-1 code. And I wonder what NRL wants to say about this.

MR. STONE:

The reason that it's different on the VLF is that we are using the FSK in order to put a CW signal out, with FSK you have a little bit of a problem, but basically what we were doing was to try to make it closer to our type of transmission.

MR. LAVANCEAU:

No, I'm sorry, maybe I didn't make myself clear. The DUT-1 code transmitted by the Navy station is sometimes not the one that is supposed to be transmitted. Sometimes they forget to change it. I wonder how to make certain that the station will transmit the correct DUT-1 code.

MR. STONE:

That's a hard one to answer. I don't know how you guard against lapse of memory, or whatever it is. But I'm sure that there could be some kind of operational procedure, maybe automatic, that would take care of that. I see no reason why not; it's just a matter of knowing whether or not it's occurring.

DR. WINKLER:

We have a problem which increases with the number of controlled messages and the number of adjustments. I think the point really is, is it necessary to have the DUT-1 code to a tenth of a second? How many people are using it? How many people are getting it from the published value in, for instance, the "Notice to Mariners"? That's really a question which has to be investigated.

DR. KLEPCZYNSKI:

This leads into another problem which I wasn't aware of, but the Manned Spacecraft Center in Houston, Texas, was really upset by the leap second. The Apollo launch can't really be delayed too much after December because if it is, then their time system will be offset by one second. And all their orbits are precomputed, so this is a very difficult operational problem to overcome. They essentially just can't schedule a launch, especially a manned launch, during the period of a leap second.

MR. WARDRIP:

This, I might add, is also true of the Skylab project. They are particularly concerned, not necessarily when they are sending up unmanned satellites, but certainly when they're having manned satellite activity.

DR. REDER:

It's sort of a legitimate question, "Why January 1?" because if you have any program or automatic system you have to work harder on January 1 to recognize the Julian date going from 365 to one, and so on. Why is it that it's done then?

DR. WINKLER:

The reason for that is that otherwise no international agreement could have been reached in the discussions about the change of the old UTC system, and I remind you about your troubles which you had when you were to be prepared to make frequency changes in multiplies of 50 parts in 10^{10}, possibly every year, also steps of one-tenth of a second, sometimes quite frequently.

Don't forget, we have been exceedingly lucky from 1966 through 1972. We had only one step and no frequency change, but the situation could have changed. Following some legitimate complaints from the physicists and from radio engineers who wanted an invariable frequency base connected to the time-signal emission, it became clear that the offset had to be dropped.

Now you cannot drop the offset without at the same time increasing the tolerance between UT-1 and the time signal. An increase of the tolerance I think was most strenuously objected to by a number of people and a number of nations. For instance, the Russians objected to that increase of tolerance vehemently for years. When it finally became clear that there was still a possibility of reaching some agreement, it was only on the condition that any change take place only at a fixed date. Now that couldn't be done. You cannot have an exact second introduced at a fixed date and still stick to a tolerance of 0.7 second.

So the solution was modified – not one fixed date, but two fixed dates. And finally everybody agreed on two fixed dates. A step second could only be introduced at the end of June or at the end of December.

There is some additional provision in the IAU recommendation – and also I think in the CCIR recommendation – that in extreme cases the step second could be introduced at another month, or at any time. And this may become necessary. Our learning period is very short; we have not seen any really violent change in the rate of rotation of the earth.

But I believe that should answer the question, "Why have these two periods been selected? Couldn't it be at any other time?" The reason is that – in brief – you should make such drastic changes only with complete international agreement. Nothing worse could

be imagined than to have these 40 or so time service stations mentioned before, meet on two different systems, or three different systems which may be half a second apart.

It's for that reason that I think the present system is a great improvement. Of course, by necessity it has to be a compromise. The impression is, "How much do we pay?" Is it intolerable, or can we still effect some improvements?

MEMBER OF THE AUDIENCE:

I am in fact very happy to hear that the leap second is going to cause some problems operationally. We have foreseen some of that. And I wonder if any progress is being made towards a uniform time scale.

The leap second is, as you say, a compromise. And most of the information that needs to be used by those users who depend on it, can be provided by radio signals. In most other cases the publications on the time difference should be adequate. Is there any further development along those lines?

DR. WINKLER:

I know for certain that there will be no change in the basic concept for at least five to ten years. Another change within only two or three years is out of the question.

MR. KEATING:

Does WWV announce shortly before the hour, five or ten minutes before the hour, for example, the maximum usable frequency?

MR. STANLEY:

No, sir, WWV does not announce maximum usable frequency. We do not have that data available to us on a day-to-day basis.

MR. KEATING:

I would like to suggest that that would be very useful.

MEMBER OF THE AUDIENCE:

We find the present system most useful, having originally developed all our equipment around WWVB, the 60-kHz station, because of the various offsets in the other signals. Is there any anticipated dropping of that station now? I have heard rumors that it was to be phased out. Is that so?

MR. STANLEY:

There is nothing definite to report at this time. There is some speculation, of course, that eventually WWVB will be phased out. As for a target data, I have heard that 1980 might be a reasonable date to look forward to now for phase-out of WWVB. But there is nothing certain. And certainly nothing definite at this time.

MR. CURTRIGHT:

I'd like to make a comment on WWV. We in the deep space net, unlike other people, do have catastrophic failures in our timing system. And we do appreciate very much being able to put on the headset or the scope, or whatever, and being able to be in the ballpark, so to speak. It's a very, very usable tool in the case of catastrophic failures.

MR. STANLEY:

I don't mean to paint a gloomy picture. Perhaps I have in talking about the shortcomings of high frequencies for time and frequency dissemination. As satellites come into the picture and become fully operational systems, perhaps WWV may be curtailed. But I think it will be many, many years before the service is stopped altogether.

MR. CURTRIGHT:

I didn't mean to sidetrack the discussion concerning WWV. We use WWV every day for setting the master time on our computers for the ranging operation. However, our master station clocks are compared and phased to WWVB, and it is for this reason I was concerned about the possible termination of that station.

DR. WINKLER:

In the absence of any further comments here, I would like to say something concerning WWV. As I said before, I am in complete agreement: This is an extremely important service, for instance, here on the east coast, in Washington and in Florida; the day-to-day variations in the time of arrival of 15-mHz signals are on the order of 0.1 millisecond. You can get that with a relatively cheap high-frequency receiver. And I think that is very difficult to beat, also in respect to the difficulty of tuning the receiver.

There are, however, a couple of comments. If any station wants to routinely monitor the signals from WWV, or from any standard-frequency time signal which is convenient and close, don't forget that one of the benefits of the new UTC system is that overseas we have quite a number of stations, including the Russian stations, which are very close to the epoch which we use here.

But if you have the signal monitored, I think it should be monitored at the same time during the day. One must insist that the operator not change the bandwidth control on his communication receiver, if he has a variable bandwidth. You should encourage him to demonstrate that to himself, to look for variation in the time of arrival, which can be several milliseconds if a different bandwidth is used.

He should be encouraged to watch the difference in time of arrival as noted when you tune in or when you adjust for the beginning of the tick, as opposed to a zero crossing later on in the tick. The reason for this is that in the first case you depend on the transient response of your receiver, and in the second one you get into the steady-state response.

I believe the beginning of the signal is more stable and less affected, in respect to tuning differences, than later on. However, it is easier to measure with a later zero crossing. Interference, I think, has been very well pointed out in the talks. After all, there are several stations, and if you can't tune in one frequency, for heaven's sake try another frequency. Maybe you are consistently on the wrong frequency.

And, last but not least, I think if different receivers are used, it is clear that the differences in receiver delay must be established and entered in a logbook. Under these provisions, and using the best available transmitter, I think we have sold short the use of high-frequency time signals for many applications. And we may have enlarged the use of much more complicated, less reliable, and more expensive systems in cases where high frequency transmissions would have been entirely satisfactory.

MR. WARD:

I think what I've been hearing here this afternoon, then, is a need for training of the operators in the proper use of high-frequency receivers. And more documentation of this, I think, is in order.

DR. WINKLER:

I very much agree, and we have felt that need, and that's why we have invited and asked NBS to please give us a plan on it.

MR. STANLEY:

I appreciate your comment. Perhaps in view of your suggestion and others I have heard, it may be worthwhile to publish a technical note on this very subject. I will give it some serious thought when I return to Fort Collins. Thank you very much.

MEMBER OF THE AUDIENCE:

I had one more thing that I think Mr. Curtright could give quite a bit of help on. The impact the leap second has on operational systems is significant, and I believe that in the two times that he has had to handle this for the deep space net, Mr. Curtright has done so. And I think he has quite a bit that he can say here.

MR. CURTRIGHT:

I do have quite a bit to say about the leap second. Operationally we have rather force-fed it to out people, particularly the overseas stations. We go through some lengthy procedure on how the operator – by the way, the operator is just a normal person; he's usually not degreed, he's just an operator – and we go through some lengthy procedures for the man to check his clocks and check his oscillators, and what-have-you, to make sure that this is done right. And we get squawks, as we call them, from most of the people overseas on, "How come you have to do it on that particular day?" or, "Why can't you do it on the 5th of December, because we're not tracking that day, and it sure would be nice."

Well, conveniently I'd assume that, there's no reason why the guy really can't change his clock on the 5th of December if he's just prone to being adverse to publications. He probably could do this. As long as he's not tracking. As long as the data that is being collected is not time-tagged.

But we do force-feed them and we tell them, "Now's the time to change. You might as well get used to it. The world is changing every day." And we do it.

DR. WINKLER:

I think that's a very good point to be mentioned here. I completely agree with you. At the observatory we still have, I would think, some eight or ten clocks which have not been changed. And I recommend to institutes in those cases when you have some which ought to be changed, and maybe others which shouldn't because of the continuity of an ongoing project, to simply tag them.

I agree, there is no need to have all the clocks changed immediately. The no-change even refers to the old frequency, the eight or ten still operate as they are set, and there is no difficulty.

MEMBER OF THE AUDIENCE:

I represent Air Force Communications Services. And as we look toward the dissemination of precise time, and we look at some of our past experiences, we find that trying to determine which people will be responsible for the operation and maintenance of the time standards at various sites is to a certain extent a problem. In the past, these communicators have been interested only in receiving and processing data; and not in receiving and processing time. And so they don't have a real empathetical approach for it.

So, to a certain extent, looking over the type of training that is going to have to be given to these people, it seems that a need might develop for automation, or perhaps, for streamlining some of the techniques we have for getting right on top of precise time identification.

And I'm wondering, do any of the technical notes published on WWV contain such information as, "Do you use coherent modulation techniques? What is the spectral power density of the tick?" Things of that nature.

MR. STANLEY:

We do have information published on the power density, the spectral power distribution of the tick. To the best of my knowledge there is no National Bureau of Standards Technical Note dealing with the other matter you brought up.

DR. KLEPCZYNSKI:

Now I would like to turn to the next topic, and introduce Mr. Folts and Mr. Stone.

In discussing the communications aspects and the requirements for frequency standard, Mr. Stone discussed briefly the accuracies which you might need in an oscillator, and I was wondering whether maybe you would make any comment as to whether the equipment that is available today satisfies the needs which you see in the future for frequency in special communications? Or is there a need for development along certain lines?

MR. STONE:

Our problem is one of how do you use your manpower? If you have a cesium beam, we assume that we can forget frequency. The only problem that we have now is the instrument for time.

If we don't do anything else, anything that has much of a drift involved in it, then you have this problem of training, the problem of the man having to update. So, the problem almost reduces itself to one at the operational situation.

We would prefer that we have as nearly an invariant standard as possible. And we only have the problem of setting time.

MR. LIEBERMAN:

As long as we have had three complimentary papers on communication and PTTI, most questions that are asked, particularly by management run something like: Why do we need the precision? More important, I think we ought to address the cost of ownership, the cost effectiveness of putting in a PTTI-coordinated system for communication. I think Hal Folts probably addressed that very slightly.

MR. FOLTS:

In reply to that, I tried to get some fundamentals out in my paper. Of course, there's much more to it than that. On cost, I mention that some of the complex processes such as – I call them complex, maybe some people don't consider them that way – bit stuffing, pulse stuffing techniques compensate for time differences between the ends. There is a report done by Dr. Patell of the DCA Systems Engineering Facility, which shows that once you get over a certain number of channels, that bit stuffing no longer is cost effective and it would be better to have even just straight cesium standards at every nodal point.

I can't remember the exact figure, but it was in the order of magnitude of 10 circuits or something like that.

As far as the accuracies go, there's always room for improvement on that. And one thing about it, things need to be automated as much as possible to minimize the amount of human intervention. For instance, we could have coherence of one part in 10^{12}, the frequency coherence of one part in 10^{12}, for a purely synchronous operation, or a fully corrective solution to the time difference would be only good for about two

megabits. And of course in the system we're addressing getting up into many multi-megabits. 20 megabits and even higher than that.

So time could be tightened up considerably more. There'll have to be a combination of techniques there, of course.

In addition, the training part of it is important. That's why I say things need to be automated as much as possible, including maximum use of servo-loops. Yet not to a point where you could get into system instability. This is the other problem, you can't have things too automated; you have to have some sort of checkpoint to prevent the wrong type of feedbacks. But educating the personnel out in the station to handle the types of accuracies and precisions, it's a very difficult concept to get across. You know, parts in 10^{12}, and so on, it's such a minute quantity that the average person doesn't seem to understand this very well.

The examples I've cited before, for instance, where we surveyed our facilities, and from one AUTODN site they came back and said, "Our clocks are absolutely perfect. We have no trouble with them whatsoever." And we said, "We don't believe you. Send us the records."

And we got the records from the VLF receiver and it was straight-line right across the recorder perfectly horizontal. From this VLF comparison – they were Sultzer 5A oscillators against a VLF signal – not even any diurnal shift in it. Of course, the receiver wasn't even working and they were just sitting there fat, dumb, and happy that they had perfect oscillators.

Education will be very important, coupled with the minimization of any human intervention. I think that's it.

MR. KEATING:

Automation is usually quite expensive. And it has been my experience that when you tell someone to retard a clock one second, there's a 50-50 chance he's going to advance it one second. And you speak here of a time-synchronized, multimode, high-precision time net. What would the leap second do to your multinode net without automation? Would you care to speculate?

MR. FOLTS:

I don't think all that much, because, well, it's a question of how much will we use actual time as opposed to the time interval. Because we have to do some synchronizing anyway to take up the path delay, so whether actual time is going to be of benefit or not Bob Stone and I have discussed this quite a bit. I haven't put that much thought into that idea.

But the question of your comment about automation being expensive, I question that point. Because in fact you have got to look at the expense overall in operation, for what

you really gain for that money. And servo-control and digital techniques are getting cheaper and cheaper all the time. I think that's one great thing. So it's not so expensive as it used to be.

In fact, if you can automate something and eliminate the human portion of it, you could be saving an awful lot of money with the increased accuracy and precision that you'll get out of it.

MR. STONE:

One of the reasons that we use the distribution system that we do with the discipline time-frequency oscillator is to get around some of these problems. If you will look at it in one sense, it is an automated system, because we have put the effort in one spot: the place where the knowledge has to be, at where to set the time. The rest is a controls system and the man does not enter the loop very often. And if you follow this on through it is very much more cost effective at the moment than it would be to put a series of cesium beams in the stations.

MR. BISHOP:

If I could comment for just a minute on what Hal Folts said, we in Air Force Communications Services are presently operationally evaluating high bulk-rate digital systems in a test facility out in Richards Gebeur Air Force Base. And I believe that what Hal said is in fact a practical line of thought. A great deal of automation will be necessary, I think. In just our initial studies we have found that if I wanted to take, say, commerically available PCM channel banks which operate at 1.544 megabits with a throughput of approximately 24 narrowband channels – if I wanted to take those and replace them – replace existing trunking systems within the Department of Defense Communications System, at a parity of channels, I would have to stack roughly 300 narrowband channel capacity links onto a wideband trunk. Consequently, this would mean I would have to have a bit structure of about 25 megabits.

Now, if I only have 15 megahertz of frequency allocation, immediately, just to achieve a parity of channels, I've got to do something in the way of clever encoding, or something like this, which automatically leads me to believe that precise time definition within the trunking system is a desirable thing.

And there is a cost tradeoff there, I think. If I use a little bit of precise time definition within the trunks I can use commercially available equipment that I don't have to obtain research and development costs for. So I think that the cost of this automation can be amortized against the cost of not having to incur research and development funds.

Regarding training personnel, I think that it is quite possible to develop a time-division multiplex (TDM) hierarchy within this system which allows asynchronous inputs to the TDM trunk network, which would enable as you get farther, and farther away from this

high-density trunk system to utilize systems which don't require quite so much time definition as you get closer and closer to the terminal consumer.

Here again it is a question of practical tradeoffs but I would estimate that they are available and it's strictly up to us, I believe, as application engineers, to investigate them and take advantage of them where possible.

DR. REDER:

I think there's a danger in overemphasizing automation versus training. I think – and this is based on many years of experience – there is no substitute for proper training, no matter how much you automize. Automation is very fine, but as the North Vietnamese said, "Computers can easily bring about a hundred fold increase in human stability."

MR. SWANSON:

I might comment, following on Dr. Reder, that this is one advantage with any automated scheme, and that is to say the check will necessarily always be made. It's quite possible in the time business to start paying a lot of attention to the microsecond business and start forgetting about seconds or days or years. Just in the ordinary course of affairs there is no need to look at these. Some years ago at one timing station, we had a slight mismatch in some OMEGA transmissions, and the trouble eventually went down to the timing station.

What they had done is they had set their adjustments and gone through all the clocks on the the very precise program to make sure they were correct, the last step of which was to look at the wall clock. And they had a little matter of 800 milliseconds loose somewhere in the course of all this. And instead of going 800, which would have taken a lot of time, they went 200 the other way. Which was fine, except that they forgot this last step of looking at the wall clock. And as it was placed at the time, it isn't hard to describe it, they were accurate to a part in 10^{11} plus or minus one second.

DR. WINKLER:

I would like to mention here that we have one clock on which can be preprogrammed to make the change – a one step-second change automatically, and the program can be put in within one year. I wonder whether anybody else has experience with such a clock?

DR. KLEPCZYNSKI:

I have a comment. Yesterday in a panel discussion, Dr. McCoubrey indicated that he felt that oscillator development would be more of a developing to the nth degree the technology we have now. But apparently, from what the radio astronomers were talking about yesterday, they need portable hydrogen masers.

Now, it's true that the masers which are around now are portable in the sense that an 85-foot radio telescope is portable, but that's not very practical. Are there any designs or technical innovations which might lead to smaller masers? Anybody care to comment?

MR. PETERS:

Well, we have one physical limitation that is the wavelength we are speaking about in our cavities, 21 centimeters. And so masers will never be smaller than that, even if they are highly loaded cavities.

Our efforts in research with masers have been directed primarily towards performance; as far as the sizes they come in, we do want to have them in one rack so that they can be moved from station to station. They are somewhat portable, but that's an engineering thing which is sort of incidental to our research efforts in that we have to make a fundamental and ultimate standard for most critical applications. Masers are never going to be portable in the conventional portable-clock sense, nor will masers be used as conventional portable clocks, I think, but for specialized application.

When maser applications are sufficiently numerous and important, then it would behoove us to put more into constructing more of them and less into moving them around. But as to making them smaller, I don't think that there is more than a factor of two to be gained and that it probably would be a very great shame to compromise any of the performance for any miniaturization.

DR. HAFNER:

We have recently started with an Army program which eventually we expect will lead up to a very small molecular frequency standard. It's a program which we expect to run for several years before we finally get what we are after. We expect, however, that the frequency stability – not accuracy stability – in the order of parts of 10^{12} can be obtained in a package of 20 to 40 cubic inches.

The basis of this program will be a CO_2 laser which is stabilized and then used as a reference. The technical difficulties are enormous, but we believe that over a few years those can be resolved. So don't expect it tomorrow, but several years from now I think those things will become available.

DR. WINKLER:

Regarding Dr. McCoubrey's statement yesterday, I found myself first in sharp disagreement that the frequency standards, molecular or atomic frequency standards represent less technology than a television receiver. But after some thought I realized that there have been 500 million or maybe a billion television receivers manufactured in the last 30 years, and the total engineering and design efforts probably were much larger than what went into atomic and molecular frequency standards.

On the other hand, I think it's possibly misleading to entertain such opinions because we ought to remember that they are the most precise instruments we have. And the acceptance of time-frequency technology, in order to accomplish certain other goals in our systems design, is necessary, as is the price which we have to pay. And there is no question that some training and some expense for automation is absolutely necessary.

On the other hand, as kind of a compensation and consolation, these clocks today are certainly exceedingly reliable. In fact they are so reliable that I think the old concept of stocking spare parts and so on may be economically not feasible. And it may be much simpler to operate simply on the basis of having two or three of these standards at a site which must be operational, and if one clock fails, the on-site personnel will simply send it back to one central repair facility. I think that is a much more economical approach.

So there are various aspects to these facts, but one cannot expect that we will have one more decade of precision, every year. I think we ought to realize that there are fundamental limits.

DR. CUTLER:

With regards to applications for long baseline interferometry, I'd like to bring up the point that either Roger Beehler or Dave Allen brought up yesterday with regards to superconducting cavity-stabilized oscillators. These offer very great promise for very high stability, which is the sort of thing that's needed for long baseline interferometry. They will not be primary standards in any sense of the word, but they will certainly serve as very good workhorses for very good short-term and medium-term stability oscillators.

MR. ALLEN:

I have a couple of comments in regard to a communications system, if I understand Dr. Folts correctly, and I thought he presented a very coherent paper. In such a net, if you require simple frequency coherence of your system, and you don't really require any external time synchronization to UTC, USNO, NBS, or anything else, it seems to me that you could utilize the very good stability of quartz oscillators as they are now available, and the learning system to go with it. Some of these units are now commercially available.

We built up one of these at NBS. It has worked beautifully for us, and it's quite inexpensive. The system would simply be that you would use time approximately every hour or so to discipline the oscillator, and it would be as good as the medium itself, and certainly the bit rate can't be higher than the medium stability. And then you would have all of the advantages of the short-term stability characteristics of the quartz oscillator, which is incidentally better than most of the cesiums, until the supertube – as it is often referred to – becomes available.

This, to me, seems to be one fairly inexpensive solution for some of the installations at the nodal points in the communications map.

I have another couple of comments. In regard to Mr. Stanley's talk, I would like to clarify one minor point.

The control of the transmitter at the WWV is done, as he said, by means of the line-10 TV sync method. The error on that is actually pretty small, on the order of 30 to 60 nanoseconds. Their control is within three microseconds, as he states.

The tie between USNO and NBS is something that I think maybe should be made clear and public. In October, 1968, the USNO and NBS agreed to coordinate their UTC scales for the convenience of users of both systems. And we agreed to try to keep the scales within five microseconds. Actually, the time deviation has been a little bit larger than that since then. But the two UTC scales have always been within six microseconds, and now the time difference between the two scales is about one microsecond. We now have a policy, at least at NBS, to maintain a synchronization of the UTC scale with the international scale, UTCBIH. But I believe that USNO is attempting to achieve the same goal. So by synchronizing to the same international scale, we essentially keep synchronizing with each other. Is that correct, Dr. Winkler?

DR. WINKLER:

I would like to try to introduce a slightly different word here. You talk about synchronization; I found that one of the greatest difficulties in my discussions with managers or assistance people is to explain the difference between synchronization, coordination, and complete independence. Synchronization and complete independence are two extremes which one can combine without the disadvantages of either, by coordination.

And we have today, as we have seen in some of these excellent slides in Mr. Stone's talk, that we are actually building networks of interacting time stations, if you will, or communications centers, or systems, which can for a day, or even for a week, be considered completely independent. They are not synchronized to each other in the strict sense; they operate free-running. They are completely independent, but from time to time you introduce a very small correction and the availability of atomic clocks of very high performance in these centers enables you to do both: to operate independently, and yet to operate on the same time. It's that third word, *coordination,* which applies.

That leads me to another point – why do we have these international frequency offsets? NBS has ten parts in 10^{13} up, and we have, I believe, four parts down from our local time scale. And maybe we ought to enlarge upon that one. The five contributors to the international time scale, which you saw on one of yesterday's slides, contribute their local independent time scales. These local scales are completely independent and must remain completely independent time scales. Otherwise, you have a loop – a dog which chases its own tail.

So these independent time scales contribute to a computed international time scale. And that, in turn, is used as a benchmark for each time center. In fact, everyone, not only these five contributors, but everyone concerned with precise time uses the time scale to generate a coordinated time. And that coordinated time attempts to be within a narrow tolerance of the BIH.

Today all five contributors agree within 10 or 15 microseconds, I believe. And there's no difficulty in accomplishing that. I believe we could probably achieve an accuracy of within

one microsecond without difficulty. However, the price to be paid for that improvement would be a more frequent adjustment in the differential rate. And that is something which we, at the observatory, do not want to introduce. In fact, we have specifically been asked by a number of systems managers not to do that unless absolutely necessary. And for these reasons, we did not make a change last January; we maintain a deliberate, very small frequency difference with the BIH, which we will bring into agreement sometime next summer.

Let's not forget there are difficulties which are larger than a discussion of the performance of the individual time scales may lead you to believe. The difficulties are in the propagation noise. Some seasonal effects have been claimed for some linkages. They may exist in fact for all different time measurements, whether they use LORAN-C or television, or what-have-you, because evidently the air pressure and the air temperature, and so on, will be expected to affect the LORAN wave similarly as it will affect microwave length over distances of several thousand miles.

So, what I am saying is that the noise level, or the noise in the intercomparison between major timing centers necessitates a deliberate, long time constant in the control loop which generates the local coordinated time, as opposed to the independent time scales where five of these form the basis of the international timing system.

DR. KLEPCZYNSKI:

We are getting close to the time of adjournment now. I'd like to thank all the speakers very much for participating in the panel discussion, and also for being so prompt with their talks. They have kept everything on time and on schedule. We appreciate that very much.

SESSION III

VLF—UHF, Propagation and Use

DELAY TIME MEASUREMENTS OF THE PROPAGATION OF RADIO WAVES IN THE ATMOSPHERE

Frederick Rohde
U.S. Army Corps of Engineers

Between 1964 and 1970 the U.S. Army Corps of Engineers established networks of accurate positions around the world. The positions were determined by means of the Geodetic Secor System. This system consists of four ground stations and a satellite. The ground stations transmit radio signals to the satellite, and the signals are then returned to the ground stations. The time between transmission and reception of the signal at the ground station is measured and used to calculate the distance between ground stations and satellite. In order to convert the time measurement into a distance it is necessary to know the wave velocity along the path of which the wave is traveling. The wave velocity depends upon the medium in which the wave is traveling.and is characterized by the refractive index. The refractive index of a medium is the ratio of the wave velocity in the vacuum to the wave velocity in medium. For all material media, the refractive index is a function of the wave frequency and some physical properties of the specific medium. The frequency dependency of the refractive index is called dispersion. The propagation of an electromagnetic wave in a dispersive medium is characterized by the phase refractive index and the group refractive index. The phase refractive index is derived from the velocity with which the phase (the crest) of a wave propagates; the group refractive index is derived from the velocity with which the energy or the signal of the wave propagates. A thorough analysis of the wave propagation in material media leads to additional concepts of the refractive index. An excellent book on this subject is *Wave Propagation and Group Velocity* by Leon Brillouin. For our considerations, however, the concepts of phase velocity and group velocity are sufficient.

The group refractive index n_g and the phase refractive index n_p are related to each other by Equation (1).

$$n_g = n_p + f_c \frac{dn_p}{df_c} \tag{1}$$

The carrier frequency in this equation is f_c. Appleton and Hartree developed the expression for the phase refractive index of a magnetoionic medium. The index is a complex function and depends on the frequency of the wave, the electron density, the magnetic field of the earth, and the collision frequency of electrons with ions and molecules. It can be shown that for frequencies above 200 MHz, the Appleton-Hartree equation can be simplified so that the group refractive index can be expressed as shown in Equation (2).

$$n_g = 1 + 40.365 \frac{N}{f_c^2} \tag{2}$$

N is the electron density. The errors resulting from this simplification are few parts in a million and are decreasing with increasing frequency.

The traveling time T of a wave between two points is given by Equation (3).

$$T = \frac{1}{c_0} \int n_g \, dr \tag{3}$$

The integral has to be taken along the wave path between the two points. If the simplified group refractive index of the ionosphere is inserted into Equation (3), the integral is split into two terms as shown in Equation (4).

$$T = \frac{r}{c_0} + \frac{40.365}{c_0 f_c^2} \int N \, dr = T_0 + \tau \tag{4}$$

The term r/c_0 represents the traveling time if the medium between the two points were vacuum. The second term represents the additional traveling time which is caused by the presence of the ionosphere. This term is called the ionospheric delay time because of the delaying influence of the ionosphere on the signal.* It is important to note that the phase refractive index of the ionosphere is smaller than one and, therefore the phase of the wave travels faster in the ionosphere than in vacuum.

The SECOR signals are transmitted on a carrier f_c from the ground stations to the satellite and transmitted back from the satellite to the ground stations on two different carriers, αf_c and βf_c.. The ratio of α to β is two to one. The round-trip time of the signal using the α carrier is T_α, and the round-trip time of the signal using the β carrier is T_β. Both times are measured by the SECOR system and subsequently subtracted from each other. The time difference ΔT is given by Equation (5) which relates the total electron content to the measured time difference and known parameters. The ionospheric delay

$$\Delta T = T_\beta - T_\alpha = \frac{40.365}{c_0 f_c^2} \left(\frac{1}{\beta^2} - \frac{1}{\alpha^2} \right) \int N \, dr \tag{5}$$

time for the α downlink can now be calculated as shown in Equation (6).

$$\tau_\alpha = \frac{\Delta T}{\alpha^2/\beta^2 - 1} \tag{6}$$

The precision of the ionospheric measurements was determined by a collocation experiment. Two SECOR stations were placed at a distance of 257 meters on an installation at Herndon, Virginia, and were used to track the same satellite. Because the two stations were so close

*The integral in equation (4) represents the total electron content along the wave path.

together the signals from each station travel through the same ionospheric region on their way to and from the satellite. The ionospheric delay times measured by the stations should therefore be identical. Figure 1 shows the results from two tracks of the collocation experiment. The satellite used was EGRS-13, a satellite in an orbital altitude of about 1100 kilometers and near 90° inclination. The table contains the ranges between satellite and ground stations and the ionospheric correction. The process of determining the distance between satellite and ground sattion is as follows: The round-trip time of the signal using the alpha-carrier is measured. This time is multiplied by the vacuum velocity of light and divided by two which yields a distance that is too large by the ionospheric correction. The true distance is obtained by subtracting the ionospheric correction from the vacuum distance. The ionospheric correction is obtained by dividing the alpha-carrier delay time by 3.118 (the delay time is measured in nanoseconds and the ionospheric correction is measured in meters). To obtain the total electron content in electrons per square meter, the ionospheric correction has to be multiplied by 4.673×10^{15}. One can see that the IC for stations 0 and 4 are not identical. Figure 2 shows the difference of the ionospheric correction of one of the preceding tracks and the deviation of the mean. The collocation experiment has shown that the standard deviation of the measured ionospheric correction is about ±3 meters. Figure 3 shows the results of three tracks of the collocation experiment. The abscissa is the elevation angle and the ordinate is the delay time for a 1600-MHz carrier. Please take note of the characteristic shape of curves 777 and 797. The points where the curves reverse is at the maximum elevation angle.

In Figure 4 you see the first geodetic network which was established by SECOR, which provides a tie between Japan and Hawaii. The orbital altitudes of the satellites used in this program were about 900 kilometers. The program was started in August 1964 and completed in July 1966. Figure 5 shows the SECOR equatorial belt network. Satellites of about 3800 kilometers altitude were used because of the large distance between stations. The program was initiated in July 1966 and completed in April 1970. Figure 6 shows the results of a track taken at the island of Woleai. In the graph at the lower left the ionospheric correction is plotted versus time. The satellite is EGRS-3, which has an orbital altitude of about 925 kilometers. The dotted line in the lower left graph is teh ionospheric correction multiplied by satellite altitude over range. This calculation was performed to obtain some extrapolated values for the total electron content above the station. The graph in the upper left of the figure shows the range to the satellite and the elevation angle of the range (dotted line) as a function of time. The right side of the figure shows the suborbital plot of the satellite orbit. At the center of the graph is the location of the station. This track was observed at 6:30 a.m. One can see that at this time the ionospheric correction is small, around five meters. Figure 7 shows similar plots. The track has been observed about noon. At this time the ionospheric correction is much larger and varies from about 90 meters to 180 meters. Figure 8 shows a four-station track in the Pacific Ocean area. Stations were located at Truk, Swallow, Kusaii, and Gizo. In this graph the delay time for a 1600-MHz carrier is plotted against the elevation angle. The local time of the track is about 9:00 p.m. The curves appear to be fairly well correllated. Figure 9 shows a similar set of curves, but taken about 6 a.m., local time.

Again, the ionospheric delay time is small. Figure 10 shows ionospheric delay times measured at a four-station track during the equatorial belt operation. These numbers are the local time of the stations at the beginning of each track. The local time is calculated from the station coordinates and is, therefore, not identical with the time of the local time zone. The track was taken on October 14, 1967. Figure 11 shows the results of a track taken at the same two stations and at about the same time, but a few days later, on October 20, 1967. Figure 12 shows the results of a four-station track taken very early in the morning. Again, at this time the ionospheric delay time is small and, consequently so is the TEC.

The diurnal variation of the total electron content was investigated. Of particular interest was the variation of the vertical total electron content above a station. Figure 13 shows such data, which were obtained from the station at Woleai. The left coordinates represent the vertical total electron content measured in electrons per square meter. The right coordinate gives the ionospheric delay time in nanoseconds for a 450-MHz carrier. The measurements were obtained from tracks having a high elevation angle. The vertical electron content was then extrapolated in the same way as described before. Figure 14 shows a diurnal region of the vertical total electron content, which contains about 70 measurements taken between September 1965 and January 1966 on the islands of Guam, Manus, Truk, Woleai, and Yap.

The noisiness of the curves was also investigated with respect to elevation angle, time of the day, geographic location, and season. Figure 15 shows a typical example. The ionospheric correction has been plotted in intervals of two seconds. Figure 16 shows another example. The standard deviation of the noise is about two meters. No correlation was found. It can therefore be concluded that the noise contribution due to the ionosphere is smaller than the noise caused by the equipment.

It has been frequently suggested that the ionosphere is a stratified medium in which the electron density is a function of altitude. An examination of the measured delay times with respect to elevation angle indicates that in addition to the altitude variation of the electron density, a variation with latitude and longitude must be included. Without latitude and longitude variation, all curves would be symmetrical with respect to the maximum elevation angle, a fact which is not confirmed by the measurements. Figure 17 shows a satellite located at S and moving from A over S_M to B. At S_M the satellite assumes the position of highest elevation angle with respect to the observing ground station. The ground station is at P_o. The center of the earth is at the point 0. It is assumed that the electron density is a function of the altitude H and the angles ψ and ω An altitude function W(h) that shows some characteristics of the layer structure of the ionosphere is selected. The functions $U(\psi)$ and $V(\omega)$ are simple expressions representing characteristic electron density gradients in the ψ and ω direction. N is then assumed to be the product of the functions, U, V, and W. The total electron content is calculated along the direction alpha, as shown in Figure 18.

A report has been prepared recently about the same subject. It contains ionospheric data from more than 400 tracks. It contains also a more detailed discussion of the Appleton-

Hartree equation and more on ionospheric modeling. I have given two copies of the report to Mr. Acrivos, and more copies are available on request. The conclusions of the report are as follows:

- Electrical signals of the 1600-MHz band will be subjected to delays of from 3 nanoseconds to more than 100 nanoseconds while traveling through the ionosphere. For radio range measurements, these delay times correspond to errors of from one meter to more than 30 meters.
- The range error due to ionospheric noise will be smaller than 25 centimeters for signals in the 1600-MHz band.
- Diurnal curves of the vertical total electron content vary considerably from day to day and location to location. Variations of 100 percent are not uncommon. The variations are most pronounced during the morning hours between 9 a.m. and 12 a.m. For this time period variations of several hundred percent can be observed when the observations are extended over a period of several months.
- If radio range measurements at 1600 MHz are used for the purpose of navigation, the error caused by the ionosphere may be of no significance or may be corrected sufficiently by relatively crude ionospheric models.
- If radio (1600 MHz) range measurements are used for precise positioning and surveying, the ionospheric error must be determined by a dual frequency method or by ionospheric models which permit the calculation of the delay time to about three nanoseconds.
- Satellites of medium orbital altitudes will provide more useful data for generating model functions than satellites in synchronous orbits. This is because radio links from the ground to medium orbital satellites sweep through a much larger portion of the ionosphere than the radio links to synchronous satellites. Model functions could then provide ionospheric corrections for stations in this area which have no dual frequency capability.

ORBIT: 703 LOCAL TIME: 10.14			ORBIT: 777 LOCAL TIME: 23.12		
RANGE [KM]	STATION 0 IC [M]	STATION 4 IC [M]	RANGE [KM]	STATION 0 IC [M]	STATION 4 IC [M]
1902	162	154	1991	102	104
1763	140	142	1912	98	97
1683	135	139	1840	95	95
1612	129	135	1669	88	86
1549	129	128	1581	81	83
1496	122	125	1633	87	87
1407	116	121	1722	91	94
1472	119	124	1780	94	98
			1846	101	104
			2084	121	118
			2174	126	122
			2269	133	130
			2367	139	139
			2469	143	143
			2573	149	153

Figure 1. Results of the collocation experiment on EGRS-13.

n	STATION 0	STATION 4	0 - 4 = Δ	m - Δ
1	102	104	-2	+1.7
2	93	97	+1	-1.3
3	95	95	0	-0.3
4	88	86	+2	-2.3
5	81	83	-2	+1.7
6	87	87	0	-0.3
7	91	94	-3	+2.7
8	94	98	-4	+3.7
9	101	104	-3	+2.7
10	121	118	+3	+3.3
11	126	122	+4	+4.3
12	133	130	+3	+3.3
13	139	139	0	-0.3
14	143	143	0	-0.3
15	149	153	-4	-3.7

Figure 2. Ionospheric correction of track and deviation from the mean.

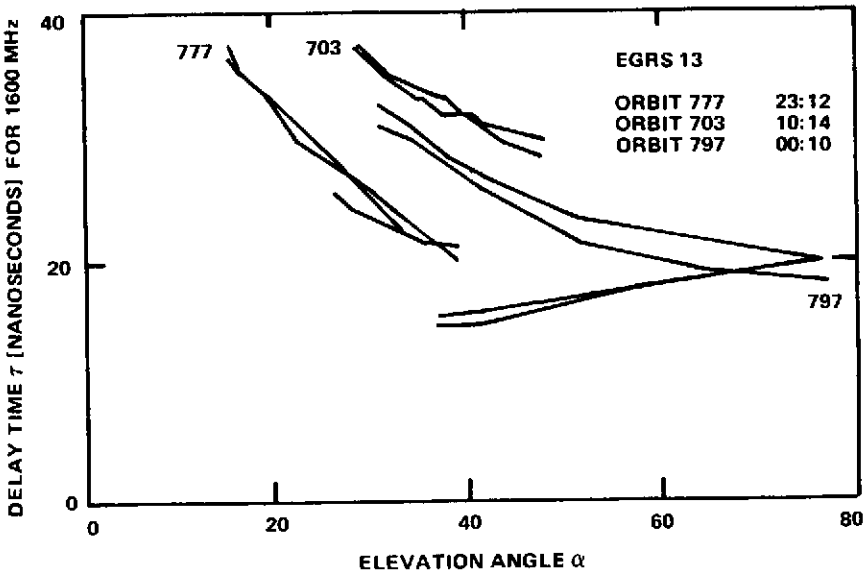

Figure 3. Results of three tracks of the collocation experiment.

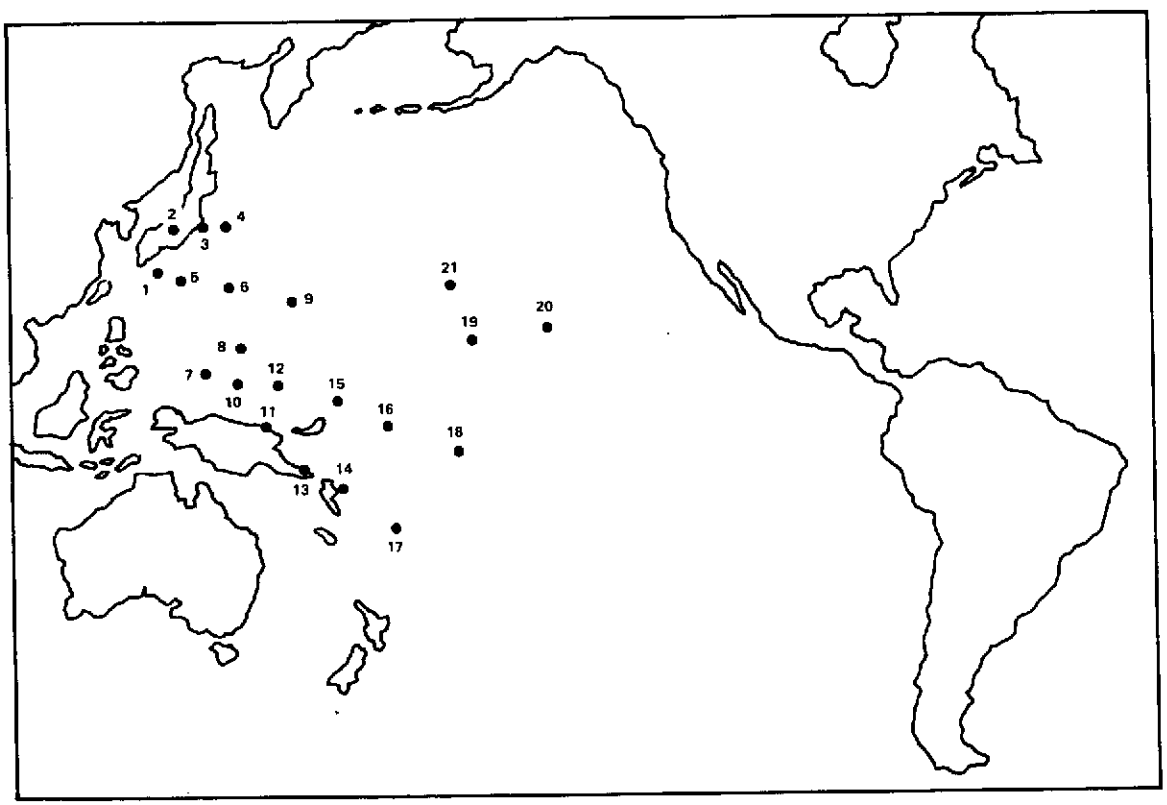

Figure 4. SECOR Pacific operations.

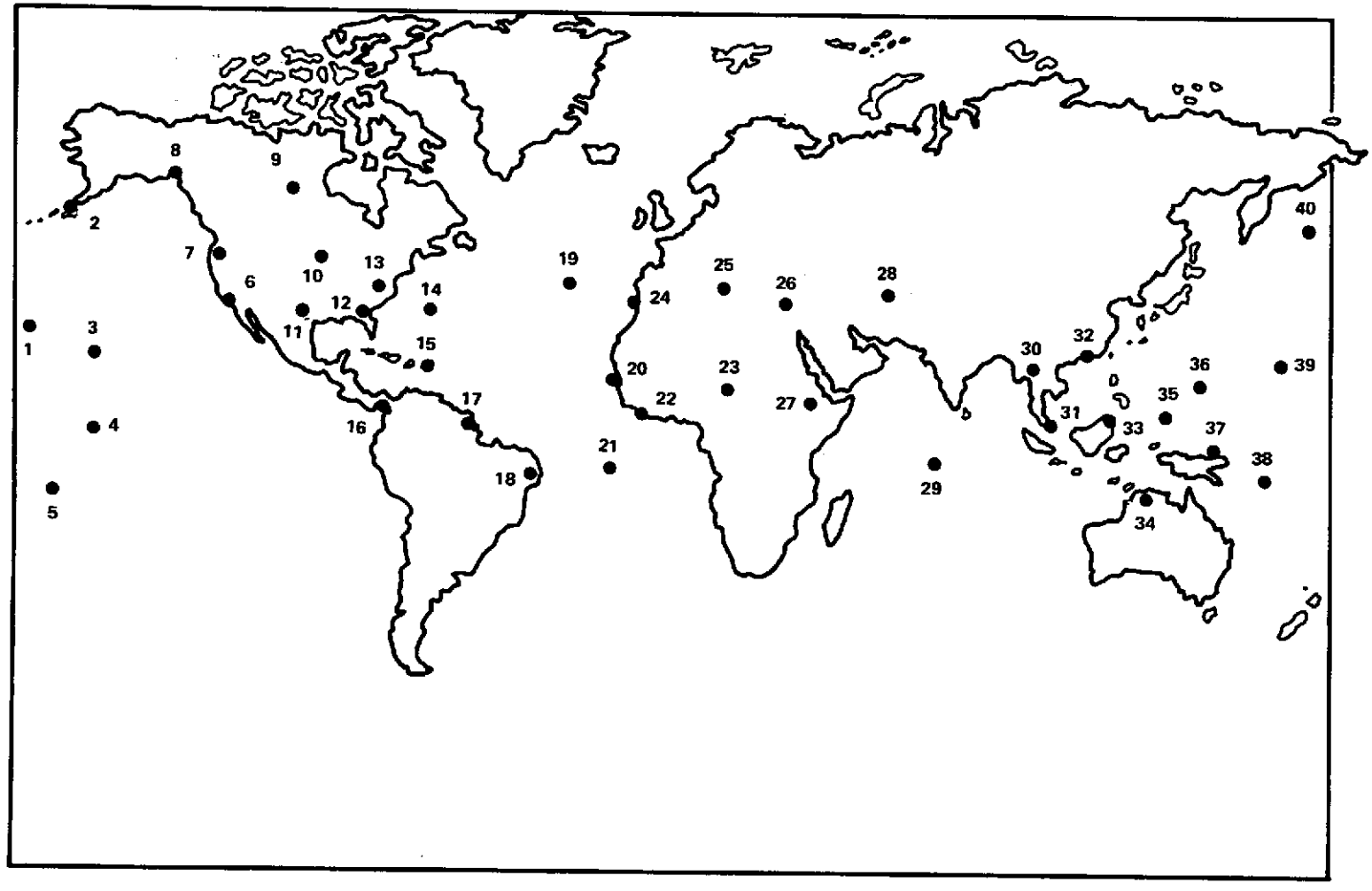

Figure 5. SECOR equatorial network.

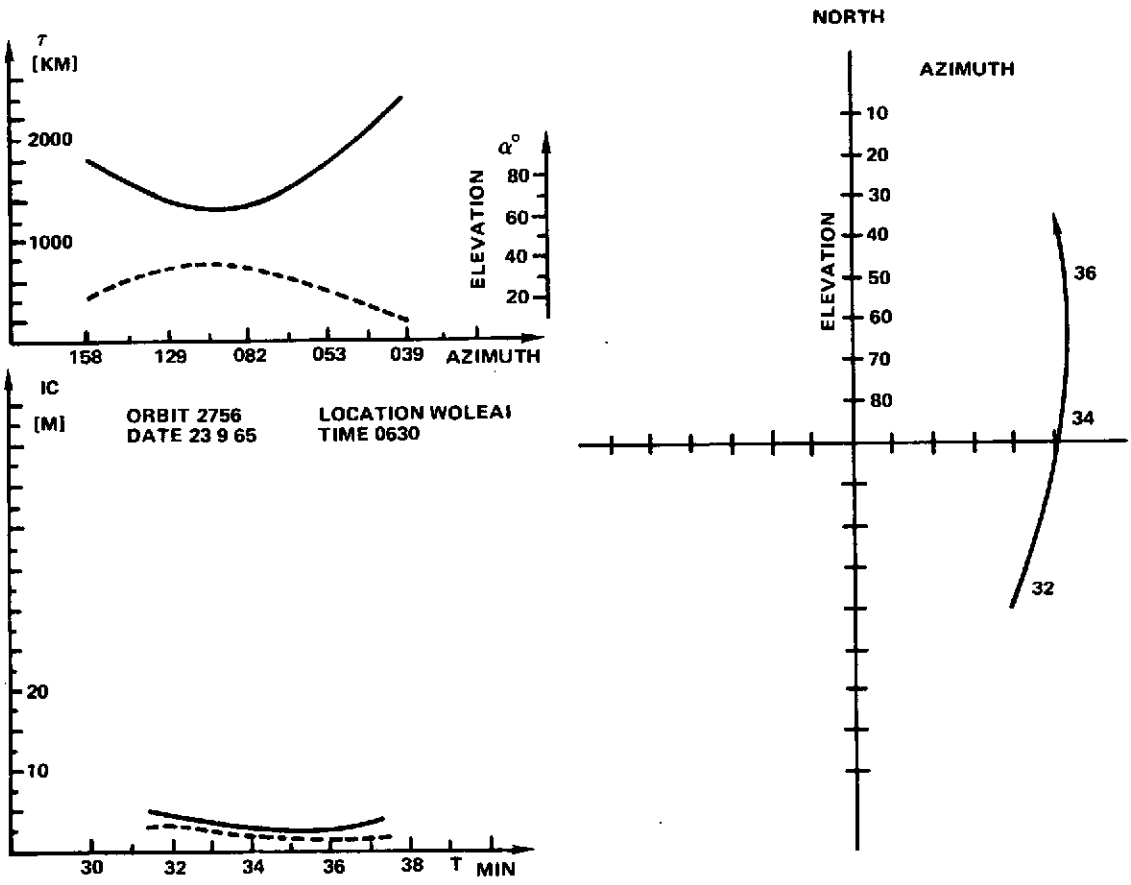

Figure 6. Results of EGRS-3 taken at the island of Woleai.

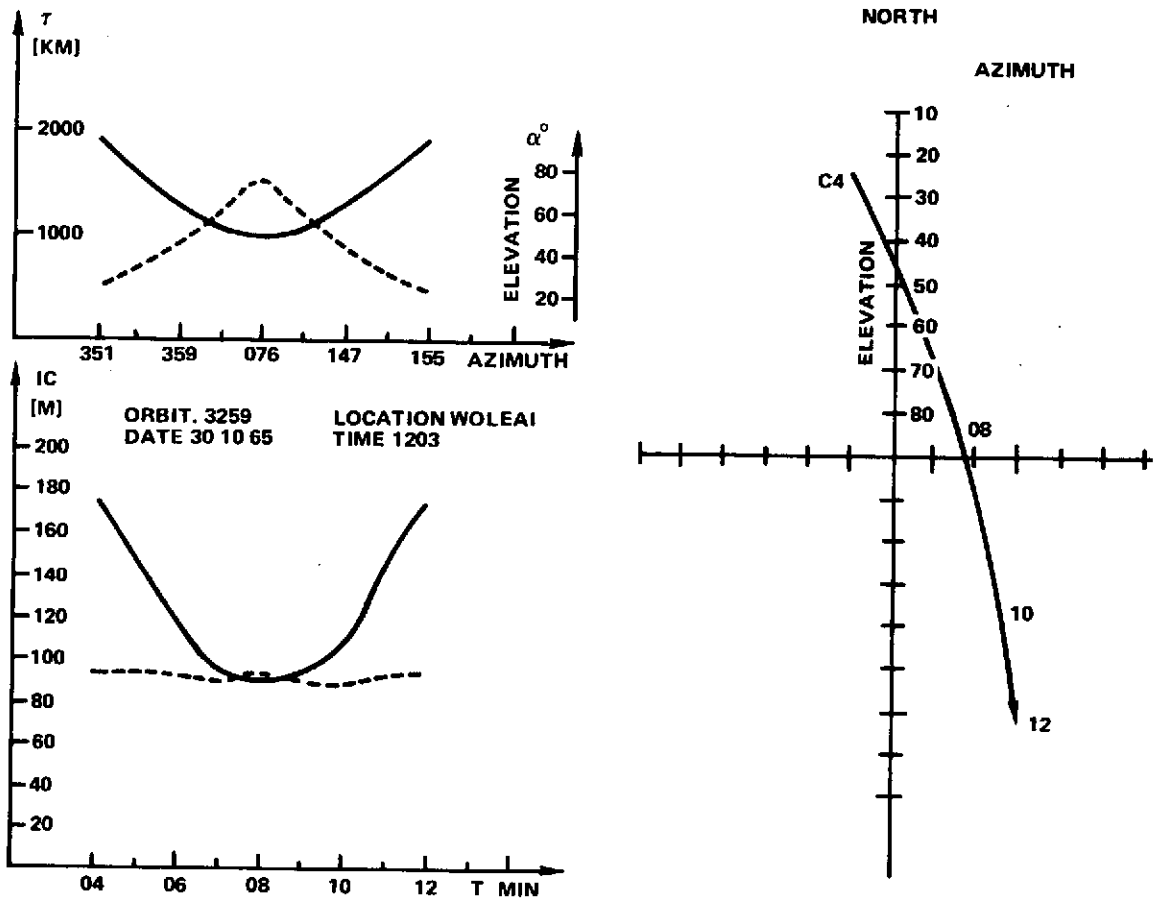

Figure 7. Results of tracks similar to those in Figure 6.

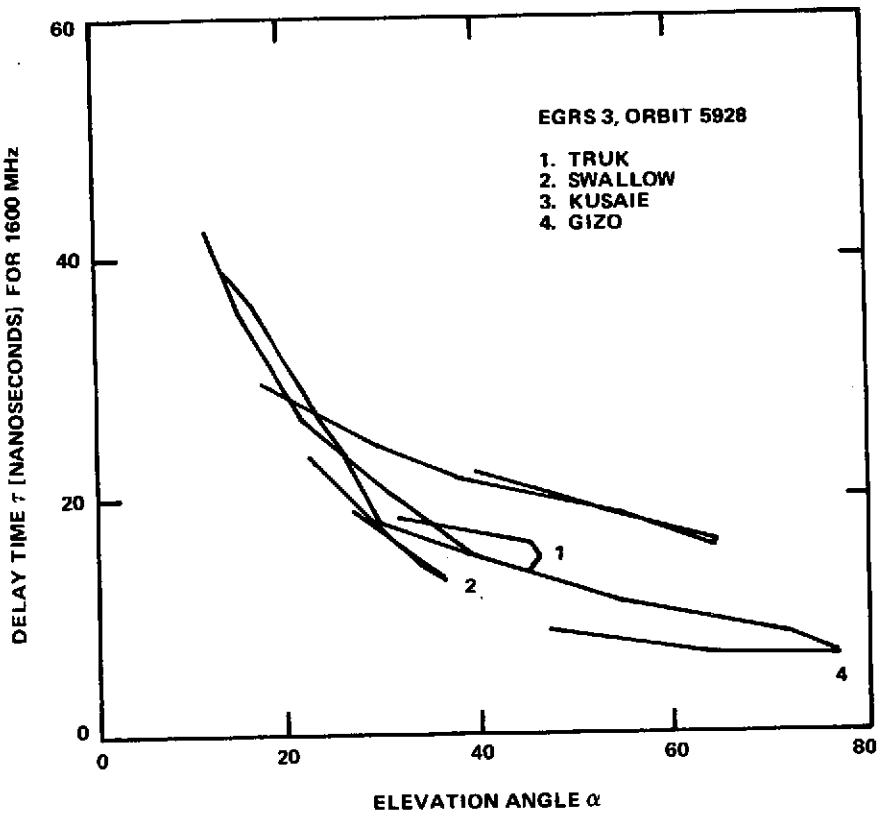

Figure 8. Results of a four-station track in the Pacific Ocean area.

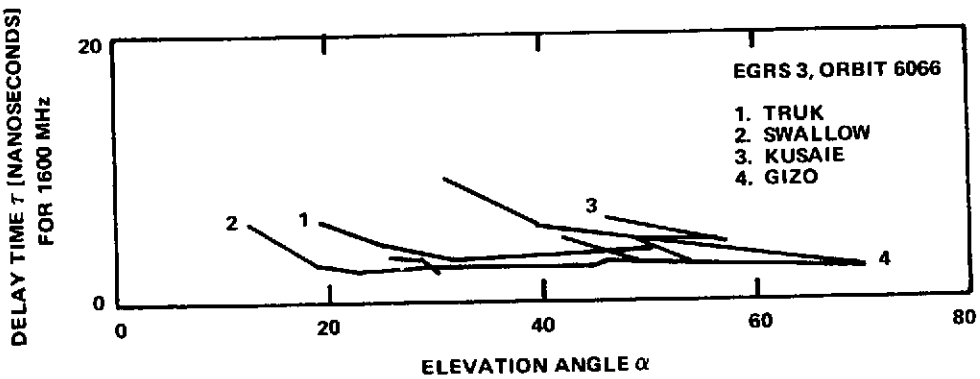

Figure 9. Curves similar to those in Figure 8.

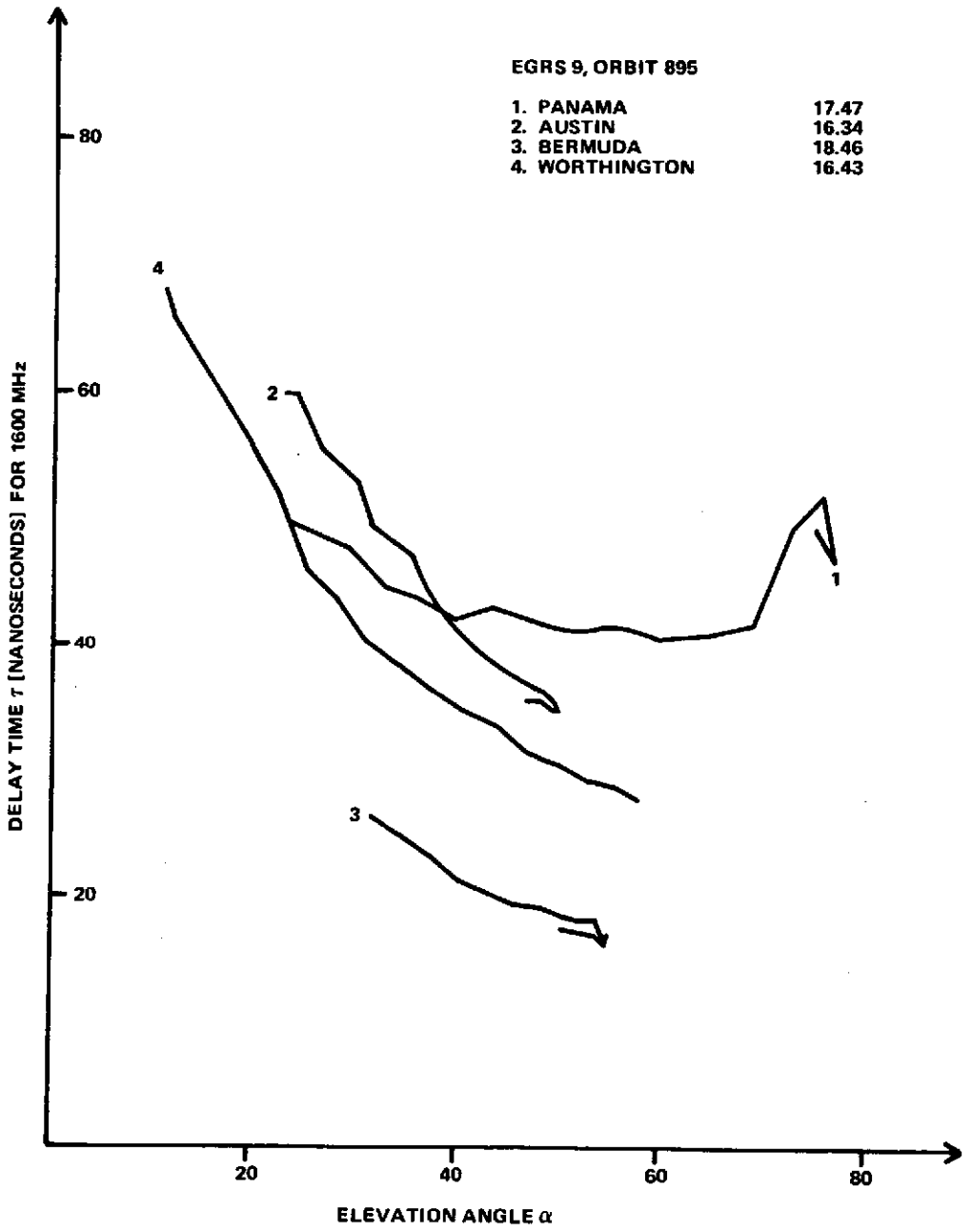

Figure 10. Ionospheric delay times measured at a four-station track during the equatorial belt operation.

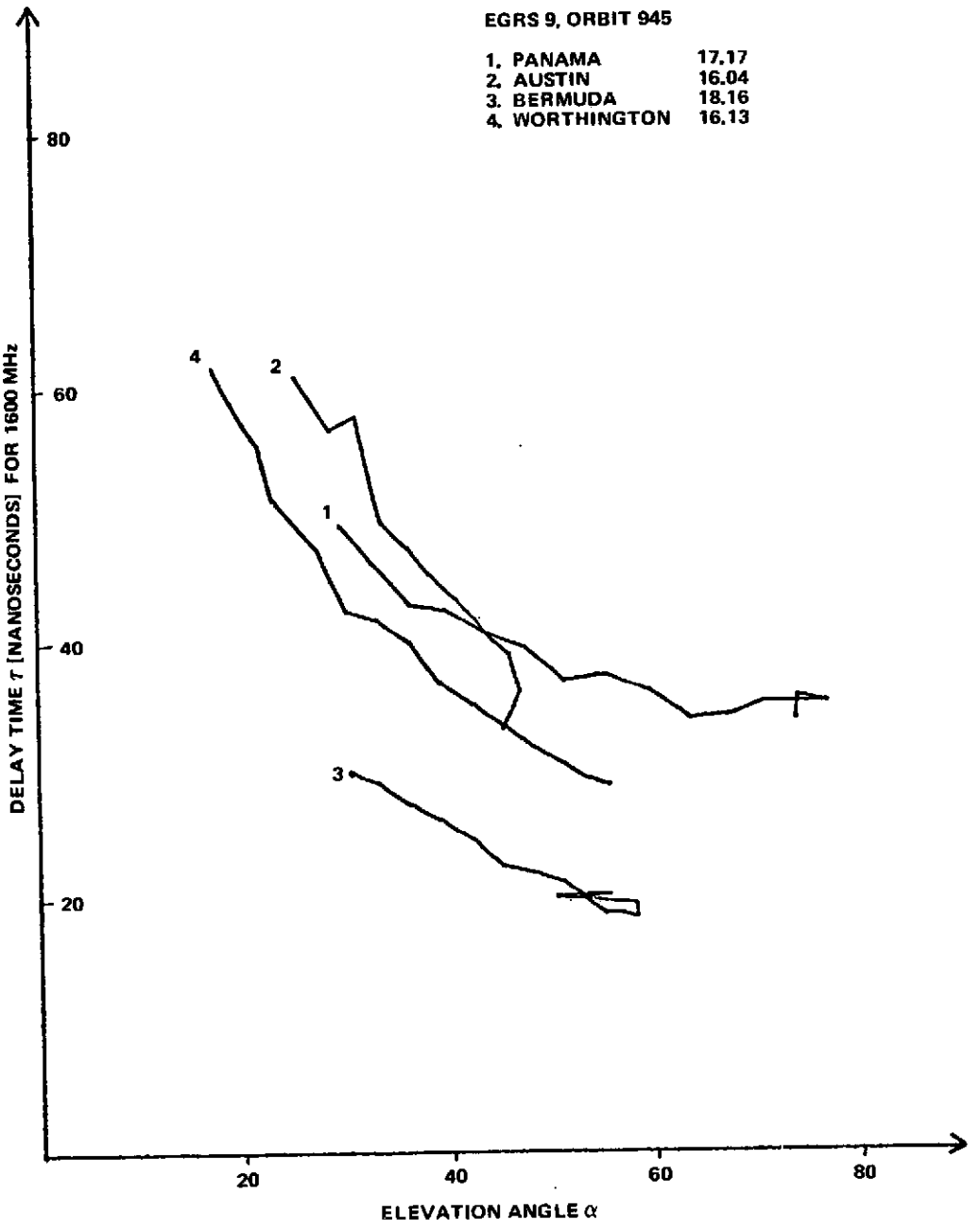

Figure 11. Results of a track taken at the same stations as those used for Figure 10, but a few days later.

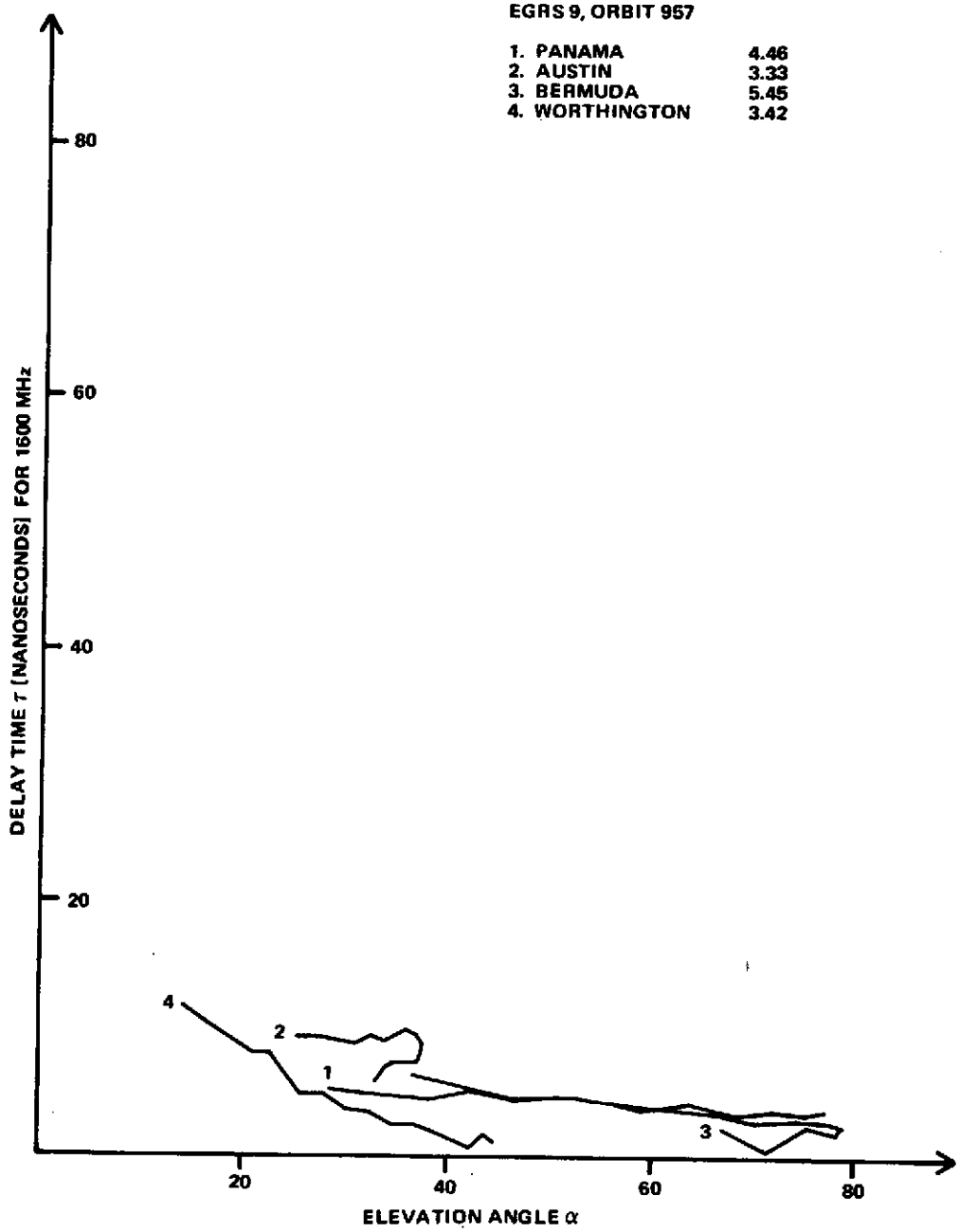

Figure 12. Results of an early morning four-station track.

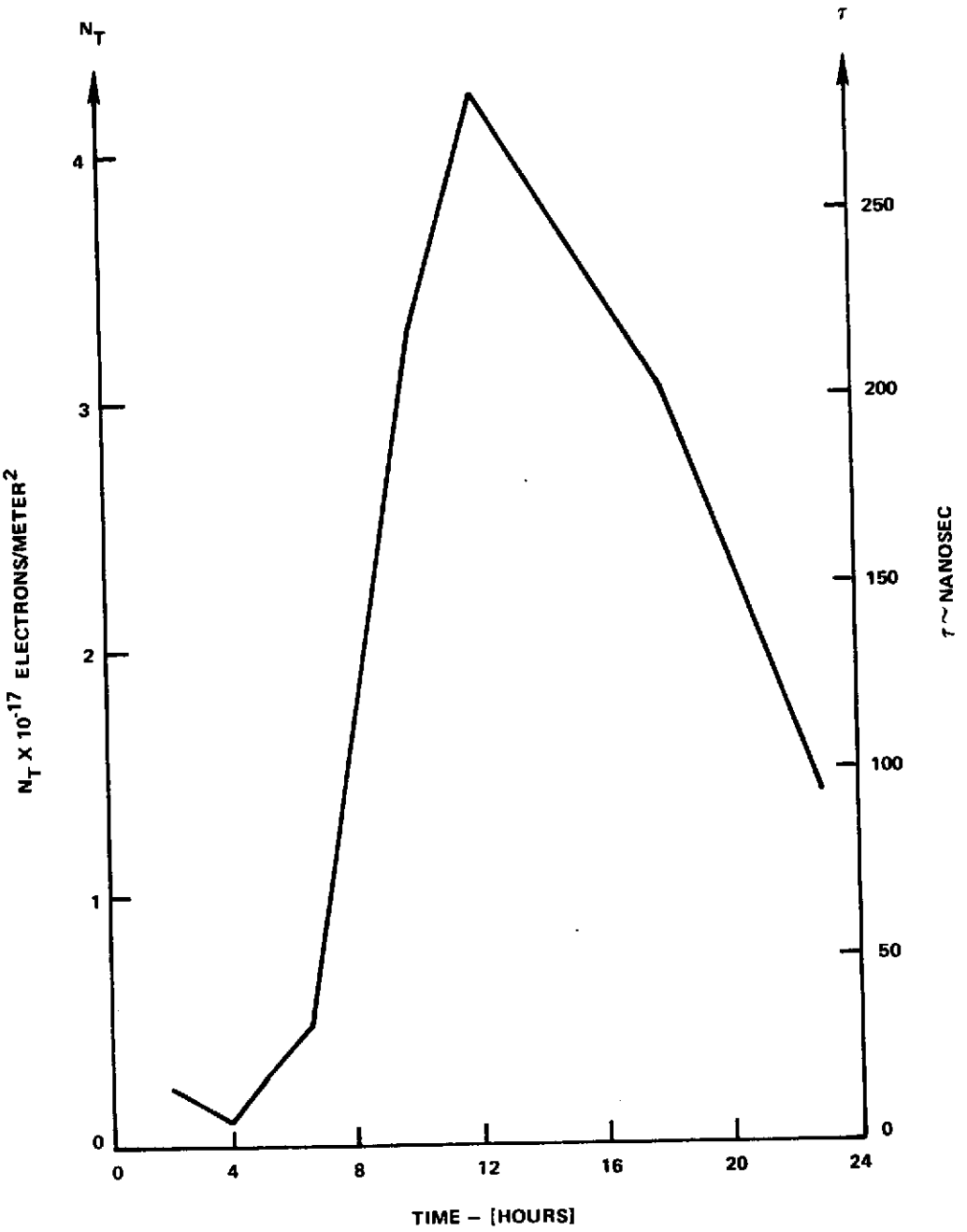

Figure 13. Results obtained from the station at Woleai.

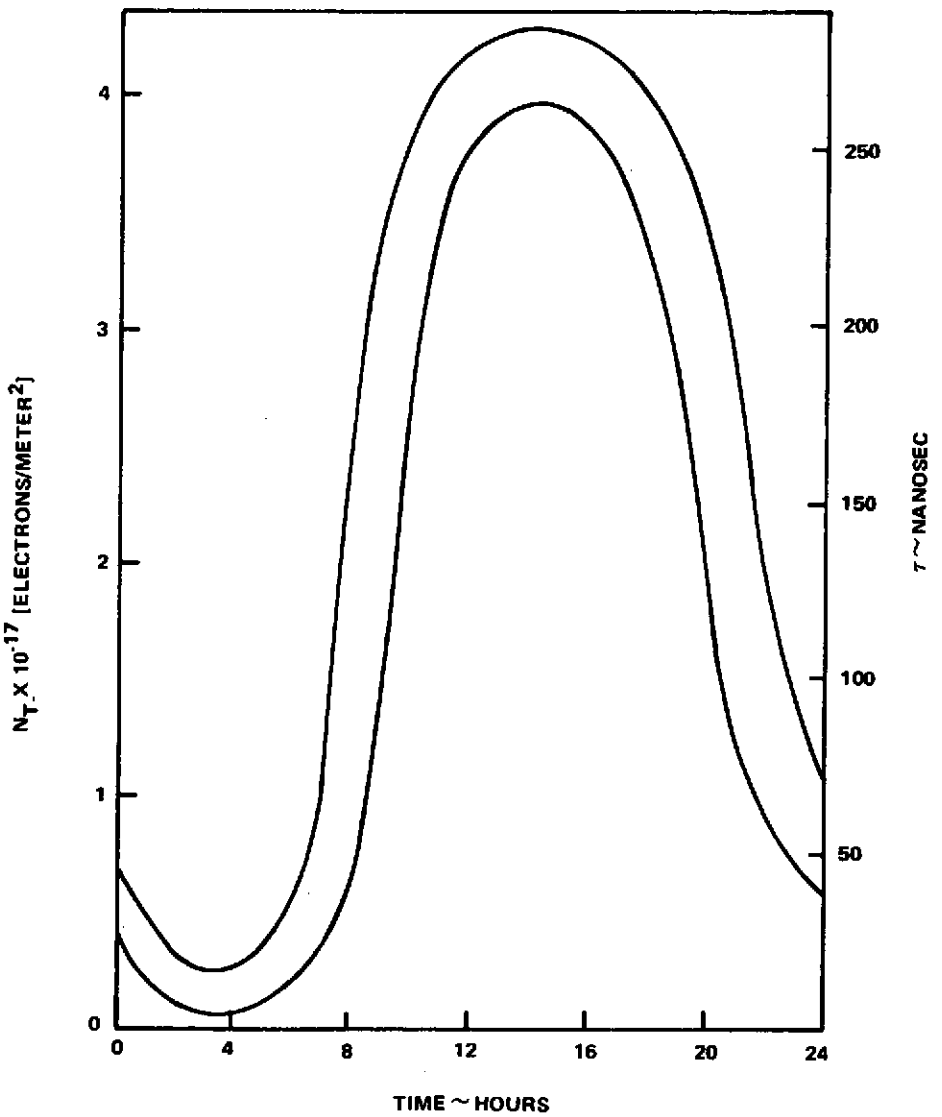

Figure 14. Diurnal region of vertical total electron count from about 70 measurements taken in the Pacific area between September 1965 and January 1966.

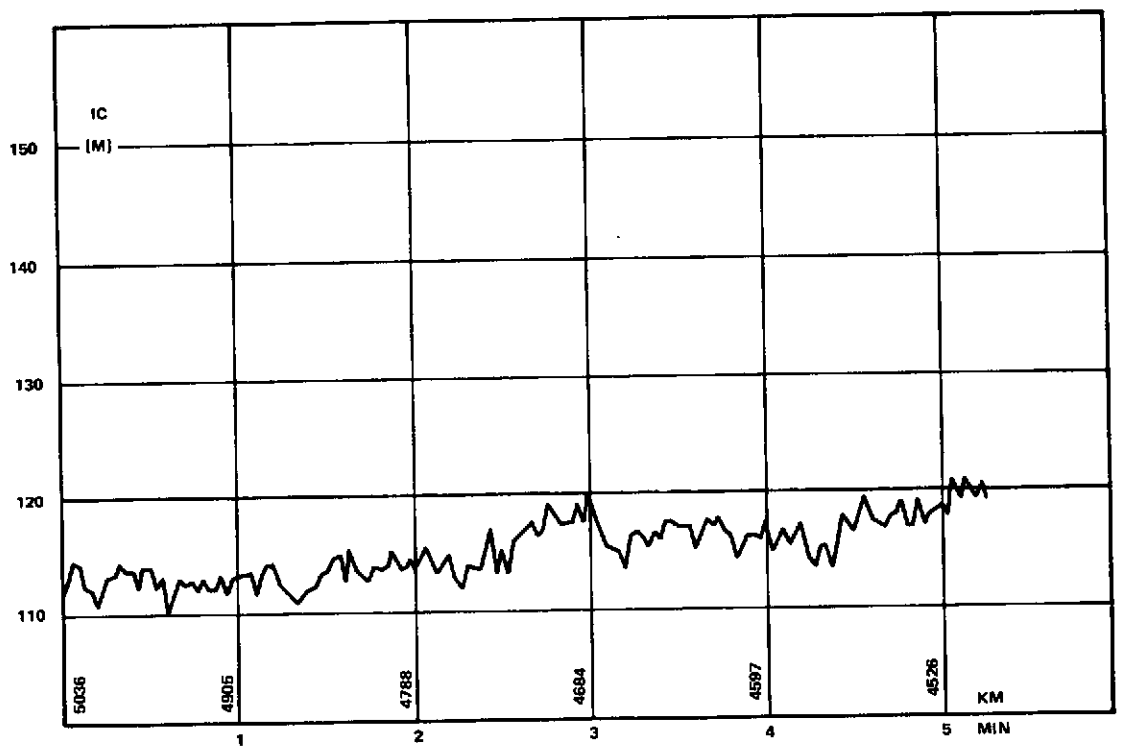

Figure 15. Typical example of noisiness of curves with respect to elevation angle, time of day, geographic location, and season.

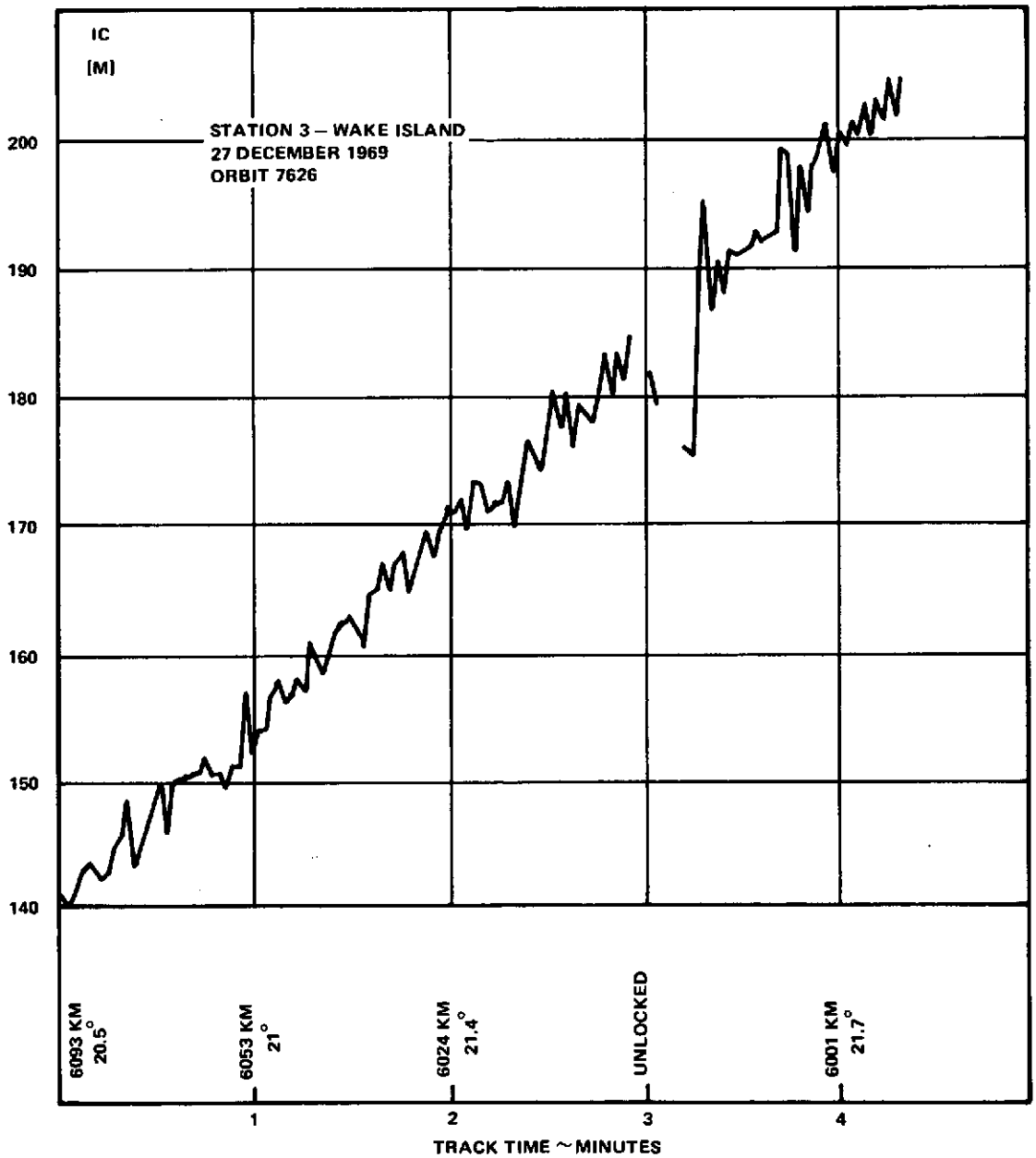

Figure 16. Another example of noisiness with same variable as those in Figure 15.

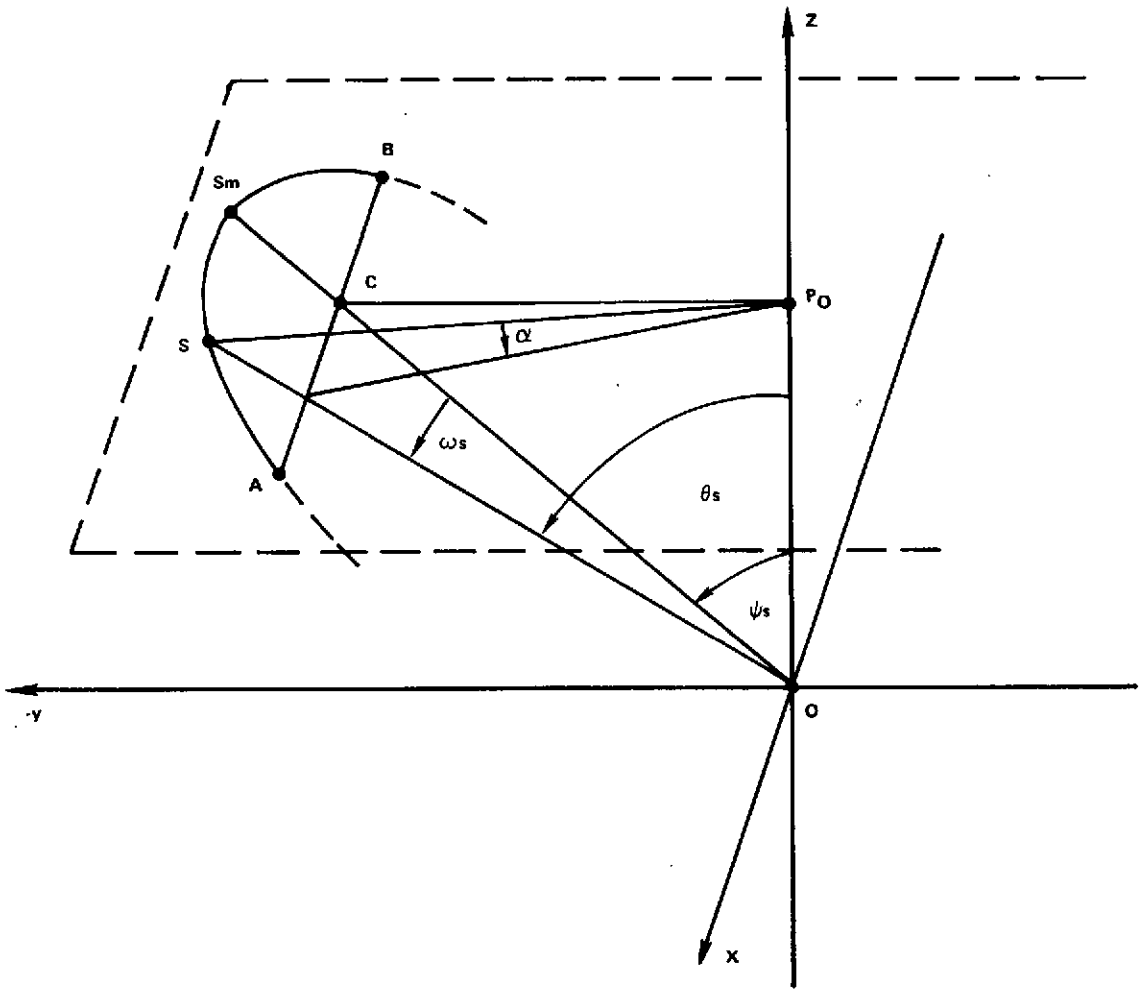

Figure 17. Plot of a satellite path.

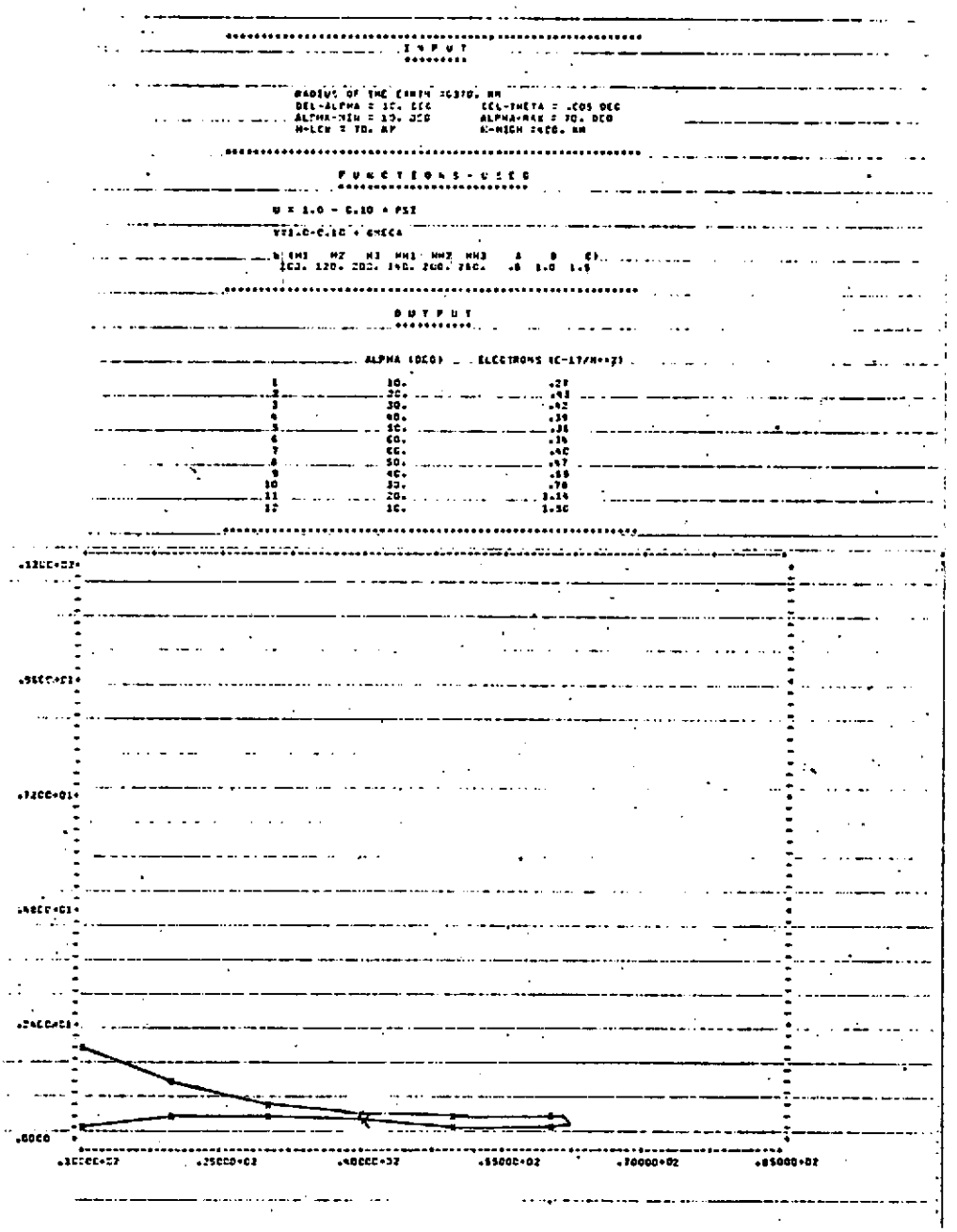

Figure 18(a). Total electron content calculated along the direction alpha (Figure 17).

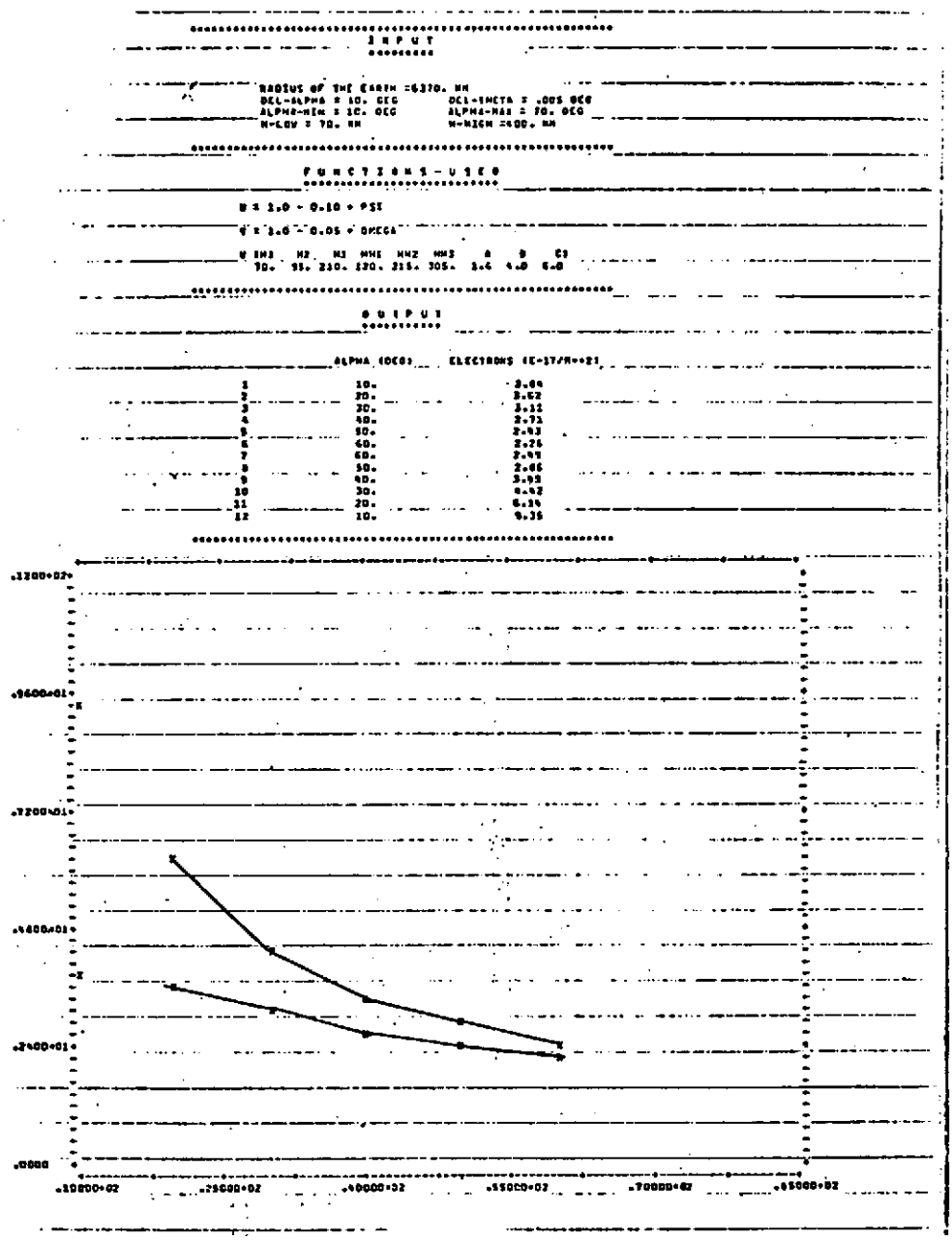

Figure 18(b). Total electron content calculated along the direction alpha (Figure 17).

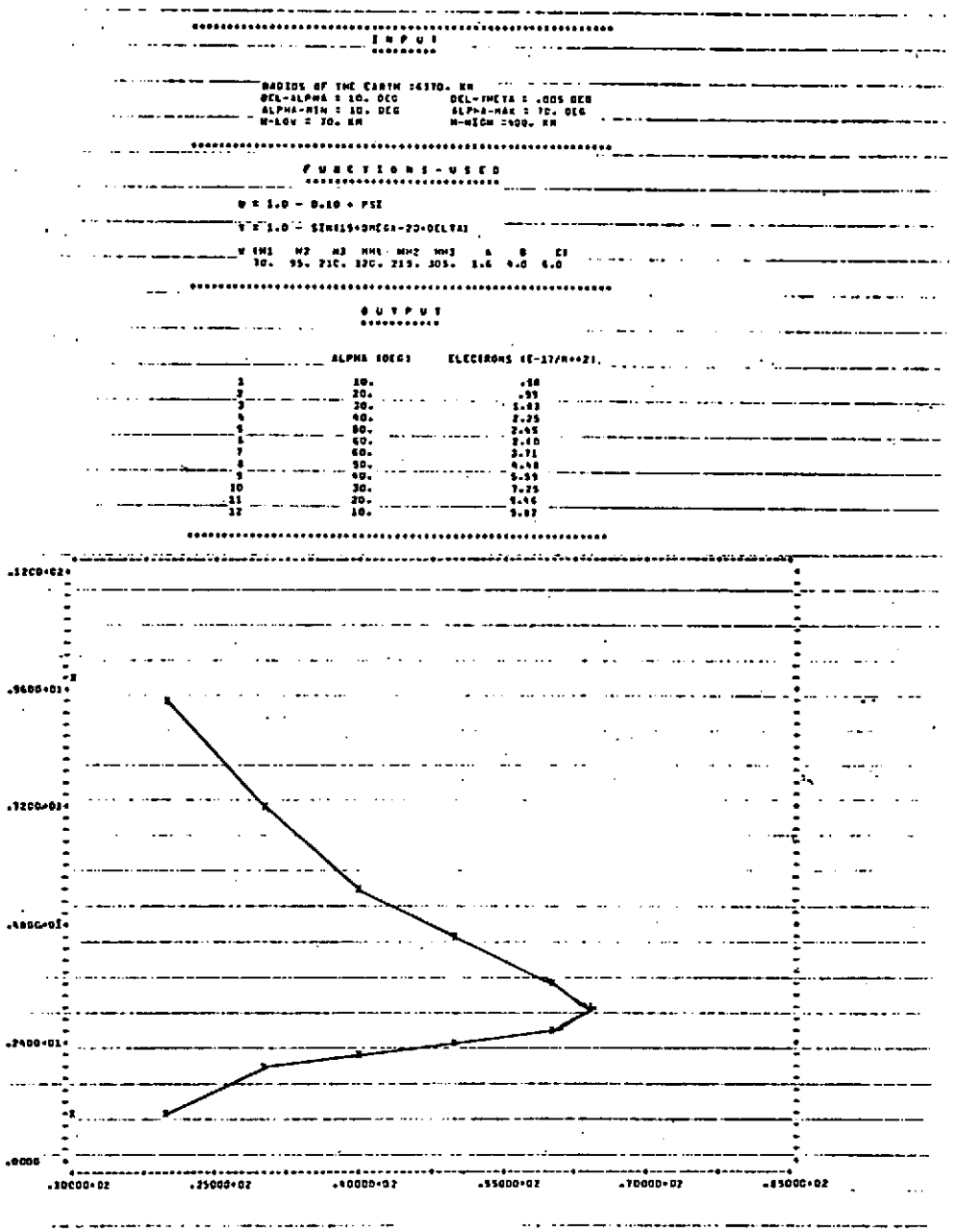

Figure 18(c). Total electron content calculated along the direction alpha (Figure 17).

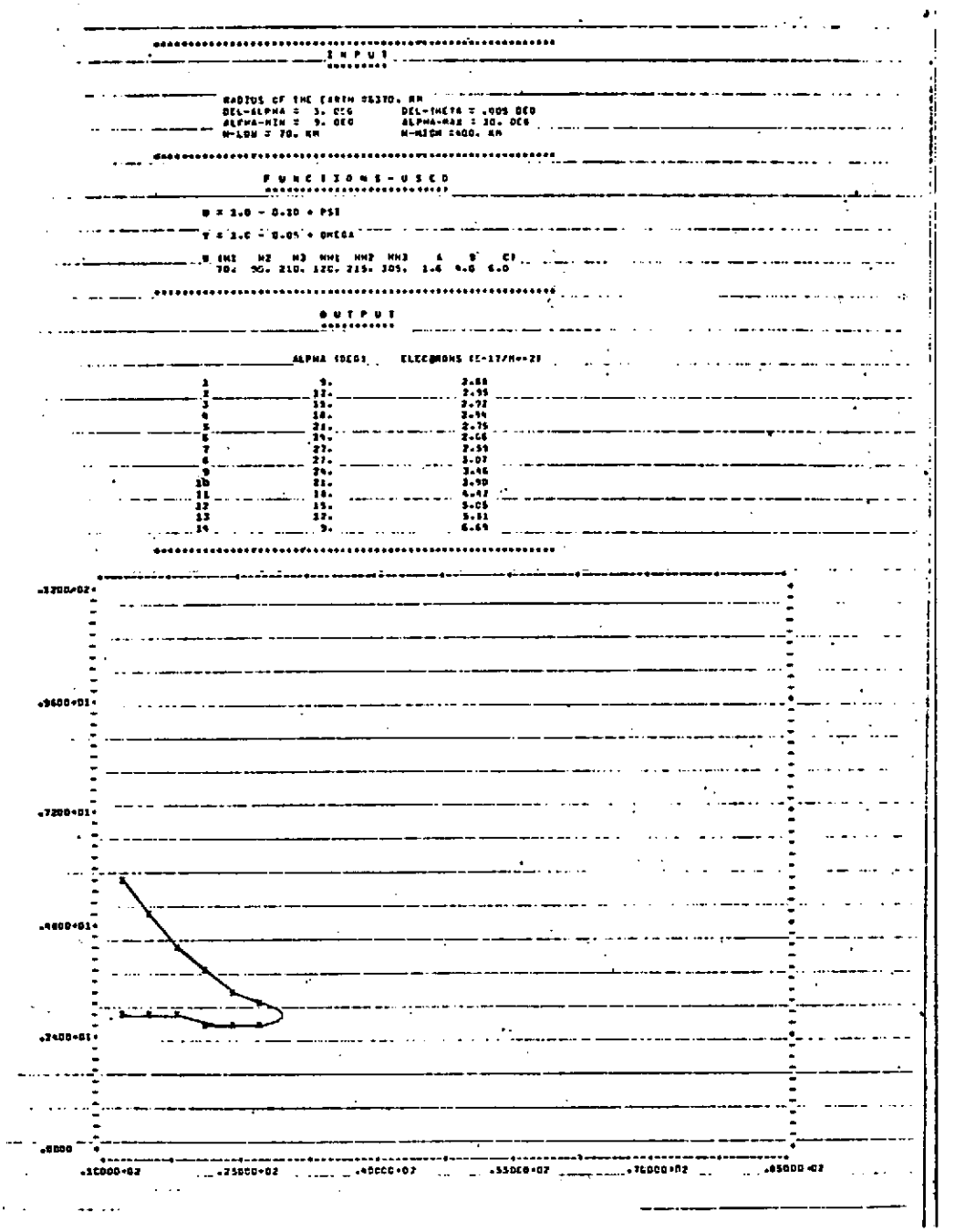

Figure 18(d). Total electron content calculated along the direction alpha (Figure 17).

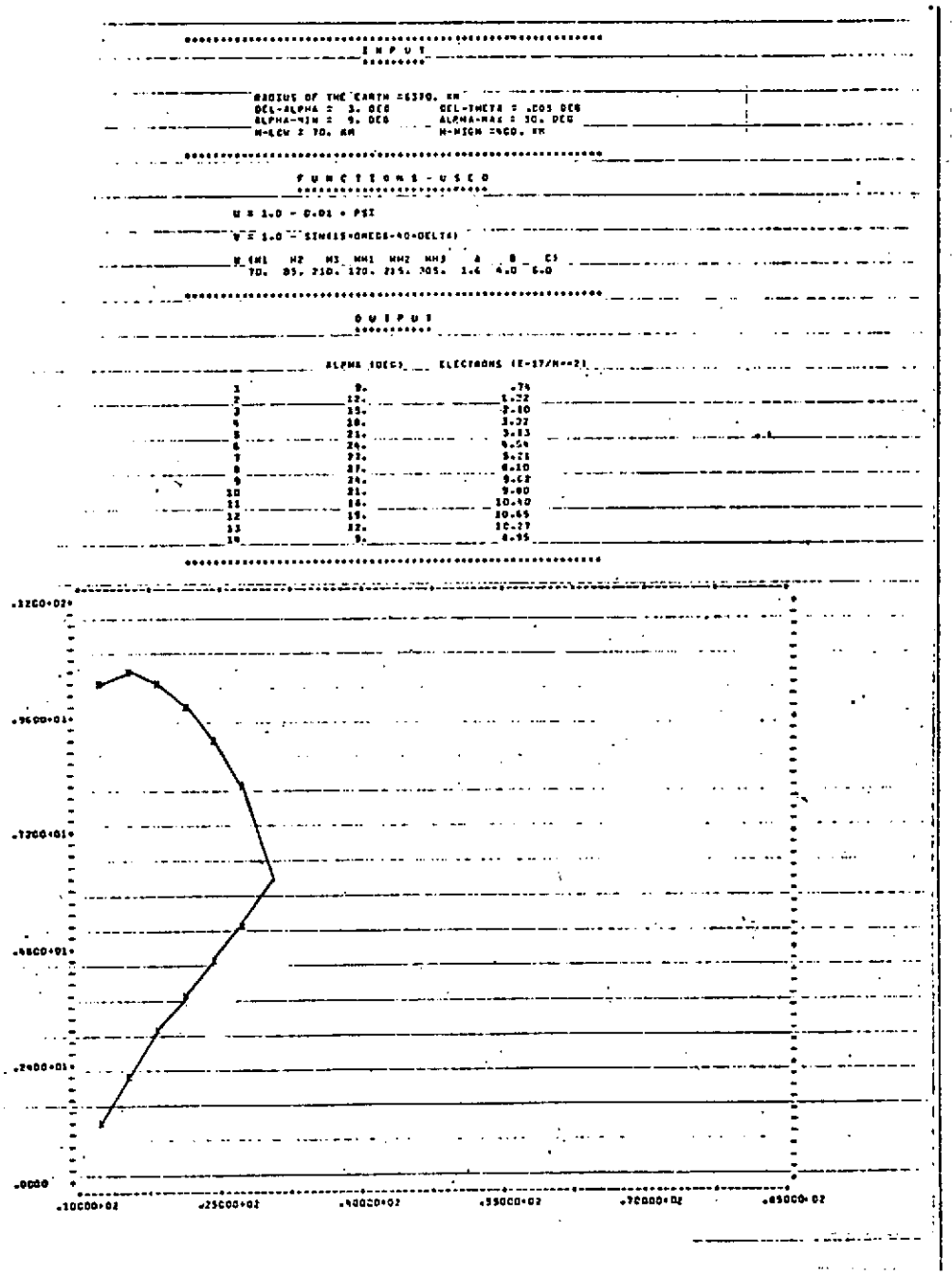

Figure 18(e). Total electron content calculated along the direction alpha (Figure 17).

REPRODUCIBILITY OF THE
ORIGINAL PAGE IS POOR

USE OF PROPAGATION CORRECTIONS FOR VLF TIMING

Eric R. Swanson
Naval Electronics Laboratory Center

ABSTRACT

The theory of VLF timing from phase measurements is briefly reviewed with attention to both frequency and epoch. Propagational aspects are noted without specific attention to predictional details. "Cycle slippage" is described. Application of propagation corrections to VLF timing is described, with particular attention to the use of available skywave corrections published for the OMEGA Navigation System.

INTRODUCTION

The past, present, and future of VLF time dissemination has recently been described simplistically as time ticks, frequency comparison, and total epoch dissemination, respectively. (1) Throughout the past decade, phase comparisions at VLF have been in general use as a method of frequency intercomparison of precision oscillators. Typically, such comparisons are made between fixed sites and at the same times of day so that phase predictions are relatively unimportant—often the "prediction" simply being the assumption that seasonal and diurnal variations are not important. Foreseen in the future is increased use of VLF for epoch dissemination as has been used over the past six years to hold the intercontinental OMEGA navigation stations in synchronization to within a few microseconds. For epoch dissemination to sites without calibration by flying clock or other ancillary means, propagation predictions will be necessary. In addition, the use of propagation corrections can improve the accuracy of frequency or epoch determination and increase flexibility through allowing signal comparison at any hour of the day.

VLF PHASE

General

A recent review of VLF timing is given in Reference 1 while a fundamental tutorial discussion of the nature of the measurement will be found in Reference 2. Briefly, we wish to compare two remote clocks. Since frequency is the derivative of phase (expressed in cycles), only the ability to disseminate epoch need be considered in order to establish capabilities for dissemination of frequency. A stabilized transmitter is assumed as the source of standard continuous wave (CW) signals of fixed frequency and known epoch. A similar frequency is derived locally at a remote site and the phase is shifted until it is in coincidence (or quadrature) with the received signal. The amount of shift is related to time by the association that one cycle of phase shift corresponds to the time represented by one period of the CW signal. The absolute shift required after allowance for propagation can be related to the epoch of the local clock. Any variation in the shift apart from

propagational changes may be associated with a frequency offset between the local oscillator and transmitter standard reference.

The repeatability and stability of VLF signal propagation has long been recognized. Figure 1 shows the average phase of Haiku, Hawaii, received in New York. Although the diurnal variation corresponds to about 100 μs (1 centicycle (cec) at 10.2 kHz $\approx$ 1 μs), the hourly standard deviation was only about 2 μs. The most common applied "predictions" for timing are probably that the phase is repeatable from day to day when examined at the same time or that phase is time independent or "flat" during the night or nearly midday (0800 and 2100 in Figure 1). In practice, the latter assumption is more nearly satisfied near 20 kHz and above rather than at 10.2 kHz, which typically exhibits a slow diurnal "curvature" during the day as shown in the figure.

Although experimental, the variation shown in Figure 1 is typical in the classical sense of being most representative of an ideal rather than being common or expected. Four main regions may be identified. Constant phase is observed from about 0600 to 0900Z when the entire propagation path is dark. This period is identified propagationally as night. Sunrise at the New York end of the path occurred near 0900Z and the phase proceeded into a ramping decrease as sunrise proceeded on path to Hawaii. About 1600, sunrise occurred in Hawaii and the phase then stabilized to a nearly constant daytime value continuing a slight decrease until noon, due to variation in the solar zenith angle. The sunset process is essentially the reverse of the sunrise process. The behavior described is expected most at the VLF navigational frequencies (10-14 kHz) over long east-west paths. Several complexities generally need to be considered. The illustration shows a situation in which propagation may be associated with only one earth-ionosphere waveguide propagation mode. Even in such a relatively simple case, some complexity is expected due to ionospheric time constants resulting in a slight lag between the nominal VLF phase variation and the zenith angle variation and an abrupt phase change presumably associated with photo detachment at sunrise. The complexities inherent even to a propagation model employing only a single propagation mode are described in detail for 10.2

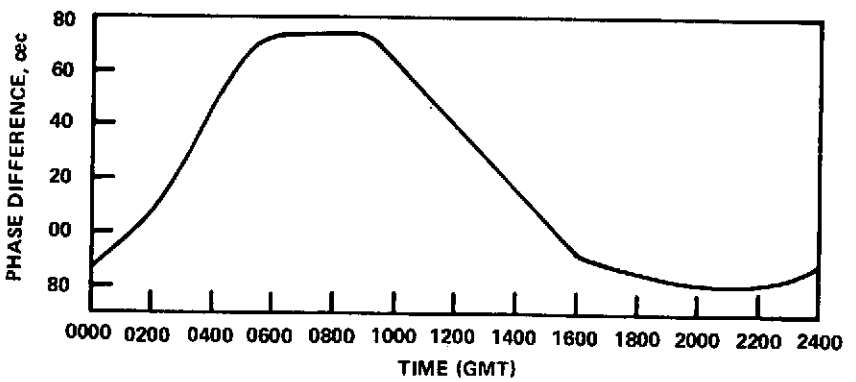

Figure 1. Average 10.2-kHz phase of Haiku, Hawaii, received at Forestport, New York, station, May 17-24, 1966. Standard deviation approximately 2 cec.

kHz by Swanson and Bradford and are more apparent on measurements over north-south paths (3). Especially above 2 kHz, multimode propagation may be important as is described in the subsequent section. It is also possible that modal conversion may occur at the sunrise or sunset terminators wherein some propagation by the first waveguide mode may be converted into the second waveguide mode or conversely. (4, 5)

Modal Variation

When two or more propagation modes are effective, the received signal will be the phasor sum of the components. Maximum and rms phase irregularity from the interference of two waveguide modes of various amplitudes have been computed by Gallenberger and are given in Reference 6. Provided one mode remains dominant, the phase irregularity will be less than quadrature; thus corresponding to a variation of 25 microseconds at 10 kHz and about eight microseconds at 30 kHz. Even with a nominal "dominance" of 5 dB, the maximum phase variations will correspond to less than ten microseconds. Typically, the first mode will be dominant by considerably more than 5 dB over long paths during the day. However, without detailed specific computation for the path considered, it is not clear what mode will be dominant at night, especially above 20 kHz. Unless the same mode is dominant throughout the 24-hour day, a phenomenon referred to as "cycle slipping" or "cycle jumps" can occur.

Cycle slippage should not be confused with failure to maintain proper phase tracking due to reduced signal. Although it is true that an amplitude minimum will usually correspond to the cycle slip, the minimum may still be quite sufficient that the receiving equipment track properly. Essentially, if modal dominance changes between day and night, then it is self-evident that the modes must be equal somewhere during sunrise and sunset transitions. The important consideration is then what the relative phase of the two modes is at equality. If the modes are in phase, then the field strength is enhanced and no unusual variation is necessarily seen in amplitude. If they are in opposition, a null will occur; the signal will disappear and a receiver will necessarily attempt to track noise. More commonly, neither of these extremes will occur.

An example will help to illustrate the possibilities. Assume a first-mode diurnal phase change of one cycle. This may be illustrated as the locus of a vector of nearly constant or slightly increasing magnitude during sunset with relatively uniform phase shift as shown in Figure 2(a). As the diurnal change in velocity and amplitude of the second mode would usually be much greater, a possible locus for the second mode contribution is represented in Figure 2(b). The observed diurnal phase change will follow the locus of the phasor sum. Both the absolute phasing and the diurnal phase change on each mode can vary slightly from one day to the next as a function of random variations in the ionosphere. As a quantitative example, on a 5000-km path with propagation conditions comparable with isotropic propagation between San Diego and Hawaii, amplitude and phasing would be as indicated in Table 1.

(a) FIRST MODE (≈ 1 CYCLE)

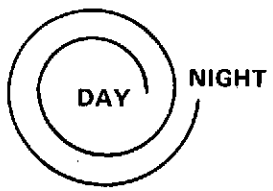

(b) SECOND MODE (≈ 2 CYCLES)

Figure 2. Vector loci for modal variation during sunset transition.

Table 1
Hypothetical Amplitude Over a 5000-km Path.

Frequency	Diurnal Period	Mode	Amplitude Phase (relative dB)
10 kHz	Day	1	-13.5
		2	-93.8
	Night	1	-8.5
		2	-58.2
20 kHz	Day	1	-8.3
		2	-29.7
	Night	1	-14.0
		2	-16.0

Propagation constants from Wait & Spies, 70 km during the day[7]; Snyder and Pappert, 84 km at night[8].

During the day, single-mode propagation is closely approximated at either frequency. At night, single-mode propagation is closely approximated at 10 kHz while the modes are nearly equal at 20 kHz. Indeed, had a slightly shorter path been considered, the second mode would have dominated at night at 20 kHz. Nominal phase values based on isotropic ionospheres of 70 and 84 km day and night, respectively, are given in Table 2.

Table 2
Nominal Phase Values Over a 5000-km Path.

Frequency	Diurnal Period	Mode	Phase (Cycles With Respect to Ground Wave)
10 kHz	Day	1	-0.6
		2	-8.3
	Night	1	-0.1
		2	5.8
20 kHz	Day	1	0.6
		2	-3.3
	Night	1	1.2
		2	-1.7

The diurnal phase change is about 0.5 cycle on the first mode but about two cycles on the second. More important, the absolute phase being received is several cycles different between the modes. Thus, if the entire propagation path should suffer an anomalous height variation corresponding to one-tenth of the diurnal height change, the relative arrival phase of 10 kHz would advance or delay about five centicycles at any time during the 24-hour day, but the second mode would suffer an anomalous variation of about 0.1 (8.3 - 5.8) = 0.25 cycles. That is, the first mode phase would be only slightly changed while the second mode phase would be shifted to quadrature. The relative phase between the modes would thus be significantly altered as would the phasor sum. Thus, as the ionosphere varies slightly from day to day, the diurnal phase variation may change quite substantially if a change in modal dominance occurs between day and night. Considering the contribution of still other modes, the phasor sum locus may circle the origin once, twice, several times or not at all depending entirely on the relative phase relations of the various modes during transitions. This can lead to several types of anomalous phase shift. The diurnal pattern could be one full cycle more or less than nominal, or it could always gain a cycle at sunrise and lose one at sunset, or any of a nearly unlimited number of alternative possibilities might apply. Further, phase shift may not repeat from day to day. Detailed 24-hour prediction and reliable use of signals experiencing a change of modal dominance would thus depend on a very careful analysis. Reliable use would be possible only under unusual circumstances.

The cycle slip phenomena is illustrated in Figures 3, 4, and 5. In each case, the assumed model is that of two modes, each of which has constant phase and amplitude both day and night, but for which the amplitudes and phases vary uniformly through an assumed ramp sunrise or sunset transition. In each case, the diurnal variation was assumed to be one cycle on the first mode and two cycles on the second mode. Figure 3 shows hypothetical amplitude and phase variation when only the first mode is present. Figure 4 shows hypothetical variations when the first mode remains dominant. Figure 5 shows variations when modal dominance changes.

Signal Selection

The foregoing illustrates some forms of diurnal phase variations which may be observed in practice and emphasizes the difficulty of quantitative explanation of the entire 24-hour

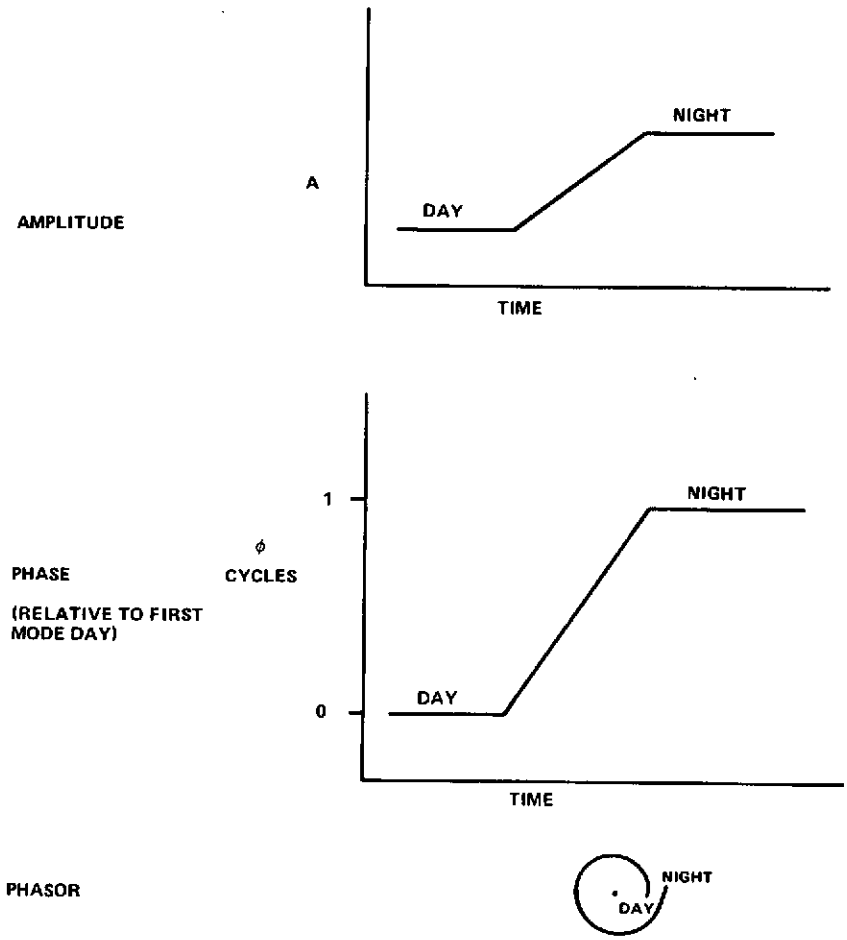

Figure 3. Sunset diurnal variation–first mode only.

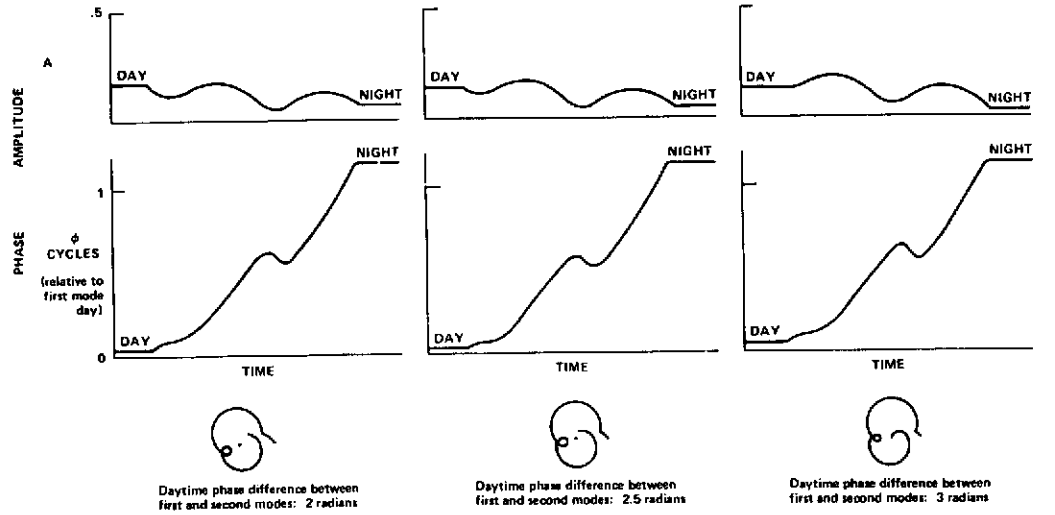

Figure 4. Sunset diurnal variation–first and second modes, first mode dominant.

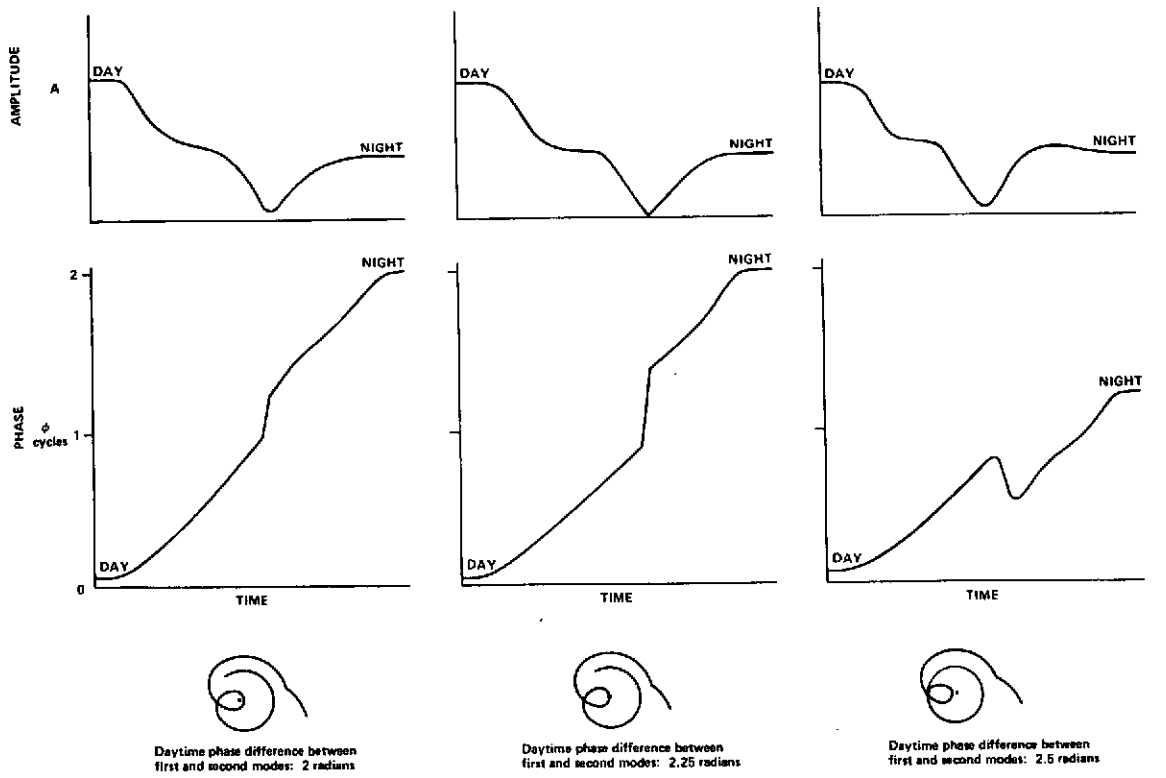

Figure 5. Sunset diurnal transition–first and second modes, change of mode dominance.

diurnal variation when modal dominance changes. Since phase repeatability may also be poor under conditions of competitive modes, the best solution in such cases is one of signal avoidance. In any conceivable location, many VLF signals will be available and it is unnecessary to attempt accurate time determinations using signals of inordinately complex structure. Signal selection is, however, a matter of considerable practical importance since, to many engineers, the best signal is the loudest—this is also likely from the closest station at the highest frequency and therefore, exhibiting the most complex structure. For the balance of this paper, the signal is assumed to be of essentially single mode character—at least during the diurnal period of observation. Signals propagated by more complex structures may also be used, but their calibration and potential seasonal variation are best obtained by ancilliary methods such as flying clock or by "boot-strap" wherein more predictable signals are used as a reference until sufficient statistical confidence is generated.

Uncertainty in the spatial prediction of phase also may be a factor in signal selection. Spatial prediction theory at the navigation frequencies is discussed in Reference 6 which shows the importance of a number of path parameters such as ground conductivity, path orientation, latitude and so forth to phase prediction. Prediction errors and signal selection at the OMEGA frequencies are discussed in detail in Appendices D and F of Reference 9. Desirable characteristics from the viewpoint of spatial resolution include daytime illumination, high ground conductivity—such as sea water or normal land—and temperate latitude propagation.

Propagation Corrections and Application

Precise propagation corrections for VLF phase are presently published only for the 10.2 kHz OMEGA frequency. Necessary computational parameters for phase prediction at 13.6 and 11.33 kHz are available and normally used within multifrequency OMEGA receivers which compute propagation corrections internally. Tabular computation at 13.6 and 11.33 kHz is occasionally produced, but not published. Propagation predictions at 10.2 kHz are widely distributed by the Defense Mapping Agency (formerly Oceanographic Office) in the series H.O. Pub 224 *et seq.* available from clearing houses in Philadelphia, Pennsylvania, and Clearfield, Utah. The series includes various volumes depending on area. In the temperate latitudes, skywave corrections are computed for every four degrees of latitude and longitude.

A sample skywave correction table is shown in Figure 6. Phase corrections are tabulated hourly for semimonthly periods. The corrections are referred to as "0.9974 X groundwave" geodetic reference, which is the circular OMEGA line of position defined by

$$G_R = \frac{0.9974\ d}{\lambda}$$

LOCATION 16°0'N 40°0'W
STATION A: NORWAY

DATE	GMT																
	00	01	02	03	04	05	06	07	08	···	18	19	20	21	22	23	24
JAN 1–15	–71	–71	–71	–71	–71	–71	–71	–71	–71		–24	–40	–61	–71	–71	–71	–71
JAN 16–31	–71	–71	–71	–71	–71	–71	–71	–71	–68		–20	–36	–57	–71	–71	–71	–71
FEB 1–14	–71	–71	–71	–71	–71	–71	–71	–71	–59		–16	–31	–52	–71	–71	–71	–71
FEB 15–28	–71	–71	–71	–71	–71	–71	–71	–67	–44		– 9	–24	–45	–71	–71	–71	–71
MAR 1–15	–71	–71	–71	–71	–71	–71	–70	–59	–32		– 5	–17	–39	–70	–71	–71	–71
···																	
DEC 16–31	–71	–71	–71	–71	–71	–71	–71	–71	–71		–26	–43	–65	–71	–71	–71	–71

Figure 6. Skywave correction table.

Referencing to the line of position removes most of the spatial variation. The most precise prediction can be obtained by interpolating from skywave corrections published for the four grid squares surrounding the receiving site. However, the published density of skywave corrections is sufficient that interpolation will only improve the predictions by five microseconds or less from assuming the nominal table for the grid square in which the receiver is located.

A detailed example of the application of skywave corrections to timing is given in Sample Procedure 1 below. A typical long-term calibration error day or night is 3.25 microseconds.

It is noteworthy that if absolute epoch is not important, the geodesic calculation can be disregarded. Hourly or semimonthly differences in the skywave corrections as tabulated are valid corrections for use in estimating nominal seasonal or diurnal propagational phase change to determine frequency.

The foregoing technique can be applied to any frequency within the navigation band by interpolating skywave corrections between computations for 10.2, 11.33, and 13.5 kHz. However, slight anomalous differences between frequencies, such as caused by modal interference when two or more modes are present, may be important when deducing propagation corrections for subsequent use in cycle determination. As an example, consider predictions at 12.0 and 12.250 kHz as might be used with the timing receiver described by Wilson, Britt, and Chi. (10) Assume interpolation of OMEGA predictions predicts both carriers to an average nominal accuracy of 3.25 microseconds, but produces a differential prediction error of two centicycles due to the presence of some second-mode contamination on the signals. Since the time associated with the differential phase prediction error on the difference frequency is referred to the difference frequency period, the error is now two centicyles referred to the four millisecond period of 250 Hz; that is, 80 microseconds. Viewed in this way, the error is gross and much too large to support

A. PREDICTED VALUES	PATH LENGTH	d	7772.487 km		
	WAVELENGTH	$\lambda_{13.6}$	22.04 km/cycle		
	REFERENCE PATH DELAY	G_R	-0.9974 d/$\lambda_{13.6\ kHz}$	-351.679 cycles	
	DIURNAL CORRECTION	SWC_R	published table	-0.950 cycles	
	E-FIELD PHASE	ϕ_{P_E}	$G_R + SWC_R$	-352.629 cycles	
	LOOP ANTENNA ADJUSTMENT	ϕ_A	¼ cycle, if applicable	+0.250 cycles	
	H-FIELD PHASE	ϕ_{P_H}	$\phi_{P_E} + \phi_A$	-352.379 cycles	-352.279 cycles

B. OBSERVED VALUES	MEASURED FRACTION	ϕ_O	$\phi_{REMOTE} - \phi_{LOCAL}$	-0.389 cycles	
	CYCLE IDENTIFICATION	ϕ_N	$\phi_{P_H} - \phi_O < 0.5$ cycle	-352.0 cycles	
	OBSERVED PHASE	ϕ_O	$\phi_O + \phi_N$	-352.389 cycles	-352.389 cycles

C. CLOCK PHASE	ERROR	E_ϕ	PREDICTED - OBSERVED, $\phi_{P_H} - \phi_O'$	+0.010 cycles
	AMBIGUITY	ϕ_T	CARRIER FREQUENCY CYCLES	±N cycles

C. CLOCK TIME	ERROR	E_T	$\frac{\text{PHASE}}{\text{FREQUENCY}} \frac{E_\phi}{f}$	+0.7 μs
	AMBIGUITY	t_T	CARRIER FREQUENCY PERIODS	±NT μs

Sample Procedure 1: phase epoch determination. Done for Hawaii signal observed at the Naval Observatory on 13.6 kHz on 112000Z November 1969 – loop antenna (refer to text on facing page).

A. PREDICTED VALUE CALCULATIONS

1. From the known propagation path length d and the wavelength λ of the specific carrier being observed, compute the reference path delay or geodesic G_R:

$$G_R = -0.9974d/\lambda_f$$

2. Look up the expected diurnal correction SWC_R in a skywave correction table. Select the value for the appropriate transmitter, frequency, year, month, day, and fraction of an hour:

$$SWC_R = \text{tabulated values}$$

3. Add the reference path delay to the diurnal correction to compute the predicted phase for the E-field vector ϕ_{P_E}:

$$\phi_{P_E} = G_R + SWC_R$$

4. If a loop antenna is used to observe the H-field vector, *reduce* the predicted E-field delay by ¼ cycle to compensate for the 90° lag of the E-field from the H-field:

$$\phi_{P_H} = \phi_{P_E} + 0.25$$

B. OBSERVED VALUE CALCULATIONS

1. Record the measured fractional cycle delay ϕ_O of the remote versus the local phase:

$$\phi_O = \phi_R - \phi_L) = \text{data}$$

2. Assume that no ambiguity exists and assign a whole cycle count ϕ_N to adjust the measured fraction to within ½ cycle of the predicted value:

$$\phi_O' = \phi_O + \phi_N$$

where ϕ_O' is defined as the observed phase.

C. CLOCK PHASE AND TIME ERROR CALCULATIONS

1. Subtract the observed from the predicted phase to compute the *phase* error of the local clock:

$$E_\phi = (\phi_{P_{(H \text{ or } E)}} - \phi_O') \pm \phi_T = \Delta\phi \pm \phi_T$$

where ϕ_T represents the ambiguity as an integral number of carrier frequency cycles.

2. Divide the clock phase error by the carrier frequency to compute the clock time or epoch error:

$$E_T = \frac{E_\phi}{f} = \Delta t \pm t_T$$

where t_T represents the ambiguity as an integral number of carrier frequency periods.

cycle resolution even though the error on either carrier was quite nominal. The problem of differential prediction error when using multiple frequencies is most severe when the frequencies are closely spaced. In such cases, the nominal prediction for one of the carriers can be obtained by interpolation of tables from 10.2, 11.33, and 13.6 kHz, but the prediction for the second should be adjusted so that the difference reflects not only the nominal dispersion, but also any structural differences in the signals as can be assessed, for example, by fullwave computation. An example of a full wave calculation for a 250 Hz difference frequency is given in Figure 7, which shows significant modal complexity to 4000 km during the day.

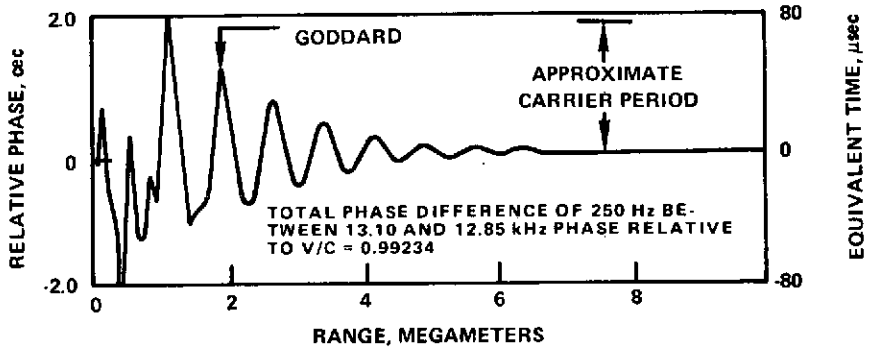

Figure 7. Relative phase of daytime OMEGA difference frequency, North Dakota to Goddard (Wait's $\beta = 0.5$ km^{-1}, H' = 70 km profile).

CONCLUSIONS

Published OMEGA skywave corrections are easily applied to determine epoch or to account for seasonal or diurnal phase variations when deducing frequency from 10.2 kHz measurements.

ACKNOWLEDGEMENT

Credit is due Miss Pamela Mallory who wrote a desk-top computer program and prepared the phasor sums shown in Figures 3, 4, and 5.

REFERENCES

1. E.R. Swanson and C.P. Kugel. "VLF Timing: Conventional and Modern Techniques Including Omega." *Proceedings IEEE.*

2. E.R. Swanson, "Time Dissemination Effects Caused by Instabilities of the Medium." North Atlantic Treaty Organization Advisory Group for Aerospace Research and Development, Electromagnetic Wave Propagation Committee, *Phase and Frequency Instabilities in Electromagnetic Wave Propagation* K. Davies, ed. Slough England Technivision Services, 1970 (AGARD Conference Proceedings No. 33). pp. 181-98.

3. E.R. Swanson and W.R. Bradford. "Diurnal Phase Variation at 10.2 kHz." Naval Electronics Laboratory Center Technical Report 1781. August 11, 1971.

4. D.D. Crombie. "Periodic Fading of VLF Signals over Long Paths During Sunrise and Sunset." *Radio Science* 68D (1) (1964).pp. 27-34.

5. Richard A. Pappert and Floyd P. Snyder. "Some Results of a Mode Conversion Program for VLF." *Radio Science*, 7 (no. 10, October 1972). pp. 913-24.

6. E.R. Swanson, "VLF Phase Prediction." *VLF Propagation: Proceedings from the VLF Symposium.* G. Bjontegaard, Norwegian Institute of Cosmic Physics Report 7201. (January 1972). pp. 8-1 to 8-36.

7. J.R. Wait and K.P. Spies. *Characteristics of the Earth-Ionosphere Waveguide for VLF Radio Waves.* NBS Technical Note 300.

8. F.P. Snyder and R.A. Pappert. "A Parametric Study of VLF Modes Below Anisotropic Ionospheres." *Radio Science*, 4 (no. 3, March 1969). pp. 213-26.

9. E. R. Swanson and C. P. Kugel. "Omega VLF Timing." Naval Electronics Laboratory Center Technical Report 1740 (also NASA S-51743A-G, revision 1, 1972).

10. J. Wilson, J. Britt, and A. Chi. "Omega Timing Receiver, Design and System Test." PTTI *Proceedings.* 1972.

INTERPRETATION OF VLF PHASE DATA

Friedrich Reder and James Hargrave
U. S. Army Electronics Technology and Devices Laboratory

James Crouchley
University of Queensland
Australia

1.0 INTRODUCTION

VLF phase tracking finds application in:

- Long-range standard frequency distribution
- Long-range clock synchronization
- Global radio navigation
- Global monitoring of the lower ionosphere and of solar activity
- Prospecting for mineral deposits

Correct interpretation of VLF phase data requires thorough training of equipment operators and data analysts since the recorded data are strongly dependent on proper equipment performance and on the interaction of all parameters describing the status of the lower ionosphere and of the ground along the path of signal propagation. Furthermore, recorded data depend on path length and signal frequency.

It is the purpose of this report to review some additional facts on the subject and to augment the information presented at the third PTTI Conference.(1) The present and previous reports are based on our experience with a global VLF-tracking network established in 1965 (Project INT-VLF). The reader is assumed to be familiar with the concepts of VLF propagation and of VLF signal tracking, and is referred to the literature for background information.(2, 3, 4)

The discussion will deal with equipment; representation of VLF waves; diurnal effects and mode interference phenomena; antipodal interference; and solar flare, galactic X-ray, and geomagnetic effects.

2.0 DISCUSSION

2.1 Equipment

Many equipment problems have been discussed previously.(1) The following figures illustrate the effects of noise and of changing control settings on the signal phase and amplitude

outputs of one popular commercial VLF receiver. Of course, these effects may differ from model to model, but it is useful to alert operators and analysts to the possible existence of such phase and amplitude variations of instrumental origin.

Figure 1 shows the experimental setup for testing a receiver. The signal generator is simply another receiver whose antenna input is disconnected and whose synthesizer output provides the signal input for the receiver being tested. The blocks marked "DB" represent fixed or variable attenuators, "noise" is a source of Gaussian noise, and the diode serves as a clipping circuit (see insert in Figure 1) to convert the Gaussian noise to some resemblance of impulsive noise of atmospheric origin.

Figure 2 depicts the influence of various S/N ratios on phase (ϕ) and amplitude (A) tracks as the receiver time-constant switch (in the phase control loop) is changed from TC = 5 to 50 and 150 seconds. (The left-hand number on top of each interval gives the signal level in dB with respect to an arbitrary dB reference; the right-hand number gives the relative noise level in dB). The amplitude recording is only slightly improved by a TC increase, but the improvement in the phase record is striking. For TC = 5 sec and S/N = -10/30, the receiver lost track. At the moments marked by vertical arrows a phase step of 10 μs was introduced in the driving signal to check whether the receiver on test was still tracking the signal. It was. This suggests a useful check—to test for correct tracking under conditions of low signal strength or high noise levels as evidenced by large fluctuations of the signal-strength meter; that is, to displace the phase of the reference signal by 10 μs using the

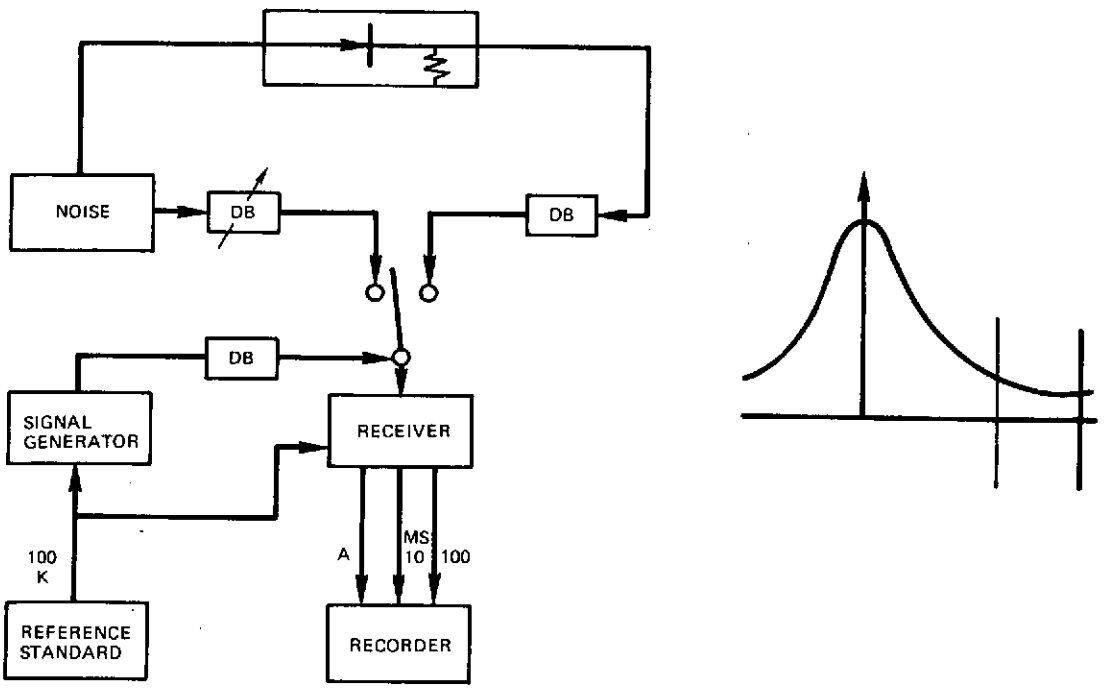

Figure 1. Block diagram of equipment set up to measure influence of S/N and equipment controls on phase and amplitude recordings.

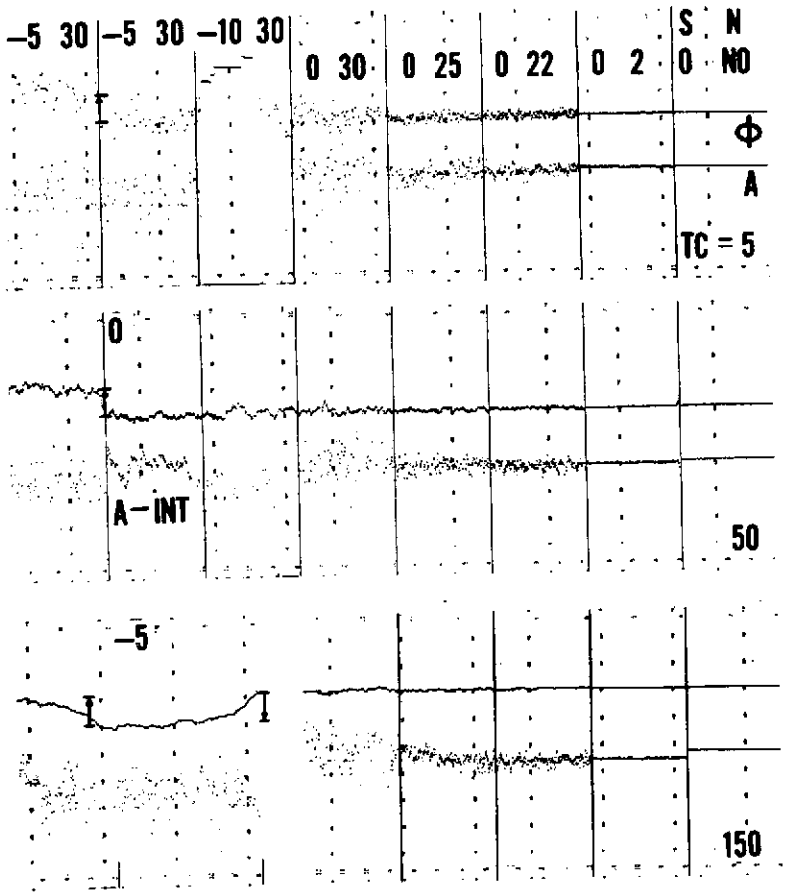

Figure 2. Influence of servo time constant, TC, and amplitude integrator on quality of phase and amplitude recordings.

slewing switch and to note if the initial phase indication is recovered. The amplitude recording for TC = 50 seconds and S/N = -5/30 was considerably improved by adding an integrator (A-INT) with a time constant of ~50 seconds at the amplitude output of the receiver. Note however that the fluctuations in this section are meaningless.

Figure 3 demonstrates the improvement of ϕ and A tracking by utilizing the blanking control of the receiver when the atmospheric noise level is high (setup of Figure 1 with noise input through the clipping diode). The blanking control is not effective with Gaussian noise.

In Figure 4 one can see that for a receiver TC = 5 seconds both the ϕ and A tracks are somewhat affected by the internal receiver noise if the signal level is reduced by 50 dB by means of an external attenuator and the receiver (internal) gain is raised by 50 dB (+50). However, internal noise would hardly be noticeable at TC = 50 seconds and larger.

The left-hand part of Figure 5 shows that the change of the TC switch causes some small

phase steps (particularly between TC = 5 and 150 seconds), but no amplitude jumps. The right-hand part reveals that changes of the electronic receiver gain are not detectable on the phase track, but that externally connected variable attenuators may be slightly reactive as evidenced by the small phase step when 10 dB attentuation was added. (If external variable attenuators are utilized for calibration, it is advisable to leave ~3 dB always in circuit in order to provide matching or else calibration readings may be in error.)

Some receiver models have synthesizer modules with an A/B switch with A for a local oscillator frequency of ($F_{SIG} + F_{IF}$), and B for ($F_{SIG} - F_{IF}$). This switch serves to increase discrimination against undesirable signals at the mirror frequency of the desired incoming signal, but the operator should be aware that changing between positions A and B may cause sizable phase and amplitude changes on the recording (Figure 6). In this connection it should be mentioned that the proper selection of the A/B switch position for interference reduction may be necessary even if the receiver has a 20 dB front-end RF filter and the

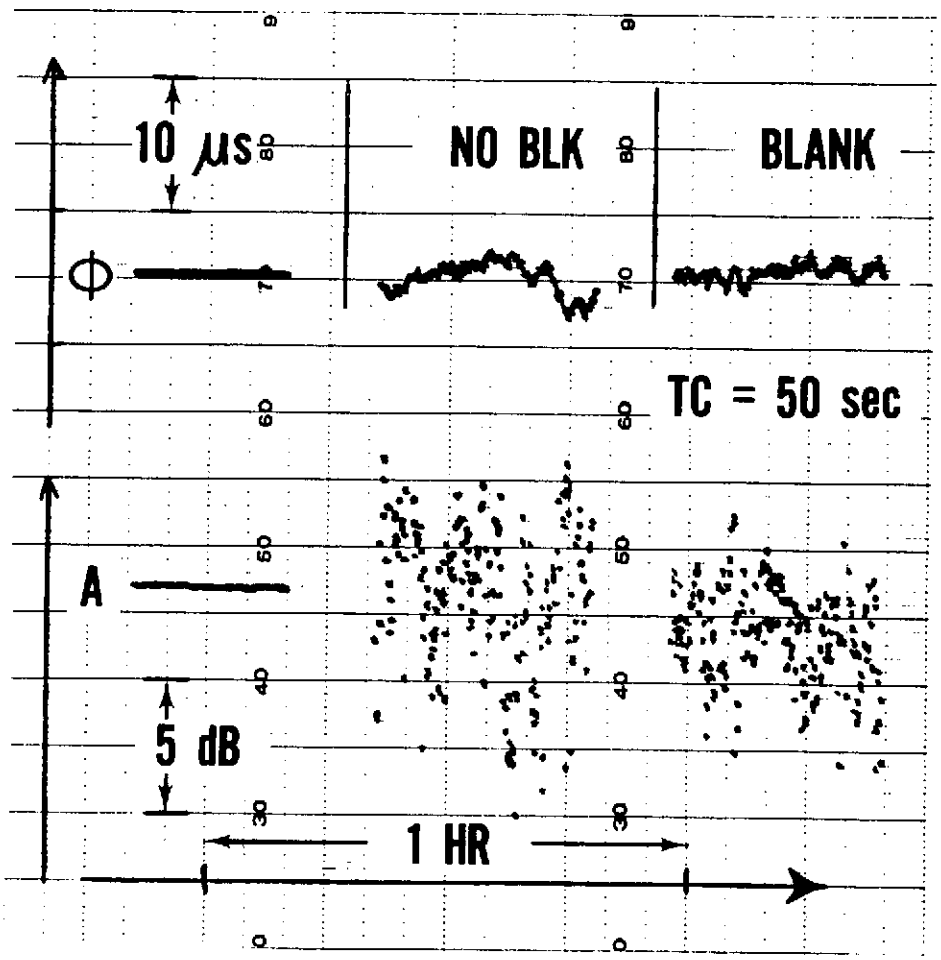

Figure 3. Effectiveness of blanking control to improve quality of phase and amplitude recordings in the presence of strong atmospheric noise.

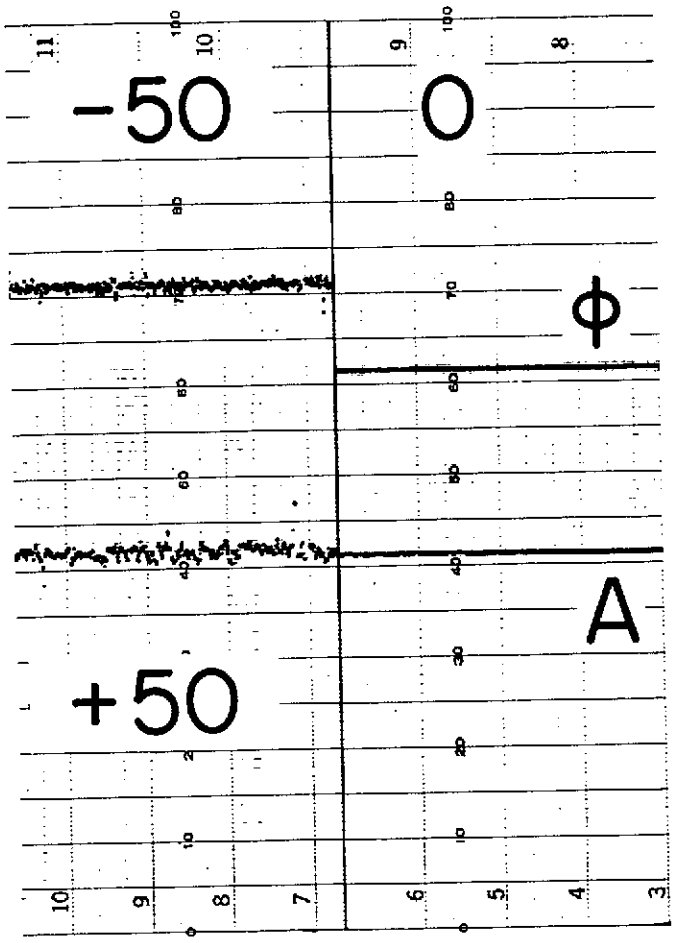

Figure 4. Effect of internal receiver noise on phase and amplitude recordings.

tuned loop antenna provides a further rejection of ~ 15 dB. For example, a Haiku-10.2 kHz receiver at Brisbane, with an IF = 1 kHz and the switch in position B (synthesizer signal at 10.2 - 1.0 = 9.2 kHz), was found to track the powerful NDT-17.4 kHz transmission with the second harmonic of the 9.2 kHz synthesizer signal (9.2 × 2 = 18.4 = 17.4 + 1 kHz). Changing to switch position A eliminated the problem. A similar problem could arise with F_{SIG} = 10.2 kHz, switch position A, and NSS (21.4 kHz) or NPM (23.4 kHz) when these transmitters are commissioned again (11.2 × 2 = 22.4 = 21.4 + 1 = 23.4 - 1 kHz).

Figure 7 depicts an experimental setup to demonstrate (Figure 8) that the coherent output from a receiver locked to a stable VLF signal and driven by a modestly-priced crystal frequency standard (e.g. internal crystal oscillator of a commercial electronic counter) can provide a 100-kHz standard reference signal of excellent accuracy to drive either a clock of microsecond precision or another VLF tracking receiver. The scope serves for a convenient adjustment of the crystal frequency to the atomically controlled frequency of a

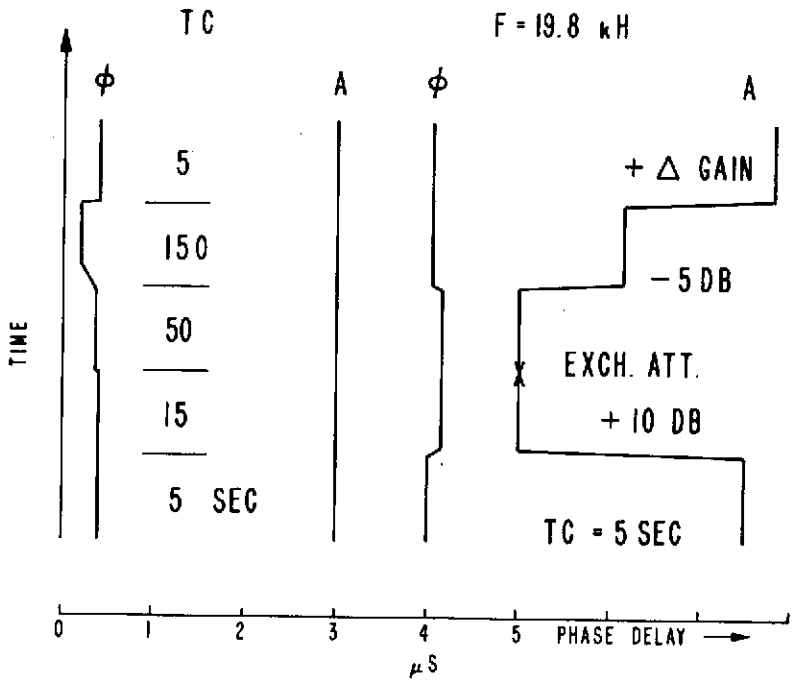

Figure 5. Phase jumps caused by changes of TC control, gain, and external attenuator settings (EXCH. ATT means external attenuator was replaced).

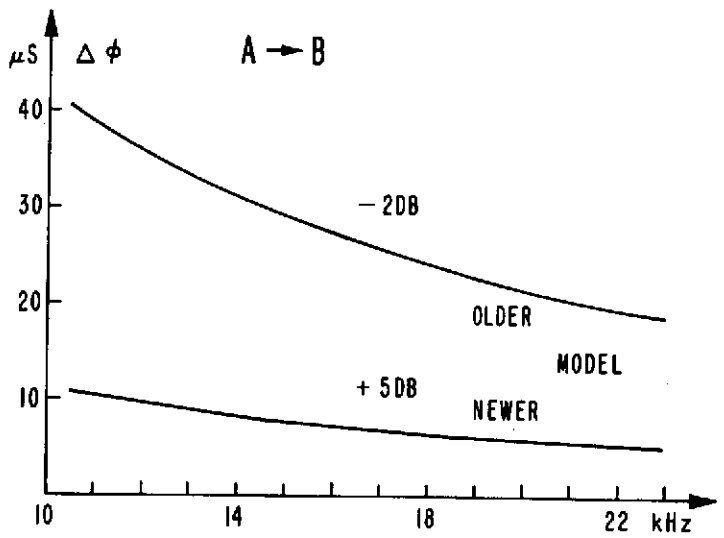

Figure 6. Phase and amplitude changes introduced by changing local reference signal from (F_S+IF) to (F_SIF). F_S is signal frequency.

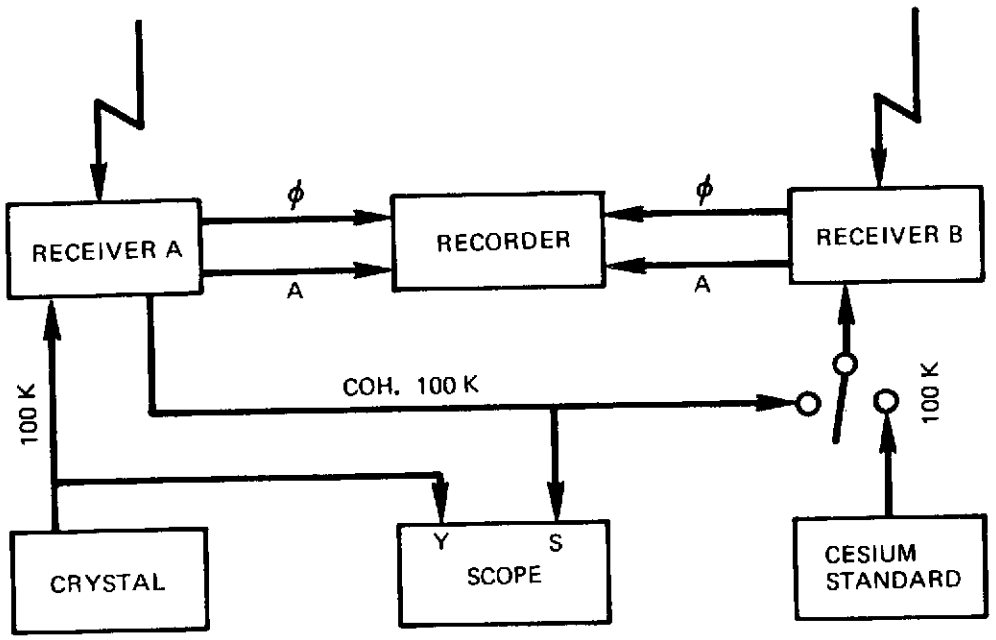

Figure 7. Block diagram for testing the usefulness of improving the accuracy of a low-cost-crystal signal by locking a VLF receiver to an atomically stabilized VLF transmission.

tracked VLF signal. The top part of Figure 8 gives the phase (lower smooth plot) and amplitude (uppermost plot) of NLK-Deal received by receiver B when driven by the 100-kHz cesium standard reference. (Time progresses to the left.) The steeply sloping lines represent the NLK-Deal phase output of the crystal-driven receiver A (crystal frequency is $\sim 5 \times 10^{-8}$ above UTC) and the middle plot is the receiver-A amplitude. It is evident that the large crystal offset does not affect the amplitude record. In the center part of Figure 8, receiver B was driven by the coherent (with NLK signal) 100-kHz output of receiver A. Since the coherent output of receiver A reproduces the diurnal shift of the NLK phase, the phase output of receiver B (100 μs full-scale at top and 10 μs full-scale at bottom) is now a horizontal line with only very small ($\sim \pm 0.2$ μs) fluctuations. Of course, the large crystal offset requires a certain phase error in the receiver in order to generate a large enough control signal to keep the receiver locked to the VLF signal. That error is larger for longer TC values of receiver A, consequently a change of the TC of receiver A changes the offset error as shown by the phase steps at the left of the figure. For TC = 150 seconds, receiver A lost track (TC values from right to left were: 50 seconds, 15 seconds [step -1.6 μs], 5 seconds [additional step of -0.6 μs], 50 seconds [back to original phase], and 150 seconds [loss of lock]). The bottom part of Figure 8 demonstrates that receiver A can provide a suitable coherent signal (provided TC_A = 5 seconds) even for a crystal offset of $\sim 24 \times 10^{-8}$ (see steep lines on right-hand side, each equivalent to a 100 μs time accumulation in $\sim$ 7 minutes). This means, that a VLF receiver driven by almost any crystal standard and locked to the VLF signal of a transmitter (preferably nearby for a small diurnal shift, e.g. NSS-Deal) can maintain synchronization of a clock to better than 5 μs. To avoid large

Table 1

Important TM Modes at Given Signal Frequencies and Distances from Transmitter for an Exponential Isotropic Ionosphere and Infinite Ground Conductivity.

F	DISTANCE (Mm)														
kHz	1	2	3	4	5	6	7	8	9	10	11	12	13	14	15
10	1	1	1	1	1	1	1	1	1	1	1	1	1	1	1
12	12	12	1	1	1	1	1	1	1	1	1	1	1	1	1
14	12	12	1	1	1	1	1	1	1	1	1	1	1	1	1
16	12	12	1	1	1	1	1	1	1	1	1	1	1	1	1
18	123	12	12	1	1	1	1	1	1	1	1	1	1	1	1
20	123	12	12	12	1	1	1	1	1	1	1	1	1	1	1
22	213	21	12	12	12	1	1	1	1	1	1	1	1	1	1
24	213	21	12	12	12	12	1	1	1	1	1	1	1	1	1
26	231	21	21	12	12	12	12	1	1	1	1	1	1	1	1

Day

10	12	12	12	1	1	1	1	1	1	1	1	1	1	1	1
12	123	12	12	12	1	1	1	1	1	1	1	1	1	1	1
14	213	123	12	12	12	12	1	1	1	1	1	1	1	1	1
16	213	123	21	12	12	12	12	12	1	1	1	1	1	1	1
18	231	213	21	21	21	12	12	12	12	12	12	1	1	1	1
20	231	231	231	21	21	21	21	21	21	12	12	12	12	12	12
22	23	23	23	21	21	21	21	21	21	21	21	21	21	21	21
24	23	23	23	2	2	2	2	2	2	2	2	2	2	2	2
26	23	23	23	2	2	2	2	2	2	2	2	2	2	2	2

Night

clock errors when the transmitter goes temporarily off the air, it is advisable to avoid large offsets and to adjust the crystal frequency (as often as once per day) against the coherent output of receiver A.

For problems encountered with antennas, cables, battery standby supplies, connectors on receiver modules, recorders, environmental conditions for atomic frequency standards, station keeping, and transmitter interference, the reader is referred to previous publications (1, 5).

2.2 Wave Propagation (1, 2, 3, 4)

For distances less than 1 Mm it is convenient to represent the observed EM field by the following components: (6)

(a) Groundwave: not influenced by ionosphere;

(b) Ordinary skywave: vertically polarized, influenced by ionosphere; and

(c) Extraordinary skywave: horizontally polarized, influenced by ionosphere, and originating from the ordinary wave upon reflection in the ionosphere in presence of the geomagnetic field.

A whip or a long-wire antenna picks up all three components; a loop directed towards the transmitter picks up the first two components; a loop oriented precisely perpendicular to the signal path picks up primarily the last component. A separation between ground and ordinary skywave is possible by means of a whip/loop arrangement.(6) Short-path skywaves at nighttime are usually strongly disturbed in phase and amplitude due to their deeper (as compared to long-path signals) penetration into the ionosphere. The presence of the extraordinary wave causes an elliptical polarization of the skywave, reduces the depth of the "loop null," and can introduce a sizable error in direction finding by means of "loop nulling."

For distances greater than ~ 1 Mm it is advantageous to describe the EM field by modes. Each mode of order, n, is characterized by 3 parameters: excitation function Ω_n in dB, attenuation rate α_n in dB/Mm, and phase velocity V_n in units of C (velocity of light).

Mode parameters for an isotropic (no geomagnetic field) exponential ionosphere (described by a reference height h, km, and a gradient km^{-1}) and a ground of infinite conductivity (good approximation for sea water) have been published. (7, 8) Computer programs for a more sophisticated anisotropic ionosphere (because of geomagnetic field) and a ground of specified conductivity are available. (9)

Table 1 [based on Reference 8, isotropic model], shows which modes should be considered at a given signal frequency and distance. For example, 213 means that the n = 2 mode predominates over the next important n = 1 mode, and a still-weaker n = 3 mode.

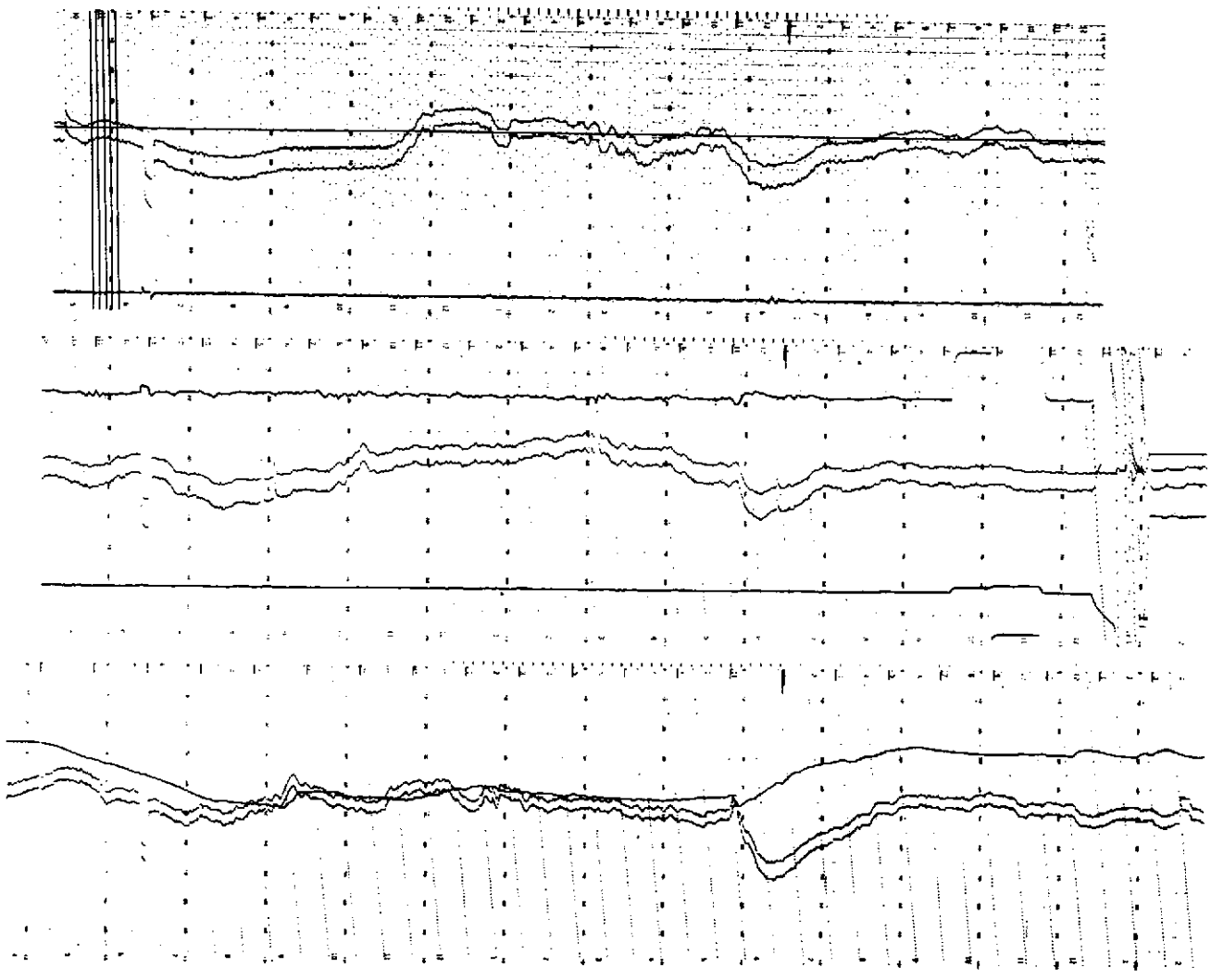

Figure 8. Demonstration of feasibility of generating precise local reference signals by phase-locking a VLF receiver, driven by a low-cost-crystal signal, to a stabilized VLF transmission.

If a VLF signal consists of two important modes with almost equal amplitudes and phase values differing by 180°, even small ionospheric changes will cause large phase fluctuations as illustrated by the phasor diagram of Figure 9. If phasor B swings further in a CCW direction with respect to phasor A, the phase deviation $\Delta\phi$ will again diminish. The plots of Figure 9 give the necessary minimum A/B ratios (in dB) for a given signal frequency in order to keep phase fluctuations due to mode interference below 1, 2, or 5 μs.

Figure 10 gives for each VLF signal frequency the minimum distance one has to be away from the transmitter in order to keep phase fluctuations, $\Delta\phi$, (as defined in Figure 9) below 1, 2, or 5 μs [based on Reference 8; h = 90 km, $\beta = 0.5$ km^{-1} for night; and h = 70 km, $\beta = 0.3$ km^{-1} for day].

The existence of the geomagnetic field gives rise to nonreciprocity of propagation losses (with reference to $\vec{NS}$, propagation losses in $\vec{EW}$ direction are larger and losses in $\vec{WE}$ direction are smaller) (3); to some variations of phase velocities as the azimuth of the path with respect to the geomagnetic field changes (10); and to the generation of TE modes and coupling between TM and TE modes. (2, 3, 9).

Low ground conductivities, as encountered in Greenland and Antarctica and somewhat less in the permafrost regions of Canada and Siberia, increase propagation losses for low ionospheric reference heights (undisturbed day, and especially during solar proton precipitations) and also affect phase velocities. (11, 12) Signal losses are also strongly increased at times when the signal path is close and nearly parallel to the solar terminator.

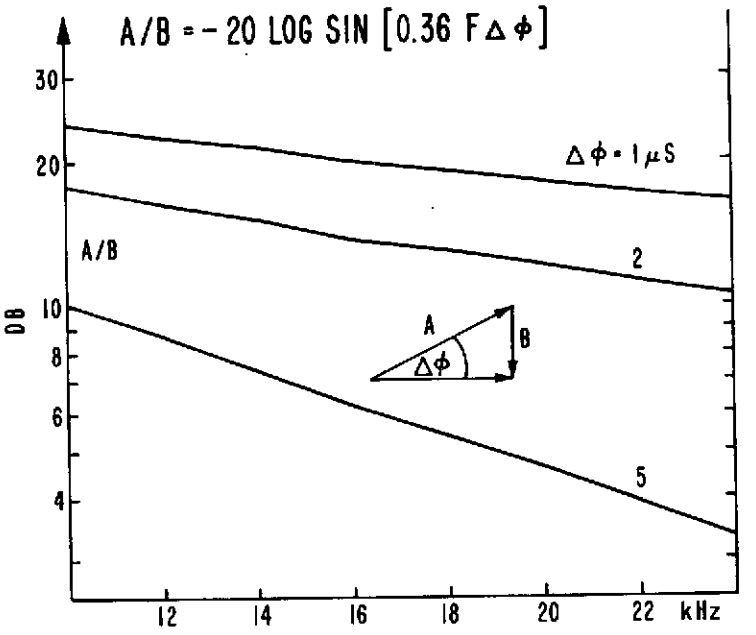

Figure 9. Maximum permissible strength B of an interfering VLF mode to keep phase anomalies due to mode interference below specified $\Delta\phi$ values at a given frequency.

2.3 Mode Interference

Values of diurnal shifts (nighttime phase is retarded with respect to daytime values) for various signal paths used in the INT-VLF Project have been quoted elsewhere.(13) Phase steps, amplitude minima and sometimes cycle slips, regularly observed during the morning hours for signal frequencies above ~ 16 kHz have been explained by Crombie (14) in terms of mode interference. Similar interference effects during the evening hours have been observed predominantly on low-latitude EW paths. (1) (15) Examples of irregular diurnal shifts observed on transequatorial paths (15) [believed to be caused by enhanced mode conversion when the terminator passes over the region where the signal crosses the geomagnetic equator (16)] may be seen in Figures 11 and 12.

The strong enhancement by mode interference of ionospheric effects on VLF phase and amplitude recordings is illustrated by the 13.6 kHz N. Dakota-Deal plots in the lower part of Figure 13 (if there were no mode interference one would expect the 10.2 kHz anomalies to be bigger than those observed at 13.6 kHz because, due to dispersion, single-mode signals are the more disturbed the lower the frequency).

The upper part of Figure 13 shows the different phase and amplitude behaviors when a signal propagating over a short distance (Forestport-Deal) is received by a loop ∥ to the path (groundwave plus ordinary sky-wave) and a loop ⊥ to the path (extraordinary wave).

2.4 Antipodal Interference

A typical example of a diurnal phase pattern obtained in the presence of antipodal signal interference (15) is shown in Figure 14. When the shorter EW path is fully sunlit, propagation losses are higher than those on the longer but nighttime WE path. Therefore, an extra hump appears during daytime along the short path.

The previously mentioned nonreciprocity of propagation losses due to the geomagnetic field extends the region of antipodal interference, in an easterly direction, from the true geographic antipode of the transmitter. Thus, signals from VLF transmitters in the U.S.A. are received at many locations in the western Pacific both along the short and long path. The geomagnetically induced nonreciprocity is so powerful that even a 14.2 kHz signal from Forestport, N.Y., was observed (15) near Guam to arrive predominantly over the long path from the west despite a path ratio of 28/12 Mm.

A peculiar antipodal interference, controlled by the large ice masses of Greenland and Antarctica, has been discussed elsewhere.(1) (15)

The effect of geomagnetic nonreciprocity on antipodal interference is enhanced if the EW path is sunlit and passes over a region of low ground conductivity. If a signal over a sunlit shorter EW path shows no signs of antipodal interference (increased phase instability, extra hump, anomalous shape of an SID) it cannot possibly show antipodal interference during nighttime along the shorter EW path. Therefore, it is unrealistic to ascribe the

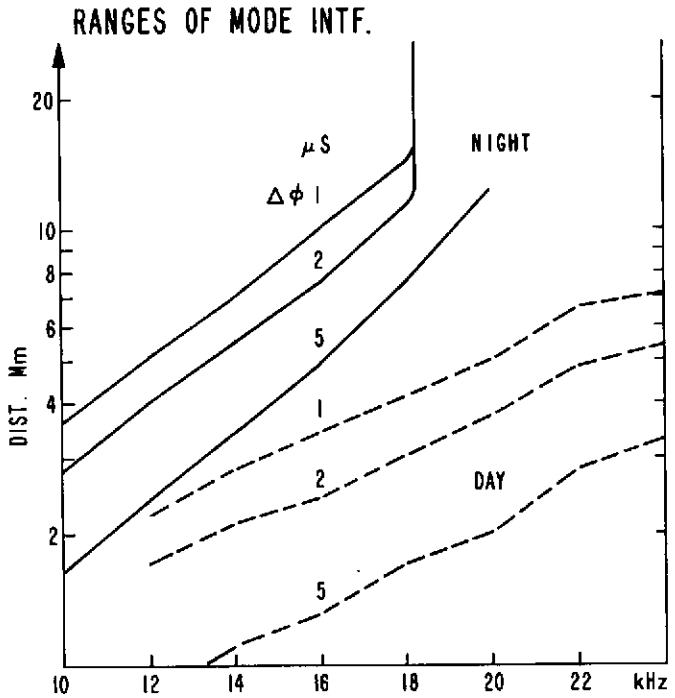

Figure 10. Minimum distances, at a given frequency, to keep mode interference effects on phase below specified limits, $\Delta\phi$. (Isotropic ionosphere.)

unusual nighttime phase behavior obtained on Haiku-Brisbane (13, 15) to antipodal interference because the short-path daytime signal reveals no evidence of such interference.

2.5 Solar Flare Effects

Solar flares cause an increased flux of X-rays and/or precipitation of electrons and/or protons in the ionosphere, giving rise to phase advances and signal amplitude changes of single-mode VLF signals.(1, 13) On short-distance signals (e.g. Forestport-13.6 kHz-Deal) composed of at least two modes and on long-distance signals affected by antipodal interference (e.g. GBR-Brisbane), phase anomalies may be reversed (delay).(1)

Solar X-ray effects (SID's) can only be observed on sunlit paths. They are detectable at all latitudes but predominantly on paths with a low-average solar zenith angle. The phase anomalies increase with illuminated path length and decreasing frequency.

In general, signal amplitude increases during an X-ray flare for signal frequencies above 16 kHz but signal decreases have been observed on GBR (16.0 kHz) and NAA (17.8 kHz) to Beirut and Tananarive during strong flares. Examples additional to those in reference (11) are shown in Figure 15. Note that GBR-Cordoba (Argentina) always experienced signal enhancements, while the strong flare on July 25, 1425 UT caused a signal decrease on NAA-TAN.

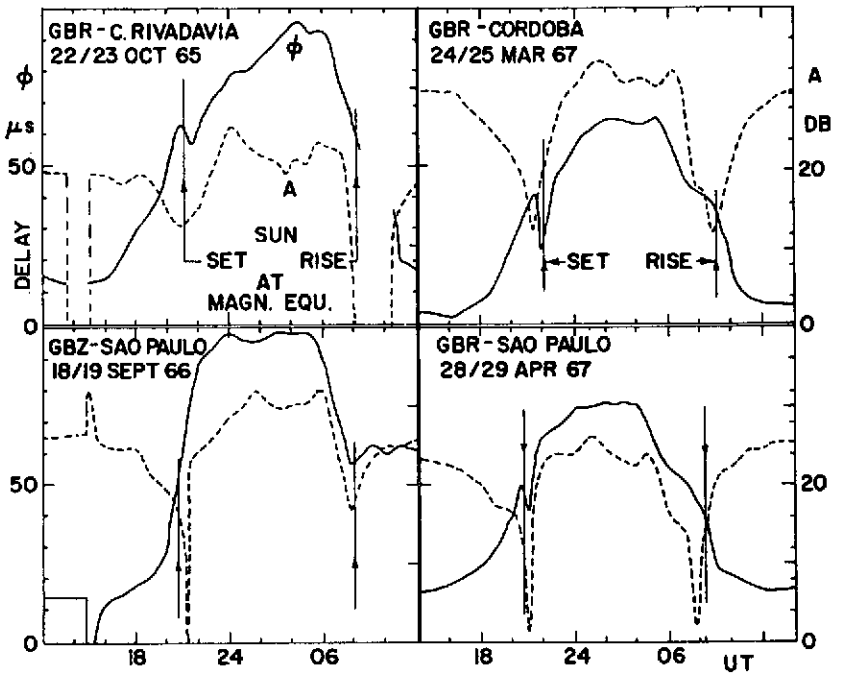

Figure 11. Examples of anomalies observed during sunrise and sunset where VLF signals cross geomagnetic equator. C. Rivadavia and Cordoba are in Argentina.

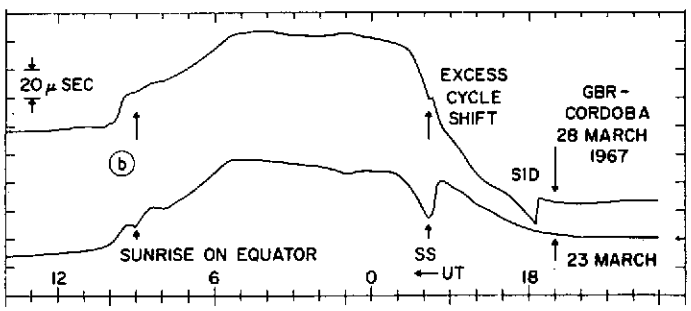

Figure 12. Another example of modal interference during sunrise and set where GBR signal crosses geomagnetic equator.

SID's usually last from 0.5 to 2 hours, in exceptional cases as long as 8 hours. Maximum deviations may be reached within a few minutes but occasionally the rise-time is as long as an hour. Maximum phase anomalies of 10 μs/Mm at 10.2 kHz have been observed a few times during 1968 and 1969.

Sometimes, the onset of a strong SID was so rapid that the receiver lost track at a TC = 50 seconds and slipped a cycle in phase. This became obvious after the ionosphere had re-

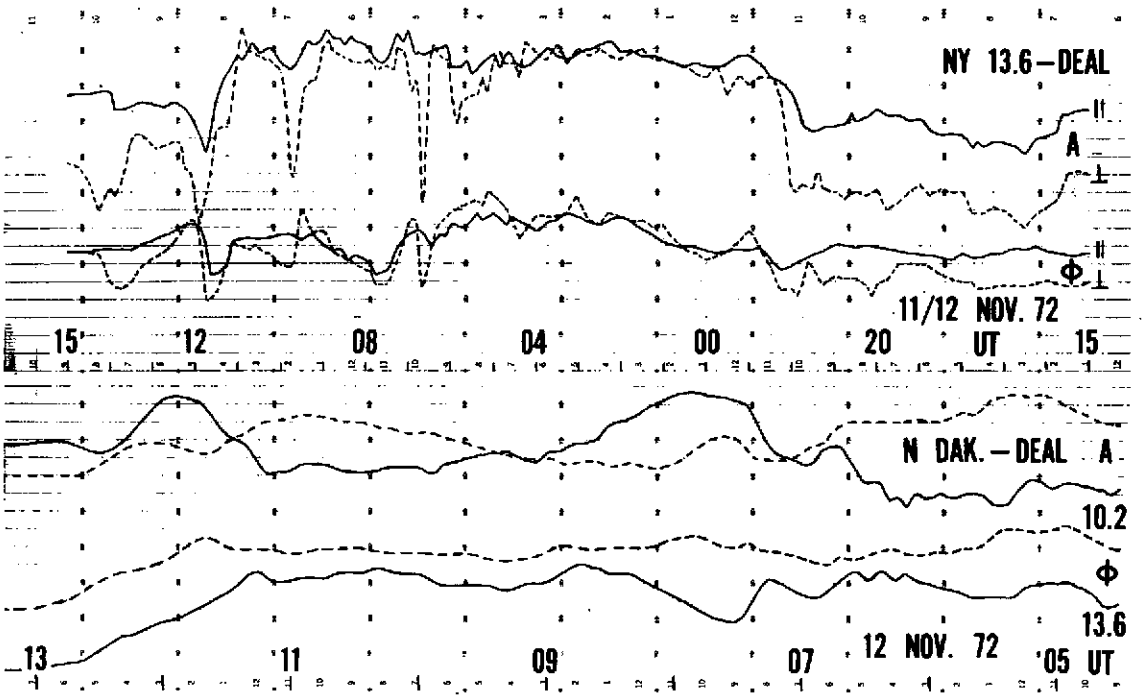

Figure 13. Difference of phase and amplitude recordings when short-distance Forestport (NY) signal is recorded with loops ∥ and ⊥ to path (top). Influence of modal interference during nighttime on N. Dakota (13.6 kHz)–Deal (NJ) transmissions (bottom).

covered and the recorded signal phase showed a delay (with respect to the phase value before SID onset) which required a correction of exactly one cycle.

VLF anomalies from electron precipitation are most frequently observed on signals passing through the auroral zone and subauroral regions.(13, 15) Electron effects are more frequently observed at night as electron energies of only about 40 keV are needed to penetrate to the nighttime reflection region (about 90 km) whereas energies of about 200 keV are needed to significantly influence the electron density in the daytime reflection region.

Electron effects typically last from one to eight hours. Figure 16 depicts some examples of electron-induced phase anomalies observed simultaneously on several signals tracked at Deal. Note the strong anomaly on the mid-latitude signal Haiku-Deal. The amplitude effects are difficult to predict. Both increases and decreases have been recorded.

Figure 17 shows a typical X-ray phase anomaly observed during daytime on NWC (22.3 kHz)-Tokyo, with a first onset at ~ 0520 UT and the dominant one at ~ 0620 UT. At ~ 0530, the signal Haiku-Deal advanced in phase. Since this path was totally in nighttime, the Haiku-Deal anomaly cannot have been due to X-rays. Furthermore, proton precipitation of such short duration is not very likely; thus electrons must be considered to be the most probable source of this disturbance.

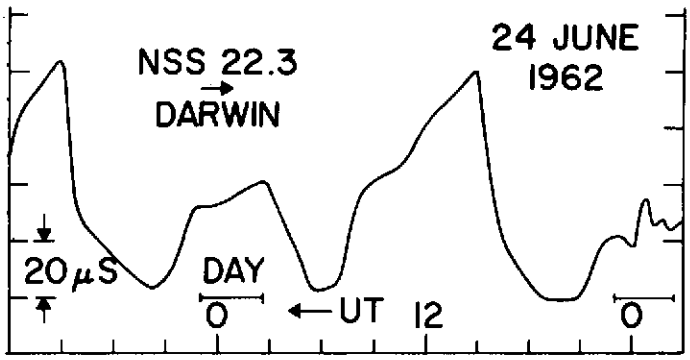

Figure 14. Example of typical antipodal interference on NSS (22.3 kHz)-Darwin (Australia).

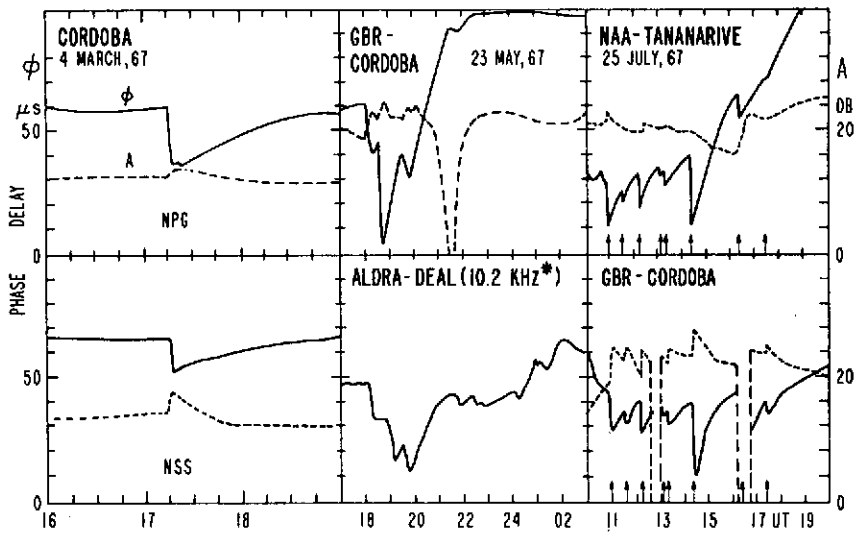

Figure 15. Examples of solar X-ray effects on long-distance VLF signals.

An interesting case of phase oscillations closely correlated with micropulsations observed by magnetometers is illustrated in Figure 18. Since oscillations of the magnetic field per se cannot affect VLF phase to that degree, the magnetic oscillations must have been accompanied by variations of the ionospheric electron density profiles. When looking at such phase oscillations, one might be tempted to suspect signal interference from another transmitter. However, signal interference requires the presence of simultaneous amplitude oscillations which are absent here. (15)

Solar proton precipitation affects the polar caps, (latitudes $>\sim 62°$ geomagnetic) only, and may last from two to ten days.(1, 11) On November 28, 1968, ALDRA(10.2 kHz)-Deal showed a phase advance of $\sim 100\,\mu s$. It usually takes a few hours to reach the maximum

of the anomaly, but in this event it took only ~ 45 min. The rise time is longer if the initiating flare occurs in the eastern solar hemisphere. During simultaneous geomagnetic storms, proton effects may be noticeable down to geomagnetic latitudes of ~ 50°.

Due to the slower onset of proton anomalies one often cannot be sure whether an observed steady phase advance is caused by proton precipitation or a malfunction of the transmitter. It is easy to determine the cause if one can observe two signals of different frequencies emitted by the same transmitter (e.g. Aldra 10.2 and 13.6 kHz). If the phase traces remain exactly parallel to each other during the phase advance, it is a malfunction of the transmitter control oscillator. On the other hand, if it is a proton event, dispersion causes a more rapid phase advance at the lower frequency.

During the first few hours of an anomaly observed on a high-latitude signal one often cannot be sure whether one observes a proton or electron event. If no recovery sets in after five hours, if the phase tracks are relatively smooth, and if other signals which propagate below ~ 62° geomagnetic latitude but near the fringes of the auroral zone show no unusual anomalies, one may be fairly sure of protons. If the auroral zone signals are also disturbed and the phase behavior of the polar cap signals is not smooth, it is likely that one observes the effects of electron precipitation.

2.6 Stellar X-ray Effects

Stellar X-ray effects on VLF signals have been discussed in detail elsewhere. (17) Only the

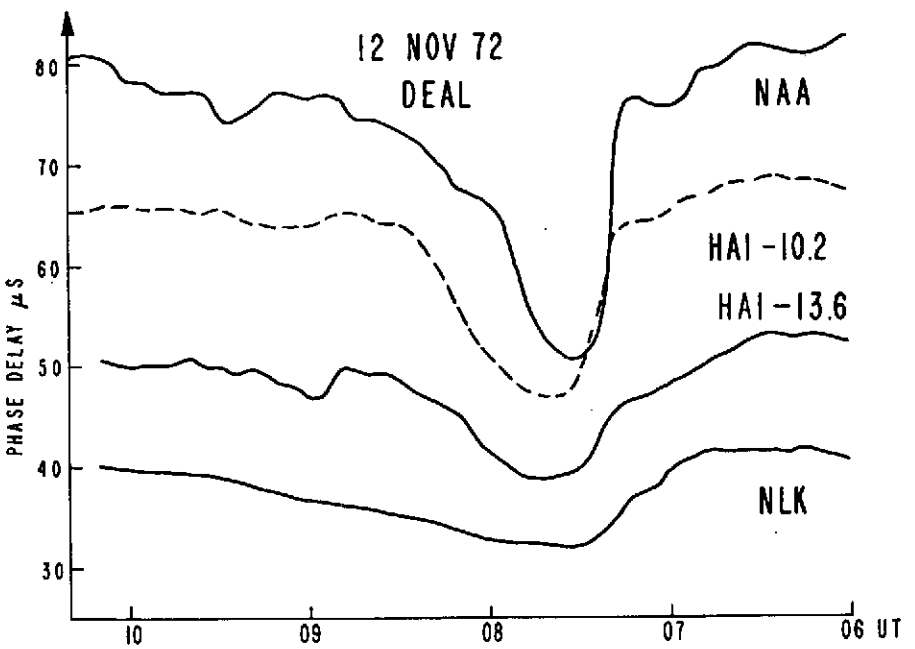

Figure 16. Examples of electron precipitation effects on VLF signals passing through subauroral regions.

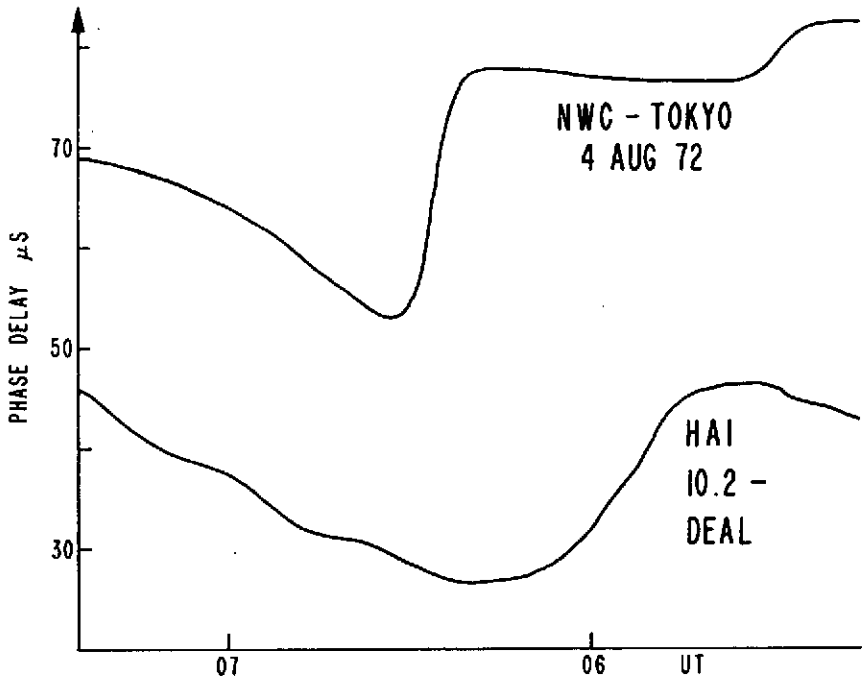

Figure 17. Example of electron precipitation effects observed on nighttime Haiku-Deal signal when daytime NWC-Tokyo showed an X-ray anomaly. It is not clear whether the correlation is accidental.

strongest stellar X-ray sources can cause a detectable phase advance during nighttime and then only provided the stellar zenith angle is very small, the night is long, and the signal frequency preferably above 20 kHz. Stellar effects must reveal a sidereal shift (occur earlier with advancing date). No detectable stellar X-ray effects were found with OMEGA navigation signals because their frequencies are well below 20 kHz.

2.7 Solar Eclipse Effects

As a solar eclipse reduces illumination along some VLF signal paths, one might expect a phase and amplitude behavior similar to that at normal nighttimes: phase delay and signal enhancement. This is illustrated by Figure 18.

3.0 CONCLUSIONS

VLF phase and amplitude tracking can be a powerful tool for frequency and time transfer, radio navigation and ionospheric monitoring provided one uses the most reliable equipment available on the market; entrusts the equipment to thoroughly trained operators; and has the data analyzed by people who are familiar with all the pitfalls of this technology and the complexity of ionospheric phenomena and multimode radio propagation.

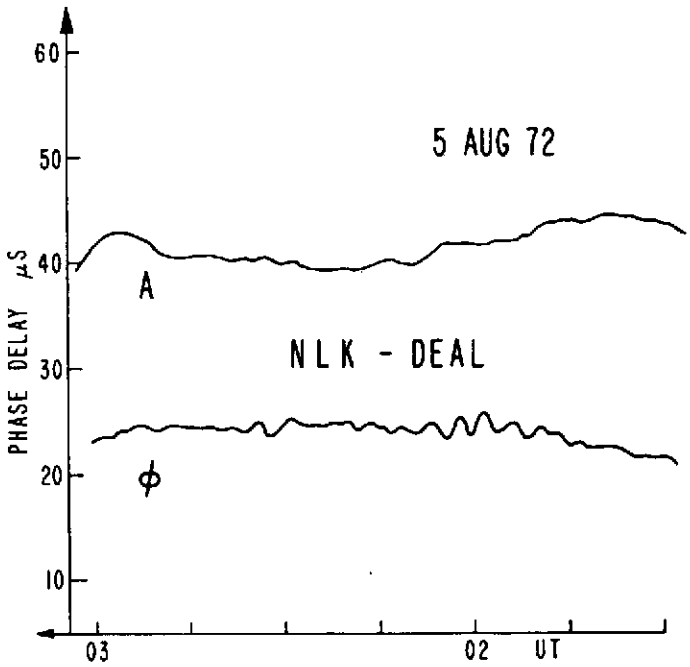

Figure 18. Example of a phase oscillation observed on NLK-Deal during period when magnetometers recorded strong micropulsations.

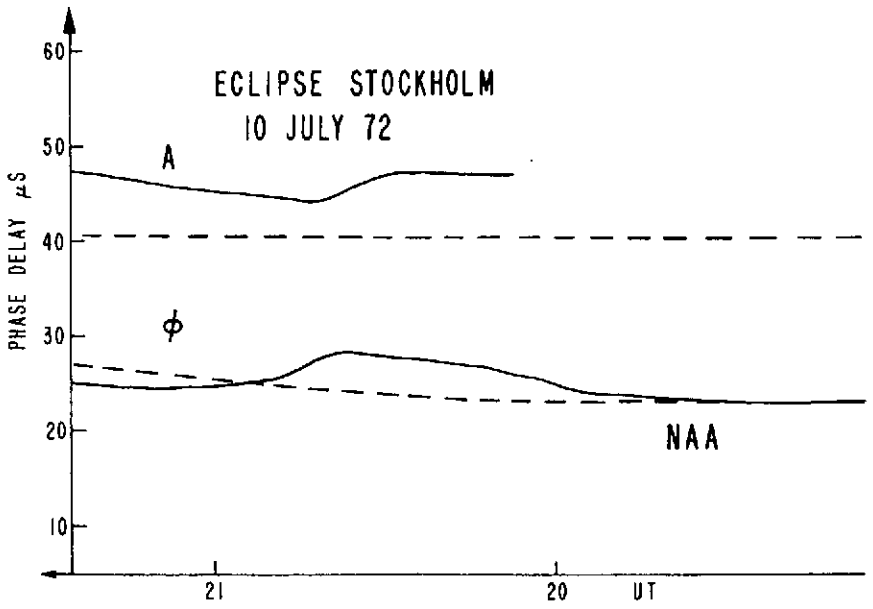

Figure 19. Phase delay and signal enhancement observed on NAA-Stockholm during solar eclipse of July 10, 1972.

ACKNOWLEDGEMENT

Some of the phase and amplitude data discussed here were provided by Col. L. Gallo of Escuella Superior de Aerotechnica, Cordoba, Argentina; Prof. P. Kaufmann, MacKenzie University, Sao Paulo, Brazil; Mr. B. Oehman, Research Institute of National Defense, Stockholm, Sweden; and Prof. R. L. Douglass, Phys. Dept., American University, Beirut, Lebanon. Figures 11 and 15 were taken from Reference 15, and Figures 12 and 14 from Reference 13.

REFERENCES

(1) F. Reder, VLF phase tracking for "precise time and time-interval" (PTTI) applications, Proc. Third PTTI Symposium, pp. 117-149, 16-18 Nov. 1971 (available from U. S. Naval Obs., Wash., D. C.).

(2) K. G. Budden, Radio Waves in the Ionosphere, Cambridge University Press, 1961.

(3) J. R. Wait, Electromagnetic Waves in Stratified Media, Pergamon Press, Oxford, 1962.

(4) A. D. Watt, VLF Radio Engineering, V. 14, International Series on Electromagnetic Waves, Pergamon Press, New York, 1967.

(5) F. Reder, Properties of VLF signals, Proc. Natl. Electronic Conf., Vol. XXVII, pp. 253-257, Oct. 9-11, 1972.

(6) R. N. Bracewell, The ionospheric propagation of radio waves of frequency 16 KC/s over distances of about 200 km, Proc. Inst. Elec. Engrs. IV, Vol. 99, pp. 217-228, 1952.

(7) J. R. Wait, K. P. Spies, Characteristics of the earth ionosphere waveguide for VLF radio waves, NBS Tech. Note 300, 1964, with 2 appendices.

(8) C. B. Brookes, J. H. McGabe, F. J. Rhoads, Theoretical VLF multimode propagation predictions, NRL Rept. 6663, 1 Dec. 1967.

(9) C. H. Sheddy, R. Pappert, Y. Gough, and W. Moler, A Fortran program for mode constants in an earth-ionosphere waveguide, Interim Rept. #683, NELC, 1968.

(10) R. J. Gallenberger, E. R. Swanson, Variations in OMEGA parameters, NELC Tech. Rept. #1773, 25 June 1971.

(11) S. Westerlund, F. Reder, C. Åbom, Effects of polar cap absorption events on VLF transmissions, Planet. Space Sci., Vol. 17, pp. 1329-1374, July 1969.

(12) S. Westerlund, F. Reder, VLF radio signals propagating over the Greenland ice-sheet, to be published in J. Atmosph. Terr. Phys., 1973 (accepted Dec 1972).

(13) F. Reder, VLF propagation phenomena observed during low and high solar activity, Prog. Radio Sci., 1966-1968, Vol. 2, pp. 113-140, URSI-Brussels, 1971.

(14) D. D. Crombie, Further observations of sunrise and sunset fading of VLF signals, Radio Sci., Vol. 1, pp. 47-51, Jan. 1966.

(15) F. Reder, S. Westerlund, VLF signal instabilities produced by propagation medium: Experimental results, AGARD Conf. Proceedings #33, pp. 103-136, Technivision Services, Slough, U.K., July 1, 1970.

(16) K. J. W. Lynn, Anomalous sunrise effects observed on a long transequatorial VLF propagation path, Radio Sci., Vol. 2, pp. 521-530, 1967.

(17) J. Svennesson, F. Reder, J. Crouchley, Effects of X-ray stars on VLF signal phase, J. Atmosph. Terr. Phys., Vol. 34, pp. 49-72, 1972.

OMEGA TIMING RECEIVER, DESIGN AND SYSTEM TEST

John J. Wilson, James E. Britt
Naval Electronics Laboratory Center

Andrew Chi
Goddard Space Flight Center

ABSTRACT

Each OMEGA Navigation Station is scheduled to transmit two unique frequencies separated by 250 Hz. These signals can be used to transfer precise time to receivers all over the world.

This paper discusses the design of a two frequency OMEGA Timing Receiver being developed by the Naval Electronics Laboratory Center (NELC). The receiver tracks the arrival time of the signals by precise phase matching at the receiving antenna. Provision is made for inserting a propagation delay correction for each signal path. Time is measured as the difference between the zero crossing coincidence of the corrected signals and the local time. This number is displayed on the front panel in microseconds. The receiver can also function as a precise phase tracking receiver for collection of propagation data essential to augmenting the propagation corrections. All phase and time information is made available in a BCD format for flexibility in interfacing with other equipment.

Results of preliminary tests run at NELC (San Diego, California) using experimental transmissions from the North Dakota OMEGA Station are given. Preliminary results indicate time may be transferred by this technique to an accuracy of a few microseconds.

I. INTRODUCTION

This paper discusses a two-frequency timing receiver being designed and built by the Naval Electronics Laboratory Center (NELC). Preliminary tests conducted at NELC, receiving OMEGA North Dakota, indicate that time transfer accurate to a few microseconds is obtainable. Section II presents a background discussion of the OMEGA transmission format, timing epoch, and defines the term *pseudo-epoch*. Effects of propagation are also addressed. Section III discusses the actual receiver design, and section IV is a discussion of results of preliminary tests conducted at NELC. Section V explains proposed system tests.

II. BACKGROUND

Transmission Format

Two unique frequencies with a 250-Hz separation will be transmitted from each OMEGA station as part of the 10-second OMEGA transmission sequence. The frequency assignments listed in Table 1 have been proposed.

Table 1
Proposed Frequency Assignments.

Station Designation	Station Location	Frequencies	
		F_1	F_2
A	Norway	12.10	12.35 kHz
B	Trinidad	12.00	12.25
C	Hawaii	11.80	11.55
D	North Dakota	13.10	12.85
E	La Reunion	12.30	12.05
F	Argentina	12.90	13.15
G	Australia	13.00	17.75
H	Japan	12.80	13.05

The approximately one-second-duration pulses of 10.2 kHz, 13.6 kHz, and 11-1/3 kHz which are radiated sequentially by each station will be followed by five pulses of F_1 and F_2. See the generalized transmission format shown in Figure 1. Several uses are being considered for the F_1 and F_2 transmission. Among them is time transmission, which is the subject of the paper.

General Discussion of Timing Epoch

Merriam-Webster defines *epoch* as: "An event or a selected time marked by an event that begins a new period . . . ." The OMEGA station epoch is defined by the positive going zero crossing of a selected cycle of 10.2 kHz. F_1 and F_2 positive going-zero crossings are held to ±100 nanoseconds of this epoch, and ±20 nanoseconds with respect to each other. Since F_1 and F_2 are both multiples of 50 Hz, a "timing epoch" can be defined which will occur at a 50-Hz rate (every 20 milliseconds) and will be marked by the coincident positive going zero crossings of F_1 and F_2. Two of the stations, B and G (Table 2), have frequencies that are multiples of 250 Hz and will have coincident positive going-zero crossings every 4 milliseconds, therefore, an epoch every 4 milliseconds.

Table 2
Pseudo-Epochs for each F_1/F_2 Pair.

Station	Frequency (kHz)	T (μsec)	Epoch (No. of cycles)	Pseudo-Epochs (No. of cycles)
C	11.55	86.58	231	46 92 139 185
	11.80	84.75	236	47 94 142 189
		diff=1.834		
B	12.00	83.33	48	
	12.25	81.63	49	
		diff=1.700		
E	12.05	82.99	241	48 96 145 193
	12.30	81.30	246	49 98 148 197
		diff=1.687		
A	12.10	82.64	242	48 97 145 194
	12.35	80.97	247	49 99 148 198
		diff=1.673		
G	12.75	78.43	51	
	13.00	76.92	52	
		diff=1.508		
H	12.80	78.125	256	51 102 154 205
	13.05	76.63	261	52 104 157 209
		diff=1.497		
D	12.85	77.82	257	51 103 154 206
	13.10	76.34	262	52 105 157 210
		diff=1.485		
F	12.90	77.52	258	52 103 155 206
	13.15	76.05	263	53 105 158 210
		diff=1.474		

The other frequency pairs will also have zero phase differences every 4 milliseconds, but zero crossing coincidence will not occur every 4 milliseconds. Adjacent to these zero phase points, a pair of zero crossings will come very close to coinciding. Only a few tenths of a microsecond separate the positive going zero crossings at these near-coincidence points. In practice they will show up as zero crossing coincidences because of system noise and the finite resolution possible. These are not genuine timing epochs; we have called them *pseudo-epochs*. We do not want to take time from a pseudo-epoch, because it will be in time error by some multiple of fifths of a cycle. Figure 2 illustrates the pseudo-epochs for station A, 12.1 kHz and 12.35 kHz. The first pseudo-epoch is displaced from the 4 millisecond timing by 2/5 cycle of the timing frequencies (-33.1 microseconds); the second by 1/5 cycle (+16.5 microseconds), and so on. The pseudo-epoch problem rules out using a four millisecond repetition rate for measuring time.

Propagation and Resolution

"OMEGA time" is indicated by a timing epoch at the transmitting station. Specifically, every 20 milliseconds F_1 and F_2 will have coincident positive going-zero crossings. To retrieve this time epoch at some receiver site, time delays introduced by propagation must be taken into account.[1,2] Dispersion complicates the process of compensating for propagation delays. Swanson and Kugel[3] develop in detail the predication accuracies to be expected, and give many examples of applicable data.

Both the cited references point out the importance of knowing the elapsed propagation time from the transmitter to the receiver. Swanson and Kugel further define the limits to which we can expect to be able to know this. This knowledge is fundamental to retrieving time at a receiver site. No matter what scheme is used, this elapsed time must be accounted for.

The OMEGA Timing Receiver looks at the positive going zero-crossings of the received signals. Timing epoch will be indicated by coincidence of these zero crossings when propagation has been properly taken into account. The propagation correction is set into the receiver via a pair of front panel thumbwheel switches. Short duration pulses with leading edges that coincide with the positive going-zero crossings are formed. These pulse trains are, in turn, examined by logic circuitry for coincidences. The duration of these pulses is important. Too short duration pulse imposes too precise requirements on knowledge of propagation, (remember, we're limited in the accuracy of our knowledge of propagation at any given time). On the other hand, too long duration pulse can result in multiple

[1] E. R. Swanson, "Use of Propagation Corrections for VLF Timing," *Proceedings of the Fourth PTTI Conference*.

[2] A. R. Chi, L. A. Fletcher, and C. J. Casselman, "OMEGA Time Transmissions and Receiving Requirements," *Proceedings of the National Electronics Conference*, 1972, pp. 268-73.

[3] E. R. Swanson and C. P. Kugel, "OMEGA VLF Timing," NELC Technical Report 1740, pp. 29ff.

coincidences. Referring to Figure 2, it can be seen (with a little thought) that the optimum pulse width is one half the difference between periods of the two frequencies. That is, it is best to make the pulse wide enough so there is always a coincidence, but narrow enough so multiple coincidences are not possible as the two pulse trains move in time with respect to one another. As implemented, the pulse widths are approximately 700 nanoseconds, which approaches the ideal for the highest frequency pair, and falls about 200 nanoseconds short for the lowest pair. This is manageable.[4]

In any time measuring system which uses two frequencies to identify epoch, the time readout will change in increments of a whole cycle of either frequency. This happens as the respective phases of the frequencies are differentially perturbed by noise or propagation. In this receiver it will be seen as steps of 76 to 86 microseconds depending upon the particular frequencies.

RECEIVER DESIGN

The OMEGA Timing Receiver performs, in brief, as follows:

- It tracks the phase of the received timing signals
- It automatically removes receiver phase effects
- It removes propagation phase effects (manual insertion of phase corrections)
- The resulting signals, which are phase equivalent to the transmitted signals, become the internal OMEGA time reference
- The time difference between OMEGA time and local time is measured and displayed
- The phase of the received signals (without manual phase corrections), with respect to local time, are provided as an output for data collection purposes.

The receiver is shown in simplified block form in Figure 3. It consists of three main groups of circuitry: the F_1 receiver, the F_2 receiver, and circuits common to both frequencies.

Each of the receiver groups contains two phase holding loops. The first holds an internally generated reference signal, F_R, in phase with the received signal as seen at the phase detector. This phase holding loop has a time constant long enough to smooth out additive noise in the received signal. The second phase holding loop holds another locally generated signal, F_S, in phase with F_R as seen at the phase detector. F_S is injected into the antenna coupler and has all the antenna and receiver circuitry in common with the

[4]OMEGA Timing Receiver Report and Instruction Manual, publication pending.

received signal. By injecting F_S like this, and holding it in phase with F_R at the phase detector, the phase of F_S at the F_S generator is compensated for any phase shifts introduced by the antenna and receiver circuitry. F_S has the true phase of the received signal; receiver phase effects have been removed.

Since F_S is a strong signal (good S/N), the F_S phase holding loop has a time constant of about one tenth that of the phase holding loop that holds F_R in phase with the received signal. F_{1S} and F_{2S} are used to measure phase with respect to local time and to generate F_{1SC} and F_{2SC} which are used to determine the time.

F_{SC} is F_S passed through a manual phase shifter to provide a means of correcting for propagation effects. The smoothed and corrected signals, F_{1SC} and F_{2SC}, are used to determine the time difference between the received OMEGA time and local time.

Front panel thumbwheel switches control the phase shifter circuits. The phase correction is entered in centicycles;* only the fractional cycle portion of the propagation delay for each frequency must be set in. The time information is conveyed by the uniqueness of the phase relationship between the two timing frequencies. This relationship will not be affected by whole cycle changes in phase of either frequency.

All the phase sensitive operations in the receiver are carried out to 0.1 cec resolution. Since all digital circuitry is used, the resolution is obtained by deriving F_R, F_S, F_{SC} (and F_L) from 1000 F_1 and 1000 F_2. In this way, step size is 0.1 cec. The 1000 F signals are generated by the frequency synthesizer. The synthesizer is a phase locked loop which may be programmed to generate any of the timing frequencies, and holds them phase stable to the one MHz input. The synthesizers and the narrow band filters required for the front end portion of the receiver are contained in one modular plug in assembly, so by changing modules all frequency sensitive circuits are changed at once. Two of the modules are mounted in the receiver, selectable by a front panel switch. Either of two (preselected) stations can thus be received by switch selecting between them.

The commutator generates the gating pulses (commutation sequence) and all other control signals for the receiver. One of these control pulses is a 4-millisecond pulse, which is used in determining the time difference. This pulse is made to begin two milliseconds before the local one-second time pulse, and to continue for two milliseconds afterwards. The receiver searches for time during this four millisecond "window."

The leading edge of the four-millisecond pulse is used to start a counter and the F_{1SC}–F_{2SC} coincidence, the timing epoch, is used to stop it. By presetting the counter to -2000 microseconds the algebraic difference between OMEGA time and local time is read out directly (to the nearest microsecond). If the received OMEGA time is sooner than local time, the time difference readout will be minus; if received time is later than local time, the time difference readout will be plus. These readings appear on a

*Centicycle (cec) = 1 percent cycle = 3.6°.

front panel readout, and are provided in BCD form on a back panel plug. They are also made available in a low resolution analog output described in detail under Preliminary Test Results.

PRELIMINARY TEST RESULTS

The timing receiver was tested October 11-13 and October 31-November 3, 1972, at NELC, San Diego, on off-the-air signals from the North Dakota station. Since the North Dakota station is not yet radiating the timing frequencies on a regular basis, special arrangements were made for these two periods of testing. Arrangements were also made for North Dakota to radiate F_1 and F_2 the week of November 13-17 so the receiver could be demonstrated at the fourth PTTI conference at NASA/GSFC.

During the tests, time was known at NELC relative to OMEGA North Dakota to ±5 microseconds. This was established by a "flying clock" in April, with subsequent monitoring of other OMEGA transmission, and represents a "best estimate."

The need to take into account propagation delays and changes in propagation delays has already been mentioned. Using their VLF propagation model, Swanson and Kugel provided predictions of the propagation delays for October 11 to 13, to be valid at noon local time ±2 hours. The result of setting in this initial propagation correction was an indicated timing error of about 76 microseconds, or one cycle of the timing frequencies (refer to discussion of resolution). Phase measurements made on the received 13.10 and 12.85 kHz signals were examined, and based on this actual propagation information the initial propagation corrections were adjusted. This change in the propagation correction was 0.7 cec (1/2 microsecond) for each frequency. These "refined" values for propagation give time difference readings as indicated in Table 3.

The five-microsecond reading for October 13 is the time measured the last day of the first test. This number was visually observed and noticed to be very constant. The same propagation corrections were maintained for the second test and a digital printer was installed to record the time measurements. The measurement updated every ten seconds and was printed. The October 31 readings ranged from -3 to +2 microseconds. It was subsequently discovered that the receiver antenna coupler box had not been properly sealed and was admitting moisture; this in turn grossly affected the local signal injection network (up to 7 cecs of phase shift). The effect was essentially the same at both frequencies; thus it shows up as a modest translation in time, rather than a large time step to another pair of zero crossings. The last three entries of the table show the time readings with the equipment functioning properly, demonstrating excellent repeatability. As was previously stated, the best estimates of receiver site time relative to transmitter site time was ±5 microseconds. This accuracy was adequate to prove that the proper pair of signal zero crossings could be identified. To make a statement as to accuracies down to the last microsecond, would require "flying clock" trips between the transmitting and receiving sites during the tests.

Table 3
Time Difference Readings Between Local Time and Received Omega Time
During Four-Hour Midday Period.

Propagation Corrections set into Receiver 13.1 kHz 79.5 cec 12.85 kHz 92.4 cec			
Test	Date	Time	Remarks
1	Oct 13	+5 μsec	Visual Observations Only
2	Oct 31	-3 to +2	Coupler Network Disturbed by Moisture
	Nov 1	+4 to +5	
	Nov 2	+1 to +3	
	Nov 3	+1 to +3	

Figures 4 and 5 present segments of the data taken during the tests conducted October 31 to November 3. The phases of 13.10 kHz and 12.85 kHz as received (F_{1S} and F_{2S}) versus local time are presented. Each phase record is made of two parts. The straight line segments represent tens of centicycles, while centicycles and tenths of centicycles are given by the dispersed meandering line. The tens of cec portion of the recording has 100 cec full scale; the units and tenths portions 10 cec full scale. The two lines are summed to get the reading. By using this split presentation, the Rustrak recordings offer resolution to 0.1 cecs. The data labeled "time difference" are a low resolution analog presentation of part of the front-panel time-difference readings. The purpose of these data is to identify the reading occurring most often among several (i.e., the statistical mode). Bearing in mind that in the presence of noise the time difference readings will vary in steps of one cycle, approximately 76 microseconds, this record assists the operator in identifying the proper time difference number. This record is the analog presentation of the least significant three figures of the time difference reading, along with the sign. Full scale is ± 1000 microseconds; positive numbers are indicated from zero at the left edge, and negative numbers are indicated from zero at the right edge.

Figure 4 shows F_1 and F_2 phase through a night to day transition. The phase of F_1 and F_2 varies through 25 cec during the transition, yet cycle identification was not lost. At the right of the figure are printouts of the time difference in microseconds at 10 second

intervals from 1557Z to 1603Z. These illustrate the constancy of the time measurements which occurred during daylight hours.

Figure 5 shows data taken mostly at night. The period of 1055Z to 1130Z when F_1 was off the air, serves to illustrate how the time difference reading runs off in steps of 76 microseconds. The time difference printouts at the right also illustrate the step runoff.

Table 4 shows the good phase stability of the difference frequency as received during stable daytime hours. These numbers were generated by subtracting the measured arrival phase of the 13.1 kHz from that of the 12.85 kHz. This can be thought of as the arrival phase of the 250 Hz difference frequency, although this frequency never exists, nor is it generated. To the extent this difference phase will stay stable and predictable within the ± 0.95 cec limit, the proper coincidence of zero crossings can be relied upon to occur, and precise time down to a few microseconds can be obtained. As can be seen, all of the data points fall well within these limits. The starred data points occurred during the previously mentioned moisture problem with the antenna coupler. As can be seen, the phase shift effect was the same for both frequencies and therefore didn't affect the difference frequency. (A word about the distribution of the stars through the data: Two antenna systems were being used alternately during the test, a troublefree one as well as the troublesome one. By the end of the test the exact manner of the trouble had been determined and corrected.)

In summary, the receiver concept and design have been proven with off-the-air tests. These preliminary tests show good correlation between the two timing signals and good correlation to the prediction model. The OMEGA timing signals appear to afford a workable system for dissemination of microsecond timing.

SYSTEM TEST

The system test is designed to demonstrate the system capability for transmitting precise time, but also to determine the limitations and the extent to which the applications can be made in the use of the transmissions.

As demonstrated, the input requirements are: the propagation delay calculations based on the coordinates of the location where time is received; a one pulse per second output from a local clock whose time is accurately known to a reference clock; and a one megahertz output signal.

With the knowledge of the difference of the local clock time relative to a standard time, we can measure the propagation delay. The measured propagation delay can, therefore, be compared with the predicted propagation delay and is used to check the theory.

Using past experience, three days to a week is needed to conduct the test. This is the minimum amount of time required for the needed data. This length of time in a location depends, of course, on the objective of the test.

Table 4
Half-Hourly Difference-Phase Measurements
Made During Daylight Hours
ϕDiff = ϕ12.85 – ϕ13.1

Time	Oct 11	Oct 12	Oct 13	Oct 31	Nov 01	Nov 02	Nov 03
1500Z		12.9	12.8		12.8*	12.7*	12.9
1530	12.9	12.8	12.7		13.1*	12.7*	13.1
1600	—	12.8	—		12.8*	12.4*	13.1
1630	12.8	12.8	—		—	12.6*	12.9
1700	13.0	12.7	12.7		—	12.8*	13.0
1730	12.8	12.9	12.7		12.8*	12.6*	12.8
1800	12.9	13.0	12.8		12.8*	12.8*	12.9
1830	12.9	12.9	12.7		12.8*	12.8*	13.1
1900	12.9	12.8	12.7	12.9*	13.0	12.8*	—
1930	12.8	12.9	12.8	13.0*	13.1	12.8	13.1
2000	13.1	12.7	12.8	13.0*	13.1*	13.0	13.0
2030	12.9	12.7		12.5*	13.2	13.0	
2100	12.9	12.6		12.7*	—	12.6	
2130	12.9	12.9		12.6*	13.0	12.7	
2200	12.7	12.8		12.5*	12.9	12.5	
2230	12.8	12.7		12.8*	12.8	12.4	
2300	12.9	12.7		12.8*	12.9	12.9	
2330	12.9	12.7		12.6*	—	12.6	
0000	13.0	12.7		12.7*	12.4	12.9	

N = 45
ϕ_{Diff} = 12.82 cec
Std Dev = 0.11 cec
Pk Dev = +0.3, –0.1

N = 55
ϕ_{Diff} = 12.82 cec
Std Dev = 0.20 cec
Pk Dev = +0.4, –0.4

Allowable Deviation for a Workable System ±0.95 cec

The objectives of the tests are the following:

1. To determine the precision of the time reception as a function of time, such as time of day or time of year, from a single transmitter
2. To identify satisfactory signal reception for determining range from the near distance to the far distance between the transmitter and the receiver for which the precision of the received time is the same
3. To test the global coverage of the system

In order to test the global coverage, one should intercompare the results of signal reception and precision obtained from all the eight stations to determine if all or only selected OMEGA transmitting stations are needed and at the same time to determine the extent they are intercontrolled.

Figure 6 illustrates the geographical locations of the eight OMEGA stations relative to our tracking network. This figure shows that most of our tracking stations are within about 5000 miles. This distance is believed to be within the good signal reception range for VLF transmissions.

Obviously, the first thing that we shall try to do is to coordinate the time transmissions from the OMEGA stations. Next we shall try to select the locations which are the most suitable for the test, in particular, the sites from our tracking stations. There have been a number of people from the Department of Defense, the National Bureau of Standards, and so on, who have participated in this program with us and with whom we certainly shall coordinate the test program.

Comment on Units for VLF Phase Recording

We would like to make one comment in regard to the units for phase recording; that is the units of microsecond and cycle. I recall some years ago when VLF receivers were designed; there was a considerable discussion on how the phase should be recorded and in what units the phase should be expressed. The decision at the time was in favor of the unit of time and furthermore the full scale of a phase record was chosen to be 100 microseconds for phase-tracking VLF receiver.

While the reason at the time was that the frequency of the VLF transmissions was not rigidly controlled and subject to change, and also that the full scale in time units would be easier for the operator to record and to read, the important reason which remains valid today is in the simplicity in receiver design and uniformity in phase records.

This decision was not made without consultation with other users. In retrospect, if one looks at the past phase records, he will find many advantages when he tries to use the phase records. Had the phase records been recorded in cycles, he would have to know the carrier frequency of the transmitter in order to know exactly what is the full scale. The disadvantage of this system is that the phase record is not continuous: unlike the cycle

recordings, the phase of a signal does not come back to the same point after a perturbation due to sudden ionospheric disturbance.

Perhaps it is time to re-examine the need of standardization in the selection of units for phase recordings. We really do not see an easy solution nor a great conflict between the navigator's unit of cycles and the time user's unit of microseconds provided the unit is clearly stated.

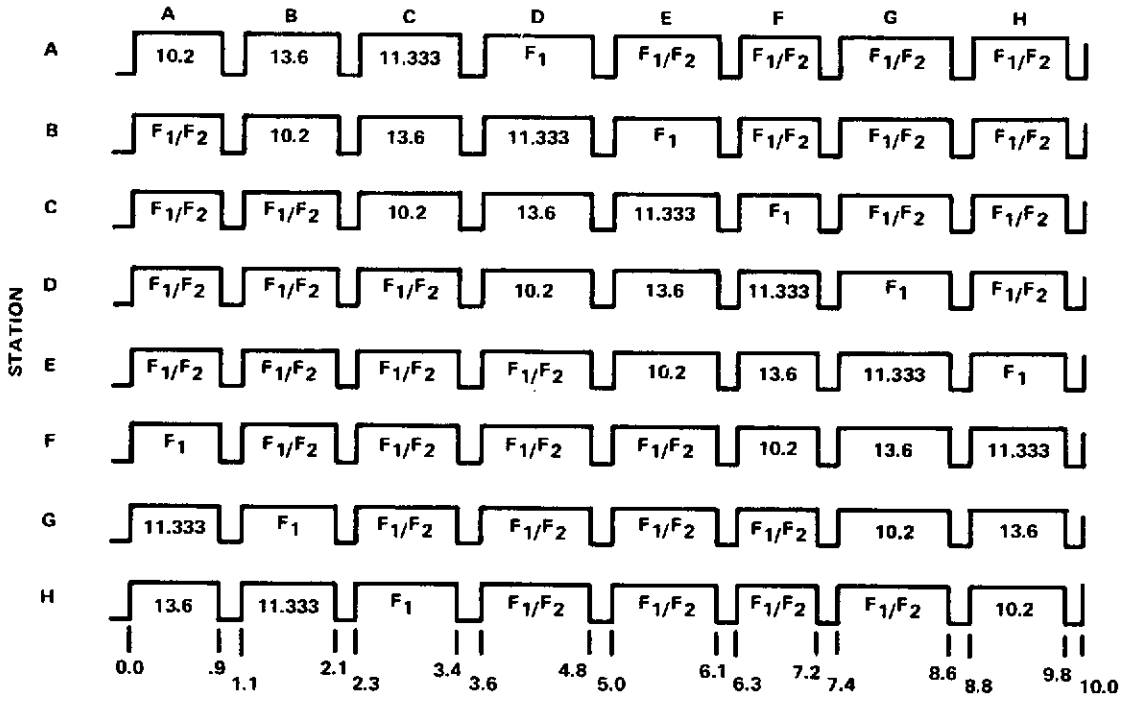

Figure 1. The ten-second OMEGA transmission sequence.

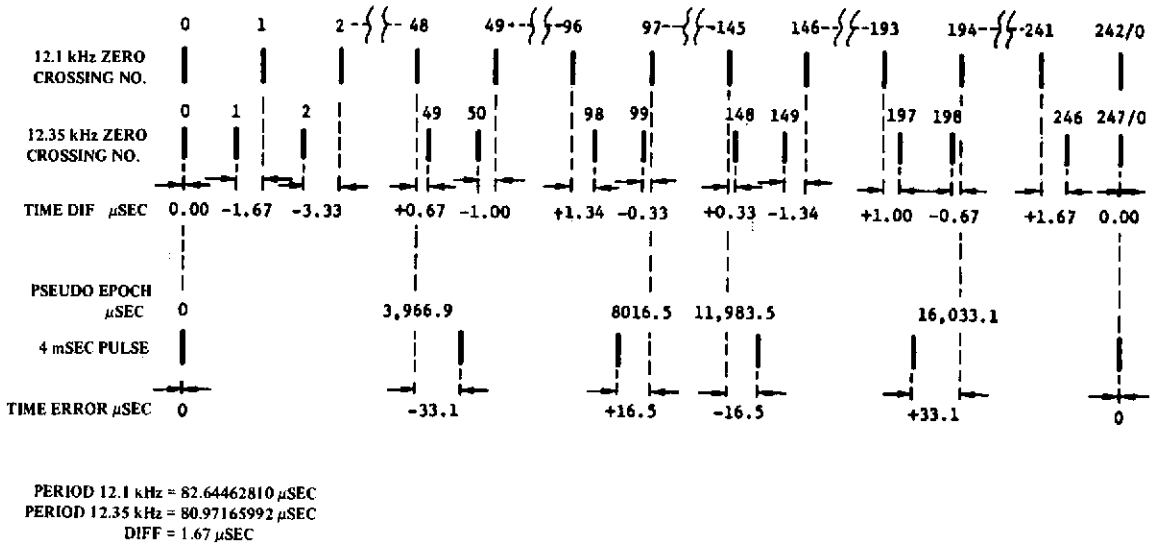

Figure 2. Example of pseudo-epochs for 12.1/12.35 kHz pair.

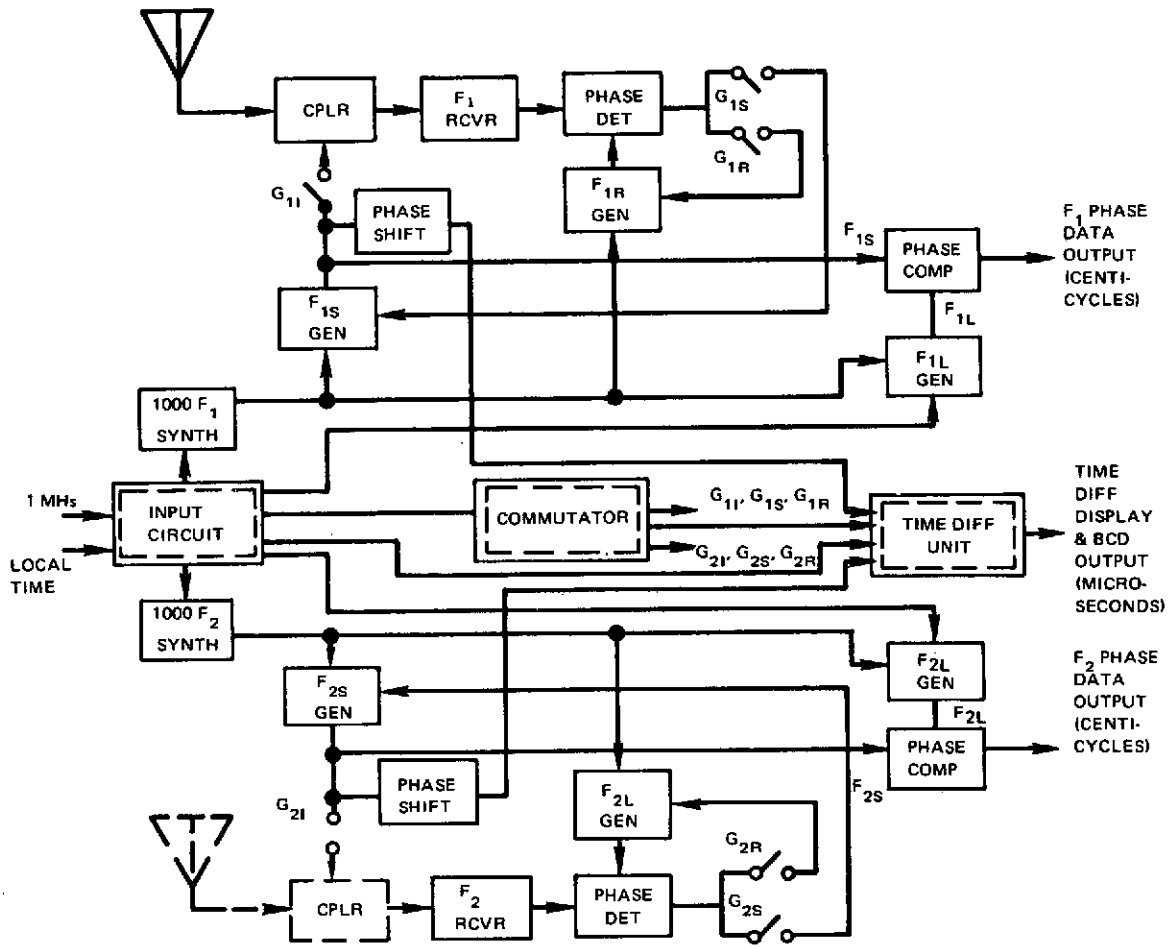

Figure 3. OMEGA Timing Receiver block diagram.

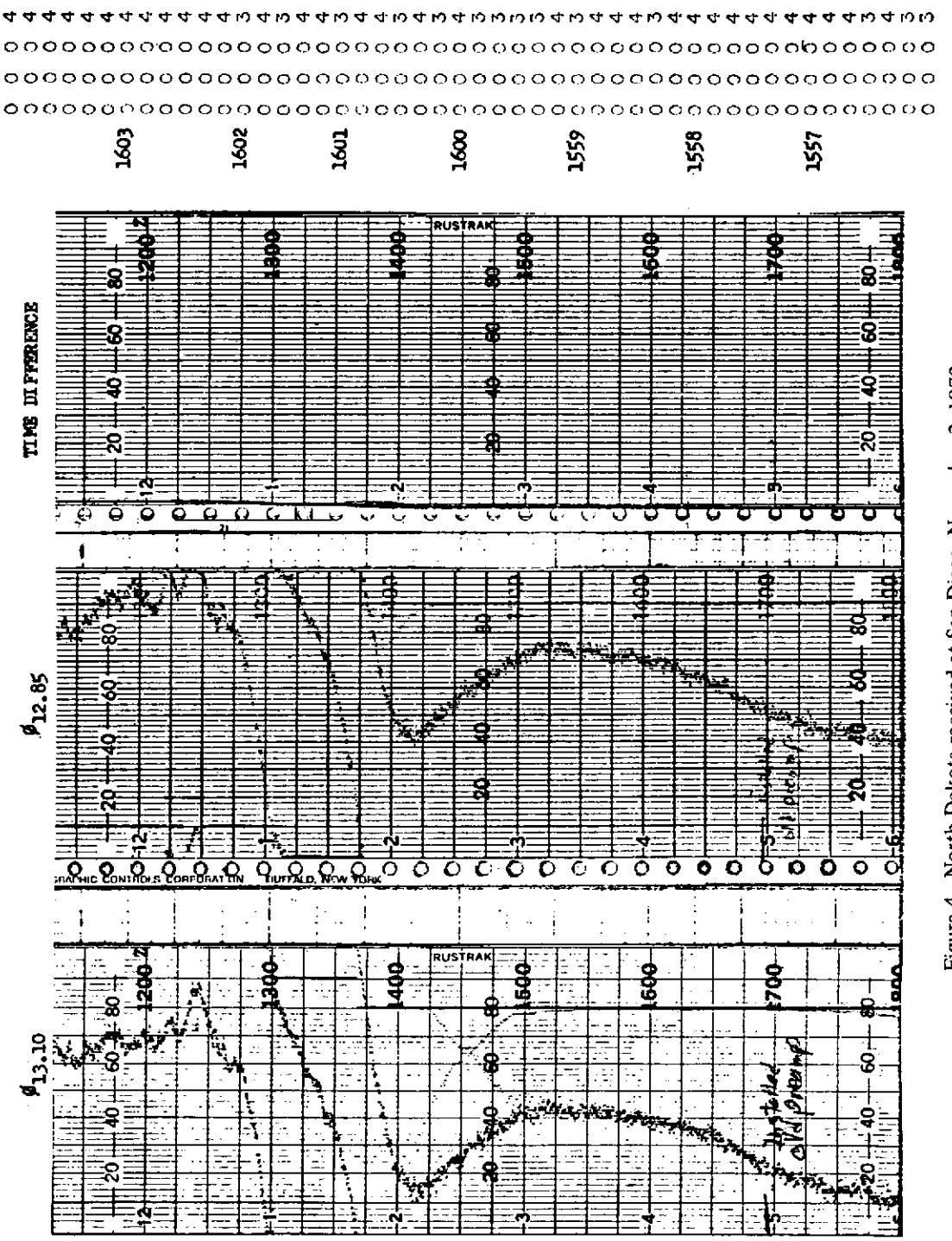

Figure 4. North Dakota received at San Diego, November 3, 1972.

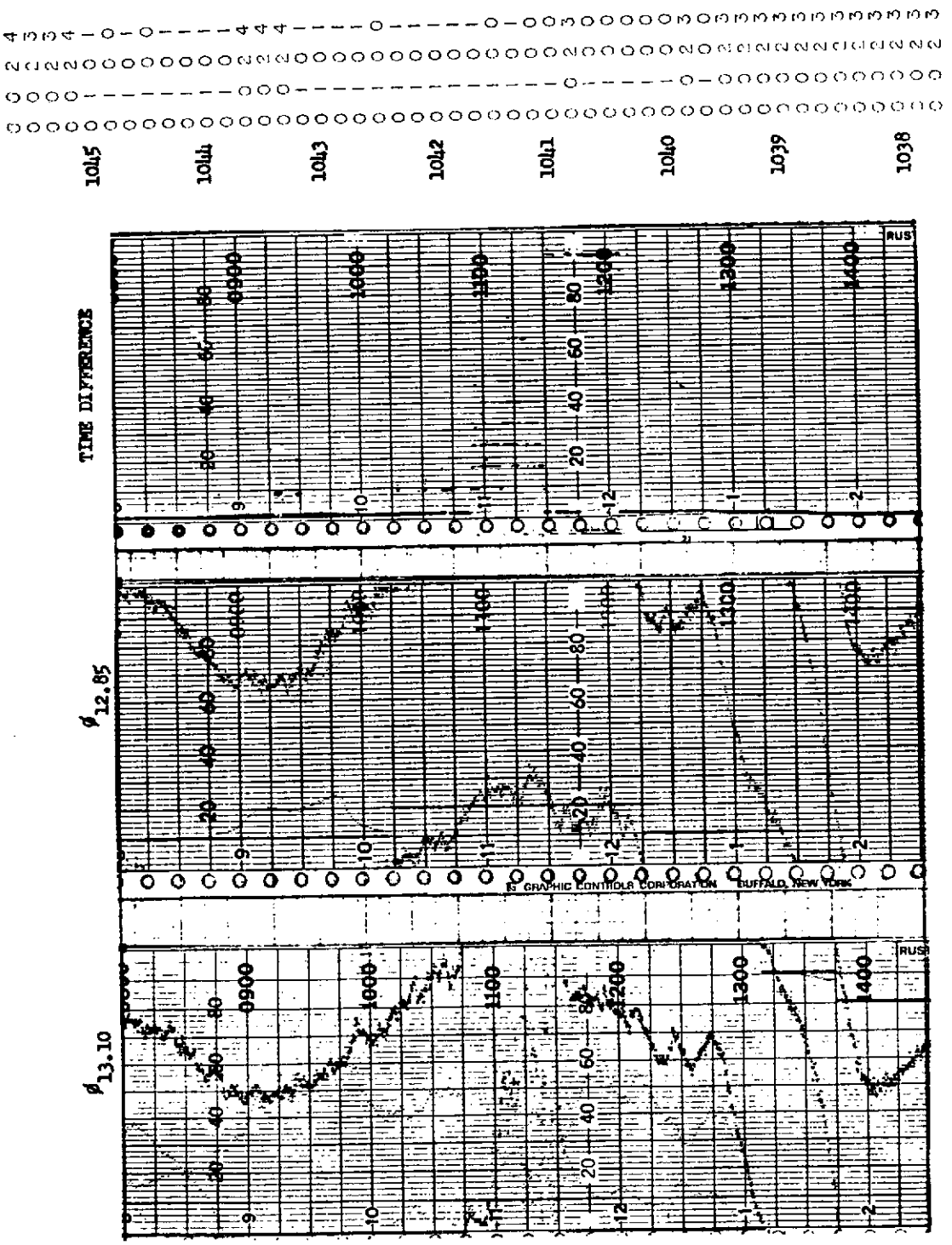

Figure 5. North Dakota received at San Diego, November 2, 1972.

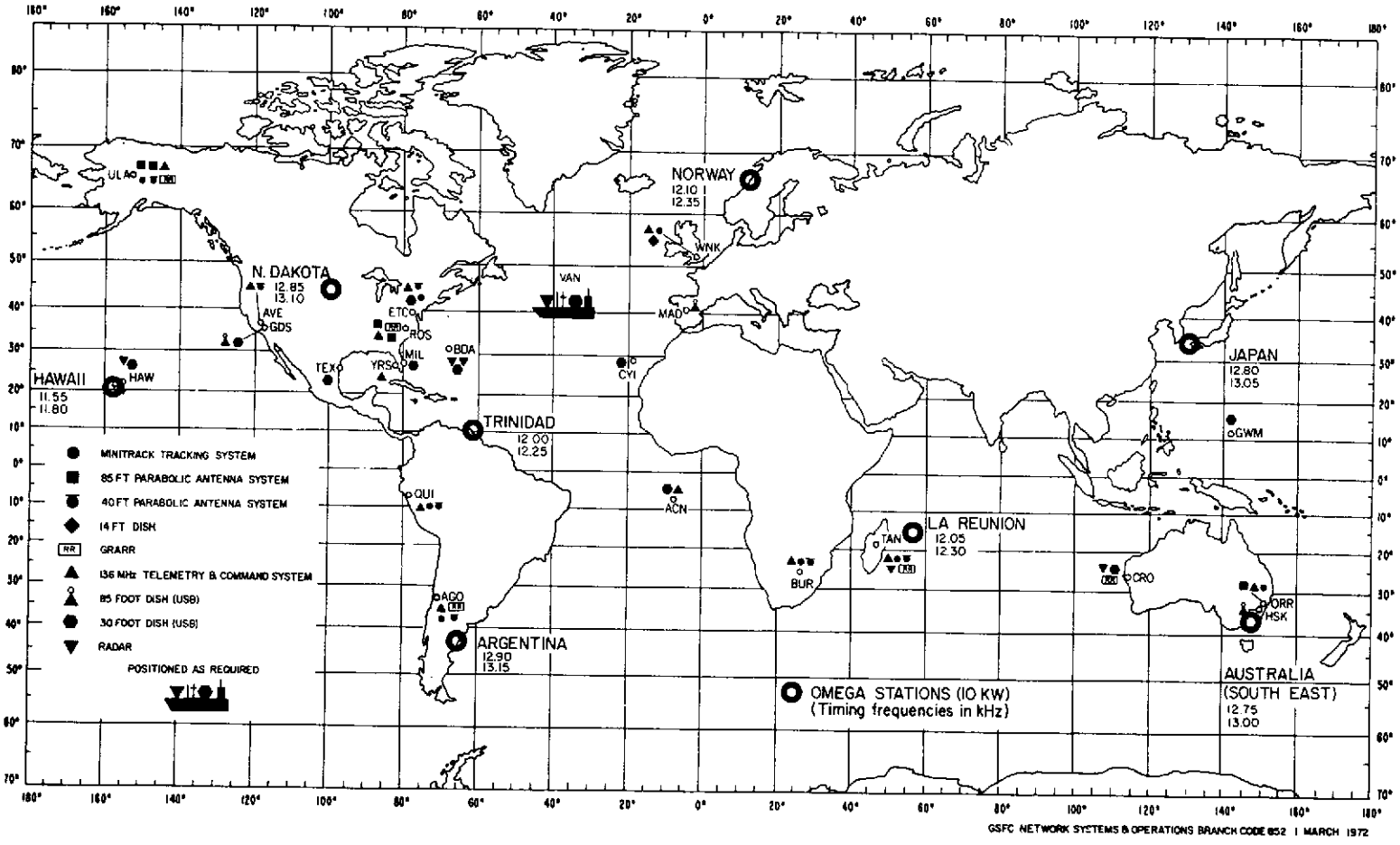

Figure 6. STDN capabilities map.

PANEL DISCUSSION

Gernot M. R. Winkler, Moderator
U. S. Naval Observatory

DR. WINKLER:

And now, while we are preparing for the panel discussion, for which we will have this morning's speakers present, I would like to invite comments on the last paper.

DR. REDER:

There is a disadvantage to using centicycles instead of microseconds. That is, if you have a rapid onset of a distrubance, you may get a cycle jump and, as was pointed out, you won't know it. And you think you don't care. The only trouble is when the distrubance slowly recedes and the previous level is reestablished, then you will introduce new cyclic advance or delay, and you won't know when it was caused previously.

I also think the notion that microseconds are completely arbitrary is very objectionable because the microsecond scale is just derived from the cycle scale by dividing phase by circular frequencies. So it's not arbitrary, and if you want to argue about that then I can give you an argument on that, too, because you can define phase propagation time, and in that case it's very useful to talk about microseconds.

DR. WINKLER:

I think the last point is also where I have strong feelings. I think for any combined use, which I envision for OMEGA stations, the measurement of propagation time in microseconds is better because it is frequency independent in the first approximation. But I propose that unless there are very strong feelings now for equal time on the other side, to go on to a different subject.

MR. WARD:

The arrival phase of F-1 and F-2 is unique for all points on a common great circle. But if you take the phase difference between these two, you now have media information because this is unique. And this changes only when the medium, when the effective path length changes. So you therefore can tell if you have cycle-slip information, and you'll also have propagation path information – everything is right there by simply taking the phase difference of the arrival phase. And as long as, for instance, the beat is 250 cycles, well within a path equivalent to the wavelength, it is unique.

MR. BRITT:

Yes, I think as Mr. Chi said, there are two ways of using this kind of system. You either have to know propagation, what to expect in the way of propagation quite well, and to be able to correct for it; or else you must start by knowing time quite well.

Now in the case of our demonstration in the back of the auditorium, we probably could have just come in, since we had very, very precise time, and we could sit at our receiver site and take data – and this is something I failed to mention in the paper – and then based on this phase data that you are talking about, we could manufacture our own propagation correction. So you could play it either way: You could make your own correction at the site, if you had good time to start with; or, if you didn't have good time, then you would need a good number to put in the receiver.

DR. WINKLER:

I'm sorry that it has not been possible to have a paper on LORAN-C. However, there is a development which is quite significant, which I would like you to know about.

We have tentative approval from various agencies to set the LORAN-D chain, which is presently operating in the western United States, on precise time. These stations are near Las Vegas and Reno, in Utah, and very close to Los Angeles. I think that the coverage is excellent and the signals can be received with a standard timing receiver.

The difference between LORAN-C and LORAN-D is mainly that LORAN-D, in order to compensate for the lesser power radiated from a smaller and more-mobile antenna, utilizes more pulses, the pulses following one-half millisecond intervals instead of one-millisecond intervals, but the one-millisecond interval pulses follow the same phase code as LORAN-C standard. And this I think will be a very significant improvement in our capability to disseminate time in the western part of the United States.

Indeed, I hope that these timing transmissions, which at this time we must consider experimental or test transmissions, nevertheless, can be continued until a more permanent LORAN-C arrangement can be developed in that area.

Now, going back into the subject of the discussions, I would like to ask, first, a very general question of our speakers here, who have been active in time and frequency applications and research. I would like them to summarize what they think is a major problem, or problems, which should be addressed in the dissemination of time or measurement of precise frequency, or the use of precision frequency and time standards.

MR. CHI:

As you know, the application of time depends on the need. In the past the requirement has always been for very coarse time, which is a problem, but not of interest to people who work at R&D activities in frequency and time.

Now, the application requirement is increasing to the order of a microsecond or below. The question is how can one be sure the time he gets is within that requirement? That is, how can one be sure that the time is correct. Furthermore, once one does have the time – I assume that he gets the time – he needs a way to verify that his time is correct. Now the next question: How can he get coarse time? Very often we work within microseconds or nanoseconds, and we lose in hours, minutes, or seconds.

So the problem is to be able to disseminate the time to the users to the point that the user can be sure that he meets his requirements. It does not require too much analysis, but if you want precise time you must exercise a certain amount of wisdom. Now the wisdom doesn't come with the users who are not in this particular field, so that some of these problems are involved in the designing of a system in a manner that people outside the field will understand exactly what they need to do.

DR. REDER:

I'm just referring to some problems which we have in VLF. I think we have learned a lot in this area during the last couple of years, but there are still some very puzzling things.

For instance, we do see antipodal interference on some paths where by all rights there shouldn't be any, and vice versa. The particular area of trouble is in the western Pacific, for instance on paths from Hawaii to Australia, as is now well known, and I think that the prediction in this area is still rather poor. So more work is needed. And I believe it could be extremely helpful if OMEGA could temporarily transmit a higher frequency on one of the segments, so that we would have three different frequencies reasonably spaced in order to get a handle on the main problems.

We have 10.2 and 13.6 kHz – if they could give us anything between, let's say 15 and 18 kHz, it would be helpful. It wouldn't have to be for a very long period of time, but as long as the segments aren't completely used anyway, and if they can do it technically, it would be very desirable.

MR. SWANSON:

May I comment on that? I believe that a signal structure question, say in the Australian area, is not really that germane to the timing problem.

The reasoning here is principally that in timing you have the choice; you can choose whatever time of day is best for you. Ordinarily, this turns out to be daytime. And actually both the 10.2- and 13.6-kilohertz signals have been monitored at the University of Queensland by Dr. Crouchley, who is here today. And the time was in fact checked by a

flying-clock arrangement; it was not exactly done specifically for the experiment, so that there was an uncertainty of some microseconds. But nonetheless, the predictions at both frequencies, from Hawaii down to the University of Queensland, agreed with the clock by about five microseconds, I believe.

MR. WILSON:

Could I add just one comment on possible experiments added to OMEGA stations? As you may or may not know, the OMEGA navigation system is in the process of becoming an operational system, and while I wouldn't say that adding experiments is impossible, I would say that it's getting harder and harder as time goes along. There is a greater and greater reluctance to take the stations off the air for any amount of time to make changes and do experiments.

MR. SWANSON:

In fact, the last series of modifications for experimental purposes I can think of occurred prior to 1966.

DR. WINKLER:

We undoubtedly move now into an era of increased application of precise time and frequency standards. I think this year's conference and last year's conference indicate that there are many systems which will eventually use precise time and frequency standards in larger numbers. Conceivably, most of these standards will be better quartz crystals, because they are still the most reliable, and probably the least expensive, precision frequency oscillators. But I do foresee a significant number of atomic frequency standards.

In this respect, I consider the equipment which we see on display here to be quite a significant accomplishment of the last two years. And the question is now: What problems can be anticipated, or where do you, as systems engineers and managers, think that problems in that critical phase may arise? I'm thinking about calibration needs. I'm thinking about training arrangements which should be made. Things along these lines. And I am wondering whether there are any comments from the audience or from the panel?

MR. SWANSON:

I'd like to express a comment on one problem that I see and have always seen, and it seems to continue. This is the confusion, I believe, between frequency and perhaps epoch or date.

A frequency standard, no matter how good – and I do think there are some superb ones available – is not in itself going to provide permanent synchronization with anything else. It necessarily will vary slightly. There will be a random walk. And sooner or later, whatever one needs in the area of synchronization, will no longer exist.

How one balances this depends on a lot of things: how good the time dissemination is; how good the standards are; what these methods cost; and how laborious they may be. But it's necessary always to balance. There's nothing wrong with buying a cesium standard simply because you don't want to bother fiddling around with adjustments for the next year, and assume that you can leave it there for a year and then adjust. This is the economic thing to do; that's perfectly reasonable.

But to buy one without recognizing the fact that you must also have a dissemination or control procedure of some kind, if you really need synchronization, is a terrible mistake. Too often one winds up with nearly impossible frequency requirements, driving one to a standard which costs at least $10,000, when perhaps dissemination methods would solve the whole thing for very much less money. But again, this is always a tradeoff. As long as it's done properly it's all one can hope for.

Another quite unrelated minor practical thing I have forgotten to mention, but John Hannah pointed out that the Naval Oceanographic Office does not exist -- they are now the Defense Mapping Agency. So if you wish to get any corrections, you had better get them from the only existing agency: the DMA.

DR. ROHDE:

There is minimum awareness in the Department of the Army of the need for precise positioning. And we in the topographic laboratories have a responsibility to provide the means, and we feel that substantial research and development should be performed in the area of providing precise timing devices such as clocks or atomic devices. But you have to realize that these equipments have to work in a dirty environment, and also they should be sufficiently cheap so that large numbers could be procured.

So there is an area where more research and development should be done, and we cannot do this in our agency. I guess it has to be done in other agencies or by industry.

Another area which causes considerable problems is the area of propagation. I indicated this morning that the ionosphere is not as simple as one may expect. In addition to ionospheric propagation, which is essentially a problem with satellite systems, there is also ground wave propagation with its attenuation problems. If one tries to get information about phase delays or time delays over ground, there is also very little material available, at least to my knowledge.

DR. WINKLER:

I think, however, that for precise time application itself, now considering the main interest of this conference, the detailed applications in navigation should be left aside.

So far as I see, the purpose of this conference is to discuss applications of technology to precise time and frequency generators, to measurements, and to certain fundamental difficulties. Well, in that respect, the propagation question is an important one, although I think of it with less seriousness because as we mentioned repeatedly, if you have to bring precision

time, or to calibrate a user's clock, you can do that in a way which takes the most advantage from the fact that he has a good clock. You can do that at the best moment, which for a satellite dissemination would be probably 4:00 o'clock in the morning local time. And for VLF or OMEGA, probably around noon.

However, there is another point in the question of systems applications, and it is the following: I think it would be a mistake if large systems which propose to use precision time technology, or TF technology, depended solely upon external systems for synchronization. I think a time and frequency autosystem should have provisions for internal synchronization. On the other hand, it must also have an interface in case of trouble. That is the main purpose of having coordinated time; in case of trouble, you must be able to get time from a variety of other sources. I think these two principles are entirely compatible and, as we discussed yesterday, that is the difference between coordination and synchronization, or immediate synchronization. It is something which is very dear to my heart, because I find that it is a most frequent cause of misunderstanding, and misunderstanding produces wrong decisions, which can be exceedingly expensive. Duplication of effort, for instance, duplication of clocks within very small application centers such as vessels or aircraft or communications centers, can be avoided or at least reduced if the whole systems aspect is kept in mind. And that is a point which maybe we have not emphasized sufficiently at this conference.

This brings me to my last concern, which is that we do depend upon feedback from you, the users. I think the conference can only be beneficial if there is substantial feedback, and criticism if available, and suggestions of what should be covered, and where the problem areas exist.

Since our discussions have to end soon, I would not like to let that end arrive without giving credit to those people who have kept the ideals of this conference alive, and who have helped to accomplish this extremely desirable coordination of our efforts, and combination of sponsorship.

And I would like to really express my gratitude to Mr. Nick Acrivos of the U.S. Naval Observatory, and Mr. Clark Wardrip from the NASA/Goddard Space Flight Center. Without these two gentlemen there would be no conference today, I can assure you.

Are there any comments in regards to what we have discussed this morning, or what may be on your mind?

DR. SONKA:

I would like to ask the panel if they would briefly discuss limitations of using VLF in our RO-RO world navigations system when you have a clock on-board.

MR. SWANSON:

I think the main limitation is the one right off the top: How do you set your clock? In essence, when you ask, "How do you set up the clock?" by the time you've answered that you're back into a hyperbolic situation.

DR. SONKA:

Well, assume you have a clock.

MR. SWANSON:

Now, to do any good in a range-to-range sense, you must have the absolute epoch, or your ticking, or whatever.

DR. SONKA:

I know. Assume you have that; you've come to the Naval Observatory and synched your clock and carried it away with you, a cesium clock, or whatever. But now all the things we have talked about this morning, all of the errors in propagation, and everything, how are these things going to limit the navigation? In other words, what will be your navigational error? It appears to me it will be several nautical miles.

MR. SWANSON:

Again it would depend on how many stations you were using. For example, the OMEGA receiver error is one specific example. In this case there is an attempt made to set the clock, at least within the epoch dealt with by the normal frequency you happen to be working with. This is not of any great use for timing because of the scales involved, but that is how the receiver is set up.

And one could, I suppose, inject, that the receiver does operate with redundant range-range lines of position. The mere fact that they're redundant is sort of getting you back more or less to some of the advantages of the hyperbolic system. In any event, its nominal accuracy, at least in the OMEGA range, would tend to be on the order of a mile, which would be that of the OMEGA system itself. This would depend on time and whatnot.

DR. WINKLER:

I would like to make a comment here. I think with all due respect for the capabilities of the OMEGA system, that from my point of view it would be advisable not to overlook capabilities which we may have entirely for free.

What Mr. Stone has described, the timing of the VLF stations, enables a user, if his equipment is sufficiently flexible, to use any combination of signals.

Also, the bit timing, which I hope will be implemented soon on the VLF stations, will provide at least a starting point. You will be able to set your clock to within probably a fraction of a millisecond in respect to that signal.

Provided one has a small computer on-board, which is entirely possible – I have seen aircraft VLF navigation systems demonstrated which utilize a small computer – the moment one has such a computer on-board, one can use a bootstrap method and a refinement in

improving the synchronization of the clock by looking at several stations, exactly the same way as has been described for LORAN-C, in which by improving the fit of the circles one can update one's clock as well as refine one's position estimation. And I see no essential difference in the case of VLF or OMEGA application except that it is harder to account for the propagation anomalies and dispersion effects.

MR. SWANSON:

I agree. I think the only reason that people have ever bothered to invent a hyperbolic navigation system in the first place is because they don't know what time it is. Had the time been known, range-range is clearly preferable. But depending on the constraints of adjusting the clock, you may work out to identically the same situation, addressing it as range-range and trying to set the clock as if you had a hyperbolic system in the first place. You can't, in essence, get something for nothing, especially if you are dealing with only three stations and an unknown clock.

DR. SONKA:

In spite of the fact that you continually refine your position and your time, aren't there fundamental limitations just because of the propagation anomalies that we've talked about this morning?

DR. WINKLER:

Yes, there are, and maybe the most serious one is if you are moving. If you yourself are moving at high speeds there are additional complications. They are the same as if you use the satellite navigation system or time dissemination system. In these applications really time and location are almost equivalent terms.

It is true, there are limitations. But I think they will essentially be comparable to the noise level which we discussed earlier in the case of VLF and OMEGA systems. That seems to be around one microsecond for very quiet periods in the polar cycle. Short-term (precision) limits of noise seem to be in the 0.1-μs range, according to the numbers which we have seen this morning in Dr. Reder's paper. Would you agree with that, Dr. Reder?

DR. REDER:

We made some experiments using a better crystal, actually an atomic clock. And then we found that we could reduce the equipment noise. I would say we could reach 0.1-μs for integration periods of about 10 s.

DR. WINKLER:

The essential principle is exactly the same in all of these applications. You have redundant data; you look at several stations, or you look at a moving satellite, and the redundancy provides a capability to update and improve your location as well as your clock. But you have to have a starting point someplace, and in practice that may mean that for many of these applications you may want to leave your clock running, even if the aircraft is on the ground or the vessel is in the harbor.

MR. SWANSON:

I'd like to make a comment that Dr. Winkler has already made twice. But I think maybe I could just second it and agree to it. And that is the little matter of differences between time scales, for example, between NBS, USNO, OMEGA, and several others. The tradeoff here is one of how often do you want to adjust and try to keep together on the basis of a rather noisy intercomparison between sources? I think this is the sort of thing where feedback is very helpful to those who have to worry about this type of problem.

You can have a nice frequency stability by simply ignoring the rest of the world. This way you don't make any epoch changes, thereby inducing discontinuities in what you are doing, and it's very nice. I believe this is undoubtedly the concern of users who said to Dr. Winkler: "Please, don't fiddle with the scale," This is what they want. They don't want these horrible changes.

At the same time, you buy this continuity of scale at the expense of the divergence between different systems. So this is, in essence, the control problem that is faced by anybody running this sort of a system. The users are those who can say, let it go hands-off and then finally adjust it by a very large amount. So do you keep making small adjustments all the time? What is really best for the application?

DR. WINKLER:

I think that is an excellent comment. And there is another application which we should mention, and that is the SATCOM ground stations. As you know, these 28 stations are being equipped with cesium beam standards. Since the satellite link provides a synchronization capability to one-tenth of a microsecond, these stations automatically become precise time reference stations.

But what are the requirements to actually step these clocks? At the present time I think we have adopted a more-or-less experimental procedure to stay within 25 microseconds for all of these. We know, of course, the time difference to a tenth of a microsecond or so. But I can foresee that as one gains experience, and as the operators become more used to the new procedures, that one can reduce that tolerance to something like one microsecond without any difficulty. And I think that's just another example for this operational question which was raised by Mr. Swanson.

MR. LIEBERMAN:

I would like to leave this conference with just one thought. We've demonstrated here, and over the years, that we have disseminated precise time and time interval over satellite stations, LORAN-C, VLF, and now OMEGA, and also TV. I think we should begin to look for applied research in using this time and time interval information, which will be available almost throughout the world. We can now talk about getting comparatively inexpensive receiving equipment to make use of the time that's available. And I disagree that

systems in the future necessarily have to have internal references, if there are sufficient sources, just like our power sources now, to keep them on time and frequency.

DR. WINKLER:

I think you will find the greatest amount of resistance for any military system to have to rely exclusively on something which is outside, because one should keep the systems separate in their operational capability. That capability should not be endangered by any failure outside of the system.

Ladies and gentlemen, I think we have come to the end of our allocated time. I would like to thank the speakers, and turn the meeting back to Mr. Clark Wardrip.

MR. WARDRIP:

It has been Goddard's pleasure to host the Fourth PTTI Conference; and on behalf of the U.S. Naval Observatory, the Naval Research Laboratory, and the Naval Electronic Systems Command, I thank you all for coming and for your participation.

Thank you very much.

APPENDIX A

List of Attendees
Fourth Precise Time and Time Interval (PTTI)
Planning Meeting
November 14-16, 1972

Name	Activity	Code	Address	Tel. No.
Acrivos, H. N.	NAVOBSY	62L	Washington, D. C. 20390	202/254-4587
Acton, B. A.	State Department	OPR/ADP	Washington, D. C. 20520	202/632-0194
Akers, O. M.	NAVOCEANO	3110	Washington, D. C. 20390	202/763-1270
Allan, D. W.	NBS	- - - - -	Boulder, Colorado 80302	303/499-1000 X3208
Allen, J. F.	Australian Embassy	- - - - -	Washington, D. C. 20036	202/797-3454
Alley, C. O.,	University of Maryland	Phy. & Ast.	College Park, Md. 20742	301/454-3405
Ashinsky, M.	Sperry Rand Corp.	Sys. Mgt. Div.	Great Neck, N. Y. 11020	516/574-2454
Bajus, J.C., CAPT	NAVELECSYSCOM	- - - - -	Washington, D. C. 20360	202/542-6410
Baldwin, C. E.	NAVELEXACT BSN	- - - - -	Boston, Mass. 02210	617/542-5100
Barnaba, J. F.	AGMC	MLPE	Newark, Ohio 43055	614/522-2171
Barnes, D. S.	AFS	CF/DVH	Los Angeles, Calif. 90009	213/643-1366
Barry, J. R.	APL	- - - - -	Silver Spring, Md. 20910	301/792-7800 X7240
Bartholomew, C.A.	NRL	7962	Washington, D.C. 20390	202/767-2595
Bartko, A.C.	NAVAIR	53343E	Washington, D.C. 20360	202/692-0758/9
Beahn, T. J.	NSA	- - - - -	Ft. Meade, Md. 20755	301/277-4190
Beard, R. L.	NRL	7969	Washington, D. C. 20390	202/767-2595
Beehler, R. E.	NBS	- - - - -	Boulder, Colorado 80302	303/499-1000 X3986
Behen, T. R.	NAVCOMM	212A	Washington, D. C. 20390	202/282-0700 202/282-0570
Berbert, J.	NASA-GSFC	550		301/982-5055
Best, J. S.	USASTRATCOM	- - - - -	Ft. Dix, N.J. 08640	609/234-6041
Biederman, D.M., LTJG	USCG	- - - - -	Washington, D. C. 20590	202/426-1242
Bigelow, H. L., Jr.	OASD(T)	TELECOM	Washington, D. C. 20301	202/697-8613
Bishop, J. W.	HQ AFCS/EPECCS	- - - - -	Richards, Mo. 64030	816/331-4400 X3813
Blackburn, W. J.	NGS	- - - - -	Rockville, Md. 20852	301/496-8307
Bodily, L. N.	Hewlett-Packard	- - - - -	Santa Clara, Calif. 95050	408/246-4300 X2248
Bourdet, J.	Hewlett-Packard	- - - - -	Santa Clara, Calif. 95050	408/246-4300 X2171
Bowman, J. A.	NRL	5424	Washington, D. C. 20390	202/767-2061
Bradley, J.	NAVAIRSYSCOM	J P-2	Washington, D. C. 20360	202/692-2511
Bruce, W. E.	WSMR	- - - - -	White Sands, N.M. 88002	915/678-1619
Breetz, L. D.	NRL	7967	Washington, D. C. 20390	202/767-2595
Brienza, N.	CSC	- - - - -	Falls Church, Va. 22046	703/533-8877
Britney, O. L.	Canadian Def. Res. Staff	- - - - -	Washington, D. C. 20008	202/483-5505 X304
Britt, J. E.	USNELC	2100	San Diego, Calif. 92152	714/225-6883
Brooks, C. C.	DOD	W1	Ft. Meade, Md. 20755	301/688-7438
Brown, C. W.	APL	- - - - -	Silver Spring, Md. 20910	301/953-7100 X7074
Buisson, J.	NRL	7965	Washington, D. C.	202/767-2595

Name	Activity	Code	Address	Tel. No.
Burman, G. A. LCDR	NAVELECSYSCOM	-----	Washington, D. C. 23060	202/692-2182
Bush, R. L.	Bendix Comm. Div.	-----	Towson, Md. 21204	301/823-2200
Butterfield, F. E.	Aerospace Corp.	-----	El Segundo, Calif. 90045	213/648-7683
Byrne, F.	NASA-KSC	-----	KSC, Fla. 32899	305/867-4432
Cain, M. L.	Nat. Comm. Sys.	4370	Arlington, Va. 22217	703/692-2815
Calkins, Jr., D. S. CDR	NAG	-----	Point Mugu, Calif. 93043	805/982-8016 805/982-8017
Casey, C. F.	CSC	-----	Falls Church, Va. 22046	703/533-8877
Casselman, C. J.	NELC	2100	San Diego, Calif. 92152	714/225-6648
Cavanagh, E. J.	NAVELECSYSCOM	412	Washington, D. C. 20360	202/282-0510
Chi, A. R.	NASA/GSFC	810	Greenbelt, Md. 20771	301/982-2502
Childers, A. A.	DCA	330	Washington, D. C. 20305	202/692-0255
Chin, J. W.	USAF	-----	Wright Patterson, O. 45433	-----
Clark, E. T.	Aerospace Corp.	-----	El Segundo, Calif. 90045	213/648-7048
Clark, M. E.	Dept. of Army	-----	Ft. Huachuca, Ariz. 85613	602/538-6061
Clark, T. A.,	NASA/GSFC	693		301/982-5957
Clements, D. E.	USCG RADSTA	-----	Alexandria, Va. 22310	703/971-1600 X46
Cloeren, J. M.	Austron Inc.	-----	Austin, Texas 78758	512/836-3523
Cole, Jr., R.W.	NRL	5458	Washington, D. C. 20390	202/767-2265
Cook, D.	DCA HQ	482	Washington, D. C. 20305	202/692-2775
Creveling, C. V.	NASA/GSFC	560		301/982-6126
Crouchley, J.	Queensland Univ.	-----	Ft. Monmouth, N. J.	201/535-1624
Currie, D. G.	Univ. of Maryland	-----	College Park, Md. 20742	301/454-3405
Curtright, J. B.	JPL	-----	Pasadena, Calif. 91103	
Cutler, L. S.	Hewlett-Packard	-----	Palo Alto, Calif. 94304	415/493-1501
Davis, G. W.	USAF (AAC)	L6MP	Elmendorf, Alaska 99506	907/753-3219
Davis, J. H.	NAVOBSY	-----	Washington, D. C. 20390	202/254-4537
DeGreck, J. A.	NSA	-----	Ft. Meade, Md. 20755	301/688-6761
Dennis, A. R.	CSC	-----	Gaithersburg, Md. 20760	301/589-1545
DeSocio, G.	NAVELECSYSCOM	05183	Washington, D. C. 20360	202/692-7573
Dieter, F.	DCA	482	Washington, D. C. 20305	202/692-2772
Di Pietro, M. A.	Army Dept.	-----	Washington, D. C. 20390	202/693-6954
Dix, W. H.	DCA	-----	Washington, D. C. 20305	202/692-6930
Donaldson, R. W.	Westinghouse Elec.	-----	Baltimore, Md. 21203	301/765-6295
Dorian, C., CAPT	COMSAT	-----	Washington, D. C. 20024	202/554-6829
Dorsey, S. L.	DCEO	-----	Reston, Va. 22090	703/437-2266
Driscoll, M. M.	Westinghouse Elec.	-----	Baltimore, Md. 21207	301/765-2701
Duckworth, D. T.	NWL	TI	Dahlgren, Va. 22448	703/663-8474
Duncan, P. I.	Australian Embassy	-----	Washington, D. C. 20036	202/797-3287
Easton, R.	NRL	7960	Washington, D. C. 20390	202/767-2595
Feldman, S.	NOL	-----	Silver Spring, Md. 20910	301/495-8174
Fey, L.	NBS	-----	Boulder, Co. 80302	303/499-1000
Fishburn, T. F.	NUSC	WM13X	Newport, R.I. 02840	401/841-3088
Fisher, L. C.	NAVOBSY	62F	Washington, D. C. 20390	202/254-4555
Fiske, P. E.	NELC	230	San Diego, Calif. 92152	714/225-7326
Fleishman, L. S.	Westinghouse Elec.	-----	Baltimore, Md. 21203	301/765-2043
Folts, H. C.	NCS	-----	Arlington, Va. 22204	703/692-2126
Fosque, H. S.	NASA HDQ	TA	Washington, D. C. 20546	202/755-2434
Foushee, W. T.	NAVELECSYSCOM	05713	Washington, D. C. 20360	202/692-8232
Foxe, M.	NASA/GSFC	509		301/982-4947
Frenkel, G.	CSC	-----	Falls Church, Va. 22046	703-533-8877
Friedl, R. S., CAPT	DCA	H830	Reston, Va. 22090	703/437-2450

Name	Activity	Code	Address	Tel. No.
Gallant, A.	NAVELECSYSCOM	044AG	Washington, D. C.	202/692-7474
Gardner, L. M.	Sperry-Rand Corp.	- - - - -	Great Neck, N.Y. 11020	516/574-2455
Gattis, T. H.	NRL	5424	Washington, D. C. 20390	202/767-2347
Gomm, N. F.	Australian Embassy	- - - - -	Washington, D. C. 20036	202/797-3382
Gordon, D. J.	DMA-TC	52323	Washington, D. C. 20315	202/227-2584
Gould, R.	Sperry-Rand Corp.	- - - - -	Great Neck, N.Y. 11020	516/574-2423
Gutleber, F. S.	USAECOM	TRI-TAC	Ft. Monmouth, N.Y. 07703	201/532-8415
Hafner, E.,	USAECOM	AMSEL-TL-SI	Ft. Monmouth, N.J. 07703	201/535-1878
Hagerman, L. L.	Aerospace Corp.	- - - - -	Los Angeles, Calif. 90045	213/648-7597
Hakkarinen, W.	NW ESA	131E	Washington, D. C. 20390	202/433-3856
Hall, R. G.	NAVOBSY	62B	Washington, D. C. 20390	202/254-4547
Halpeny, O. S.,	DCA	330	Washington, D. C. 20305	202/692-0256
Hamilton, M. A.	NAG	- - - - -	Pt. Mugu, Calif. 93043	805/982-8702
Hanna, J. E., Jr.	DMA	NT2	Washington, D. C. 20390	301/763-1504
Harper, H. M.	CSC	- - - - -	Falls Church, Va. 22046	703/533-8577
Harris, H. C.	DMAAC	- - - - -	F. E. Warren, Wy. 82001	307/775-2894
Hartell, W. K., CDR	NAVELECSYSCOM	- - - - -	Washington, D. C. 20360	202/692-8863
Hathaway, J. D.	DMA	52323	Washington, D. C. 20315	202/227-2587
Haupt, R. F.	NAVOBSY	61B	Washington, D. C. 20390	202/254-4598
Healey, D. J., III	Westinghouse Elec.	- - - - -	Baltimore, Md. 21203	301/765-2054
Heinmiller, D. R.	NRL	7967A	Washington, D. C. 20390	202/767-2595
Herring, J. C., MAJOR	USAF	- - - - -	Bedford, Ma. 01730	617/861-4550
Hibbs, R.	NASA/GSFC	814	Greenbelt, Md. 20771	301/982-5046
Hickey, C. B.	USCG	- - - - -	Alexandria, Va. 22310	703/971-1600 X11
Hocking, W. M.	NASA/GSFC	814	Greenbelt, Md. 20771	301/982-5046
Holman, W.	NELC	- - - - -	San Diego, Calif. 92152	714/225-7064
Holt, J. M.	McDonnell-Douglas	- - - - -	St. Charles, Mo. 63301	314/232-0232
Hoover, H. D.	Bendix	814	Riverdale, Md. 20840	301/277-0952
Horowitz, M. W.	DCA/DCEO	- - - - -	Reston, Va. 22090	703/437-2316
Howatt, R. C.	NASA/GSFC	814	Greenbelt, Md. 20771	301/982-6461
Howell, W. R., Jr.	Army Dept.	DACE-EDC-E	Washington, D. C. 20314	202/693-6954
Hurd, W. J.,	JPL	M/S 238/420	Pasadena, Calif. 91103	213/354-2748
Hurst, W. O.	USASTRATCOM	- - - - -	Ft. Huachuca, Ariz. 85613	602/538-6511
Janiczek, P. M.	NAVOBSY	- - - - -	Washington, D. C. 20390	202/254-4595
Jespersen	NBS	273.01	Boulder, Colo. 80302	303/499-1000
Johnston, K.	NRL	7130J	Washington, D. C. 20390	202/767-2351
Jones, H. H., Jr.	DCA/DCEO	- - - - -	Reston, Va. 22090	703/437-2316
Jones, J. K.	NASA/GSFC	852	Greenbelt, Md. 20770	301/982-5353
Jones, M. E.	CSC	- - - - -	Falls Church, Va. 22046	703/533-8877 X544
Kahn, W. D.	NASA/GSFC	550	Greenbelt, Md. 20770	301/982-4554
Kaufmann, D.	NASA/GSFC	814	Greenbelt, Md. 20771	301/982-4031
Kern, R. H.	Freq. & Time Sys.	- - - - -	Danvers, Mass. 01923	617/777-1255
Kitchen, W. L.	NASA/LRC	M.S. 488	Hampton, Va. 23365	703/827-3701
Kleyczynski, W. J.	NAVOBSY	62K	Washington, D. C. 20390	202/254-4023
Knowles, S. H.	NRL	7132	Washington, D. C. 20390	202/767-2257
Kohler, R. E.	NOAA-NOS	- - - - -	Rockville, Md. 20852	301/496-8907
Krutenat, R. A.	NAVTORPSTA	7034	Keyport, Wn. 98345	206/697-4544
Krutz, R. A.	DCA	H610	Reston, Va. 22090	703/437-2261
Kuldell, P. D.	DMA-HC	- - - - -	Washington, D. C. 20390	202/763-1212
Kushmeider, P.	NASA/GSFC	814	Greenbelt, Md. 20771	301/982-4031

Name	Activity	Code	Address	Tel. No.
LaRochelle, P. J.	FAA	RD-630	Washington, D. C. 20591	202/426-8684
Lavanceau, J. D.	NAVOBSY	62E	Washington, D. C. 20390	202/254-4548
Lavery, J.	NASA-GSFC	814	Greenbelt, Md. 20771	301/982-5975
Lee, B.	MIT	- - - - -	Cambridge, Mass. 02138	617/258-4087
Leeuwenburg, B.	DCEO	H710	Reston, Va. 22090	703/437-2266
Lieberman, T.	NAVELEX	05183	Arlington, Va. 22217	202/692-7367
Looney, C. H.	NASA/GSFC	540	Greenbelt, Md. 20771	301/982-4623
Love, J. D.	DMATC	- - - - -	Washington, D. C. 20315	202/227-2249
Luciani, V. J.	FAA-NAFEC	- - - - -	Atlantic City, N.J. 08405	609/646-9089
Lynch, D. W.	NRL	7965	Washington, D. C. 20390	202/767-2294
MacDoran, P. F.	JPL	- - - - -	Pasadena, Calif. 91103	213/354-7118
Madrid, G. A.	JPL	- - - - -	Pasadena, Calif. 91103	213/354-6754
Mallet, R. L.	SMAMA/MMEES	- - - - -	McClellan, Calif. 95652	916/643-5060
Malone, D. R.	Austron, Inc.	- - - - -	Austin, Texas 78753	512/836-3523
Martin, A. J.	NRL	7937	Washington, D. C. 20390	202/767-2891
Mazur, W. E.	NASA/GSFC	814	Crownsville, Md. 21032	301/982-6587
McCaskill, T.	NRL	7965	Washington, D. C. 20390	202/767-2595
McClain, E.D.	NAVOBSY	- - - - -	Washington, D. C. 20390	202/254-4415
McConnell, V.	NSA	- - - - -	Ft. Meade, Md. 20755	301/688-6551
McCoubrey, A. O.	Freq. & Time Sys.	- - - - -	Danvers, Mass. 01923	617/777-1255
McDonald, K. D.	DOD	- - - - -	Arlington, Va. 22203	202/692-4891
McFadden, G. R., CDR	DMA	PRA	Washington, D. C. 20305	202/254-4455
McIntire, O. E.	FAA	RD241	Washington, D. C. 20591	202/426-3225
McNair, M. L., LCDR	OTEF	- - - - -	Norfolk, Va. 23511	
McNeece, J. O.	NAVOBSY	- - - - -	Washington, D. C. 20390	202/254-4423
Michelini, R. D.	SAO	- - - - -	Cambridge, Ma. 02138	617/864-7910 X486
Miller, P. K.	NAVOBSY	- - - - -	Washington, D. C. 20390	202/254-4415
Moore, R. T.	Vitro Lab	- - - - -	Silver Spring, Md. 20910	301/871-2749
Moore, R. B.	NRL	7962	Washington, D. C. 20890	202/767-2595
Morakis, J.	NASA/GSFC	752	Greenbelt, Md. 20771	301/982-2180
Morcerf, L. A., Jr. LCDR	COMNAVCOMM	- - - - -	Washington, D. C. 20390	202/282-0573
Murray, J. A., Jr.	NRL	5425	Washington, D. C. 20390	202/767-3155
Nolan, T. P., CDR	USCG	- - - - -	Bedford, Mass. 01730	617/861-3941 617/861-4394
Nugent, M. J.	NSA	- - - - -	Ft. Meade, Md. 20755	301/688-6396
O'Brien, E.	FAA	ARD-330	Washington, D. C. 20591	202/360-5055
O'Neill, J.	NRL	5424C	Washington, D. C. 20390	202/767-2061
Orr, C. B., Jr.	DCA	- - - - -	Reston, Va. 22090	703/437-2266
Parsons, P. H.	NSA	R-904	Ft. Meade, Md. 20755	301/688-7054 301/688-7135
Percival, D. B.	NAVOBSY	62F4	Washington, D. C. 20390	202/254-4555
Perfetto, H. A.	Booz-Allen	- - - - -	Bethesda, Md. 20014	301/656-2200
Perry, J. C.	NASA/GSFC	814	Greenbelt, Md. 20771	301/982-4051
Peters, H. E.	NASA/GSFC	524	Greenbelt, Md. 20771	301/982-4682
Petrey, H. E.	DMA	52251	Washington, D. C. 20315	703/756-5165
Pfeiffer, G. C.	NSSNF	SPY-91	Brooklyn, N.Y. 11251	212/625-4500 X357
Phillips, D. H.	NRL	5424C	Washington, D. C. 20390	202/767-2061
Phillips, G. K.	NSA	- - - - -	Ft. Meade, Md. 20755	301/688-6127
Phillips, R. E.	NRL	5424C	Washington, D. C. 20390	202/767-2061 202/767-3262
Phipps, P.	Sandia Labs	- - - - -	Albuquerque, N. M. 87115	505/264-7531

Name	Activity	Code	Address	Tel. No.
Pitsenberger, J. W.	Navy Dept.	SP 2701	Washington, D. C. 22202	202/695-0775
Plotkin. I. P.	DCEO	- - - - -	Reston, Va. 22090	703/437-2266
Priddy, N. B., CAPT	SAMTEC	- - - - -	Vandenberg, Calif. 93437	805/866-8772
Putkovich, K.	NAVOBSY	62E1	Washington, D. C. 20370	202/254-4437
Quinn, G.	FAA	- - - - -	Washington, D. C. 20591	202/426-8412
Raines, M.	NAVOBSY	- - - - -	Washington, D. C. 20390	202/254-4551
Ramasastry, J.,	NASA/GSFC	553	Greenbelt, Md. 20771	301/982-5462
Reder, F. H.,	USAECOM	AMSEL-TL-A	Ft. Monmouth, N.J. 07703	201/535-1624
Ricketts, J. C.	NAVELECSYSCOM	0345	Washington, D. C. 20360	202/692-6093
Rivamonte, J.	USAMCC	AMSMI-MME	Redstone Arsenal, Ala. 35809	205/876-4969
Robinson, T. A.	DMA-TC	TPCTP(14220)	Washington, D. C. 20315	202/227-2158
Roeber, J. F., Jr., LCDR	USCG-HQ	EEE-4	Washington, D. C. 20590	202/426-1193
Rohde, F. W.,	USATOPOCOM-ETL	TPCTL-TD-EA	Ft. Belvoir, Va. 22060	703/664-6994
Rosenbaum, B.	NASA/GSFC	553	Greenbelt, Md. 20771	301/982-5462
Rountree, R. D.	USACEEIA	SCCC-CED-XET	Ft. Huachuca, Ariz. 85613	602/879-6829
Rousseau, E. W.	SAMTEC	- - - - -	Vandenberg, Calif. 93437	805/866-8772
Rubino, J.	FAA	AEM-200	Washington, D. C. 20590	202/426-8794
Rueger, L. J.	APL	- - - - -	Silver Spring, Md. 20910	301/953-7100
Sable, T. J.	NAVELEX	05623	Washington, D. C. 20360	202/282-0280
Schmid, J. G.	SAMTEC	ENDS	Vandenberg, Calif. 93437	805/866-4871
Schoone, G.	NASA-WS	- - - - -	Wallops Island, Va. 23337	703/824-3411
Schultz, D. O.	DCEO	701	Reston, Va. 22090	703/437-2266
Scott, T.	NASA/WS	- - - - -	Wallops Island, Va. 23337	703/824-3411 X565
Scott, W. V.	Sierra Research	- - - - -	Buffalo, N.Y. 14225	716/632-8823
Selland, D. A.	DCEO	H-710	Reston, Va. 22090	703/437-2266
Severo, F. E.	USAF	TSG	Washington, D. C. 20332	202/693-0593
Sgro, D.	Hughes Aircraft Co.	- - - - -	Aurora, Colo. 80010	303/343-7575
Shames, O.	NADC	- - - - -	Johnsville Warminster, Pa. 18974	215/672-9000 X2227 X2951
Shnidman, D.	BENDIX/GSFC	832	Greenbelt, Md. 20771	
Smith, L. E.	DMATC	52332	Washington, D. C. 20315	202/227-2262
Sokol, S.	NASA-LRC	- - - - -	Hampton, Va. 23365	703/827-3701
Stanley, J. T.	NBS-WWV	- - - - -	Ft. Collins, Co 80521	303/484-2372
Stelter, L. R.	NASA-GSFC	800	Greenbelt, Md. 20771	301/982-6727
Stern, W.	General Time	- - - - -	Stamford, Conn. 06902	203/325-1587
Sterrett, D. T.	NSA	- - - - -	Ft. Meade, Md. 20755	301/688-7905
Stetina, F.	NASA-GSFC	831	Greenbelt, Md. 20771	301/982-2357
Stone, R. R., Jr.	NRL	5424	Washington, D. C. 20390	202/767-3454
Stonestreet, W.	MIT	- - - - -	Cambridge, Mass. 02138	617/258-4087
Stover, H. A.	DCA-SEF	T213	Reston, Va. 22090	703/437-2346
Strain, J. T.	Freq. Elec.	- - - - -	Rockville, Md. 20850	301/762-6210
Strucker, P. P.	MEC NAVPRU	- - - - -	Pomona, Calif. 91766	714/629-5111 X3012
Sutorik, G. J.	COMNAVCOMM	- - - - -	Washington, D. C. 20390	202/282-0561
Suttle, R. V., III	NAVOBSY	- - - - -	Washington, D. C. 20390	202/254-4437
Swaims, T.	Gulton Indus. Inc.	- - - - -	Albuquerque, N.M. 87123	505/299-7601
Swanson, E. R.	NELC	2250	San Diego, Calif. 92101	714/225-6365
Swift, E.	NWL	- - - - -	Dahlgren, Va. 22448	703/663-8209
Sydnor, R. L.,	JPL	M/S 238/420	Pasadena, Calif. 91103	213/354-2763

Name	Activity	Code	Address	Tel. No.
Thornburg, C.	Booz-Allen	-----	Bethesda, Md. 20014	301/656-2200
Tollefson, G.	DAFC	-----	Washington, D. C. 20332	202/693-0593
Tomlin, J. W.	Hughes Aircraft	-----	Aurora, Colo. 80010	303/341-3247
Toms, J. L.	T E Corp.	-----	Rockville, Md. 20850	301/340-0303
Troutt, D. W., LT	USCG	-----	Washington, D. C. 20590	202/426-1193
Turner, K. M.	COMNAVCOMM	-----	Washington, D. C. 20390	202/282-0533
Tymczyszyn, J. J.	FAA-WR	AWE-105	Los Angeles, Calif. 90045	213/670-7030 X259
Viars, T. C.	USAECOM	AMSEL-VL-G	Ft. Monmouth, N.J. 07762	201/535-2490
von Bun, F.	NASA/GSFC	550	Greenbelt, Md. 20771	301/982-5201
Wachob, J. R.	NAVOBSY	-----	Washington, D. C. 20390	202/254-4474
Walch, M.	NSA	W83	Ft. Meade, Md. 20755	301/688-6127
Walls, J. E.	FAA/NAFEC	-----	Atalntic City, N.Y. 08405	609/641-8200 X2618
Walton, F. W.	NOAA-NOS	-----	Rockville, Md. 20852	301/496-8907
Ward, S. C.	JPL	-----	Pasadena, Calif. 91103	213/354-4638
Wardrip, C.	NASA/GSFC	814	Greenbelt, Md. 20771	301/982-6587
Watson, F. D.	McDonnell Douglas	-----	St. Charles, Missouri 63301	314/232-0232
Weber, D. G.	Hayes Intl.	-----	Huntsville, Ala. 35807	205/453-1770
Webster, H. C.	Australian Embassy	-----	Washington, D. C. 20036	202/797-3258
Wendel, T. B.	FAA	-----	Washington, D. C. 20591	202/426-8684
West, J. S.	NRL	5424	Washington, D. C. 20390	202/767-3161
White, F. C.	ATA	-----	Washington, D. C. 20006	202/872-4026
White, H. L.	DMAAC/RDGS	-----	St. Louis, Mo. 63118	314/268-4061
Wick, R. J.	Sperry-Rand	-----	Great Neck, N.Y. 11020	516/574-2577
Williams, R. E.	Univ. of Md.	-----	College Park, Md. 20742	301/454-3405
Wills, A., Jr.	Sperry-Rand	-----	Great Neck, N.Y. 11020	516/574-2577
Wilson, J.	NELC	2100	San Diego, Calif. 92152	714/225-6783
Winkler, G. M. R.	NAVOBSY	62	Washington, D. C. 20360	202/254-4546
Wipff, F. P.	ANC	-----	Prescott, Az. 86301	602/445-5711
Workman, J. P., CAPT	USAF-AGMC	-----	Newark, Ohio 43055	614/522-2171 X549
Wyatt, J. A.	NAVELECSYSCOM	05183	Washington, D. C. 20390	202/692-7368
Young, W. R.	NASA-LRC	M.S. 488	Hampton, Va. 23365	703/827-3701
Zirm, R. R.	NRL	7964	Washington, D. C. 20390	202/767-2595